

EXPERIMENTAL AND NUMERICAL STUDIES ON BLOCK TYPE QUAY WALLS
UNDER DYNAMIC LOADING

A THESIS SUBMITTED TO
THE GRADUATE SCHOOL OF NATURAL AND APPLIED SCIENCES
OF
MIDDLE EAST TECHNICAL UNIVERSITY

BY

HÜLYA KARAKUŞ

IN PARTIAL FULFILLMENT OF THE REQUIREMENTS FOR
THE DEGREE OF DOCTOR OF PHILOSOPHY

IN

CIVIL ENGINEERING

MARCH 2013

Approval of the thesis:

**EXPERIMENTAL AND NUMERICAL STUDIES ON BLOCK TYPE QUAY WALLS UNDER
DYNAMIC LOADING**

submitted by **HÜLYA KARAKUŞ** in partial fulfillment of the requirements for the degree of
Doctor of Philosophy in Civil Engineering, Middle East Technical University by,

Prof.Dr. Canan ÖZGEN
Dean, **Graduate School of Natural and Applied Sciences**

Prof. Dr. Ahmet Cevdet Yalçiner
Head of Department, **Civil Engineering, METU**

Prof. Dr. Ayşen Ergin
Supervisor, **Civil Engineering, METU**

Examining Committee Members:

Prof. Dr. Yalçın Yüksel
Civil Engineering, YTÜ

Prof. Dr. Ayşen Ergin
Civil Engineering, METU

Prof. Dr. Can Elmar Balas
Civil Engineering, Gazi University

Prof. Dr. Ahmet Cevdet Yalçiner
Civil Engineering, METU

Prof. Dr. Kemal Önder Çetin
Civil Engineering, METU

Date: 29.03.2013

I hereby declare that all information in this document has been obtained and presented in accordance with academic rules and ethical conduct. I also declare that, as required by these rules and conduct, I have fully cited and referenced all material and results that are not original to this work.

Name, Last name: Hülya KARAKUŞ

Signature: _____

ABSTRACT

EXPERIMENTAL AND NUMERICAL STUDIES ON BLOCK TYPE QUAY WALLS UNDER DYNAMIC LOADING

Karakuş, Hülya
Ph.D., Department of Civil Engineering
Supervisor: Prof. Dr. Ayşen Ergin

March 2013, 338 pages

Block type quay walls are one of the most important gravity quay wall which would suffer during earthquakes; although, this truth is known clearly, seismic design of this kind of structures have not studied yet in depth.

Most generally used approaches for design of gravity quay walls can be categorized into two groups namely, "Conventional Seismic Design Method" and "Performance Based Design Method". Conventional seismic design methodology does not give any information about the performance of structure when the limit of the force-balance is exceeded. In performance based design methodology, the design parameters (deformation; overturning, horizontal and vertical displacement) which are identified before the design stage are used as design parameters.

In this study, the dynamic response of block type quay wall was investigated by 1 g shaking table tests for one, two, three block(s) for different frequencies using two different saturated granular backfill materials (Soil 1 and Soil 2). During the experiments accelerations, pore pressures, soil pressures and displacements are measured. Distribution of the fluctuating component of total saturated soil pressure and application point, friction coefficients between the rubble-block and block-block are determined experimentally to form a base for the "performance based design method".

The experimental studies completed with numerical studies carried out using PLAXIS V8.2 software program. Comparisons of all soil pressure and horizontal displacement results show that experimental conditions are simulated succesfully with numerical study.

A case study was carried out with the site data of Derince Port, block type quay wall which is damaged during Eastern Marmara Earthquake, 1999. Horizontal displacement result obtained by PLAXIS V8.2 for Derince Port, block type quay wall is in very close agreement with the site measurements.

Results of measurements for displacement are discussed in view of "acceptable level of damage in performance based design" given in PIANC (2001). The result of the study performed for Derince Port, block type quay wall using numerical model is a good evidence of the reliability of the definitions of damaged levels given in PIANC (2001) to be used in performance based methods for seismic design of block type quay walls.

Keywords: Block Type Quay Walls, 1 G Shaking Table Tests, Numerical Modeling, Performance Based Design, Friction Coefficient

ÖZ

DİNAMİK YÜKLEME ALTINDA BLOK TİPİ KIYI YAPILARI ÜZERİNE DENEYSEL VE SAYISAL ÇALIŞMALAR

Karakuş, Hülya
Doktora, İnşaat Mühendisliği Bölümü
Tez Yöneticisi: Prof. Dr. Ayşen Ergin

Mart 2013, 338 sayfa

Blok tip kıyı yapıları deprem sonucu zarar gören en önemli ağırlık tipi kıyı yapılarından biridir. Bu gerçeğin açıkça bilinmesine rağmen, bu tip yapıların sismik tasarımı henüz detaylı olarak çalışılmamıştır.

Ağırlık tipi kıyı yapılarının tasarımında en çok kullanılan yaklaşımlar “geleneksel sismik tasarım yöntemi” ve “davranışa dayalı tasarım yöntemi” olarak iki grupta sınıflandırılabilir. Geleneksel sismik tasarım yöntemi, kuvvet-denge sınırı aşıldığında oluşan yapı performansı hakkında herhangi bir bilgi vermemektedir. Performansa dayalı tasarımda ise, sismik tasarımdan önce tanımlanan parametreler (deformasyon, dönme, yatay ve düşey yer değiştirme) tasarım parametreleri olarak kullanılmaktadır.

Bu çalışmada, blok tipi kıyı yapısının dinamik davranışı iki farklı suya doymuş granüler geri dolgu malzemesi (Dolgu Malzemesi 1 ve Dolgu Malzemesi 2) kullanılarak farklı frekanslar için 1 g sarsma tablası testleri ile araştırılmıştır. Deneyler sırasında, ivmeler, boşluk suyu basınçları, zemin basınçları ve yer değiştirmeler ölçülmüştür. Suya doymuş zemin basıncının düzenli bileşinin dağılımı ve etki noktası, anroşman-blok ve blok-blok arasındaki sürtünme katsayıları performansa dayalı tasarım yönteminin temel parametrelerini elde etmek amacıyla deneysel olarak belirlenmiştir.

Deneysel çalışmalar, PLAXIS V8.2 bilgisayar programı kullanılarak gerçekleştirilen sayısal çalışma ile bütünleştirilmiştir. Suya doymuş toplam zemin basınçları ve yatay yer değiştirme sonuçlarının karşılaştırması, sayısal çalışmanın deney koşullarını başarıyla benzeştirdiğini göstermektedir.

1999, Doğu Marmara Depremi'nde hasar gören Derince Limanı'ndaki blok tipi kıyı yapısının saha verileri kullanılarak bir durum çalışması yapılmıştır. PLAXIS V8.2 ile Derince Limanı için elde edilen yatay yer değiştirmeler, referans değerler ile oldukça uyumludur.

Yatay yer değiştirme ölçüm sonuçları, PIANC (2001)'de verilen “davranışa dayalı tasarımda kabul edilebilir hasar seviyeleri” göz önünde tutularak tartışılmıştır. Derince Limanı, blok tipi kıyı yapısı için gerçekleştirilen sayısal çalışmanın sonuçları, PIANC (2001)'de verilen performansa dayalı tasarım için öngörülen hasar parametrelerinin blok tipi kıyı yapılarının sismik tasarımında uygulanabilirliğinin bir göstergesidir.

Anahtar Kelimeler: Blok Tipi Kıyı Yapısı, 1 G Sarsma Tankı Testleri, Numerik Modelleme, Davranışa Dayalı Tasarım, Sürtünme Katsayısı.

dedicated to my family...

ACKNOWLEDGEMENTS

It is too difficult to express my appreciation in just few words to all the people who helped me to accomplish this compulsory study.

First and foremost, I express sincere appreciation to my supervisor Prof. Dr. Ayşen Ergin for her guidance, motivation and insight throughout this study since beginning of my graduate studies. I am really glad and proud that I have had an opportunity to work closely with such an incredible person. She inspired and enriched my growth not only as a researcher but also as a person.

I would like to thank my cosupervisor Dr. Işıkhan Güler for interesting and significant discussions on my study. He always encouraged me throughout this study.

I would like to attend my thanks to Prof. Dr. Ahmet Cevdet Yalçın who supported me with his valuable guidance. He could not even imagine how much I have learned from him.

I would like to thank Prof. Dr. Yalçın Yüksel for giving me the full support throughout my experimental studies carried out at Hydraulics and Coastal and Harbor Lab., Civil Engineering Faculty at Yıldız Technical University as a part of “Simplified Dynamic Analysis of Block Type Quay Wall” project sponsored by Scientific and Technological Research Council of Turkey (TUBITAK) (Project Number: 111Y006).

Thanks to Yıldız Technical University members especially Dr. Kubilay Cihan, Anıl Uluşan and Gazi Kurt. And special thanks to TUBİTAK for their supports.

This study is very meaningful for me since I found my love whom I will share my life. Words fail me to express my appreciation to Dr. Kubilay Cihan first of all for his willingness to share his bright thoughts with me during this study as well as for his endless love which always give me a reason to smile.

I would like to thanks to my family, it was impossible to finish this challenging study without their love and good wishes.

My deepest and sincere gratitude to my colleague Mustafa Esen, for his dedicated efforts in our business life for both during the time while my leg was broken and I was writing my thesis.

Special thanks to Baki Arslan, his unflinching courage and conviction always inspired me.

Special thanks to Dr. Ceren Özer, Dr. Cüneyt Baykal, Dr. Gülizar Özyurt, Gökhan Güler, Çağdaş Bilici, Rosita Kian, Damla Atalay, Koray Özdemir, Işıl İnsel, Aykut Ayça, Nuray Sefa, Pelin Öğünç, Arif Kayışlı and Yusuf Korkut.

TABLE OF CONTENTS

ABSTRACT	iii
ÖZ	iv
ACKNOWLEDGMENTS	vi
TABLE OF CONTENTS	vii
CHAPTERS	
1 INTRODUCTION.....	1
2 LITERATURE REVIEW	3
2.1 Conventional Seismic Design Methodology	10
2.1.1 Analytical Studies.....	10
2.1.1.1 Rigid Plastic Methods.....	10
2.1.1.1.1 Pseudo-static Analysis.....	10
2.1.1.1.1.1 Mononobe Okabe Method	12
2.1.1.1.1.2 Seed – Whitman Method	12
2.1.1.1.2 Pseudo-Dynamic Analysis	12
2.1.1.1.2.1 Steedman and Zeng	12
2.1.1.2 Elastic Methods.....	13
2.1.1.2.1 Wood.....	13
2.2 Performance Based Design	17
2.2.1 Analytical Studies.....	17
2.2.1.1 Displacement Based Studies	17
2.2.1.1.1 Newmark Sliding Method	18
2.2.1.1.2 Richard and Elms.....	18
2.2.1.1.3 Whitman and Liao	18
2.2.1.1.4 Nadim and Whitman	18
2.2.2 Numerical Studies	23
2.2.3 Experimental Studies	25
2.2.3.1 Shaking Table Tests	25
2.2.3.2 Centrifuge Tests.....	28
2.2.3.3 Large Scale Prototype Field Tests.....	28
2.3 Block Type Quay Walls	29
2.4 Conclusion	30
2.4.1 Earth Pressure	30
2.4.2 Soil Pressure Distribution.....	31
2.4.3 Friction Coefficients.....	33

2.4.4 Displacement	34
2.4.5 Hydrodynamic Forces and Pore Pressures	35
3 QUAYWALLS	37
3.1 General	37
3.2 Scope of this Study	41
4 EXPERIMENTAL SET-UP	45
4.1 Experimental Set-up	45
4.1.1 Known Parameters	46
4.1.1.1 Soil parameters	46
4.1.1.2 Block(s) dimensions and Scaling	46
4.1.1.3 Dynamic Loading Frequencies	48
4.1.2 Instruments Used in Measuring the Unknown Parameters	48
4.1.2.1 1g Shaking Table	48
4.1.2.2 Raining System	50
4.1.2.3 Soil Pressure Cells	51
4.1.2.4 Position Transducers	51
4.1.2.5 Accelerometer	51
4.1.2.6 Pore Pressure Cells	52
4.1.2.7 Software and Hardware System	52
4.2 Dynamic Loading Experiments	52
4.3 One Block Test Set Up	58
4.3.1 One Block Test Set Up for Soil 1 and for Soil 2	58
4.4 Two Blocks Test Set Up	60
4.4.1 Two Blocks Test Set Up for Soil 1 and for Soil 2	60
4.5 Three Blocks Test Set Up	62
4.5.1 Three Blocks Test Set Up for Soil 1 and for Soil 2	62
5 PRESENTATION AND DISCUSSION OF THE RESULTS OF ACCELERATION MEASUREMENTS	65
5.1 One Blok Acceleration Measurements (Test 1.1 and Test 1.2)	65
5.1.1 One Blok, Soil 1: Acceleration Measurements (Test 1.1)	66
5.1.1.1 Results of Acceleration Measurements (Soil 1)	69
5.1.2 One Blok, Soil 2: Acceleration Measurements (Test 1.2)	70
5.1.2.1 Results of Acceleration Measurements (Soil 2)	71
5.2 Two Blocks Acceleration Measurements (Test 2.1 and Test 2.2)	73
5.2.1 Two Blocks, Soil 1: Acceleration Measurements (Test 2.1)	73
5.2.1.1 Results of Acceleration Measurements (Soil 1)	74
5.2.2 Two Blocks, Soil 2: Acceleration Measurements (Test 2.2)	76
5.2.2.1 Results of Acceleration Measurements (Soil 2)	77
5.3 Three Blocks Acceleration Measurements (Test 3.1 and Test 3.2)	78
5.3.1 Three Blocks, Soil 1: Acceleration Measurements (Test 3.1)	78
5.3.1.1 Results of Acceleration Measurements (Soil 1)	79

5.3.2 Three Blocks, Soil 2: Acceleration Measurements (Test 3.2).....	81
5.3.2.1 Results of Acceleration Measurements (Soil 2)	81
5.3.3 Summary and Discussion of the Acceleration Measurement	83
6 PRESENTATION AND DISCUSSION OF THE RESULTS OF SOIL PRESSURE AND PORE PRESSURE MEASUREMENTS.....	89
6.1 Results of Pore Pressure Measurements (Soil 1 and Soil 2).....	92
6.2 One Blok Soil Pressure Measurements (Test 1.1 and Test 1.2)	92
6.2.1 One Blok, Soil 1: Total Saturated Soil Pressure Measurements (Test 1.1).....	92
6.2.1.1 Results of Soil Pressure Cell Measurements (Soil 1)	96
6.2.1.2 One Block- Fluctuating and Non-fluctuating Components of Total Saturated Soil Pressure Soil 1	98
6.2.1.2.1 One Block- Fluctuating and Non-fluctuating Components of Total Saturated Soil Pressure for 2 Hz for Soil 1	98
6.2.1.2.1.1 One Block- Fluctuating and Non-Fluctuating Components of Total Lateral Soil Pressure for 3 Hz for Soil 1	101
6.2.1.2.1.2 One Block- Fluctuating and Non-Fluctuating Components of Total Saturated Soil Pressure for 4 Hz for Soil 1	103
6.2.1.2.1.3 One Block- Fluctuating and Non-Fluctuating Components of Total Lateral Soil Pressure for 5 Hz for Soil 1	105
6.2.1.2.1.4 One Block- Fluctuating and Non-Fluctuating Components of Total Lateral Soil Pressure for 6 Hz for Soil 1	107
6.2.1.2.1.5 Maximum Fluctuating Components of Total Saturated Soil Pressures for Soil 1	109
6.2.1.2.1.6 Maximum Non-Fluctuating Components of Total Saturated Soil Pressures for Soil 1	110
6.2.2 One Blok, Soil 2: Total Saturated Soil Pressure Measurements (Test 1.2).....	112
6.2.2.1 Results of Soil Pressure Measurements (Soil 2)	114
6.2.2.2 One Block- Fluctuating and Non-fluctuating Components of Total Saturated Soil Pressures for Soil 2.....	116
6.2.2.2.1 One Block- Fluctuating and Non-fluctuating Components of Total Saturated Soil Pressure for 4 Hz for Soil 2	116
6.2.2.2.2 One Block- Fluctuating and Non-Fluctuating Components of Total Soil Pressure for 5 Hz for Soil 2.....	118
6.2.2.2.3 One Block- Fluctuating and Non-Fluctuating Components of Total Soil Pressure for 6 Hz for Soil 2.....	120
6.2.2.2.3.1 Maximum Fluctuating Components of Total Saturated Soil Pressures for Soil 2	122
6.2.2.2.3.2 Maximum Non-Fluctuating Components of Total Saturated Soil Pressures for Soil 2	123
6.3 Two Blocks, Soil 1: Soil Pressure Measurements (Test 2.1 and Test 2.2).....	124
6.3.1 Two Blocks, Soil 1: Soil Pressure Measurements (Test 2.1).....	124
6.3.1.1 Results of Soil Pressure Measurements (for Soil 1)	128
6.3.1.2 Two Blocks- Fluctuating and Non-fluctuating Components of Total Saturated Soil Pressure for Soil 1	131
6.3.1.2.1 Two Blocks- Fluctuating and Non-Fluctuating Components of Total Soil Pressure for 5 Hz for Soil 1	131

6.3.1.2.1.1 Maximum Fluctuating Components of Total Saturated Soil Pressures for Soil 1	135
6.3.1.2.1.2 Maximum Non-Fluctuating Components of Total Saturated Soil Pressures for Soil 1	137
6.3.2 Two Blocks, Soil 2: Soil Pressure Measurements (Test 2.2)	139
6.3.2.1 Results of Soil Pressure Measurements (Soil 2).....	141
6.3.2.2 Two Blocks- Fluctuating and Non-fluctuating Components of Total Saturated Soil Pressure for Soil 2	143
6.3.2.2.1 Maximum Fluctuating Components of Saturated Total Soil Pressures.....	143
6.3.2.2.1.1 Maximum Non-Fluctuating Components of Total Saturated Soil Pressures for Soil 2	144
6.4 Three Blocks, Soil 1: Total Saturated Soil Pressure Measurements (Test 3.1 and Test 3.2).....	146
6.4.1 Three Blocks, Soil 1: Soil Pressure Measurements (Test 2.1)	146
6.4.1.1 Results of Soil Pressure Measurements (Soil 1).....	149
6.4.1.2 Three Blocks- Fluctuating and Non-fluctuating Components of Total Saturated Soil Pressure for Soil 1	151
6.4.1.2.1 Maximum Fluctuating Components of Total Saturated Soil Pressures for Soil 1	151
6.4.1.2.2 Maximum Non-Fluctuating Components of Total Saturated Soil Pressures for Soil 1	153
6.4.2 Three Blocks, Soil 2: Soil Pressure Measurements (Test 3.2)	155
6.4.2.1 Results of Soil Pressure Measurements (Soil 2).....	157
6.4.2.2 Three Blocks- Fluctuating and Non-fluctuating Components of Total Saturated Soil Pressure for Soil 2	159
6.4.2.2.1 Maximum Fluctuating Components of Saturated Total Soil Pressures for Soil 2	159
6.4.2.2.2 Maximum Non-Fluctuating Components of Total Saturated Soil Pressures for Soil 2	160
6.4.2.2.3 Presentation and Discussion of the Soil Pressure Measurement Results	162
7 PRESENTATION AND DISCUSSION OF THE RESULTS OF POSITION TRANSDUCERS MEASUREMENTS	167
7.1 One Block: Position Transducers Measurements (Test 1.1 and Test 1.2)	167
7.1.1 One Blok, Soil 1: Position Transducers Measurements (Test 1.1)	167
7.1.1.1 Horizontal, Vertical Displacements Measurements and Tilting Degree	171
7.1.2 One Block, Soil 2: Position Transducers Measurements (Test 1.2)	172
7.1.2.1 Horizontal, Vertical Displacements and Tilting Degree	173
7.1.3 Comparisons of Results for Position Transducers for One Block for Soil 1 and Soil 2	174
7.2 Two Blocks: Position Transducers Measurements (Test 2.1 and Test 2.2).....	174
7.2.1 Two Blocks, Soil 1: Position Transducers Measurements (Test 2.1).....	175
7.2.1.1 Horizontal, Vertical Displacements and Tilting Degree	178
7.2.2 Two Blocks, Soil 2: Position Transducers Measurements (Test 2.2).....	180
7.2.2.1 Horizontal, Vertical Displacements and Tilting Degree	180
7.2.3 Comparisons of Results for Position Transducers for Two Blocks for Soil 1 and Soil 2	181
7.3 Three Block: Position Transducers Measurements (Test 3.1 and Test 3.2).....	181

7.3.1 Three Blocks, Soil 1: Position Transducers Measurements (Test 3.1).....	181
7.3.1.1 Horizontal, Vertical Displacements and Tilting Degree.....	184
7.3.2 Three Blocks, Soil 2: Position Transducers Measurements (Test 3.2).....	185
7.3.2.1 Horizontal, Vertical Displacements and Tilting Degree.....	186
7.3.3 Comparisons of Results for Position Transducers for Three Blocks for Soil 1 and Soil 2	187
7.4 Summary and Discussion of the Position Measurements	187
7.4.1 Evaluation of the Position Transducers Results	190
7.4.1.1 For One Block	190
7.4.1.2 For Two Blocks	191
7.4.1.3 For Three Blocks.....	192
8 FRICTION COEFFICIENTS.....	195
8.1 Static Friction Coefficient	195
8.1.1 One Block.....	197
8.1.1.1 Rubble – Block	197
8.1.2 Two Blocks.....	201
8.1.2.1 Static Friction Coefficient: Rubble - Block 1	201
8.1.2.2 Static Friction Coefficient: Block 1 - Block 2	202
8.1.3 Three Blocks	202
8.1.3.1 Static Friction Coefficient: Rubble - Block 1	202
8.1.3.2 Static Friction Coefficient: Block 1 - Block 2	203
8.1.3.3 Static Friction Coefficient: Block 2 - Block 3	203
8.2 Dynamic Friction Coefficient	204
8.3 Comparisons Of Static And Dynamic Friction Coefficients	206
9 NUMERICAL MODELING.....	209
9.1 Modeling of the System.....	209
9.1.1 Subprogram 1 : Input	209
9.1.2 Subprogram 2 : Calculation	214
9.1.3 Subprogram 3 : Outputs.....	214
9.1.3.1 Soil Pressure Outputs	216
9.1.3.2 Displacement Outputs.....	219
9.2 Comparisons of the Experimental and Numerical Results	220
9.2.1 Comparisons of Soil Pressure Results	220
9.2.2 Comparisons of Displacements Results	223
9.3 A Case Study on Derince Port Block Type Quay Wall	225
9.3.1 Derince Port	225
9.3.2 Numerical Modeling of Derince Port, Block Type Quay Wall.....	227
9.3.2.1 Result of Derince Port, Block Type Quay Wall	230
9.3.2.2 Discussions on Acceptable Level of Damage Derince Port, Block Type Quay Wall.....	230
10 RESULTS AND CONCLUSIONS	233
10.1 Experimental Studies	234

10.1.1 Acceleration	234
10.1.2 Pore Pressure.....	234
10.1.3 Saturated Soil Pressures.....	234
10.1.4 Displacements	235
10.1.5 Friction Coefficient Results.....	235
10.2 Numerical Analysis	235
10.3 Case Study	235
10.4 Acceptable Level of Damage	235
10.5 Future Studies	236
REFERENCES	237
APPENDICES	
A. Advantages and Disadvantages.....	242
B. Scaling.....	244
C. Relative Density.....	246
D. Instruments.....	247
E. Mathcad Software Program.....	250
F. Acceleration Results.....	254
G. Two Blocks: Fluctuating and Non-Fluctuating Components	263
H. Three Blocks: Fluctuating and Non-Fluctuating Components	293
I. Position Measurements for One Block	322
J. Position Measurements for Two Blocks	324
K. Position Measurements for Three Blocks	326
L. Material Properties	328
M. August 17, 1999 Earthquake Data	334
CURRICULUM VITAE	335

LIST OF TABLES

TABLES

Table 2.1: General types of quay walls.....	4
Table 2.2: Past strong earthquakes and quay wall damage level (References are given in parenthesis)	5
Table 2.3: Methods generally used in the design of gravity type quay walls.....	11
Table 2.4: Generally used methods for pseudo-static analysis	14
Table 2.5: Generally used methods for pseudo-dynamic analysis	15
Table 2.6: Generally used methods for elastic analysis	16
Table 2.7: General used methods based on displacement, analytical studies.....	19
Table 2.8: Friction Coefficients.....	34
Table 3.1: Levels of earthquake motions (PIANC, 2001)	39
Table 3.2: Acceptable level of damage in performance based design (PIANC, 2001)	41
Table 3.3: Performance grades S, A, B and C. (PIANC, 2001)	41
Table 3.4: Performance grade based on the importance category of port structures (PIANC, 2001)	41
Table 3.5: Several questions to be answered under dynamic loading	42
Table 3.6: 1 g shaking table tests	42
Table 3.7: Flow chart of this study	44
Table 4.1: Parameters of this study	45
Table 4.2: Soil parameters for backfill and foundation (Soil 1)	46
Table 4.3: Soil parameters for backfill for Soil 2	46
Table 4.4: Prototype and model properties.....	47
Table 4.5: Scaling factors in present model.....	48
Table 4.6: Acceptable level of damage in performance-based design* (PIANC, 2001)	55
Table 4.7: Proposed damage criteria for gravity quay walls (PIANC, 2001)	56
Table 4.8: Limit of performance for gravity wall (Technical Seismic Specifications on Construction of Coastal and Harbor Structures, Railways And Airports, 2008)	56
Table 4.9: Model studies under dynamic loading.....	57
Table 5.1: Maximum accelerations at base (Acc 1) and on block 1 (Acc 2) for Soil 1 with respect to frequencies.....	69
Table 5.2: Acceleration measurements for one block for Soil 1	70
Table 5.3: Maximum accelerations at base (Acc 1) and on block (Acc 3) for Soil 2 with respect to frequencies.....	72
Table 5.4: Acceleration measurements for one block for Soil 2	73
Table 5.5: Maximum accelerations at Base (Acc 1), at Block 1 (Acc 3) and on Block 2 (Acc 2) for Soil 1 with respect to frequencies	74
Table 5.6: Ratios between Block 2 / Block 1, Block 1 / Base, Block 2 / Base	75
Table 5.7: Acceleration measurements for two blocks for Soil 1	76

Table 5.8: Maximum accelerations at Base (Acc 1), at Block 1 (Acc 3) and at Block 2 (Acc 2) for Soil 2 with respect to frequencies	77
Table 5.9: Ratios (Block 2 / Block 1, Block 1 / Base, Block 2 / Base) versus frequency for Soil 2.....	77
Table 5.10: Acceleration measurements for two blocks for Soil 2	78
Table 5.11: Frequency and relations of maximum acceleration measurements of base and block for Soil 1	79
Table 5.12: Ratios (Block 3 / Block 2, Block 2 / Block 1, Block 1 / Base, Block 3 / Base) versus frequency for Soil 1	80
Table 5.13: Acceleration measurements for three blocks for Soil 1.....	80
Table 5.14: Frequency and relations of maximum acceleration measurements of base and blocks for Soil 2	82
Table 5.15: Ratios (Block 3 / Block 2, Block 2 / Block 1, Block 1 / Base, Block 3 / Base) versus frequency for Soil 2	82
Table 5.16: Acceleration measurements for three blocks for Soil 2.....	83
Table 5.17: $ a_{max} $ and frequency relations for Soil 1 and Soil 2 for Base (duration is 30 sec.).....	84
Table 5.18: Maximum acceleration $ a_{max} $ and frequency relations for Soil 1 and Soil 2.....	85
Table 5.19: $ a_{max} $ and frequency relations for Soil 1 and Soil 2 for Block 1 (duration is 30 sec.).....	86
Table 5.20: $ a_{max} $ and frequency relations for Soil 1 and Soil 2 for Block 2 (duration is 30 sec.).....	86
Table 5.21: $ a_{max} $ and frequency relations for Soil 1 and Soil 2 for Block 3 (duration is 30 sec.).....	86
Table 6.1: Total saturated soil pressure measurements ranges for 2 Hz – 6 Hz for Soil 1 ...	93
Table 6.2: Total saturated soil pressure measurements for different frequencies before and after dynamic loading for Soil 1	96
Table 6.3: Maximum fluctuating components of total saturated soil pressures and before dynamic loading pressure measurements for SP1 and SP2 for Soil 1	109
Table 6.4: Maximum non-fluctuating components of total saturated soil pressures and before dynamic loading pressure measurements for SP1 and SP2 for Soil 1	111
Table 6.5: Total saturated soil pressure measurements ranges for 2 Hz – 6 Hz for Soil 2 .	112
Table 6.6: Total saturated soil pressure measurements for different frequencies before and after dynamic loading for Soil 2	114
Table 6.7: Maximum fluctuating components of total saturated soil pressures and before dynamic loading pressure measurements for SP1 and SP2 for Soil 2	122
Table 6.8: Maximum non- fluctuating components of total saturated soil pressures and before dynamic loading pressure measurements for SP1 and SP2 for Soil 2	123
Table 6.9: Total saturated soil pressure measurements ranges for 2 Hz – 6 Hz for Soil 1 .	125
Table 6.10: Total saturated soil pressure measurements for different frequencies before and after dynamic loading	129
Table 6.11: Maximum fluctuating components of total saturated soil pressures and before dynamic loading pressure measurements for SP1, SP2, SP3 and SP4 for Soil 1.....	135
Table 6.12: Maximum non-fluctuating components of total saturated soil pressures and before dynamic loading pressure measurements for SP1, SP2, SP3 and SP4 for Soil 1 ...	137
Table 6.13: Total saturated soil pressure measurements ranges for 2 Hz – 6 Hz for Soil 2	139

Table 6.14: Saturated soil pressure measurements for different frequencies before and after dynamic loading for Soil 2	141
Table 6.15: Maximum fluctuating components of total saturated soil pressures and before dynamic loading pressure measurements for SP1, SP2, SP3 and SP4 for Soil 2	143
Table 6.16: Maximum non-fluctuating components of total saturated soil pressures and before dynamic loading pressure measurements for SP1, SP2, SP3 and SP4 for Soil 2 ...	145
Table 6.17: Total saturated soil pressure measurements ranges for 3 Hz – 6 Hz for Soil 1	147
Table 6.18: Total saturated soil pressure measurements for different frequencies before and after dynamic loading for Soil 1	149
Table 6.19: Maximum fluctuating components of total saturated soil pressures and before dynamic loading pressure measurements for SP1, SP2, SP3 and SP4 for Soil 1	151
Table 6.20: Maximum non-fluctuating components of total saturated soil pressures and before dynamic loading pressure measurements for SP1, SP2, SP3 and SP4 for Soil 1 ...	153
Table 6.21: Soil pressure measurements ranges for 4 Hz – 6 Hz for Soil 2.....	155
Table 6.22: Total saturated soil pressure measurements for different frequencies before and after dynamic loading for Soil 2.....	157
Table 6.23: Maximum fluctuating components of total saturated soil pressures and before dynamic loading pressure measurements for SP1, SP2, SP3 and SP4 for Soil 2	159
Table 6.24: Maximum non-fluctuating components of total saturated soil pressures and before dynamic loading pressure measurements for SP1, SP2, SP3 and SP4 for Soil 2 ...	161
Table 7.1: Horizontal, vertical displacement measurements results and calculated tilting values for each frequency for one block for Soil 1	171
Table 7.2: Horizontal displacement measurements for each frequency for one block tests for Soil 2	173
Table 7.3: Comparisons of tests results of one block for Soil 1 and Soil 2.....	174
Table 7.4: Horizontal, vertical displacement measurements and tilting values for each frequency for one block for Soil 1	179
Table 7.5: Horizontal, vertical displacement measurements and tilting values for each frequency for one block for Soil 2	180
Table 7.6: Horizontal displacement measurements and tilting values for each frequency for three blocks for Soil 1	184
Table 7.7: Horizontal displacement measurements and tilting values for each frequency for three blocks for Soil 2.....	186
Table 7.8: Horizontal displacement measurements for one block, two blocks and three blocks for Soil 1 and Soil 2.....	188
Table 7.9: Calculated tilting degree for one block, two blocks and three blocks for Soil 1 and Soil 2	189
Table 7.10: Damage level of block(s) for Soil 1 and Soil 2	194
Table 8.1: The computation steps of the static friction coefficients for one block, two blocks and three blocks.....	196
Table 8.2: Sliding time of block for 4 Hz for Soil 1	198
Table 8.3: Base and block accelerations for specified sliding time for Soil 1	198
Table 8.4: The soil pressure measurements for 11.426 sec for SP1 and SP2 for Soil 1	199
Table 8.5: Total soil pressure measurements versus elevation for 4 Hz for Soil 1	200
Table 8.6: Results of the static friction coefficients calculations for rubble-block 1 for 5 Hz	201
Table 8.7: Results of the static friction coefficients calculations for block 1-block 2 for 5Hz	202

Table 8.8: Results of the static friction coefficients calculations for rubble-block 1 for 5Hz.	202
Table 8.9: Results of the static friction coefficients calculations for block 1-block 2 for 5Hz	203
Table 8.10: Results of the static friction coefficients calculations for block 2 - block 3 for 5 Hz	203
Table 8.11: Static friction coefficients for rubble-block and block-block for one block, two blocks and three blocks.....	206
Table 8.12: Comparisons of static friction coefficients with the standards.....	207
Table 9.1: Material models given in PLAXIS V8.2 (PLAXIS GID, Material Models Manual)	212
Table 9.2: The properties of interface and all other material properties	213
Table 9.3: The displacement results obtained from PLAXIS V8.2 for one block, two blocks and three blocks for 5 Hz for Soil 1	220
Table 9.4: Maximum deviation between experimental and numerical studies for one block	223
Table 9.5: Maximum deviation between experimental and numerical studies for two blocks	223
Table 9.6: Maximum deviation between experimental and numerical studies for three blocks	223
Table 9.7: Comparisons of displacements results	223
Table 9.8: Properties of the materials used in PLAXIS V8.2.....	228

LIST OF FIGURES

FIGURES

Figure 2.1: General cross-sections of quay walls (PIANC, 2001).....	4
Figure 2.2: Damage of Block Type Quay Walls After a) 1985, Chile Earthquake (see Table 2.2 no: 11) b) 1986, Kalamata Earthquake (no: 12) c) 1989, Chenoua Earthquake (no: 13) d) 1999, Kocaeli Earthquake (no: 20) (PIANC, 2001)	8
Figure 2.3: Damage of Caisson Type Quay Walls and Sheet Pile Quay Walls After e) 1995, Hyogoken-Nambu Earthquake (no: 19) f) 1993, Kushiro-Okai Earthquake (no: 15) g) 1993, Kushiro-Okai Earthquake (no: 15) h) 1999, Ji-Ji earthquake (no: 21) i) 1983, Nihonkai-Chubu Earthquake (no: 10) j) 1993, Kushiro-Okai Earthquake (no: 15) (PIANC, 2001).....	9
Figure 2.4: Typical section of block type wall.....	29
Figure 2.5: Elastic dynamic earth-pressure distribution of a pseudo-statically excited one-layer system for a non-sliding wall, (Gazetas et al., 2004)	31
Figure 2.6: Seismic soil pressure for 4m height wall (a) Bridge abutment, (b) flexible wall, (c) rigid wall, (Anastasopoulos et al., 2010).	32
Figure 2.7: Suggested approximate seismic soil pressure distribution (a) typical distribution suggested here for rigid walls and semi-rigid walls, such as bridge abutment and propped bridge abutment, (b) distribution suggested for flexible walls such as cantilever retaining walls taller than 5 m, (Maleki and Mahjoubi, 2010).....	32
Figure 2.8: Total soil pressure distribution during earthquake (a) Rigid or semi-rigid wall, (b) Flexible wall, (Maleki and Mahjoubi, 2010).	32
Figure 2.9: Earth-pressure distribution of a quasi-statically excited retaining system with varying relative flexibility, $d\theta$, of the base rotational spring for different values of relative wall flexibility, $d\omega$ (Psarropoulos et al., 2004)	33
Figure 2.10: Illustration of the force equilibrium for the sliding block on a slope	34
Figure 3.1: Deformation/failure modes of gravity quay wall on firm foundation (PIANC, 2001)	37
Figure 3.2: Deformation/failure modes of gravity quay wall on loose sandy formation (PIANC, 2001)	38
Figure 3.3: Flowchart for seismic performance evaluation	40
Figure 4.1: General view of 1g shaking table.....	48
Figure 4.2: General view of one block experiment set-up (top view).....	49
Figure 4.3: Raining system	50
Figure 4.4: Raining system	51
Figure 4.5: Raining system and shaking table	51
Figure 4.6: Force components acting on block during dynamic loading (Kim et al., 2005) ..	52
Figure 4.7: Fluctuating and non-fluctuating component of total saturated soil pressure (Kim et al., 2004)	53
Figure 4.8: Displacement and tilting for one block.....	54
Figure 4.9: Displacement and tilting for two blocks	54
Figure 4.10: Displacement and tilting for three blocks.....	55
Figure 4.11: Block and dummies	58

Figure 4.12: Block and instruments	58
Figure 4.13: Measuring instruments and general view of one block tests	59
Figure 4.14: Blocks, dummies and instruments	60
Figure 4.15: Measuring instruments and general view of two blocks tests	61
Figure 4.16: Blocks, dummies and instruments	62
Figure 4.17: Measuring instruments and general view of three blocks tests	63
Figure 5.1: General view of two accelerometers Acc 1 (base) and Acc 2 or Acc 3 (block 1) for one block tests for Soil 1 and Soil 2	65
Figure 5.2: Acceleration measurements for Acc 1 and Acc 2 for 2 Hz for Soil1 (Test 1.1.1)	66
Figure 5.3: Acceleration measurements for Acc 1 and Acc 2 for 3 Hz for Soil1 (Test 1.1.2)	66
Figure 5.4: Acceleration measurements for Acc 1 and Acc 2 for 4 Hz for Soil1	67
Figure 5.5: Acceleration measurements for Acc 1 and Acc 2 for 5 Hz for Soil1 (Test 1.1.4)	67
Figure 5.6: Acceleration measurements for Acc 1 and Acc 2 for 6 Hz for Soil1 (Test 1.1.5)	68
Figure 5.7: Acceleration measurements for Acc 1 and Acc 2 for 7 Hz for Soil1 (Test 1.1.6)	68
Figure 5.8: Maximum accelerations at base and on block 1 for 2 Hz - 6 Hz for Soil 1	69
Figure 5.9: Ratio (Block 1/Base) versus frequency for Soil 1	69
Figure 5.10: Acceleration measurements for Acc 1 and Acc 3 for 4 Hz for Soil 2 (Test 1.2.1)	70
Figure 5.11: Acceleration measurements for Acc 1 and Acc 3 for 5 Hz for Soil 2 (Test 1.2.2)	71
Figure 5.12: Acceleration measurements for Acc 1 and Acc 3 for 6 Hz for Soil 2 (Test 1.2.3)	71
Figure 5.13: Maximum accelerations at base and on block 1 for 4Hz - 6 Hz for Soil 2	72
Figure 5.14: Ratio (Block 1 / Base) versus frequency for Soil 2	72
Figure 5.15: General view of three accelerometers (Acc 1, Acc 2, Acc 3) for two blocks tests	73
Figure 5.16: Acceleration values of Base (A 1), Block 1 (A 3) and Block 2 (A 2) for 4 Hz (Test 2.1.3)	74
Figure 5.17: Maximum acceleration measurements of Base and Block for 2 Hz - 6 Hz for Soil 1	75
Figure 5.18: Ratios (Block 2 / Block 1, Block 1 / Base, Block 2 / Base) versus frequency for Soil 1	75
Figure 5.19: Acceleration values of Base (Acc 1), Block 1 (Acc 3) and Block 2 (Acc 2) for 5 Hz (Test 2.2.2)	76
Figure 5.20: Maximum acceleration measurements of Base and Blocks for 4 Hz - 6 Hz for Soil 2	77
Figure 5.21: Ratios (Block 2 / Block 1, Block 1 / Base, Block 2 / Base) versus frequency for Soil 2	77
Figure 5.22: General view of three accelerometers (Acc 1, Acc 2, Acc 3, Acc 4) for three blocks tests	78
Figure 5.23: Acceleration values of base (Acc 1), block 1 (Acc 2) and block 2 (Acc 3) and block 3 (Acc 4) for 5 Hz (Test 3.1.3)	79
Figure 5.24: Maximum acceleration measurements of base and blocks for 3 Hz - 6 Hz for Soil 1	80

Figure 5.25: Ratios (Block 3/ Block 2, Block 2 / Block 1, Block 1 / Base, Block 3 / Base) versus frequency for Soil 1.....	80
Figure 5.26: Acceleration values of base (Acc 1), block 1 (Acc 2) and block 2 (Acc 3) and block 3 (Acc 4) for 5 Hz (Test 3.2.3)	81
Figure 5.27: Maximum acceleration measurements of base and blocks for 3 Hz, 4 Hz, 5 Hz for Soil 2	82
Figure 5.28: Ratios (Block 3/ Block 2, Block 2 / Block 1, Block 1 / Base, Block 3 / Base) versus frequency for Soil 1.....	83
Figure 6.1: Pore Pressure values of Pore P1 and Pore P2 located at 15 cm and 1 cm for 3 Hz	89
Figure 6.2: Pore Pressure values of Pore P1 and Pore P2 located at 12.5 cm and 1 cm for 6 Hz	90
Figure 6.3: Pore Pressure values of Pore P1 and Pore P2 located at 12.3 cm and 3 cm for 6 Hz	90
Figure 6.4: Pore Pressure values of Pore P1 and Pore P2 located at 28.5 cm and 7.7 cm for 5 Hz	91
Figure 6.5: Pore Pressure values of Pore P1 and Pore P2 located at 28.4 cm and 11.1 cm for 4 Hz.....	91
Figure 6.6: Total saturated soil pressure measurements for SP1 and SP2 for 2 Hz for Soil 1 (Test 1.1.1)	93
Figure 6.7: Total saturated soil pressure measurements for SP1 and SP2 for 3 Hz for Soil 1 (Test 1.1.2)	94
Figure 6.8: Total saturated soil pressure measurements for SP1 and SP2 for 4 Hz for Soil 1 (Test 1.1.3)	94
Figure 6.9: Total saturated soil pressure measurements for SP1 and SP2 for 5 Hz for Soil 1 (Test 1.1.4)	95
Figure 6.10: Total saturated soil pressure measurements for SP1 and SP2 for 6 Hz for Soil 1 (Test 1.1.5)	95
Figure 6.11: Total saturated soil pressure measurements acting on block for 2, 3, 4, 5, 6 Hz for Soil 1	97
Figure 6.12: Total saturated soil pressure for SP1 for 2 Hz for Soil 1	98
Figure 6.13: Total saturated soil pressure, non-fluctuating and fluctuating components of total saturated soil pressure for SP1 for 2 Hz for Soil 1	99
Figure 6.14: Fluctuating components of total saturated soil pressures for SP1 for 2 Hz for Soil 1	99
Figure 6.15: Non-fluctuating components of total saturated soil pressures for SP1 for 2 Hz for Soil 1	99
Figure 6.16: Total saturated soil pressures for SP2 for 2 Hz for Soil 1	100
Figure 6.17: Total saturated soil pressure, non-fluctuating and fluctuating components of total saturated soil pressures for SP2 for 2 Hz for Soil 1	100
Figure 6.18 : Fluctuating components of total saturated soil pressures	100
Figure 6.19: Non-Fluctuating components of total saturated soil pressures for SP2 for 2 Hz for Soil 1	100
Figure 6.20: Total saturated soil pressures for SP1 for 3 Hz for Soil 1	101
Figure 6.21: Total saturated soil pressures, non-fluctuating and fluctuating components of total saturated soil pressures for SP1 for 3 Hz for Soil 1	101

Figure 6.22: Fluctuating components of total saturated soil pressures for SP1 for 3 Hz for Soil 1	101
Figure 6.23: Non-fluctuating components of total saturated soil pressures for SP1 for 3 Hz for Soil 1	101
Figure 6.24: Total saturated soil pressures for SP2 for 3 Hz for Soil 1	102
Figure 6.25: Total soil pressures, non-fluctuating and fluctuating components of total saturated soil pressures for SP2 for 3 Hz for Soil 1	102
Figure 6.26: Fluctuating components of total saturated soil pressures for SP2 for 3 Hz for Soil 1	102
Figure 6.27: Non-fluctuating components of total saturated soil pressures for SP2 for 3 Hz for Soil 1	102
Figure 6.28: Total saturated soil pressures for SP1 for 4 Hz for Soil 1	103
Figure 6.29: Total saturated soil pressures, non-fluctuating and fluctuating components of total saturated soil pressures for SP1 for 4 Hz for Soil 1	103
Figure 6.30: Fluctuating components for total saturated soil pressures for SP1 for 4 Hz for Soil 1	103
Figure 6.31: Non-fluctuating components of total saturated soil pressures for SP1 for 4 Hz for Soil 1	103
Figure 6.32: Total saturated soil pressures for SP2 for 4 Hz for Soil 1	104
Figure 6.33: Total saturated soil pressures, non-fluctuating and fluctuating components of total saturated soil pressures for SP2 for 4 Hz for Soil 1	104
Figure 6.34: Fluctuating components for total saturated soil pressures for SP1 for 4 Hz for Soil 1	104
Figure 6.35: Non-fluctuating components of total saturated soil pressures	104
Figure 6.36: Total saturated soil pressures for SP1 for 5Hz for Soil 1	105
Figure 6.37: Total saturated soil pressures, non-fluctuating and fluctuating components of total saturated soil pressures for SP1 for 5 Hz for Soil 1	105
Figure 6.38: Fluctuating components for total saturated soil pressures for SP1 for 5 Hz for Soil 1	105
Figure 6.39: Non-fluctuating components for total saturated soil pressures for SP1 for 5 Hz for Soil 1	105
Figure 6.40: Total saturated soil pressures for SP2 for 5 Hz for Soil 1	106
Figure 6.41: Total saturated soil pressures, non-fluctuating and fluctuating components of total saturated soil pressures for SP2 for 5 Hz for Soil 1	106
Figure 6.42: Fluctuating components of total saturated soil pressures for SP2 for 5 Hz for Soil 1	106
Figure 6.43: Non-fluctuating components of total saturated soil pressures for SP2 for 5 Hz for Soil 1	106
Figure 6.44: Total saturated soil pressures of SP1 for 6 Hz for Soil 1	107
Figure 6.45: Total saturated soil pressures, non-fluctuating and fluctuating components of total saturated soil pressures for SP1 for 6 Hz for Soil 1	107
Figure 6.46: Fluctuating components of total saturated soil pressures.....	107
Figure 6.47: Non-fluctuating component s of total saturated soil pressures for SP1 for 6 Hz for Soil 1	107
Figure 6.48: Total saturated soil pressures of SP1 for 6 Hz for Soil 1	108

Figure 6.49: Total saturated soil pressures, non-fluctuating and fluctuating components of total saturated soil pressures for SP2 for 6 Hz for Soil 1	108
Figure 6.50: Fluctuating components of total saturated soil pressures for SP2 for 6 Hz for Soil 1	108
Figure 6.51: Non-fluctuating components of total saturated soil pressures for SP2 for 6 Hz for Soil 1	108
Figure 6.52: Relation between maximum fluctuating components of total saturated soil pressures and depth for Soil 1	109
Figure 6.53: Maximum fluctuating components of total saturated soil pressures for SP1 vs. frequency for Soil 1	110
Figure 6.54: Maximum fluctuating components of total saturated soil pressure for SP2 vs. frequency for Soil 1	110
Figure 6.55: Maximum non-fluctuating components of total saturated soil pressure and total saturated soil pressure before dynamic loading for Soil 1	111
Figure 6.56: Soil pressure measurements for SP1 and SP2 for 4 Hz for Soil 2 (Test 1.2.1)	112
Figure 6.57: Soil pressure measurements for SP1 and SP2 for 5 Hz for Soil 2 (Test 1.2.2)	113
Figure 6.58: Soil pressure measurements for SP1 and SP2 for 6 Hz for Soil 2 (Test 1.2.3)	113
Figure 6.59: Saturated soil pressure measurements acting on block for 4, 5, 6 Hz for Soil 2	115
Figure 6.60: Total saturated soil pressure for SP1 for 4 Hz for Soil 2	116
Figure 6.61: Total saturated soil pressure, non-fluctuating and fluctuating components of total saturated soil pressure for SP1 for 4 Hz for Soil 2	116
Figure 6.62: Fluctuating components of total saturated soil pressures for SP1 for 4 Hz for Soil 2	116
Figure 6.63: Non-fluctuating components of total saturated soil pressures for SP1 for 4 Hz for Soil 2	116
Figure 6.64: Total saturated soil pressures for SP2 for 4 Hz for Soil 2	117
Figure 6.65: Total saturated soil pressure, non-fluctuating and fluctuating components of total saturated soil pressures for SP2 for 4 Hz for Soil 2	117
Figure 6.66: Fluctuating components of total saturated soil pressures for SP2 for 4 Hz for Soil 2	117
Figure 6.67: Non-fluctuating components of total saturated soil pressures for SP2 for 4 Hz for Soil 2	117
Figure 6.68: Total saturated soil pressures for SP1 for 5 Hz for Soil 2	118
Figure 6.69: Total saturated soil pressure, non-fluctuating and fluctuating components of total saturated soil pressures for SP1 for 5 Hz for Soil 2	118
Figure 6.70: Fluctuating components of total saturated soil pressures for SP1 for 5 Hz for Soil 2	118
Figure 6.71: Non-fluctuating components of total saturated soil pressures for SP1 for 5 Hz for Soil 2	118
Figure 6.72: Total saturated soil pressures for SP2 for 5 Hz for Soil 2	119
Figure 6.73: Total saturated soil pressure, non-fluctuating and fluctuating components of total saturated soil pressures for SP2 for 5 Hz	119
Figure 6.74: Fluctuating components of total saturated soil pressures for SP2 for 5 Hz ...	119

Figure 6.75: Non-fluctuating components of total saturated soil pressures for SP2 for 5 Hz for Soil 2	119
Figure 6.76: Total saturated soil pressures for SP1 for 6 Hz for Soil 2	120
Figure 6.77: Total saturated soil pressure, non-fluctuating and fluctuating components of total saturated soil pressures for SP1 for 6 Hz for Soil 2	120
Figure 6.78: Fluctuating components of total saturated soil pressures for SP1 for 6 Hz for Soil 2	120
Figure 6.79: Non-fluctuating components of total saturated soil pressures for SP1 for 6 Hz for Soil 2	120
Figure 6.80: Total saturated soil pressures for SP2 for 6 Hz for Soil 2	121
Figure 6.81: Total saturated soil pressure, non-fluctuating and fluctuating components of total saturated soil pressures for SP2 for 6 Hz for Soil 2	121
Figure 6.82: Fluctuating components of total saturated soil pressures for SP2 for 6 Hz for Soil 2	121
Figure 6.83: Non - fluctuating components of total saturated soil pressures for SP2 for 6 Hz for Soil 2	121
Figure 6.84: Relation between maximum fluctuating component of total saturated soil pressure versus depth for Soil 2	122
Figure 6.85: Maximum non-fluctuating components of total saturated soil pressure and total saturated soil pressure before dynamic loading for Soil 2	123
Figure 6.86: General view of four soil pressure cells (SP1, SP2, SP3, and SP4) and pore pressure cells (PP1, PP2) for two blocks tests for Soil 1 and Soil 2	124
Figure 6.87: Block, instruments, dummies and Soil 1	124
Figure 6.88: Soil pressure measurements for SP1, SP2, SP3 and SP4 for 2 Hz for Soil 1 (Test 2.2.1)	126
Figure 6.89: Soil pressure measurements for SP1, SP2, SP3 and SP4 for 3 Hz for Soil 1 (Test 2.2.2)	126
Figure 6.90: Soil pressure measurements for SP1, SP2, SP3 and SP4 for 4 Hz for Soil 1 (Test 2.2.3)	127
Figure 6.91: Soil pressure measurements for SP1, SP2, SP3 and SP4 for 5 Hz for Soil 1 (Test 2.2.4)	127
Figure 6.92: Soil pressure measurements for SP1, SP2, SP3 and SP4 for 6 Hz for Soil 1 (Test 2.2.5)	128
Figure 6.93: Total saturated soil pressure measurements acting on Block 1 and Block 2 for 2, 3, 4, 5, 6 Hz for Soil 1	130
Figure 6.94: Total saturated soil pressure for SP1 for 5 Hz for Soil 1	131
Figure 6.95: Total saturated soil pressure, non-fluctuating and fluctuating components of total saturated soil pressure for SP1 for 5 Hz for Soil 1	131
Figure 6.96: Fluctuating components of total saturated soil pressures for SP1 for 5 Hz for Soil 1	131
Figure 6.97: Non-Fluctuating components of total saturated soil pressures for SP1 for 5 Hz for Soil 1	131
Figure 6.98: Total saturated soil pressure for SP2 for 5 Hz for Soil 1	132
Figure 6.99: Total saturated soil pressure, non-fluctuating and fluctuating components of total saturated soil pressure for SP2 for 5 Hz for Soil 1	132
Figure 6.100: Fluctuating components of total saturated soil pressures for SP2 for 5 Hz for Soil 1	132

Figure 6.101: Non-Fluctuating components of total saturated soil pressure for SP1 for 5 Hz for Soil 1	132
Figure 6.102: Total saturated soil pressures for SP3 for 5 Hz for Soil 1	133
Figure 6.103: Total saturated soil pressure, non-fluctuating and fluctuating components of total saturated soil pressure for SP3 for 5 Hz for Soil 1	133
Figure 6.104: Fluctuating components of total saturated soil pressures	133
Figure 6.105: Non-Fluctuating components of total saturated soil pressures for SP3 for 5 Hz for Soil 1	133
Figure 6.106: Total saturated soil pressure for SP4 for 5 Hz for Soil 1	134
Figure 6.107: Total saturated soil pressure, non-fluctuating and fluctuating components of total saturated soil pressure for SP4 for 5 Hz for Soil 1	134
Figure 6.108: Fluctuating components of total saturated soil pressures for SP4 for 5 Hz for Soil 1	134
Figure 6.109: Non-fluctuating components of total saturated soil pressures for SP4 for 5 Hz for Soil 1	134
Figure 6.110: Relation between maximum fluctuating component of total lateral earth pressure and depth for Soil	136
Figure 6.111: Maximum non-fluctuating components of total saturated soil pressure and total saturated soil pressure before dynamic loading for Soil 1	138
Figure 6.112: Block, instruments, dummies and Soil 2.....	139
Figure 6.113: Soil pressure measurements for SP1, SP2, SP3 and SP4 for 4 Hz for Soil 2 (Test 2.2.1)	140
Figure 6.114: Soil pressure measurements for SP1, SP2, SP3 and SP4 for 5 Hz for Soil 2 (Test 2.2.2)	140
Figure 6.115: Soil pressure measurements for SP1, SP2, SP3 and SP4 for 6 Hz for Soil 2 (Test 2.2.2)	141
Figure 6.116: Saturated soil pressure measurements acting on Block 1 and Block 2 for 4, 5, 6 Hz for Soil 2.....	142
Figure 6.117: Relation between maximum fluctuating component of total lateral earth pressure and depth for Soil 2	144
Figure 6.118: Maximum non-fluctuating components of total saturated soil pressure and total saturated soil pressure before dynamic loading	145
Figure 6.119: General view of four soil pressure cells (SP1, SP2, SP3, and SP4) and pore pressure cells (PP1, PP2) for three blocks tests for Soil 1 and Soil 2	146
Figure 6.120: Block, instruments, dummies and Soil 1	146
Figure 6.121: Soil pressure measurements for SP1, SP2, SP3 and SP4 for 3 Hz for Soil 1 (Test 3.1.1)	147
Figure 6.122: Soil pressure measurements for SP1, SP2, SP3 and SP4 for 4 Hz for Soil 1 (Test 3.1.2)	148
Figure 6.123: Soil pressure measurements for SP1, SP2, SP3 and SP4 for 5 Hz for Soil 1 (Test 3.1.3)	148
Figure 6.124: Soil pressure measurements for SP1, SP2, SP3 and SP4 for 6 Hz for Soil 1 (Test 3.1.4)	149
Figure 6.125: Saturated soil pressure measurements acting on block 1, block 2 and block 3 for 3, 4, 5, 6 Hz for Soil 1	150
Figure 6.126: Relation between maximum fluctuating component of total lateral earth pressure and depth for Soil 1	152

Figure 6.127: Maximum non-fluctuating components of total saturated soil pressure and total saturated soil pressure before dynamic loading for Soil 1	154
Figure 6.128: Block, instruments, dummies and Soil 2	155
Figure 6.129: Soil pressure measurements for SP1, SP2, SP3 and SP4 for 4 Hz for Soil 2 (Test 3.2.1)	156
Figure 6.130: Soil pressure measurements for SP1, SP2, SP3 and SP4 for 5 Hz for Soil 2 (Test 3.2.2)	156
Figure 6.131: Soil pressure measurements for SP1, SP2, SP3 and SP4 for 6 Hz for Soil 2 (Test 3.2.3)	157
Figure 6.132: Total saturated soil pressure measurements acting on block 1, block 2 and block 3 for 4, 5, 6 Hz for Soil 2	158
Figure 6.133: Relation between maximum fluctuating component of total saturated soil pressure and depth for Soil 2	160
Figure 6.134: Maximum non-fluctuating components of total saturated soil pressure and total saturated soil pressure before dynamic loading for Soil 2	161
Figure 6.135: Maximum fluctuating component of total saturated soil pressure for Soil 1 and Soil 2 for one block	163
Figure 6.136: Maximum fluctuating component of total saturated soil pressure distribution acting on two blocks	164
Figure 6.137: Maximum fluctuating component of total saturated soil pressure distribution acting on three blocks.....	165
Figure 7.1: General view of position transducers (P1 and P2) for one block tests for Soil 1	167
Figure 7.2: Position transducers for one block tests for Soil 1	168
Figure 7.3: Horizontal and vertical displacement measurements for one block for 2 Hz.....	168
Figure 7.4: Horizontal and vertical displacement measurements for one block for 3 Hz.....	169
Figure 7.5: Horizontal and vertical displacement measurements for one block for 4 Hz....	169
Figure 7.6: Horizontal and vertical displacement measurements for one block for 5 Hz....	170
Figure 7.7: Horizontal and vertical displacement measurements for one block for 6 Hz....	170
Figure 7.8: Position transducers for one block tests for Soil 1	171
Figure 7.9: Horizontal displacement measurements for one block for Soil 1	171
Figure 7.10: Vertical displacement measurements for one block for Soil 1	172
Figure 7.11: Tilting degree for one block for Soil 1	172
Figure 7.12: General view of position transducers (P2) for one block tests for Soil 2	172
Figure 7.13: Position transducer for one block test for Soil 2.....	173
Figure 7.14: Horizontal displacement measurements for one block tests for Soil 2	173
Figure 7.15: General view of position transducers (P1, P2, P3) for two blocks tests for Soil 1 and Soil 2.....	175
Figure 7.16: Position transducers for two blocks for Soil 1 and Soil 2	175
Figure 7.17: Horizontal and vertical displacement measurements for two blocks for 2 Hz	175
Figure 7.18: Horizontal and vertical displacement measurements for two blocks for 3 Hz	176
Figure 7.19: Horizontal and vertical displacement measurements for two blocks for 4 Hz	176
Figure 7.20: Horizontal and vertical displacement measurements for two blocks for 5 Hz .	177
Figure 7.21: Horizontal and vertical displacement measurements for two blocks for 6 Hz	177

Figure 7.22: Horizontal displacement measurement for two blocks (Block 2) for Soil 1	178
Figure 7.23: Horizontal displacement measurement for two blocks (Block 2) for Soil 1	178
Figure 7.24: Position of the Block 2 after dynamic loading (after 5 Hz).....	178
Figure 7.25: Horizontal displacement measurements for two blocks for Soil 1	179
Figure 7.26: Vertical displacement measurements for two blocks for Soil 1	179
Figure 7.27: Tilting degree for two blocks for Soil 1	179
Figure 7.28: Horizontal displacement measurements for two blocks for Soil 2	180
Figure 7.29: Vertical displacement measurements for two blocks for Soil 2	180
Figure 7.30: Tilting degree for two blocks for Soil 2.....	180
Figure 7.31: Two blocks experimental results for Soil 2	181
Figure 7.32: General view of position transducers (P1, P2 and P3) for three blocks tests for Soil 1	182
Figure 7.33: Placements of the position transducers (P1, P2, P3) for three block tests for Soil 1	182
Figure 7.34: Horizontal and vertical displacement measurements for three blocks for 3 Hz	182
Figure 7.35: Horizontal and vertical displacement measurements for three blocks for 4 Hz	183
Figure 7.36: Horizontal and vertical displacement measurements for three blocks for 5 Hz	183
Figure 7.37: Horizontal and vertical displacement measurements for three blocks for 6 Hz	184
Figure 7.38: Horizontal displacement measurements for three blocks for Soil 1	185
Figure 7.39: Tilting degree for three blocks for Soil	185
Figure 7.40: Horizontal displacement measurement for two blocks (Block 2) for Soil 1.....	185
Figure 7.41: General view of position transducers (P1, P2, P3, P4) for three blocks tests for Soil 2	186
Figure 7.42: Horizontal displacement measurements for three blocks for Soil 2	186
Figure 7.43: Tilting degree for three blocks for Soil 2	186
Figure 7.44: Horizontal displacement measurement vs. acceleration for Soil 1 and Soil 2 for one block (one block tests)	190
Figure 7.45: Horizontal displacement measurement vs. acceleration for Soil 1 and Soil 2 for Block 1 (two blocks tests).....	191
Figure 7.46: Horizontal displacement measurement vs. acceleration for Soil 1 and Soil 2 for Block 2 (two blocks tests).....	192
Figure 7.47: Horizontal displacement measurement vs. acceleration for Soil 1 and Soil 2 for Block 1 (three blocks tests)	192
Figure 7.48: Horizontal displacement measurement vs. acceleration for Soil 1 and Soil 2 for Block 2 (three blocks tests)	193
Figure 7.49: Horizontal displacement measurement vs. acceleration for Soil 1 and Soil 2 for Block 3 (three blocks tests)	193
Figure 8.1: Schematic form of yield acceleration, initiation time of sliding, temporal relative displacement of block to the base (Hsieh et al., (2011)).....	196
Figure 8.2: "Base displacement and horizontal acceleration time history for typical results of second series of shake table tests" (Mohajeri et al., 2004)	197

Figure 8.3: Base and block acceleration and start of sliding point	199
Figure 8.4: Total soil pressure versus depth	200
Figure 8.5: Forces acting on rigid block sliding on an inclined plane (Hsieh et al., 2011) ..	204
Figure 8.6: Dynamic and static friction coefficients between rubble-block 1 for one block for 4 Hz.	205
Figure 8.7: Dynamic and static friction coefficients between rubble-block 1 for two blocks for 5 Hz	205
Figure 8.8: Dynamic and static friction coefficients between block 1- block 2 for two blocks for 5 Hz.	206
Figure 9.1: Numerical model for one block.....	210
Figure 9.2: Numerical model for two blocks	210
Figure 9.3: Numerical model for three blocks.....	210
Figure 9.4: Input motion for one block.....	210
Figure 9.5: Input motion for two blocks	211
Figure 9.6: Input motion for three blocks.....	211
Figure 9.7: Outputs of PLAXIS V8.2 computer program for one block for Soil 1	214
Figure 9.8: Outputs of PLAXIS V8.2 computer program for two blocks for Soil 1.....	214
Figure 9.9: Outputs of PLAXIS V8.2 computer program for three blocks for Soil 1	214
Figure 9.10: Contours of total displacement for one block for Soil 1	215
Figure 9.11: Contours of total displacement for two blocks for Soil 1	215
Figure 9.12: Contours of total displacement for three blocks for Soil 1	215
Figure 9.13: Soil profile measurements for three blocks for 5 Hz for Soil 1	216
Figure 9.14: Total saturated soil pressure results (SP1 and SP2) for one block for 5 Hz for Soil 1	216
Figure 9.15: Total saturated soil pressure results (SP1, SP2, SP3 and SP4) for two blocks for 5 Hz for Soil 1	217
Figure 9.16: Total saturated soil pressure results (SP1, SP2, SP3 and SP4) for three blocks for 5 Hz for Soil 1	218
Figure 9.17: Displacement results for one block for 5 Hz for Soil 1	219
Figure 9.18: Displacement results for two blocks for 5 Hz for Soil 1	219
Figure 9.19: Displacement results for three blocks for 5 Hz for Soil 1	219
Figure 9.20: Comparisons of soil pressure cells (SP1 and SP2) measurements for one block	220
Figure 9.21: Comparisons of soil pressure cells (SP1, SP2, SP3, SP4) measurements for two blocks.....	221
Figure 9.22: Comparisons of soil pressure cells (SP1, SP2, SP3, SP4) measurements for three blocks	222
Figure 9.23: Displacements results comparisons between 1 g shaking table tests and PLAXIS V8.2 computer program for one block for 5 Hz for Soil 1.	224
Figure 9.24: Displacements results comparisons between 1 g shaking table tests and PLAXIS V8.2 computer program for two blocks for 5 Hz for Soil 1.....	224
Figure 9.25: Displacements results comparisons between 1 g shaking table tests and PLAXIS V8.2 computer program for three blocks for 5 Hz for Soil 1.	224
Figure 9.26: Derince Port	226

Figure 9.27: Cross section of block type quay walls (Yüksel et al., 2002).....	226
Figure 9.28: Cross section of block type quay walls (Yüksel et al., 2002).....	226
Figure 9.29: Acceleration data for Kocaeli Earthquake, 1999	228
Figure 9.30: The geometric model of Derince Port block type quay wall	228
Figure 9.31: Crossection of the Derince Port, block type quay wall	229
Figure 9.32: Outputs of PLAXIS V8.2 computer program for Derince Port, block type quay wall	230
Figure 9.33: The horizontal displacement results	230

LIST OF SYMBOLS

$ a_{\max} $	maximum accelerations
A	maximum acceleration of design earthquake (inch/s ²)
Acc	accelerometer
c	cohesion of soil (kN/m ²)
CD	controlled damage
d_R	maximum displacement (inch) according to 5% exceedence probability
D_{n50}	nominal diameter (cm)
D_r	relative density
f	earthquake design frequency
Ff	exerted by friction.
Fn	normal force
FS _s	factor of safety against sliding
FS _o	factor of safety against overturning
g	gravity acceleration
h	water depth for each block
H	wall height
k_h	horizontal seismic coefficient
k_v	vertical seismic coefficient
k_h^I	modified seismic coefficient
KA	active earth pressure coefficient
KAE	dynamic active earth pressure coefficient
m	mass of the sliding block
M, Mw	the moment magnitude scale
Mj	Japan Meteorological Agency seismic intensity scale (JMA) magnitude
Ms	surface wave magnitude
ML	Richter magnitude scale

MD	minimum damage
N	design acceleration coefficient (inch/s ²)
\vec{N}	normal force exerted on the slope by the sliding block
m	mass of the sliding block
P _A	active earth pressure
P _{ad}	dynamic active force due to the weight of the soil
SP	soil pressure
PP	pore pressure
PT	position transducer
V	maximum ground velocity (inch/s)
V _s	velocity of shear (m/s),
ΔP_{AE}	dynamic component
q _{sur}	uniformly distributed surcharge
W	weight of the failure mass
W _{dry}	dry weight of the block or soil
W _{sub}	submerged weight of the block or soil
$\ddot{\vec{X}}_g(t)$	absolute temporal acceleration at the base
$\ddot{\vec{X}}_b(t)$	absolute temporal acceleration of sliding block
α_A	inclination of the ground surface behind the wall
α_{ae}	active angle of failure
β	inclined angle with the horizontal
γ	unit weight of soil (kN/m ³)
γ_{b-conc}	submerged unit weight of concrete
γ_{conc}	unit weight of concrete
γ_d	dry unit weight of soil (kN/m ³)
γ_{eq}	equivalent unit weight

γ_j	dry unit weight of soil for soil class j^{th}
γ_s	submerged unit weight of soil (kN/m^3)
γ_{sat}	saturated total unit weight (kN/m^3)
γ_w	unit weight of seawater
δ	friction angle between wall and soil
θ	angle between the back of the retaining wall and the vertical plane
λ	coefficient
μ	friction coefficient
μ_c	critical friction coefficient
λ	internal friction angle
ψ	seismic inertia angle

CHAPTER 1

INTRODUCTION

In coastal engineering applications for gravity quay walls, block type quay walls are mostly used type in practice. Design of the block type quay walls should be made considering stability, serviceability and safety as well as economy where the design guidelines available to give necessary recommendations especially under dynamic loads. These guidelines use several approaches ranging from simple to complex and these approaches can be presented basically by two primary methods, these methods are; “conventional seismic design method”, and “performance based design method”.

The conventional seismic design method is based on providing a capacity to resist the design seismic force, but it does not provide information on the performance of a structure when the limit of the force-balance is exceeded. In conventional seismic design method in case of relatively high intensity ground motions associated with a very rare seismic event, it is required that limit state (force- balance design) not to be exceeded, resulting in very high construction costs. If force-balance design is based on a more frequent seismic event, since it is difficult to estimate the seismic performance of the structure when subjected to ground motions that are greater than those used in design, risk of the failure of the structure becomes very high (PIANC, 2001).

In practice, existing block type quay wall mostly designed by using conventional seismic design methods. However, in recent years due to failure of block type quay walls all around the world and also in Turkey, for example İzmit, Derince Port, block type quay wall, a need for a complete review of the dynamic response of the block type quay walls was raised leading to a performance based design.

Performance based design come into picture where the design is based on behavior of the elements of the structure under dynamic loading (PIANC, 2002). In performance based design, the parameters (deformation; overturning, horizontal and vertical displacements) are identified before the design stage and they are used as “design parameters”.

Yet, there exist no detailed method for the design of block type quay walls where soil pressure (backfill) distribution, friction between block-block and block-bottom under dynamic loading have to be given as basic inputs.

In Turkey, “Technical Seismic Specifications on Construction of Coastal and Harbor Structures, Railways And Airports, (2008)” is used as technical specifications for the design of block type quay walls which based on several similar standards and specifications such as OCDI (2002), PIANC (2002).

In applications for the design of block type quay walls however, the existing technical specification based on conventional seismic design method caused some difficulties and uncertainties mainly due to oversized blocks which raised questions in minds. Not only that but also the most important concern for block type quay walls was on the new seismic design trend named as “performance based design” was not being presented in any technical specifications in the world and in Turkey (Technical Seismic Specifications on Construction of Coastal and Harbor Structures, Railways And Airports, (2008)).

In this study, in view of these discussions, the dynamic response of block type quay wall is investigated considering basically accelerations, pore pressures, soil pressures and displacements experimentally to form the base for the “performance based design for block type quay walls under dynamic loadings”. The experimental studies were carried out with 1 g shaking table for one, two, three block(s). During the experiments fluctuating component of dynamic loading and friction coefficient were obtained which are the main inputs of the design of block type quay walls under dynamic loading. The experimental studies completed with numerical studies and case study were carried out for block type quay wall under dynamic loading.

In Chapter 2, literature review is carried out on the seismic design approaches for the gravity type quay walls. Discussion is emphasized on the very few studies existing on dynamic response of block type quay walls to highlight the uncertainties and important parameters in the seismic design of such coastal structures.

In Chapter 3, basic definitions of the quay walls and specifically for the block type quay walls together with the scope of this study are presented.

In Chapter 4, experimental set-up and test equipment of the dynamic response of the block type quay walls is presented to perform 1 g shaking table tests. Input parameters such as backfill properties (for Soil 1 and Soil 2), scaling procedure, and method of evaluation of the test results on soil pressure, acceleration and displacement-tilting measurements are given.

In Chapter 5, results of acceleration measurements for 1 g shaking table tests are presented and discussed for each frequency for Soil 1 and Soil 2 for one block, two blocks, three blocks, separately.

In Chapter 6, in Part 1 and in Part 2 of this chapter, results of pore pressure measurements and soil pressure measurements are presented and discussed for one block, two blocks for each frequency for Soil 1 and Soil 2, respectively.

In Chapter 7, results of position transducers measurements (horizontal and tilting) are presented and discussed for one block, two blocks and three blocks for each frequency for Soil 1 and Soil 2.

In Chapter 8, comparisons of the static friction coefficients and dynamic friction coefficients computed by using 1 g shaking table tests results are presented and discussed.

In Chapter 9, comparison of the results of the experimental studies (1 g shaking table tests) on displacements and soil pressures obtained by numerical modelling (by selecting PLAXIS V8.2 software computer program) are presented.

Finally, the verification of the results of numerical modelling and site measurements considering the horizontal displacements of the block type quay wall are carried out, using the recorded bedrock motions of the August 17, 1999, Eastern Marmara Earthquake, which caused serious damaged on Derince Port, block type quay wall.

In Chapter 10, conclusions and future research studies are discussed highlighting the importance of the determination of the design parameters of block type quay walls under dynamic loading together with recommendations for the future studies on the seismic design of block type quay walls.

CHAPTER 2

LITERATURE REVIEW

Block type quay wall is the simplest type of gravity type quay wall, which consists of concrete blocks or natural stone placed on top of each other on a foundation consisting of a layer of gravel or crushed stone. Blocks designed with certain weight to maintain their stability against static and dynamic loading through friction develop between blocks and between the bottom block and the seabed.

Although number of dynamic response studies of quay walls, mostly on single block, increased after 2005, there is still not enough studies for the design of block type quay wall. Four basic elements, namely: rigid block – backfill – water – subsoil, are the main parameters forming a system for block type quays. When such a system is subjected to dynamic loading, extremely complex problem is formed due to complicated couplings between these elements is still not well understood.

The scope of this study is to investigate, the dynamic response of block type quay wall considering basically accelerations, pore pressures, soil pressures and displacements for one block, two blocks, three blocks for different frequencies for Soil 1 and Soil 2 experimentally to form the base for the “performance based design for block type quay walls under dynamic loads” in which the aim is to overcome the limitations of conventional seismic design. The experimental studies completed with numerical studies and case study were carried out for block type quay wall under dynamic loading. Site data of Derince Port, block type quay wall damaged during Eastern Marmara Earthquake, 1999 were used as input carried for case study.

In view of the scope of this study the below given literature survey is carried out.

“Ports are very important nodes of national and international transportation networks and play a crucial role in economic activity of the nation. They provide shipping, distribution, and other functions for the transport of cargoes via water. In many countries, trade through ports is most dominant mode compared to other modes such as land and air. Ports are often regional economic centers and important components of regional and local transportation lifeline systems. Because of these reasons, the downtime of the ports due to natural disaster such as an earthquake results in severe economic loss” (Na et al., 2008).

“Quay walls are used as the earth retaining structures for the mooring of ships in ports. Due to the demanding big amount of investment in port structures, the seismic design and construction of a quay wall becomes more important day by day” (Karakuş, 2007).

Table 2.1 and Figure 2.1 show the general types and general cross-sections of quay walls, respectively.

Table 2.1: General types of quay walls

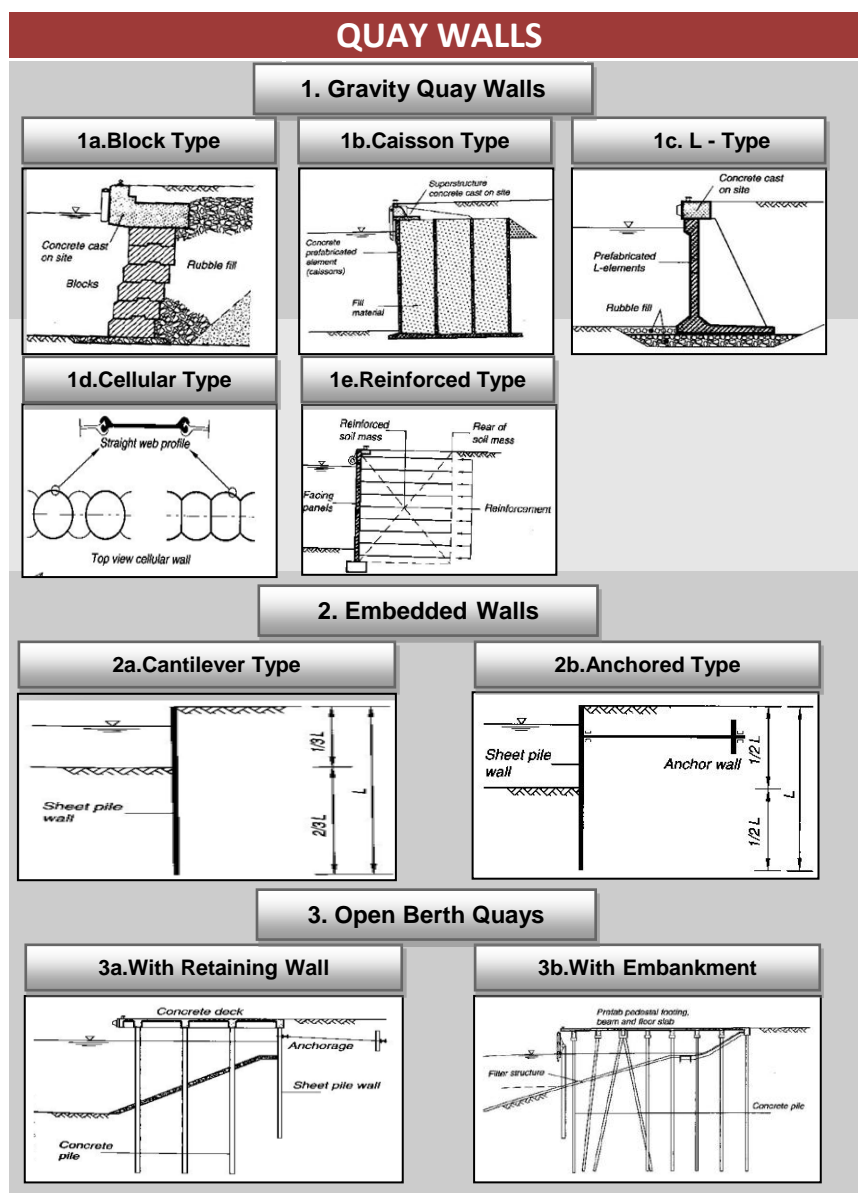
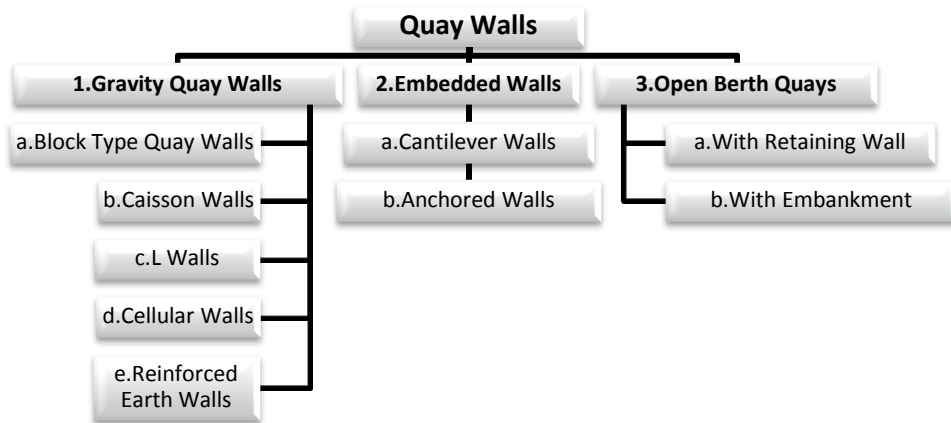


Figure 2.1: General cross-sections of quay walls (PIANC, 2001)

In the seismic design stages of quay walls; stability and safety as well as economy is considered and three basic design criteria namely, sliding, overturning and allowable bearing stress are taken into consideration for designing stage. Quay walls can suffer significantly due to earthquake and economical and social impacts of this natural event can be devastating. It is very difficult to categorize all the earthquake damages observed on quay walls; however it is possible to classify this earthquake damages considering these three basic design criteria (sliding, overturning and allowable bearing stress). "For rational design methods of retaining structures that has been pursued for several decades, deformations ranging from slight displacement to catastrophic failure have been observed in many earth retaining structures during the recent major earthquakes" (Li et al., 2010).

Table 2.2 shows the observed damages on retaining structures due to the past strong earthquakes between 1930 and 2000.

Table 2.2: Past strong earthquakes and quay wall damage level
(References are given in parenthesis)

Earthquake	Date	Magnitude	PGA	Damage Level
1.Kitaizu, Japan	1930	*M _w : 7.1 ⁽¹⁾	Unknown	Failure of gravity walls (app. 26 ft of mvt) ⁽¹⁾
2.Tonankai, Japan	1944	M _w : 8.2 ⁽¹⁾	Unknown	Sliding of retaining wall. Outward movement of bulkhead with relieving platform (10-13 ft. of mvt.) ⁽¹⁾
3.Tokachi-Oki, Japan	1952	M _w : 7.8 ⁽¹⁾	Unknown	Outward movement of gravity wall (approx. 18 ft. of mvt) ⁽¹⁾
4.Chile	1960	M _w : 9.5 ⁽²⁾	0.25g - 0.3g ⁽³⁾	Complete overturning of gravity walls (>15 ft of mvt.) Outward movement of anchored bulkheads ⁽¹⁾
5.Alaska, USA	1964	M _w : 9.2 ⁽²⁾	0.18g ⁽⁴⁾ 0.25g ⁽⁵⁾	Lateral displacement of bridge abutments. Spreading and settlement of abutment fills ⁽¹⁾
6.Niigata, Japan	1964	M _w : 7.5 ⁽¹⁾	0.2g ⁽⁵⁾	Complete failure of 4.4 miles of earth retaining waterfront structures (sheet pile and gravity walls) ⁽¹⁾
7.San Fernando, USA	1971	M _w : 6.61 ⁽⁶⁾	0.16g ⁽⁶⁾	Severely damaged flood control channels (L-type reinforced concrete sections) ⁽¹⁾
8.Friuli, Italy	1976	M _L : 6.5 ⁽⁶⁾	0.08 g ⁽⁹⁾	Complete collapse of retaining wall due to liquefied backfill ⁽¹⁾
9.Tangshan, China	1976	M _w : 7.8 ⁽¹⁾	0.1g -0.2g ⁽⁷⁾	Lateral movement of bridge abutments. Buckling of superstructures ⁽¹⁾

10.Nihonkai-Chubu, Japan	1983	$^{**}M_J: 7.7^{(8)}$	$0.24\text{ g}^{(8)}$	At the Ohama No. 2 Wharf, the sheet pile wall suffered significant damage due to liquefaction of the backfill but in Ohama No. 1 no liquefaction occurred and the quay wall didn't. The crane in Akita Port derailed on liquefied backfill of a sheet pile quay wall, resulting in a 20° landward inclination. ⁽⁸⁾
11.San Antonia Port, Chile	1985	$^{***}M_S: 7.8^{(8)}$	$0.67\text{ g}^{(8)}$	Collapse of block type quay wall over 60% of wharf length (452 m) due to strong earthquake motion and backfill liquefaction (Tsuchida et al., (1986), Wyllie et al., (1986)) Tilting and overturning of cranes on the gravity quay wall. ⁽⁸⁾
12.Kalamata Port, Greece	1986	$M_S: 6.2^{(8)}$	$0.2\text{ g} - 0.3\text{ g}^{(8)}$	Seaward displacement ($0.15 \pm 0.05\text{ m}$) with tilt (4 to 5 degrees) of block type quay wall ⁽⁸⁾
13.Chenoua, Algeria	1989	$M_W: 6.0^{(8)}$	Unknown	Ground ruptures and slides happened around the block quay wall with a horizontal displacement of 0.5 m and vertical displacement 0.3 m observed. ⁽⁸⁾
14.Loma Prieta, USA	1989	$M_L: 6.93^{(6)}$	$0.45\text{ g}^{(10)}$	Vertical cracking of reinforced concrete walls. Formation of gaps between top of walls and backfill soil.
15.Kushiro-Oki, Japan	1993	$M_J: 7.8^{(8)}$	$0.47\text{ g}^{(8)}$	Seaward displacement (0.75 m horizontally and 0.2 m vertically) with a tilt (2%) of caisson type quay wall at West Port. Seaward displacement (1.9 m horizontally and 0.2-0.5 m vertically) of caisson type quay wall at East Quay. Liquefaction of backfill resulted in opening of a crack and a displacement (0.4 m horizontally and 0.1-0.3 m vertically) in the sheet pile quay wall ⁽⁸⁾
16.Hokkaido-Nansei-Oki, Japan	1993	$M_J: 7.8^{(8)}$	$0.12\text{ g}^{(8)}$	Significant deformation (5.2 m horizontally and 1.6 m vertically) and a tilt (15 degrees) occurred on sheet pile quay wall due to liquefaction of backfill. ⁽⁸⁾
17.Guam, USA	1993	$M_S: 8.1^{(8)}$	$0.15\text{ g} - 0.25\text{ g}^{(8)}$	Displacement (0.6 m) of sheet pile quay wall ⁽⁸⁾
18.Northridge, USA	1994	$M_W: 6.7^{(8)}$	$1.7\text{ g}^{(11)}$	Continuous cracking and differential settlement of concrete crib walls ⁽⁸⁾ .

19. Hyogoken-Nanbu, Japan	1995	$M_L: 7.2^{(8)}$	$0.83\text{ g}^{(12)}$ $0.53\text{ g}^{(8)}$	Overturning and outward tilting with subsequent backfill settlement of gravity walls. Complete failure of stem of reinforced concrete cantilever retaining walls. Displacement (horizontally 1.5-2.9 m vertically 0.6-1.3 m) with tilt (11 degrees) of cellular quay wall. Buckling at upper portion of crane legs due to the movement of the caisson wall toward the sea. ⁽⁸⁾
20. Kocaeli, Turkey	1999	$M_W=7.4^{(8)}$	$0.2\text{g}-0.25\text{ g}^{(8)}$	Displacement (0.7 m) of block quay wall. Cranes derailed due to rocking response. ⁽⁸⁾
21. Ji-Ji, Taiwan	1999	$M_s=7.7^{(8)}$	$0.16\text{ g}^{(8)}$	Displacement (horizontally 1.5 m and vertically 0.1 m) of caisson quay wall and liquefaction of backfill ⁽⁸⁾

*M, Mw : The moment magnitude scale

**Mj : Japan Meteorological Agency seismic intensity scale (JMA) magnitude

***Ms : Surface wave magnitude

M_L : Richter magnitude scale

- (1) Ertugrul O., (2006), "A Finite Element Modeling Study on the Seismic Response of Cantilever Retaining Walls" (The Degree of Master of Science).
- (2) http://earthquake.usgs.gov/earthquakes/world/events/1960_05_22.php
- (3) "Unfortunately, no acceleration records are available; however, Weischet (1963) mentioned estimations about 0.25g and 0.3g according to a Mercalli intensity of X. These values are obviously not accurate and hence arguable", Villalobos, 2010
- (4) "The great Alaska earthquake of 1964", National Research Council (U.S.). Committee on the Alaska Earthquake, Volume 1, Part 1, National Academies, 1968 p. 285
- (5) Corigliano M., (2007), "Seismic Response of Deep Tunnels in Near-fault Conditions" (Research Doctorate in Geotechnical Engineering)
- (6) <http://peer.berkeley.edu/nga/data?doi=NGA0125>
- (7) R. E. S. Moss; R. E. Kayen; L.-Y. Tong; S.-Y. Liu; G.-J. Cai; and J. Wu, "Retesting of Liquefaction and Nonliquefaction Case", JOURNAL OF GEOTECHNICAL AND GEOENVIRONMENTAL ENGINEERING © ASCE , APRIL 2011
- (8) International Navigation association (PIANC), (2001), "Seismic Design Guidelines for Port Structures", 474 pages, ISBN 90 265 1818 8.
- (9) D. Leynoud; J Mienert; F. Nadim, "Slope Stability Assessment of the Hellandd Hansen Area Offshore the Mid-Norwegian Margin", INTERNATIONAL JOURNAL OF MARINE GEOLOGY, GEOCHEMISTRY AND GEOPHYSICS SEPTEMBER/2004
- (10) Master of Science Thesis in Civil Engineering, Christian H. Girsang, A Numerical Investigation of the Seismic Response of the Aggregate Pier Foundation System, December 20, 2001
- (11) <http://www.latimes.com/news/local/la-me-quake-california-20110226.0.1231448.story> and http://en.wikipedia.org/wiki/1994_Northridge_earthquake
- (12) O. Matsuo; T. Tsutsumi; K. Yokoyama and Y. Saito, (1998), "Shaking Table Tests and Analyses of Geosynthetic-Reinforced Soil Retaining Walls", GEOSYNTHETICS INTERNATIONAL.

Figure 2.2 shows the cross sections and damages on block type quay walls after earthquakes given in Table 2.2.

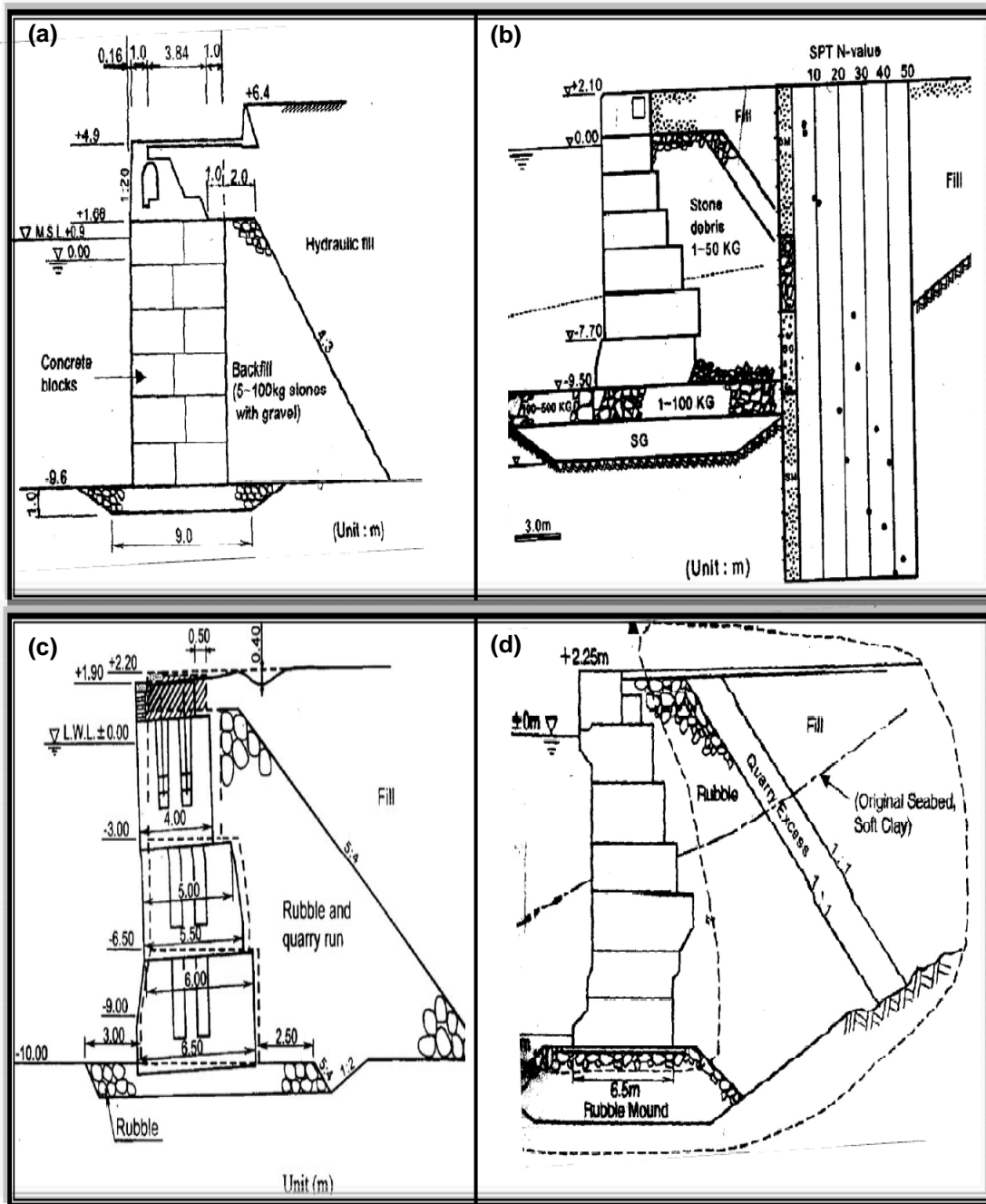


Figure 2.2: Damage of Block Type Quay Walls After a) 1985, Chile Earthquake (see Table 2.2 no: 11) b) 1986, Kalamata Earthquake (no: 12) c) 1989, Chenoua Earthquake (no: 13) d) 1999, Kocaeli Earthquake (no: 20) (PIANC, 2001)

Figure 2.3 shows the cross sections and damages of caisson type quay walls and sheet pile quay walls after earthquakes given in Table 2.2.

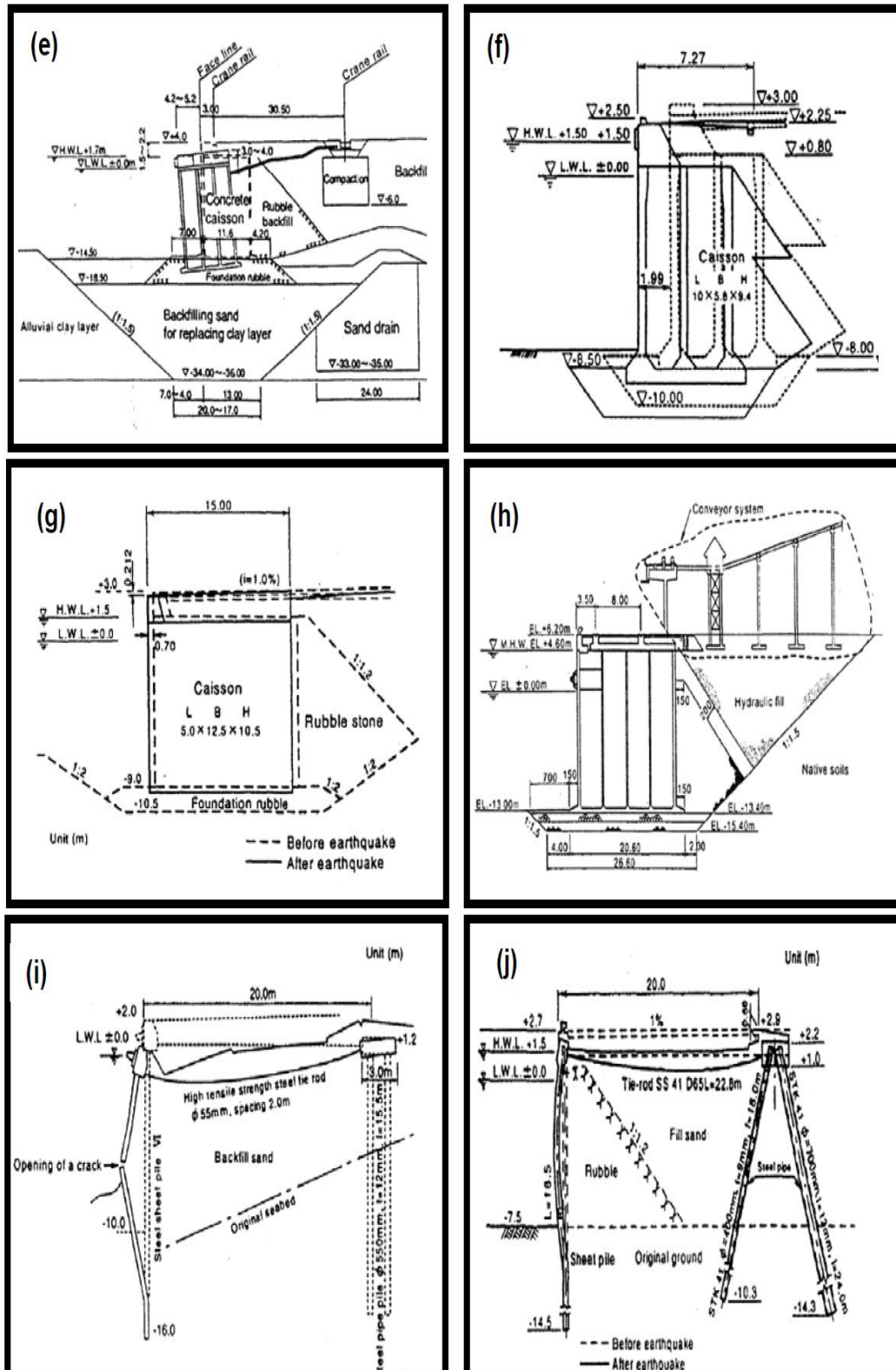


Figure 2.3: Damage of Caisson Type Quay Walls and Sheet Pile Quay Walls After e) 1995, Hyogoken-Nambu Earthquake (no: 19) f) 1993, Kushiro-Oki Earthquake (no: 15) g) 1993, Kushiro-Oki Earthquake (no: 15) h) 1999, Ji-Ji earthquake (no: 21) i) 1983, Nihonkai-Chubu Earthquake (no: 10) j) 1993, Kushiro-Oki Earthquake (no: 15) (PIANC, 2001)

Gravity quay walls are the most widely used type of quay walls. Although, the static design of gravity quay walls is well understood, the dynamic response of this type of coastal structure due to the strong ground motion is still being developed. Slight to severe deformations can be observed on this kind of coastal structures during the earthquakes. Thus, to give recommendations for the seismic design of gravity quay walls, several design methods have been developed. These design methods use several approaches ranging from simple to complex (Table 2.3).

Most generally used approaches for design of gravity quay walls can be categorized into two groups namely, “*Conventional Seismic Design Method*” and “*Performance Based Design Method*”.

The Conventional Seismic Design Method is based on providing capacity to resist a design seismic force, but it does not provide information on the performance of a structure when the limit of the force-balance is exceeded. In conventional design for the relatively high intensity ground motions associated with a very rare seismic event, it is required that limit state not to be exceeded, if the construction cost will be too high. If force-balance design is based on a more frequent seismic event, then it is difficult to estimate the seismic performance of the structure when subjected to ground motions that are greater than those used in design” (PIANC, 2001) (Table 2.3).

“In order to effectively mitigate disasters due to earthquake, tsunamis, storm surges and high waves, coastal structures with high amenity and high disaster prevention effect have been tested and new conceptual design called as “Performance Based Design Method” has been developed. Thereby, even if the force balance exceeds the limit values, it can be possible to get some information about the performance of structure” (Karakuş et. al., 2007). Performance based design consist of numerical studies, displacement based studies and experimental studies (Table 2.3).

2.1 Conventional Seismic Design Methodology

Conventional seismic design methodology includes several types of analytical studies. Analytical studies are based on rigid plastic and elastic methods. Pseudo static and pseudo dynamic analysis are mostly preferred types of rigid plastic methods and these analysis generally use Mononobe-Okabe, Seed-Whitman, Wood and Steedman-Zeng Methods (Table 2.3). Matsuo-Ohara (1960), Tajimi (1973), Scott (1973), Wood (1973) are mostly used types of elastic methods.

2.1.1 Analytical Studies

Analysis type which will be used in design of gravity quay walls is determined according to wall deflection. For example, for the very big displacements, rigid plastic methods are used however for the very small displacements elastic methods are used. For the displacements between these two extremes, usage of elasto-plastic and nonlinear methods are suggested by Nazarian and Hadjian, (1979).

2.1.1.1 Rigid Plastic Methods

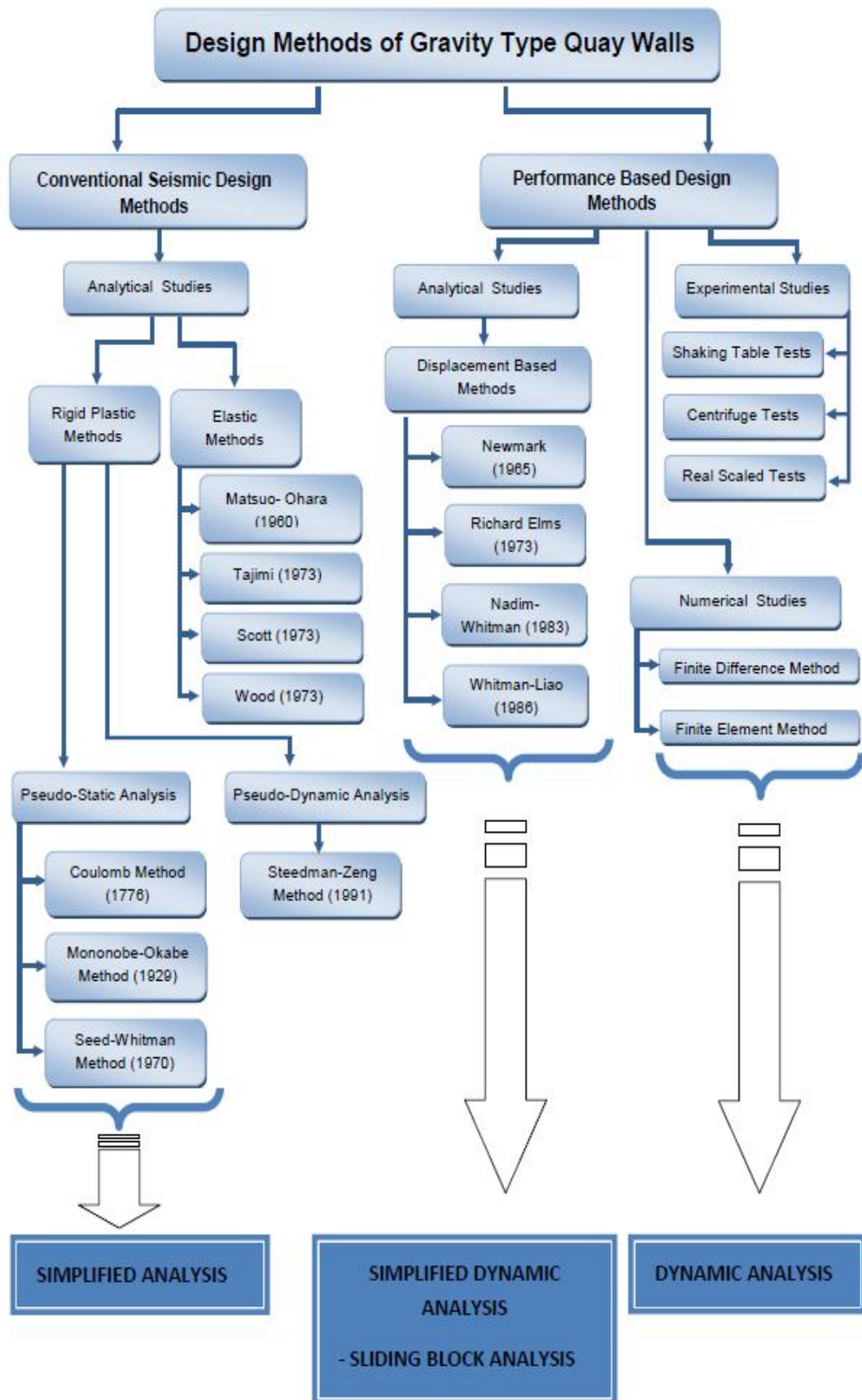
2.1.1.1.1 Pseudo-static Analysis

The most common approach based on limit state methods is pseudo-static analysis. Terzaghi (1950) developed the first explicit application of the pseudo-static approach to analyze the seismic slope stability. Horizontal inertia force (F_h) and vertical inertia force (F_v) act centered of the failure mass and the magnitudes of these forces are:

$$F_h = \frac{a_h W}{g} = k_h W$$

$$F_v = \frac{a_v W}{g} = k_v W$$

Table 2.3: Methods generally used in the design of gravity type quay walls



Where, F_h and F_v are horizontal and vertical pseudo-static forces; a_h and a_v are horizontal and vertical pseudo-static accelerations; k_h and k_v are dimensionless horizontal and vertical pseudo-static coefficients; W is weight of the failure mass.

“Similar to static limit equilibrium design methods, pseudo-static analyses provide a factor of safety against failure, but no information regarding permanent slope deformations. The vertical pseudo-static force has less effect on the factor of safety, it can reduce or increase (depending on the direction) both the driving force and resisting force. Thus, the influence of vertical acceleration is ignored in pseudo-static analysis” (Kramer, 1996).

The most generally used rigid plastic methods are Mononobe-Okabe (1929) and Steedman-Zeng Methods (1991).

2.1.1.1.1.1 Mononobe Okabe Method

“Coulomb (1776) first proposed the failure-wedge method by assuming a plane-failure surface and imposing the equilibrium conditions. Based on the Coulomb-wedge method, MueUer Breslau (1906) derived a closed-form solution for the active earth pressure coefficient taking into account the slope of the ground profile and the friction between the wall and the soil. Successively, Mononobe (1929) and Okabe (1926) extended the Coulomb solution taking also into account the earthquake-induced pressure in a pseudo-static way” (Motta, 1994).

Seed and Whitman (1970) in Green et al. (2003) indicates the method entails three fundamental assumptions:

- “1. Wall movement is sufficient to ensure either active or passive conditions, as the case may be.
2. The driving soil wedge inducing the lateral earth pressures is formed by a planar failure surface starting at the heel of the wall and extending to the free surface of the backfill. Along this failure plane the maximum shear strength of the backfill is mobilized.
3. The driving soil wedge and the retaining structure act as rigid bodies and therefore experience uniform accelerations throughout the respective bodies”.

The formulations of Mononobe-Okabe Method are shown in Table 2.4. Although this method is used to evaluate lateral earth pressure acting on retaining wall in all over the world since 1920's, Steedman (1998) pointed out “rocking, bearing and dynamic effects were important modes of response which were not effectively addressed using the Mononobe–Okabe approach of pseudo-static force-based method”.

2.1.1.1.1.2 Seed – Whitman Method

Seed and Whitman (1970) developed an empirical method to evaluate the lateral earth thrust acting on retaining wall. According to Seed-Whitman Method, maximum dynamic active earth pressure (E_{AE}) is the summation of the static and dynamic pressure increment (Table 2.4).

2.1.1.1.2 Pseudo-Dynamic Analysis

2.1.1.1.2.1 Steedman and Zeng

In pseudo-static approach, it is assumed that dynamic effect due to earthquake loading is time independent. According to this assumption, the acceleration is taken as uniform throughout the backfill during the shaking. In order to avoid the negative effects of this assumption, Steedman and Zeng (1990) improved pseudo-dynamic approach to evaluate the seismic earth pressure acting on a retaining wall considering the changes in acceleration value throughout the backfill. The formulations and detailed explanations of pseudo-dynamic method are given in Table 2.5.

“It is interesting to note that the distribution of seismic active earth pressure along the depth is non-linear in nature and this fact signifies the acceptability of the pseudo-dynamic method in comparison to pseudo-static method” (Ghosh, 2010).

Several studies based on pseudo-static analysis and pseudo-dynamic analysis, have been developed to predict the dynamic response of quay wall.

2.1.1.2 Elastic Methods

2.1.1.2.1 Wood

The two methods mentioned above is based on limit-equilibrium state, however Wood method is based on elastic method. The elastic methods regard the soil as a visco-elastic continuum, while limit-equilibrium methods assume rigid plastic behavior (Table 2.6)

Literature Surveys of Analytical Studies:

Li, Wu, and He (2010) developed a method to analyze the seismic stability of gravity type quay walls with backfill under the category of upper bound theorem of limit analysis. During this analysis, the retaining wall and the backfill soil were taken as a whole system and formulas were provided to calculate directly the yield acceleration and the inclination of the failure surface. They proved that i) proposed method and classical Mononobe–Okabe solutions coincidence to each other and ii) the influence of wall roughness on the critical acceleration factor was remarkable.

Ghosh (2010), used pseudo-dynamic approach, forming basic principles of the Steedman-Zeng Method, instead of pseudo-static approach, forming basic principles of the Mononobe-Okabe Method. Ghosh found that magnitude of seismic active earth pressure (K_{AE}) increases with the increase in the values of wall inclination (θ), horizontal and vertical seismic accelerations (k_h and k_v) but decreases with increase in the value of soil friction (Φ). The seismic active earth thrust is highly sensitive to the friction angle of soil (Φ) but comparatively less sensitive to the wall friction angle (δ) according to results of pseudo-dynamic approach. Additionally, unlike the pseudo-static analysis, the seismic active earth pressure distribution was found to be non-linear behind the retaining wall in pseudo-dynamic analysis.

Trandafir, Kamai, Sidle (2009) compared the seismic performance of gravity type quay walls and anchor reinforced slopes for dry homogeneous fill slope subjected to horizontal seismic shaking. They used Mononobe-Okabe, Bishop and Newton's second law to define the yield coefficient. According to these methodologies, they obtained different yield coefficient (k) values with respect to assumed different wall thrust (P) values for the minimum factor of safety (FS) of 1.0 and they estimated the yield coefficient according to this safety value. They also found a nonlinear relationship between the permanent displacement and the peak earthquake acceleration coefficient and they stated that especially for peak earthquake accelerations greater than 0.5g, anchor systems gave better results than earth structures.

Mylonakis, Kloukinas and Papantonopoulos (2007) also suggested some analytical solutions based on closed form stress plasticity to define the gravitational and earthquake induced earth pressures on retaining wall. They pointed out the i) importance of the weight and friction angle of the soil material, ii) wall inclination, iii) backfill inclination, iv) wall roughness, v) surcharge at soil surface, vi) horizontal and vertical seismic acceleration. They stated that this proposed method was simpler than the classical Coulomb and Mononobe-Okabe equations because by using single equation it was possible to describe both active and passive pressures regarding the appropriate signs for friction angle and wall roughness. They also assumed that the distribution of earth pressures on the back of the wall was linear with depth for both gravitational and seismic conditions.

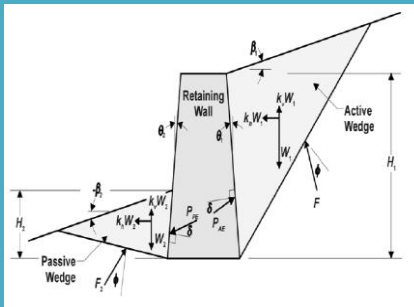
Table 2.4: Generally used methods for pseudo-static analysis

ANALYTICAL STUDIES- RIGID PLASTIC METHODS:

PSEUDO-STATIC ANALYSIS

METHOD NAME

MONONOBE-OKABE



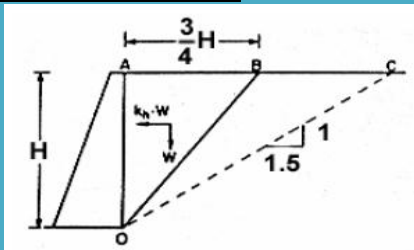
METHODOLOGY

$$K_{AE} = \frac{(1 - k_v) \cos^2(\phi - \theta - \psi)}{\cos \psi \cos^2(\theta) \cos(\theta + \delta + \psi) \left[1 + \sqrt{\frac{\sin(\phi + \delta) \sin(\phi - \beta - \psi)}{\cos(\delta + \theta + \psi) \cos(\beta - \theta)}} \right]^2} \quad P_{AE} = \frac{1}{2} K_{AE} \gamma H^2 (1 - k_v)$$

$$h = [P_A H_1 / 3 + \Delta P_{AE} \times 0.6 H_1] / P_{AE}$$

K_{AE} : dynamic active earth pressure coefficient, P_{AE} : total active thrust (kN/m), P_A : static active thrust, ΔP_{AE} : dynamic thrust, γ : unit weight of soil (kN/m^3), ϕ : internal friction angle of soil (deg), θ : angle between the back of the retaining wall, β : angle of inclination of the backfill, ψ : seismic inertia angle, δ : friction angle between wall and soil, k_v : vertical seismic coefficient and H : height of the structure.

SEED - WHITMAN



$$E_{AE} = \frac{1}{2} K_A \gamma H^2 + \Delta E_{AE}$$

$$\Delta E_{AE} = \frac{1}{2} \gamma H^2 \frac{3}{4} k_h \quad h = \frac{E_A \frac{H}{3} + \Delta E_{AE} (0.6H)}{E_{AE}}$$

K_A : static active earth pressure coefficient, E_{AE} : total active thrust (kN/m), ΔE_{AE} : dynamic thrust (kN/m), γ : unit weight of soil (kN/m^3), k_h : horizontal seismic coefficient, H : height of the structure, E_A : static active thrust

Table 2.5: Generally used methods for pseudo-dynamic analysis

ANALYTICAL STUDIES - RIGID PLASTIC METHODS:	
PSEUDO-DYNAMIC ANALYSIS	
METHOD NAME	METHODOLOGY
<u>STEEDMAN-ZENG</u>	$a(z,t) = a_h \sin \left[\omega \left(t - \frac{H-z}{V_s} \right) \right], \quad \lambda = \frac{2\pi V_s}{\omega} \quad \text{and} \quad \zeta = t - \frac{H}{V_s}$ $m(z) = \frac{\gamma}{g} t - \frac{H-z}{\tan \alpha} dz$ $Q_h(t) = \int_0^H m(z) a(z,t) dz = \frac{\lambda \gamma a_h}{4\pi^2 g \tan \alpha} [2\pi H \cos \omega \zeta + \lambda (\sin \omega \zeta - \sin \omega t)]$ $P_{AE}(t) = \frac{Q_h(t) \cos(\alpha - \phi) + W \sin(\alpha - \phi)}{\cos(\delta + \phi - \alpha)}$ $p_{AE}(t) = \frac{\partial P_{AE}(t)}{\partial z} = \frac{\gamma z}{\tan \alpha} \frac{\sin(\alpha - \phi)}{\cos(\delta + \phi - \alpha)} + \frac{k_h \gamma z}{\tan \alpha} \frac{\cos(\alpha - \phi)}{\cos(\delta + \phi - \alpha)} \sin \left[\omega \left(t - \frac{z}{V_s} \right) \right]$ $h_d = H - \frac{2\pi^2 H^2 \cos \omega \zeta + 2\pi \lambda H \sin \omega \zeta - \lambda^2 (\cos \omega \zeta - \cos \omega t)}{2\pi H \cos \omega \zeta + \pi \lambda (\sin \omega \zeta - \sin \omega t)}$ <p> $a(z, t)$: acceleration at depth z, time t, a_h: seismic acceleration, ω: angular frequency of base, $m(z)$: mass of thin element, t: time in seconds, H: height of the wall, ω: cyclic frequency of harmonic input motion, V_s: velocity of shear, γ_s, γ_w: unit weight of the soil and wall material, ϕ: internal friction angle of soil, Q_h: horizontal inertia force, $P_{AE(t)}$: Earth pressure inactive state at any time t, δ: angle of internal friction of soil and angle of wall friction respectively, θ: inclination of wall with vertical, α: angle of wedge surface with horizontal, h_d: application point </p>

Table 2.6: Generally used methods for elastic analysis

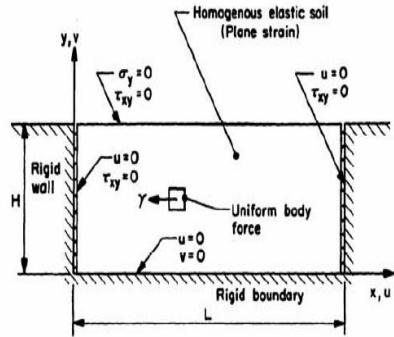
ANALYTICAL STUDIES

PSEUDO-STATIC ANALYSIS

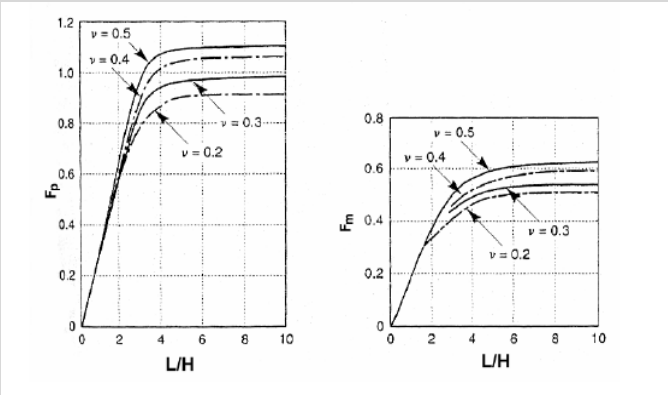
WOOD

$$\Delta P_{eq} = \gamma H^2 \frac{a_h}{g} F_p, \Delta M_{eq} = \gamma H^3 \frac{a_h}{g} F_M, h_{eq} = \frac{\Delta M_{eq}}{\Delta P_{eq}} = H \frac{F_M}{F_p}$$

ΔP_{eq} is additional dynamic drive, γ is the unit weight of soil (kN/m³), a_h is the maximum horizontal acceleration (m/s²), g gravitational acceleration (m/s²), F_p is the dimensionless drive factor, ΔM_{eq} is max seismic moment, F_M is the dimensionless moment factor, h_{eq} is the application point of dynamic drive increment



Wood's Model (after Nazarian and Hadjian, 1979)



Choudhury and Ahmad (2008) investigated the stability of the waterfront retaining wall subjected to pseudo-dynamic earthquake forces and tsunamis. They emphasized the effect of the tsunami wave height on the value of the factor of safety in sliding mode of failure and they mentioned that about 92 % decrease observed on the factor of safety against sliding when the tsunami wave height increased from 0 to 1.5. In this study, based on pseudo-dynamic analysis, nearly 16 % increase was formed on the factor of sliding mode of failure with respect to previous study (Choudhury and Ahmad (2007)) based on pseudo-static analysis. Choudhury, Nimbalkar (2007) researched the rotational displacement of retaining wall under the passive condition by using the pseudo-dynamic method. The effects of soil friction angle, wall friction angle, period of lateral shaking, horizontal and vertical seismic accelerations, amplification factor, time of input motion on the rotational displacement were studied and it was discovered that the rotational displacement increased when period of lateral shaking, horizontal and vertical seismic accelerations, amplification factor, time of input motion increase. However, the rotational displacement of the wall decreased with increase in both the soil friction and wall friction angle. Choudhury and Ahmad (2007) also researched the stability of the retaining wall by using pseudo-static analysis in terms of sliding and overturning modes of failure considering the combined of tsunami and earthquake forces. They stated that factor of safety values decreased if the tsunami water height, horizontal and vertical seismic acceleration coefficients and pore pressure ratio increased. However, on increasing soil friction angle, wall friction angle and submergence of the backfill caused increasing on stability of the retaining wall.

Literature surveys verify that conventional practice for evaluating seismic stability of retaining wall is based on pseudo-static approaches (PIANC, 2001). In PIANC, (2001), simplified analysis which based on pseudo-static approaches (Table 2.3) is defined as “this procedure, a seismic coefficient, expressed in terms of the acceleration of gravity, is used to compute an equivalent pseudo-static inertia force for use in analysis and design. The actual dynamic behavior of retaining walls is much more complex than treated in the pseudo-static approach. However, this approach has been the basis for the design of many retaining structures”.

In 1990s, in order to mitigate the damage level of gravity type quay walls during a strong earthquake, new conceptual design methods have been developed. These methods are based on determination of displacement of gravity quay. In contrary to conventional method (simplified analysis) within this study, even if the force balance exceeds the limit values, it can be possible to get some information about the performance of a structure. This conceptual design method is called as “Performance Based Design”.

2.2 Performance Based Design

2.2.1 Analytical Studies

2.2.1.1 Displacement Based Studies

“As well known, design based on pseudo-static and pseudo-dynamic approaches are generally considered conservative, since even when the safety factor drops below one the soil structure could experience only a finite displacement rather than a complete failure” (Newmark, 1965 and Ausilio, 2000). Thus, displacement based studies have been developed.

Pseudo-static and pseudo-dynamic approaches are used for defining the dynamic active or passive earth pressure values. However, due to the importance of rigidity of the wall and effects of the wall displacements on the lateral earth pressure, some approaches are also developed (Table 2.3). Over the past several decades, analytical methods have been developed to estimate the displacement of retaining walls under earthquake loading for specific applications. These methods are Richard-Elms Method (1973), Nadim-Whitman Method (1983), and Whitman-Liao Method (1986). After calculating the value and application point of the lateral earth thrust using the pseudo-static or pseudo-dynamic analysis, it is possible to define the horizontal displacement of the quay wall subjected to earthquake motion. These approaches are based on Newmark Sliding Method.

2.2.1.1.1 Newmark Sliding Method

“The Newmark sliding block method defines the yield or threshold acceleration (a_t) as the amplitude of the block acceleration when the factor of safety for sliding becomes 1.0, and evaluates the block displacement by double integration of the ground acceleration, which exceeds the yield acceleration” (Kim et al., 2005).

The coastal structures such as caisson type, L type, block type quay walls act as a retaining wall and these coastal structures are composed of a system including structure-soil-water. During the earthquake, this system moves along the base of the wall when the ground motion acceleration exceeds the threshold acceleration. The twice integration method is used to define the displacement of the wall relative to the firm base. By using the acceleration-time diagram, the velocity of the wall is computed with the first integration then according to velocity-time diagram the displacement of the wall is computed with the second integration (Table 2.7).

2.2.1.1.2 Richard and Elms

Richards and Elms (Elms, 1979) employed the Newmark sliding method to evaluate the earthquake induced displacements of gravity type quay walls. Richards and Elms (1979) suggested that by using the Mononobe–Okabe analysis based on limit equilibrium of the retaining wall, the yield acceleration of the backfill-structure system is calculated (Table 2.7).

2.2.1.1.3 Whitman and Liao

Whitman and Liao (1985) also employed the Newmark sliding method. However, differently from the Richard-Elms Methods, considering the effects of factors such as the deformation on the backfill, kinematics of backfill wedge, earthquake ground motion and possible tilting of the wall, the earthquake induced displacements of gravity retaining walls can be evaluated (Table 2.7)

2.2.1.1.4 Nadim and Whitman

Nadim and Whitman (1983) studied the influence of ground amplification on wall displacement using a two-dimensional plane-strain finite element model. They claimed that ground amplification cause more pressure and displacement on retaining wall. Nadim and Whitman suggested some criteria to include the ground amplification into the available design methodologies (Table 2.7). All these displacement based studies “cannot consider the variation of wall thrust due to the development of excess pore pressure in the backfill while determining the yield acceleration; therefore, this analysis is inappropriate for the design of quay walls with saturated backfill soils where high excess pore pressure can develop during earthquakes” (Kim et al., 2005).

Simplified dynamic analysis (Table 2.3) is categorized into three groups for seismic design of gravity wall, these are: i) sliding block analysis ii) simplified chart based on parametric study and iii) evaluation of liquefaction remediation based on parametric study (PIANC, 2001). And, Newmark, Richard and Elms, Whitman and Liao, Nadim and Whitman approaches are based on sliding block analysis. Over the last decade, very important development has been performed in hardware and numerical software which can be used in analysis and design of gravity quay walls. These numerical programs generally based on finite element analysis, boundary element analysis and finite difference techniques.

Dynamic analysis (Table 2.3), “generally using finite element or finite difference techniques, involves coupled soil-structure interaction, wherein, the response of the foundation and backfill soils is incorporated in the computation of the structural response. A structure is idealized as either a linear or non-linear model, depending on the level of earthquake motion relative to the elastic limit of the structure. The stress-strain behavior of the soil is commonly idealized with either equivalent linear or effective stress constitutive models, depending on the anticipated strain level within the soil deposit. Fairly comprehensive results can be obtained from soil-structure interaction analysis, possibly including failure modes of the soil-structure systems, extent of displacement, and stress/strain states in soil and structural components” (PIANC, 2001).

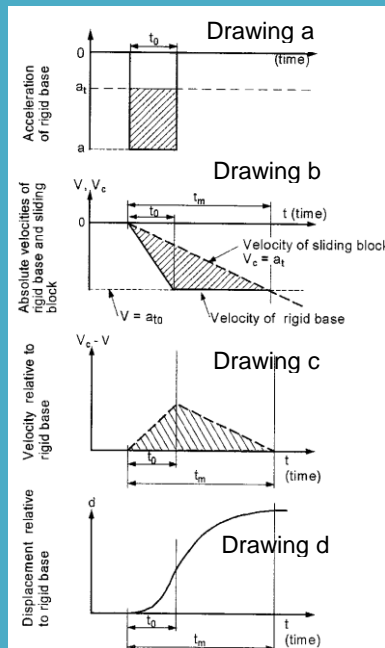
Table 2.7: General used methods based on displacement, analytical studies

PERFORMANCE BASED DESIGN

ANALYTICAL STUDIES

METHOD NAME

Newmark Sliding Method:



METHODOLOGY

“The Newmark model is basically a one-block translational or rotational mechanism along a rigid-plastic sliding surface, activated when the ground shaking acceleration exceeds a critical level” (Trandafir et al., 2009). Newmark improved this method to estimate the displacement of earth embankment and rock fill dams.

If the rectangular earthquake impulse is applied to the plane, the plane maximum acceleration is equal to “a” and the maximum acceleration transmitted to the block due to friction forces is a_t (Drawing a)

The velocity profile of the plane and block accelerations are shown in drawing b and c. Velocity of the rigid base increases to $V = a_{t0}$ in t_0 time and velocity of the sliding block ($V_c = a_t$) reaches the rigid base velocity in t_m time (Drawing b).

Velocity relative to rigid base ($V_c - V$) is shown in Drawing c.

The displacement relative to rigid base is shown as shaded area (Drawing d).

Table 2.7: General used methods based on displacement, analytical studies (continued)

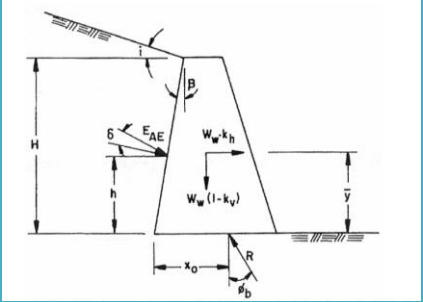
PERFORMANCE BASED DESIGN	
ANALYTICAL STUDIES	
METHOD NAME	METHODOLOGY
<p>Richard Elms Method:</p> 	<p>The procedure of the Richard and Elms Method:</p> <ol style="list-style-type: none"> Decide acceptable maximum displacement (d_R) Calculate N using; $N = A \left[\frac{0.087 V^2}{Ag} \frac{1}{d_R} \right]^{1/4}$ <p>N: design acceleration coefficient (inch/s^2), A: maximum acceleration of design earthquake (inch/s^2), V: maximum ground velocity (inch/s), d_R: maximum displacement (inch)</p> <ol style="list-style-type: none"> Use Mononobe-Okabe eq. to calculate P_{AE}. Calculate the weight of the wall for factor of safety 1.5; $W_w = \frac{1}{2} \gamma H^2 K_{AE} \left[\frac{\cos(\delta + \beta) - \sin(\delta + \beta) \tan \phi_b}{(\tan \phi_b - \tan \theta)} \right]$ <p>K_{AE} : dynamic active earth pressure coefficient, γ : the unit weight of soil (kN/m^3), ϕ_b : internal friction angle of soil (deg), θ: the angle between the back of the retaining wall, Ψ: seismic inertia angle, β : angle of inclination of the backfill, δ : friction angle between wall and soil, H: : height of the structure</p> <p>*To calculate the K_{AE} use N value instead of k_h</p>

Table 2.7: General used methods based on displacement, analytical studies (continued)

PERFORMANCE BASED DESIGN	
ANALYTICAL STUDIES	
METHOD NAME	METHODOLOGY
<u>Whitman- Liao Method:</u>	<p>The procedure of the Whitman and Liao Method:</p> <ol style="list-style-type: none"> 1. Decide acceptable maximum displacement (d_R) 2. Calculate N using; $\frac{N}{A} = 0.66 - \frac{1}{9.4} \ln \frac{d_R A}{V^2}$ <p>N: design acceleration coefficient (inch/s^2), A: maximum acceleration of design earthquake (inch/s^2), V: maximum ground velocity (inch/s), d_R: maximum displacement (inch) according to <u>5% exceedence probability</u>.</p> <ol style="list-style-type: none"> 3. Use Mononobe-Okabe eq. to calculate P_{AE}. 4. Calculate the weight of the wall. $W_w = \frac{1}{2} \gamma H^2 K_{AE} \left[\frac{\cos(\delta + \beta) - \sin(\delta + \beta) \tan \phi_b}{(\tan \phi_b - \tan \theta)} \right]$ <p>K_{AE} : dynamic active earth pressure coefficient, γ : the unit weight of soil (kN/m^3), ϕ_b : internal friction angle of soil (deg), θ: the angle between the back of the retaining wall, Ψ: seismic inertia angle, β : angle of inclination of the backfill, δ: friction angle between wall and soil, H: : height of the structure</p> <p>*To calculate the K_{AE} use N value instead of k_h</p>

Table 2.7: General used methods based on displacement, analytical studies (continued)

PERFORMANCE BASED DESIGN							
ANALYTICAL STUDIES							
METHOD NAME	METHODOLOGY						
<u>Nadim-Whitman Method:</u>	<p>The procedure of the Nadim and Whitman Method:</p> <ol style="list-style-type: none"> 1. The first shaking frequency (f_1) is ; $f_1 = \frac{V_s}{4H}$ <p>V_s: velocity of shear (m/s), H: height of the soil layer</p> <ol style="list-style-type: none"> 2. If; <table> <tr> <td>$f / f_1 < 0.25$</td><td>ignore ground amplification</td></tr> <tr> <td>$f / f_1 \approx 0.50$</td><td>increase maximum ground acceleration 25-30 % increase maximum ground velocity 25-30 %</td></tr> <tr> <td>$f / f_1 = 0.70 - 1.00$</td><td>increase maximum ground acceleration 50 % increase maximum ground velocity 50 %</td></tr> </table> <p>f: earthquake design frequency</p> 3. These new A and V values are used in Richard-Elms Method (1979). 	$f / f_1 < 0.25$	ignore ground amplification	$f / f_1 \approx 0.50$	increase maximum ground acceleration 25-30 % increase maximum ground velocity 25-30 %	$f / f_1 = 0.70 - 1.00$	increase maximum ground acceleration 50 % increase maximum ground velocity 50 %
$f / f_1 < 0.25$	ignore ground amplification						
$f / f_1 \approx 0.50$	increase maximum ground acceleration 25-30 % increase maximum ground velocity 25-30 %						
$f / f_1 = 0.70 - 1.00$	increase maximum ground acceleration 50 % increase maximum ground velocity 50 %						

2.2.2 Numerical Studies

Finite difference method (FDM) and finite element method (FEM) are the two main types of numerical studies and several studies have been performed by using the FDM and FEM. "The finite element method is certainly the most comprehensive approach to analyze the performance of soil structures subjected to seismic loading. Certainly, the finite element method has some advantages in considering the natural failure mechanisms and the interaction of structure–soil system, however, its use usually requires high numerical costs and accurate measurements of the properties of the component materials, which are often difficult to achieve" (Li et al., 2010).

Literature surveys of Numerical Studies:

Tiznado and Rodriguez-Roa (2011), obtained some results by using a series of finite element (FE) analyses (commercial FE code PLAXIS) to understand the behavior of gravity retaining walls on granular soils under strong seismic motions observed in the Chilean subductive environment. Different wall heights and sand deposits with different thicknesses and geotechnical properties were considered. It was found that permanent displacements of the wall depend on seismic amplification in both soil foundation and backfill. Although, analysis results showed that an increase of the accelerations induced on the soil behind the wall caused an increase of the seismic lateral pressures acting on the retaining structure, the traditional methods based on the simple sliding-block procedure could not consider this seismic amplification phenomenon. Thus, Tiznado and Rodriguez-Roa developed an approximate method for a given earthquake in Chilean expressed as a function of a unique design factor (F_d) including the effects of most significant variables such as seismic pressures, earthquake characteristics, ground motion amplification, and dynamic properties of the involved soils and they used design charts according to numerical analyses to predict both absolute lateral displacements at the base and top of gravity retaining walls located at sites with similar seismic characteristics to the Chilean subduction zone. The proposed charts matched well with available experimental data.

Maleki and Mahjoubi (2010) used a simple finite element model to understand the seismic behavior of retaining wall and they proposed new seismic soil pressure distributions for different soil and boundary conditions. They performed different earthquake parameters for the different wall heights and wall types such as bridge abutment, flexible wall, and rigid wall. They suggested three kinds of formulations and two kinds of pressure distributions for the rigid and flexible walls with different end conditions. At the end of these studies, the proposed methods and the finite element model (SASSI) results and also the other offered methods' results were compared and it was realized that the results were in good accordance with each other. They stated that i) although Mononobe Okabe method was not accurate, it could be used for practical purposes, ii) seismic soil pressure is more related to area under PSA spectrum than the PGA, iii) maximum soil pressure happened for the rigid fixed-base wall.

Na, Chaudhuri, Shinozuka (2009) used FLAC 2D computer program to investigate the effect of liquefaction and lateral spread on the seismic response of caisson type quay walls for the different soil systems. They classified soil systems into two groups namely, homogenous non-Gaussian random field sample and random field sample. Probabilistic responses were characterized in the Monte Carlo sense and they found that uniform models results were unconservative however due to nonlinear behavior of the soil-structure system random field model results provided better prediction response. Na, Chaudhuri, Shinozuka (2008) used FLAC 2D explicit finite difference computer program for performing soil-structure interaction analysis under static and seismic loading conditions. To investigate the sensitivity of the performance of port structures with respect to uncertainties of geotechnical parameters, tornado diagram and FOSM analyses have been conducted with nine geotechnical uncertain parameters, and choosing their values from available literature. They found that the uncertainties in the friction angle and the shear modulus of reclaimed soil contribute most to the variability of the residual horizontal displacement (RHD) response of the quay wall of port structures. They also stated that there was a significant fluctuation of pore pressure in the replaced soil however there was a little or negligible fluctuation of pore pressure in the reclaimed soil.

A two dimensional, effective stress finite element procedure in conjunction with a generalized and slightly modified elasto-plastic constitutive model was studied by Alyami, Rouainia and Wilkinson (2009). The model, which was initially evaluated by simulating the published monotonic tests, provided that the experimental results and numerical simulations perfectly matched. Then, a finite element program (UWLC) was used to apply the calibrated model to Kobe Port quay, it was found out that the computed horizontal and vertical displacements were within the range of displacements observed on the site. Additionally, the results showed that when permeability increases the accumulation of excess pore pressure is reduced and it was found that improving the backfill and the foundation soils reduced the vertical settlement at the toe of the wall by over 200%, while the horizontal displacement was reduced by over 350 %.

Ma, An, Wang (2009), studied about the dynamic friction mechanism in blocky rock systems. In this study, the blocky rock system was simplified into a multiple-degree-of-freedom mass–spring–dashpot system and the interactions of the rock blocks were considered. Newmark's sliding block theory was extended to calculate the lateral displacement of the blocky rock system, which is caused by the lateral force and the axial pulse load. They found that in a static case, the friction force applied on a rock block was a constant value, and the rock block could move when the pushing force exceeds this value. However, in a dynamic case with a pulse loading applied, the dynamic friction force vibrated around the static friction force, and the rock block could move as soon as the pushing force was larger than the minimum dynamic friction force, which was definitely smaller than that in the static case. It was also found that it was easiest to move the block in the lateral direction when the loading frequency ratio reaches a critical value; these results were obtained for both a single-block system and multiple block system.

C., F., Leung and R., F., Shen (2007) studied on performance of gravity caisson on sand compaction piles (SCPs) using a nonlinear finite analysis program (PLAXIS). Back analysis using the finite element method showed that the observed caisson movements at different construction stages could be reasonably replicated. The numerical results were also used to evaluate the caisson tilt angle, which could not be measured in the present field study and which is found to be independent of the length of SCPs underneath a caisson. Authorities in Morocco have launched construction of the Tangiers Mediterranean Harbor where the breakwater consists of precast reinforced concrete caissons having four cells shape (shamrock shape) filled with sand. Plaxis, as a finite elements analysis program, was used to estimate the settlements (both global and differential). When the behavior observed during caisson construction and results of Plaxis calculation were compared, they appeared to be consistent. Furthermore, a dynamic soil structure interaction was performed to verify the pseudo static calculation and to quantify caisson settlements and rotations during earthquake. Similar displacements were found out on the basis of the dynamic calculation.

Dynamic response of gravity type quay wall during earthquake and soil-sea-structure interaction were studied by Gharabaghi, Arablouei, Ghalandarzadeh and Abedi (2006) using finite element program (ADINA) to investigate the effects of fluid-structure interaction on residual displacement of wall after a real earthquake. The results proved that fluid-structure interaction would not significantly affect permanent displacement of a gravity quay wall during strong ground motions, if the wall is constructed on relatively non-liquefiable soil.

Psarropoulos, Klonaris and Gazetas (2005) stated that dynamic earth pressures obtained with elastic methods were more than two times higher than the dynamic earth pressures obtained with the limit equilibrium methods. They used both numerical (finite element program ABAQUAS) and analytical (Veletsos and Younan) models for rigid and flexible walls by considering the condition of the soil homogeneity and in homogeneity. They discovered that dynamic pressures depended on not only the wall flexibility but also the foundation rotational compliance and dynamic pressure values of flexible wall' were lower than the pressures for a rigid, fixed based wall for homogeneous and inhomogeneous soil.

Georgia Kastranta (2000) studied seismic effective-stress deformation analysis of waterfront retaining structures, e.g. Kobe Port quay as a case study, including modeling using finite element program (FLAC). Based on well-predicted deformation modes, the computed

horizontal and vertical displacements were consistent with those observed in Kobe Port after earthquake. The computed data was also consistent with the result obtained by similar analysis performed by Lai et al. (1996, 1998) using a different constitutive model.

Chen (1995) studied about the dynamic forces due to hydrodynamic pressure of sea water and dynamic pore pressure of backfill soil on offshore breakwaters using a finite difference method (FDM). They obtained distribution of hydrodynamic pressure for different sea bottom slope and they found that hydrodynamic pressure increases as the slope of the sea bottom increases. Chen, Huang (2002) made similar study considering the effects of sediment layer and backfill soil and they evaluated the hydrodynamic forces on concrete sea wall and breakwater during earthquakes. They stated that the simple empirical formulas can be used to predict hydrodynamic force acting on a breakwater with small error however they stated that instead of using empirical formulas for the seismic design of sea wall, their proposed study should be performed.

Sasumu and Ichii (1998) studied on the performance based design for port structures. In this method, the required performance of a structure specified in terms of displacements and stress levels. This method contributes that the requirements of the seismic performance of a structure against the probabilistic occurrence of earthquake motions. PIANC (2001) published a book named as "Seismic Design Guidelines for Port Structures". This book addresses the limitations of conventional seismic design, and performance based design of port structures and simulation techniques are discussed by Sasumu (2003). Basic earthquake engineering knowledge and a strategy for seismic performance based design is explained by using the figures and tables. The technical commentaries illustrate that specific aspects of seismic analysis and design, and provide examples of various applications of the guidelines. Ahmed Ghobarah (2001) is worked on state of development for performance based design in earthquake engineering.

As it is seen that, FDM method and FEM method are generally used for seismic design of gravity quay walls. However, results of these analyses should also be compared for the verification with the experimental studies.

2.2.3 Experimental Studies

Three types of experimental tests have been used for evaluating the dynamic response of retaining wall: the shaking table test, the centrifuge test and real scaled modeling tests.

2.2.3.1 Shaking Table Tests

The main goal of performance based design is to determine the design parameters (deformation; overturning, horizontal and vertical displacement) of the structure. However, it is not possible to estimate the distribution of the nonlinear soil behavior, changes in acceleration and pore pressure values with an acceptable accuracy during an earthquake. All the methods explained above are not adequate to determine the design parameters, correctly. Thus, "the development of performance based design requires shaking model tests to validate and improve prediction of seismically generated displacement" (Torisu et al., 2010). Another important aspect which have to be remembered that there are also some advantages and disadvantages of shaking table tests.

Literature Survey of Shaking Table Tests (and also Analytical-Numerical Studies):

Anastasopoulos, Georgarakos, Georgiannou, Drosos, Kourkoulis (2010) investigated the seismic performance of a typical bar-mat reinforced-soil retaining wall by using shaking table tests (experimentally) and by using model developed and encoded in ABAQUS (numerically). At the end of this study, a combined experimental-numerical methodology had been used to extrapolate the results of shaking table testing to prototype conditions. And it was understood that for small to medium intensity seismic motions, typical of $M_s = 6.0$ earthquakes the response of the reinforced soil walls were "quasi-elastic" and permanent lateral displacements do not exceed a few centimeters (at prototype scale). For larger intensity seismic motions, typical of $M_s = 6.5-7.0$ earthquakes permanent lateral displacement of the bar-mat is of the order 10–15cm (at prototype scale), lastly for the unrealistically large amplitude ($A=1.0$ g) is required for the active failure wedge behind the reinforced soil block to develop completely. In such a case, the permanent lateral

displacements may be excessively large. And they stated that the seismic response of reinforced earth structures was better than the standard type of earth structures, the largest lateral displacement took place at the middle height of the wall.

Toritsu, Sato, Towhata and Honda (2010) performed experimental studies by using 1g shaking table to understand the performance and nature of fill dams subjected to a dynamic loading. They found that deformation of a dam body increases with the decrease of relative density of soil and deformations in the upstream side of the dam were greater than in the downstream although the slope was gentler at the upstream side. This is because excess pore water pressure developed to some extent and reduced the effective stress in the upstream part, which led to greater deformations. Additionally, they claimed that the performance-based seismic design of geotechnical structures is possible if the time and cost necessary for laboratory tests, analyses, and, etc. are spent, and if the required accuracy of prediction is reasonable.

Hsieh, Lee, Jeng and Huang (2010), (article in press) discussed the results of tilt tests -used to define friction coefficient for static conditions and shaking table tests -used to define friction coefficient for dynamic conditions according to three different materials (aluminum, sandstone, and synthetic sandstone). They investigated variations of the friction coefficients with respect to different frequencies and the different applied normal forces regarding the different slope angle. Both tilt tests and shaking table tests showed that static friction coefficients was larger than the dynamic friction coefficients and increment in frequency caused an increase in the ratio between dynamic and static friction coefficients, however increment in normal stresses caused decrease in the ratio between the dynamic and static friction coefficient regardless of the frequency. Their observations suggested that the Coulomb friction model could not be described the real measured behaviors, thus sliding threshold should be measured using dynamic tests such as shaking table tests. Although this study considered only dry condition sliding surface, the obtained results can be significant to our study in order to define dynamic sliding threshold.

Moghadam, Ghalandarzad, Towhata, Moradi, Ebrahimian, and Hajjalikhani (2009) investigated the seismic performance of gravity quay walls by using the deformable panels. They used a series of shaking table 1g tests with two different seabed interface conditions as 0.3 and 0.6. They also performed a series of two dimensional finite difference effective-stress analyses to support the results obtained by physical modeling tests. They showed the numerical and analytical results according to maximum residual values of wall seismic response parameters, including lateral displacement, vertical settlement, seaward rotation and total thrust increment. They found that the time history of total pressure increment was recorded at the middle height of the wall and the panels reduced the seismic responses of gravity quay wall. They stated that maximum displacement vector value as 1.907 and 1.116 for the no mitigation case and mitigation case by panel respectively. It is understood that all the results obtained by using the experimental and numerical analysis were consistent.

Mendez, Botero, and Romo (2009) used shaking table, accelerometers and an LVDT to investigate how the transition from static to kinetic friction develops for a rigid block sliding down an inclined plane under the action of gravity. They also used commercial 3D distinct element code 3DEC to numerically reproduce the experiments carried out, thus validating the friction law. Three cases namely, constant friction coefficient, Coulomb friction law and the proposed friction law were analyzed and the results were compared to shaking table experiments' results. They stated that proposed friction law was reliable to define the block sliding analysis. This proposed friction law based on the static and dynamic test results, according to static tests results the friction coefficient had a gradual transition from static to kinetic conditions and similarly according to dynamic tests results friction varies smoothly as a function of excitation rate velocity and based on the experimental results a non linear exponential model was proposed. They stated that if the Coulomb's law or other single friction angle were performed, dynamic analysis involving friction results might be deceptive.

Hazarika, Kohama, Sugano (2008), made a series of underwater shaking table experiments to test a cushioning technique on a gravity type model caisson. Imparting three different earthquake loadings to the soil-structure system, the seismic load on the wall, the dynamic

increment of the earth pressure acting along the wall, the residual displacement of the wall, as well as the water pressures at various locations of the backfill were investigated for each earthquake motion. The results indicated that the observed residual horizontal displacement at the top is bigger than the bottom and reduction of seismic load and the residual displacement of structures were confirmed due to the cushioning technique.

A partially coupled effective stress analysis was performed by A. Arablouei, A. Ghalandarzadeh and A.R.M. Gharabaghi (2008), using a nonlinear finite difference program (FLAC), to estimate the seismic performance of caisson type quay wall. The study involved a numerical study of shaking table tests at Tokyo University, description of formulation of the adopted computational code and comparison of the numerical simulation results with the numerical records. Results of the study demonstrated that quay wall trend magnitude of vertical and horizontal displacements can be predicted reasonably well.

Sawichi, Chybicki, Kulczykowski (2007) emphasized the effect of the vertical ground motion on seismic induced displacements of gravity structures by using the numerical and experimental results. They claimed that rectangular acceleration pulses considered by Newmark were greatly different from real records, instead of rectangular pulse, triangular or sinusoidal acceleration pulse should be considered. They improved a computer program written in FORTRAN and the results obtained from this computer program were compared with the shaking table test results. Results were compatible to each other thus they believed that their method should replace Newmark's approach for the determination of seismic - induced displacements of gravity structures. They encountered three basic important problems, namely, i) predict the exact frequencies of horizontal and vertical accelerations and phase shifts, ii) choose the friction coefficient between the structure and subsoil, iii) the determine the dynamic parts of horizontal forces.

There are three analysis methods proposed in performance based design concept called as simplified analysis, simplified dynamic analysis and dynamic analysis. Simplified dynamic analysis method is studied by Kim et al. (2005) by taking into consideration the variation of wall thrust which is influenced by the excess pore pressure developed in backfill during earthquakes, the seismic sliding displacement of quay walls is estimated. Newmark sliding block concept is used for this method and by using the variable yield acceleration which varies according to the wall thrust, the quay wall displacement is calculated. The shaking table tests verify that the wall displacement can be predicted by using this method.

Mohajeri, Ichii, Tamura (2004) performed two series of shaking table tests, in the first series, gravity walls modeled by applying horizontal force and 20 cycles sinusoidal waves with different amplitudes and in the second part of the tests three caisson type composite breakwater were tested with different water levels. They found that considering the single yield acceleration during the dynamic analysis may cause the misleading results because tests results showed that when sliding occurred yield acceleration decreased immediately, therefore, they suggested that two different level of yield accelerations namely static and dynamic yield acceleration should be used during the displacement analysis. Furthermore, they suggested correction factor values on the conventional yield acceleration as α and β to define the static and dynamic yield accelerations

Kim, Kwon and Kim (2004) evaluated the force components acting on gravity type quay wall during earthquakes by using analytical and experimental studies. Modified Mononobe-Okabe method and Westergaard method as analytical studies are used to define dynamic forces and small and large scale shaking table tests as experimental studies are performed to compare the results. They tried to obtain the forces with low and high excess pore pressure ratio and they found that the modified Mononobe-Okabe method could not simulate the phase relationship between the wall inertia force and the dynamic thrust, additionally for the high excess pore pressure condition the dynamic thrust as much as 4.5 times of real value. In addition, Kim, Jang, Chung and Kim (2005) proposed a new simplified dynamic analysis to evaluate the displacement of quay wall considering the pore pressure effect in backfill during earthquake. They also used 1g shaking table tests to verify the results of proposed method. 1g shaking table tests showed that proposed method predicted the wall displacement correctly.

2.2.3.2 Centrifuge Tests

The centrifuge test utilizes the gravity force as the scale factor to simulate a prototype slope. "The principle behind centrifuge modeling is to create a stress field in a geometrically similar model, identical to that in a real or hypothetical prototype so that the stress-strain relationships at homologous points in the two systems will be the same if prototype materials are used in the model" (Dewoolkar, 2000).

"For any modeling of geotechnical elements or systems it is essential to know and to be able to control the past, the present and the future stress changes to which the soils are subjected. The first stage, covering the past and the present, represents the formation of the soil test bed and the establishment of some initial condition from which the effects of subsequent perturbation can be studied" (Wood, 2004).

Literature Survey of Shaking Table Tests (and also Analytical-Numerical Studies):

Dewoolkar, Ko and Pak (2000) used centrifuge tests to understand the static and seismic behavior of retaining wall with liquefiable backfills. They measured the static and dynamic lateral earth pressures directly by using the earth pressure transducers. They also determined the accelerations, bending strains and deflections. It was observed that linear regression distribution occurred along the depth of the wall at each time instances during lateral earth pressure measurements and it was seen that there were no significant effects of vertical acceleration on lateral thrust, strain and deflection. They found that at the end of shaking, after complete liquefaction, 50% increment occurred on the static thrust measurement made before shaking, thus dynamic thrust could be expected to be about 50% of the static thrust for the liquefiable soils.

Zeng (1998) investigated the seismic response of gravity quay walls by using centrifuge modeling considering the effect of pore pressure. They claimed that for dry backfill condition to calculate the lateral displacement of the retaining wall, Newmark sliding method might be used. However, for saturated backfill, due to the excess pore pressure it was impossible to compute correct displacement values of the retaining wall by the sliding block method. They also emphasized that excess pore pressure had a significant effect both on the angle of backfill wedge and horizontal thrust thus, when excess pore pressure developed in the backfill, comprehensive numerical procedures should be made to understand the response of gravity quay walls. Madabhushi and Zeng (1998) also investigated seismic response of gravity quay walls with numerical modeling, they used finite element code SWANDYNE to simulate the response of gravity quay walls under earthquake loading. By using the numerical code and special numerical techniques, it was more understandable the seismic response of gravity type quay walls for dry and saturated backfill conditions.

The dynamic response of caisson type quay wall was also worked by Yang, Elgamal, Abdoun and Lee (2001) by using the numerical and experimental studies. They used CYCLIC 2D finite element program and 100 g centrifuge tests and the results showed that increasing in the density and/or permeability of backfill/base material can improve the overall system stability.

2.2.3.3 Large Scale Prototype Field Tests

"Whenever the size and complexity of a project warrant, large-scale, prototype test programs can yield information unavailable by any other method. Because these investigations are expensive and require the services of a construction contractor in most cases, they are commonly included as part of a main contract to confirm design assumptions" (EM 1110-1-1804, 2001).

Lateral earth pressure distribution acting on retaining wall was defined by Matsuo et al., (1978) by using the large scale prototype field tests. According to Matsuo et al., (1978) "distribution of the lateral earth pressure behind the wall was not triangular and larger lateral pressure values were observed at the lower part of the wall".

Although gravity type quay walls have structural simplicity, due to the interaction between soil-structure and fluid system is complicated. Thus, the dynamic response of this structure has not been fully understood.

One of the most generally used types of gravity quay walls is block type quay wall. As it seen from the literature survey, there are numerous kinds of studies about seismic design of caisson type or L type quay walls; however, there are a few studies about seismic design of block type quay walls.

2.3 Block Type Quay Walls

“Block type quay wall is the simplest type of gravity wall, which consists of blocks of concrete or natural stone placed from the water side on a foundation consisting of a layer of gravel or crushed stone on top of each other. After placing, the blocks a reinforced concrete cap is placed as cast in situ. Block walls require much building material however labor necessity is relatively little. The height of this structure exceeds 20 m. It is important to have a good filter structure behind the wall to prevent the leakage of soil. This filter structure should involve thick filling of rock fill material with a good filter structure” (CUR, 2005)

Blocks maintain their stability through friction between themselves and between the bottom block and the seabed. Typical failure modes during earthquakes involve seaward displacement, settlement, and tilting of blocks. Figure 2.4 shows typical section of block type wall.

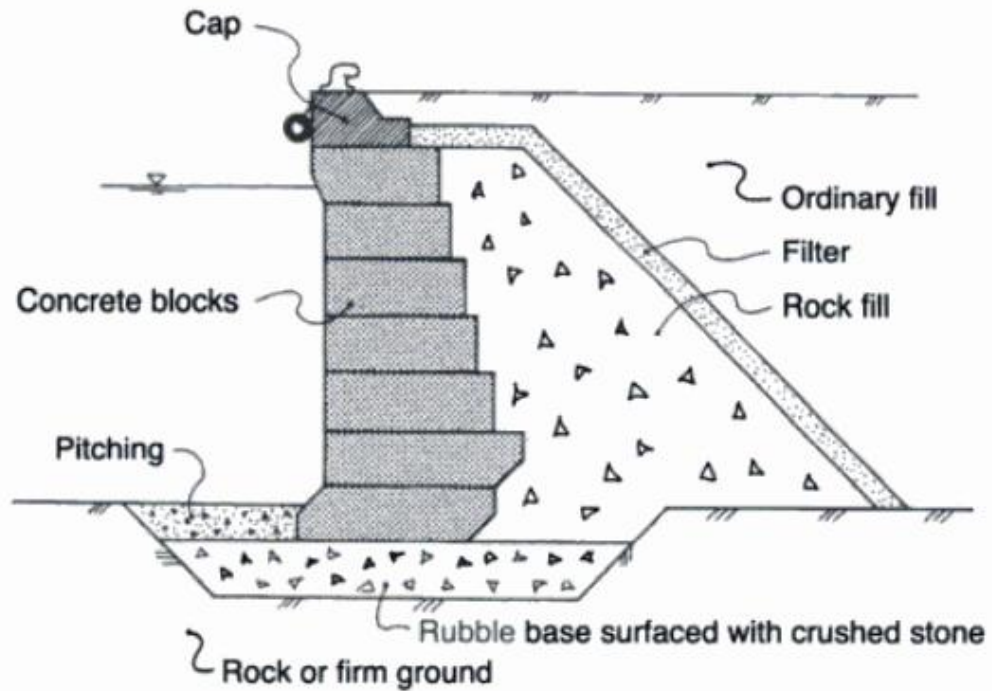


Figure 2.4: Typical section of block type wall

“The heavy damage was observed on coastal structures such as refineries, petrochemical plants and ports the eastern Marmara earthquake occurred on 17 August 1999 with an $M_w=7.4$ and İzmit Bay and north-west Turkey had been seriously affected from this earthquake. Especially, earthquake was caused crucial damage mostly on block type quay walls at Derince Port in İzmit” (Yüksel et al., 2002).

The design of block type quay walls should be performed considering stability, serviceability and safety as well as economy. Conventional seismic design methodology is generally used for block type quay walls. However, this traditional design method cannot provide the required design data and also can not provide any information about the performance of the structure after dynamic loading.

Literature Survey of Block Type Quay Walls:

Sumer, Kaya, Hansen (2002) prepared an inventory including the observations of damage to marine structures caused by liquefaction in the 17 August, 1999 Kocaeli, Turkey earthquake. According to this study, backfills behind quay walls and sheet-piled structures were almost invariably liquefied; quay walls and sheet-piled structures were displaced seaward; storage tanks near the shoreline were tilted; there were cases where the seabed settled, and structures settled and collapsed; the observations also showed that the rubble-mound breakwaters survived the earthquake with very little or no damage. However, in Tuzla Port, the block type quay wall was displaced seaward by O (40 cm) and backfill settled by O (10 cm). There was no direct evidence of liquefaction (i.e., no sand boils) in this area.

“New design approaches which are based on conventional methodologies are examined for the seismic design of block type quay walls. Within the development of the new design methodologies an inverse triangular dynamic pressures distributions are applied to define both seismic earth pressures and seismic surcharge pressures. It is assumed that soil improvement techniques are used for the site. The hydrodynamic forces are taken into consideration and equivalent unit weight concept is used during the both static and dynamic calculations. Compatibility of this new design approaches are tested by case studies and it is seen that the numerical results are in good agreement qualitatively with field measurements” (Karakuş, 2007).

Stability analysis of block type quay wall is carried out by using a computer program named QSAP (using Excel spreadsheet) has been developed by Nergis, (2010). QSAP has been prepared based on the rules of Technical Seismic Specifications on Construction of Coastal and Harbor Structures, Railways And Airports (2008). Reliability of this program is verified by a comparative study of Derince Port block type quay wall, damaged in Marmara earthquake (1999), with manual solution and field measurements. A newly introduced placement methodology “Knapsack” is also studied with QSAP and the results are compared with the conventional placement method.

Sadrekarimi, Ghalandarzadeh and Sadrekarimi (2008) investigated the both static and dynamic behavior of hunchbacked gravity quay wall by using the 1g shaking table tests for various base accelerations on models with different subsoil relative densities. The results revealed that i) negative back-slope (elevations below the breaking point of the hunch) reduces the lateral earth pressure however positive back-slope (elevations above the breaking point of the hunch) increases the lateral earth pressure, ii) relative density of sea bed affected the movement of the wall significantly, the wall moved more with large acceleration when the sea bed was softer, iii) if the model was exposed to same earthquake again, due to the subsoil densification less wall movement was observed, iv) application point of the lateral thrust fluctuated within the mid-third of wall's height and finally v) larger the height provided safer area behind the wall.

2.4 Conclusion

A review of existing literature show that; i) available methods used for analysis of the dynamic response of the block type quay walls are not adequate enough; ii) the most important step is to investigate the dynamic soil-wall interaction when studying the seismic behavior of block type quay walls; iii) one of the most important design parameters is the displacement value of the blocks after dynamic loading; iv) the influence of wall roughness between the boundaries effect the design parameters; v) system is very complicated due to including four elements, namely soil, structure, water and earthquake. All the literature surveys' results are categorized and summarized into five subtitles.

2.4.1 Earth Pressure

- “Increasing in the density and/or permeability of backfill/base material can improve the overall system stability”, (Yang et al., 2001).
- “Mononobe-Okabe method could not simulate the phase relationship between the wall inertia force and the dynamic thrust, additionally for the high excess pore pressure condition the dynamic thrust as much as 4.5 times of real value”, (Kim et al., 2004).

- “Dynamic pressures depended on not only the wall flexibility but also the foundation. Rotational compliance and dynamic pressure values of flexible walls were lower than the pressures for a rigid, fixed based wall for homogeneous and inhomogeneous soil”, (Psarropoulos et al., 2005)
- “On pseudo-dynamic analysis, nearly 16 % increase was formed on the factor of sliding mode of failure based on pseudo-static analysis”, (Choudhury and Ahmad, 2008).
- “Although Mononobe Okabe method is not accurate enough, it can be used for practical purposes”, (Maleki and Mahjoubi, 2010).
- “Magnitude of seismic active earth pressure (K_{AE}) increases with the increase in the values of wall inclination (θ), horizontal and vertical seismic accelerations (k_h and k_v) but decreases with increase in the value of soil friction (Φ)”, (Ghosh, 2010).
- “The seismic active earth thrust is highly sensitive to the friction angle of soil (Φ) but comparatively less sensitive to the wall friction angle (δ) by using the pseudo-dynamic approach”, (Ghosh, 2010).
- “Additionally, unlike the pseudo-static analysis the seismic active earth pressure distribution was found to be non-linear behind the retaining wall in pseudo-dynamic analysis”, (Ghosh, 2010).
- “The influence of wall roughness on the critical acceleration factor was remarkable”, (Li et al., 2010).
- “An increase of the accelerations induced on the soil behind the wall caused an increase of the seismic lateral pressures acting on the retaining structure, the traditional methods based on the simple sliding-block procedure could not consider this seismic amplification phenomenon”, (Tiznado and Rodriguez-Roa, 2011).

2.4.2 Soil Pressure Distribution

Several seismic soil pressure distributions along the wall height are suggested by researchers :

- “Lateral earth pressure distribution behind the wall was not triangular and relatively large lateral pressures were measured at the lower part of the wall”, (Matsuo et al., 1978).
- “Static active lateral stress had a linear distribution up to about 80% of the height of the wall and the results were compatible with the Coulomb and Mononobe-Okabe approaches. However at deeper depths the stress distribution became non-linear and increasing in the acceleration levels increased to non-linearity in the stress distribution. Additionally, for dynamic case non-linearity of the lateral earth pressure increased according to increment of the acceleration level and high stress values developed at the top of the structure”, (Sherif and Fang., 1984).
- For different wall flexibilities, the dynamic earth pressure distributions as proposed by Gazetas, (2004) are shown in Figure 2.5. Remarkable changes were obtained with respect to increasing flexibilities. “High dynamic earth pressures proposed by elastic methods decrease substantially if the structural flexibility of the wall and the rotational compliance at its base are taken into account” (Gazetas, 2004). Smaller pressure values were obtained according to Wood’s solution.

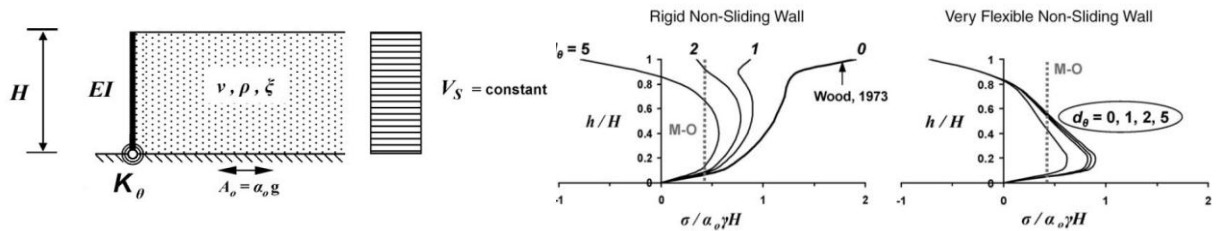


Figure 2.5: Elastic dynamic earth-pressure distribution of a pseudo-statically excited one-layer system for a non-sliding wall, (Gazetas et al., 2004)

- “The distribution of earth pressures on the back of the wall was linear with depth for both gravitational and seismic conditions”, Mylonakis et al., (2007).

- v) “M-O method suggests a linear distribution, but the Seed and Whitman method suggests no distribution and only defines $0.6 H$ as the seismic thrust point of action”, (Maleki and Mahjoubi, 2010).
- vi) “The time history of total pressure increment was recorded at the middle height of the wall” (Figure 2.6), Anastasopoulos et al., (2010).

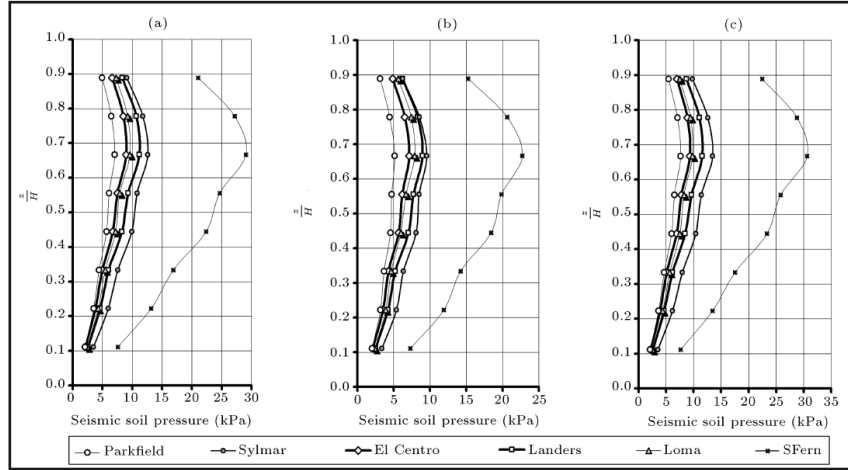


Figure 2.6: Seismic soil pressure for 4m height wall (a) Bridge abutment, (b) flexible wall, (c) rigid wall, (Anastasopoulos et al., 2010).

- vi) The seismic soil pressure distribution is proposed as given in Figure 2.7 by Maleki and Mahjoubi, (2010).

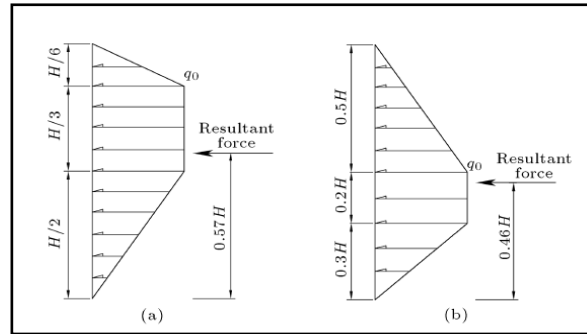


Figure 2.7: Suggested approximate seismic soil pressure distribution (a) typical distribution suggested here for rigid walls and semi-rigid walls, such as bridge abutment and propped bridge abutment, (b) distribution suggested for flexible walls such as cantilever retaining walls taller than 5 m, (Maleki and Mahjoubi, 2010).

- vii) Total soil pressure distribution is proposed as given in Figure 2.8 by Maleki and Mahjoubi, (2010).

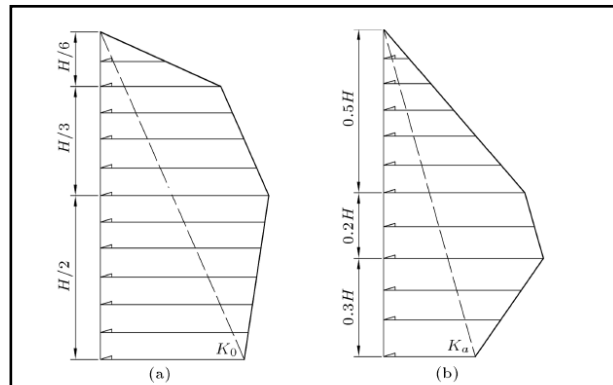
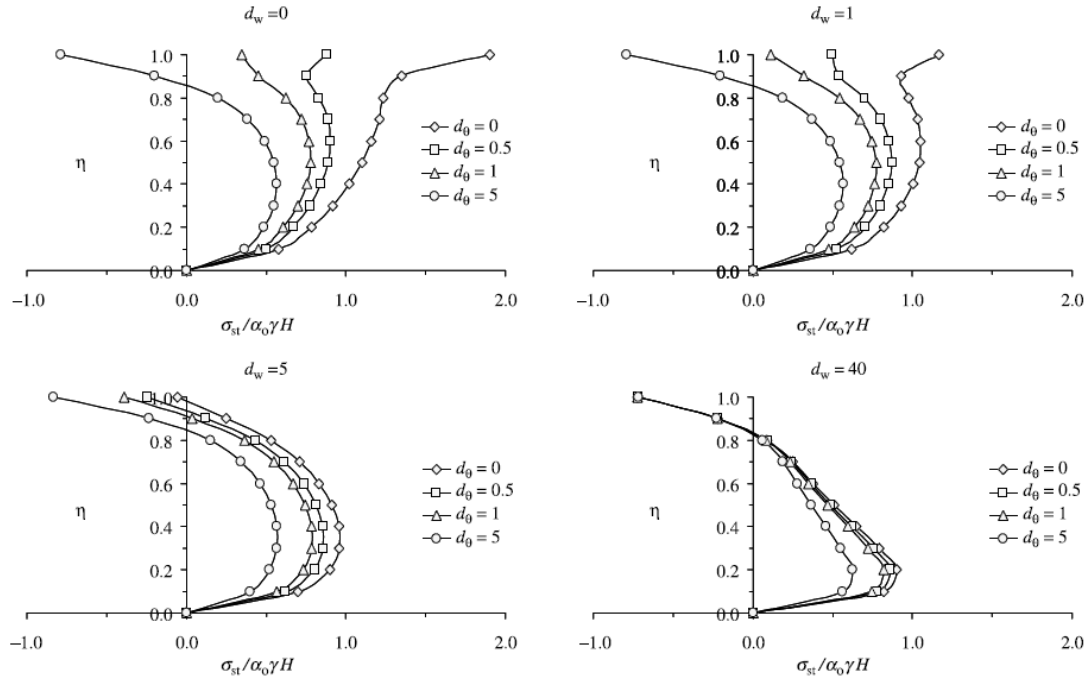


Figure 2.8: Total soil pressure distribution during earthquake (a) Rigid or semi-rigid wall, (b) Flexible wall, (Maleki and Mahjoubi, 2010).

ix) Dynamic earth pressures for different wall flexibilities proposed by Psarropoulos et al., (2004) are shown in Figure 2.9. As it is seen from the figure, dynamic earth pressure distribution depend on the wall flexibilities and the rotational base constraints of the modeled walls.



$d_w=0$ (rigid wall), 1, 5, and 40; $d_\theta=0$ (fixed against rotation), 0.5, 1, and 5

Figure 2.9: Earth-pressure distribution of a quasi-statically excited retaining system with varying relative flexibility, d_θ , of the base rotational spring for different values of relative wall flexibility, d_w (Psarropoulos et al., 2004)

2.4.3 Friction Coefficients

- “considering the single yield acceleration during the dynamic analysis may cause the misleading results because tests results showed that when sliding occurred yield acceleration decreased immediately, therefore, they suggested that two different level of yield accelerations namely static and dynamic yield acceleration should be used during the displacement analysis” (Mohajeri et al., 2004).
- “the friction angle between the wall and the retained soil can be taken as $\delta=\phi/2$, where ϕ is the internal friction angle of the soil. For typical values of ϕ (30–35°) sliding does not occur when the following condition is satisfied: $\tan \delta \approx 0.3$ ”, (Psarropoulos et al., 2005).
- “the displacements calculated by the proposed model are very sensitive to the interface friction angle. Therefore, it is important to properly evaluate the frictional resistance between a wall and foundation. The average value of the interface friction angle for the velocity range of the wall movement in the shaking table tests was about 28°” (Kim et al., 2005).
- “the uncertainties in the friction angle and the shear modulus of reclaimed soil contribute most to the variability of the residual horizontal displacement (RHD) response of the quay wall of port structures” (Na et al., 2008).
- “in a static case, the friction force applied on a rock block was a constant value, and the rock block could move when the pushing force exceeds this value. However, in a dynamic case with a pulse loading applied, the dynamic friction force vibrated around the static friction force, and the rock block could move as soon as the pushing force was larger than the minimum dynamic friction force, which was definitely smaller than that in the static case. It was also found that it was easiest to move the block in the lateral direction when the loading frequency ratio reaches a critical value” (Ma et al., 2009).

- “if the Coulomb’s law or other single friction angle were performed, dynamic analysis involving friction results might be deceptive” (Mendez et al., 2009).
- “static friction coefficients was larger than the dynamic friction coefficients and increment in frequency caused an increase in the ratio between dynamic and static friction coefficients, however increment in normal stresses caused decrease in the ratio between the dynamic and static friction coefficient regardless of the frequency” (Hsieh et al., 2010).
- “the Coulomb friction model could not be described the real measured behaviors, thus sliding threshold should be measured using dynamic tests such as shaking table tests” (Hsieh et al., 2010).
- The friction coefficients can be calculated by using tilting test as known Coulomb Theorem and the formulas developed by Hsieh et al., 2010 (Table 2.8, Figure 2.10).

Table 2.8: Friction Coefficients

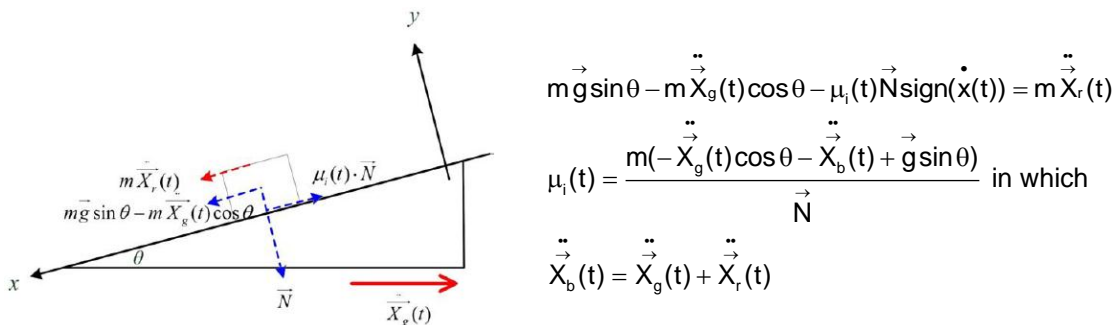
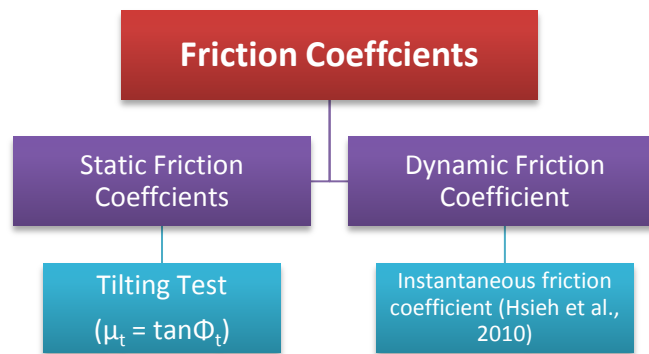


Figure 2.10: Illustration of the force equilibrium for the sliding block on a slope (Hsieh et al., 2010)

\vec{N} is the normal force exerted on the slope by the sliding block, m is the mass of the sliding block, g is the gravitational acceleration, θ is the slope angle, $\ddot{X}_g(t)$ is the absolute temporal acceleration at the base and $\ddot{X}_b(t)$ is the absolute temporal acceleration of sliding block (Figure 2.10).

2.4.4 Displacement

- “the rotational displacement increased when period of lateral shaking, horizontal and vertical seismic accelerations, amplification factor, time of input motion increased. However, the rotational displacement of the wall decreased with increase in both the soil friction and wall friction angle”, (Choudhury, Nimbalkar, 2007).
- “rectangular acceleration pulse considered by Newmark were greatly different from real records, instead of rectangular pulse triangular or sinusoidal acceleration pulse should be considered”, (Sawichi et al., 2007).
- “residual horizontal displacement at the top is bigger than the bottom”, (Hazarika et al., 2008).

- “a nonlinear relationship between the permanent displacement and the peak earthquake acceleration coefficient”, (Trandafir et al., 2009).
- “deformation of a dam body increases with the decrease of relative density of soil and deformations in the upstream side of the dam were greater than in the downstream although the slope was gentler at the upstream side. This is because excess pore water pressure developed to some extent and reduced the effective stress in the upstream part, which led to greater deformations”, (Torisu et al., 2010).
- “permanent displacements of the wall depend on seismic amplification in both soil foundation and backfill”, (Tiznado and Rodriguez-Roa, 2011).

2.4.5 Hydrodynamic Forces and Pore Pressures

- “simple empirical formulas could be used to predict hydrodynamic force acting on a wall with small error but for the seismic design of sea wall instead using empirical formulas detailed studies should be performed. Both studies emphasized the significance of the hydrodynamic analysis incorporating the effect of an earthquake should be considered for the coastal structures” (Chen, Huang, 2002).
- “fluid-structure interaction would not significantly affect permanent displacement of a gravity quay wall during strong ground motions, if the wall is constructed on relatively non-liquefiable soil” (Arablouei et al., 2006).
- “when permeability increases the accumulation of excess pore pressure is reduced it was found that improving the backfill and the foundation soils reduced the vertical settlement at the toe of the wall by over 200%, while the horizontal displacement was reduced by over 350%” (Alyami et al., 2009).

CHAPTER 3

QUAYWALLS

3.1 General

As it is well known that ports are critical civil infrastructure system for centuries, yet it is only since the mid-twentieth century that seismic provisions for port structures have been adopted in design practices. However, historical data reveal that lots of ports such as Kushiro Port, Kobe Port, Oakland Port, Port Vila and Derince Port were damaged seriously from earthquake; unfortunately, seismic risks at ports have not already received the proper amount of attention.

“Quay walls are earth retaining structures for the mooring of ships. Due to the demanding big amount of investment and the large loads on the structure, which will increase in the future because of the trade, the design and construction of a quay wall becomes more important day by day (Karakuş, 2007).

There are three kinds of quay walls name as gravity quay walls, embedded walls, open berth quays (Chapter 2, Table 2.1).

Gravity quay walls are the most generally used type of quay walls. For a gravity quay wall constructed on a firm foundation, an increase in earth pressure from the backfill plus the effect of an inertia force on the body of the wall result in the seaward movement of the wall as shown in Figure 3.1. If the width to height ratio of the wall is small, tilt may also be involved.

When the subsoil below the gravity wall is loose and excess pore water pressure increases in the subsoil, however, the movement of the wall is associated with significant deformation in the foundation soil, resulting in a large seaward movement involving tilt and settlement as shown in Figure 3.2.

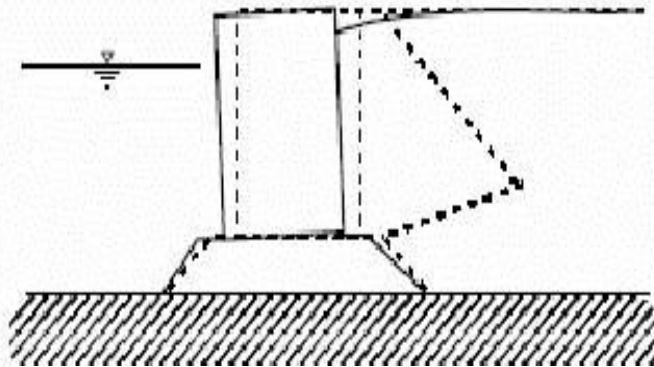


Figure 3.1: Deformation/failure modes of gravity quay wall on firm foundation (PIANC, 2001)

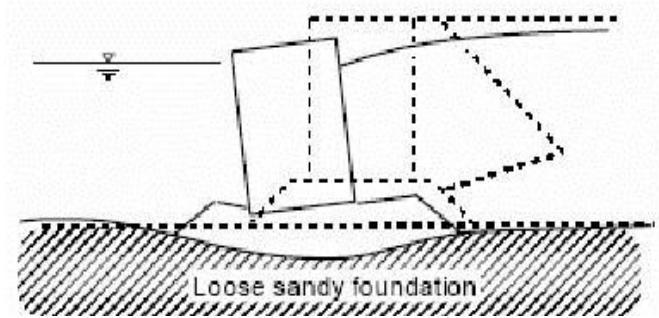


Figure 3.2: Deformation/failure modes of gravity quay wall on loose sandy formation (PIANC, 2001)

The evidence of damage to gravity quay walls suggests that:

1. most damage to gravity quay walls is often associated with significant deformation of a soft or liquefiable soil deposit, and, hence, if liquefaction is an issue, implementing appropriate remediation measures against liquefaction may be "an effective approach to attaining significantly better seismic performance;
2. most failures of gravity quay walls in practice result from excessive deformations, not catastrophic collapses, and, therefore, design methods based on displacements and ultimate stress states are desirable for defining the comprehensive seismic performance; and
3. overturning/collapse of concrete block type walls could occur when tilting is excessive, and this type of wall needs careful consideration in specifying damage criteria regarding the overturning/collapse mode" (PIANC, 2001).

In 1990s, in order to effectively mitigate the damage level of gravity type coastal structures which should be designed carefully to guarantee their survival during a strong earthquake, new conceptual design methodologies have been developed. In the seismic design of gravity type coastal structures, the most common approaches are force-based approach and displacement-based approach.

Force- based approaches are the most generally used type of method to analyze the seismic stability of gravity type quay walls. In this approach the lateral earth pressure behind the wall is expressed and force balanced equations are generated to define the stability of the gravity type quay walls. And Mononobe-Okabe equations (1929) are used as most known method to compute the total soil pressure acting on the quay walls.

Methodologies concerned with the displacement-based design of gravity type quay walls have signed up much progress and significant experimental and theoretical research studies have been performed related to this type of design methodology. Thereby, even if the force balance exceeds the limit values, it can be possible to get some information about the performance of a structure.

"The seismic design guidelines for gravity type quay walls address the limitations inherent in conventional design, and establish the framework for a new design approach. In particular, the guidelines intended to be:

- the key design parameters for the performance-based methodology which provides engineers with new design tools are the deformations in ground and foundation soils.
- performance-based, allowing a certain degree of damage depending on the specific functions and response characteristics of a port structure and probability of earthquake occurrence in the region;
- user-friendly, offering design engineers a choice of analysis methods, which range from simple to sophisticated, for evaluating the seismic performance of structures;
- general enough to be useful throughout the world, where the required functions of port structures, economic and social environment, and seismic activities may differ from region to region" (PIANC, 2001).

Conventional limit equilibrium-based methods are not well suited to evaluating these parameters.

“In performance based design, appropriate levels of design earthquake motions are defined and corresponding acceptable levels of structural damage are clearly identified. Two levels of earthquake motions are typically used as design reference motions, defined in Table 3.1” (PIANC, 2001).

Table 3.1: Levels of earthquake motions (PIANC, 2001)

Level 1 (L1)	Level 2 (L2)
<ul style="list-style-type: none"> •the level of earthquake motions that are likely to occur during the life-span of the structure •a probability of exceedance of 50% during the life-span of a structure •If the life-span of a port structure is 50 years, the return periods for L1 is 75 years 	<ul style="list-style-type: none"> •the level of earthquake motions associated with infrequent rare events, that typically involve very strong ground shaking •probability of exceedance of 10% during the life-span) •If the life-span of a port structure is 50 years, the return periods for L2 is 475 years

“The acceptable level of damage is specified according to the specific needs of the users/owners of the facilities and may be defined on the basis of the acceptable level of structural and operational damage. The structural damage category is directly related to the amount of work needed to restore the full functional capacity of the structure and is often referred to as direct loss due to earthquakes. The operational damage category is related to the length of time and cost associated with the restoration of full or partial serviceability (PIANC, 2001). “The principal steps in performance-based design are shown in Figure 3.3.

1) Performance grade is determined (S, A, B, C) selecting the damage level consistent with the needs of the users/owners according to Table 3.2 and Table 3.3. Another procedure for choosing a performance grade is to base the grade on the importance of the structure presented in Table 3.4.

2) Damage criteria is defined: the level of acceptable damage in engineering parameters such as displacements, limit stress states, or ductility factors are specified.

3) Seismic performance of a structure is evaluated: Evaluation is typically done by comparing the response parameters from a seismic analysis of the structure with the damage criteria. If the results of the analysis do not meet the damage criteria. the proposed design or existing structure should be modified. Soil improvement including remediation measures against liquefaction may be necessary at this stage” (PIANC, 2001).

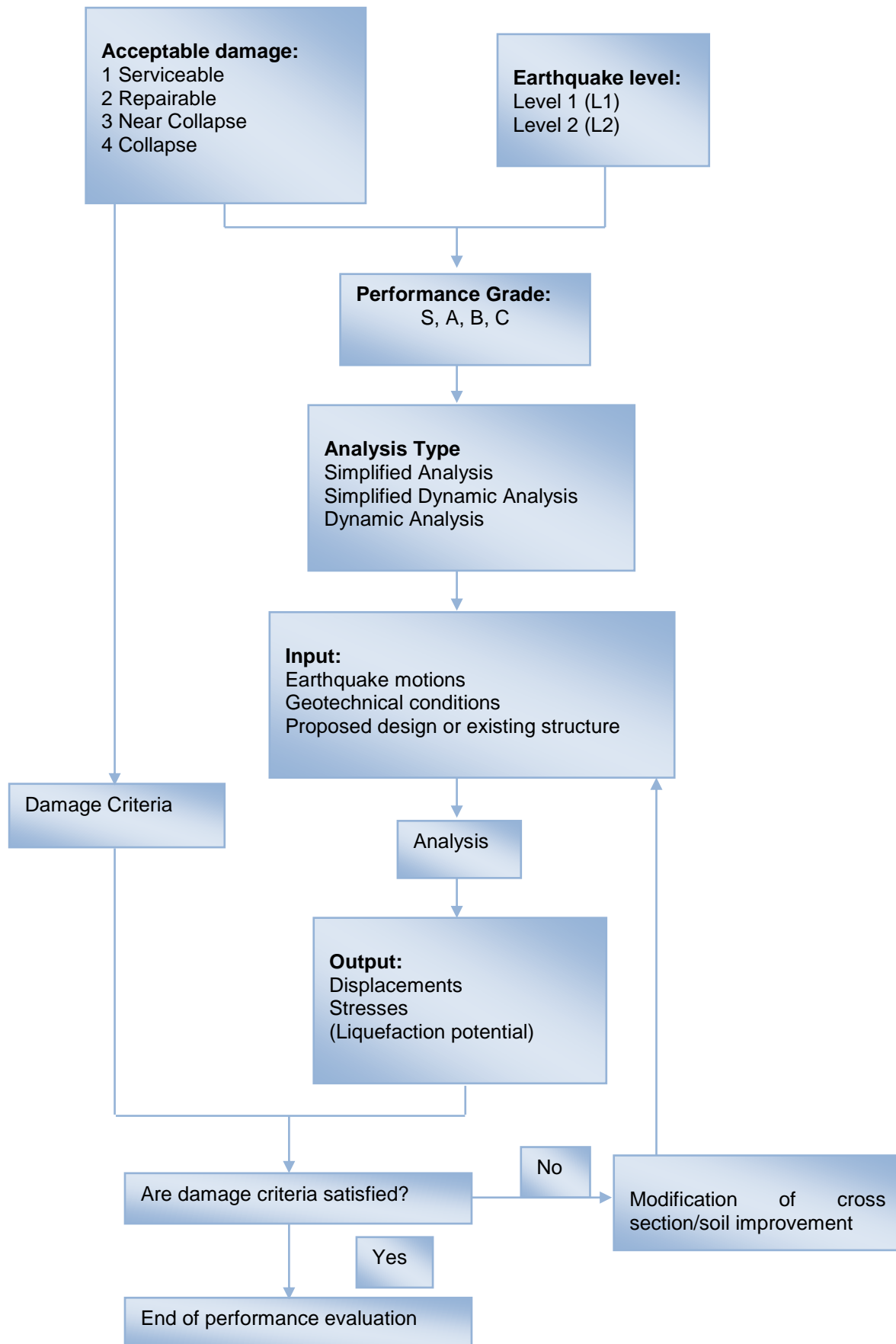


Figure 3.3: Flowchart for seismic performance evaluation

Table 3.2: Acceptable level of damage in performance based design (PIANC, 2001)

LEVEL OF DAMAGE	STRUCTURAL	OPERATIONAL
Degree 1: Serviceable	Minor or no damage	Little or no loss of serviceability
Degree 2: Repairable	Controlled damage**	Short-term loss of serviceability***
Degree 3: Near collapse	Extensive damage in near collapse	Long-term or complete loss of serviceability
Degree 4: Collapse****	Complete loss of structure	Complete loss of serviceability

* Considerations: Protection of human life and property, functions as an emergency base for transportation, and protection from spilling hazardous materials, if applicable, should be considered in defining the damage criteria in addition to those shown in this table

** With limited inelastic response and/or residual deformation.

*** Structure out of service for short to moderate time for repairs.

**** Without significant effects on surroundings.

Table 3.3: Performance grades S, A, B and C. (PIANC, 2001)

Performance grade	Design earth quake	
	Level 1 (L1)	Level 2 (L2)
Grade S	Degree 1:Serviceable	Degree 1:Serviceable
Grade A	Degree 1:Serviceable	Degree 2:Repairable
Grade B	Degree 1:Serviceable	Degree 3:Near collapse
Grade C	Degree 2:Repairable	Degree 4:Collapse

Table 3.4: Performance grade based on the importance category of port structures (PIANC, 2001)

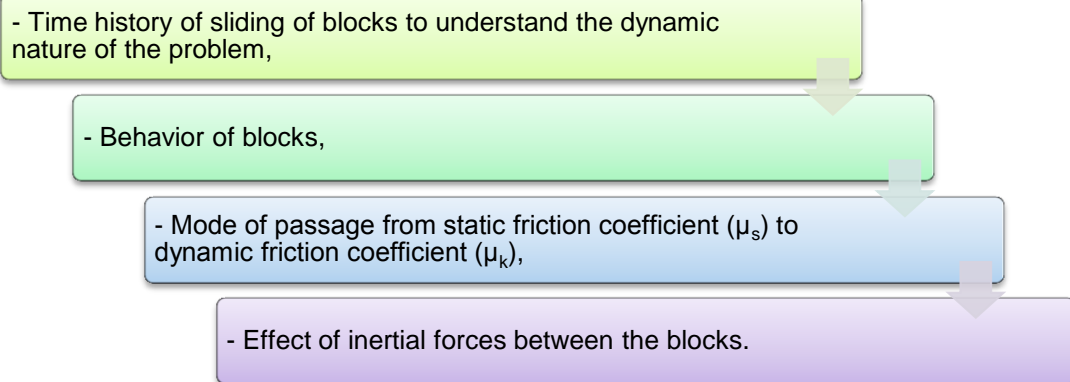
Performance grade	Definition based on seismic effects on structures
Grade S	1-Critical structures with potential for extensive loss of human life and property upon seismic damage 2-Key structures that are required to be service able for recovery from earthquake disaster 3-Critical structures that handle hazardous materials 4- Critical structures that, if disrupted, devastate economic and social activities in the earthquake damage area
Grade A	Primary structures having less serious effects for 1 through 4 than Grade S structures or 5-structures that, if damaged, are difficult to restore
Grade B	Ordinary structures other than those of Grades S,A and C
Grade C	Small easily restorable structures

3.2 Scope of this Study

The mostly used method to determine the dynamic response of block type quay wall is the **theoretical approach** where in seismic conditions, the stability of the blocks are checked by the factor of safeties using the lateral earth thrust acting on the blocks computed by the Mononobe-Okabe method or its extensions (Chapter 2, Table 2.4).

Several questions to be answered to design the block type quay walls given in Table 3.5.

Table 3.5: Several questions to be answered under dynamic loading



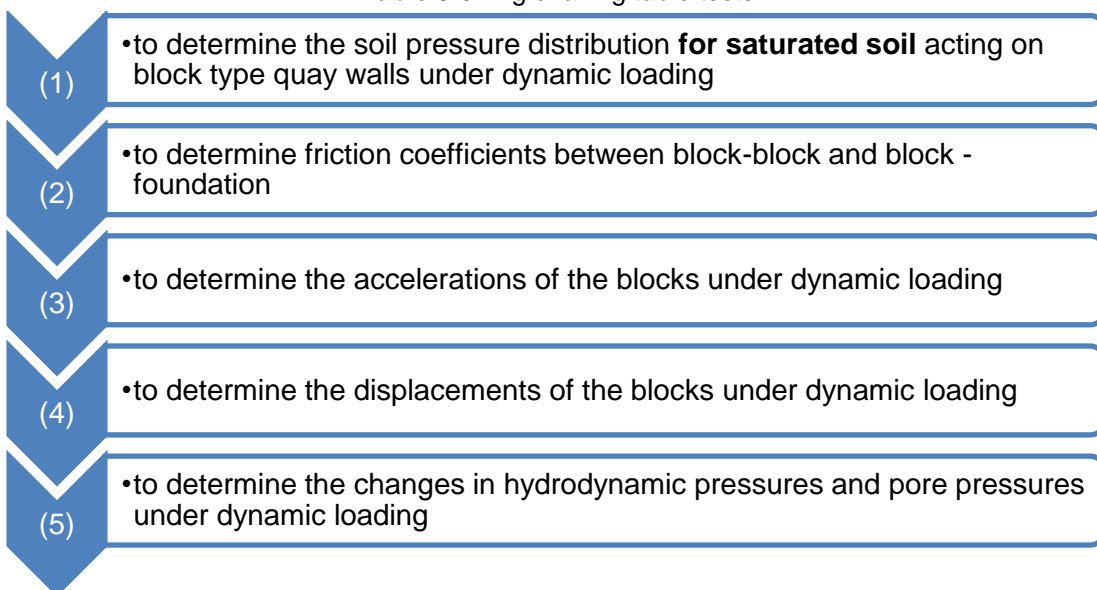
Since, it was not possible to answer all these questions (Table 3.5) only by using theoretical studies, the best approach to understand the dynamic response of block type quay walls would have been the field measurements under real seismic events. However, since the real seismic events are unpredictable and field conditions are often characterized with significant uncertainties which unable to capture the complete scenario, in the first stage of this study, the effective methodologies were selected as laboratory model studies and numerical studies.

In general, three types of laboratory model studies are available for evaluating the dynamic response of block walls: the 1g shaking table test, the centrifuge test and real scaled modeling tests.

Real scaled modeling tests investigations are expensive and require the services of a construction contractor in most cases and as if centrifuge tests are said to be more reliable than the 1g tests due to point of reduced stress level which affected the soil behavior significantly. On the other hand, relatively small model scale is recommended to be used for the centrifuge tests and it affects the soil grain size which is not practical.

In this study, after reviewing the advantage and disadvantage of all the laboratory model studies (APPENDIX A), it was decided to use 1 g shaking table. 1 g shaking table tests to obtain the results given in Table 3.6.

Table 3.6: 1 g shaking table tests



To reduce the negative effect of 1 g shaking table tests (scale effect), granular material were used as backfill material to define the dynamic response of block type quay walls **for the first time** in such type of experiments

For numerical studies, finite element and finite difference method can be used for dynamic response of block type quay walls. There are many software programs as given in Chapter 3 that can be used in the design of block type quay walls. Among these methodologies “PLAXIS” software program which gives the behavior of the structures (displacements and soil pressures) under dynamic loading is selected as a user friendly numerical program. After defining the necessary parameters by using 1 g shaking table tests, Plaxis V8.2 was performed for the comparison of the model studies’ results with the experimental studies’ results.

Damages can be observed not only in the case of strong earthquakes but also in the case of moderate earthquakes. Design of block type quay walls generally carried out by considering stability; serviceability and safety as well as economy. Therefore several design guidelines are available to give recommendations for the design and construction of block type quay walls. These guidelines use several approaches to evaluate the seismic stability of the structure, ranging from simple to complex.

Finally, a case study were performed with the numerical modeling, the recorded bedrock motions of the August 17, 1999 the eastern Marmara earthquake, which caused serious damaged on Derince Port block type quay wall, were input into the Plaxis V8.2 software program and to compare the horizontal displacement results of numerical model and site observations.

Table 3.7 gives flow chart of this study.

Throughout this study, retaining backfill and foundation (base) soil characteristics is based on the following assumptions:

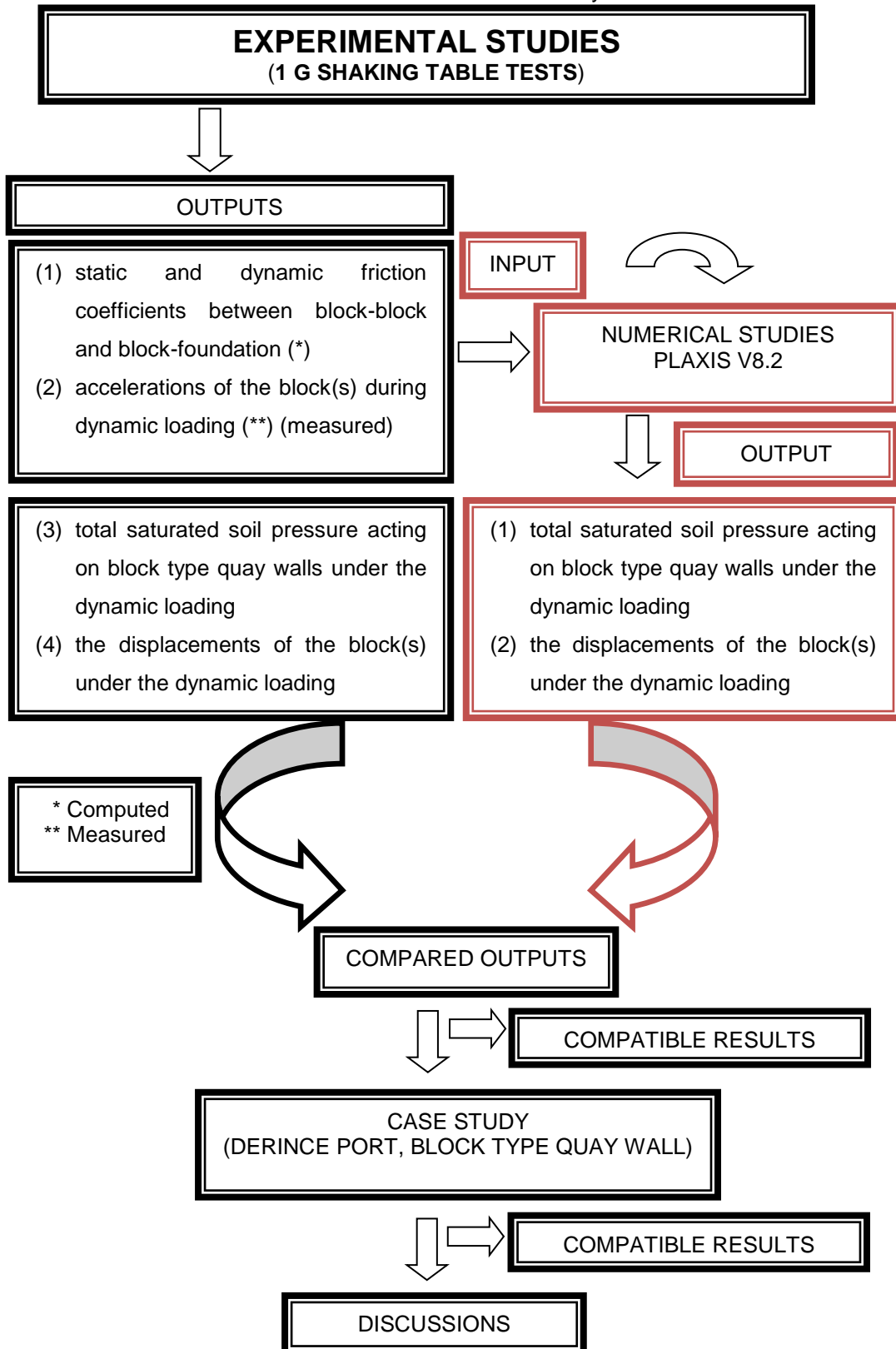
- the backfill and foundation is homogeneous, dry and cohesionless;
- the failure wedge is a plane;
- It is assumed that soil improvement techniques are used for the site as backfill and foundation where the existing soil conditions are expected to lead to unsatisfactory performance. Usually, under dynamic loading large soil movements are accepted as unsatisfactory performance. In general, port structures are designed to prevent the liquefaction in backfill. “The most common soil improvement techniques can be classified into 4 parts: densification techniques, reinforcement techniques, grouting/mixing techniques, and drainage techniques”, (Kramer, 1996).
- the ratio of backfill width to the wall height is recommended to be equal or larger than 3 (Tiznado and Roa, 2011).
- the soil-wall system is assumed to be 2D to satisfy the “plane-strain conditions”.

Regarding the experimental set up;

- The wave and current loads on the wall are not taken into considerations regarding the calm water condition inside the harbor where the block type quay walls are located. Water elevation is kept equal on both sides of the quay wall, and no tidal changes applied.
- All the acting loads due to mooring, berthing and crane operation and live loads are not taken into consideration.

Experimental results obtained in this study mainly; fluctuating component of total saturated soil pressure, application point of the fluctuating component of total saturated soil pressure and friction coefficient between block-block and block-base form the base for the performance based design of block type quay walls. These results also viewed in discussions by considering the stability; serviceability and safety as well as economy as given in the guidelines for performed based design of block type quay walls (PIANC, 2001).

Table 3.7: Flow chart of this study



CHAPTER 4

EXPERIMENTAL SET-UP

In this chapter, experimental set-up prepared to carry out dynamic response of the block type quay walls will be presented in detail.

The model tests were carried out at Hydraulics and Coastal and Harbor Lab., Civil Engineering Faculty at Yıldız Technical University as a part of “Simplified Dynamic Analysis of Block Type Quay Wall” project sponsored by Scientific and Technological Research Council of Turkey (TUBITAK) (Ref: Blok Tipi Kıyı Yapılarının Basitleştirilmiş Dinamik Analiz Yöntemi ile Tasarımı, Project Number: 111Y006, TÜBİTAK).

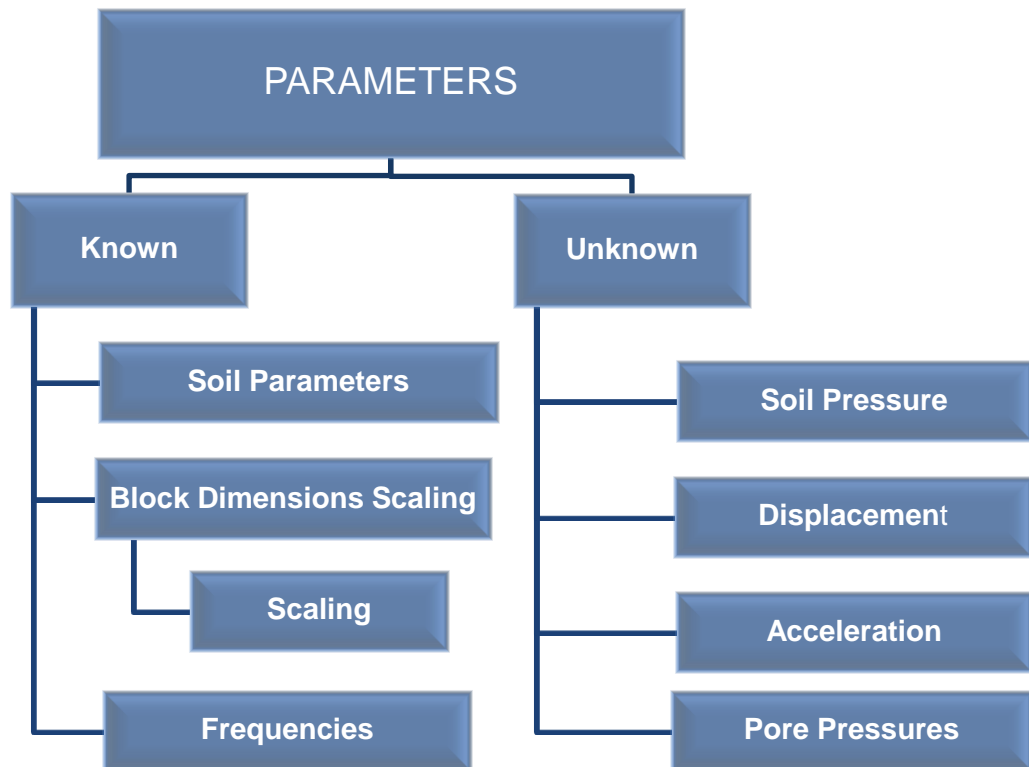
4.1 Experimental Set-up

In the preparation of experimental set up for this study parameters to be used mainly are viewed in two groups (Table 4.1):

- i) known parameters,
- ii) unknown parameters

Using the known parameters experiments are carried out in 1 g shaking table to obtain the unknowns as will be explained in the following parts.

Table 4.1: Parameters of this study



4.1.1 Known Parameters

4.1.1.1 Soil parameters

“Various advanced numerical techniques are developed on the basis of experimental studies and field observations and used in the design and seismic performance evaluation of the port structures. Through these numerical, experimental, and field studies, it is found that the seismic behavior of port structures is largely governed by the local soil conditions” (Na et al., 2009). Thus, the selected soil parameters used in 1 g shaking table tests was defined clearly for each experiment.

In this study, two different soil types were used as a backfill and one type of foundation. The first type of soil properties (Soil 1) are given in Table 4.2 and the second type of soil properties (Soil 2) which is finer than the first one are also given in Table 4.3.

Table 4.2: Soil parameters for backfill and foundation (Soil 1)

Soil 1 Parameters	(γ_{dry})(kN/m ³)	(ϕ)(°)	D _{n50} (cm)
Foundation and backfill	17	40-42	2.2

Table 4.3: Soil parameters for backfill for Soil 2

Soil2 Parameters	(γ_{dry})(kN/m ³)	(ϕ)(°)	D _{n50} (cm)
Backfill	17	40-42	1.0

Where:

γ_{dry} : Dry unit weight of the soil (foundation or backfill); Φ : internal friction angle (degree),
D_{n50}: nominal diameter (cm)

Granular material were used as backfill material to define the dynamic response of block type quay walls for the first time in such type of experiments. In practical, the weight of the granular material which is used as backfill is given 5 kg -100 kg for San Antonia Port, block type quay wall, Chile and 1 kg-50kg for Kalamata Port, block type quay wall in PIANC, (2001) and 3kg-50kg for San Pedro, block type quay wall in Handbook Quay Walls, (2005). This means that nominal diameter of the backfill can be taken as $7\text{ cm} < D_{n50} < 34\text{ cm}$. In this study the D_{n50} of Soil 1 and Soil 2 were selected as 22 cm, 10 cm respectively in prototype.

4.1.1.2 Block(s) dimensions and Scaling

Block dimensions of block type quay wall were determined by considering to;

- real block(s) dimensions which are generally used in practice in Turkey
- dimensions of the shaking table device.
- portability of the block(s) during the preparation of the experiment set- up,

Thus, the general block dimensions were determined as 3m-2m-2.5m. And scale was determined as 1/10, respectively (Table 4.4). During the experiments all the blocks had same dimensions.

Table 4.4: Prototype and model properties

PROTOTYPE	MODEL
SCALE 1/10	
<p>2 m</p> <p>3 m</p> <p>2.5 m</p> <p>Weight : 375 kN</p>	<p>Unit : meter</p> <p>0.2 m</p> <p>0.3 m</p> <p>0.25 m</p> <p>Weight : 0.375 kN</p>

“In general the similitude is necessary to interpret the results of the model tests. However, the similitude for the saturated soil-structure-fluid system is not clearly understood for the shaking table tests in the 1g gravitational field. There is a study on the similitude of soil structures under dynamic loadings by using the ratios of the forces (Kagawa, 1978). There is another study on the similitude of nonlinear dynamic responses of grounds by using Buckingham’s π -theorem (Kokusho and Iwatate, 1979). Both of the studies resulted in the same similitude. However, the results of their studies are applicable only to the shear deformation of soil structures. There is a need to extend their similitude to a more general form in order to interpret the dynamic model tests of the saturated soil-structure-fluid system.

In deriving the basic equations, the following idealization or approximations have been adopted; (1) soil skeleton is regarded as continuum, (2) deformation is regarded small so that the equilibrium equation after deformation is the same as that before the deformation, and (3) strain of the soil skeleton is regarded small so that the linear approximation of displacement-strain relation ($d\epsilon = L du$) holds true.

Consequently, there are following limitations in the applicability of the similitude; (1) the similitude is not applicable to the phenomenon at which soil particles completely lose contacts among themselves such as ultimate state of liquefaction, and (2) the similitude is not applicable to the phenomenon at which the deformation or the strain is too large to satisfy the above mentioned approximations” (Iai, 1989).

The corresponding scaling of parameters between the prototype and model used in this experiment are shown in Table 4.5. Similitude for model tests in 1g gravitational field in the special case in which $\lambda_p = 1$ and $\lambda_\epsilon = \lambda^{0.5}$. Since the scale is 1/10, λ is taken as 10 (APPENDIX B).

Table 4.5: Scaling factors in present model

Items	Scaling factors in general	Scaling factors for the present model (prototype / model)
Length	λ	10
Time	$\lambda^{0.5}$	3.16
Acceleration	1	1
Displacement	$\lambda^{1.5}$	31.62
Force	λ^3	1000
Density	1	1

4.1.1.3 Dynamic Loading Frequencies

“Measurements of earthquake motions on rock sites indicate that dominant frequencies are normally in the range of 0.1 Hz to 10.0 Hz” (Ashford and Sitar, 2002; Bhasin and Kaynia, 2004). The frequency range of interest in civil engineering for a typical real (prototype) earthquake is approximately 0-15 Hz. In this study the frequencies were taken as 2 Hz to 7 Hz with sine wave form under horizontal bed surface (slope angles $\theta=0^\circ$).

4.1.2 Instruments Used in Measuring the Unknown Parameters

To obtain the **unknown parameters**; accelerations, displacements of the block(s), soil and pore pressures of the backfill, the performance of models were tested by measuring and monitoring by electronic instruments in 1g shaking table tests:

- (1) 1g shaking table
- (2) Raining system
- (3) Soil pressure cells
- (4) Position transducers
- (5) Accelerometer
- (6) Pore pressure cells
- (7) Software and hardware computer system

4.1.2.1 1g Shaking Table

A series of 1g shaking table tests were carried out to investigate the dynamic response of block type quay walls. For this purpose, the one dimensional 1g shaking table facility located at Hydraulics and Coastal and Harbor Lab., Civil Engineering Faculty at Yıldız Technical University was used, (Figure 4.1 and Figure 4.2).



Figure 4.1: General view of 1g shaking table

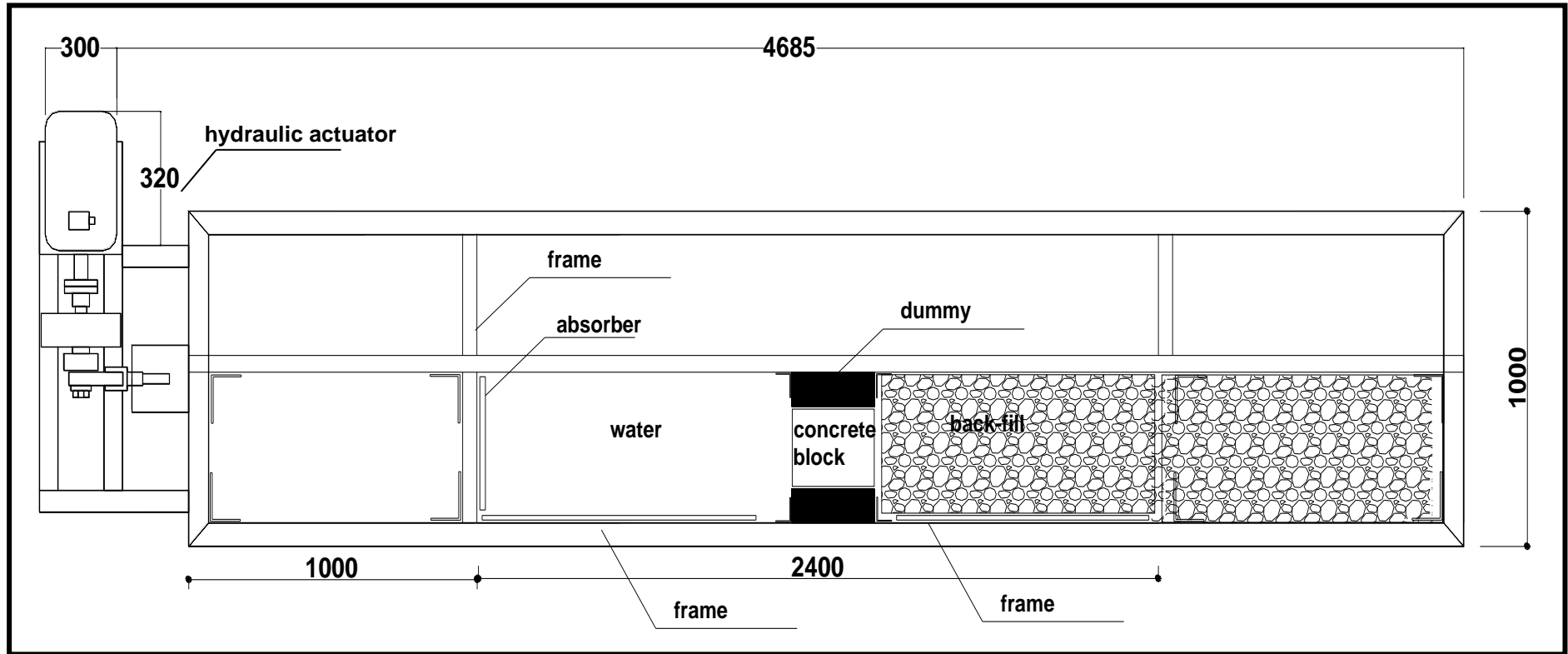


Figure 4.2: General view of one block experiment set-up (top view)

The one degree of freedom 1g shaking table had deck dimensions of 400cm-100cm-100cm with a 4 ton load capacity. It was driven by a 100-kN capacity hydraulic actuator with operator controlling and PC software.

Shaking table was one dimensional in its motion. Thus only longitudinal components of accelerations were obtained omitting the transverse and vertical components.

As shown in Figure 4.2;

- Frames were constructed within the 1g shaking table facility to divide the system into two parts to facilitate to use only the half of the 1g shaking table.
- The blocks were placed on the shaking table between dummies. Dummies were used to give the side effects from the adjacent blocks as in the prototype conditions.
- Backfill material (Soil 1 and Soil 2) was placed behind the blocks and dummies.
- The system was filled with water before starting the experiments and the absorbers were used to prevent the end effects due to reflections caused by dynamic loading.

4.1.2.2 Raining System

The method of raining was used to prepare the backfill behind the model wall. Porosity, initial velocity of soil particles, deposition height and falling height are the major factors affecting the relative density of the soil particles prepared by raining method. Falling height was chosen as 65 cm and was kept constant by lifting the sieve at each stage during backfilling (Figure 4.3).

Relative density of the Soil 1 and Soil 2 were computed between 60 % and 70 % respectively, (APPENDIX C) and according to 6 different frequencies, displacements, soil pressures, pore pressures, accelerations and the friction coefficients were measured or calculated (Figure 4.4 and Figure 4.5)

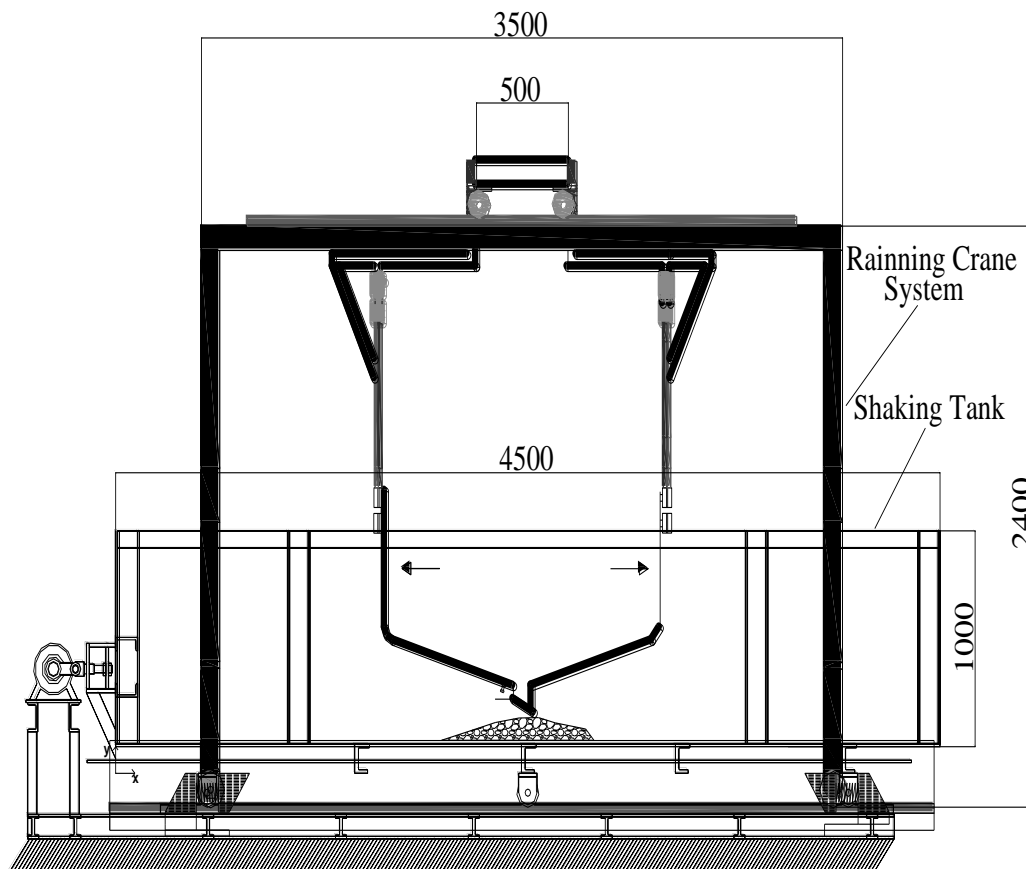


Figure 4.3: Raining system

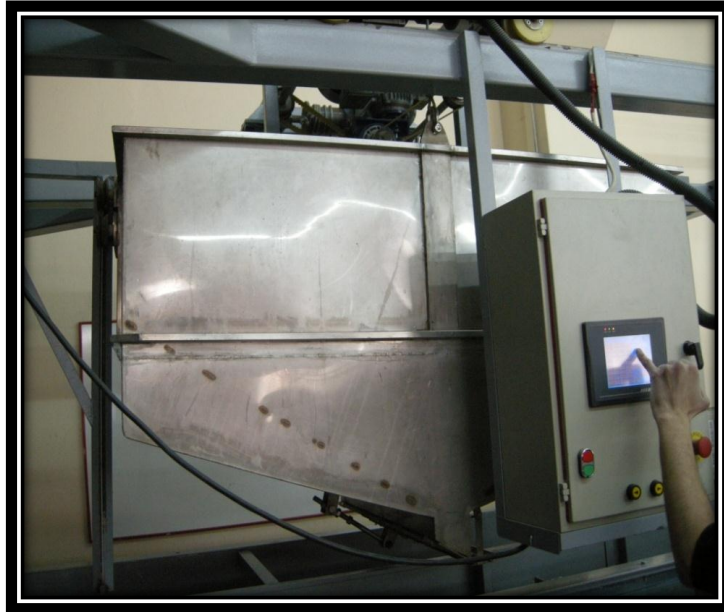


Figure 4.4: Raining system



Figure 4.5: Raining system and shaking table

4.1.2.3 Soil Pressure Cells

To obtain the soil pressure distribution acting on block type quay walls, soil pressure cells were located between the backfill and block(s). There are several kinds of soil pressure cells, KDE-PA-200 kpa were selected for this study. The technical specifications of selected soil pressure cells are given in APPENDIX D.

4.1.2.4 Position Transducers

To obtain the displacement of the block(s) during and/or after shaking, position transducers were used. There were also several kinds of position transducers, in this study HX-PA-20-SS-L5M type position transducers was used. The technical specifications of selected position transducers are given in APPENDIX D.

4.1.2.5 Accelerometer

In this study, in addition to soil pressure and position measurements, accelerations were also evaluated. The technical specifications of selected accelerometer (IMC 626B13) are given in APPENDIX D.

4.1.2.6 Pore Pressure Cells

Zeng and Madabhushi, 1998 stated that “If the structures are founded on saturated sandy soils, the earthquake loading may result in generation of excess pore pressure and, in the most severe situation, liquefaction of soils. The excess pore pressure causes degradation of soil stiffness and strength, which has severe impact on dynamic stability of earth structures. Under such circumstances, conventional design methods are not capable of producing satisfactory results. Due to the complex nature of soil behavior and soil-structure interaction under cyclic loading, comprehensive numerical procedures need to be used”. As it is known that liquefaction is very important subject, in this study, it was assumed that soil improvement techniques had to be used to improve the existing soil conditions to obtain the satisfactory conditions for backfill and foundation. The series of pore pressure measurements were carried out to verify the assumption that pore pressure in the aggregate material used in the experiments were very small. The technical specifications of selected pore pressure cells are given in APPENDIX D.

4.1.2.7 Software and Hardware System

In this study a software and hardware system were also used. The technical specification is given in APPENDIX D.

4.2 Dynamic Loading Experiments

The experiments are summarized under the title of i) Model condition, ii) Duration of each experiment, iii) Forces acting on block(s), iv) Dynamic saturated soil forces, v) Displacements and tilting of each block, vi) Experimental procedure.

- Model condition

In the preparation of the model, it was intended to simulate a plane strain condition. The main concern in simulating a plane strain condition was to avoid the side effects of the test container as stated by Hazarika et al., (2008), “in order to achieve the plane strain conditions, the side wall of the container must be rigid”.

- Duration for each experiment

During the experiments, the dynamic loading duration was selected as 30 s, long enough to observe the dynamic response of block(s), and it was kept constant in all tests. Based on the similitude relations, it was corresponding to a seismic event with time duration of approximately 90 s in the real scale (scale: 1/10) (Table 4.5).

- Forces acting on block(s)

As it is known, before dynamic loading there are only static soil pressure and hydrostatic pressure causing static soil and hydrostatic forces respectively. During dynamic loading additional forces; the inertia force of the block(s), the dynamic soil force, and the hydrodynamic force develop (Figure 4.6).

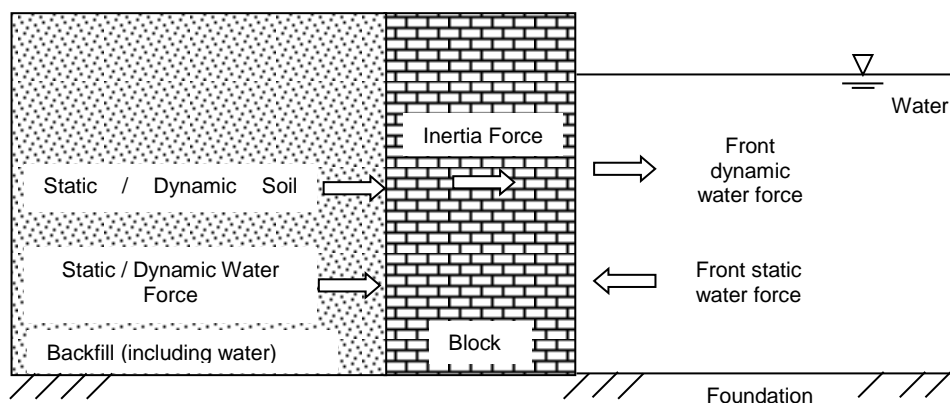


Figure 4.6: Force components acting on block during dynamic loading (Kim et al., 2005)

- **Dynamic saturated soil forces**

In principal, the total saturated soil pressure under dynamic loading can be separated into a fluctuating component and a non-fluctuating component, as shown in Figure 4.7.

Fluctuating component of the total saturated soil pressure is important for sand if it is used as backfill soil due to changes in the excess pore pressure during dynamic loading. If the excess pore pressure increases in backfill, the soil behaves like a fluid (liquefaction condition) and the water force increases while the soil forces are decreasing. Since, in this study the granular material was used as backfill soil, it was expected that the non-fluctuating component of the dynamic saturated soil pressure to remain almost constant with no excess pore pressure development during the experiments.

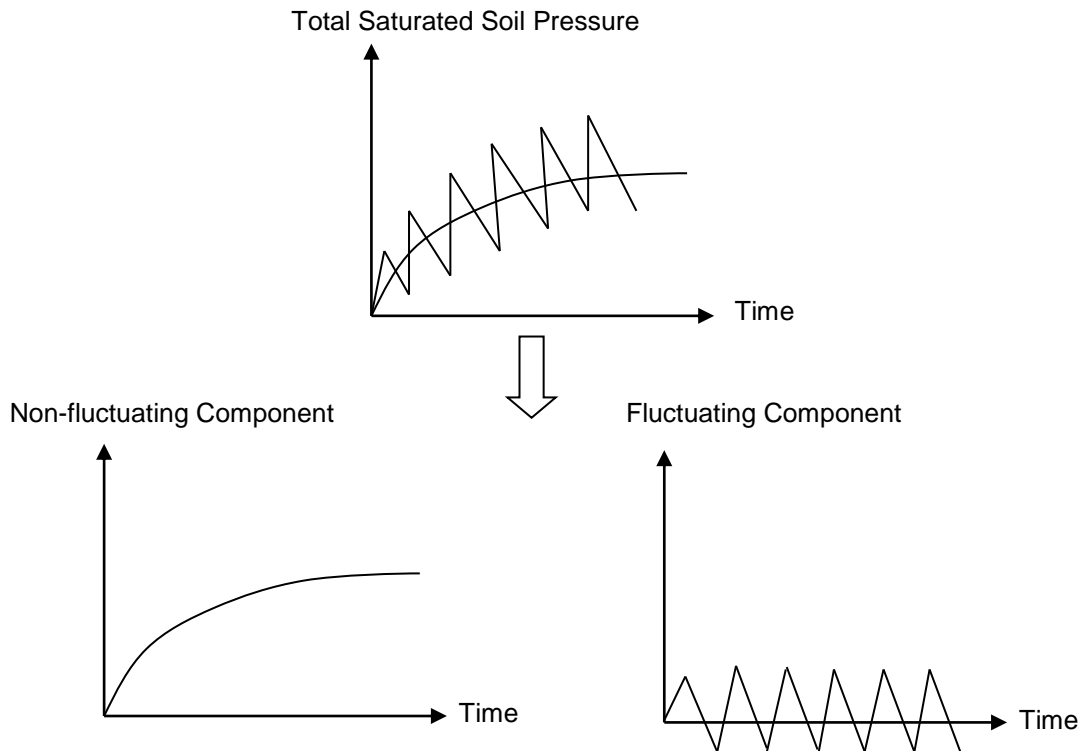


Figure 4.7: Fluctuating and non-fluctuating component of total saturated soil pressure
(Kim et al., 2004)

In this study, the measurements of the total saturated soil pressure under dynamic loading were viewed in accordance with the fluctuating and non-fluctuating components using MATHCAD computer program given in APPENDIX E.

- **Acceleration of blocks**

Experiments for acceleration of block(s) under dynamic loading with different frequencies resulted in sinusoidal shape. In the evaluation of experimental results, to determine the base acceleration, peak ground acceleration (PGA) which is defined as maximum absolute acceleration $|a_{max}|$ reached by ground horizontal acceleration during the earthquake is used. Peak ground acceleration (PGA) is also called peak acceleration or maximum acceleration (PIANC, 2001). Similar to base acceleration definition, to define the acceleration value of the block(s), maximum absolute acceleration $|a_{max}|$ measured during the experiment is used.

- **Displacements and tilting of blocks**

Displacement and tilting measurements in the experiments of the single and multiple blocks were defined as described below. In case of single block quay walls, initial position of the block (ABCD) before dynamic loading and the displaced position of the block (A', B', C', D') as observed after dynamic loading are shown in Figure 4.8. Typical wall movements combine rotation (tilting angle) and displacements (Δy). Tilting of the one block will be computed by assuming that almost no settlement will occur at the firm foundation of the

structure (Figure 4.8). As it is seen from Figure 4.8, A and B points will be displaced around AB axes, taken as an reference, with positive Δy distance (point A') and negative Δy distance (point B') in vertical direction respectively (PIANC, 2001). Since, the total vertical distance is $2\Delta y$, tilting angle α , can be calculated as:

$$\sin \alpha = \sin^{-1}(2\Delta y/a) \quad (4.1)$$

where; α : tilting degree, Δy : vertical distance, a: block width in model

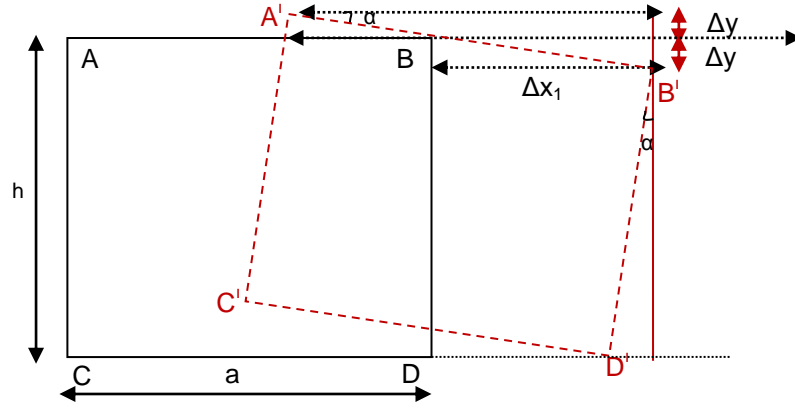


Figure 4.8: Displacement and tilting for one block

Tilting of the quay wall composed of **two and three blocks** again are computed on the assumption that almost no settlement will occur at the firm foundation of the structure (Figure 4.9 and Figure 4.10). If the seismic horizontal movement of the wall is characterized by the horizontal displacement at the wall base, Δx_2 , and at the wall top, Δx_1 , then the tilting of the upper block, α , is expressed as (Tiznado et. al., 2011):

$$\alpha = \tan^{-1}((\Delta x_2 - \Delta x_1)/H) \quad (4.2)$$

where H is the block height

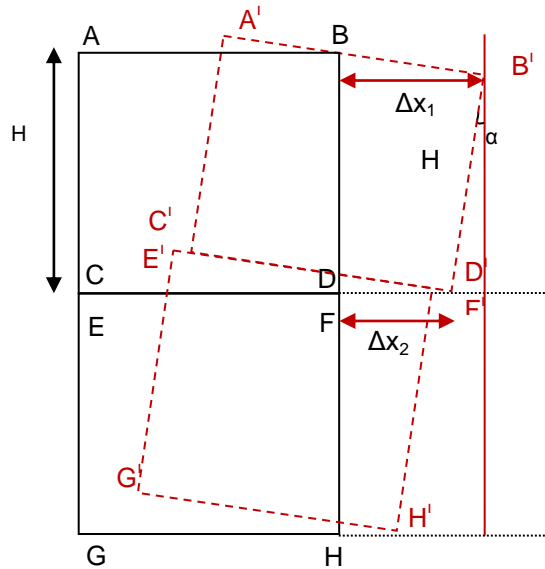


Figure 4.9: Displacement and tilting for two blocks

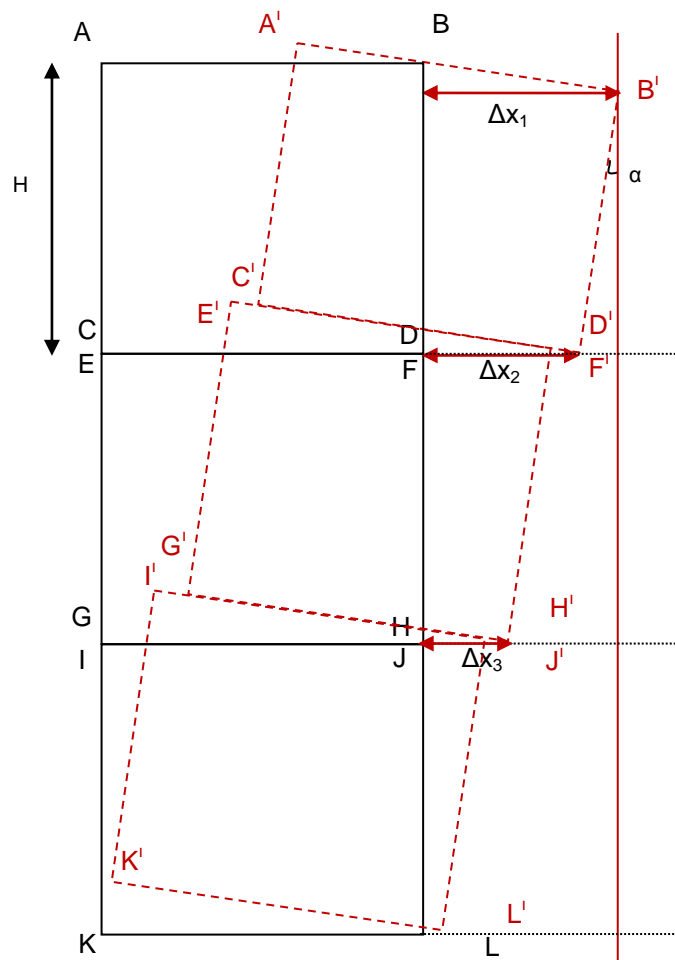


Figure 4.10: Displacement and tilting for three blocks

Results of measurements for displacement and tilting were evaluated and discussed in view of “acceptable level of damage in performance-based design” (PIANC, 2001). In the design of quay walls, the normalized residual horizontal displacement defined as $(d/H)^*$ and tilting degree values are controlled by using the “acceptable level of damage in performance-based design” and “proposed damage criteria” in (Table 4.6 and Table 4.7) given in PIANC (2001).

Table 4.6: Acceptable level of damage in performance-based design* (PIANC, 2001)

LEVEL OF DAMAGE	STRUCTURAL	OPERATIONAL
Degree I Serviceable	Minor or no damage	Little or no loss of serviceability
Degree II Repairable	Controlled damage**	Short-term loss of serviceability***
Degree III Near Collapse	Extensive damage in near collapse	Long term or complete loss of serviceability
Degree IV Collapse****	Complete loss of structure	Complete loss of serviceability

* Considerations: Protection of human life and property, functions as an emergency base for transportation, and protection from spilling hazardous materials, if applicable, should be considered in defining the damage criteria in addition to those shown in this table

** With limited inelastic response and/or residual deformation.

*** Structure out of service for short to moderate time for repairs.

**** Without significant effects on surroundings.

Table 4.7: Proposed damage criteria for gravity quay walls (PIANC, 2001)

LEVEL OF DAMAGE	Degree I	Degree II	Degree III	Degree IV
Gravity Wall Normalized residual horizontal displacement (d/H)*	Less than 1.5%**	1.5-5 %	5-10 %	Larger than 10 %
Residual tilting towards the sea	Less than 3°	3-5°	5-8°	Larger than 8°

*d: residual horizontal displacement at the top of the wall; H: height of gravity wall

** Alternative criterion is proposed with respect to differential horizontal displacement less than 30 cm.

Similar to PIANC, (2001) the level of damage for gravity wall is also given in “Technical Seismic Specifications on Construction of Coastal and Harbor Structures, Railways And Airports (2008)”. The ‘sliding block analysis’ method or empirical approaches based on this method can be used to calculate the approximate rigid horizontal displacements of the gravity wall under the dynamic loading. Permitted levels of the performance for the displacement / strain limits for minimum and controlled damage level is given in Table 4.8.

Table 4.8: Limit of performance for gravity wall
(Technical Seismic Specifications on Construction of Coastal and Harbor Structures, Railways And Airports, 2008)

LEVEL OF DAMAGE	Minimum Damage	Controlled Damage
Gravity Wall Ratio of the permanent displacement to height of the gravity wall (%)	< 1.5%	1.5-5 %
Residual tilting towards the sea	< 3°	3-5°
Different settlement between behind and top of the gravity wall	30-70	-
Different settlement behind the wall (cm)	3-10	-

- Experiment procedure

The experiments on accelerations and displacements of the block(s), pore pressures, soil pressures of the backfill under dynamic loading were carried out in three series; one block, two blocks and three blocks. For each series Soil 1 and Soil 2 conditions were tested under sinusoidal base motions with constant amplitude perpendicular to the structure alignment with either 6 tests: (2Hz, 3 Hz, 4 Hz, 5 Hz, 6 Hz, 7Hz) or 3 tests: (4 Hz, 5 Hz, 6 Hz):

1. One block tests: Soil 1: (6 tests) ; Soil 2: (3 tests)
2. Two blocks tests: Soil 1, (6 tests) ; Soil 2, (3 tests)
3. Three blocks tests: Soil 1, (6 tests) ; Soil 2, (3 tests)

Model studies are given in Table 4.9.

Table 4.9: Model studies under dynamic loading

MODEL STUDIES ON ACCELERATIONS, PORE AND EARTH PRESSURES, DISPLACEMENTS UNDER DYNAMIC LOADING

1. One Block Tests

Soil 1

Test 1.1

Test 1.1.1. , 2 Hz,
Test 1.1.2. , 3 Hz,
Test 1.1.3. , 4 Hz,
Test 1.1.4. , 5 Hz,
Test 1.1.5. , 6 Hz,
Test 1.1.6. , 7 Hz

Soil 2

Test 1.2

Test 1.2.1. , 4 Hz,
Test 1.2.2. , 5 Hz,
Test 1.2.3. , 6 Hz

2. Two Blocks Tests

Soil 1

Test 2.1

Test 2.1.1. , 2 Hz,
Test 2.1.2. , 3 Hz,
Test 2.1.3. , 4 Hz,
Test 2.1.4. , 5 Hz,
Test 2.1.5. , 6 Hz,
Test 2.1.6. , 7 Hz

Soil 2

Test 2.2

Test 2.2.1. , 4 Hz,
Test 2.2.2. , 5 Hz,
Test 2.2.3. , 6 Hz

3. Three Blocks Tests

Soil 1

Test 3.1

Test 3.1.1. , 3 Hz,
Test 3.1.2. , 4 Hz,
Test 3.1.3. , 5 Hz,
Test 3.1.4. , 6 Hz,

Soil 2

Test 3.2

Test 3.2.1. , 3 Hz,
Test 3.2.2. , 4 Hz,
Test 3.2.3. , 5 Hz

4.3 One Block Test Set Up

One block (Figure 4.13) tests were performed by using 1g shaking table for Soil 1 (Table 4.2) and Soil 2 (Table 4.3).

4.3.1 One Block Test Set Up for Soil 1 and for Soil 2

Figure 4.11 and Figure 4.12 show the general view of the experiment set up (one block and 2 dummies) of the one block tests for Soil 1 (Test 1.1) and for Soil 2 (Test 1.2).

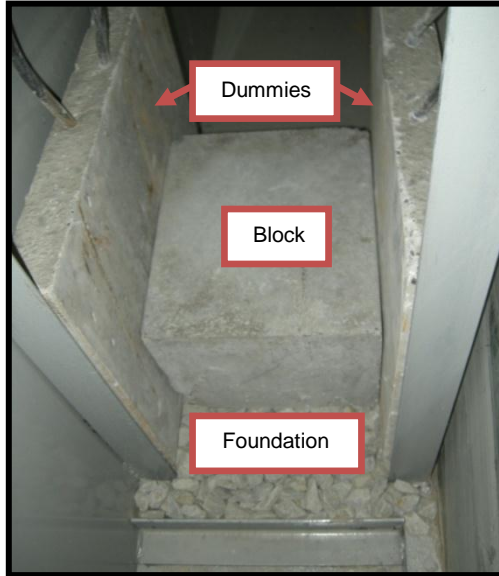


Figure 4.11: Block and dummies

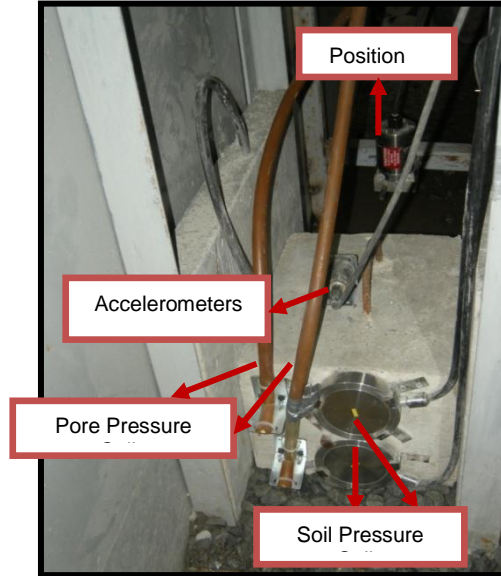


Figure 4.12: Block and instruments

Figure 4.13 shows general view of the one block tests for Soil 1 (Test 1.1) and for Soil 2 (Test 1.2) and the position of the measuring instruments; 2 soil pressure cells, 2 accelerometers, 2 pore pressure cells and 2 position transducers.

Tests 1.1 were carried out with 2 Hz (Test 1.1.1), 3 Hz (Test 1.1.2), 4 Hz (Test 1.1.3), 5 Hz (Test 1.1.4), 6 Hz (Test 1.1.5), 7 Hz (Test 1.1.6), and Tests 1.2 were carried out with 4 Hz (Test 1.2.1), 5 Hz (Test 1.2.2), 6 Hz (Test 1.2.3) (Table 4.9).

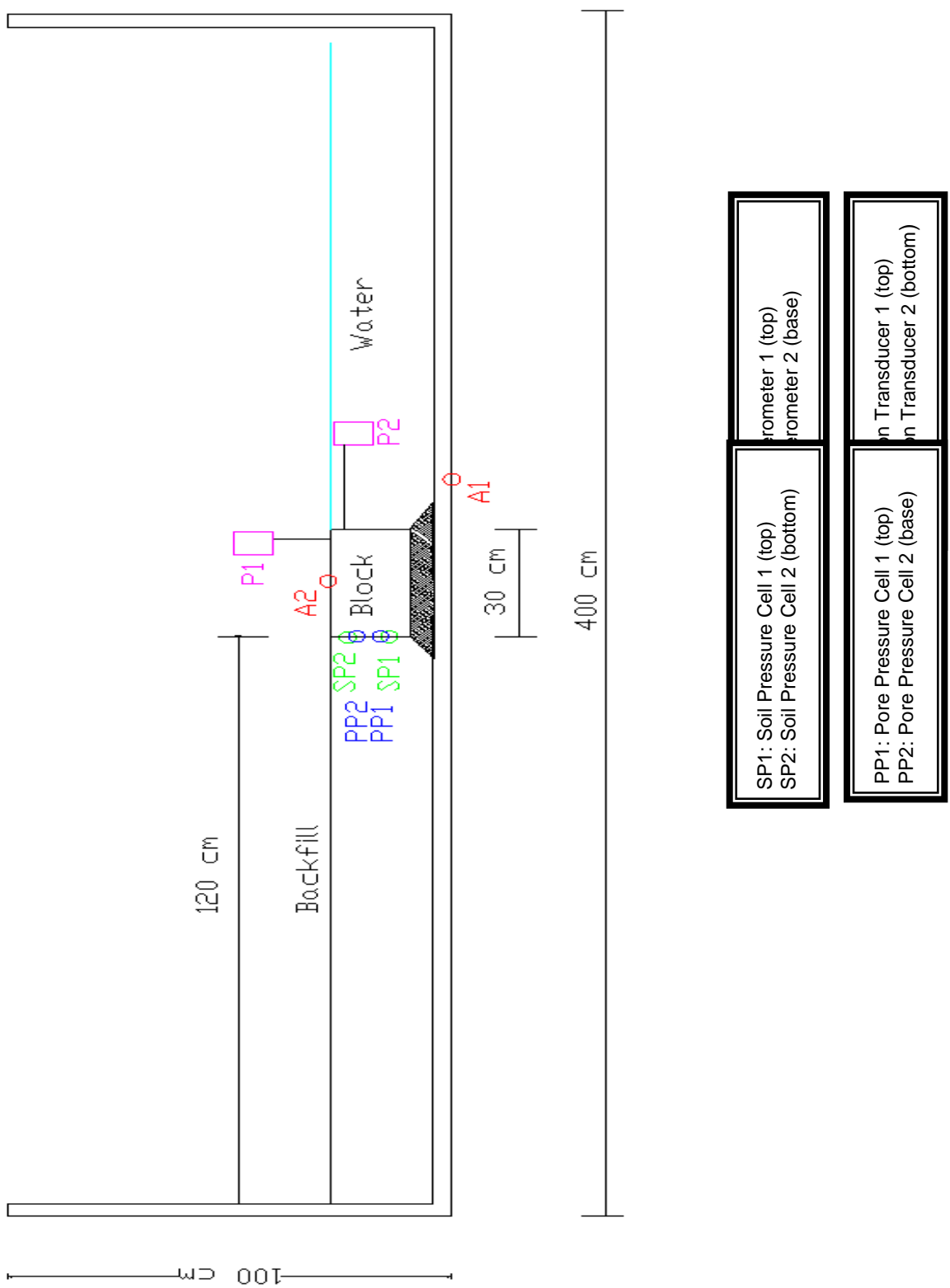


Figure 4.13: Measuring instruments and general view of one block tests

4.4 Two Blocks Test Set Up

Two blocks (Figure 4.15) tests were performed by using 1g shaking table for Soil 1 (Table 4.2) and Soil 2 (Table 4.3).

4.4.1 Two Blocks Test Set Up for Soil 1 and for Soil 2

Figure 4.14 shows the general view of the experimental set up (two blocks and 2 dummies) of the two blocks tests for Soil 1 and Soil 2.

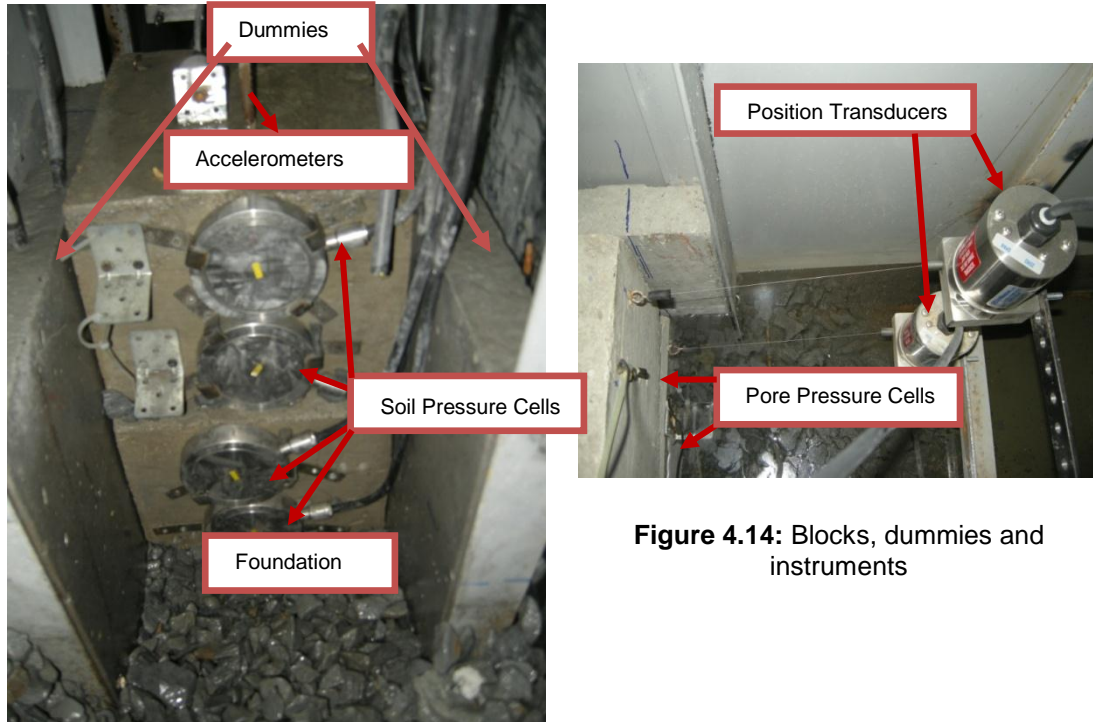
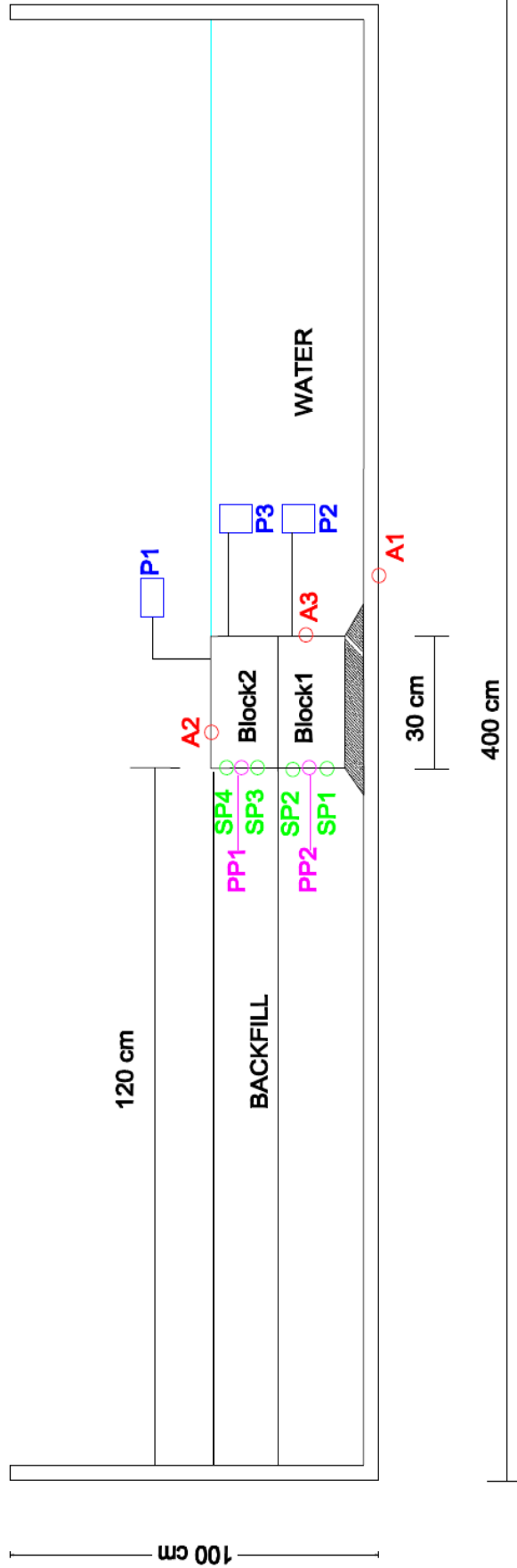


Figure 4.14: Blocks, dummies and instruments

Figure 4.15 shows general view of the two blocks tests for Soil 1 and for Soil 2 and the position of the measuring instruments; 4 soil pressure cells, 3 accelerometers, 2 pore pressure cells and 3 position transducers.

Tests 2.1 were carried out with 2 Hz (Test 2.1.1), 3 Hz (Test 2.1.2), 4 Hz (Test 2.1.3), 5 Hz (Test 2.1.4), 6 Hz (Test 2.1.5), 7 Hz (Test 2.1.6), and Tests 2.2 were carried out with 4 Hz (Test 2.2.1), 5 Hz (Test 2.2.2), 6 Hz (Test 2.2.3) (Table 4.9).



SP1: Soil Pressure Cell 1 (bottom) SP2: Soil Pressure Cell 2 (middle) SP3: Soil Pressure Cell 3 (middle) SP4: Soil Pressure Cell 4 (top)	A1: Accelerometer 1 (base) A2: Accelerometer 2 (top) A3: Accelerometer 3 (on block 1)
PP1: Pore Pressure Cell 1 PP2: Pore Pressure Cell 2 (base)	P1: Position Transducer 1 (top) P2: Position Transducer 2 (bottom) P3: Position Transducer 2 (block 2)

Figure 4.15: Measuring instruments and general view of two blocks tests

4.5 Three Blocks Test Set Up

Three blocks (Figure 4.17) tests were performed by using 1g shaking table for Soil 1 (Table 4.2) and Soil 2 (Table 4.3)

4.5.1 Three Blocks Test Set Up for Soil 1 and for Soil 2

Figure 4.16 shows the general view of the experimental set up (three blocks and 2 dummies) of the three blocks tests for Soil 1 and Soil 2.

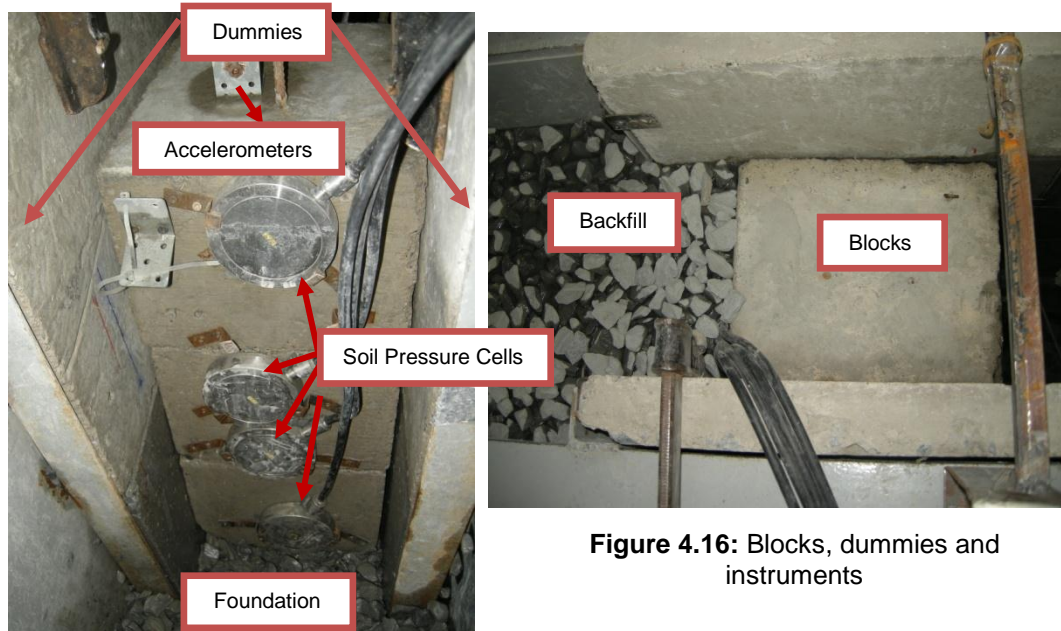


Figure 4.16: Blocks, dummies and instruments

Figure 4.17 shows general view of the three blocks tests for Soil 1 and for Soil 2 and the position of the measuring instruments; 4 soil pressure cells, 3 accelerometers, 2 pore pressure cells and 3 position transducers.

Tests 3.1 were carried out with 2 Hz (Test 3.1.1), 3 Hz (Test 3.1.2), 4 Hz (Test 3.1.3), 5 Hz (Test 3.1.4), 6 Hz (Test 3.1.5), 7 Hz (Test 3.1.6), and Tests 3.2 were carried out with 3 Hz (Test 3.2.1), 4 Hz (Test 3.2.2), 5 Hz (Test 3.2.3) (Table 4.9).

Experimental data on acceleration measurements, pore and soil pressure measurements, and displacement measurements for one block, two blocks and three blocks for Soil 1 and Soil 2, will be given in Chapters 5, 6 and 7 respectively.

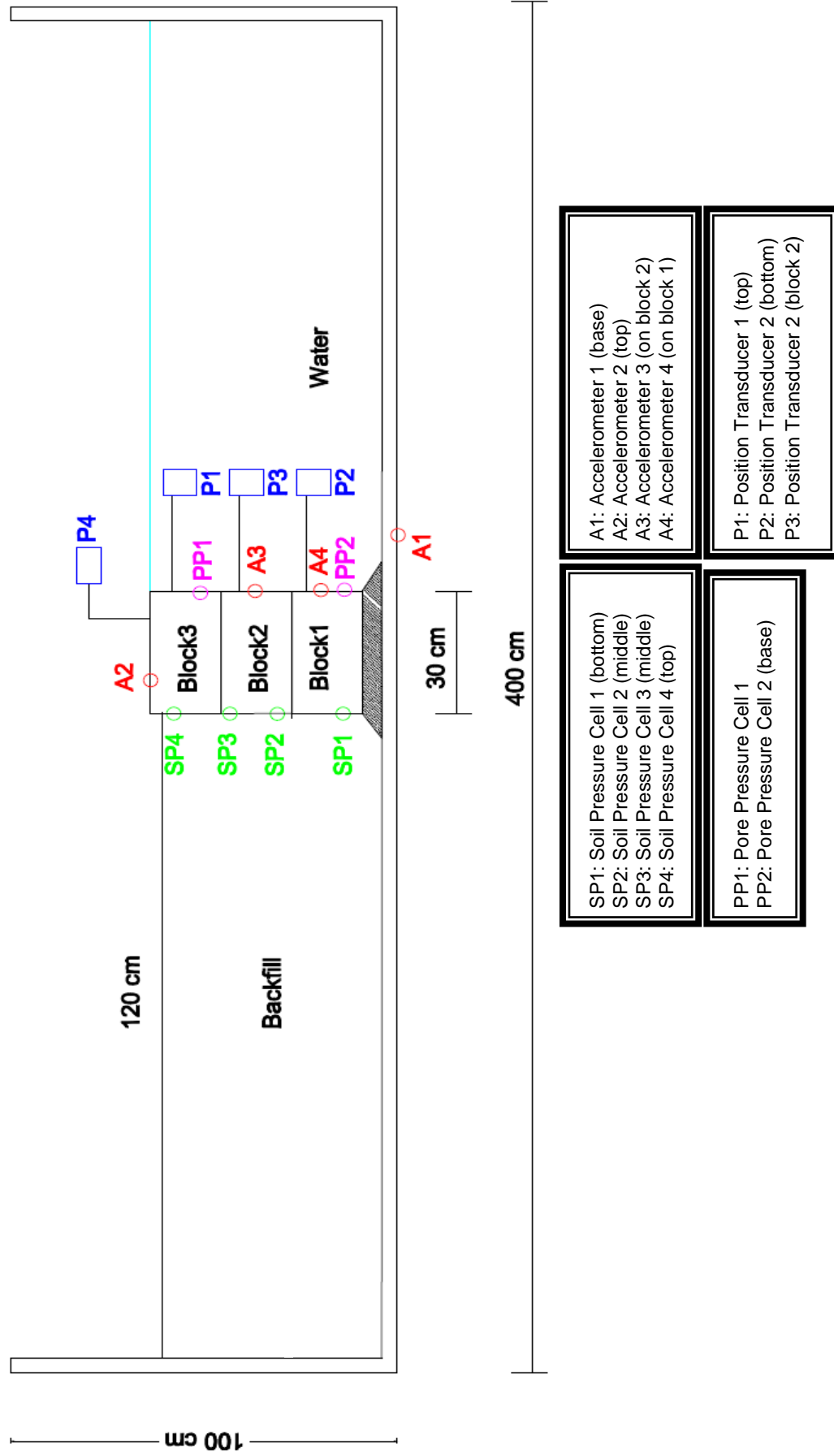


Figure 4.17: Measuring instruments and general view of three blocks tests

CHAPTER 5

PRESENTATION AND DISCUSSION OF THE RESULTS OF ACCELERATION MEASUREMENTS

The experiments for acceleration measurements were carried out in three series: one block, two blocks and three blocks under dynamic loadings. In deciding the number of tests to be carried out with the selected test frequencies, the limitations of the experimental set up and the time requirement were the basic parameters. Accordingly, some frequencies were not included in the test based on the significance of the test results or the experimental set up limitations.

In this chapter acceleration measurements and results are presented for each series for Soil 1 with 6 tests (2 Hz, 3 Hz, 4 Hz, 5 Hz, 6 Hz, 7 Hz) for one block and two blocks, 5 tests (3 Hz, 4 Hz, 5 Hz, 6 Hz, 7 Hz) for three blocks. Test with 2 Hz frequency for three blocks were omitted seeing that it had insignificant effect (e.g. no displacement) for one block and two block tests.

Similarly, same decisions made for Soil 2 experiments. Acceleration measurements and results are presented for each series for Soil 2 with 3 tests (4 Hz, 5 Hz, 6 Hz) for one block and two blocks, 3 tests (3 Hz, 4 Hz, 5 Hz) for three blocks. 3 Hz tests were omitted for one block and two blocks and 6 Hz tests were omitted for three blocks due to the limitations of the experimental set up and the difficulties faced during the measurements.

5.1 One Blok Acceleration Measurements (Test 1.1 and Test 1.2)

General view of two accelerometers for one block tests for Soil 1- Tests 1.1 (Acc 1 and Acc 2) and for Soil 2 - Test 1.2 (Acc 1 and Acc 3) are shown in Figure 5.1a and Figure 5.1b respectively.

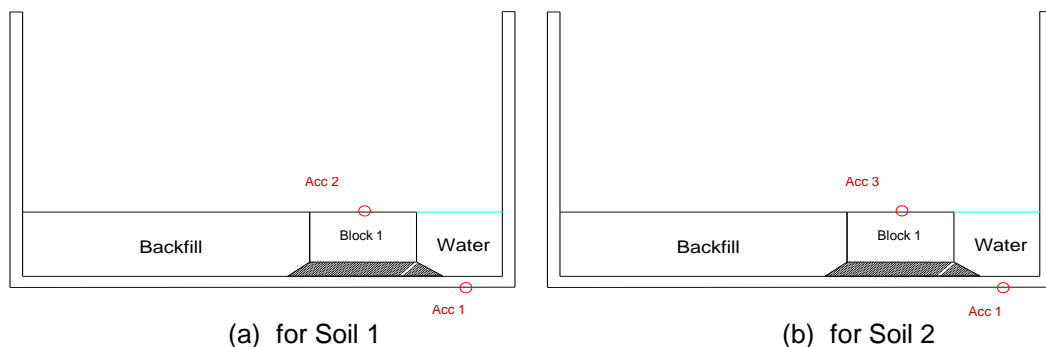


Figure 5.1: General view of two accelerometers Acc 1 (base) and Acc 2 or Acc 3 (block 1) for one block tests for Soil 1 and Soil 2

Results of acceleration measurements of Test 1.1 (Soil 1) and Test 1.2 (Soil 2) are presented between Figure 5.2 - Figure 5.9 and Figure 5.10 - Figure 5.14.

5.1.1 One Blok, Soil 1: Acceleration Measurements (Test 1.1)

In Figure 5.2 - Figure 5.7 acceleration measurements for each frequency are presented as acceleration (g) versus time (second) for the accelerometers placed at the base of the set-up (Acc 1) and at the block 1 (Acc 2) (Figure 5.1a).

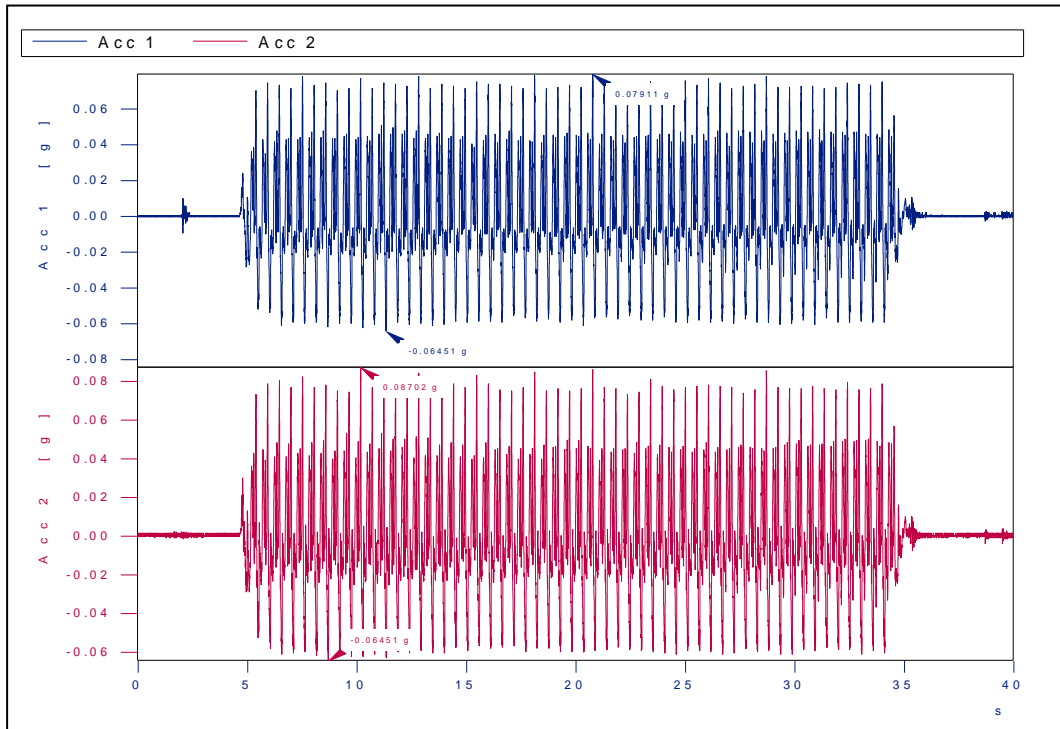


Figure 5.2: Acceleration measurements for Acc 1 and Acc 2 for 2 Hz for Soil1 (Test 1.1.1)

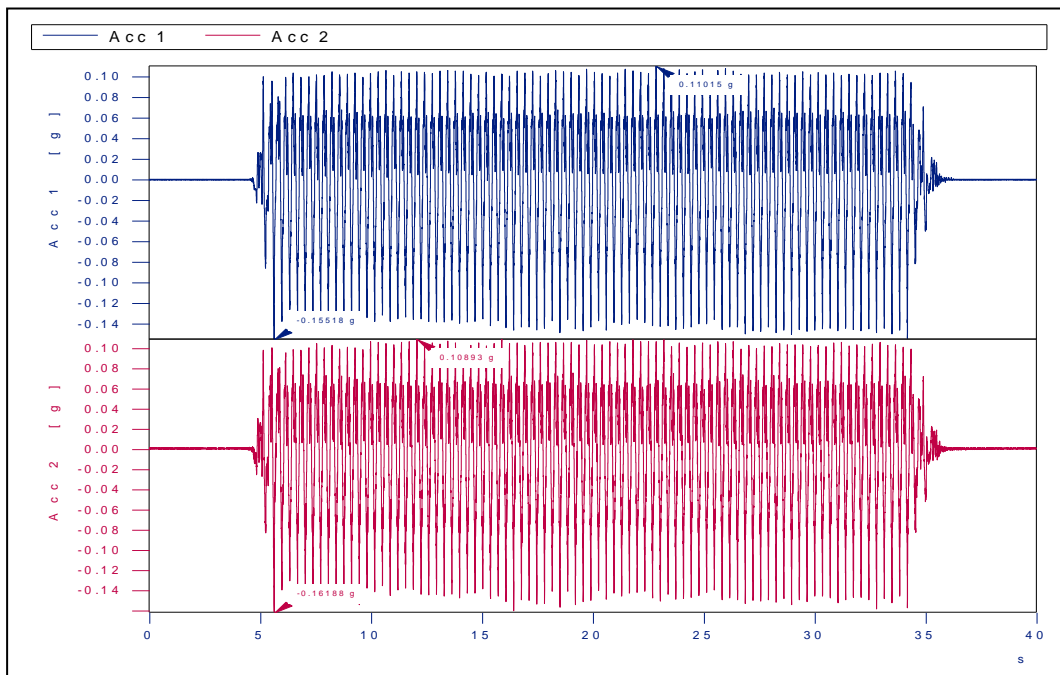


Figure 5.3: Acceleration measurements for Acc 1 and Acc 2 for 3 Hz for Soil1 (Test 1.1.2)

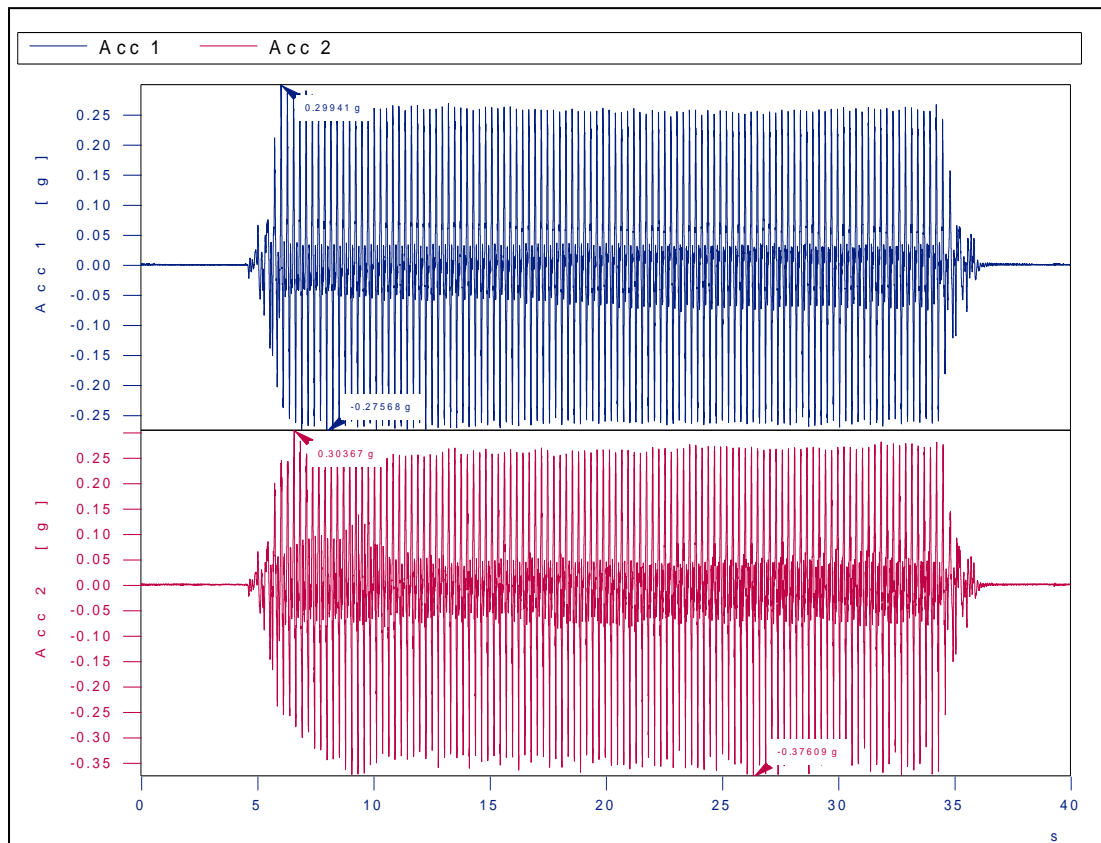


Figure 5.4: Acceleration measurements for Acc 1 and Acc 2 for 4 Hz for Soil1 (Test 1.1.3)

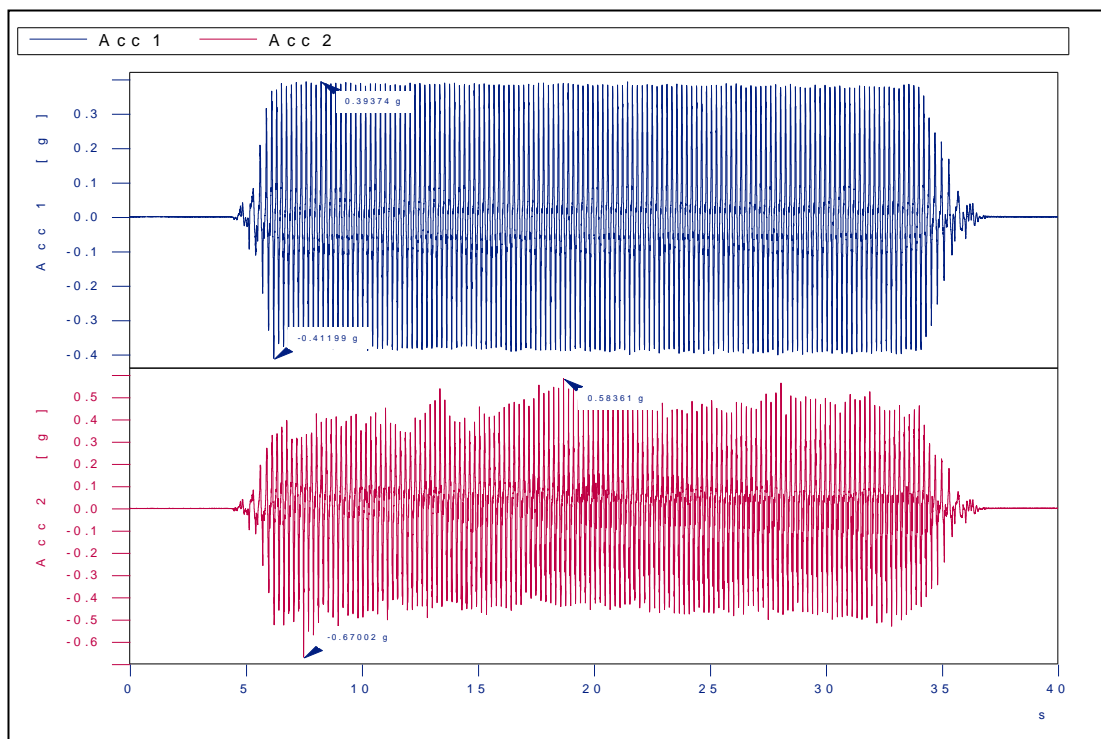


Figure 5.5: Acceleration measurements for Acc 1 and Acc 2 for 5 Hz for Soil1 (Test 1.1.4)

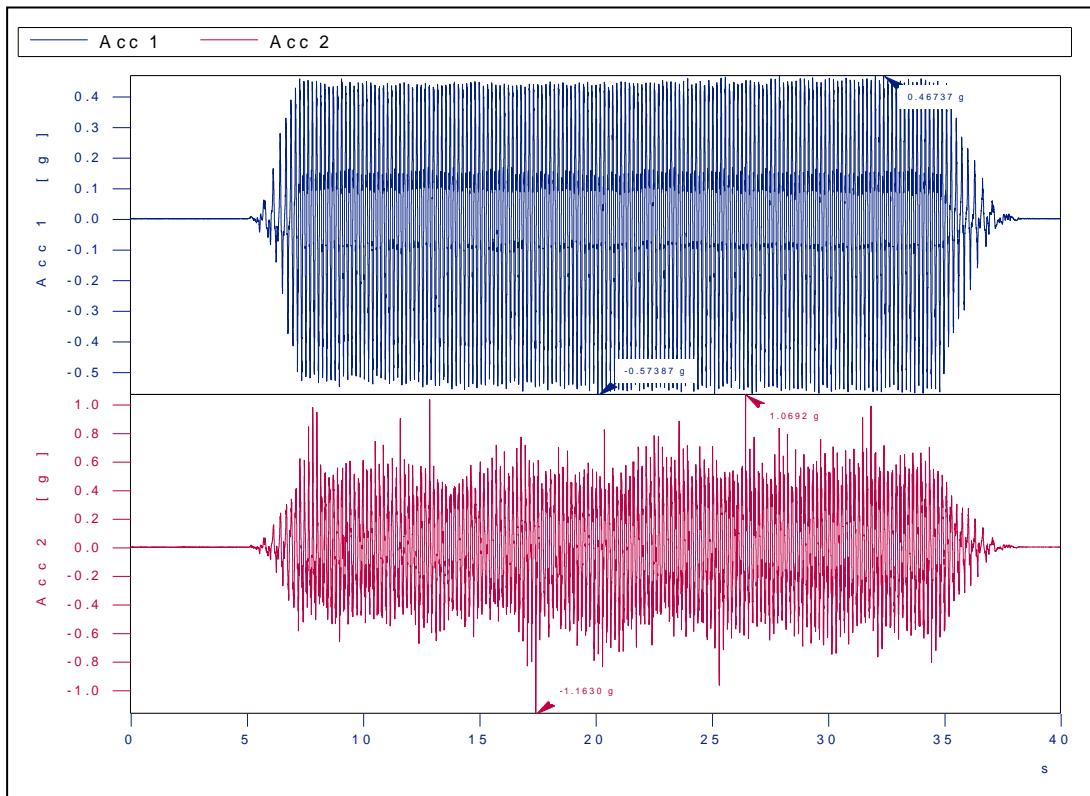


Figure 5.6: Acceleration measurements for Acc 1 and Acc 2 for 6 Hz for Soil1 (Test 1.1.5)

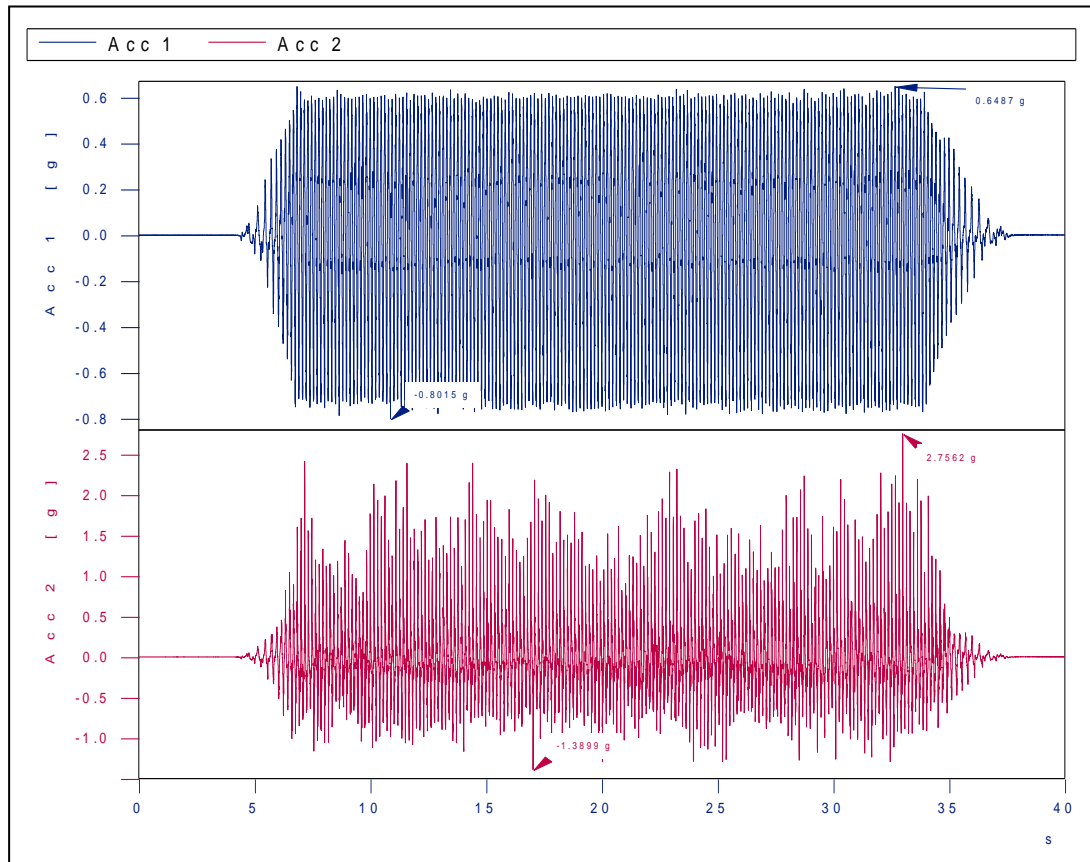


Figure 5.7: Acceleration measurements for Acc 1 and Acc 2 for 7 Hz for Soil1 (Test 1.1.6)

5.1.1.1 Results of Acceleration Measurements (Soil 1)

Maximum accelerations $|a_{\max}|$ recorded at 2 accelerometers (Acc 1 for Base, Acc 2 for Block 1) for Soil 1 for each frequency (2 Hz - 7 Hz) are presented in Table 5.1 and Figure 5.8. Ratios between Block 1 / Base are also presented in Figure 5.9.

Results of experiments for frequency 6 Hz, causing maximum acceleration 0.57 g corresponds to highest level of the events recorded as given in Table 2.2. In the experiments frequency 7 Hz, causing maximum acceleration 0.80g has also been tested, which corresponded to the highest event ever recorded once (Table 2.2). Therefore, in this study the results of 7 Hz causing full damage condition was not found reliable to investigate the soil pressure distribution accurately.

Table 5.1: Maximum accelerations at base (Acc 1) and on block 1 (Acc 2) for Soil 1 with respect to frequencies

Frequency (Hz)	BASE	BLOCK 1	RATIO (Block 1 / Base)
	Maximum Acceleration (g)	Maximum Acceleration (g)	
2	0.08	0.087	1
3	0.16	0.16	1
4	0.30	0.38	1.3
5	0.41	0.67	1.6
6	0.57	1.16	2.0
7	0.80	2.76	3.5

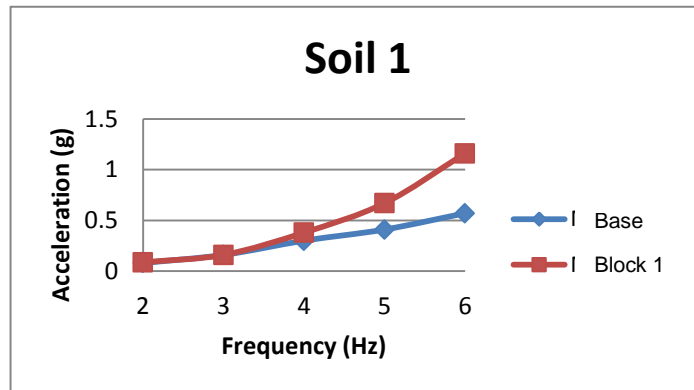


Figure 5.8: Maximum accelerations at base and on block 1 for 2 Hz - 6 Hz for Soil 1

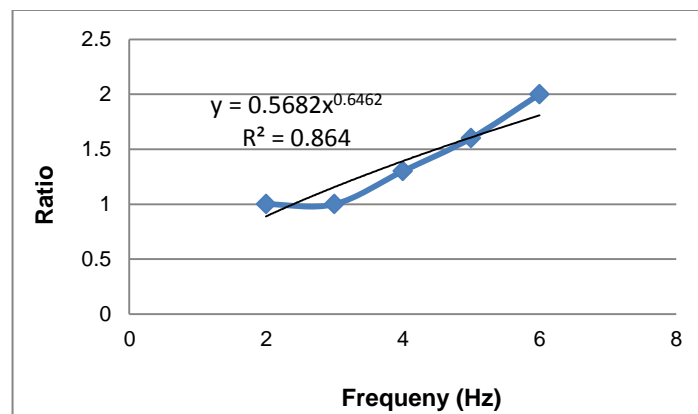


Figure 5.9: Ratio (Block 1/Base) versus frequency for Soil 1

Overall view of the acceleration measurements for one block for Soil 1 is presented in Table 5.2.

Table 5.2: Acceleration measurements for one block for Soil 1

FREQUENCY	RESULTS
Frequency increases	$ a_{\max} _{\text{base}}$ and $ a_{\max} _{\text{block}}$ increase
For a given frequency	<p>$a_{\max} _{\text{block}}$ values are always greater than the $a_{\max} _{\text{base}}$ values</p> <p>The ratio between block/base maximum acceleration increases while frequency is increasing ($R^2=0.864$)</p>
For small frequencies (for 2 Hz - 3 Hz)	<p>there is no significant change between $a_{\max} _{\text{base}}$ and $a_{\max} _{\text{block}}$</p> <p>there is no significant change of the ratio of $a_{\max} _{\text{block}} / a_{\max} _{\text{base}}$</p>
For larger frequencies (for 4 Hz - 6 Hz)	<p>difference between $a_{\max} _{\text{base}}$ and $a_{\max} _{\text{block}}$ values increases rapidly</p> <p>the ratio of $a_{\max} _{\text{block}} / a_{\max} _{\text{base}}$ ranges between (1.3 - 2.0) respectively.</p>

5.1.2 One Blok, Soil 2: Acceleration Measurements (Test 1.2)

In Figure 5.10 - Figure 5.12 acceleration measurements for 4 Hz, 5 Hz and 6 Hz are presented as acceleration (g) versus time (second) for the accelerometers placed at the base of the set-up (Acc 1) and at the block 1 (Acc 3) (Figure 5.1b).

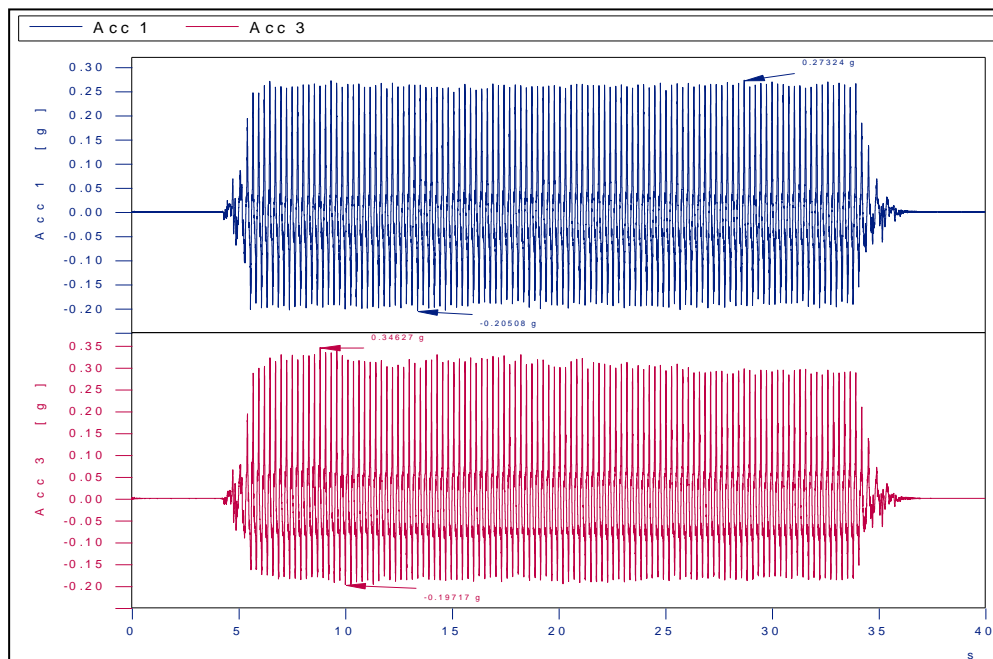


Figure 5.10: Acceleration measurements for Acc 1 and Acc 3 for 4 Hz for Soil 2 (Test 1.2.1)

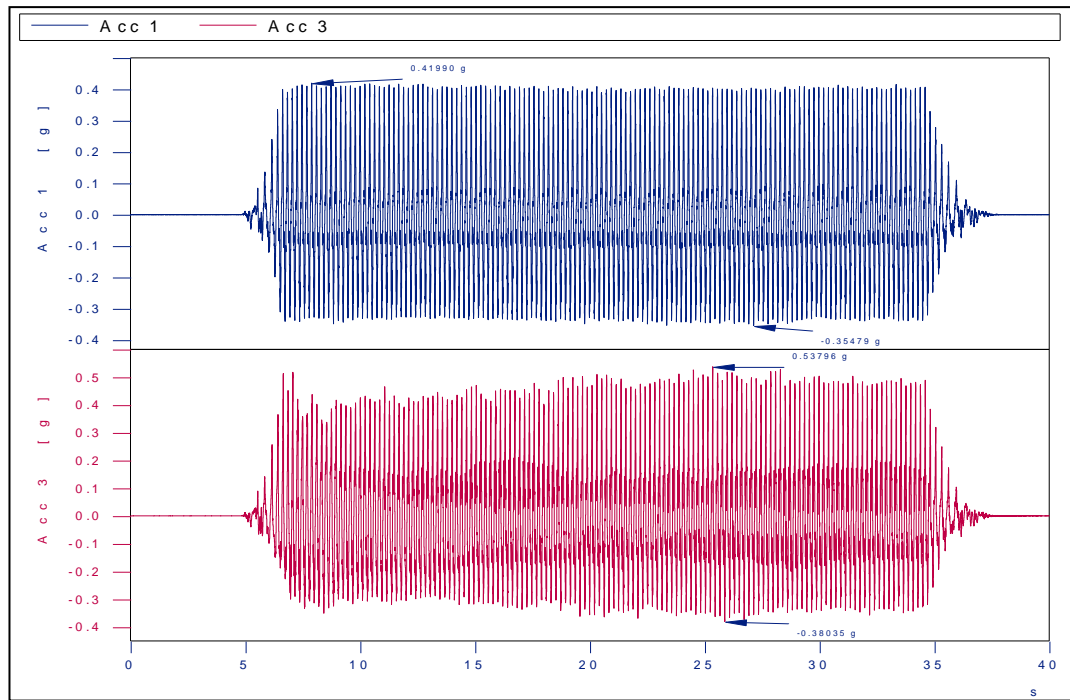


Figure 5.11: Acceleration measurements for Acc 1 and Acc 3 for 5 Hz for Soil 2 (Test 1.2.2)

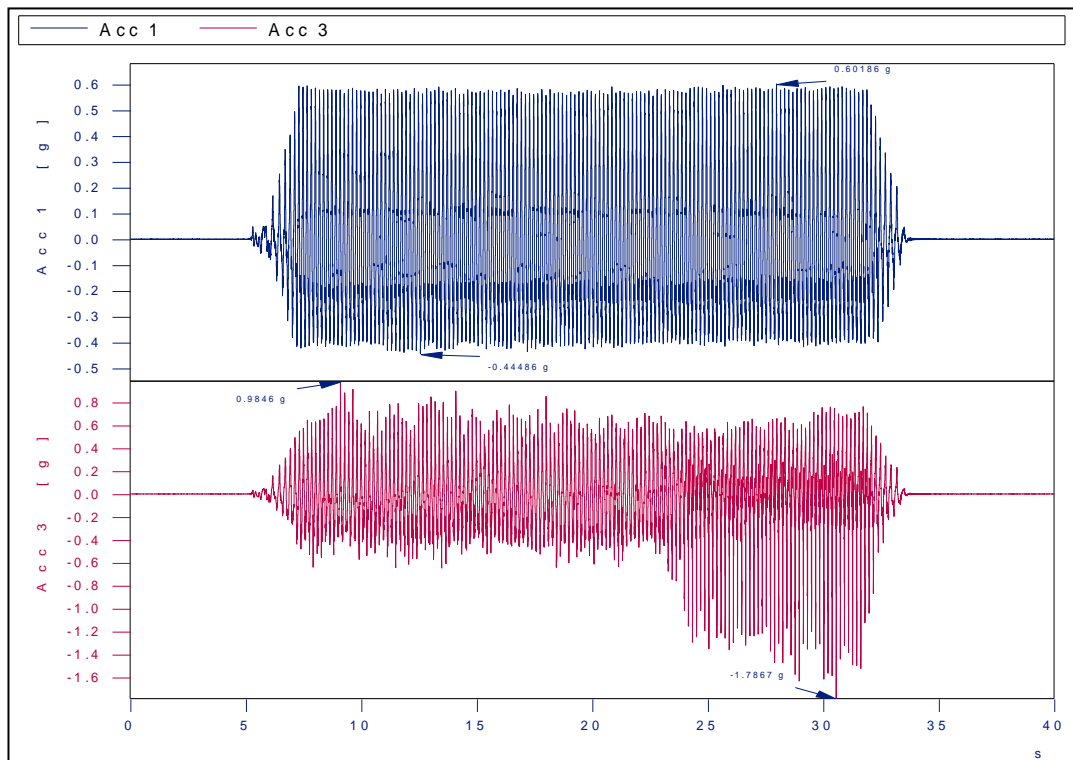


Figure 5.12: Acceleration measurements for Acc 1 and Acc 3 for 6 Hz for Soil 2 (Test 1.2.3)

5.1.2.1 Results of Acceleration Measurements (Soil 2)

Maximum accelerations $|a_{\max}|$ recorded at 2 accelerometers (Acc 1 for Base, and Acc 3 for Block 1) for Soil 2 for each frequency (4 Hz - 6 Hz) are presented in Table 5.3 and Figure 5.13. Ratios between Block 1 / Base are also presented in Figure 5.14.

Table 5.3: Maximum accelerations at base (Acc 1) and on block (Acc 3) for Soil 2 with respect to frequencies

Frequency (Hz)	BASE	BLOCK 1	RATIO (Block 1 / Base)
	Maximum Acceleration (g)	Maximum Acceleration (g)	
4	0.27	0.35	1.29
5	0.42	0.54	1.29
6	0.60	1.77	2.95

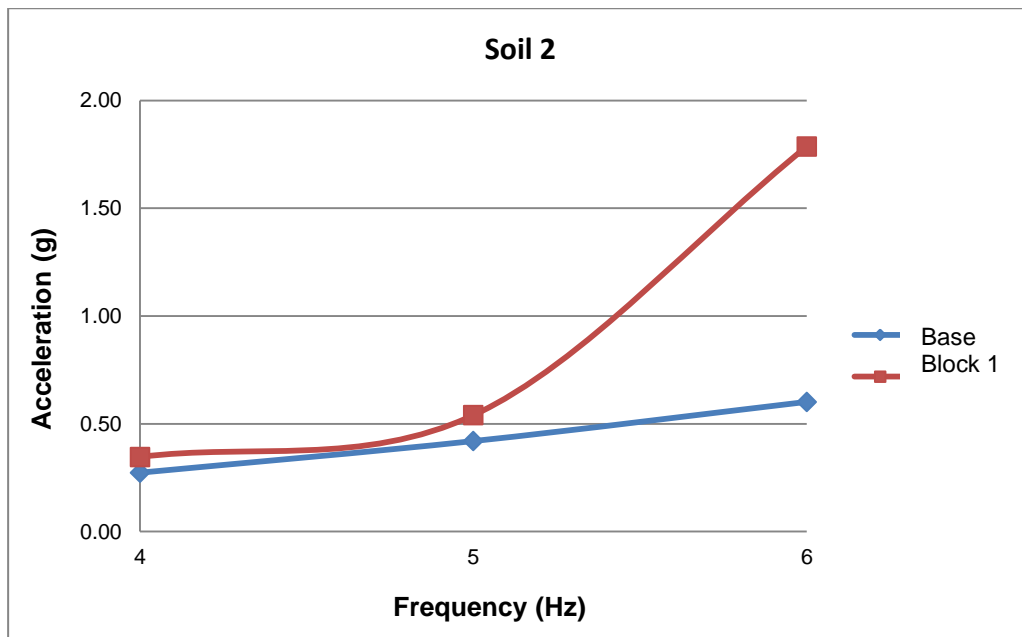


Figure 5.13: Maximum accelerations at base and on block 1 for 4Hz - 6 Hz for Soil 2

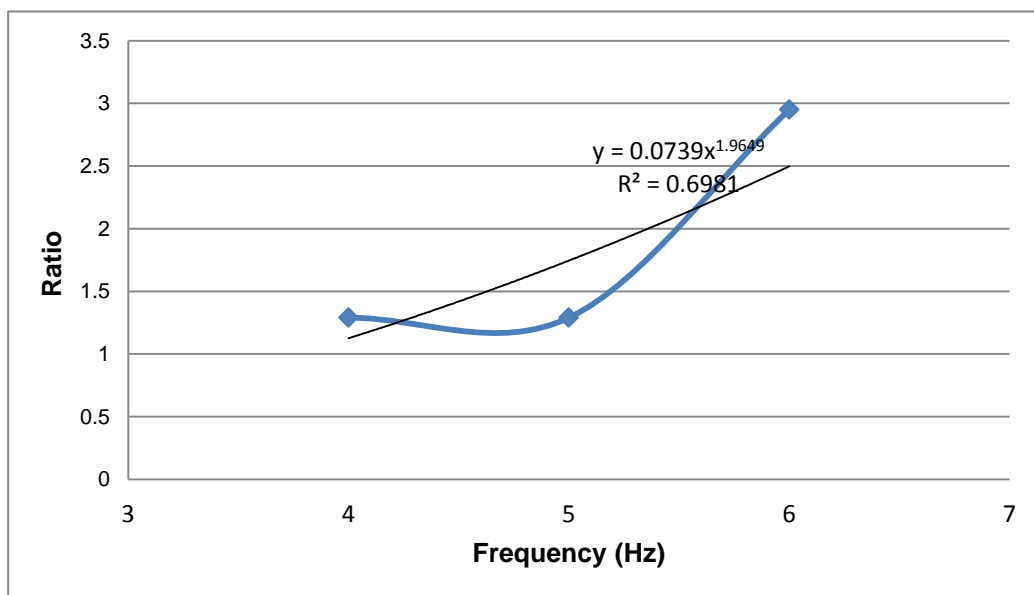


Figure 5.14: Ratio (Block 1 / Base) versus frequency for Soil 2

Overall view of the acceleration measurements for one block for Soil 2 is presented in Table 5.4.

Table 5.4: Acceleration measurements for one block for Soil 2

FREQUENCY	RESULTS
Frequency increases	$ a_{\max} _{\text{base}}$ and $ a_{\max} _{\text{block}}$ increase
For a given frequency	$ a_{\max} _{\text{block}}$ values are always greater than the $ a_{\max} _{\text{base}}$ values The ratio between block/base maximum acceleration increases while frequency is increasing ($R^2=0.70$)
For 4 Hz, 5 Hz, 6 Hz	difference between $ a_{\max} _{\text{base}}$ and $ a_{\max} _{\text{block}}$ values increases rapidly
For 4 Hz, 5 Hz, 6 Hz	difference between $ a_{\max} _{\text{base}}$ and $ a_{\max} _{\text{block}}$ values increases rapidly,
For 4 Hz, 5 Hz, 6 Hz	the ratio of $ a_{\max} _{\text{block}} / a_{\max} _{\text{base}}$ ranges between (1.3 - 2.95) respectively.
For 6 Hz	increased and irregular acceleration measurements after 15 sec.

5.2 Two Blocks Acceleration Measurements (Test 2.1 and Test 2.2)

General view of three accelerometers (Acc 1, Acc 2, Acc 3) used for two blocks tests for Soil1- Tests 2.1 and for Soil 2 - Test 2.2 are shown in Figure 5.15.

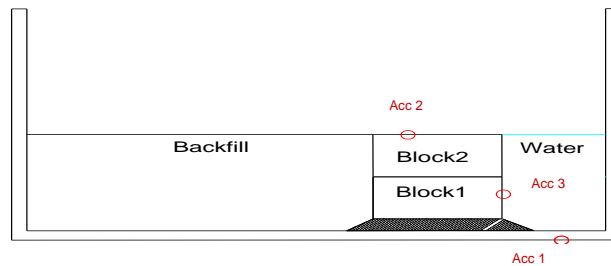


Figure 5.15: General view of three accelerometers (Acc 1, Acc 2, Acc 3) for two blocks tests

Test 2.1 was carried out with 2 Hz, 3 Hz, 4 Hz, 5 Hz, 6 Hz for Soil 1 and Test 2.2 was carried out and 4 Hz, 5 Hz, 6 Hz for Soil 2 and acceleration measurements are presented as an example for Soil 1 in Figure 5.16 and for Soil 2 in Figure 5.18. Results of acceleration measurements for two blocks for Soil 1 (Test 2.1) and for Soil 2 (Test 2.2) under dynamic loading are presented in APPENDIX F.

5.2.1 Two Blocks, Soil 1: Acceleration Measurements (Test 2.1)

As an example, in Figure 5.16 maximum acceleration measurements $|a_{\max}|$ for each frequency are presented as acceleration (g) versus time (second) for the accelerometers placed at the base of the set-up (Acc 1), at the block 2 (Acc 2) and on the block 1 (Acc 3) (Figure 5.15).

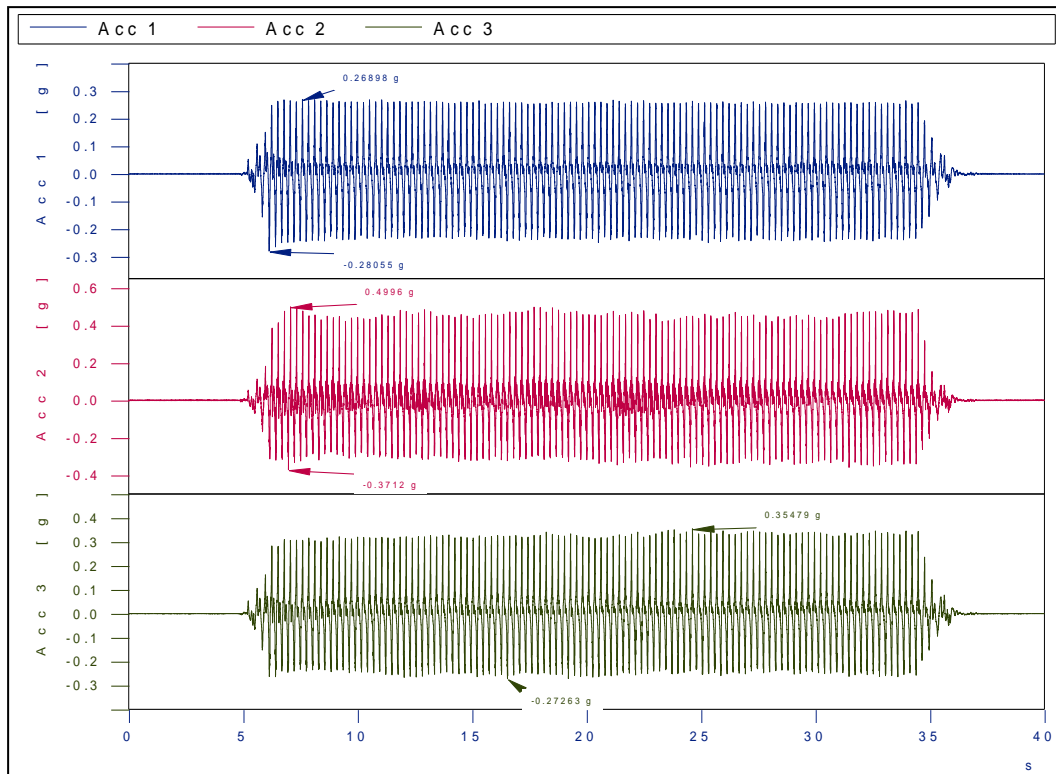


Figure 5.16: Acceleration values of Base (A 1), Block 1 (A 3) and Block 2 (A 2) for 4 Hz (Test 2.1.3)

5.2.1.1 Results of Acceleration Measurements (Soil 1)

Maximum accelerations $|a_{\max}|$ recorded at 3 accelerometers (Acc 1 base, Acc 2 block 2 and Acc 3 block 1) for Soil 1 for each frequency (2 Hz - 6 Hz) are presented in Table 5.5 and Figure 5.17. Ratios between Block 2 / Block 1, Block 1 / Base, Block 2 / Base are also presented in Table 5.6 and Figure 5.18.

Table 5.5: Maximum accelerations at Base (Acc 1), at Block 1 (Acc 3) and on Block 2 (Acc 2) for Soil 1 with respect to frequencies

Frequency (Hz)	Maximum Base Acceleration (g)	Maximum Block 1 Acceleration (g)	Maximum Block 2 Acceleration (g)
2	0.07	0.07	0.07
3	0.18	0.18	0.18
4	0.28	0.35	0.50
5	0.4	0.69	0.81
6	0.55	1.14	1.28

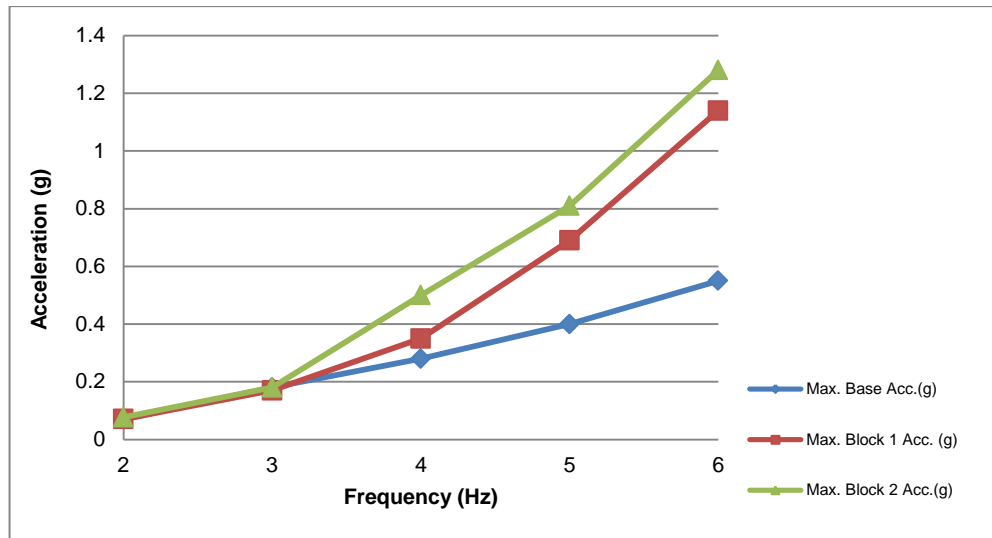


Figure 5.17: Maximum acceleration measurements of Base and Block for 2 Hz - 6 Hz for Soil 1

Table 5.6: Ratios between Block 2 / Block 1, Block 1 / Base, Block 2 / Base

Frequency (Hz)	RATIOS		
	Block 2 / Block 1	Block 1 / Base	Block 2 / Base
2	1	1	1
3	1	1	1
4	1.43	1.25	1.79
5	1.17	1.73	2
6	1.12	2	2.32

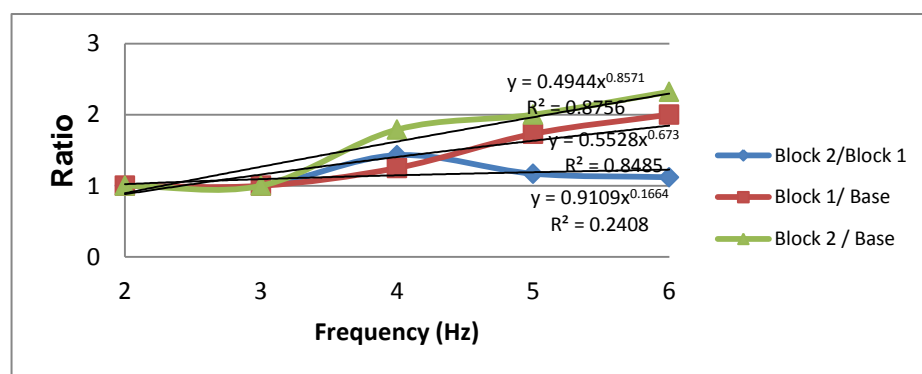


Figure 5.18: Ratios (Block 2 / Block 1, Block 1 / Base, Block 2 / Base) versus frequency for Soil 1

Overall view of the acceleration measurements for two blocks for Soil 1 is presented in Table 5.7.

Table 5.7: Acceleration measurements for two blocks for Soil 1

FREQUENCY	RESULTS
Frequency increases	$ a_{\max} _{\text{base}}$, $ a_{\max} _{\text{block1}}$, $ a_{\max} _{\text{block2}}$ increase
For a given frequency	$ a_{\max} _{\text{block}(n)}$ values are always greater than the $ a_{\max} _{\text{block}(n-1)}$ for $n=2$ $ a_{\max} _{\text{block1}}$ values are always greater than the $ a_{\max} _{\text{base}}$
For small frequencies (for 2 Hz - 3 Hz)	there is no significant change between $ a_{\max} _{\text{base}}$, $ a_{\max} _{\text{block1}}$, $ a_{\max} _{\text{block2}}$ there is no change of the ratio between $ a_{\max} _{\text{block2}} / a_{\max} _{\text{block1}}$, $ a_{\max} _{\text{block1}} / a_{\max} _{\text{base}}$, $ a_{\max} _{\text{block2}} / a_{\max} _{\text{base}}$
For larger frequencies (for 4 Hz - 6 Hz)	$ a_{\max} _{\text{block2}} / a_{\max} _{\text{block1}}$ ranges between (1.43-1.12) $ a_{\max} _{\text{block1}} / a_{\max} _{\text{base}}$ ranges between (1.25-2.00) $ a_{\max} _{\text{block2}} / a_{\max} _{\text{base}}$ ranges between (1.79-2.32) $ a_{\max} _{\text{base}}$, $ a_{\max} _{\text{block1}}$ and $ a_{\max} _{\text{block2}}$ values increases rapidly Increment of $ a_{\max} _{\text{block1}} / a_{\max} _{\text{base}}$ and $ a_{\max} _{\text{block2}} / a_{\max} _{\text{base}}$ is almost linear Increment of $ a_{\max} _{\text{block2}} / a_{\max} _{\text{block1}}$ is not linear, and decrement was observed after 4 Hz

5.2.2 Two Blocks, Soil 2: Acceleration Measurements (Test 2.2)

As an example, in Figure 5.19 acceleration measurements for each frequency are presented as acceleration (g) versus time (second) for the accelerometers placed at the base of the set-up (Acc 1), at the block 2 (Acc 2) and on the block 1 (Acc 3) (Figure 5.19).

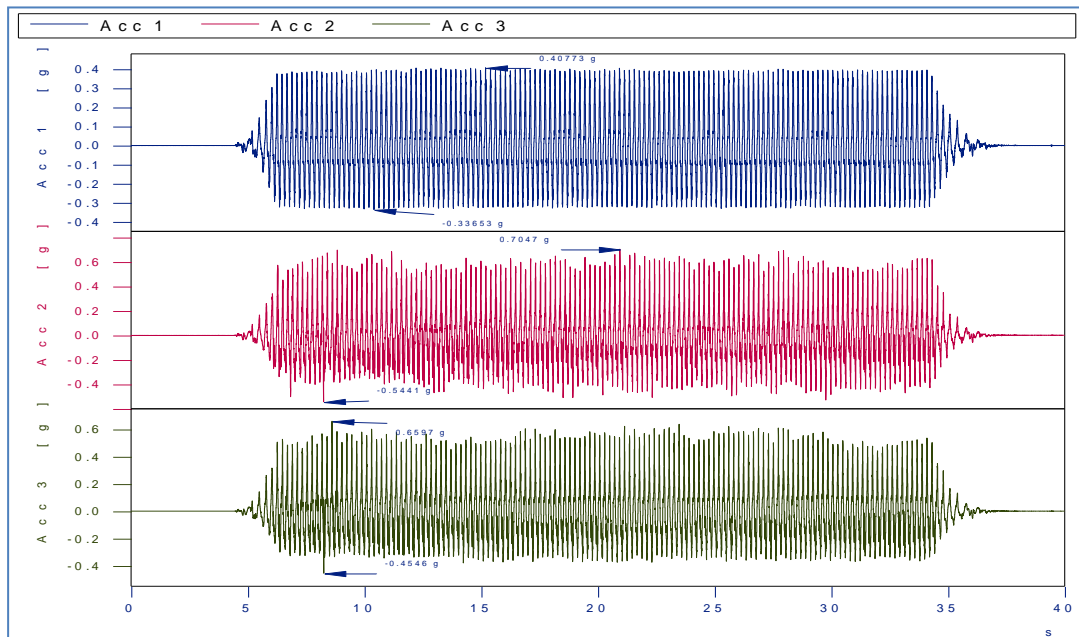


Figure 5.19: Acceleration values of Base (Acc 1), Block 1 (Acc 3) and Block 2 (Acc 2) for 5 Hz (Test 2.2.2)

5.2.2.1 Results of Acceleration Measurements (Soil 2)

Maximum accelerations $|a_{\max}|$ recorded at 3 accelerometers (Acc 1 for Base, Acc 2 for Block 2 and Acc 3 for Block 1) for Soil 2 for each frequency (4 Hz - 6 Hz) are presented in Table 5.8 and Figure 5.20. Ratios between Block 2 / Block 1, Block 1 / Base, Block 2 / Base are also presented in Table 5.9 and Figure 5.21.

Table 5.8: Maximum accelerations at Base (Acc 1), at Block 1 (Acc 3) and at Block 2 (Acc 2) for Soil 2 with respect to frequencies

Frequency (Hz)	Maximum Base Acceleration (g)	Maximum Block 1 Acceleration (g)	Maximum Block 2 Acceleration (g)
4	0.24	0.27	0.35
5	0.41	0.66	0.70
6	0.60	1.79	1.67

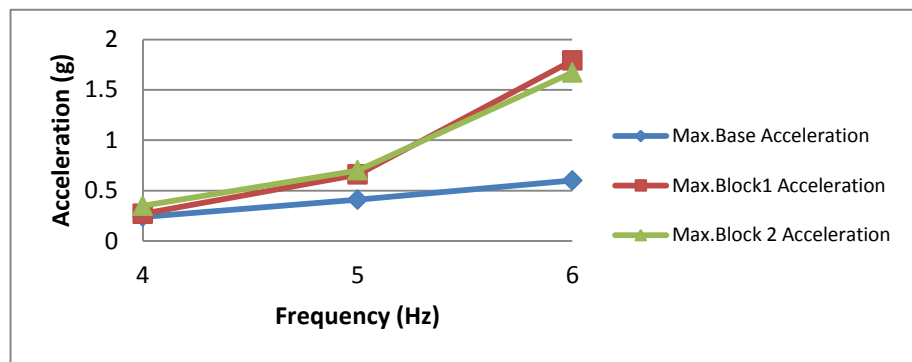


Figure 5.20: Maximum acceleration measurements of Base and Blocks for 4 Hz - 6 Hz for Soil 2

Table 5.9: Ratios (Block 2 / Block 1, Block 1 / Base, Block 2 / Base) versus frequency for Soil 2

Frequency (Hz)	RATIOS		
	Block 2 / Block 1	Block 1 / Base	Block 2 / Base
4	1.30	1.13	1.45
5	1.06	1.61	1.70
6	0.93	2.98	2.79

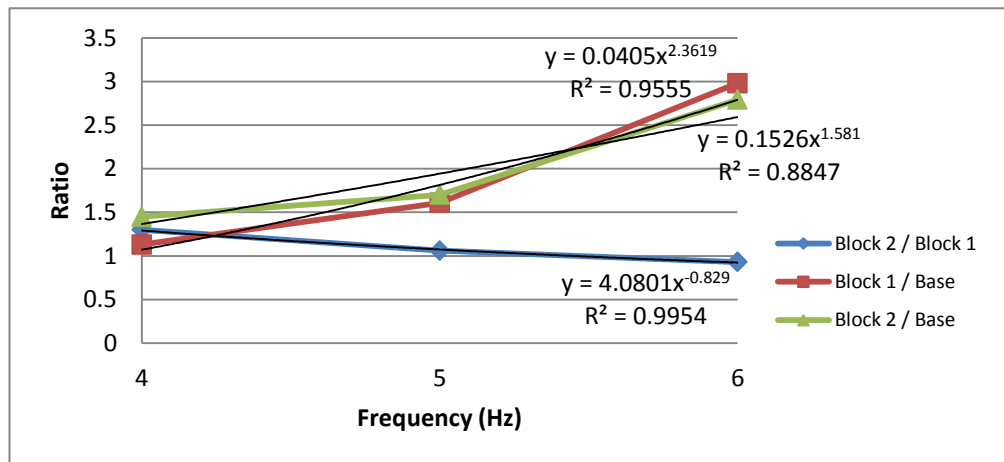


Figure 5.21: Ratios (Block 2 / Block 1, Block 1 / Base, Block 2 / Base) versus frequency for Soil 2

Overall view of the acceleration measurements for two blocks for Soil 2 is presented in Table 5.10.

Table 5.10: Acceleration measurements for two blocks for Soil 2

FREQUENCY	RESULTS
Frequency increases	$ a_{\max} _{\text{base}}$, $ a_{\max} _{\text{block1}}$, $ a_{\max} _{\text{block2}}$ increase
For a given frequency	$ a_{\max} _{\text{block}(n)}$ values are always greater than the $ a_{\max} _{\text{block}(n-1)}$ for $n=2$ $ a_{\max} _{\text{block1}}$ values are always greater than the $ a_{\max} _{\text{base}}$
For larger frequencies (for 4 Hz - 6 Hz)	$ a_{\max} _{\text{block2}} / a_{\max} _{\text{block1}}$ ranges between (1.30-0.93) $ a_{\max} _{\text{block1}} / a_{\max} _{\text{base}}$ ranges between (1.13-2.98) $ a_{\max} _{\text{block2}} / a_{\max} _{\text{base}}$ ranges between (1.45-2.79) $ a_{\max} _{\text{base}}$, $ a_{\max} _{\text{block1}}$ and $ a_{\max} _{\text{block2}}$ values increases rapidly Increment of $ a_{\max} _{\text{block1}} / a_{\max} _{\text{base}}$ and $ a_{\max} _{\text{block2}} / a_{\max} _{\text{base}}$ is almost linear Increment of $ a_{\max} _{\text{block2}} / a_{\max} _{\text{block1}}$ is not linear, and decrement was observed for 4 Hz-6Hz

5.3 Three Blocks Acceleration Measurements (Test 3.1 and Test 3.2)

General view of four accelerometers (Acc 1, Acc 2, Acc 3, Acc 4) used for three blocks tests for Soil 1- Tests 3.1 and for Soil 2 - Test 3.2 are shown in Figure 5.22.

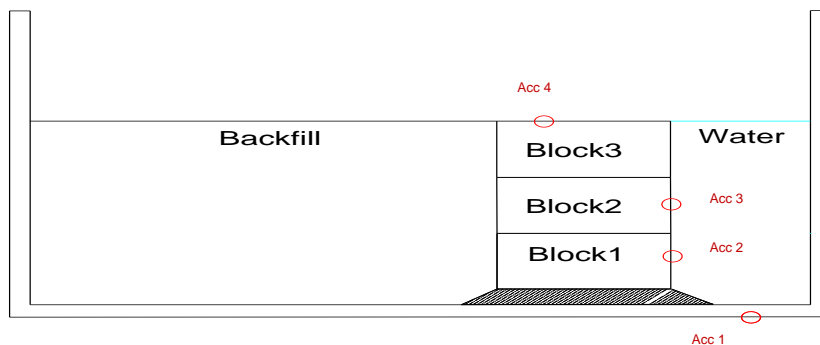


Figure 5.22: General view of three accelerometers (Acc 1, Acc 2, Acc 3, Acc 4) for three blocks tests

Test 3.1 was carried out with 3 Hz, 4 Hz, 5 Hz, 6 Hz for Soil 1 and Test 3.2 was carried out and 3 Hz, 4 Hz, 5 Hz for Soil 2. For Soil 2, 6 Hz frequency test was omitted due to the limitations of the experimental set up and the difficulties faced during the measurements. Acceleration measurements are presented as an example for Soil 1 in Figure 5.23 and for Soil 2 in Figure 5.24. Results of acceleration measurements for three blocks for Soil 1 (Test 3.1) and for Soil 2 (Test 3.2) under dynamic loading are presented in APPENDIX F.

5.3.1 Three Blocks, Soil 1: Acceleration Measurements (Test 3.1)

As an example, in Figure 5.23 acceleration measurements for each frequency are presented as acceleration (g) versus time (second) for the accelerometers placed at the base (Acc 1), at the Block 1 (Acc 2), at the Block 2 (Acc 3) and at the Block 3 (Acc 4).

5.3.1.1 Results of Acceleration Measurements (Soil 1)

Maximum accelerations $|a_{\max}|$ recorded at 4 accelerometers (Acc 1 Base, Acc 2 Block 1 and Acc 3 Block 2, Acc 4 Block 3) for Soil 1 for each frequency (3 Hz - 6 Hz) are presented in Table 5.11 and Figure 5.24. Ratios between Block 3 / Block 2, Block 2 / Block 1, Block 1 / Base, Block 3 / Base are also presented in Table 5.12 and Figure 5.25.

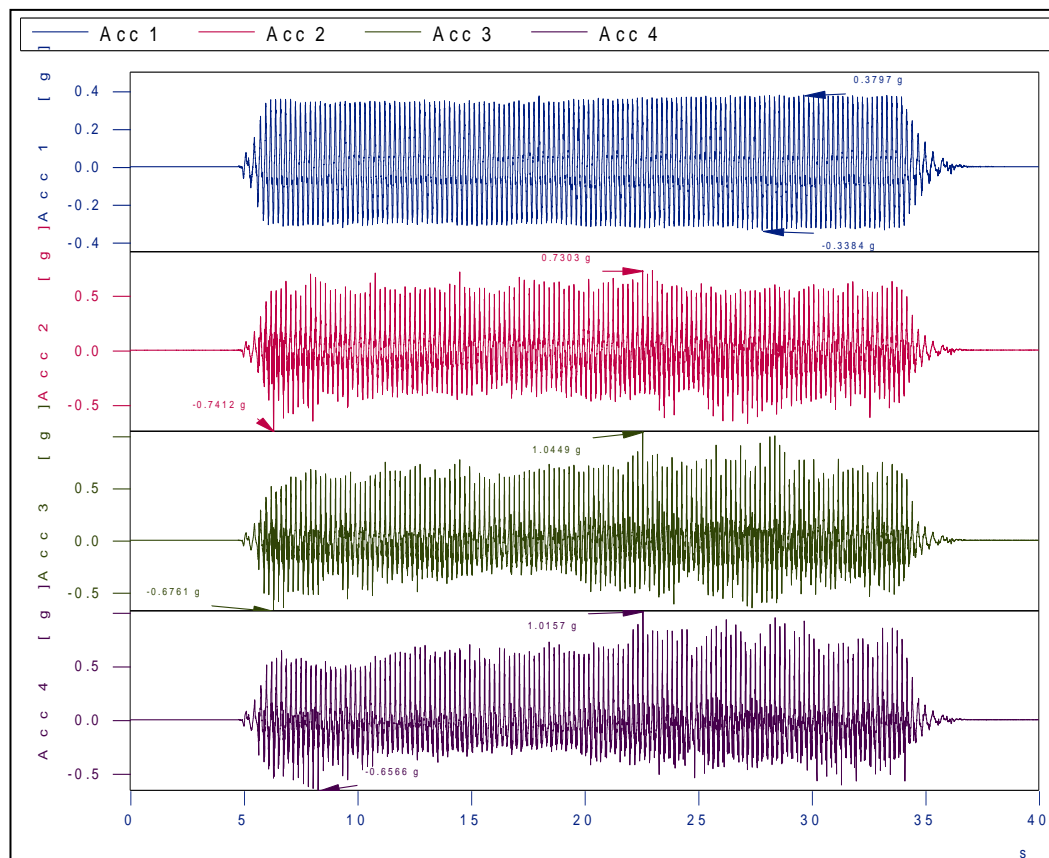


Figure 5.23: Acceleration values of base (Acc 1), block 1 (Acc 2) and block 2 (Acc 3) and block 3 (Acc 4) for 5 Hz (Test 3.1.3)

Table 5.11: Frequency and relations of maximum acceleration measurements of base and block for Soil 1

Frequency (Hz)	Maximum Base Acceleration (g)	Maximum Block 1 Acceleration (g)	Maximum Block 2 Acceleration (g)	Maximum Block 3 Acceleration (g)
3	0.13	0.13	0.13	0.13
4	0.27	0.30	0.34	0.43
5	0.38	0.74	1.05	1.02
6	0.58	1.54	1.65	2.43

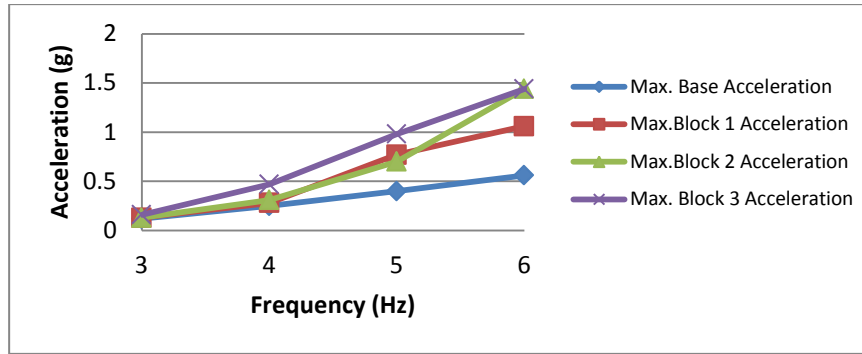


Figure 5.24: Maximum acceleration measurements of base and blocks for 3 Hz - 6 Hz for Soil 1

Table 5.12: Ratios (Block 3 / Block 2, Block 2 / Block 1, Block 1 / Base, Block 3 / Base) versus frequency for Soil 1

Frequency (Hz)	RATIOS			
	Block 3 / Block 2	Block 2 / Block 1	Block 1 / Base	Block 3 / Base
3	1	1	1	1
4	1.26	1.13	1.11	1.59
5	0.97	1.42	1.94	2.68
6	1.47	1.07	2.65	4.20

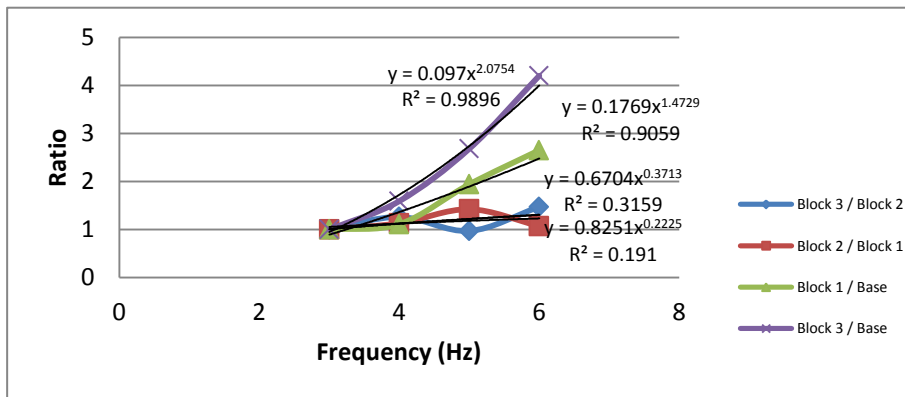


Figure 5.25: Ratios (Block 3 / Block 2, Block 2 / Block 1, Block 1 / Base, Block 3 / Base) versus frequency for Soil 1

Overall view of the acceleration measurements for three blocks for Soil 1 is presented in Table 5.13.

Table 5.13: Acceleration measurements for three blocks for Soil 1

FREQUENCY	RESULTS
Frequency increases	$ a_{\max} _{\text{base}}$, $ a_{\max} _{\text{block1}}$, $ a_{\max} _{\text{block2}}$, $ a_{\max} _{\text{block3}}$ increase
For a given frequency	$ a_{\max} _{\text{block}(n)}$ values are generally greater than the $ a_{\max} _{\text{block}(n-1)}$ for $n=3$ $ a_{\max} _{\text{block1}}$ values are always greater than the $ a_{\max} _{\text{base}}$
For small frequencies (for 3 Hz)	there is no significant change between $ a_{\max} _{\text{base}}$, $ a_{\max} _{\text{block1}}$, $ a_{\max} _{\text{block2}}$, $ a_{\max} _{\text{block3}}$

	there is no change of the ratio between $ a_{\max} _{\text{block3}} / a_{\max} _{\text{block2}}$, $ a_{\max} _{\text{block2}} / a_{\max} _{\text{block1}}$, $ a_{\max} _{\text{block1}} / a_{\max} _{\text{base}}$, $ a_{\max} _{\text{block3}} / a_{\max} _{\text{base}}$
For larger frequencies (for 4 Hz - 5 Hz)	$ a_{\max} _{\text{block3}} / a_{\max} _{\text{block2}}$ ranges between (1.26-0.97) $ a_{\max} _{\text{block2}} / a_{\max} _{\text{block1}}$ ranges between (1.13-1.42) $ a_{\max} _{\text{block1}} / a_{\max} _{\text{base}}$ ranges between (1.11-1.94) $ a_{\max} _{\text{block2}} / a_{\max} _{\text{base}}$ ranges between (1.59-2.68) $ a_{\max} _{\text{base}}$, $ a_{\max} _{\text{block1}}$, $ a_{\max} _{\text{block2}}$ and $ a_{\max} _{\text{block3}}$ values increases rapidly Increment of $ a_{\max} _{\text{block1}} / a_{\max} _{\text{base}}$, $ a_{\max} _{\text{block2}} / a_{\max} _{\text{base}}$, $ a_{\max} _{\text{block3}} / a_{\max} _{\text{base}}$ is almost linear Increment of $ a_{\max} _{\text{block3}} / a_{\max} _{\text{block2}}$ is not linear, and decrement was observed after 4 Hz
for 6 Hz	$ a_{\max} _{\text{base}}$, $ a_{\max} _{\text{block1}}$, $ a_{\max} _{\text{block2}}$ and $ a_{\max} _{\text{block3}}$ values increases rapidly the ratio of $ a_{\max} _{\text{block3}} / a_{\max} _{\text{block2}}$ is 1.47 the ratio of $ a_{\max} _{\text{block2}} / a_{\max} _{\text{block1}}$ is 1.07 the ratio of $ a_{\max} _{\text{block1}} / a_{\max} _{\text{base}}$ is 2.65

5.3.2 Three Blocks, Soil 2: Acceleration Measurements (Test 3.2)

As an example, in Figure 5.26 acceleration measurements for frequencies are presented as acceleration (g) versus time (second) for the accelerometers placed at the base of the set-up (Acc 1), at the block 1 (Acc 2), at the block 2 (Acc 3) and on the block 3 (Acc 4) (Figure 5.26).

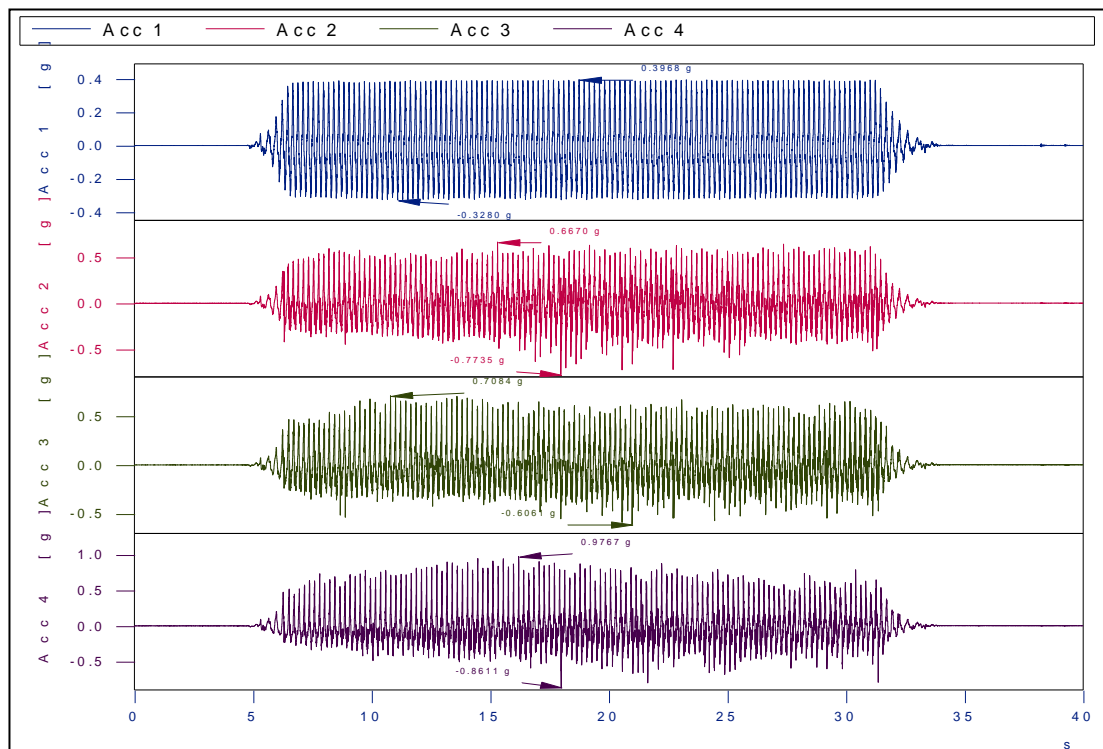


Figure 5.26: Acceleration values of base (Acc 1), block 1 (Acc 2) and block 2 (Acc 3) and block 3 (Acc 4) for 5 Hz (Test 3.2.3)

5.3.2.1 Results of Acceleration Measurements (Soil 2)

Maximum accelerations $|a_{\max}|$ recorded at 4 accelerometers (Acc 1 Base, Acc 2 Block 1 and Acc 3 Block 2, Acc 4 Block 3) for Soil 2 for each frequency (3 Hz - 5 Hz) are presented in Table 5.14 and Figure 5.27. Ratios between Block 3 / Block 2, Block 2 / Block 1, Block 1 / Base, Block 3 / Base are also presented in Table 5.15 and Figure 5.28.

Table 5.14: Frequency and relations of maximum acceleration measurements of base and blocks for Soil 2

Frequency (Hz)	Maximum Base Acceleration (g)	Maximum Block 1 Acceleration (g)	Maximum Block 2 Acceleration (g)	Maximum Block 3 Acceleration (g)
3	0.12	0.13	0.13	0.16
4	0.25	0.28	0.31	0.47
5	0.40	0.77	0.7	0.98

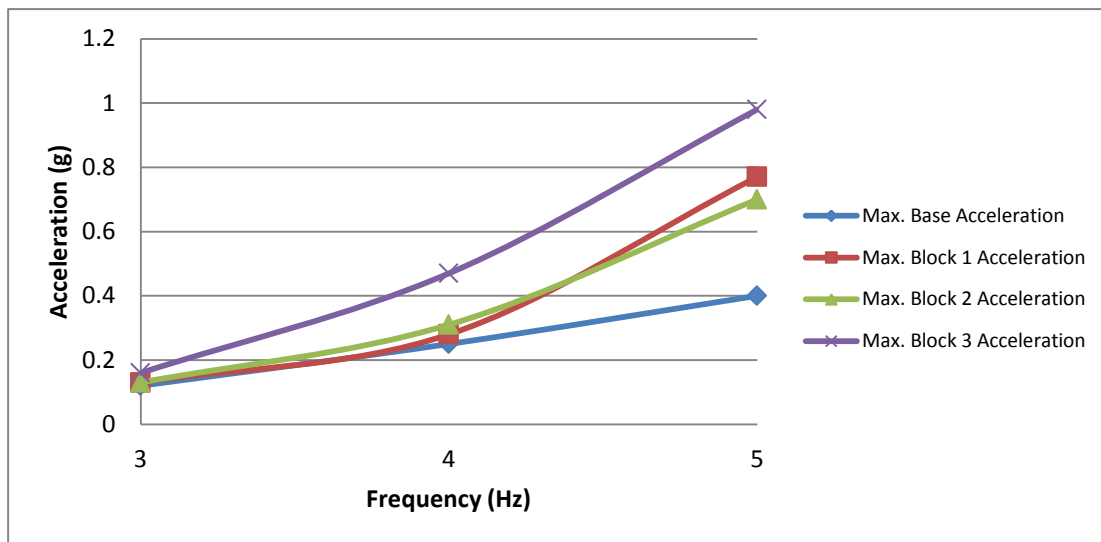


Figure 5.27: Maximum acceleration measurements of base and blocks for 3 Hz, 4 Hz, 5 Hz for Soil 2

Table 5.15: Ratios (Block 3 / Block 2, Block 2 / Block 1, Block 1 / Base, Block 3 / Base) versus frequency for Soil 2

Frequency (Hz)	RATIOS			
	Block 3 / Block 2	Block 2 / Block 1	Block 1 / Base	Block 3 / Base
3	1.23	1	1.08	1.33
4	1.51	1.10	1.12	1.88
5	1.40	0.91	1.93	2.45

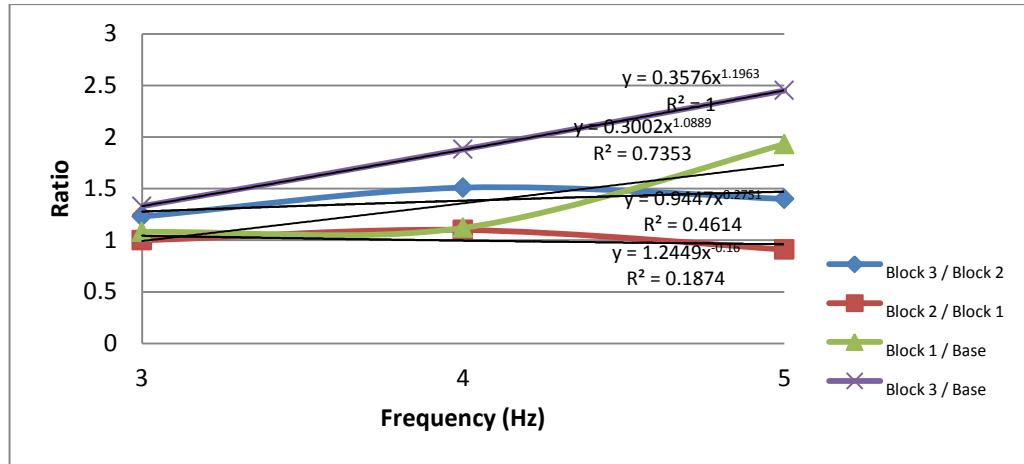


Figure 5.28: Ratios (Block 3/ Block 2, Block 2 / Block 1, Block 1 / Base, Block 3 / Base) versus frequency for Soil 1

Overall view of the acceleration measurements for three blocks for Soil 2 is presented in Table 5.16.

Table 5.16: Acceleration measurements for three blocks for Soil 2

FREQUENCY	RESULTS
Frequency increases	$ a_{\max} _{\text{base}}$, $ a_{\max} _{\text{block1}}$, $ a_{\max} _{\text{block2}}$, $ a_{\max} _{\text{block3}}$ increase
For a given frequency	$ a_{\max} _{\text{block}(n)}$ values are generally greater than the $ a_{\max} _{\text{block}(n-1)}$ for $n=3$ $ a_{\max} _{\text{block1}}$ values are always greater than the $ a_{\max} _{\text{base}}$
For small frequencies (for 3 Hz, 4 Hz)	there is no significant change between $ a_{\max} _{\text{base}}$, $ a_{\max} _{\text{block1}}$, $ a_{\max} _{\text{block2}}$, $ a_{\max} _{\text{block3}}$ for 3 Hz. Increment of $ a_{\max} _{\text{block1}} / a_{\max} _{\text{base}}$, $ a_{\max} _{\text{block2}} / a_{\max} _{\text{base}}$, $ a_{\max} _{\text{block3}} / a_{\max} _{\text{base}}$ is almost linear
For larger frequencies (for 5 Hz)	$ a_{\max} _{\text{base}}$, $ a_{\max} _{\text{block1}}$, $ a_{\max} _{\text{block2}}$ and $ a_{\max} _{\text{block3}}$ values increases rapidly $ a_{\max} _{\text{block3}} / a_{\max} _{\text{block2}}$ is 1.40, the ratio decreases compared to smaller frequencies $ a_{\max} _{\text{block2}} / a_{\max} _{\text{block1}}$ is 0.91, the ratio decreases compared to smaller frequencies Increment of $ a_{\max} _{\text{block1}} / a_{\max} _{\text{base}}$, $ a_{\max} _{\text{block2}} / a_{\max} _{\text{base}}$, $ a_{\max} _{\text{block3}} / a_{\max} _{\text{base}}$ is almost linear

5.3.3 Summary and Discussion of the Acceleration Measurement

Table 5.17 shows the summary of the acceleration measurements with different frequencies for Soil 1 and Soil 2 for one block, two blocks and three blocks. Table 5.18, Table 5.19, Table 5.20 and Table 5.21: $|a_{\max}|$ and frequency relations for Soil 1 and Soil 2 for Block 3 (duration is 30 sec.) show the general results of maximum acceleration $|a_{\max}|$ measurements for Base, Block 1, Block 2 and Block 3 for each frequency for Soil 1 and for Soil 2, respectively.

During the evaluation of the results, the observations given below should be taken into consideration.

- During these experiments after 20 sec. test duration, it was observed that as the frequency increases behavior of the finer backfill (Soil 2) changed totally compared to coarser material (Soil 1).
- After 20 sec. which corresponds to approximately 60 sec in prototype, Soil 2 slumped down towards the structure causing higher and irregular acceleration measurement on the block contrary to Soil 1 behavior.
- For comparison of the results, a time based was selected as 30 sec. All the discussions based on 30 sec which is taken as a representative duration for a devastating earthquake which might be taken as representative of the most critical condition. For shorter durations the available measurements presented in APPENDIX F could be used for the any required duration.

Table 5.17: $|a_{\max}|$ and frequency relations for Soil 1 and Soil 2 for Base (duration is 30 sec.)

BASE	Soil 1	Soil 2
Frequency increases	$ a_{\max} $ increases	$ a_{\max} $ increases
For a given frequency, as block number (n) increases (n=1 to 3)	$ a_{\max} $ decreases	$ a_{\max} $ decreases
a_{\max} values are close to each other for test frequencies.		

Table 5.18: Maximum acceleration $|a_{max}|$ and frequency relations for Soil 1 and Soil 2

BLOCK (S)	SOIL 1						SOIL 2			
	FREQ.	2 Hz	3 Hz	4 Hz	5 Hz	6 Hz	3 Hz	4 Hz	5 Hz	6 Hz
One Block	BASE ACC.(g)	0.08	0.16	0.30	0.41	0.57		0.27	0.42	0.60
	BLOCK1 ACC.(g)	0.08	0.16	0.38	0.67	1.16		0.35	0.54	1.77
Two Blocks	BASE ACC.(g)	0.07	0.14	0.28	0.40	0.55		0.24	0.41	0.60
	BLOCK1 ACC.(g)	0.07	0.14	0.35	0.69	1.14		0.27	0.66	1.79
	BLOCK2 ACC.(g)	0.07	0.14	0.50	0.81	1.28		0.35	0.70	1.67
Three Blocks	BASE ACC.(g)		0.13	0.27	0.38	0.58	0.12	0.25	0.40	
	BLOCK1 ACC.(g)		0.13	0.30	0.74	1.54	0.13	0.28	0.77	
	BLOCK2 ACC.(g)		0.13	0.34	1.05	1.65	0.13	0.31	0.70	
	BLOCK3 ACC.(g)		0.13	0.43	1.02	2.43	0.16	0.47	0.98	

Table 5.19: $|a_{\max}|$ and frequency relations for Soil 1 and Soil 2 for Block 1
(duration is 30 sec.)

BLOCK 1	Soil 1	Soil 2
Frequency increases	$ a_{\max} $ increases	$ a_{\max} $ increases
For a given frequency, block number increases (2-3-4 Hz for Soil 1) (4 Hz for Soil 2)	$ a_{\max} $ decreases	$ a_{\max} $ decreases
For 5 and 6 Hz, block number increases	$ a_{\max} $ increases	$ a_{\max} $ increases
For 4 Hz and 5 Hz, in general $ a_{\max} $ of Soil 1 is greater than $ a_{\max} $ of Soil 2 For 6 Hz $ a_{\max} $ of Soil 1 is smaller than $ a_{\max} $ of Soil 2		

Table 5.20: $|a_{\max}|$ and frequency relations for Soil 1 and Soil 2 for Block 2
(duration is 30 sec.)

BLOCK 2	Soil 1	Soil 2
Frequency increases	$ a_{\max} $ increases	$ a_{\max} $ increases
For 4 Hz, block number increases	$ a_{\max} $ decreases	$ a_{\max} $ decreases
For 5 Hz, block number increases	$ a_{\max} $ increases	$ a_{\max} $ increases
For 6 Hz, block number increases	$ a_{\max} $ increases	-
For 4 Hz and 5 Hz, in general $ a_{\max} $ of Soil 1 is greater than $ a_{\max} $ of Soil 2 For 6 Hz $ a_{\max} $ of Soil 1 is smaller than $ a_{\max} $ of Soil 2		

Table 5.21: $|a_{\max}|$ and frequency relations for Soil 1 and Soil 2 for Block 3
(duration is 30 sec.)

BLOCK 3	Soil 1	Soil 2
Frequency increases	$ a_{\max} $ increases	$ a_{\max} $ increases
In general, for 4 Hz and 5 Hz, $ a_{\max} $ measurements are close to each other except 5 Hz, 3 blocks (Block 2)		

In conclusion, increase in frequency means that number of cycles of dynamic loading increases which causes an increase in acceleration measurements.

Using Soil 1 (coarser) or Soil 2 (finer) backfill material does not cause significant difference in the behavior of the material during seismic loading between 2 Hz-5 Hz. However, for larger frequency (6 Hz) this difference becomes significant.

The choice of the backfill material in case of smaller peak ground acceleration depends on the cost optimization of the material however in case of regions where the seismic loading is critical then the choice of the coarser backfill material (Soil 1) is recommended.

CHAPTER 6

PRESENTATION AND DISCUSSION OF THE RESULTS OF SOIL PRESSURE AND PORE PRESSURE MEASUREMENTS

In Part 1 of this chapter, pore pressure measurements are presented and discussed for one block, two blocks for each frequency for Soil 1 and Soil 2.

In Part 2 of this chapter, soil pressure measurements are presented and discussed for one block, two blocks and three blocks for each frequency for Soil 1 and Soil 2.

PART 1 PRESENTATION AND DISCUSSION OF THE RESULTS OF PORE PRESSURE MEASUREMENTS

General view of two pore pressure cells (Pore P1 and Pore P2) for one block and two blocks tests for Soil 1 and for Soil 2 are shown in Figure 4.13 and Figure 4.15. Pore pressure measurements for one block and two blocks for selected frequencies for Soil 1 and Soil 2 are shown between Figure 6.1– Figure 6.5.

- ONE BLOCK- SOIL 1

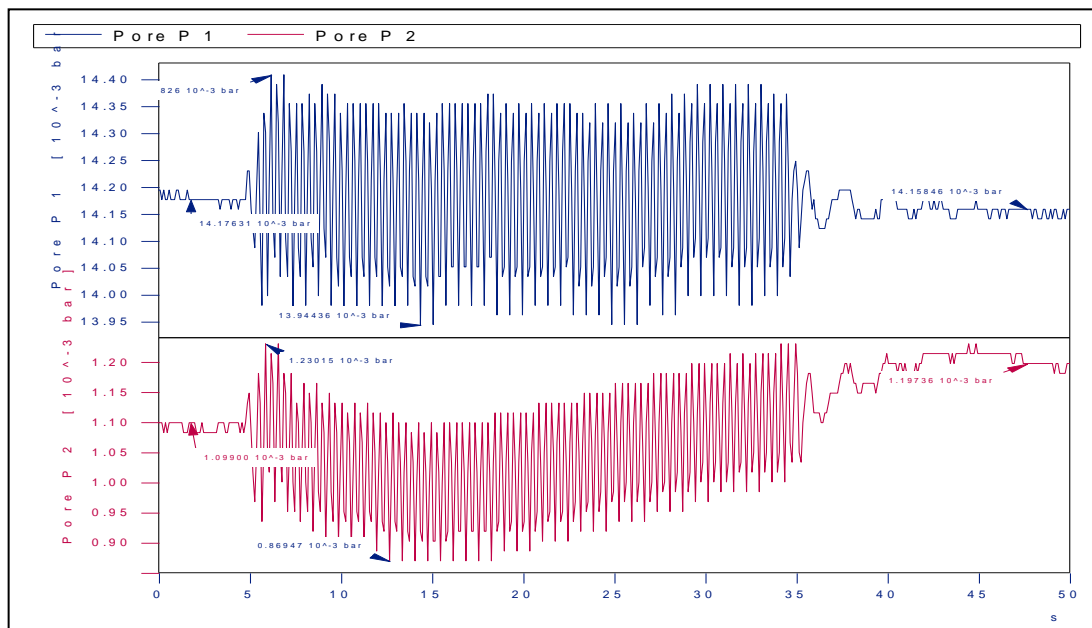


Figure 6.1: Pore Pressure values of Pore P1 and Pore P2 located at 15 cm and 1 cm for 3 Hz

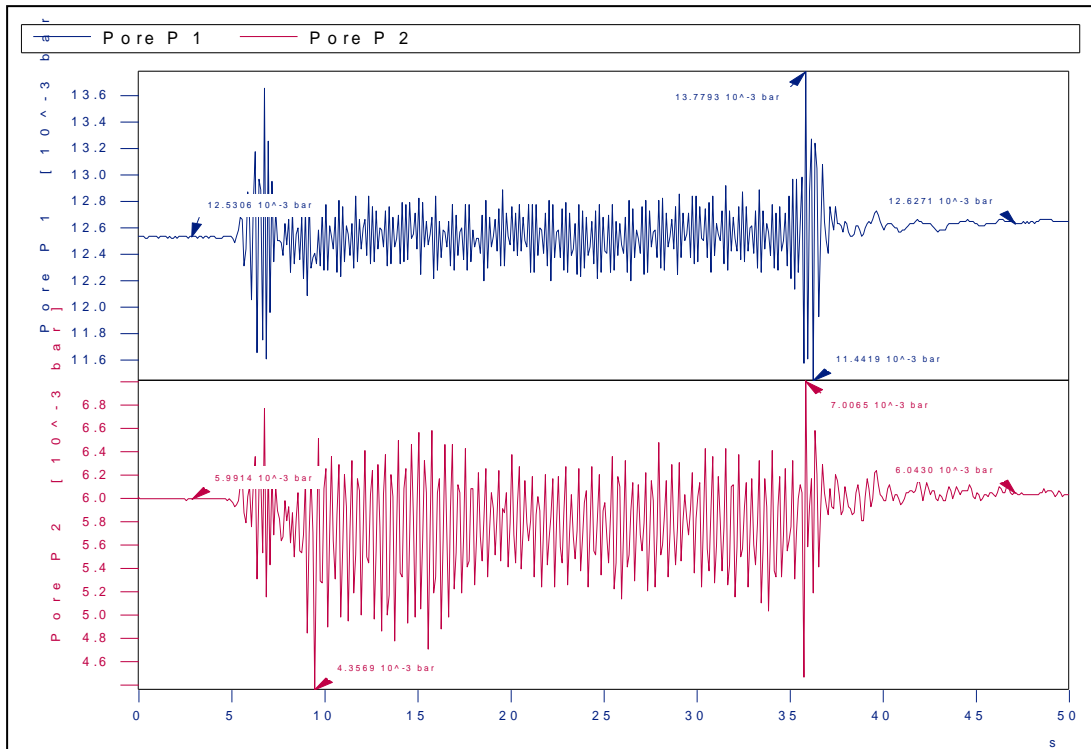


Figure 6.2: Pore Pressure values of Pore P1 and Pore P2 located at 12.5 cm and 1 cm for 6 Hz

- ONE BLOCK- SOIL 2

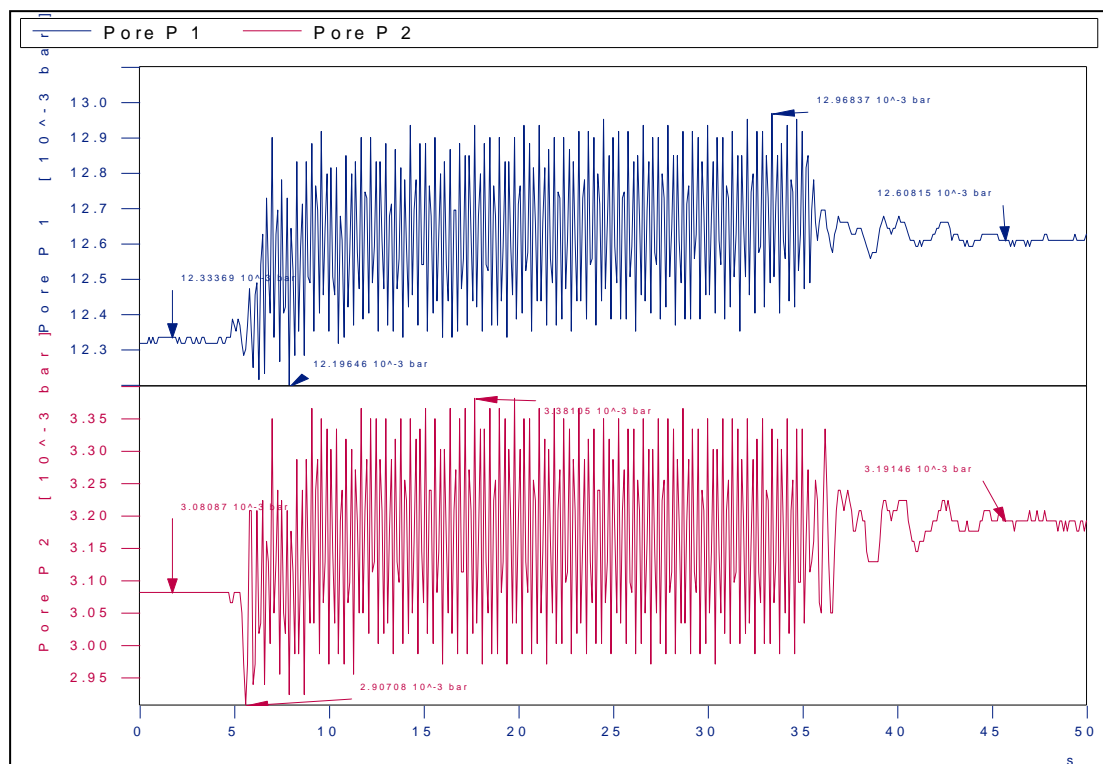


Figure 6.3: Pore Pressure values of Pore P1 and Pore P2 located at 12.3 cm and 3 cm for 6 Hz

- TWO BLOCKS- SOIL 1

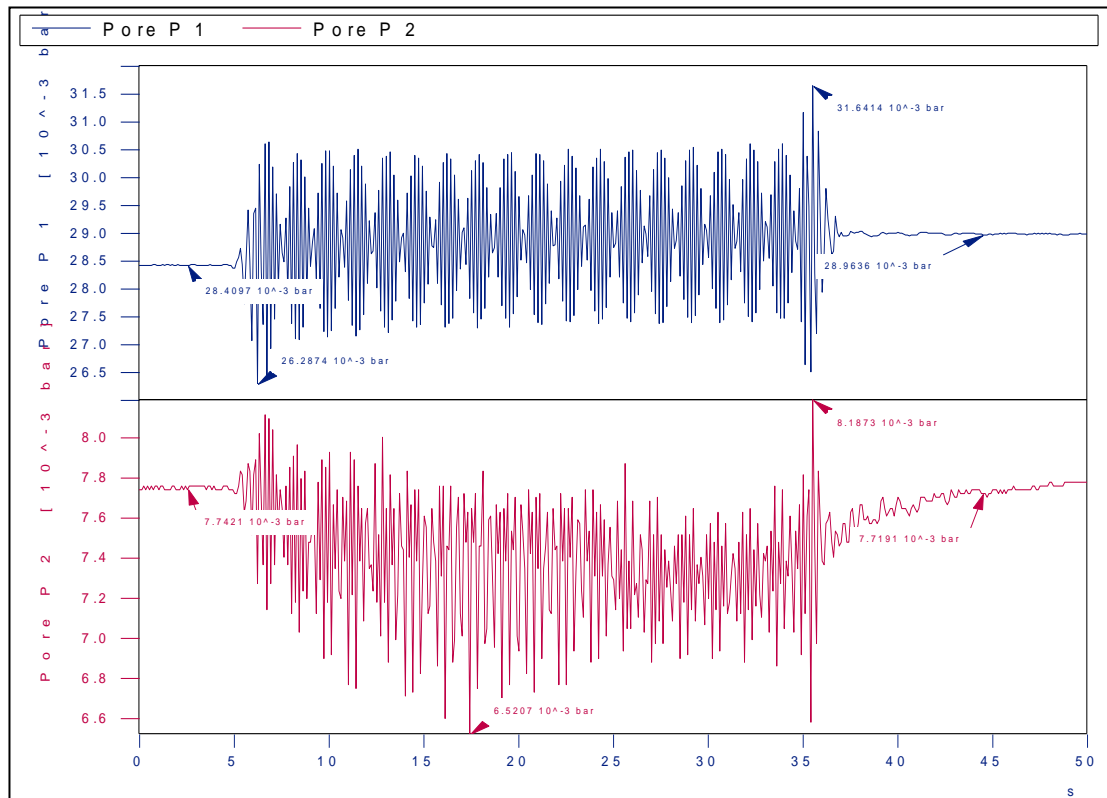


Figure 6.4: Pore Pressure values of Pore P1 and Pore P2 located at 28.5 cm and 7.7 cm for 5 Hz

- TWO BLOCKS- SOIL 2

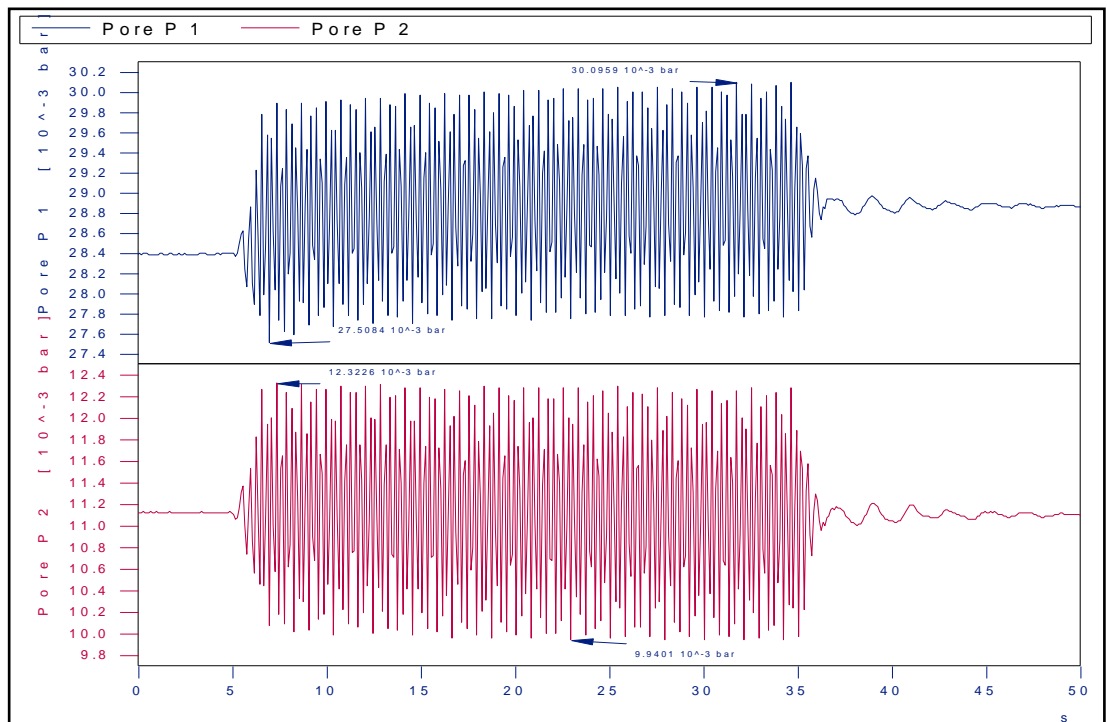


Figure 6.5: Pore Pressure values of Pore P1 and Pore P2 located at 28.4 cm and 11.1 cm for 4 Hz

6.1 Results of Pore Pressure Measurements (Soil 1 and Soil 2)

The excess pore pressure has significant effects on soil pressure and horizontal displacements on block type quay walls under dynamic loading. Kim et al., (2005) stated that "If the excess pore pressure increases, the backfill soil behaves increasingly like a fluid, thus the mobility of the soil increases". Zeng (1998) emphasized that excess pore pressure had a significant effect both on the angle of backfill wedge and horizontal thrust thus, when excess pore pressure developed in the backfill, comprehensive numerical procedures should be made to understand the response of gravity quay walls.

Experimental, numerical and analytical results showed that when permeability increases the accumulation of excess pore pressure is reduced.

In this study;

- gravel type backfill materials (Soil 1 and Soil 2, see Table 4.2 and Table 4.3) are used and since gravels are more permeable, significant excess pore pressures usually do not generate for this kind of backfill. The excess pore pressures occurred under dynamic loading disappears immediately.
- it is assumed that soil improvement techniques are used for the selected project site as backfill and foundation where the existing soil conditions are expected to lead to unsatisfactory performance. Alyami, Rouainia and Wilkinson (2009) found that "improving the backfill and the foundation soils reduced the vertical settlement at the toe of the wall by over 200%, while the horizontal displacement was reduced by over 350%".

According to assumption and studies explained above and the 1 g shaking table tests results for one block, two blocks and three blocks for Soil 1 and Soil 2 given between Figure 6.1- Figure 6.5, there is no significant effect of excess pore pressure on block(s). Based on these results, experiments for pore pressure measurements are not carried out for three blocks.

In conclusion, in this study, effect of excess pore pressure is neglected in accordance with the technical requirements of backfill properties are selected as Soil 1 and Soil 2.

PART 2 PRESENTATION AND DISCUSSION OF THE RESULTS OF SOIL PRESSURE MEASUREMENTS

Total saturated soil pressure measurements results are presented and discussed for each series for Soil 1 and Soil 2 (Table 4.9). 3 Hz tests were omitted for one block and two blocks and 6 Hz tests were omitted for three blocks due to the limitations of the experimental set up.

6.2 One Blok Soil Pressure Measurements (Test 1.1 and Test 1.2)

General view of two soil pressure cells (SP1 and SP2) for one block tests for Soil 1- Tests 1.1 and for Soil 2 - Test 1.2 are shown in Figure 4.13.

6.2.1 One Blok, Soil 1: Total Saturated Soil Pressure Measurements (Test 1.1)

In Figure 6.6 - Figure 6.10 total saturated soil pressure measurements for each frequency are presented as soil pressure cells placed at 15 cm below the top of the block (SP1) and 5 cm below the top of the block (SP2) for Soil 1 (Figure 4.13)

Total saturated soil pressure measurements ranges under dynamic loading for 2 Hz – 6 Hz are shown in Table 6.1 with respect to results of the total saturated soil pressure measurements given in Figure 6.6 - Figure 6.10 for Soil 1.

Table 6.1: Total saturated soil pressure measurements ranges for 2 Hz – 6 Hz for Soil 1

Frequency	Soil Pressure Cells	Ranges of Total Saturated Soil Pressure Measurements
2 Hz	SP2	0.90 kpa – 1.65 kpa
	SP1	1.86 kpa - 2.40 kpa
3 Hz	SP2	0.65 kpa - 1.93 kpa
	SP1	1.57 kpa - 2.88 kpa
4 Hz	SP2	0.59 kpa - 1.88 kpa
	SP1	1.81 kpa – 3.91 kpa
5 Hz	SP2	0.77 kpa - 1.35 kpa
	SP1	1.77 kpa – 5.77 kpa
6 Hz	SP2	0.56 kpa - 1.23 kpa
	SP1	1.50 kpa – 6.05 kpa

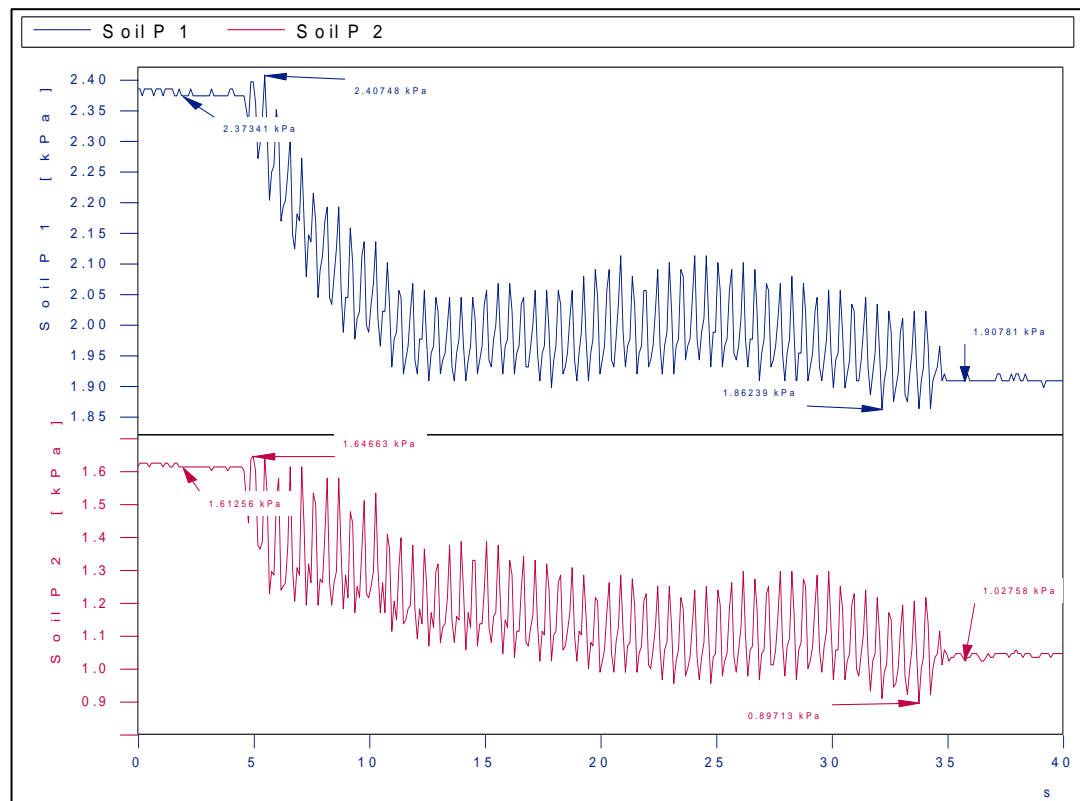


Figure 6.6: Total saturated soil pressure measurements for SP1 and SP2 for 2 Hz for Soil 1 (Test 1.1.1)

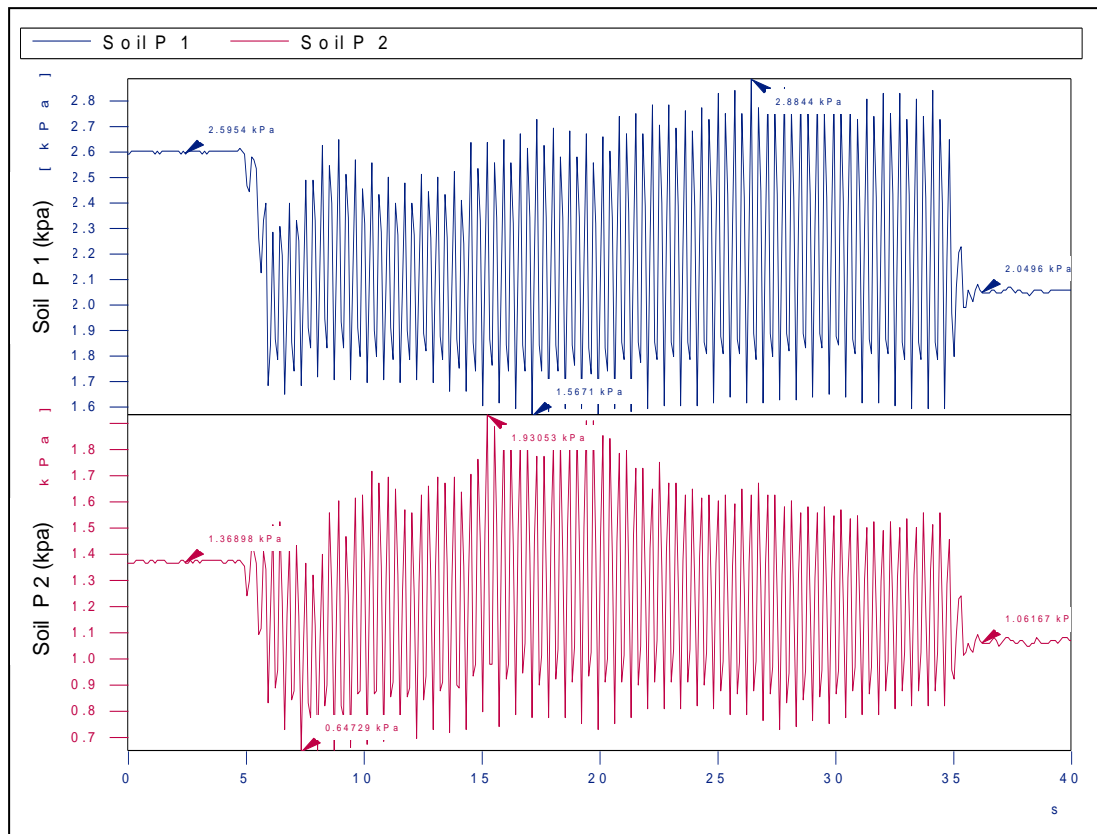


Figure 6.7: Total saturated soil pressure measurements for SP1 and SP2 for 3 Hz for Soil 1 (Test 1.1.2)

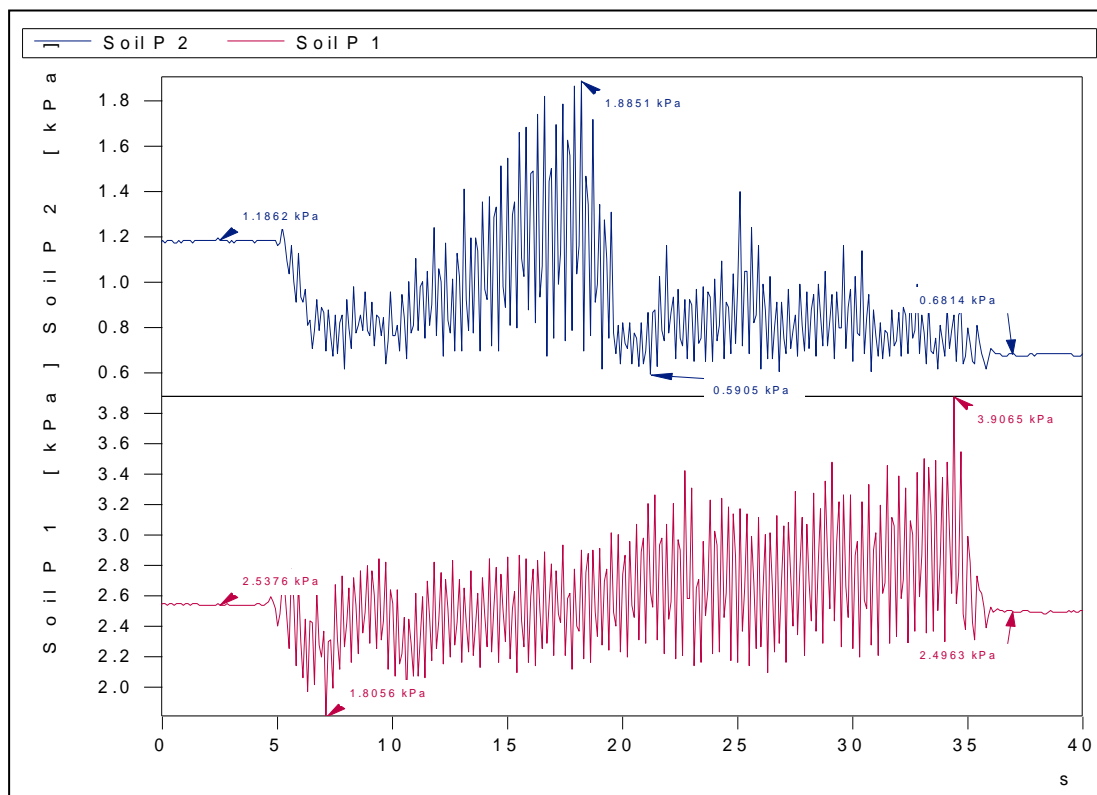


Figure 6.8: Total saturated soil pressure measurements for SP1 and SP2 for 4 Hz for Soil 1 (Test 1.1.3)

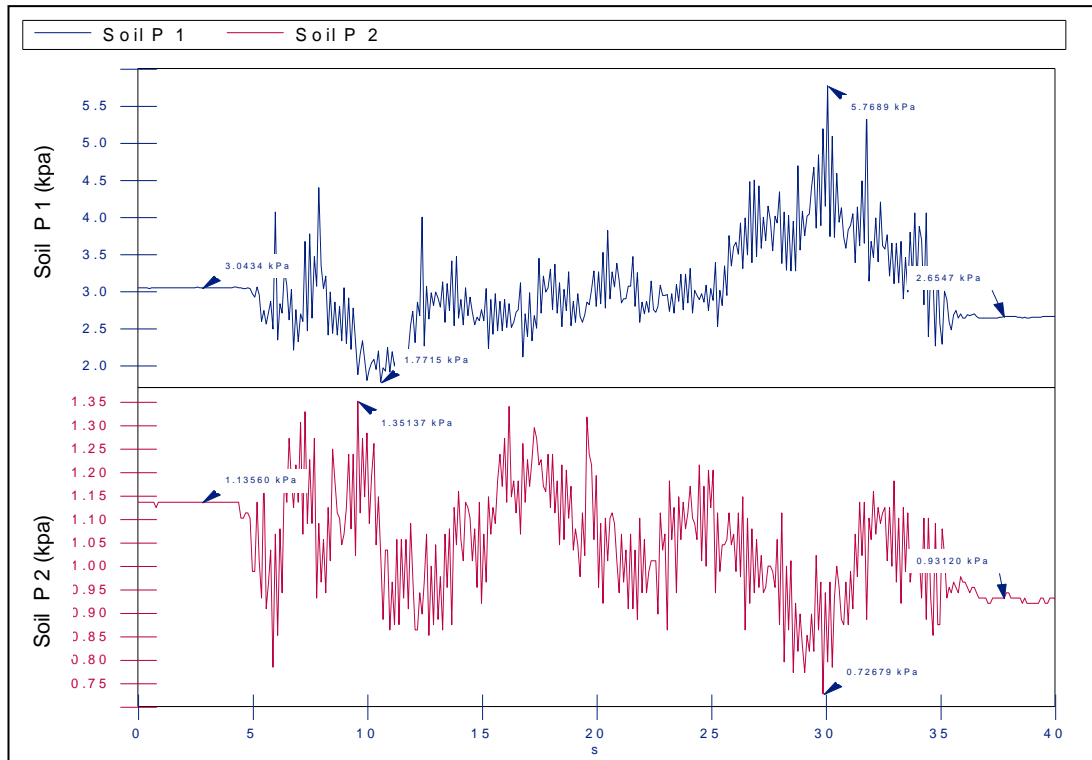


Figure 6.9: Total saturated soil pressure measurements for SP1 and SP2 for 5 Hz for Soil 1 (Test 1.1.4)

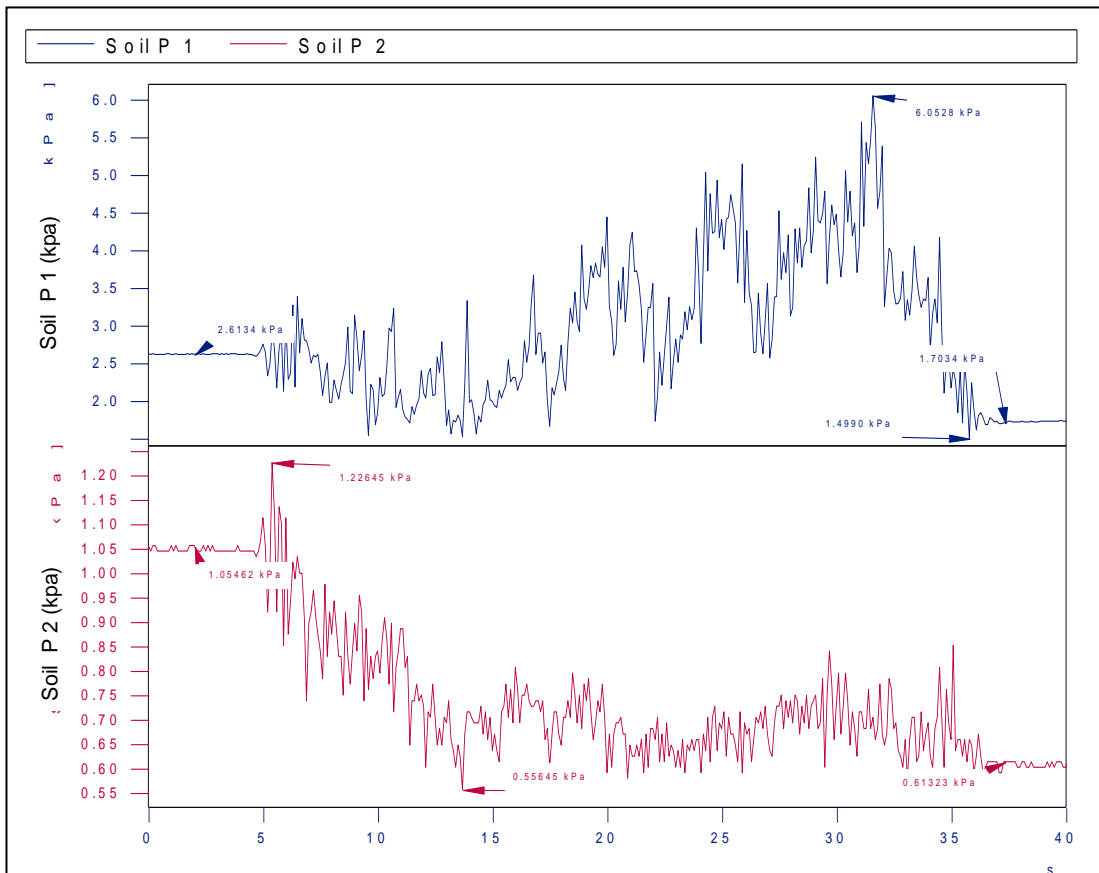


Figure 6.10: Total saturated soil pressure measurements for SP1 and SP2 for 6 Hz for Soil 1 (Test 1.1.5)

6.2.1.1 Results of Soil Pressure Cell Measurements (Soil 1)

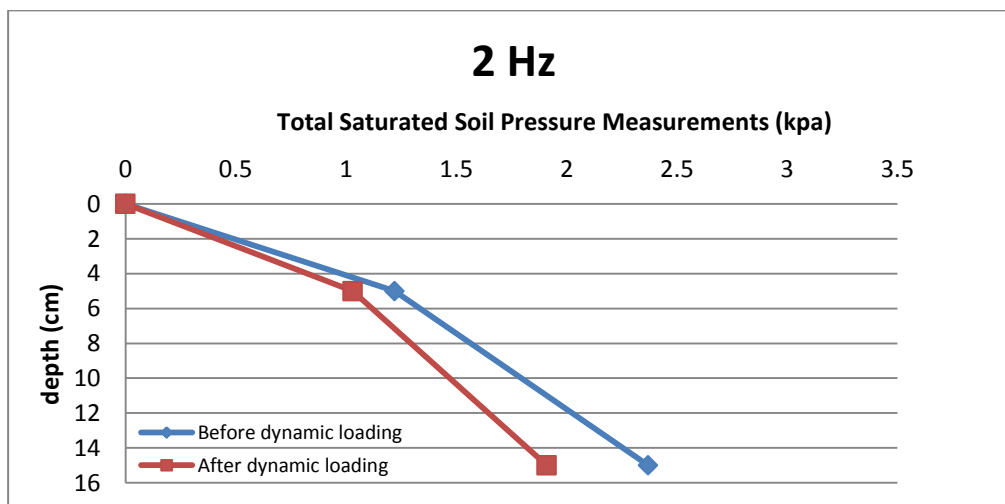
2 soil pressure cells namely SP1 (placed at 15 cm below the top of the block) and SP2 (5 cm below the top of the block) were used to define the total saturated soil pressure distribution acting on block for Soil 1 for each frequency (2 Hz - 6 Hz).

For the frequencies 2 Hz - 6 Hz, the total saturated soil pressure measured for two different conditions -before dynamic loading and at the end of (after) dynamic loading- are given in Table 6.2 for Soil 1.

Total saturated soil pressure measurements for before dynamic loading (beginning of the tests) and after dynamic loading (30 sec, corresponding to the end of the tests) acting on block for each frequency (2 Hz, 3 Hz, 4 Hz, 5 Hz, 6 Hz) for Soil 1 versus depth relations are given in Figure 6.12.

Table 6.2: Total saturated soil pressure measurements for different frequencies before and after dynamic loading for Soil 1

Frequency (Hz)	Soil Pressure Numbers	Total Saturated Soil Pressures (kpa)		
		Before Dynamic Loading (kpa)	After Dynamic Loading (kpa)	Ratio
2	SP2	1.67	1.03	1.62
	SP1	2.37	1.91	1.24
3	SP2	1.37	1.06	1.29
	SP1	2.6	2.05	1.27
4	SP2	1.18	0.68	1.74
	SP1	2.53	2.49	1.02
5	SP2	1.13	0.93	1.22
	SP1	3.09	2.65	1.17
6	SP2	1.05	0.6	1.75
	SP1	2.61	1.7	1.54



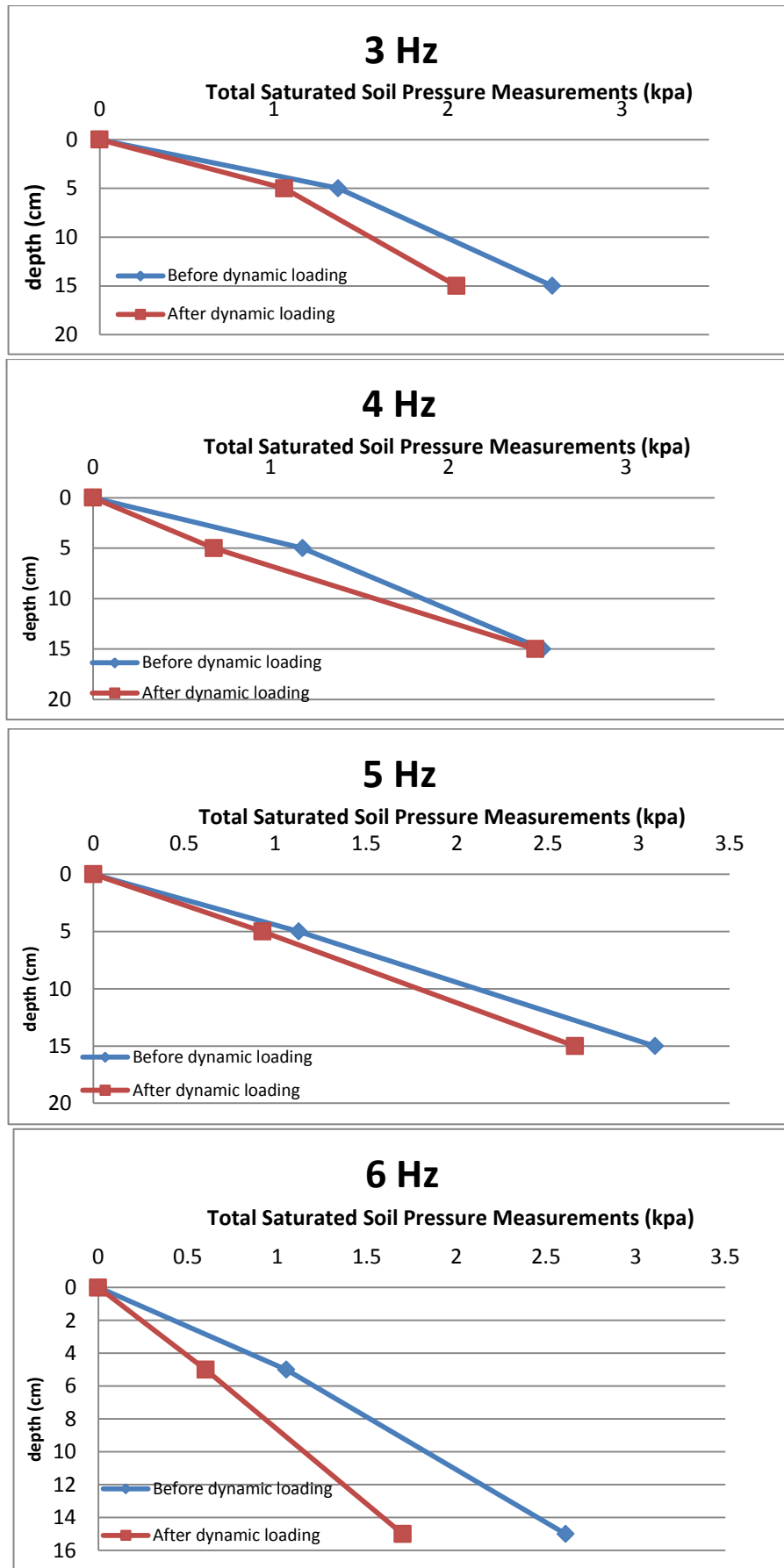


Figure 6.11: Total saturated soil pressure measurements acting on block for 2, 3, 4, 5, 6 Hz for Soil 1

As it is seen from the Figure 6.11 and Table 6.2 for Soil 1,

- The total saturated soil pressure measurements increase while depth is increasing for both before and after dynamic loading for each frequency.
- Total saturated soil pressures measured before dynamic loading almost 1.5 times larger than the total saturated soil pressures measured after dynamic loading for SP1. This result shows that compaction of the soil causes increment in relative density (D_r) and increment in relative density (D_r) causes decrement in measured total saturated soil pressures.
- Total saturated soil pressures measured before dynamic loading almost 1.2 times larger than the total saturated soil pressures measured after dynamic loading for SP2. This result is not only related to compaction of the soil but also related to reduced backfill height behind the block.

In the measurements for Soil 1 ($D_{n50}=2.2$ cm) sudden decrease of the soil pressure measurements was observed clearly during the experiments. This was due to sudden compaction of the soil particles under dynamic loadings within few seconds which changed the contact points of the pressure cells with the soil particles of the backfill material effecting the sensitivity of the measurements. Therefore, sudden decrease was disregarded during the evaluations of test results. In view of the objective of these experiments, soil distribution on block(s) under dynamic loading were determined successfully by omitting the sudden decrease on the pressure measurements. This discussion holds true for two and three blocks soil pressure measurements for Soil 1.

6.2.1.2 One Block- Fluctuating and Non-fluctuating Components of Total Saturated Soil Pressure Soil 1

There are two components namely, fluctuating and non-fluctuating components (Part 4.2) of total saturated soil pressure measurements. By using MathCAD software program (Appendix E), these components were computed. Total saturated soil pressures and fluctuating and non-fluctuating components are shown between Figure 6.13 – Figure 6.51 these values are shown for different frequencies Soil 1.

6.2.1.2.1 One Block- Fluctuating and Non-fluctuating Components of Total Saturated Soil Pressure for 2 Hz for Soil 1

Figure 6.12 - Figure 6.15 show the total saturated soil pressure, non-fluctuating and fluctuating components of total saturated soil pressure for **SP1 for 2 Hz for Soil 1**.

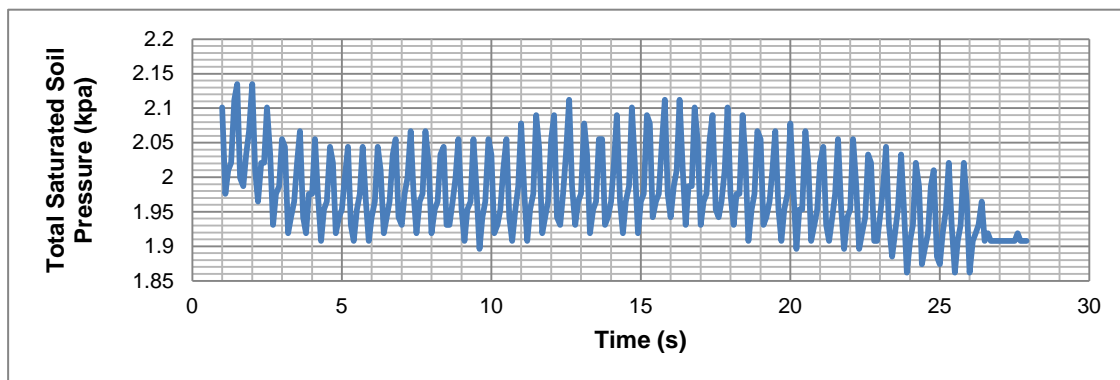


Figure 6.12: Total saturated soil pressure for SP1 for 2 Hz for Soil 1

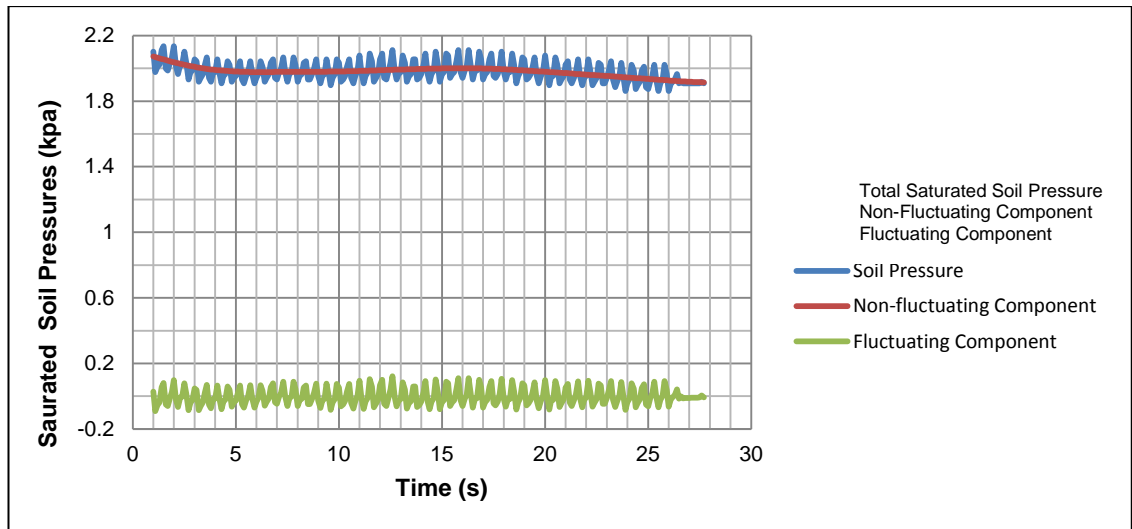


Figure 6.13: Total saturated soil pressure, non-fluctuating and fluctuating components of total saturated soil pressure for SP1 for 2 Hz for Soil 1

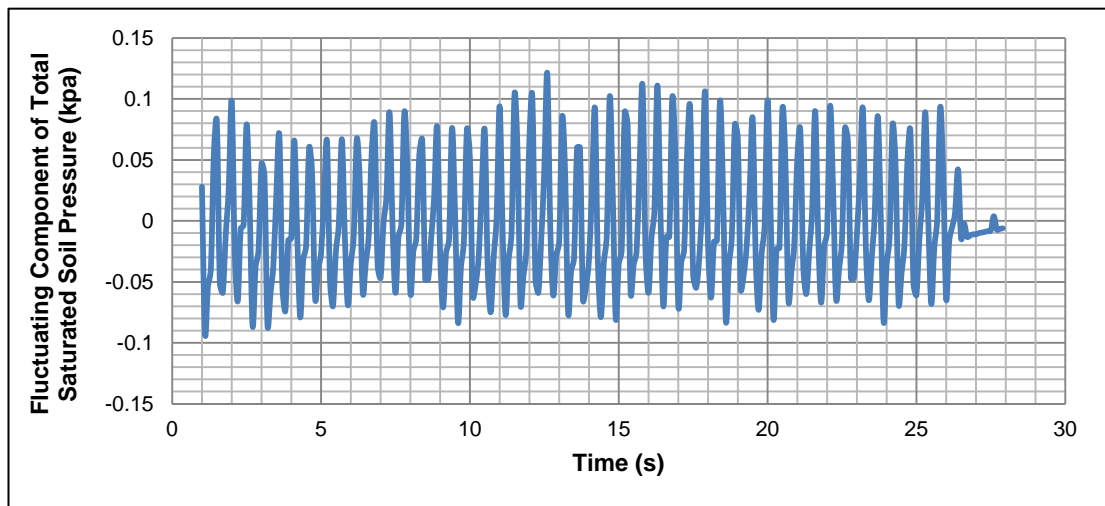


Figure 6.14: Fluctuating components of total saturated soil pressures for SP1 for 2 Hz for Soil 1

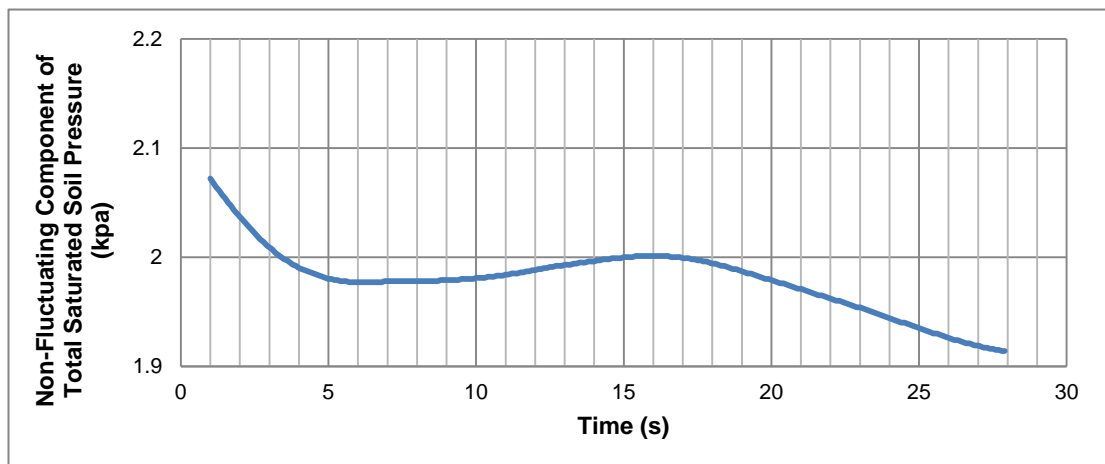


Figure 6.15: Non-fluctuating components of total saturated soil pressures for SP1 for 2 Hz for Soil 1

Figure 6.16 - Figure 6.19 show the total soil pressure, non-fluctuating and fluctuating components of total saturated soil pressure of **SP2 for 2 Hz for Soil 1**.

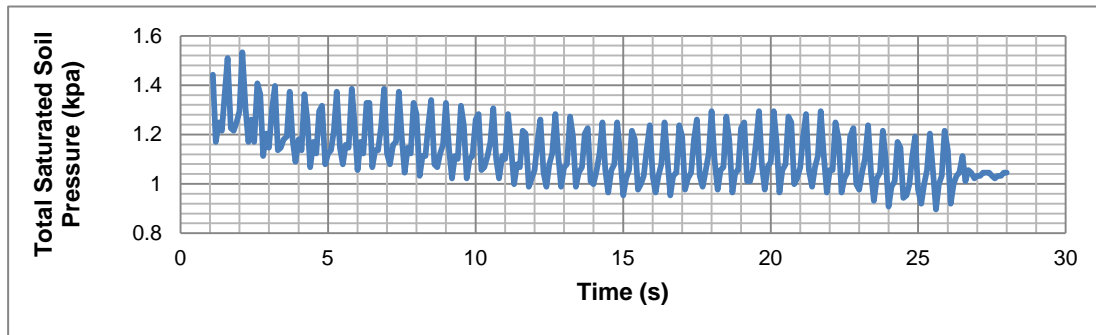


Figure 6.16: Total saturated soil pressures for SP2 for 2 Hz for Soil 1

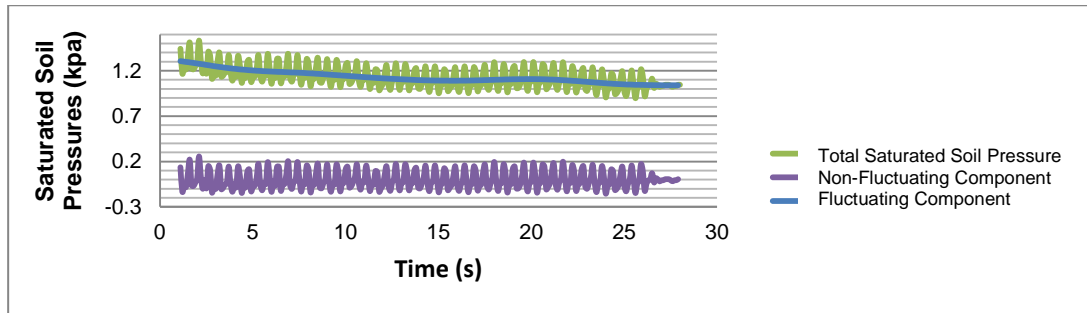


Figure 6.17: Total saturated soil pressure, non-fluctuating and fluctuating components of total saturated soil pressures for SP2 for 2 Hz for Soil 1

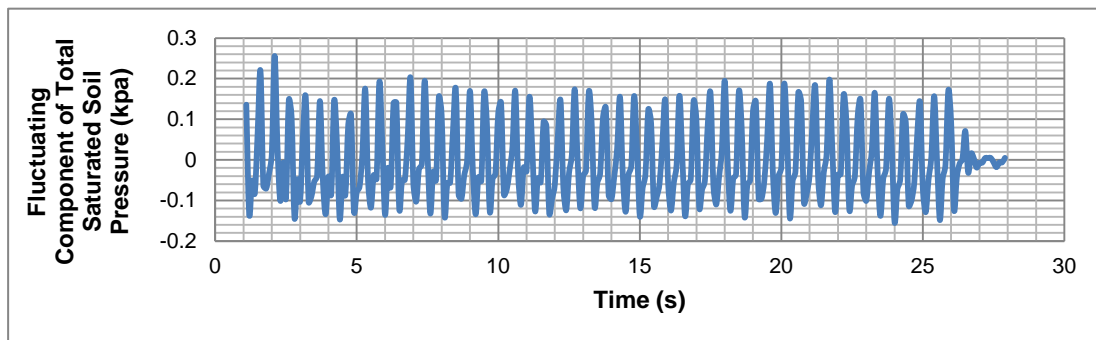


Figure 6.18 : Fluctuating components of total saturated soil pressures for SP2 for 2 Hz for Soil 1

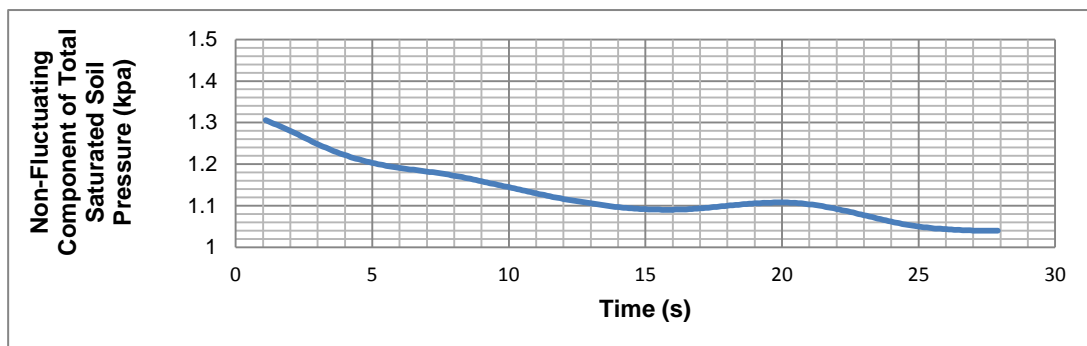


Figure 6.19: Non-Fluctuating components of total saturated soil pressures for SP2 for 2 Hz for Soil 1

6.2.1.2.1.1 One Block- Fluctuating and Non-Fluctuating Components of Total Lateral Soil Pressure for 3 Hz for Soil 1

Figure 6.20 - Figure 6.23 show the total saturated soil pressure, non-fluctuating and fluctuating components of total saturated soil pressure of SP1 for 3 Hz for Soil 1.

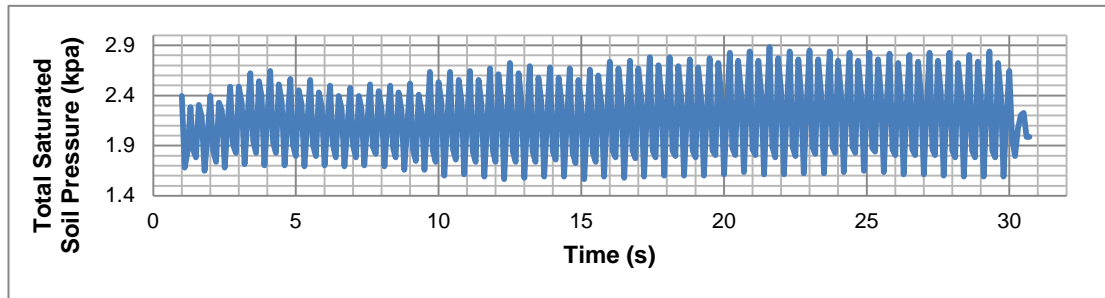


Figure 6.20: Total saturated soil pressures for SP1 for 3 Hz for Soil 1

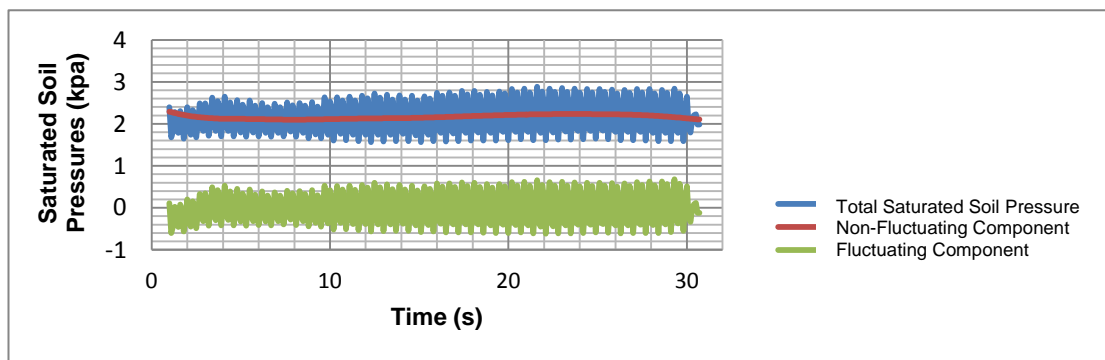


Figure 6.21: Total saturated soil pressures, non-fluctuating and fluctuating components of total saturated soil pressures for SP1 for 3 Hz for Soil 1

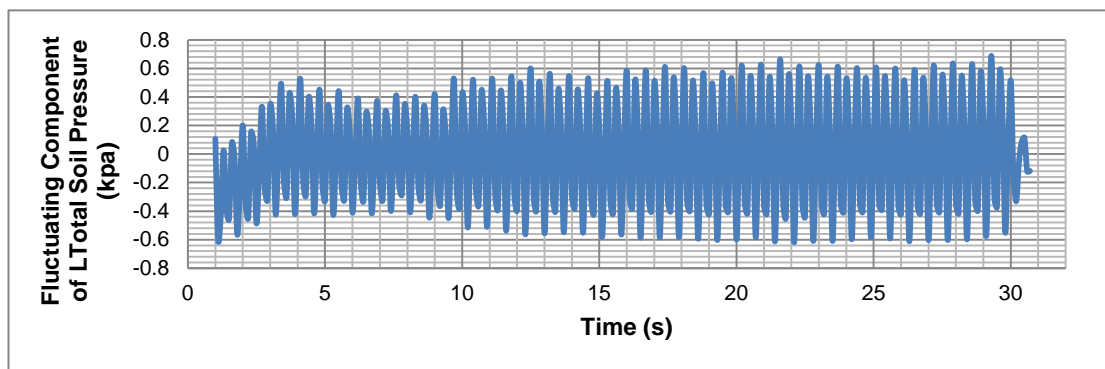


Figure 6.22: Fluctuating components of total saturated soil pressures for SP1 for 3 Hz for Soil 1

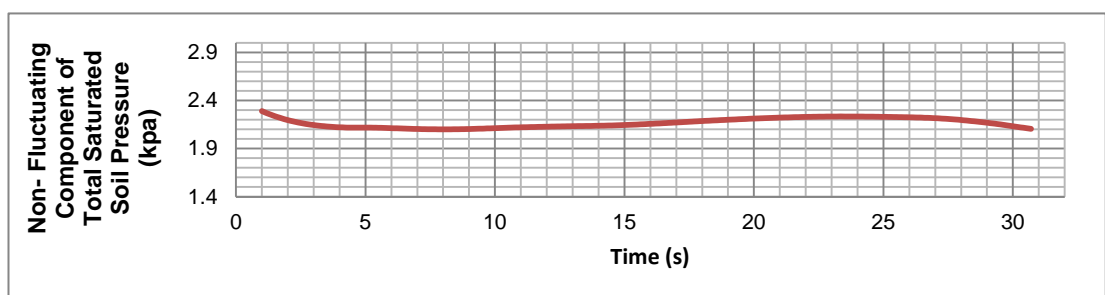


Figure 6.23: Non-fluctuating components of total saturated soil pressures for SP1 for 3 Hz for Soil 1

Figure 6.24-Figure 6.27 show the total saturated soil pressures, non-fluctuating and fluctuating components of total saturated soil pressures of **SP2 for 3 Hz for Soil 1**.

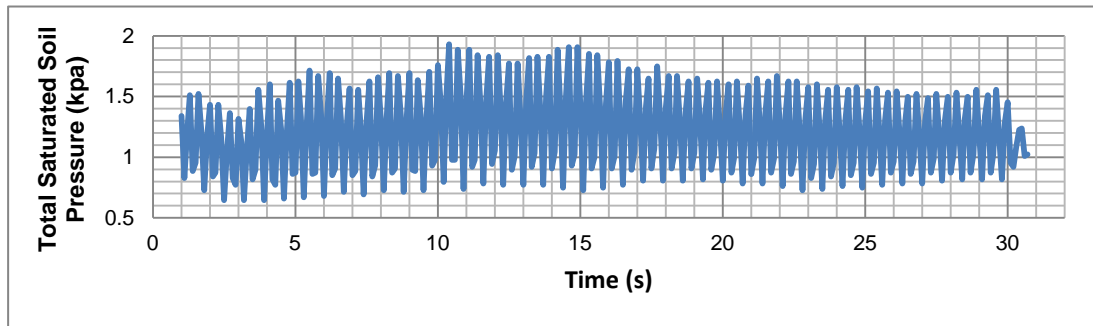


Figure 6.24: Total saturated soil pressures for SP2 for 3 Hz for Soil 1

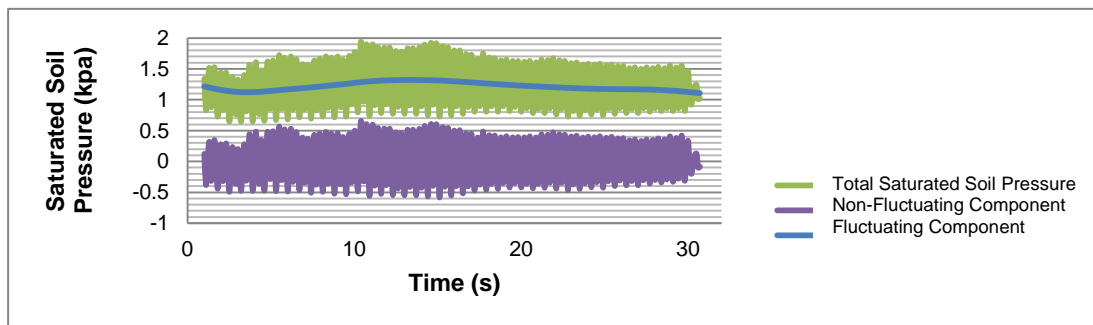


Figure 6.25: Total soil pressures, non-fluctuating and fluctuating components of total saturated soil pressures for SP2 for 3 Hz for Soil 1

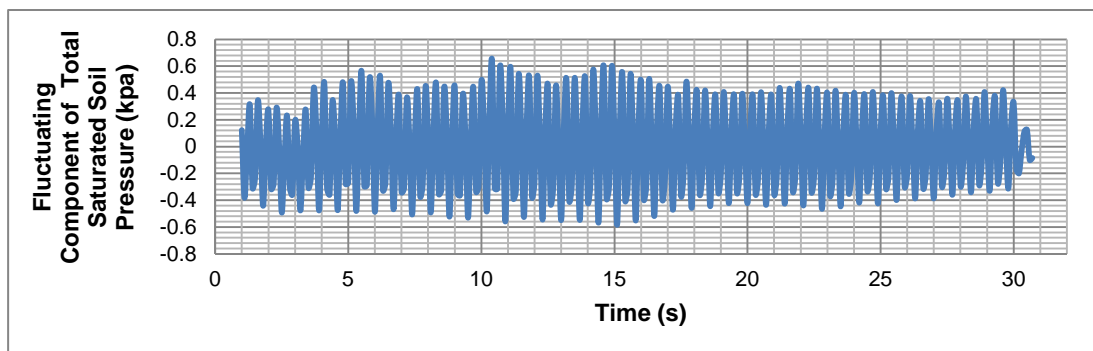


Figure 6.26: Fluctuating components of total saturated soil pressures for SP2 for 3 Hz for Soil 1

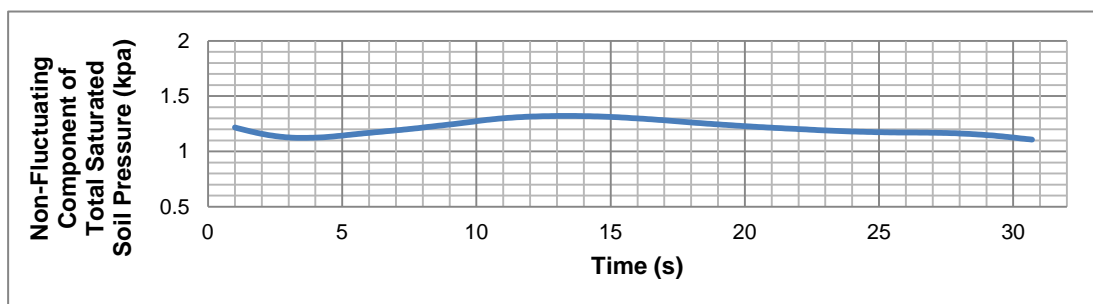


Figure 6.27: Non-fluctuating components of total saturated soil pressures for SP2 for 3 Hz for Soil 1

6.2.1.2.1.2 One Block- Fluctuating and Non-Fluctuating Components of Total Saturated Soil Pressure for 4 Hz for Soil 1

Figure 6.28-Figure 6.31 show the total saturated soil pressures, non-fluctuating and fluctuating components of total saturated soil pressures of **SP1 for 4 Hz for Soil 1**.

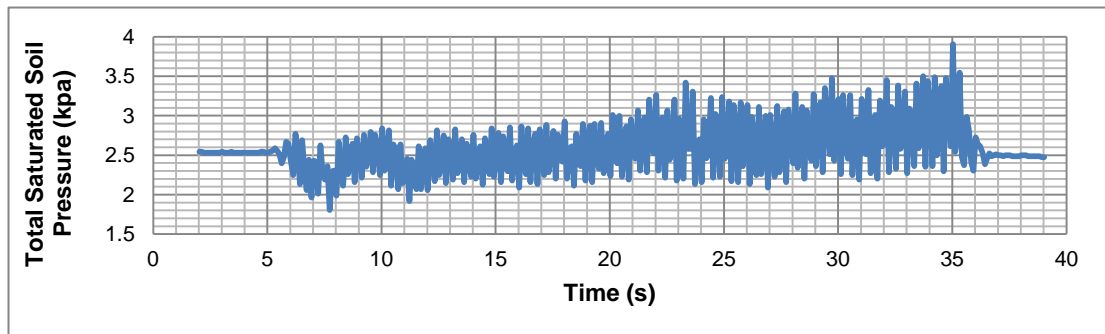


Figure 6.28: Total saturated soil pressures for SP1 for 4 Hz for Soil 1

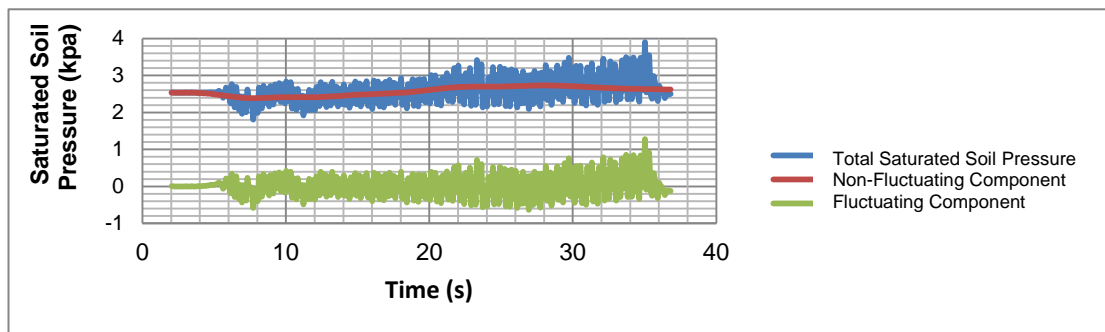


Figure 6.29: Total saturated soil pressures, non-fluctuating and fluctuating components of total saturated soil pressures for SP1 for 4 Hz for Soil 1

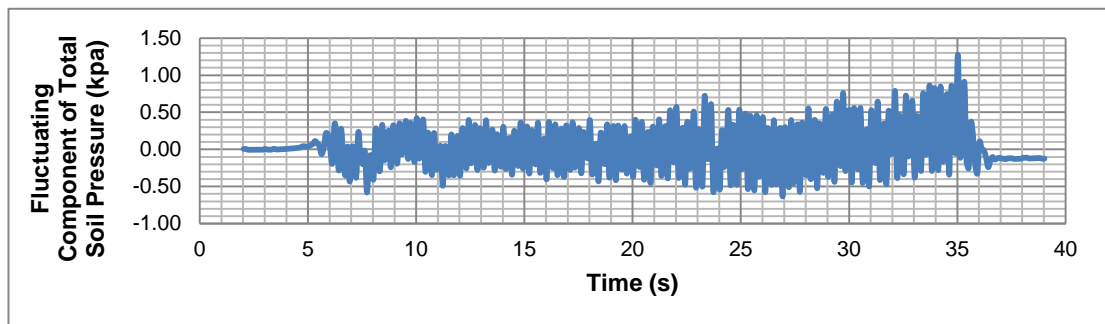


Figure 6.30: Fluctuating components for total saturated soil pressures for SP1 for 4 Hz for Soil 1

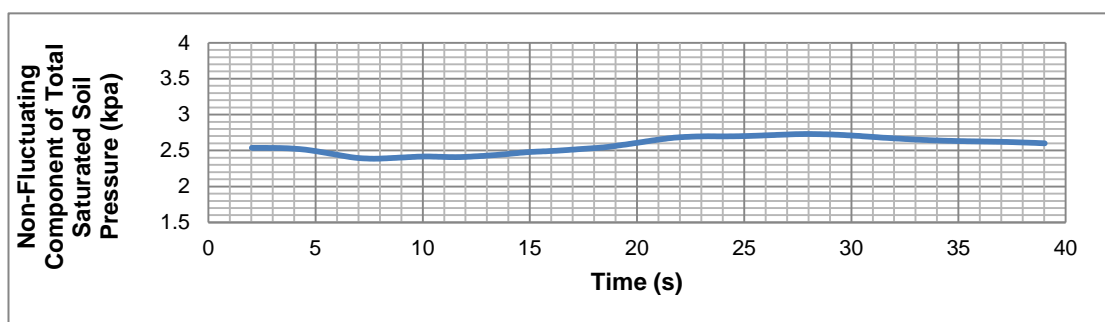


Figure 6.31: Non-fluctuating components of total saturated soil pressures for SP1 for 4 Hz for Soil 1

Figure 6.32-Figure 6.35 show the total saturated soil pressures, non-fluctuating and fluctuating components of total saturated soil pressures of **SP2 for 4 Hz for Soil 1**.

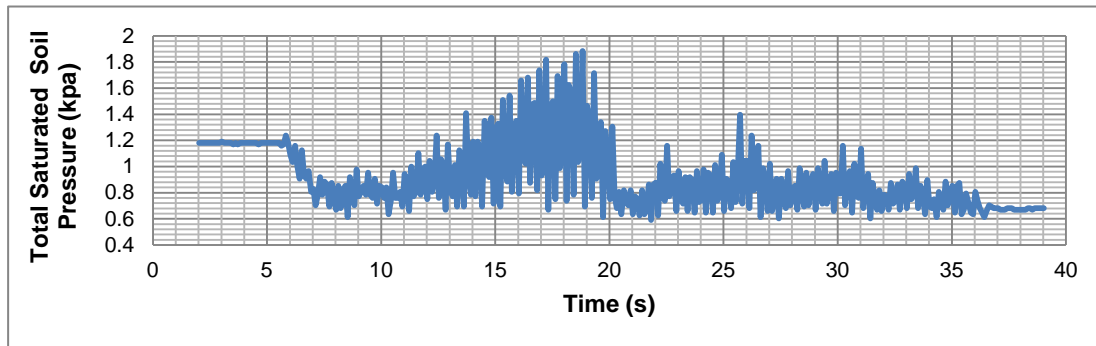


Figure 6.32: Total saturated soil pressures for SP2 for 4 Hz for Soil 1

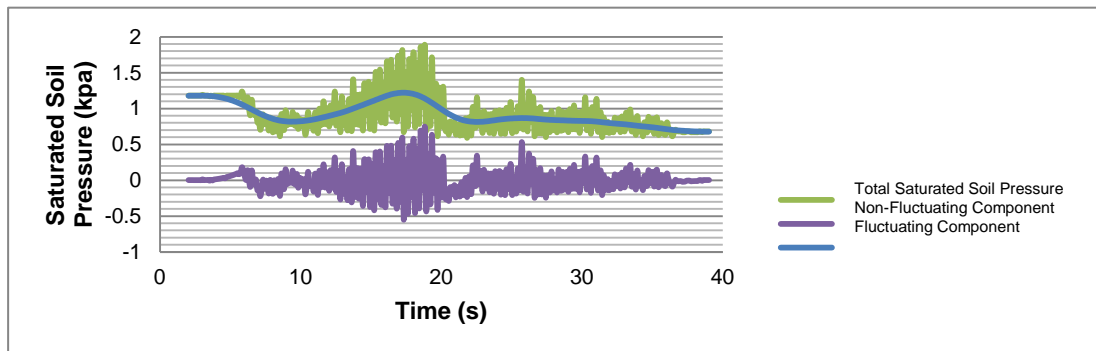


Figure 6.33: Total saturated soil pressures, non-fluctuating and fluctuating components of total saturated soil pressures for SP2 for 4 Hz for Soil 1

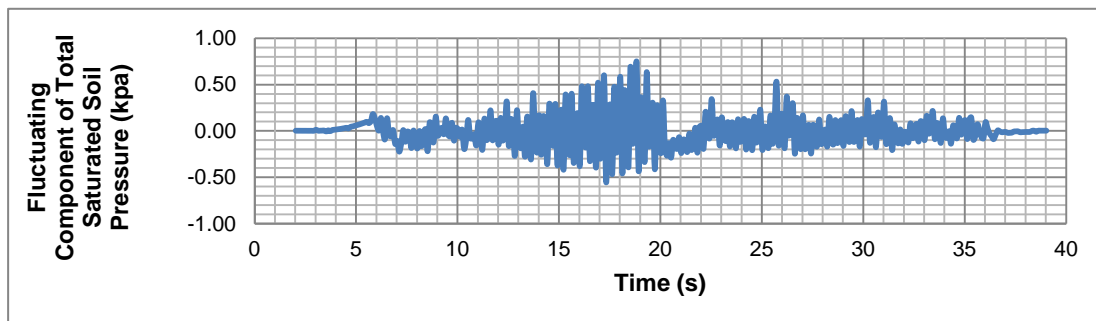


Figure 6.34: Fluctuating components for total saturated soil pressures for SP1 for 4 Hz for Soil 1

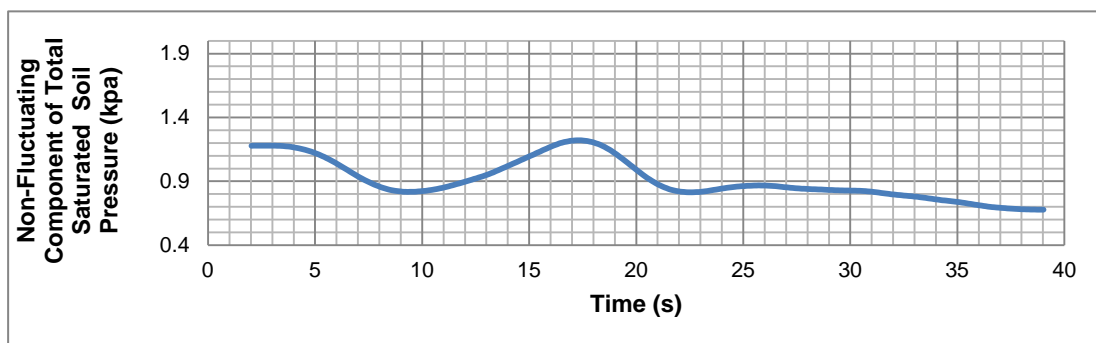


Figure 6.35: Non-fluctuating components of total saturated soil pressures for SP2 for 4 Hz for Soil 1

6.2.1.2.1.3 One Block- Fluctuating and Non-Fluctuating Components of Total Lateral Soil Pressure for 5 Hz for Soil 1

Figure 6.36-Figure 6.39 show the total saturated soil pressures, non-fluctuating and fluctuating components of total saturated soil pressures of **SP1 for 5 Hz for Soil 1**.

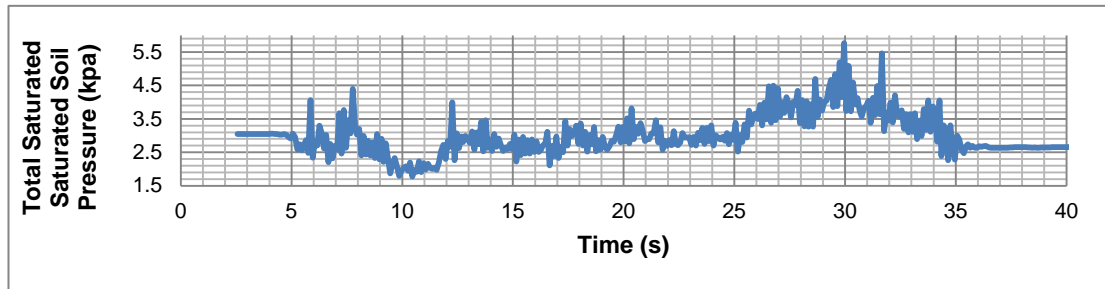


Figure 6.36: Total saturated soil pressures for SP1 for 5Hz for Soil 1

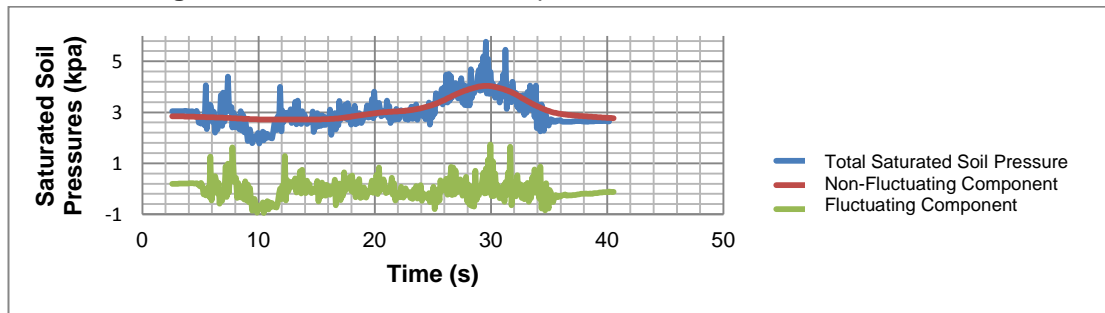


Figure 6.37: Total saturated soil pressures, non-fluctuating and fluctuating components of total saturated soil pressures for SP1 for 5 Hz for Soil 1

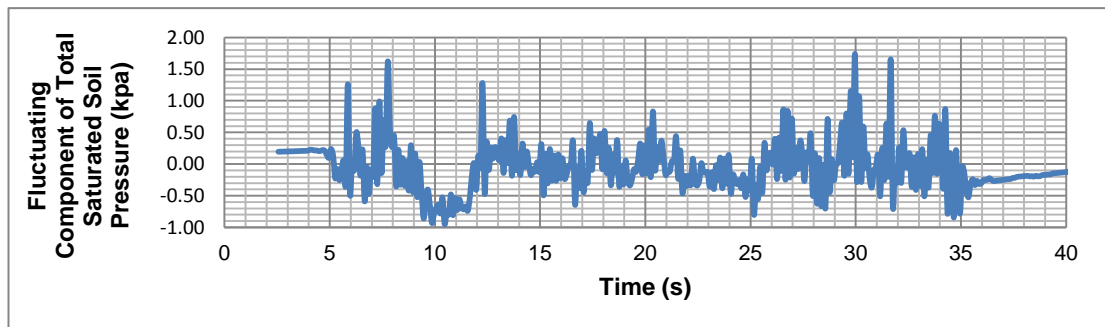


Figure 6.38: Fluctuating components for total saturated soil pressures for SP1 for 5 Hz for Soil 1

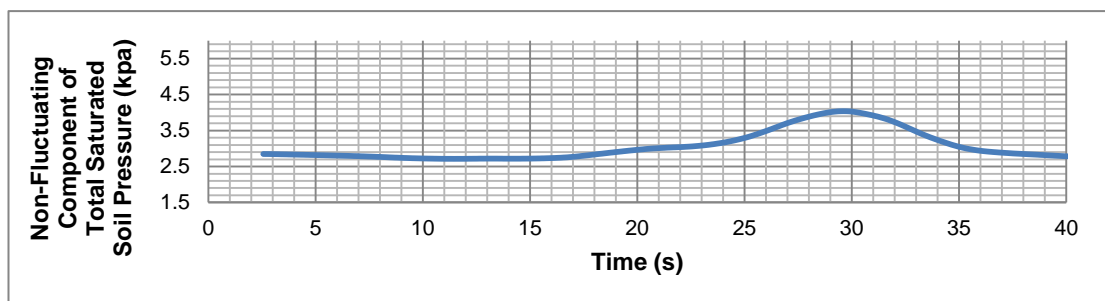


Figure 6.39: Non-fluctuating components for total saturated soil pressures for SP1 for 5 Hz for Soil 1

Figure 6.40-Figure 6.43 show the total saturated soil pressures, non-fluctuating and fluctuating components of total saturated soil pressures of **SP2 for 5 Hz for Soil 1**.

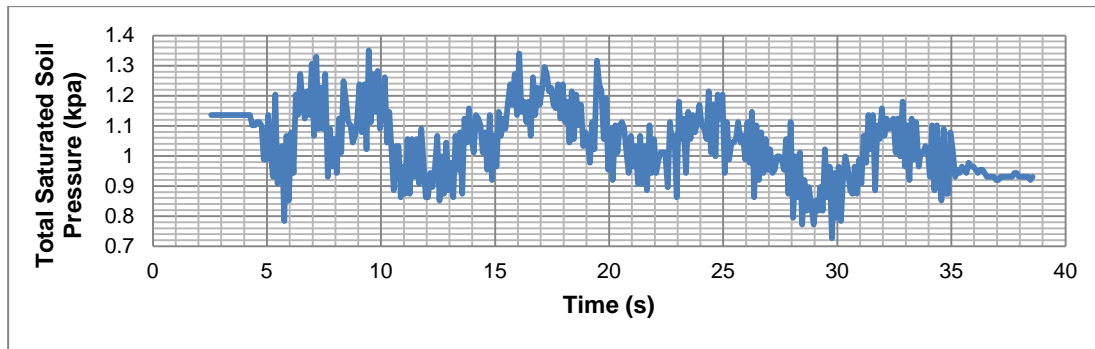


Figure 6.40: Total saturated soil pressures for SP2 for 5 Hz for Soil 1

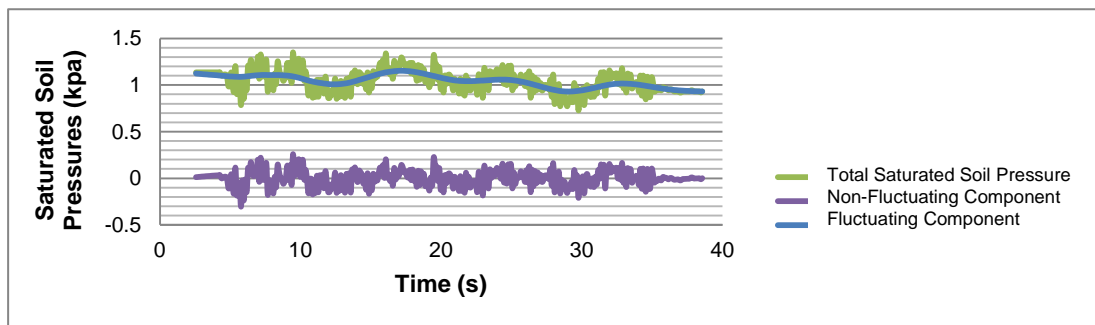


Figure 6.41: Total saturated soil pressures, non-fluctuating and fluctuating components of total saturated soil pressures for SP2 for 5 Hz for Soil 1

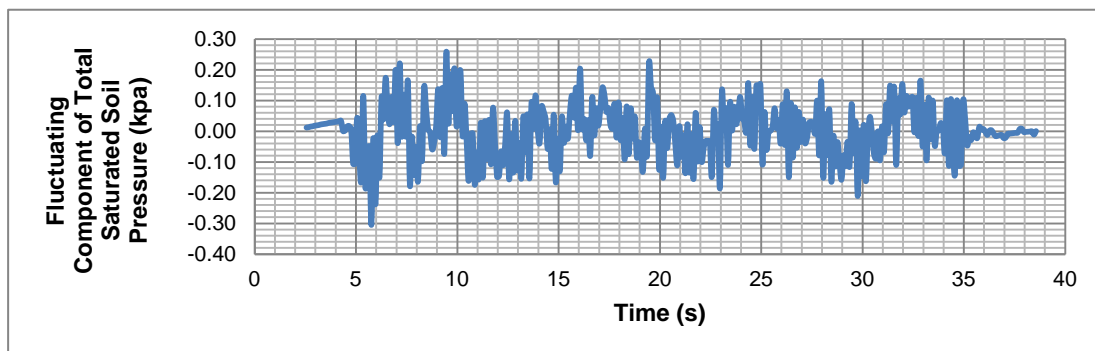


Figure 6.42: Fluctuating components of total saturated soil pressures for SP2 for 5 Hz for Soil 1

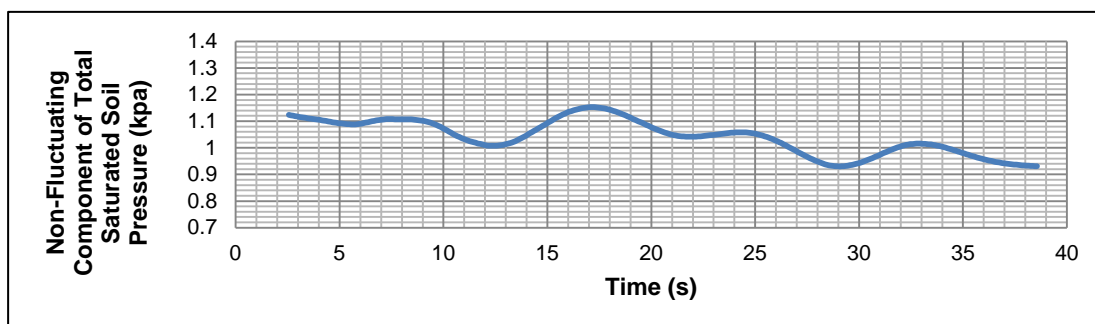


Figure 6.43: Non-fluctuating components of total saturated soil pressures for SP2 for 5 Hz for Soil 1

6.2.1.2.1.4 One Block- Fluctuating and Non-Fluctuating Components of Total Lateral Soil Pressure for 6 Hz for Soil 1

Figure 6.44 - Figure 6.47 show the total saturated soil pressures, non-fluctuating and fluctuating components of total saturated soil pressures of **SP1 for 6 Hz for Soil 1**.

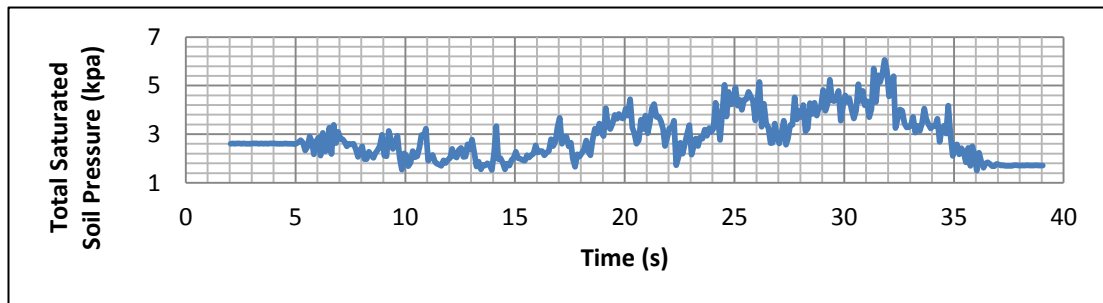


Figure 6.44: Total saturated soil pressures of SP1 for 6 Hz for Soil 1

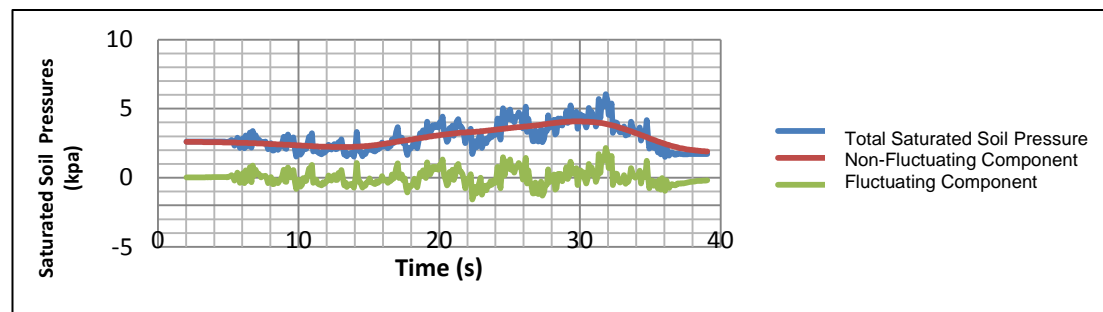


Figure 6.45: Total saturated soil pressures, non-fluctuating and fluctuating components of total saturated soil pressures for SP1 for 6 Hz for Soil 1

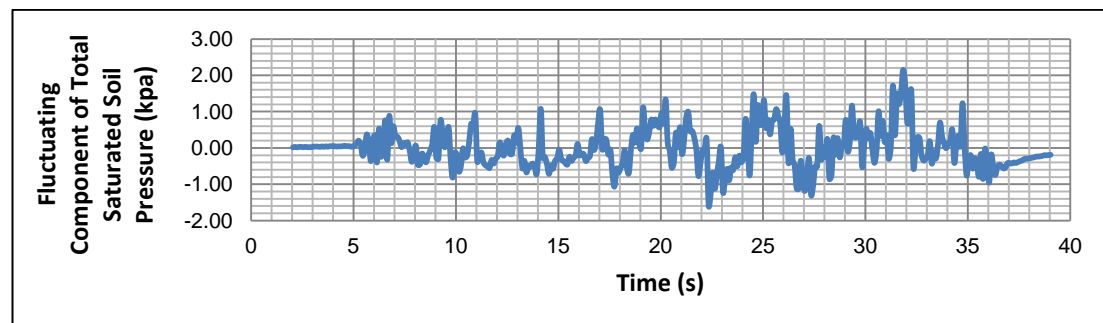


Figure 6.46: Fluctuating components of total saturated soil pressures for SP1 for 6 Hz for Soil 1

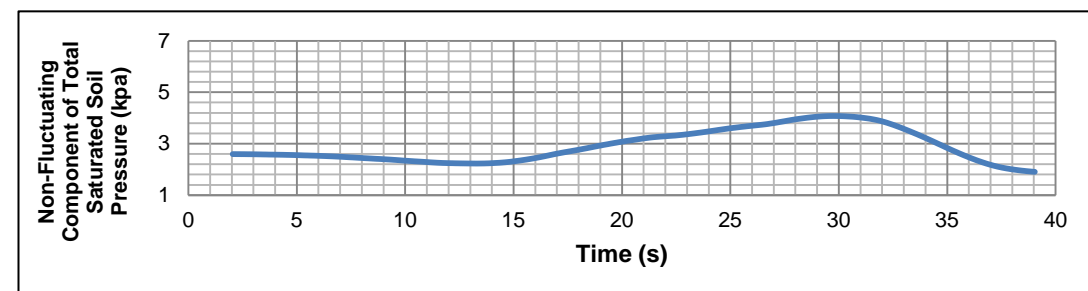


Figure 6.47: Non-fluctuating component s of total saturated soil pressures for SP1 for 6 Hz for Soil 1

Figure 6.48 - Figure 6.51 show the total saturated soil pressures, non-fluctuating and fluctuating components of total saturated soil pressures of **SP2 for 6 Hz for Soil 1**.

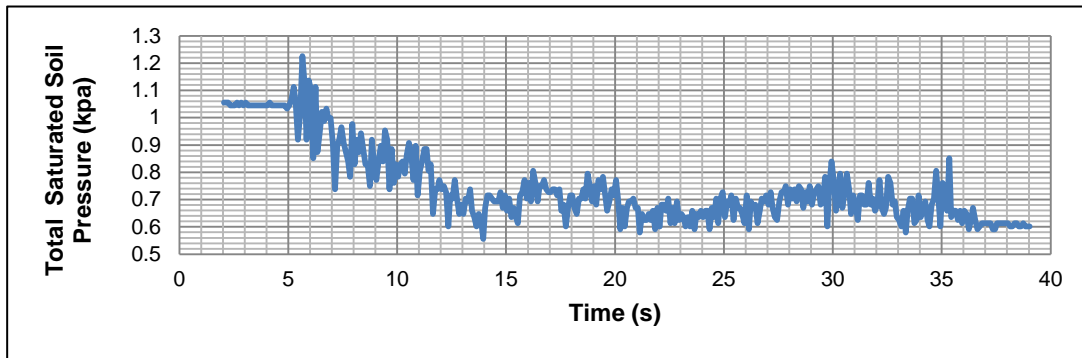


Figure 6.48: Total saturated soil pressures of SP1 for 6 Hz for Soil 1

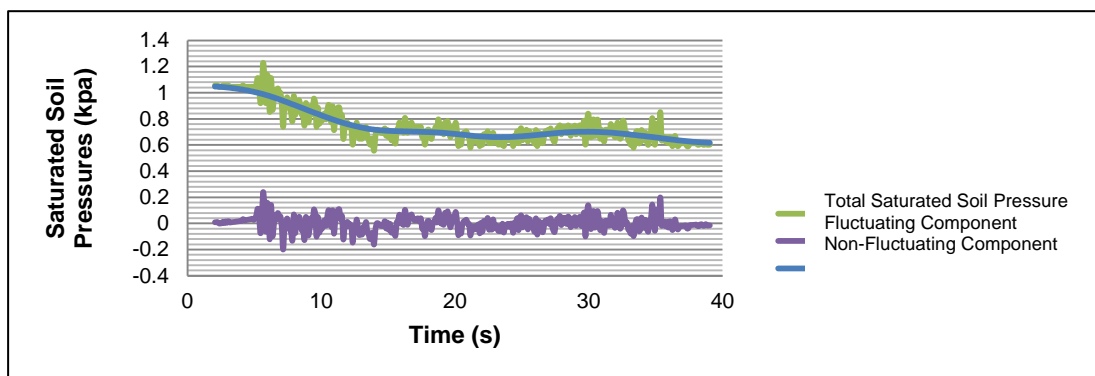


Figure 6.49: Total saturated soil pressures, non-fluctuating and fluctuating components of total saturated soil pressures for SP2 for 6 Hz for Soil 1

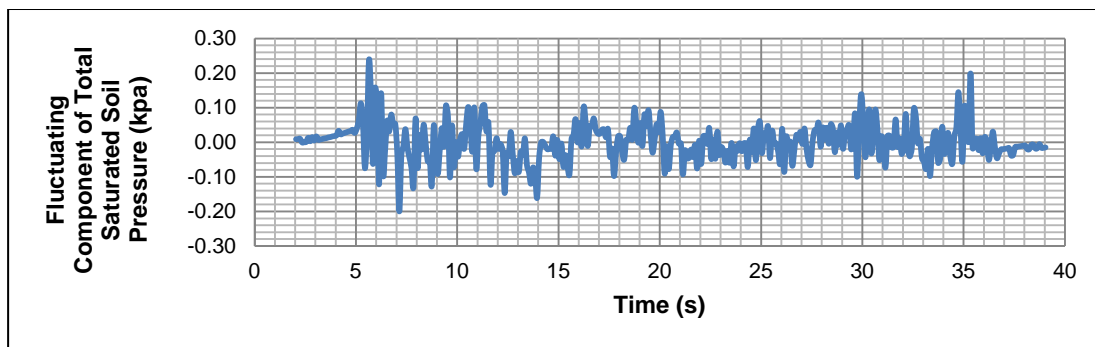


Figure 6.50: Fluctuating components of total saturated soil pressures for SP2 for 6 Hz for Soil 1

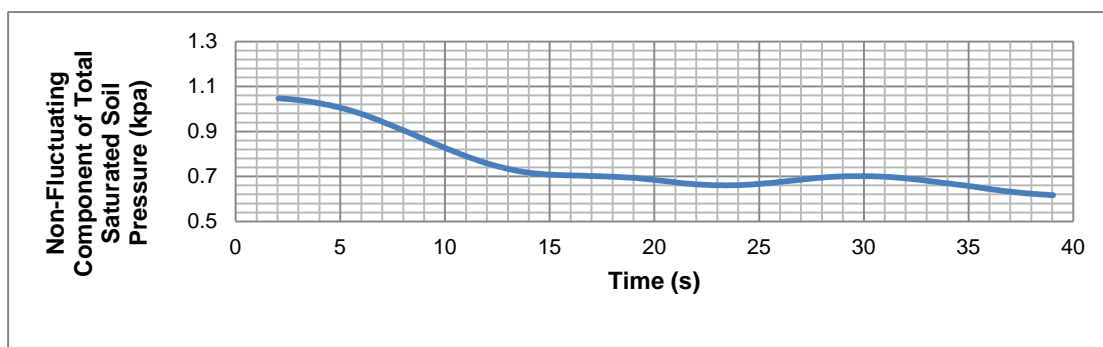


Figure 6.51: Non-fluctuating components of total saturated soil pressures for SP2 for 6 Hz for Soil 1

6.2.1.2.1.5 Maximum Fluctuating Components of Total Saturated Soil Pressures for Soil 1

For the determination of the application point of the soil pressure under dynamic loading, maximum fluctuating component was taken as a reference. Relation between maximum fluctuating components of total saturated soil pressures and depth for each frequency are shown in Table 6.3 and Figure 6.52 for Soil 1.

Table 6.3: Maximum fluctuating components of total saturated soil pressures and before dynamic loading pressure measurements for SP1 and SP2 for Soil 1

Hz	Max Fluctuating Comp. SP1	Max Fluctuating Comp. SP2
2	0.12	0.26
3	0.68	0.65
4	1.28	0.75
5	1.74	0.26
6	2.15	0.24

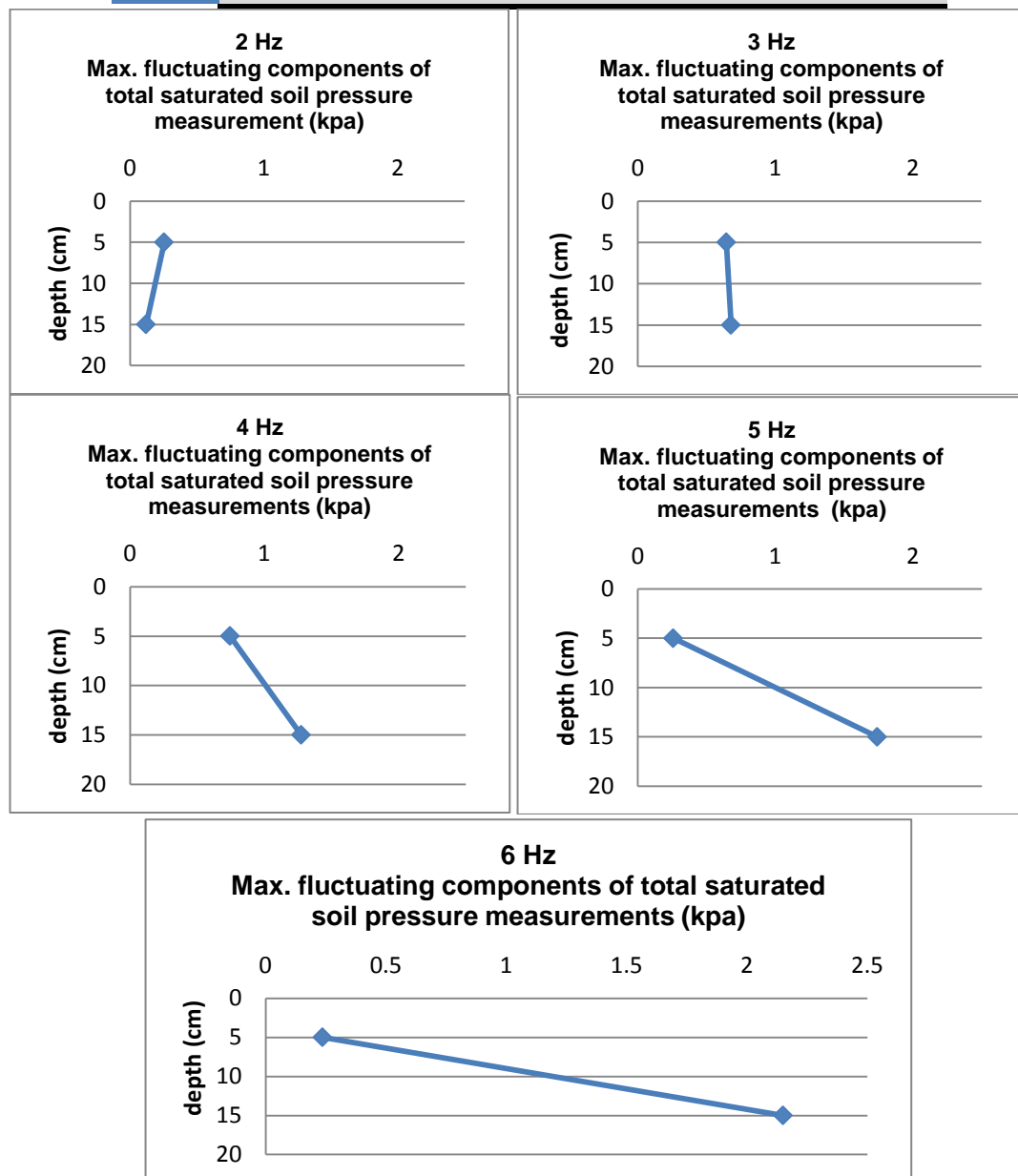


Figure 6.52: Relation between maximum fluctuating components of total saturated soil pressures and depth for Soil 1

As it is seen from Table 6.3 and Figure 6.52 for Soil 1;

- Maximum fluctuating components of total saturated soil pressures increase while depth is increasing for 3, 4, 5 and 6 Hz. Only for 2 Hz, maximum fluctuating components of total saturated soil pressures decrease while depth is increasing since block cannot move during dynamic loading.
- The maximum fluctuating components of total saturated soil pressure of SP1, placed at the bottom side of the block, increases almost linearly (Figure 6.53).

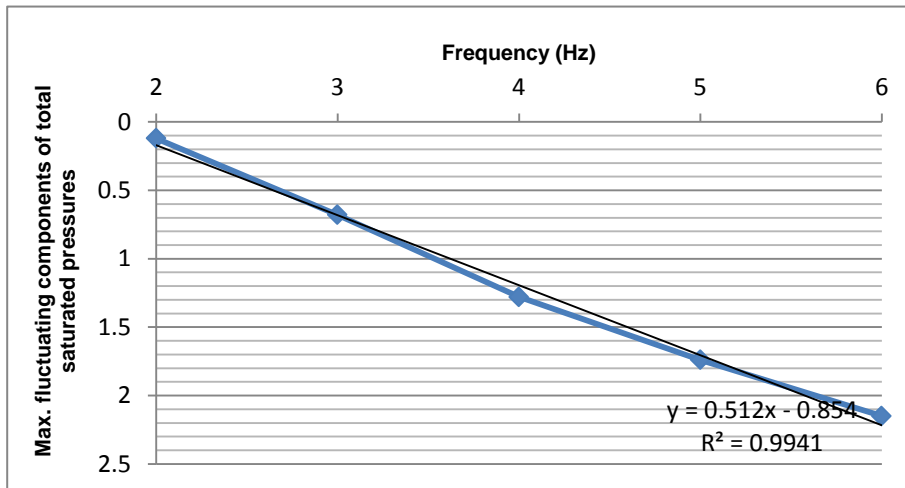


Figure 6.53: Maximum fluctuating components of total saturated soil pressures for SP1 vs. frequency for Soil 1

- However, the maximum fluctuating components of total saturated soil pressure of SP2, placed at the upper side of the block, does not show same trend with SP1 (Figure 6.54). This situation can be explained by the gradual increase of displacements measured on the block during dynamic loading, especially after 4 Hz. Height of the backfill behind the block decreases and the total saturated soil pressures and also fluctuating components of total saturated soil pressure decreases.

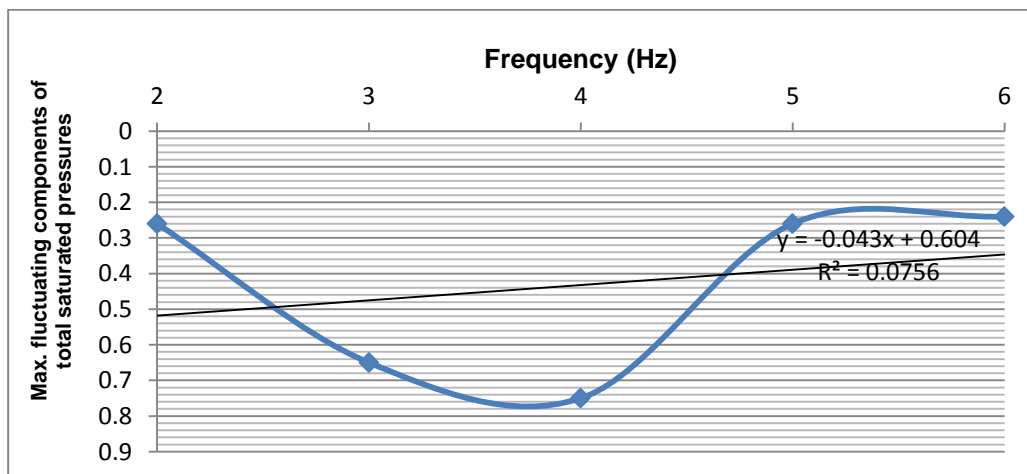


Figure 6.54: Maximum fluctuating components of total saturated soil pressure for SP2 vs. frequency for Soil 1

6.2.1.2.1.6 Maximum Non-Fluctuating Components of Total Saturated Soil Pressures for Soil 1

Relation between maximum non-fluctuating components of total saturated soil pressures and depth for each frequency are shown in Table 6.4 and Figure 6.55.

Table 6.4: Maximum non-fluctuating components of total saturated soil pressures and before dynamic loading pressure measurements for SP1 and SP2 for Soil 1

Hz	Before Dynamic Loading (SP1)	Max Non-Fluctuating Comp. (SP1)	Before Dynamic Loading (SP2)	Max Non-Fluctuating Comp. (SP2)
2	2.37	2.07	1.67	1.31
3	2.60	2.29	1.37	1.32
4	2.53	2.73	1.18	1.22
5	3.09	4.04	1.13	1.15
6	2.61	4.08	1.05	1.05

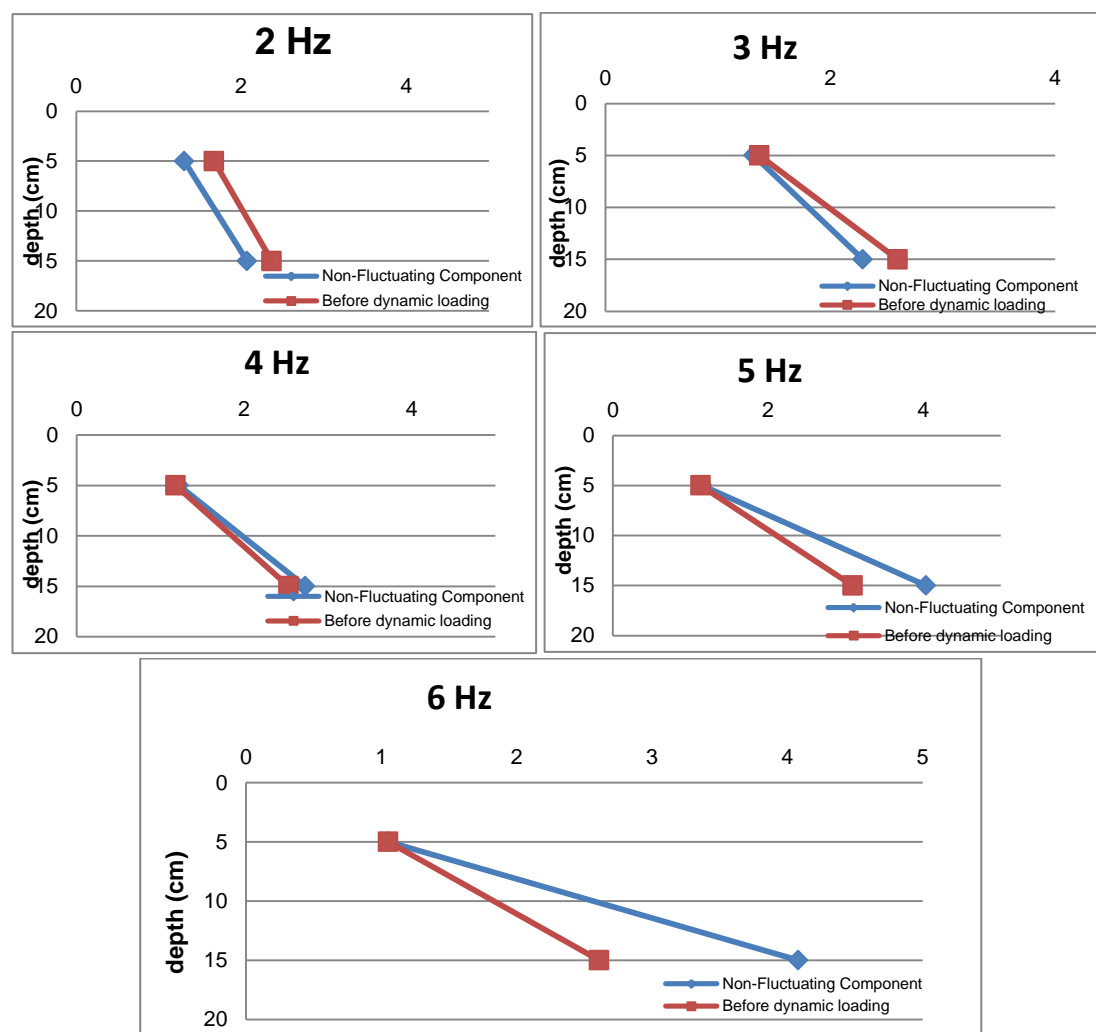


Figure 6.55: Maximum non-fluctuating components of total saturated soil pressure and total saturated soil pressure before dynamic loading for Soil 1

As it is seen from Table 6.4 and Figure 6.55 for Soil 1;

- Maximum non-fluctuating components of total saturated soil pressures and the total saturated soil pressures before dynamic loading increase while depth and frequency is increasing.

- Maximum non-fluctuating components of total saturated soil pressures are greater than the total saturated soil pressure before dynamic loading for 4 Hz, 5 Hz and 6 Hz.
- Maximum non-fluctuating components of total saturated soil pressures are smaller than the total saturated soil pressure before dynamic loading for 2 Hz and 3 Hz. That is simply because no motion is observed on block for 2 Hz and 3 Hz.

6.2.2 One Blok, Soil 2: Total Saturated Soil Pressure Measurements (Test 1.2)

General view of two soil pressure cells (SP1 and SP2) for one block tests for Soil 2- Tests 1.2 is shown in Figure 4.13. In Figure 6.56 - Figure 6.58 soil pressure measurements for each frequency are presented as soil pressure cells placed at 15 cm below the top of the block (SP1) and 5 cm below the top of the block (SP2) (Figure 4.13). As it is seen from the Figure 6.56 - Figure 6.58, soil pressure measurements ranges for 4 Hz – 6 Hz are shown in Table 6.5 for Soil 2.

Table 6.5: Total saturated soil pressure measurements ranges for 2 Hz – 6 Hz for Soil 2

Frequency	Soil Pressure Cells	Ranges of Total Saturated Soil Pressure Measurements
4 Hz	SP1	1.61 kpa - 2.65 kpa
	SP2	0.50 kpa – 1.08 kpa
5 Hz	SP1	1.64 kpa – 2.35 kpa
	SP2	0.45 kpa – 0.72 kpa
6 Hz	SP1	1.50 kpa – 6.05 kpa
	SP2	0.56 kpa - 1.23 kpa

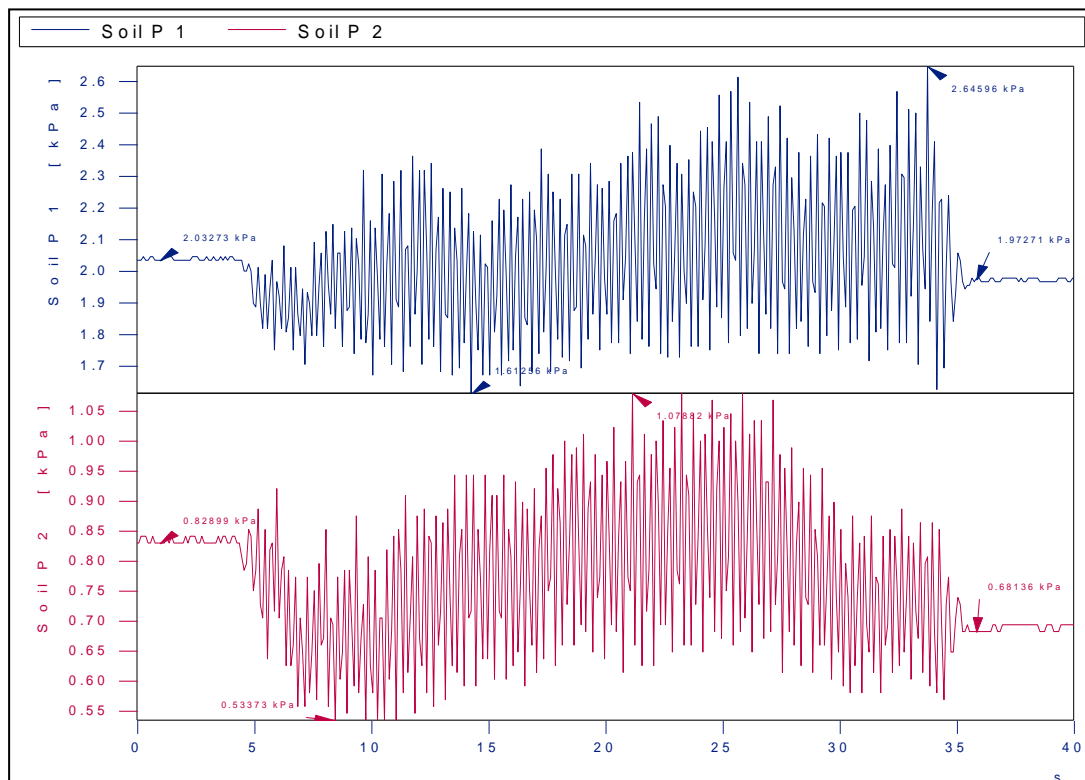


Figure 6.56: Soil pressure measurements for SP1 and SP2 for 4 Hz for Soil 2 (Test 1.2.1)

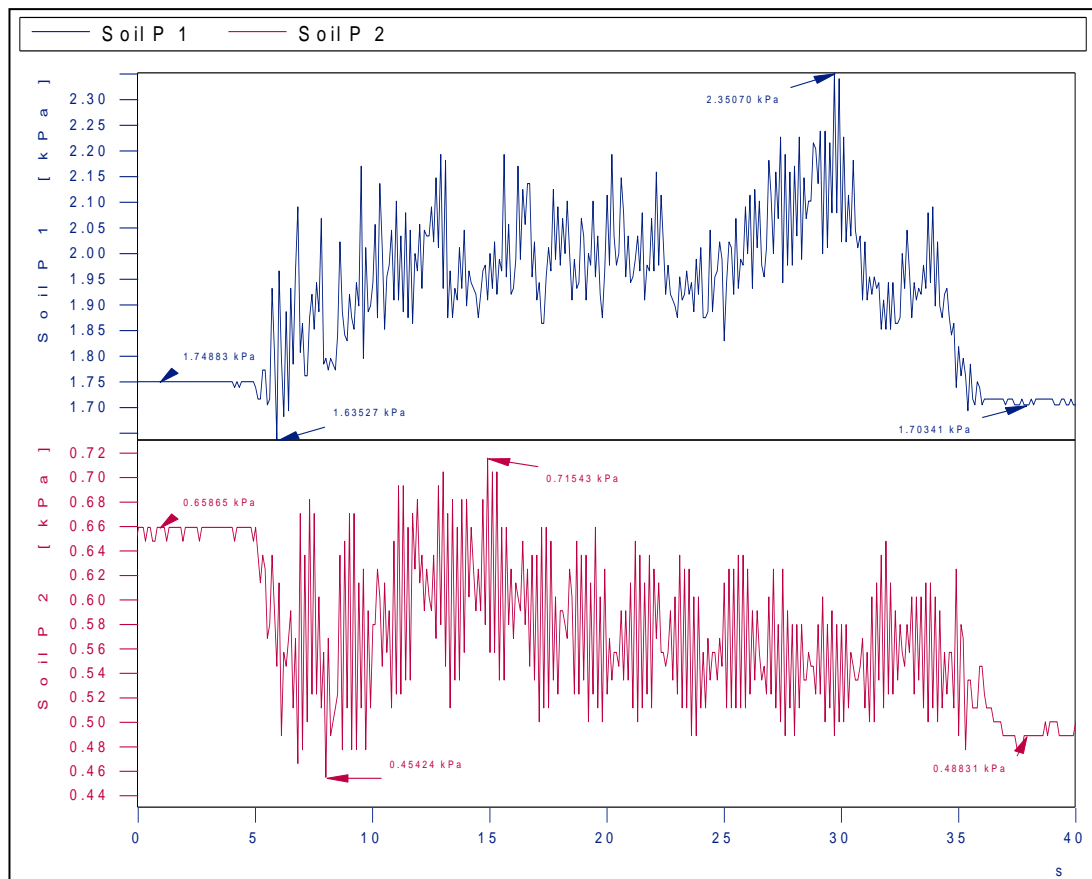


Figure 6.57: Soil pressure measurements for SP1 and SP2 for 5 Hz for Soil 2 (Test 1.2.2)

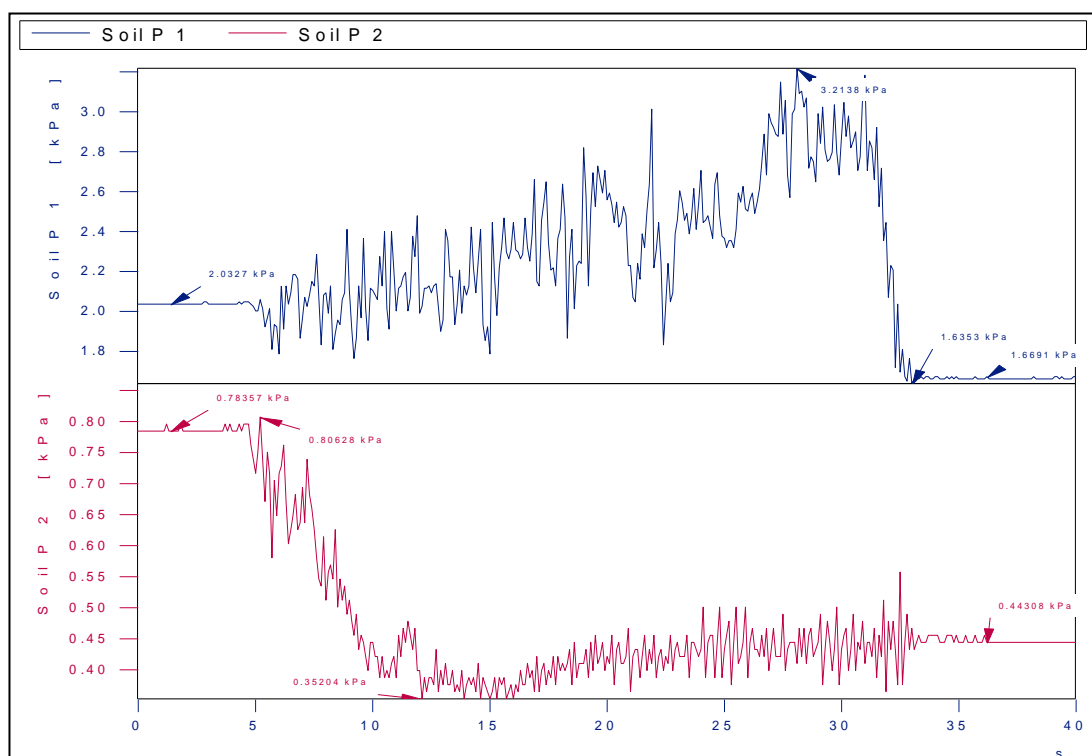


Figure 6.58: Soil pressure measurements for SP1 and SP2 for 6 Hz for Soil 2 (Test 1.2.3)

6.2.2.1 Results of Soil Pressure Measurements (Soil 2)

2 soil pressure cells namely SP1 (located at the bottom of the block) and SP2, (located at the top of the block) were used to define the total saturated soil pressure distribution acting on block for Soil 2 for each frequency (4 Hz - 6 Hz).

For the frequencies 4 Hz - 6 Hz, the total saturated soil pressure measured for two different conditions - before dynamic loading and at the end of (after) dynamic loading - are given in Table 6.6 for Soil 2.

Table 6.6: Total saturated soil pressure measurements for different frequencies before and after dynamic loading for Soil 2

Frequency (Hz)	Soil Pressure Numbers	Total Saturated Soil Pressures (kpa)		
		Before Dynamic Loading (kpa)	After Dynamic Loading (kpa)	Ratio
4	SP1	2.03	1.97	1.03
	SP2	0.83	0.68	1.22
5	SP1	1.75	1.70	1.03
	SP2	0.66	0.49	1.35
6	SP1	2.03	1.67	1.22
	SP2	0.78	0.44	1.77

Total saturated soil pressure measurements for before dynamic loading and after dynamic loading acting on block for each frequency (4 Hz, 5 Hz, 6 Hz) for Soil 2 versus depth relations are given in Figure 6.59.

In contrary to Soil 1 (coarser material), for Soil 2 (finer material), there is no significant sudden decrease are observed within a few seconds on total saturated soil pressure measurements obtained before dynamic loading.

As it is seen from the Figure 6.59 and Table 6.6, for Soil 2;

- The total saturated soil pressure measurements increase while depth is increasing for both before and after dynamic loading for each frequency.
- Total saturated soil pressures measured before dynamic loading almost same with total saturated soil pressures measured after dynamic loading for Soil 2.
- Total saturated soil pressures measured before dynamic loading slightly larger than the total saturated soil pressures measured after dynamic loading for SP1.
- Total saturated soil pressures measured before dynamic loading larger than the total saturated soil pressures measured after dynamic loading for SP2. This result is not only related to compaction of the soil but also related to decrement of backfill height behind the block.

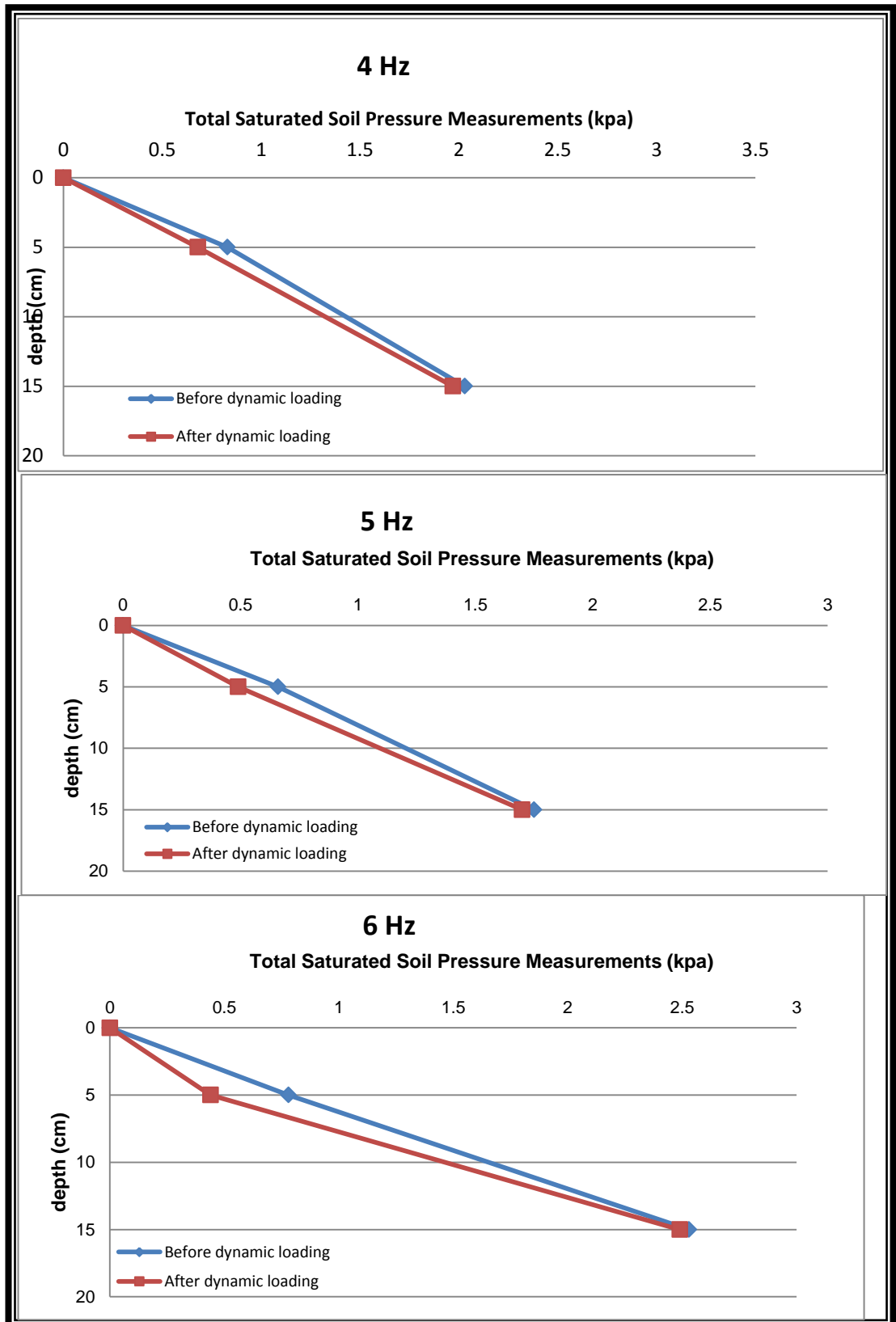


Figure 6.59: Saturated soil pressure measurements acting on block for 4, 5, 6 Hz for Soil 2

6.2.2.2 One Block- Fluctuating and Non-fluctuating Components of Total Saturated Soil Pressures for Soil 2

Total saturated soil pressures, fluctuating and non-fluctuating components of total saturated soil pressures are shown between Figure 6.60 - Figure 6.83 these values are shown for different frequencies for Soil 2.

6.2.2.2.1 One Block- Fluctuating and Non-fluctuating Components of Total Saturated Soil Pressure for 4 Hz for Soil 2

Figure 6.60–Figure 6.63 show the total saturated soil pressures, non-fluctuating and fluctuating components of total saturated soil pressures of SP1 for 4 Hz for Soil 2.

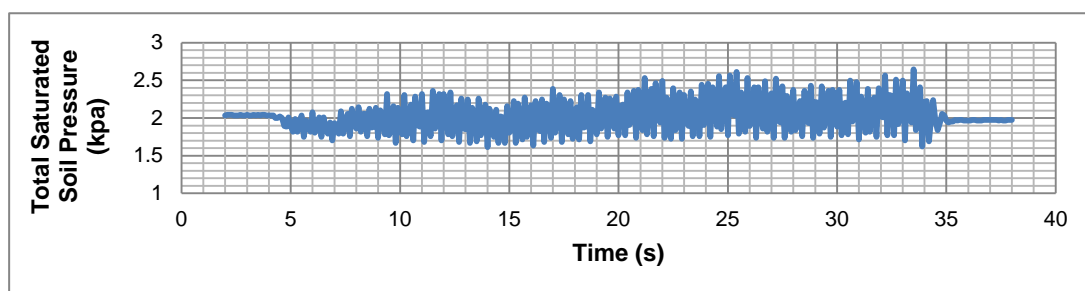


Figure 6.60: Total saturated soil pressure for SP1 for 4 Hz for Soil 2

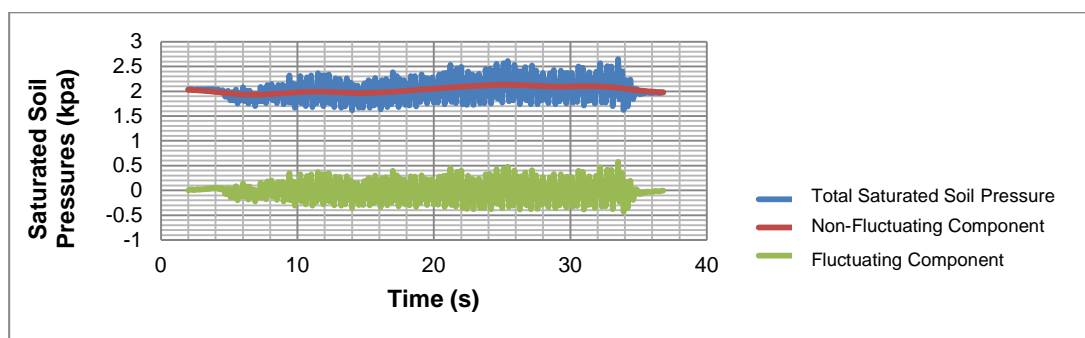


Figure 6.61: Total saturated soil pressure, non-fluctuating and fluctuating components of total saturated soil pressure for SP1 for 4 Hz for Soil 2

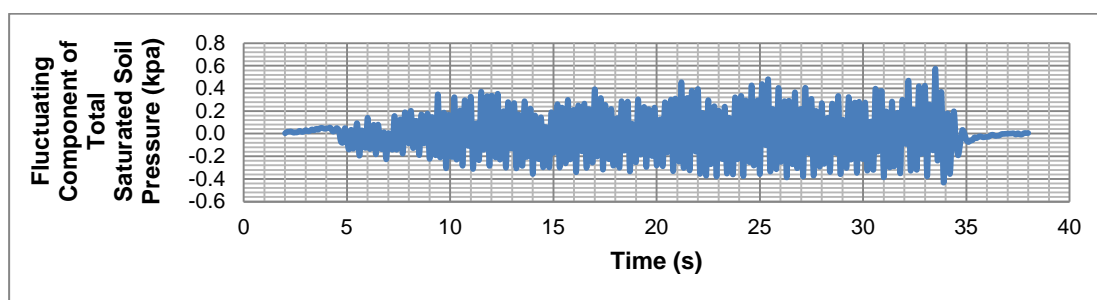


Figure 6.62: Fluctuating components of total saturated soil pressures for SP1 for 4 Hz for Soil 2

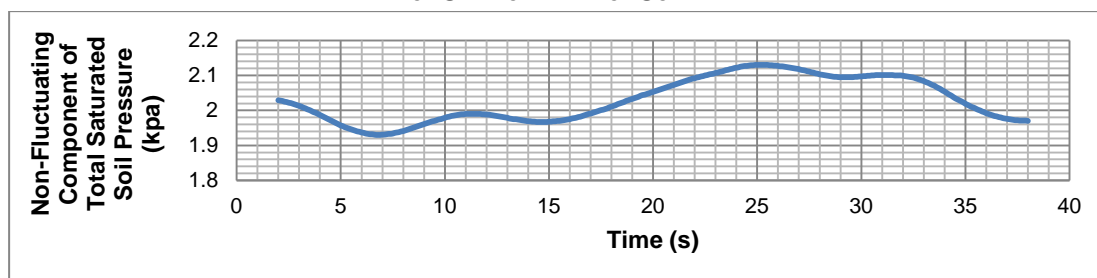


Figure 6.63: Non-fluctuating components of total saturated soil pressures for SP1 for 4 Hz for Soil 2

Figure 6.64 - Figure 6.67 show the total saturated soil pressures, non-fluctuating and fluctuating components of total saturated soil pressures of **SP2 for 4 Hz for Soil 2.**

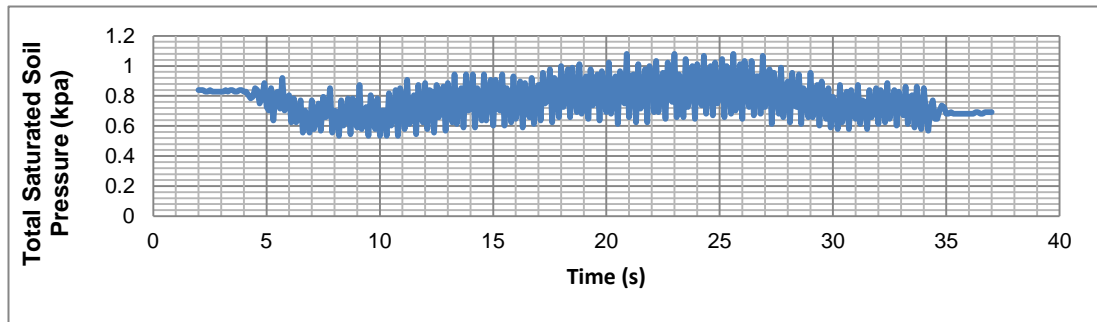


Figure 6.64: Total saturated soil pressures for SP2 for 4 Hz for Soil 2

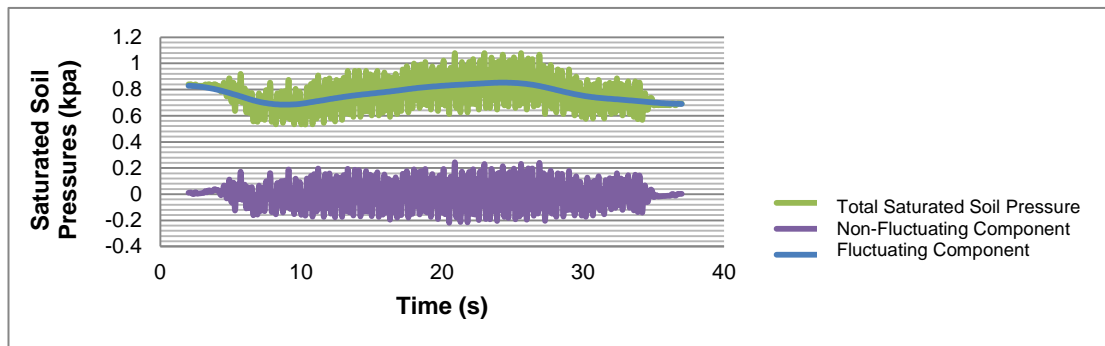


Figure 6.65: Total saturated soil pressure, non-fluctuating and fluctuating components of total saturated soil pressures for SP2 for 4 Hz for Soil 2

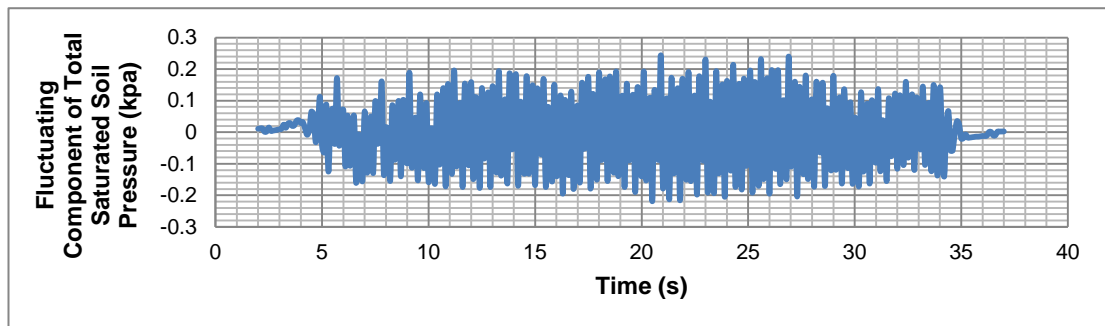


Figure 6.66: Fluctuating components of total saturated soil pressures for SP2 for 4 Hz for Soil 2

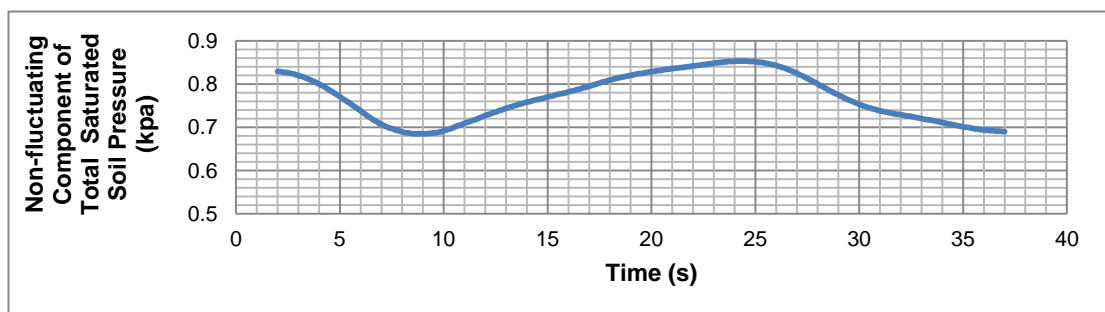


Figure 6.67: Non-fluctuating components of total saturated soil pressures for SP2 for 4 Hz for Soil 2

6.2.2.2.2 One Block- Fluctuating and Non-Fluctuating Components of Total Soil Pressure for 5 Hz for Soil 2

Figure 6.68 - Figure 6.71 show the total saturated soil pressures, non-fluctuating and fluctuating components of total saturated soil pressures of **SP2 for 5 Hz for Soil 2**.

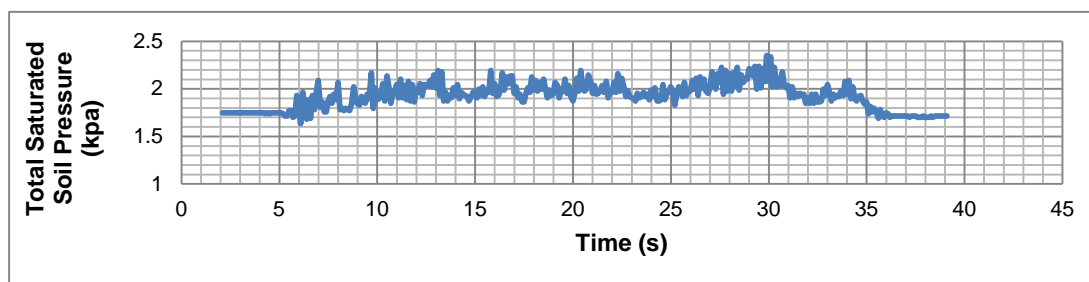


Figure 6.68: Total saturated soil pressures for SP1 for 5 Hz for Soil 2

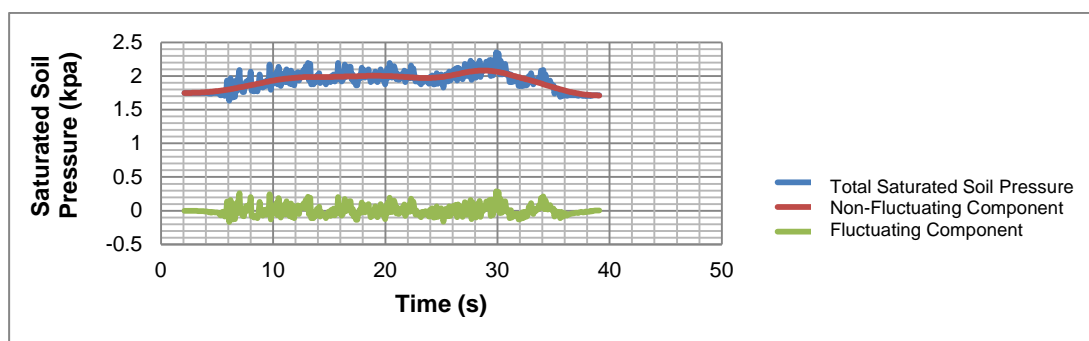


Figure 6.69: Total saturated soil pressure, non-fluctuating and fluctuating components of total saturated soil pressures for SP1 for 5 Hz for Soil 2

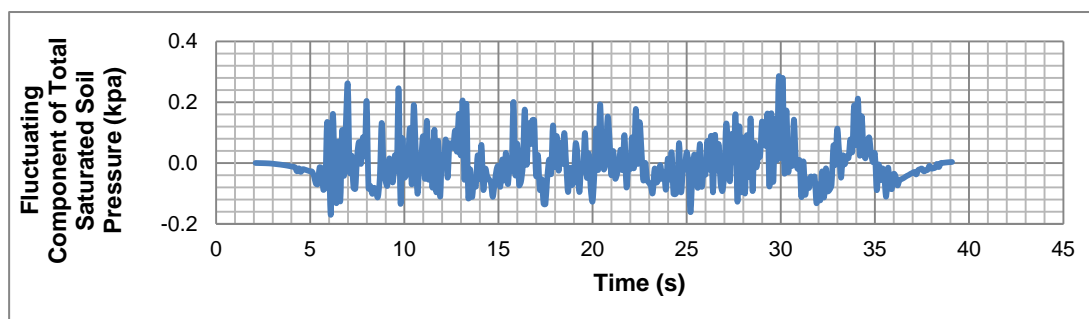


Figure 6.70: Fluctuating components of total saturated soil pressures for SP1 for 5 Hz for Soil 2

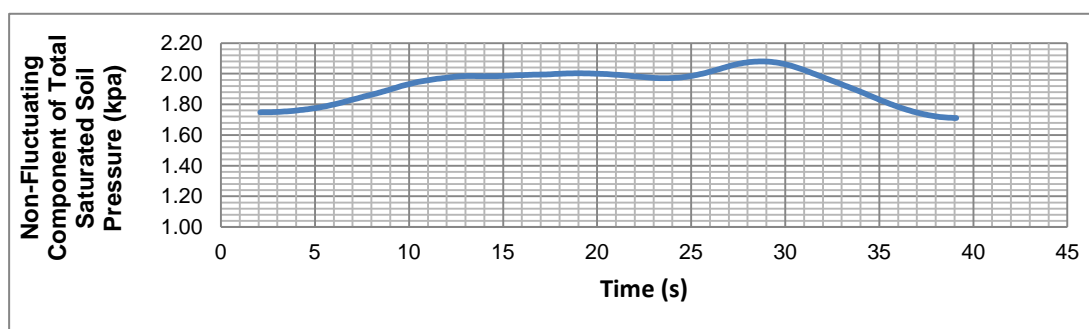


Figure 6.71: Non-fluctuating components of total saturated soil pressures for SP1 for 5 Hz for Soil 2

Figure 6.72 - Figure 6.75 show the total saturated soil pressures, non-fluctuating and fluctuating components of total saturated soil pressures of **SP2 for 5 Hz for Soil 2**.

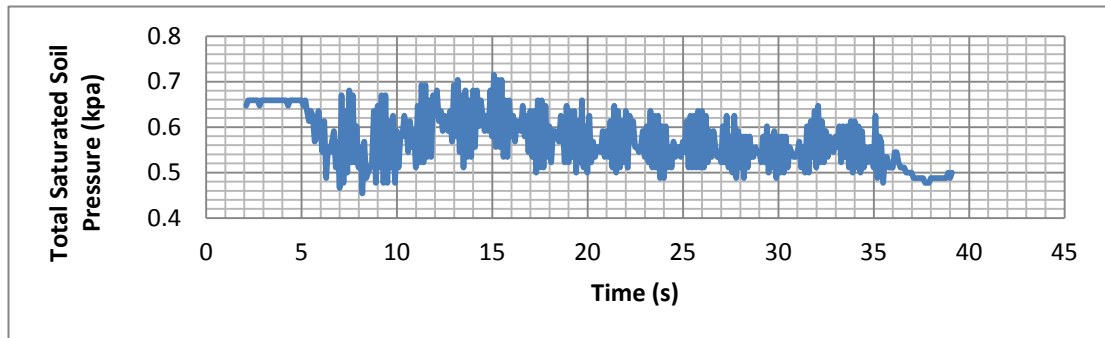


Figure 6.72: Total saturated soil pressures for SP2 for 5 Hz for Soil 2

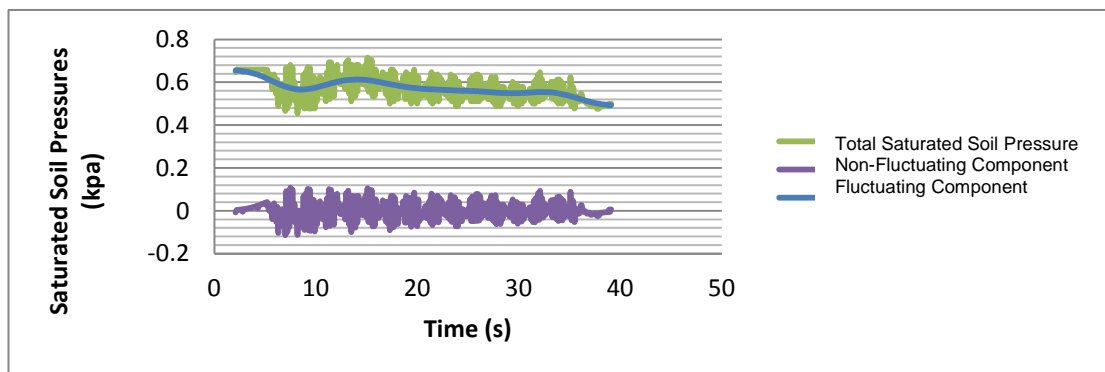


Figure 6.73: Total saturated soil pressure, non-fluctuating and fluctuating components of total saturated soil pressures for SP2 for 5 Hz

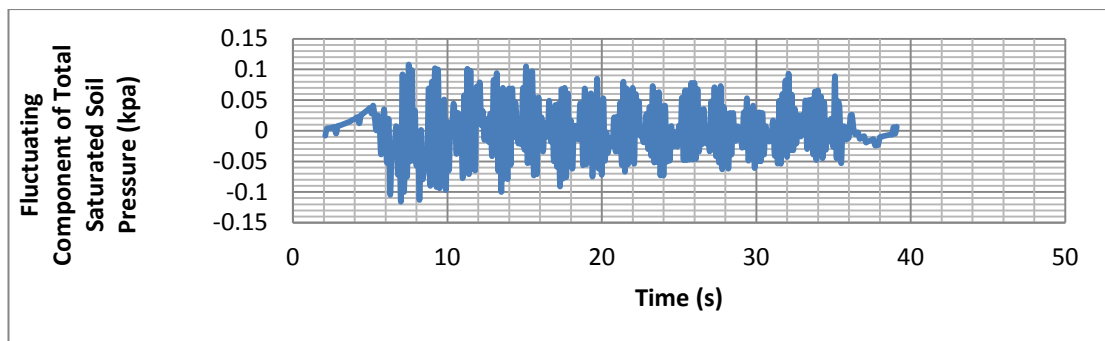


Figure 6.74: Fluctuating components of total saturated soil pressures for SP2 for 5 Hz

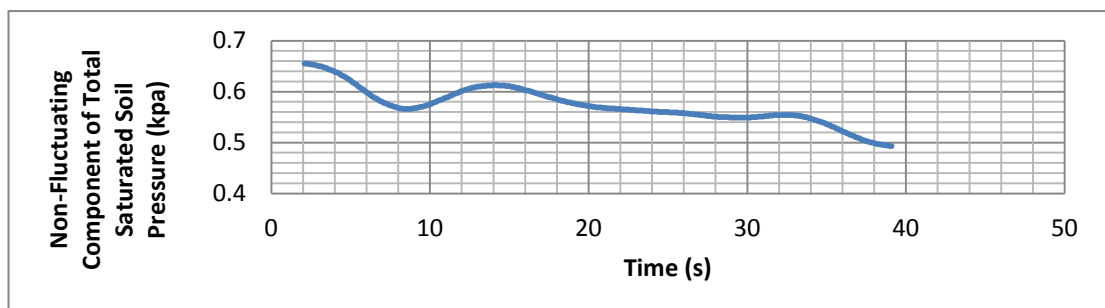


Figure 6.75: Non-fluctuating components of total saturated soil pressures for SP2 for 5 Hz for Soil 2

6.2.2.2.3 One Block- Fluctuating and Non-Fluctuating Components of Total Soil Pressure for 6 Hz for Soil 2

Figure 6.76 - Figure 6.79 show the total saturated soil pressures, non-fluctuating and fluctuating components of total saturated soil pressures of SP1 for 6 Hz for Soil 2.

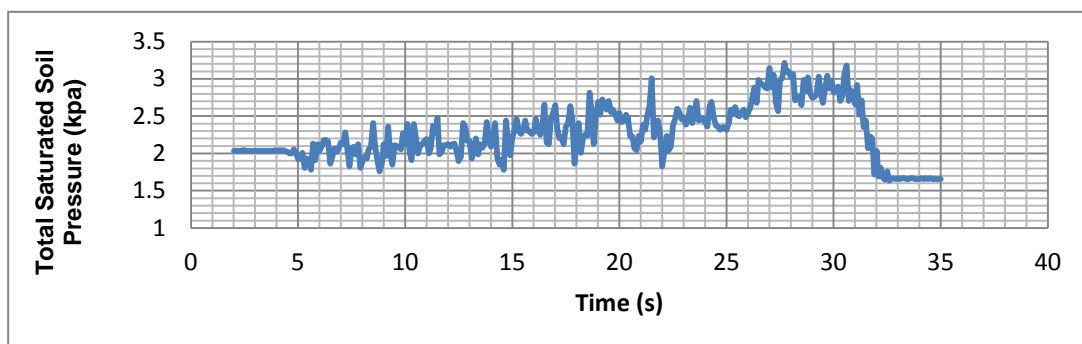


Figure 6.76: Total saturated soil pressures for SP1 for 6 Hz for Soil 2

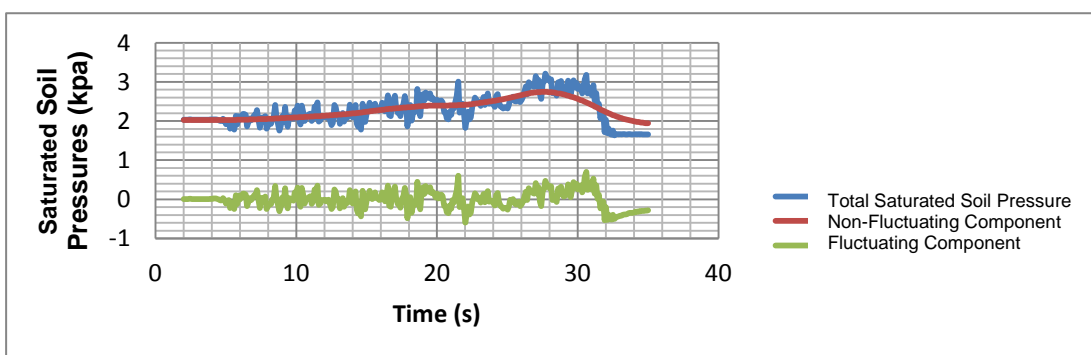


Figure 6.77: Total saturated soil pressure, non-fluctuating and fluctuating components of total saturated soil pressures for SP1 for 6 Hz for Soil 2

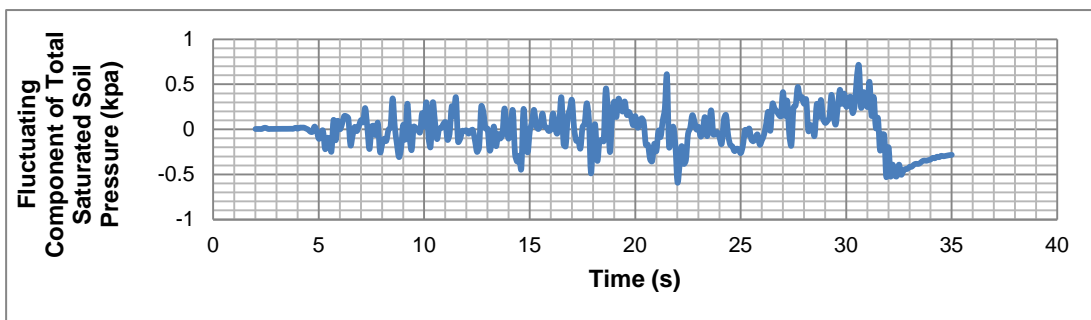


Figure 6.78: Fluctuating components of total saturated soil pressures for SP1 for 6 Hz for Soil 2

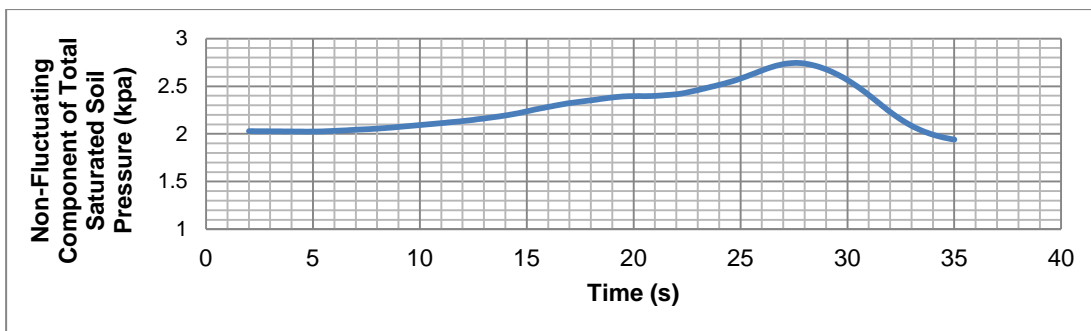


Figure 6.79: Non-fluctuating components of total saturated soil pressures for SP1 for 6 Hz for Soil 2

Figure 6.80 - Figure 6.83 show the total saturated soil pressures, non-fluctuating and fluctuating components of total saturated soil pressures of SP2 for 6 Hz for Soil 2.

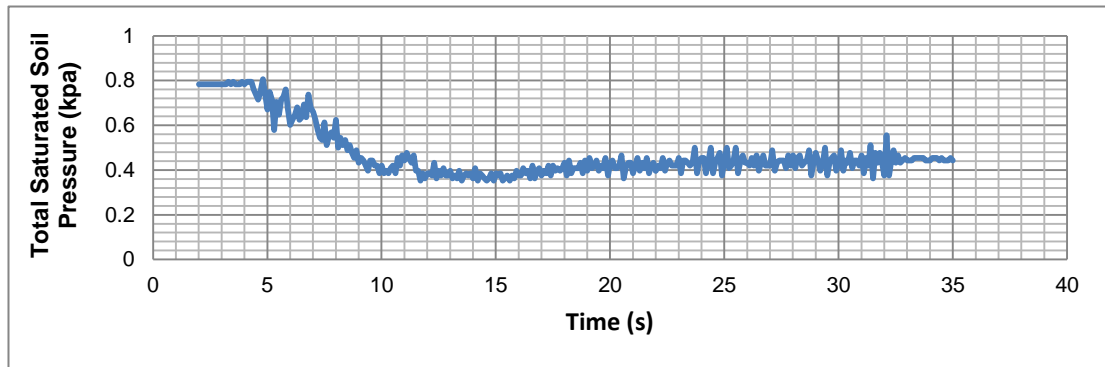


Figure 6.80: Total saturated soil pressures for SP2 for 6 Hz for Soil 2

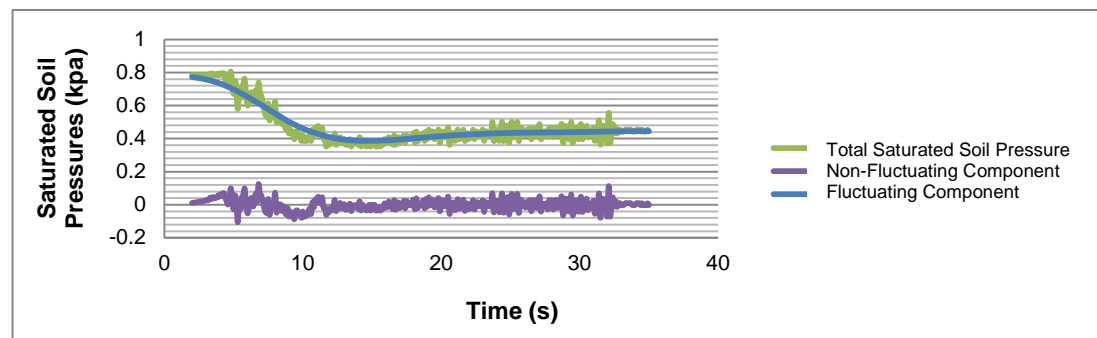


Figure 6.81: Total saturated soil pressure, non-fluctuating and fluctuating components of total saturated soil pressures for SP2 for 6 Hz for Soil 2

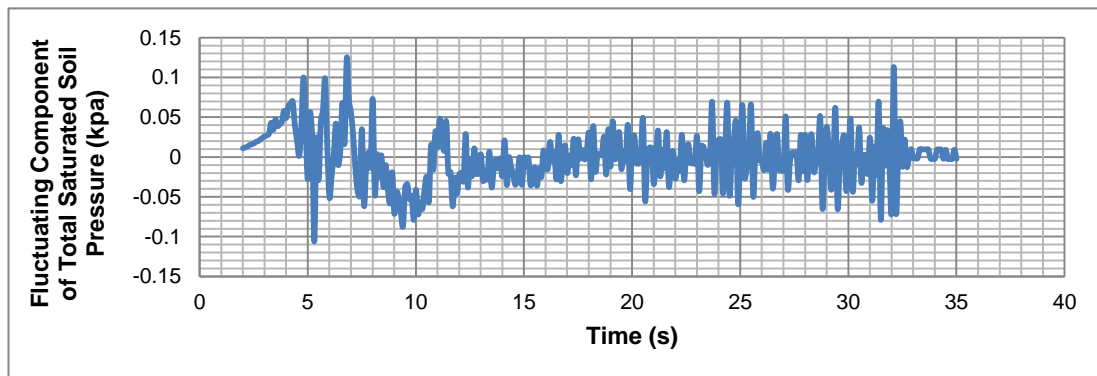


Figure 6.82: Fluctuating components of total saturated soil pressures for SP2 for 6 Hz for Soil 2

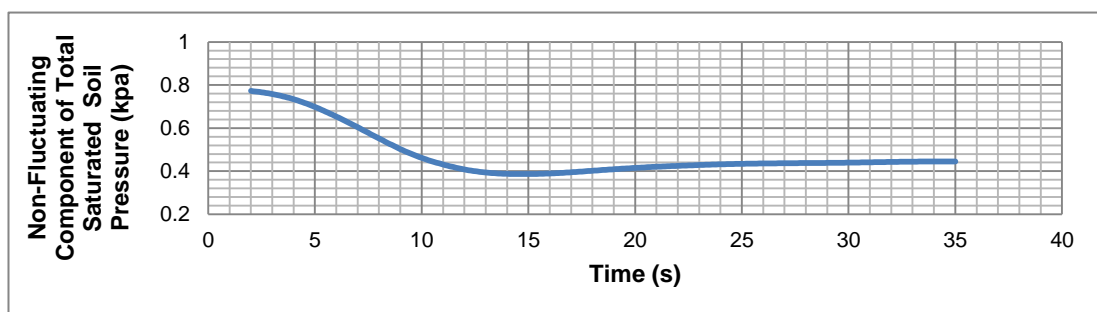


Figure 6.83: Non - fluctuating components of total saturated soil pressures for SP2 for 6 Hz for Soil 2

6.2.2.2.3.1 Maximum Fluctuating Components of Total Saturated Soil Pressures for Soil 2

Relation between maximum fluctuating components of total saturated soil pressures and depth for each frequency are shown in Table 6.7 and Figure 6.84 for Soil 2.

Table 6.7: Maximum fluctuating components of total saturated soil pressures and before dynamic loading pressure measurements for SP1 and SP2 for Soil 2

Hz	Max Fluctuating Comp. SP1	Max Fluctuating Comp. SP2
4	0.58	0.24
5	0.29	0.11
6	0.71	0.12

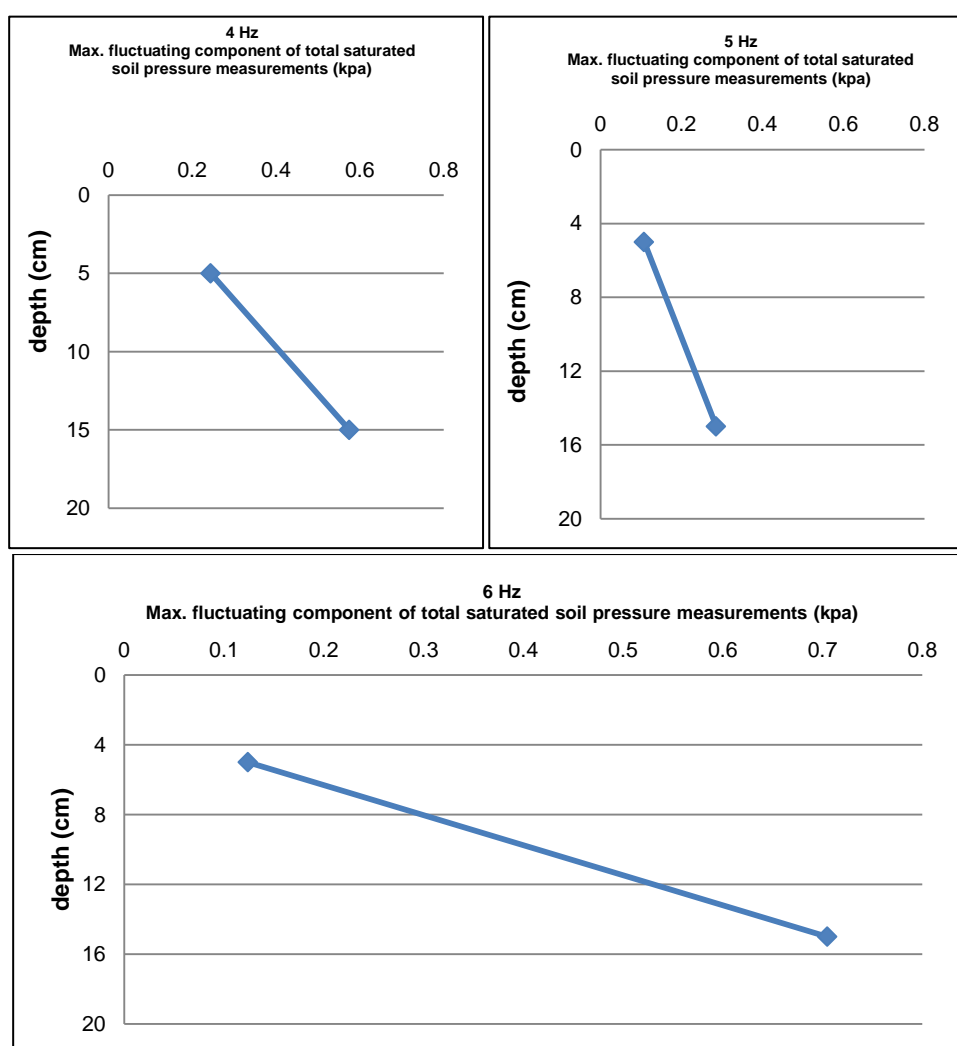


Figure 6.84: Relation between maximum fluctuating component of total saturated soil pressure versus depth for Soil 2

As it is seen from Table 6.7– Figure 6.84 for Soil 2;

- Maximum fluctuating components of total saturated soil pressures increase while depth is increasing for 4, 5 and 6 Hz.

6.2.2.2.3.2 Maximum Non-Fluctuating Components of Total Saturated Soil Pressures for Soil 2

Relation between maximum non-fluctuating components of total saturated soil pressures and depth for each frequency are shown in Table 6.8 and Figure 6.85.

Table 6.8: Maximum non- fluctuating components of total saturated soil pressures and before dynamic loading pressure measurements for SP1 and SP2 for Soil 2

Hz	Before Dynamic Loading SP1	Max Non-Fluctuating Comp. SP1	Before Dynamic Loading SP2	Max Non-Fluctuating Comp. SP2
4	2.03	2.13	0.83	0.85
5	1.75	2.08	0.66	0.66
6	2.03	2.75	0.78	0.77

As it is seen from Table 6.8 and Figure 6.85 for Soil 2;

- Maximum non-fluctuating components of total saturated soil pressures and the total saturated soil pressures before dynamic loading increase while depth and frequency is increasing.
- Maximum non-fluctuating components of total saturated soil pressures are greater than the total saturated soil pressure before dynamic loading for 4 Hz, 5 Hz and 6 Hz.

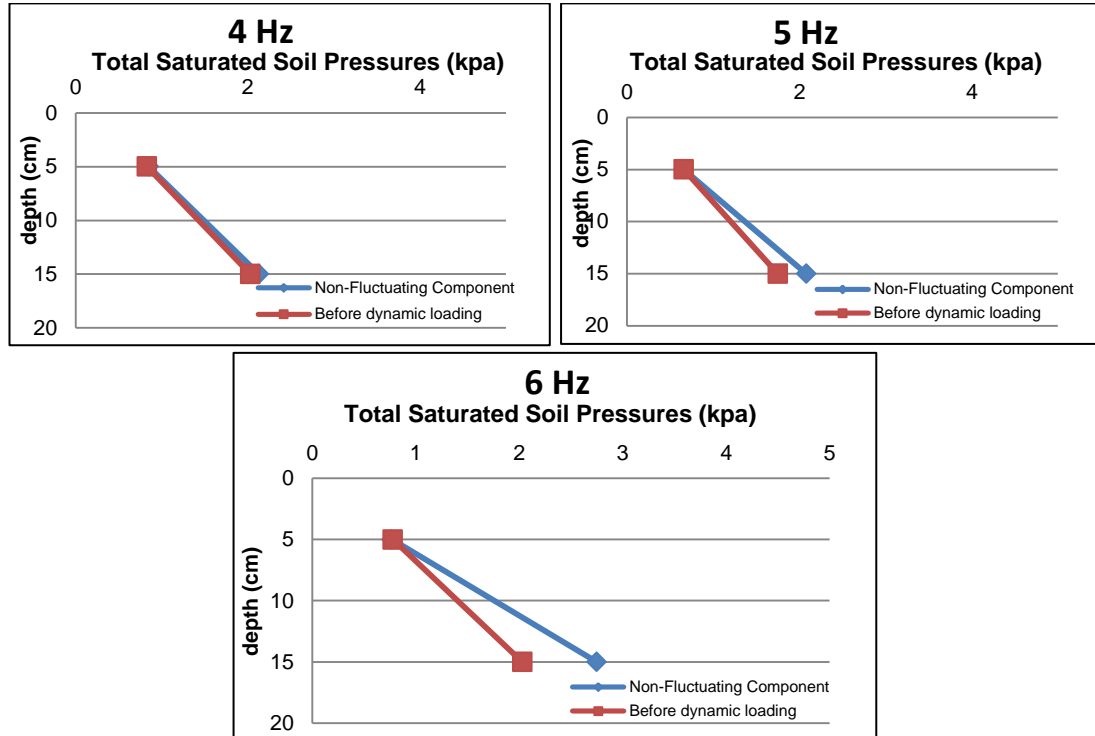


Figure 6.85: Maximum non-fluctuating components of total saturated soil pressure and total saturated soil pressure before dynamic loading for Soil 2

6.3 Two Blocks, Soil 1: Soil Pressure Measurements (Test 2.1 and Test 2.2)

Soil pressure measurements and results are presented for each series for Soil 1 with 5 tests (2 Hz, 3 Hz, 4 Hz, 5 Hz, 6 Hz) and for Soil 2 with 3 tests (4 Hz, 5 Hz, 6 Hz) for two blocks.

General view of four soil pressure cells (SP1, SP2, SP3, and SP4) for two blocks tests for Soil 1- Tests 2.1 and for Soil 2 - Test 2.2 are shown in Figure 6.86.

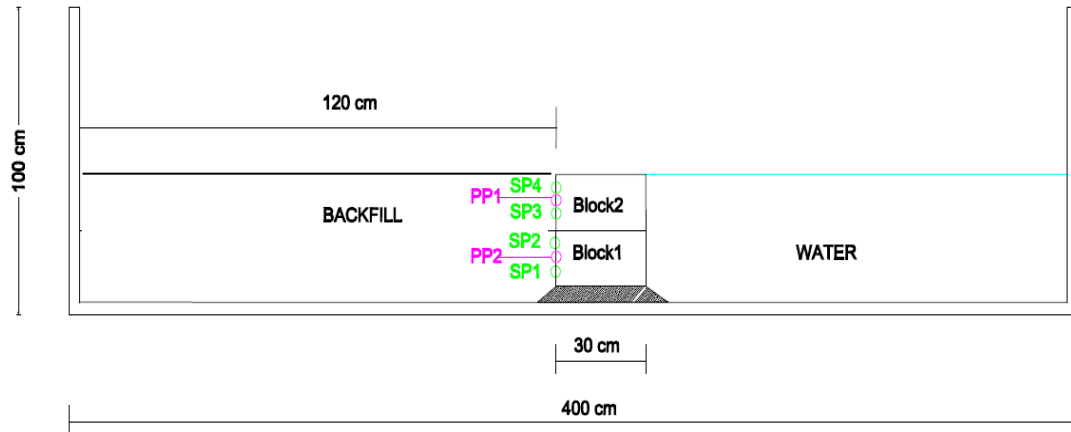


Figure 6.86: General view of four soil pressure cells (SP1, SP2, SP3, and SP4) and pore pressure cells (PP1, PP2) for two blocks tests for Soil 1 and Soil 2

6.3.1 Two Blocks, Soil 1: Soil Pressure Measurements (Test 2.1)

In Figure 6.88 - Figure 6.92 total saturated soil pressure measurements for each frequency are presented as soil pressure cells placed at 5 cm -15 cm below the top of the Block 2 (SP4 and SP3) and 25 cm – 35 cm below the top of the Block 2 (SP2 and SP1) (Figure 6.86).

Figure 6.87 Figure 6.87 show the general view of the experiment set up of the two blocks tests for Soil 1.



Figure 6.87: Block, instruments, dummies and Soil 1

As it is seen from the Figure 6.88 - Figure 6.92, total saturated soil pressure measurements ranges under dynamic loading for 2 Hz – 6 Hz are shown in Table 6.9 for Soil 1.

Table 6.9: Total saturated soil pressure measurements ranges for
2 Hz – 6 Hz for Soil 1

Frequency	Soil Pressure Cells	Ranges of Total Saturated Soil Pressure Measurements
2 Hz	SP1	4.59 kpa – 5.04 kpa
	SP2	3.60 kpa – 3.76 kpa
	SP3	2.03 kpa – 2.43 kpa
	SP4	0.90 kpa – 1.32 kpa
3 Hz	SP1	4.11 kpa – 4.87 kpa
	SP2	3.17 kpa – 3.93 kpa
	SP3	1.68 kpa – 2.23 kpa
	SP4	0.81 kpa – 1.28 kpa
4 Hz	SP1	7.54 kpa – 3.66 kpa
	SP2	2.85 kpa – 4.47 kpa
	SP3	1.59 kpa – 3.45 kpa
	SP4	0.60 kpa – 1.42 kpa
5 Hz	SP1	3.63 kpa – 5.98 kpa
	SP2	2.68 kpa – 6.84 kpa
	SP3	1.37 kpa – 4.07 kpa
	SP4	0.63 kpa – 1.64 kpa
6 Hz	SP1	3.74 kpa – 5.72 kpa
	SP2	2.67 kpa – 4.82 kpa
	SP3	1.37 kpa – 4.66 kpa
	SP4	0.49 kpa – 1.07 kpa

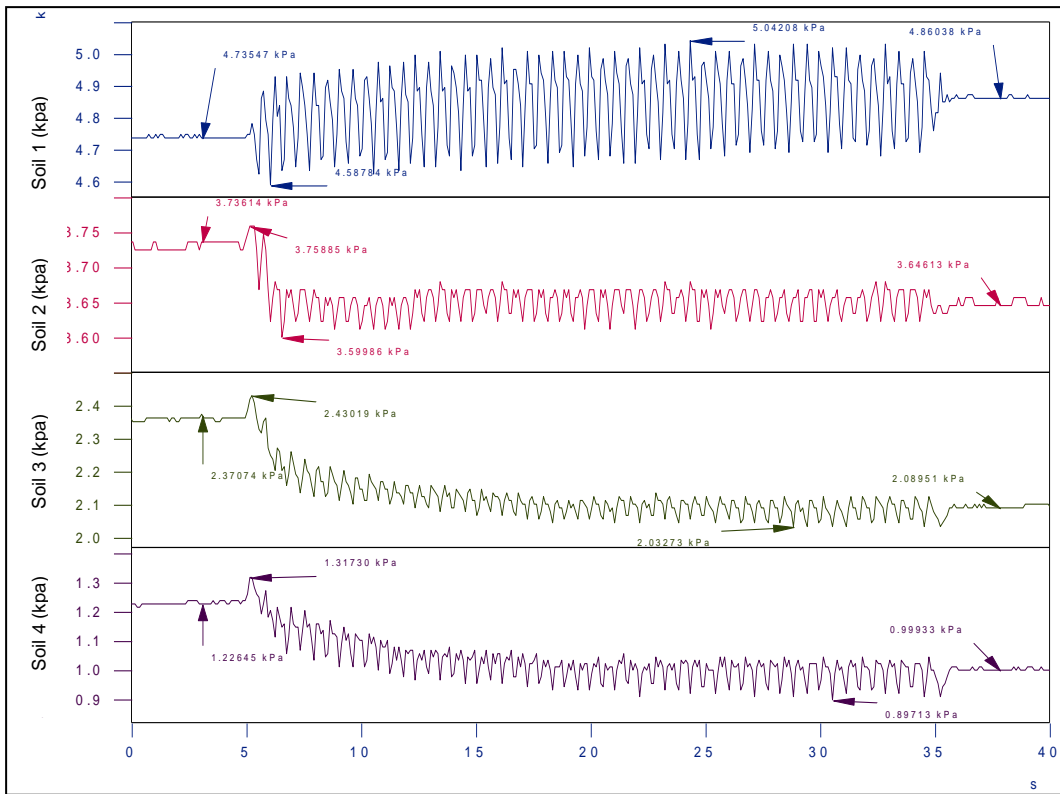


Figure 6.88: Soil pressure measurements for SP1, SP2, SP3 and SP4 for 2 Hz for Soil 1 (Test 2.2.1)

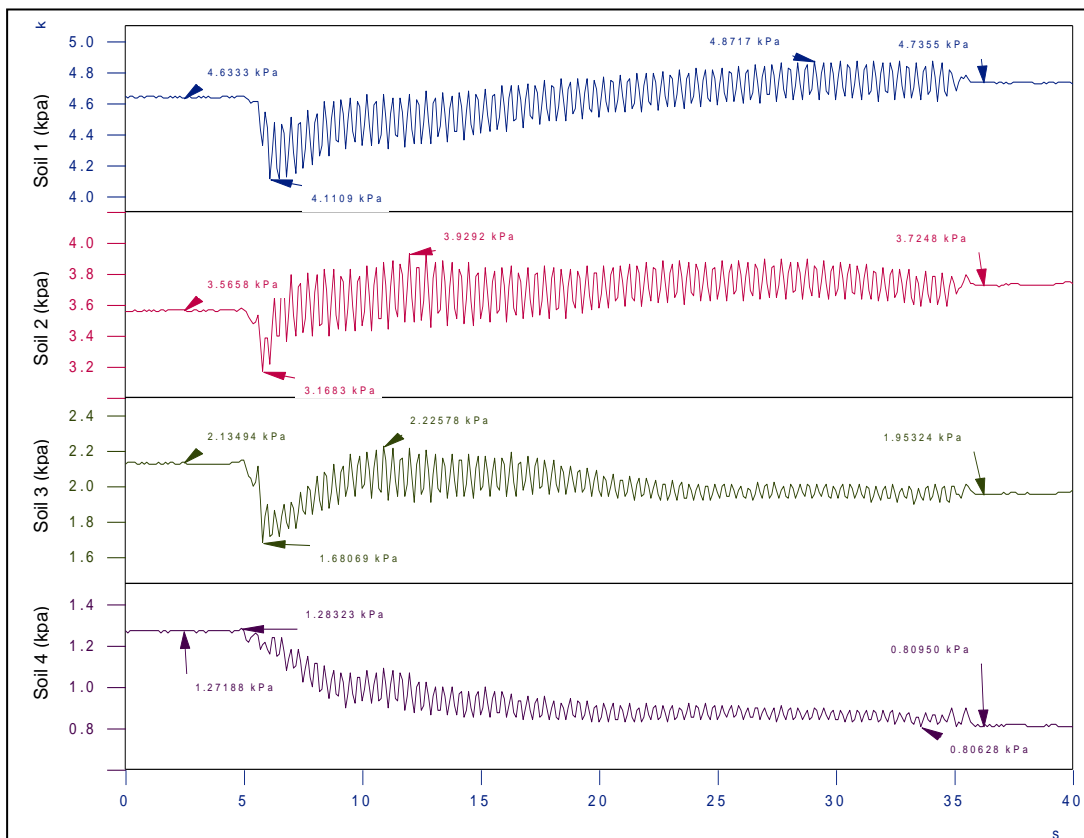


Figure 6.89: Soil pressure measurements for SP1, SP2, SP3 and SP4 for 3 Hz for Soil 1 (Test 2.2.2)

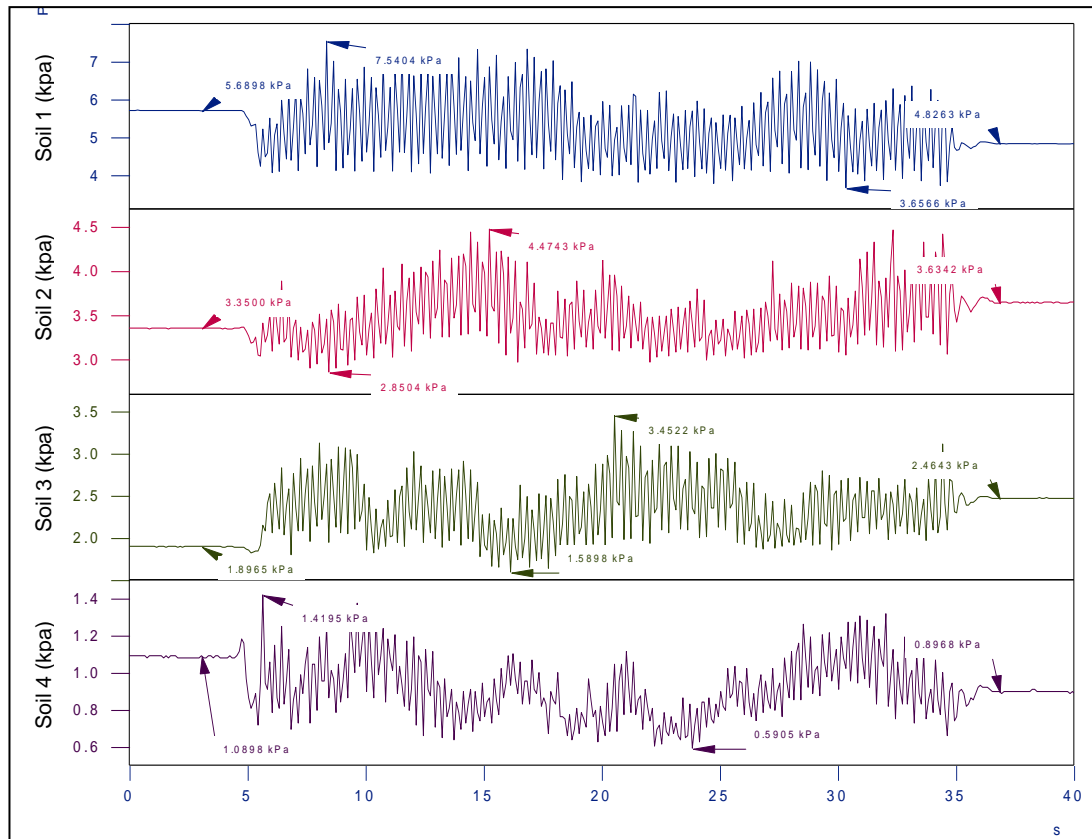


Figure 6.90: Soil pressure measurements for SP1, SP2, SP3 and SP4 for 4 Hz for Soil 1 (Test 2.2.3)

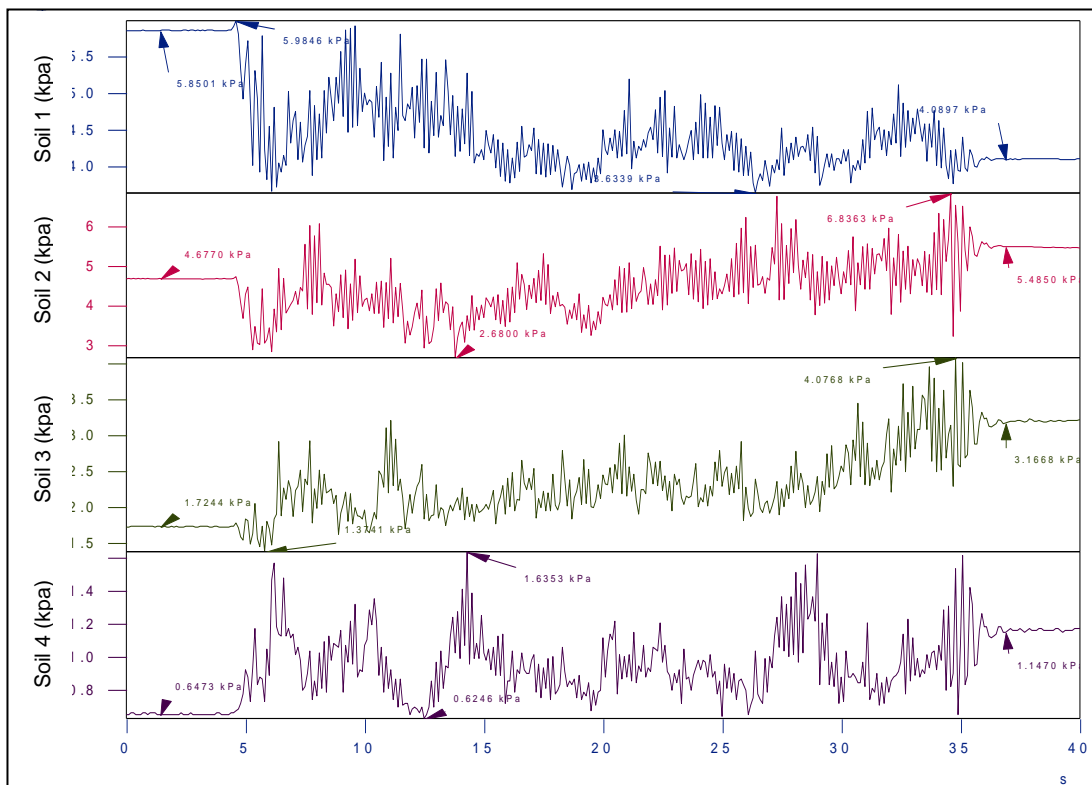


Figure 6.91: Soil pressure measurements for SP1, SP2, SP3 and SP4 for 5 Hz for Soil 1 (Test 2.2.4)

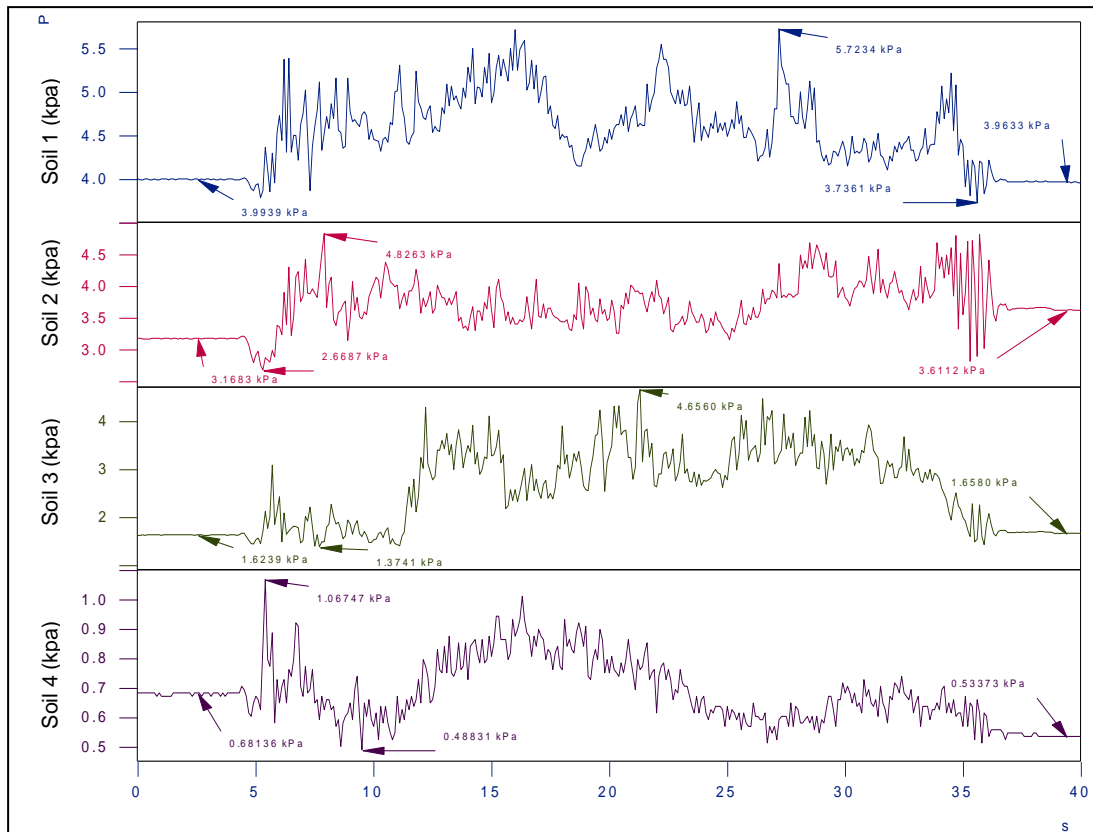


Figure 6.92: Soil pressure measurements for SP1, SP2, SP3 and SP4 for 6 Hz for Soil 1 (Test 2.2.5)

6.3.1.1 Results of Soil Pressure Measurements (for Soil 1)

4 soil pressure cells namely SP1 and SP2, located on the Block 1, and SP3 and SP4, located on the Block 2, were used to define the total saturated soil pressure distribution acting on two blocks for Soil 1 for each frequency (2 Hz - 6 Hz).

For the frequencies 2 Hz - 6 Hz, the total saturated soil pressure measured for two different conditions - before dynamic loading and at the end of (after) dynamic loading - are given in Table 6.10.

Total saturated soil pressure measurements for before dynamic loading and after dynamic loading acting on blocks for each frequency (2 Hz, 3 Hz, 4 Hz, 5 Hz, 6 Hz) for Soil 1 versus depth relations are given in Figure 6.93.

As it is seen from the Figure 6.93 and Table 6.10 for Soil 1;

- The total saturated soil pressure measurements increase while depth is increasing for both before and after dynamic loading for each frequency.
- Total saturated soil pressure measurements for both before and after dynamic loading are almost same and these values increase while depth is and frequency are increasing for 2 Hz and 3 Hz,
- If the final pressures are compared, the pressure values for before dynamic loading is greater than the pressure values for after dynamic loading for 4 Hz, 5 Hz and 6 Hz.
- Total saturated soil pressures measured before dynamic loading is almost 1.3 times larger than the total saturated soil pressures measured after dynamic loading for SP2. This result is not only related to compaction of the soil but also related to decrement of backfill height behind the block.
- There is no significant difference between the before and after measurements of total saturated soil pressure for SP 1, SP 2 and SP3.

Table 6.10: Total saturated soil pressure measurements for different frequencies before and after dynamic loading

Frequency (Hz)	Soil Pressure Numbers	Total Saturated Soil Pressures (kpa)		
		Before Dynamic Loading (kpa)	After Dynamic Loading (kpa)	Ratio
2	SP1	4.73	4.86	0.97
	SP2	3.74	3.65	1.02
	SP3	2.37	2.08	1.14
	SP4	1.22	0.99	1.23
3	SP1	4.63	4.74	0.98
	SP2	3.57*	3.73	0.96
	SP3	2.14*	1.95	1.10
	SP4	1.27	0.81	1.57
4	SP1	5.69*	4.83	1.18
	SP2	3.35	3.63	0.92
	SP3	1.89	2.46	0.77
	SP4	1.09	0.9	1.21
5	SP1	5.85*	4.09	1.17
	SP2	4.67*	5.49	0.85
	SP3	1.72	3.17	0.54
	SP4	0.65	1.15	0.57
6	SP1	4.00	3.96	1.01
	SP2	3.17	3.61	0.88
	SP3	1.62	1.66	0.98
	SP4	0.68	0.53	1.28

* sudden decrease is observed in measurements.

In case of two blocks experiments, sudden changes were observed during the measurements as explained for one block case.

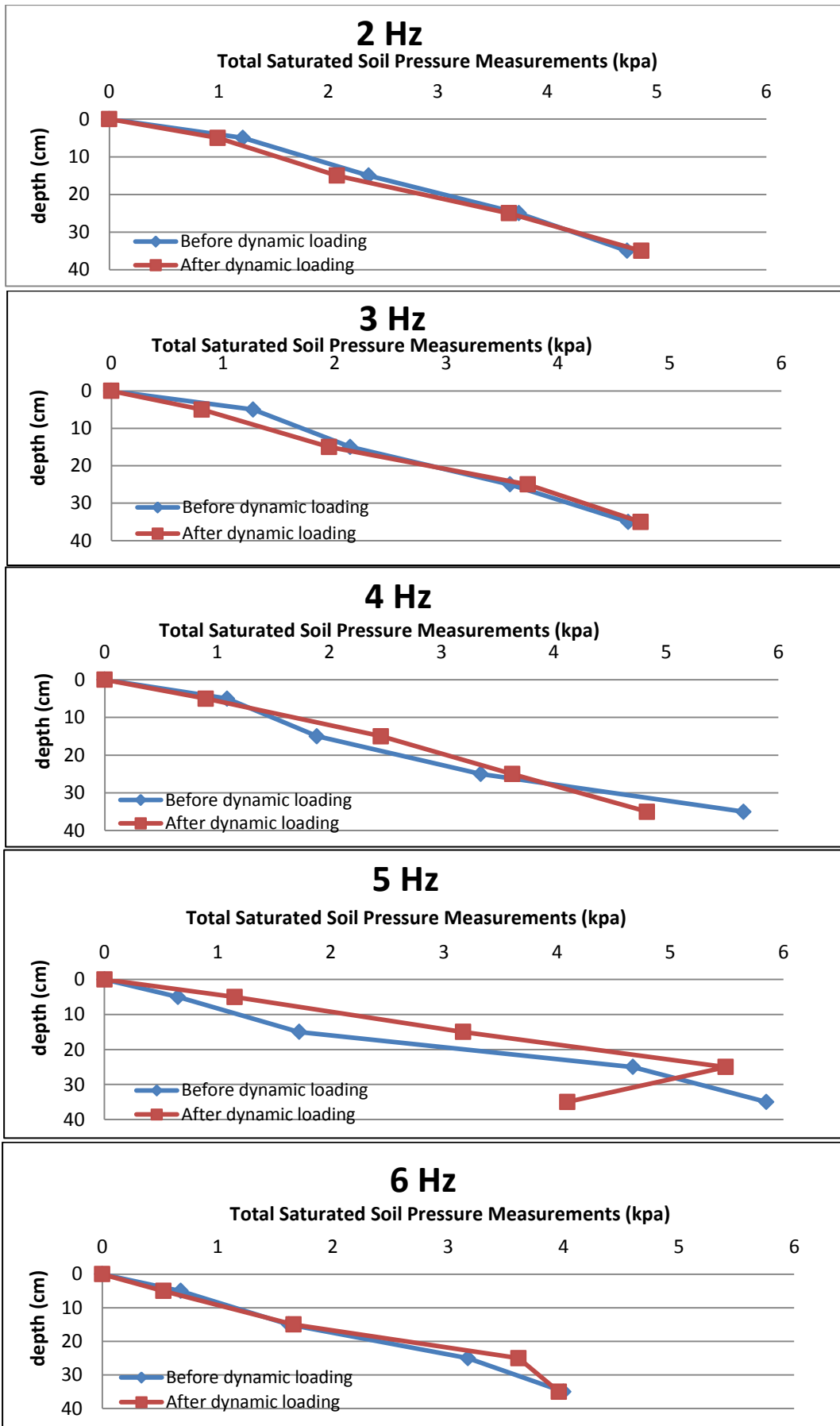


Figure 6.93: Total saturated soil pressure measurements acting on Block 1 and Block 2 for 2, 3, 4, 5, 6 Hz for Soil 1

6.3.1.2 Two Blocks- Fluctuating and Non-fluctuating Components of Total Saturated Soil Pressure for Soil 1

Total saturated soil pressures, fluctuating and non-fluctuating components of total saturated soil pressures are shown between Figure 6.94 - Figure 6.109 for 5 Hz as an example. The results for 2, 3, 4 and 6 Hz are given in APPENDIX G for Soil 1.

6.3.1.2.1 Two Blocks- Fluctuating and Non-Fluctuating Components of Total Soil Pressure for 5 Hz for Soil 1

Figure 6.94 - Figure 6.97 show the total saturated soil pressures, non-fluctuating and fluctuating components of total saturated soil pressures for **SP1 for 5 Hz for Soil 1**.

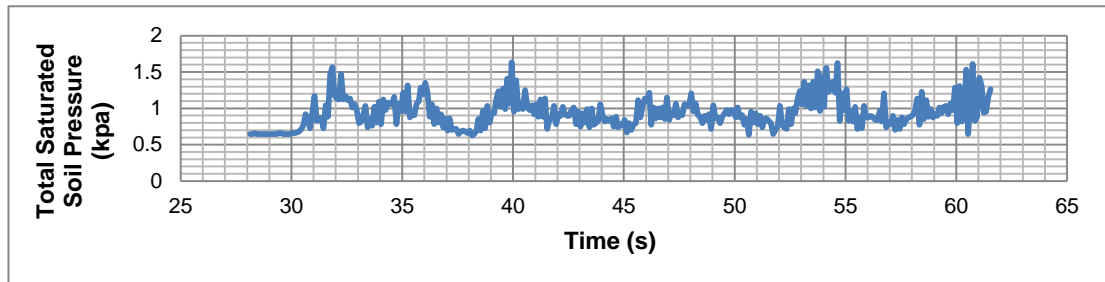


Figure 6.94: Total saturated soil pressure for SP1 for 5 Hz for Soil 1

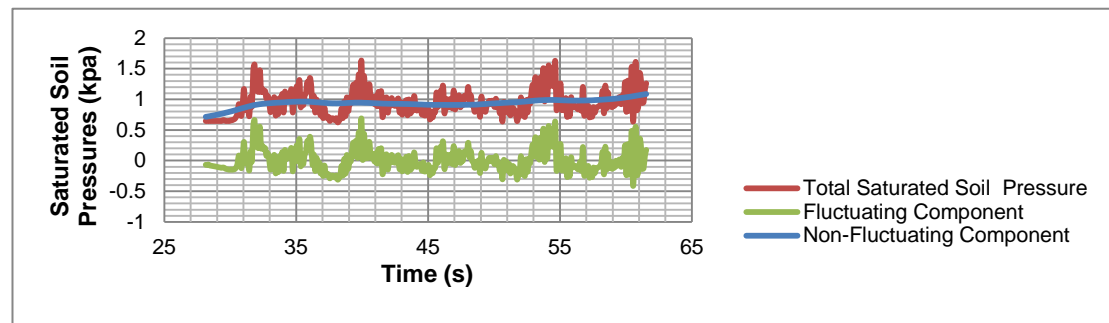


Figure 6.95: Total saturated soil pressure, non-fluctuating and fluctuating components of total saturated soil pressure for SP1 for 5 Hz for Soil 1

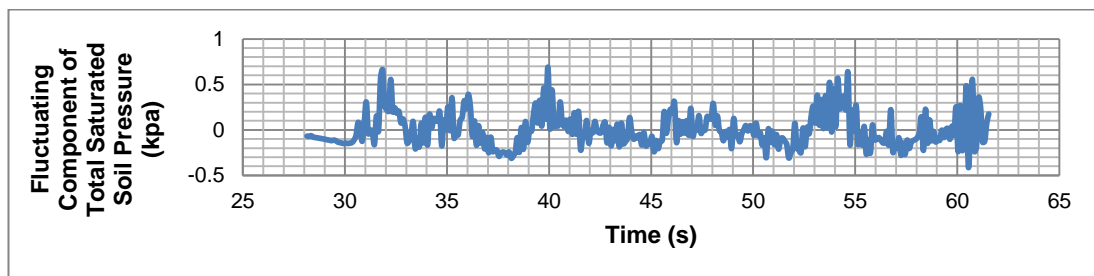


Figure 6.96: Fluctuating components of total saturated soil pressures for SP1 for 5 Hz for Soil 1

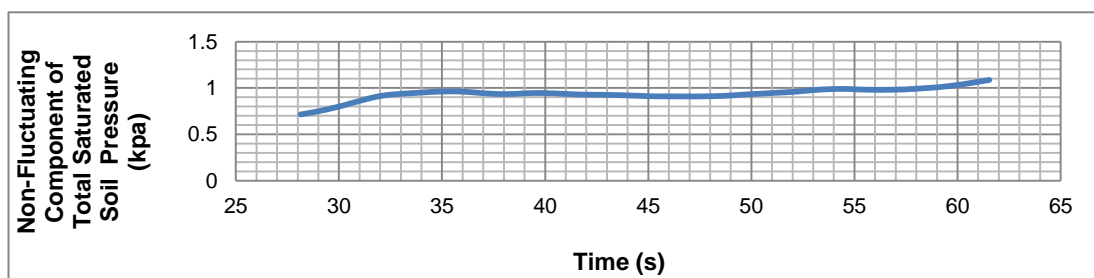


Figure 6.97: Non-Fluctuating components of total saturated soil pressures for SP1 for 5 Hz for Soil 1

Figure 6.98 - Figure 6.101 show the total saturated soil pressures, non-fluctuating and fluctuating components of total saturated soil pressures for **SP2 for 5 Hz for Soil 1.**

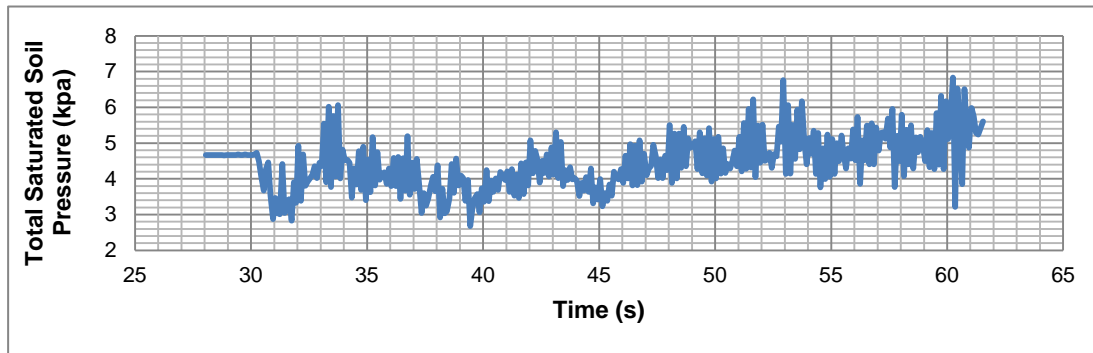


Figure 6.98: Total saturated soil pressure for SP2 for 5 Hz for Soil 1

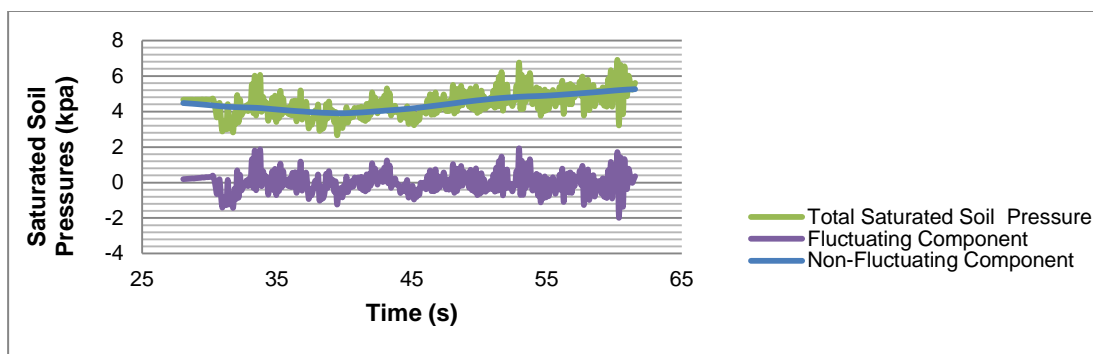


Figure 6.99: Total saturated soil pressure, non-fluctuating and fluctuating components of total saturated soil pressure for SP2 for 5 Hz for Soil 1

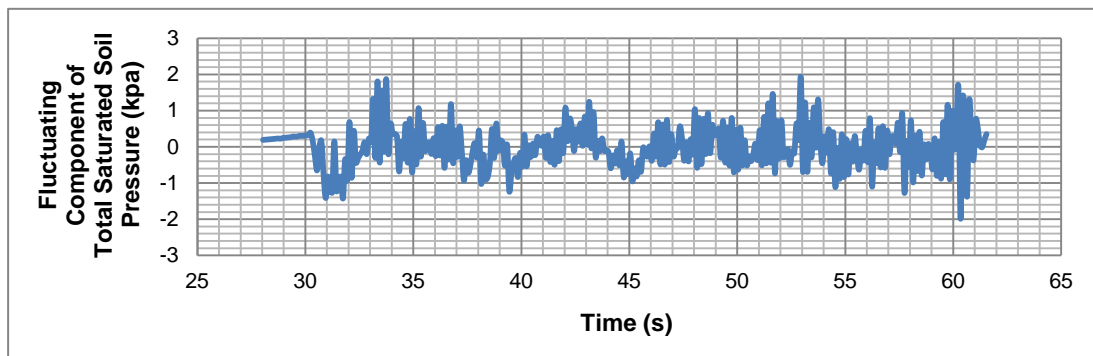


Figure 6.100: Fluctuating components of total saturated soil pressures for SP2 for 5 Hz for Soil 1

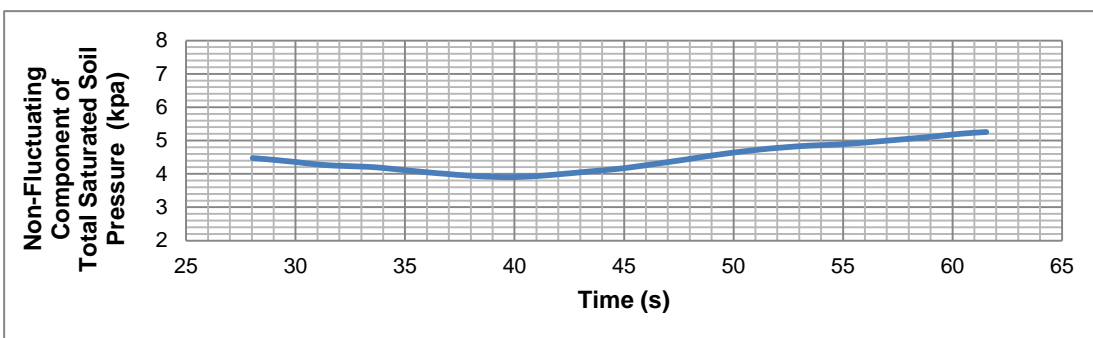


Figure 6.101: Non-Fluctuating components of total saturated soil pressure for SP1 for 5 Hz for Soil 1

Figure 6.102 - Figure 6.105 show the total saturated soil pressures, non-fluctuating and fluctuating components of total saturated soil pressures of **SP3 for 5 Hz for Soil 1**.

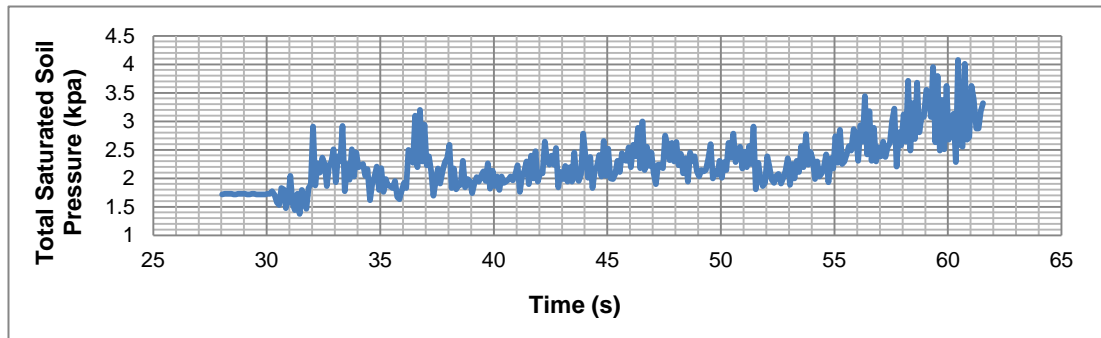


Figure 6.102: Total saturated soil pressures for SP3 for 5 Hz for Soil 1

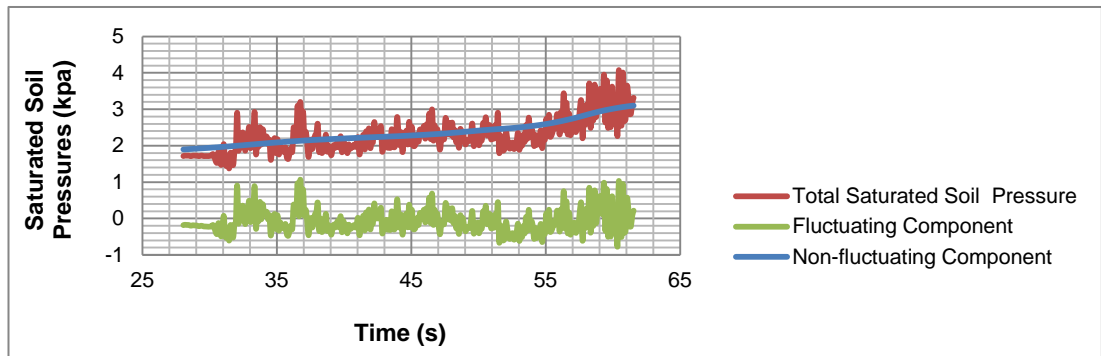


Figure 6.103: Total saturated soil pressure, non-fluctuating and fluctuating components of total saturated soil pressure for SP3 for 5 Hz for Soil 1

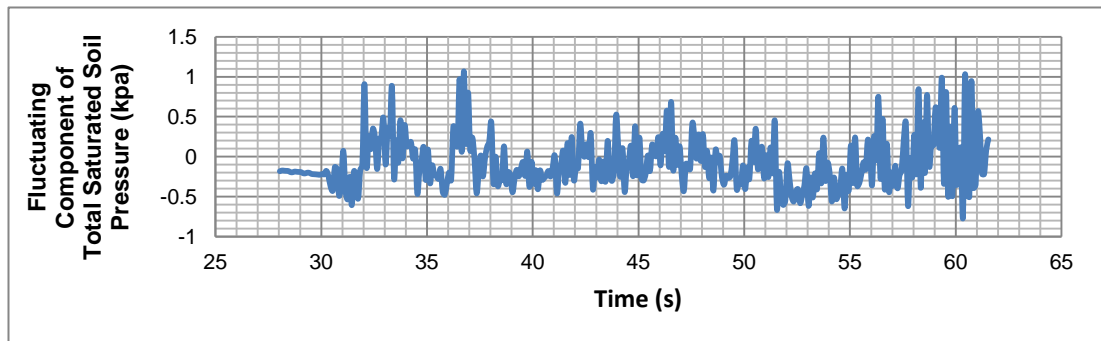


Figure 6.104: Fluctuating components of total saturated soil pressures for SP3 for 5 Hz for Soil 1

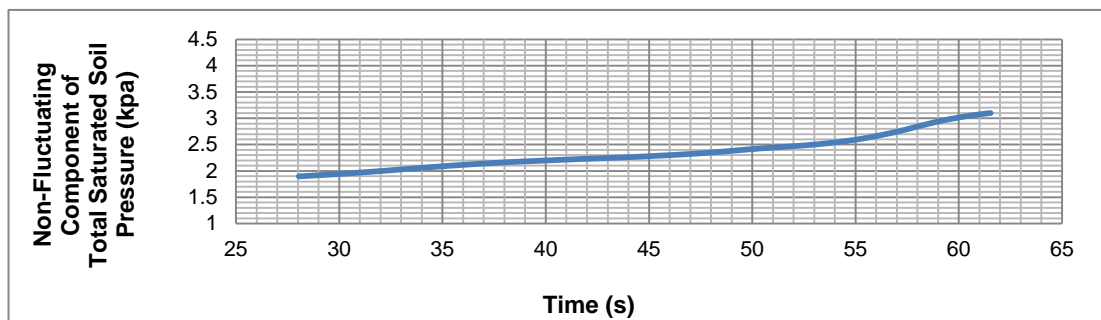


Figure 6.105: Non-Fluctuating components of total saturated soil pressures for SP3 for 5 Hz for Soil 1

Figure 6.106 - Figure 6.109 show the total saturated soil pressures, non-fluctuating and fluctuating components of total saturated soil pressures of **SP4 for 5 Hz for Soil 1.**

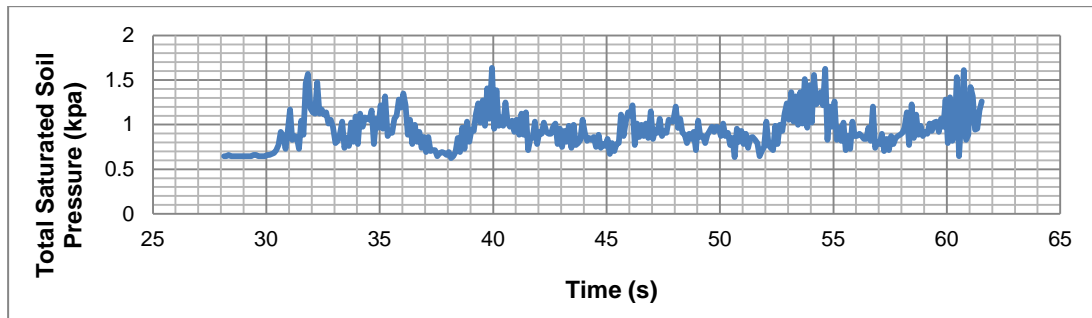


Figure 6.106: Total saturated soil pressure for SP4 for 5 Hz for Soil 1

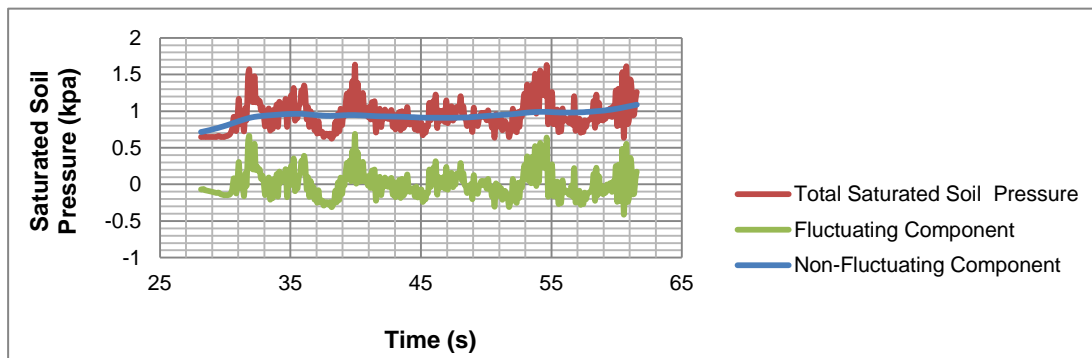


Figure 6.107: Total saturated soil pressure, non-fluctuating and fluctuating components of total saturated soil pressure for SP4 for 5 Hz for Soil 1

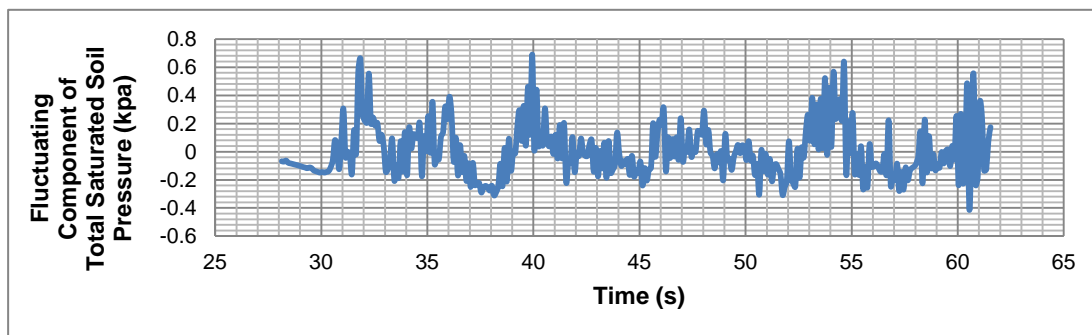


Figure 6.108: Fluctuating components of total saturated soil pressures for SP4 for 5 Hz for Soil 1

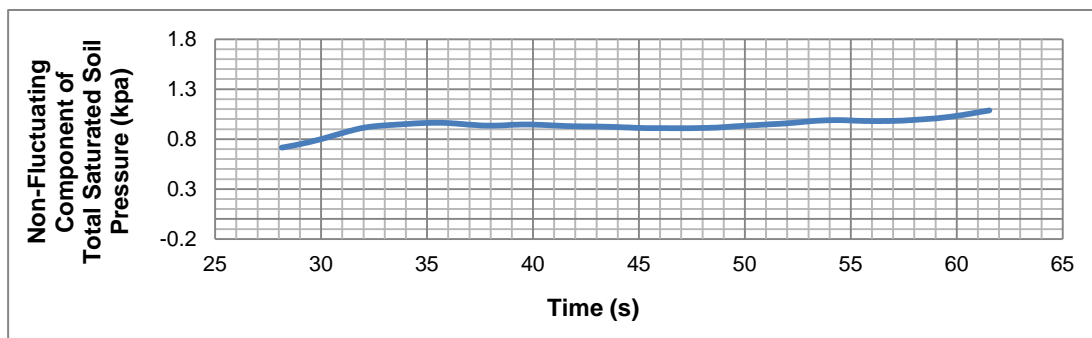


Figure 6.109: Non-fluctuating components of total saturated soil pressures for SP4 for 5 Hz for Soil 1

6.3.1.2.1.1 Maximum Fluctuating Components of Total Saturated Soil Pressures for Soil 1

The relation between maximum fluctuating components of total saturated soil pressures and depth for each frequency are shown in Table 6.11 and Figure 6.110 for Soil 1.

Table 6.11: Maximum fluctuating components of total saturated soil pressures and before dynamic loading pressure measurements for SP1, SP2, SP3 and SP4 for Soil 1

Frequency (Hz)	Soil Pressure Numbers	Before Dynamic Loading (kpa)	Maximum Fluctuating Comp. of Total Saturated Soil Pressure (kpa)
2	SP1	4.73	0.18
	SP2	3.74	0.03
	SP3	2.37	0.04
	SP4	1.22	0.06
3	SP1	4.63	0.20
	SP2	3.57	0.26
	SP3	2.14	0.19
	SP4	1.27	0.10
4	SP1	5.69	2.1
	SP2	3.35	0.86
	SP3	1.89	0.94
	SP4	1.09	0.44
5	SP1	4.80	1.13
	SP2	4.67	1.93
	SP3	1.72	1.07
	SP4	0.65	0.69
6	SP1	4.00	1.18
	SP2	3.17	1.17
	SP3	1.62	1.70
	SP4	0.68	0.38

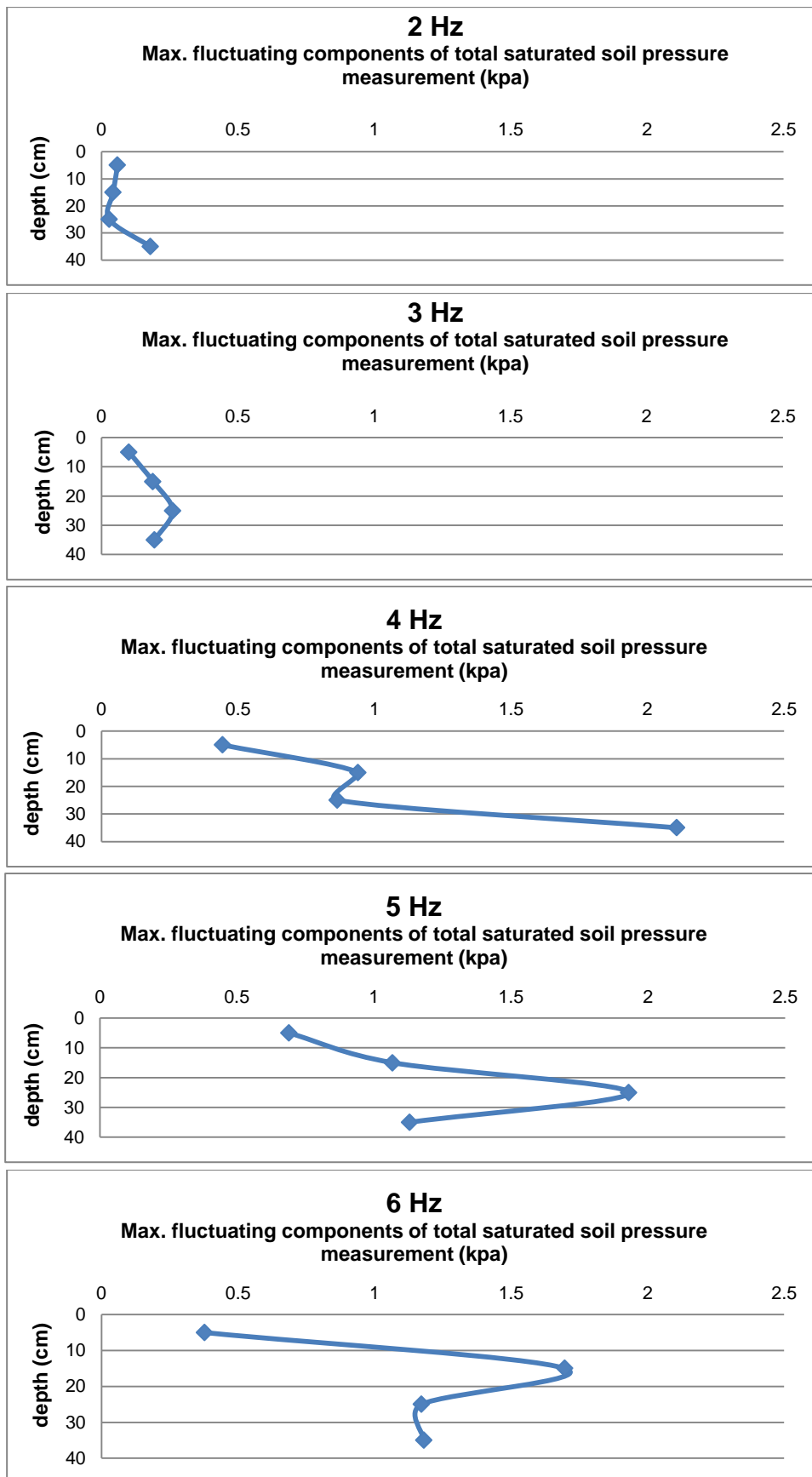


Figure 6.110: Relation between maximum fluctuating component of total lateral earth pressure and depth for Soil

As it is seen from Table 6.11 – Figure 6.110 for Soil 1;

- Only for 2 Hz, there is no motion under dynamic loading, maximum fluctuating components of total saturated soil pressure firstly decreases and then increases while depth is increasing. Thus, it is not possible to define the distribution of fluctuating components of total saturated soil pressure.
- Maximum fluctuating components of total saturated soil pressures increases until a “certain depth” for 3 Hz, 4 Hz, 5 Hz and 6 Hz.
After a certain depth, maximum fluctuating components of total saturated soil pressures decrease and in general the pressure values at the bottom of the blocks are greater than the pressure values at the top of the blocks.
The depth where this change in pressure take place can be defined as;

Frequency (Hz)	Depth (cm)
3 Hz	25 cm
4 Hz	16 cm
5 Hz	25 cm
6 Hz	17 cm

Depth ranges are defined as 16 cm – 25 cm. The total height of the blocks (H) is 40 cm, thus the application point of the fluctuating components of total saturated soil pressure (a) is;

$$40 \text{ cm} \times a = 16 \text{ cm} \quad a = 0.40$$

$$40 \text{ cm} \times a = 25 \text{ cm} \quad a = 0.63$$

“Application point of the fluctuating components of total saturated soil pressure is between 0.40 H – 0.63 H”

6.3.1.2.1.2 Maximum Non-Fluctuating Components of Total Saturated Soil Pressures for Soil 1

The relation between maximum non-fluctuating components of total saturated soil pressures and depth for each frequency are shown in Table 6.12 and Figure 6.111 for Soil 1.

Table 6.12: Maximum non-fluctuating components of total saturated soil pressures and before dynamic loading pressure measurements for SP1, SP2, SP3 and SP4 for Soil 1

Frequency (Hz)	Soil Pressure Numbers	Before Dynamic Loading (kpa)	Maximum Non-Fluctuating Comp. of Total Saturated Soil Pressure (kpa)
2	SP4	1.22	1.18
	SP3	2.37	2.27
	SP2	3.74	3.68
	SP1	4.73	4.87
3	SP4	1.27	1.16
	SP3	2.14	2.06
	SP2	3.57	3.76
	SP1	4.63	4.75
4	SP4	1.09	1.17
	SP3	1.89	2.06
	SP2	3.35	3.76
	SP1	5.69	4.75
5	SP4	0.65	1.09
	SP3	1.72	3.10
	SP2	4.67	5.26
	SP1	4.80	5.60
6	SP4	0.68	0.83
	SP3	1.62	3.35
	SP2	3.17	4.02
	SP1	4.00	4.78

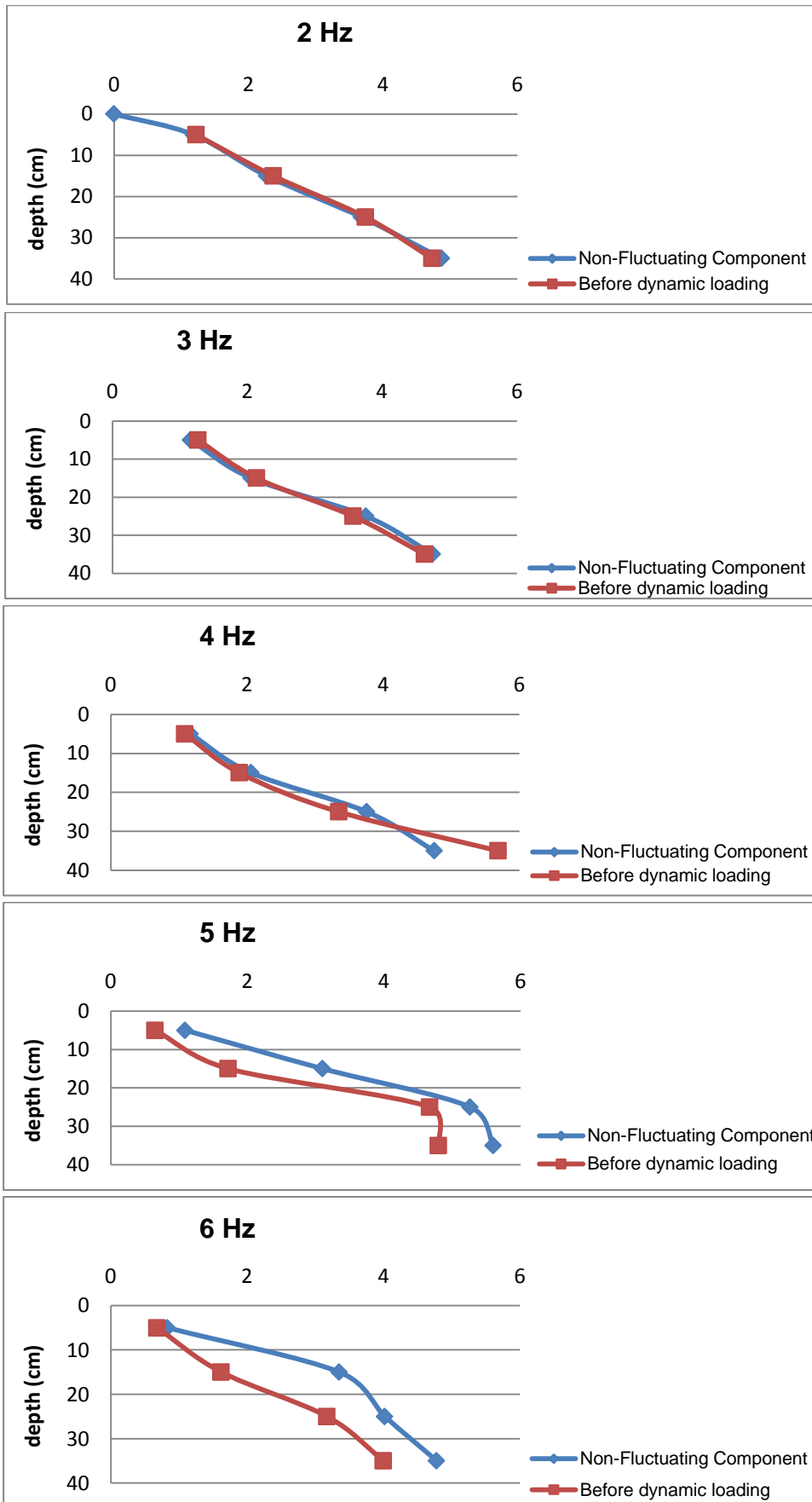


Figure 6.111: Maximum non-fluctuating components of total saturated soil pressure and total saturated soil pressure before dynamic loading for Soil 1

As it is seen from Table 6.12 and Figure 6.111 for Soil 1;

- *Maximum non-fluctuating components of total saturated soil pressures and the total saturated soil pressures before dynamic loading increase while depth and frequency are increasing.*
- *Maximum non-fluctuating components of total saturated soil pressures and total saturated soil pressure before dynamic loading are so close to each other for 2 Hz and 3 Hz and also for 4 Hz. That is simply because no motion is occurred on block for 2 Hz and 3 Hz.*
- *Maximum non-fluctuating components of total saturated soil pressures are greater than the total saturated soil pressure before dynamic loading for 4 Hz, 5 Hz and 6 Hz.*

6.3.2 Two Blocks, Soil 2: Soil Pressure Measurements (Test 2.2)

Soil pressure measurements and results are presented for each series for Soil 2 with 3 tests (4 Hz, 5 Hz, and 6 Hz) for two blocks.

In Figure 6.113 - Figure 6.117, total saturated soil pressure measurements for each frequency are presented as soil pressure cells placed at 5 cm -15 cm below the top of the block 2 (SP4 and SP3) and 25 cm – 35 cm below the top of the Block 2 (SP2 and SP1) (Figure 6.86) Figure 6.112 show the general view of the experiment set up of the two blocks tests for Soil 2.



Figure 6.112: Block, instruments, dummies and Soil 2

As it is seen from the Figure 6.113 - Figure 6.115, total saturated soil pressure measurements ranges under dynamic loading for 4 Hz – 6 Hz are shown in Table 6.13 for Soil 2.

Table 6.13: Total saturated soil pressure measurements ranges for 2 Hz – 6 Hz for Soil 2

Frequency	Soil Pressure Cells	Ranges of Total Saturated Soil Pressure Measurements
4 Hz	SP1	3.57 kpa – 4.86 kpa
	SP2	2.66 kpa – 3.45 kpa
	SP3	1.53 kpa – 2.32 kpa
	SP4	0.53 kpa – 1.11 kpa
5 Hz	SP1	4.25 kpa – 6.35 kpa
	SP2	2.88 kpa – 3.91 kpa
	SP3	1.57 kpa – 2.70 kpa
	SP4	0.39 kpa – 0.92 kpa
6 Hz	SP1	3.74 kpa – 6.42 kpa
	SP2	2.93 kpa – 7.34 kpa
	SP3	1.14 kpa – 2.49 kpa
	SP4	0.16 kpa – 0.95 kpa

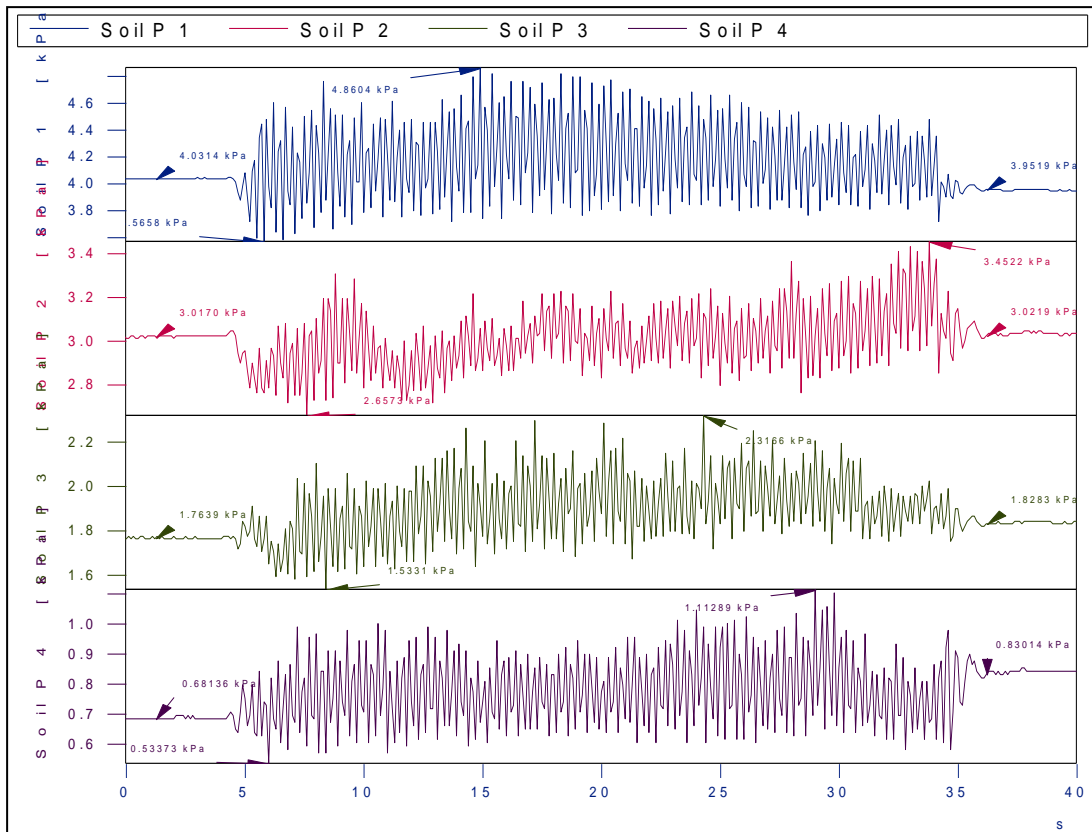


Figure 6.113: Soil pressure measurements for SP1, SP2, SP3 and SP4 for 4 Hz for Soil 2 (Test 2.2.1)

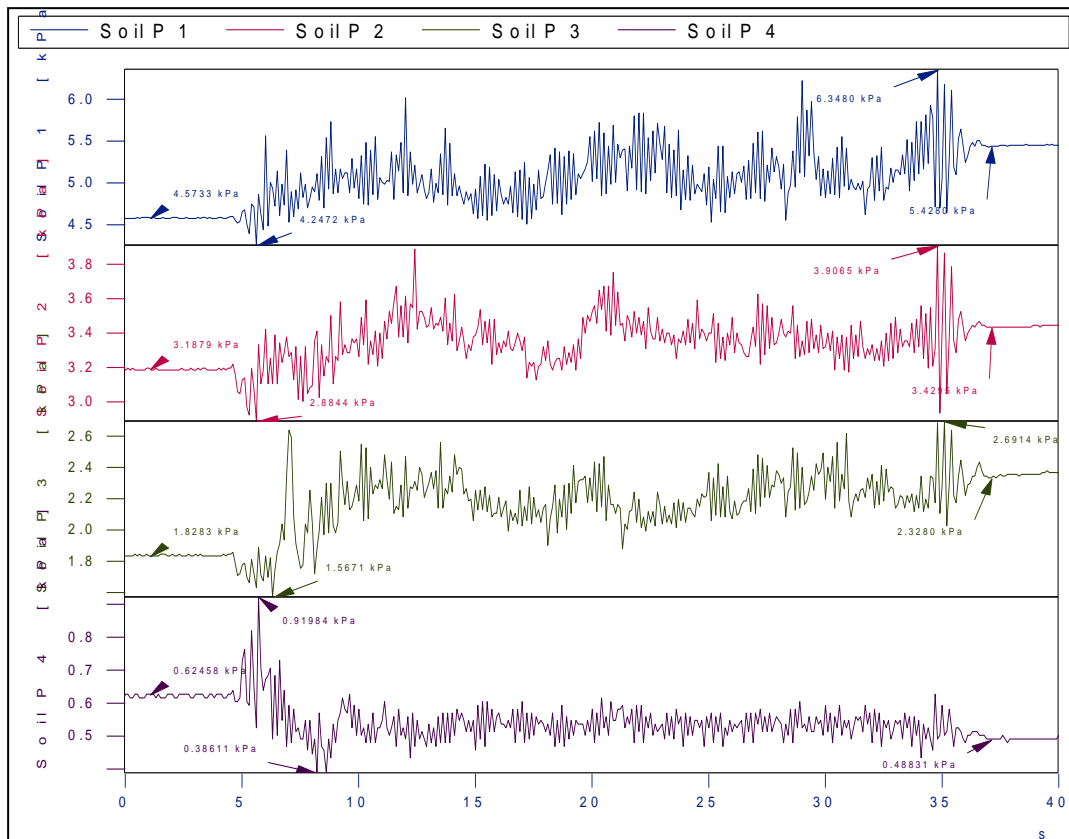


Figure 6.114: Soil pressure measurements for SP1, SP2, SP3 and SP4 for 5 Hz for Soil 2 (Test 2.2.2)

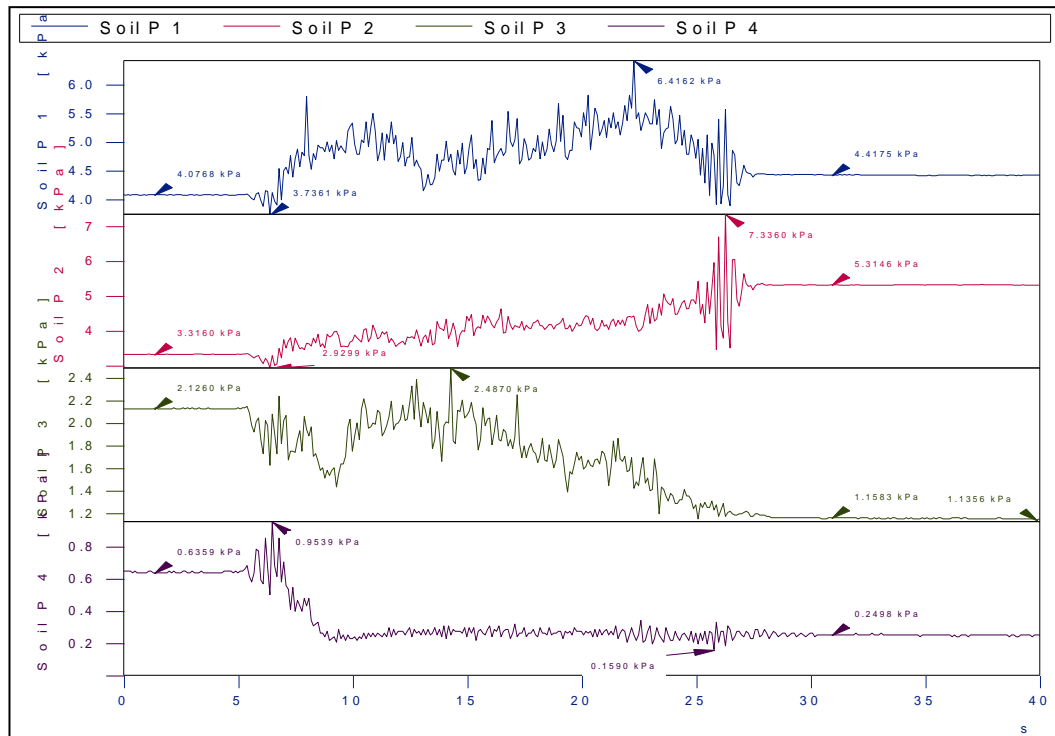


Figure 6.115: Soil pressure measurements for SP1, SP2, SP3 and SP4 for 6 Hz for Soil 2 (Test 2.2.2)

6.3.2.1 Results of Soil Pressure Measurements (Soil 2)

4 soil pressure cells namely SP1 and SP2, located on the Block 1, and SP3 and SP4, located on the Block 2, were used to define the soil pressure distribution acting on blocks for Soil 2 for each frequency (4 Hz - 6 Hz).

In contrary to Soil 1, for Soil 2, there is no significant abrupt decrement are observed within a few seconds on total saturated soil pressure measurements obtained before dynamic loading. Because of this, finer material was used as backfill material.

For the frequencies 4 Hz - 6 Hz, the total saturated soil pressure measured for two different conditions - before dynamic loading and at the end of (after) dynamic loading - are given in Table 6.14.

Table 6.14: Saturated soil pressure measurements for different frequencies before and after dynamic loading for Soil 2

Frequency (Hz)	Soil Pressure Numbers	Total Saturated Soil Pressures (kpa)		
		Before Dynamic Loading (kpa)	After Dynamic Loading (kpa)	Ratio
4	SP1	4.03	3.95	1.02
	SP2	3.01	3.02	1.00
	SP3	1.76	1.83	0.96
	SP4	0.68	0.83	0.82
5	SP1	4.57	5.43	0.84
	SP2	3.19	3.43	0.93
	SP3	1.83	2.33	0.79
	SP4	0.63	0.49	1.29
6	SP1	4.08	4.42	0.92
	SP2	3.32	5.31	0.63
	SP3	2.13	1.14	1.87
	SP4	0.64	0.25	2.56

Total saturated soil pressure measurements for before dynamic loading and after dynamic loading acting on blocks for each frequency (4 Hz, 5 Hz, 6 Hz) for Soil 2 versus depth relations are given in Figure 6.116.

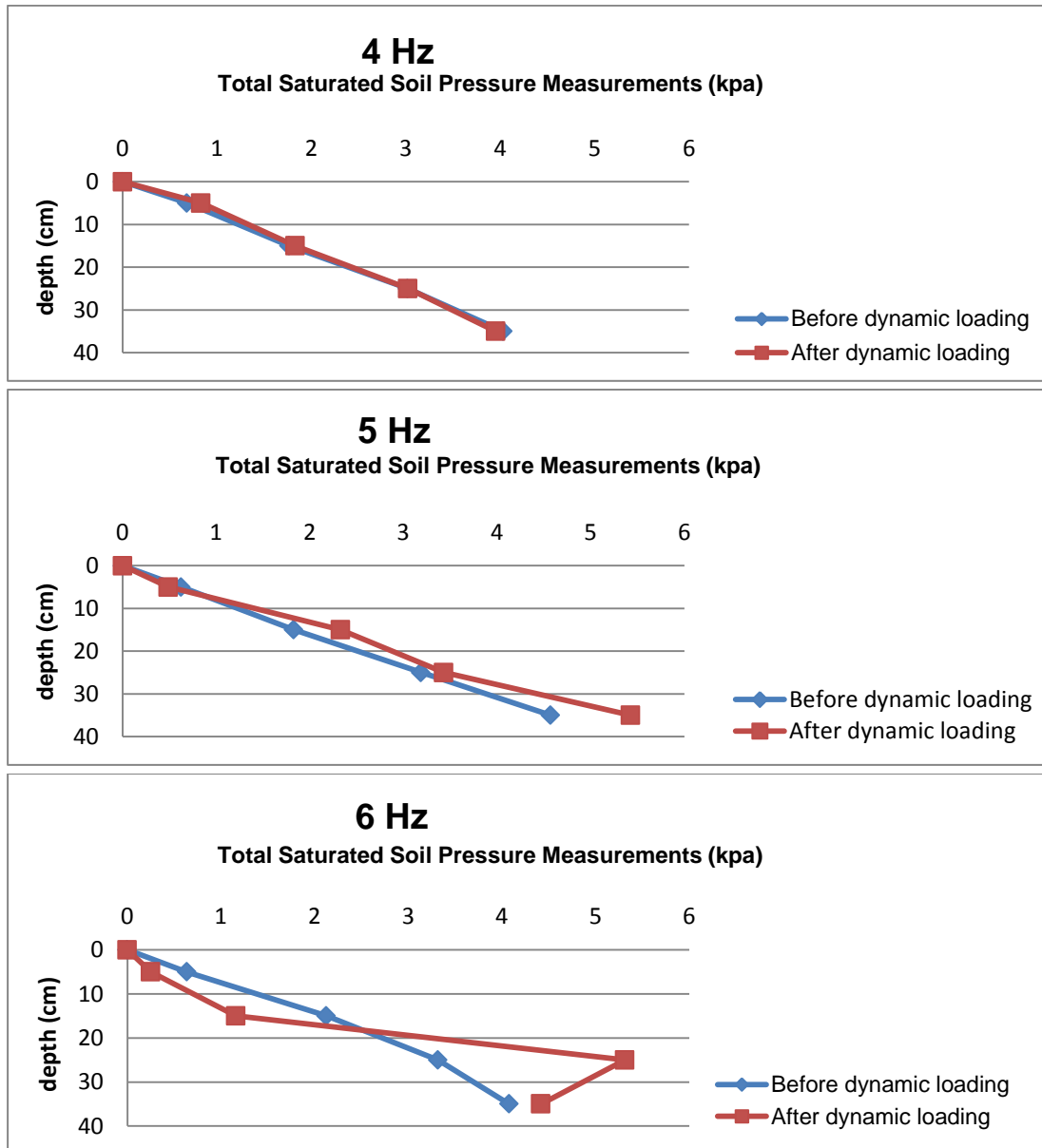


Figure 6.116: Saturated soil pressure measurements acting on Block 1 and Block 2 for 4, 5, 6 Hz for Soil 2

As it is seen from the Figure 6.116 and Table 6.14 for Soil 2;

- The total saturated soil pressure measurements increase while depth is increasing for both before and after dynamic loading for each frequency.
- Total saturated soil pressure measurements for both before and after dynamic loading are almost same and these values increase while depth is and frequency are increasing for 4 Hz,
- In contrary to Soil 1 (coarser), for Soil 2 (finer), if the final pressures are compared, the pressure values for before dynamic loading is smaller than the pressure values for after dynamic loading for 5 Hz and 6 Hz. This result shows that Soil 2 (finer) behavior completely changes after 5 Hz, due to significant horizontal displacement measurements. Dissipation of the Soil 2 (finer) causes decrement in relative density (D_r) and decrement in relative density causes increment in soil pressures.

6.3.2.2 Two Blocks- Fluctuating and Non-fluctuating Components of Total Saturated Soil Pressure for Soil 2

Total saturated soil pressures, fluctuating and non-fluctuating components of total saturated soil pressures are shown in APPENDIX G for different frequencies for Soil 2.

6.3.2.2.1 Maximum Fluctuating Components of Saturated Total Soil Pressures

The relation between maximum fluctuating components of total saturated soil pressures and depth for each frequency are shown in Table 6.15 and Figure 6.117 for Soil 2.

Table 6.15: Maximum fluctuating components of total saturated soil pressures and before dynamic loading pressure measurements for SP1, SP2, SP3 and SP4 for Soil 2

Frequency (Hz)	Soil Pressure Numbers	Maximum Fluctuating Comp. of Total Saturated Soil Pressure (kpa)
4	SP1	0.65
	SP2	0.37
	SP3	0.37
	SP4	0.31
5	SP1	1.06
	SP2	0.43
	SP3	0.68
	SP4	0.30
6	SP1	1.53
	SP2	2.32
	SP3	0.48
	SP4	0.40

As it is seen from Table 6.15 – Figure 6.117;

- *Fluctuating components of total saturated soil pressures increase until a “certain depth” for 5 Hz and 6 Hz. After a certain depth, fluctuating components of total saturated soil pressures decrease*

This certain depth is;

Frequency (Hz)	Depth (cm)
5 Hz	26 cm
6 Hz	15 cm

The total height of the blocks (H) is 40 cm, thus the application point of the fluctuating components of total saturated soil pressure (a) is;

$$40 \text{ cm} \times a = 26 \text{ cm} \quad a = 0.65$$

$$40 \text{ cm} \times a = 15 \text{ cm} \quad a = 0.375$$

“Application point of the fluctuating components of total saturated soil pressure is between 0.375H and 0.65 H for 6 Hz and 5 Hz”.

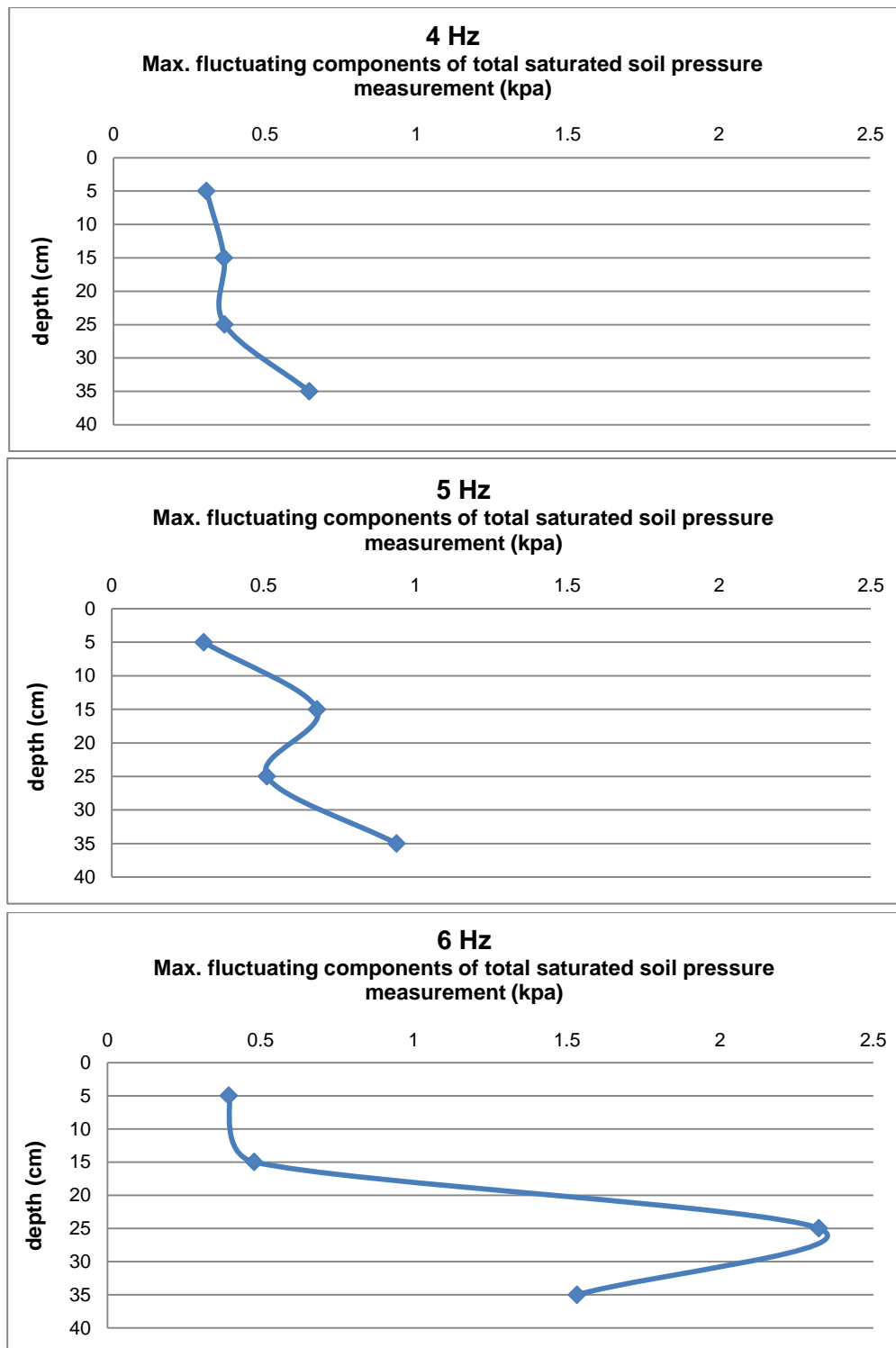


Figure 6.117: Relation between maximum fluctuating component of total lateral earth pressure and depth for Soil 2

6.3.2.2.1.1 Maximum Non-Fluctuating Components of Total Saturated Soil Pressures for Soil 2

The relation between maximum non-fluctuating components of total saturated soil pressures and depth for each frequency are shown in Table 5.16 and Figure 6.118.

Table 6.16: Maximum non-fluctuating components of total saturated soil pressures and before dynamic loading pressure measurements for SP1, SP2, SP3 and SP4 for Soil 2

Frequency (Hz)	Soil Pressure Numbers	Before Dynamic Loading (kpa)	Maximum Non-Fluctuating Comp. of Total Saturated Soil Pressure (kpa)
4	SP1	4.03	4.27
	SP2	3.01	3.10
	SP3	1.76	1.97
	SP4	0.68	0.81
5	SP1	4.57	5.34
	SP2	3.19	3.45
	SP3	1.83	2.30
	SP4	0.63	0.63
6	SP1	4.08	4.94
	SP2	3.32	5.23
	SP3	2.13	2.12
	SP4	0.64	0.65

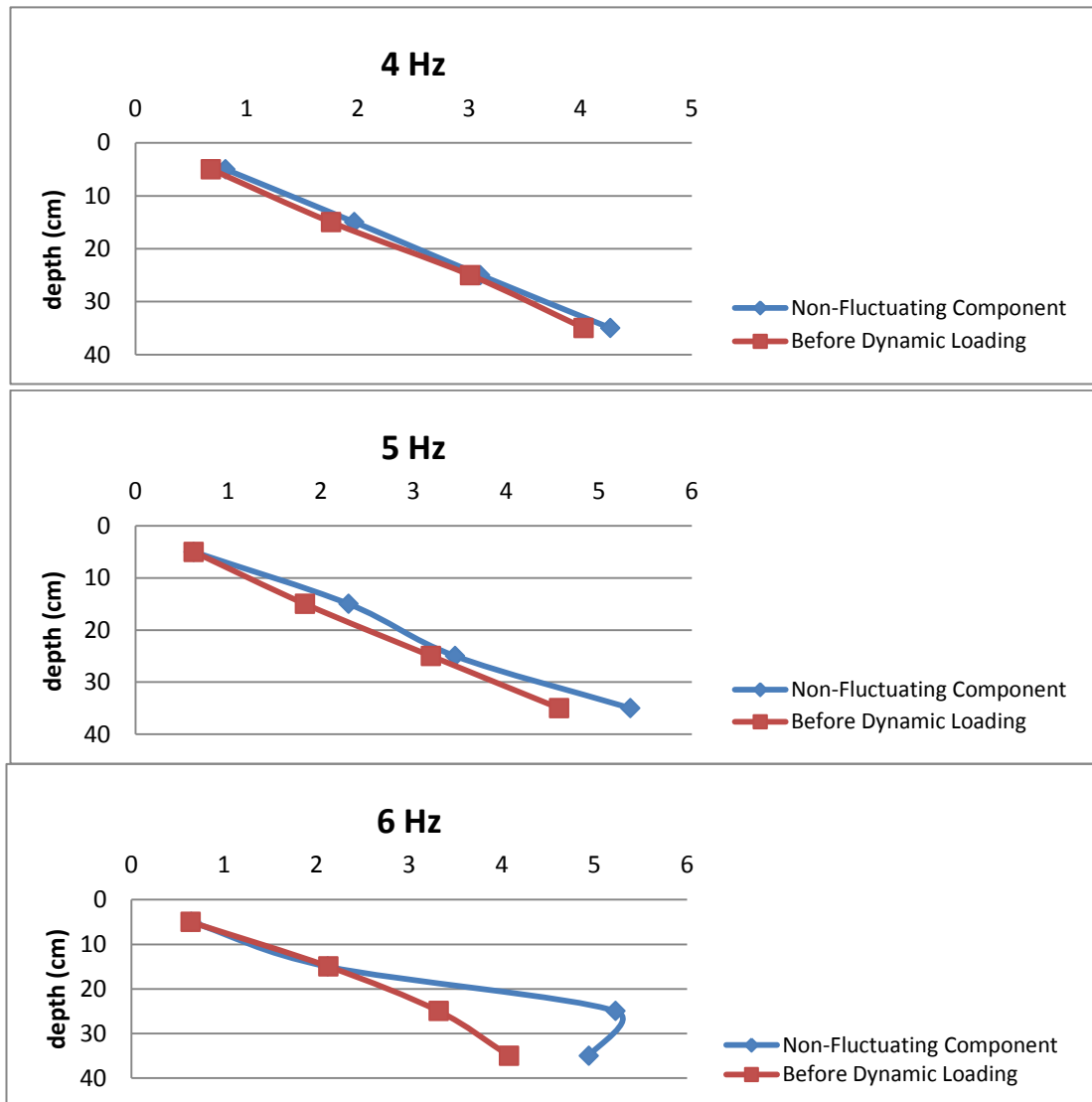


Figure 6.118: Maximum non-fluctuating components of total saturated soil pressure and total saturated soil pressure before dynamic loading

As it is seen from Table 6.16 and Figure 6.118;

- *Maximum non-fluctuating components of total saturated soil pressures and the total saturated soil pressures before dynamic loading increase while depth and frequency is increasing.*
- *Maximum non-fluctuating components of total saturated soil pressures and total saturated soil pressure before dynamic loading are so close to each other for 4 Hz.*
- *Maximum non-fluctuating components of total saturated soil pressures are greater than the total saturated soil pressure before dynamic loading for 5 Hz and 6 Hz.*

6.4 Three Blocks, Soil 1: Total Saturated Soil Pressure Measurements (Test 3.1 and Test 3.2)

Soil pressure measurements and results are presented for each series for Soil 1 with 5 tests (3 Hz, 4 Hz, 5 Hz, 6 Hz and for Soil 2 with 3 tests (4 Hz, 5 Hz, 6 Hz) for three blocks.

General view of four soil pressure cells (SP1, SP2, SP3, and SP4) placed at 5 cm -25 cm below the top of the block 2 (SP4 and SP3) and 35 cm – 55 cm below the top of the block 2 (SP2 and SP1) and two pore pressure cells (PP1 and PP2) for three blocks tests for Soil 1- Tests 3.1 and for Soil 2 - Test 3.2 are shown in Figure 6.119.

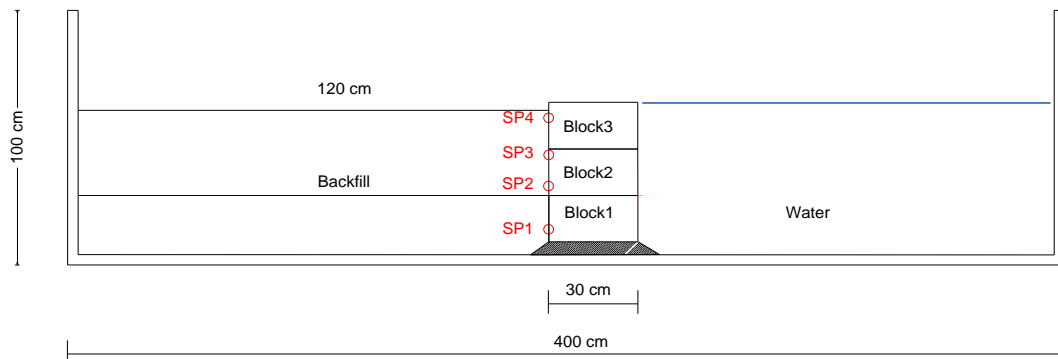


Figure 6.119: General view of four soil pressure cells (SP1, SP2, SP3, and SP4) and pore pressure cells (PP1, PP2) for three blocks tests for Soil 1 and Soil 2

6.4.1 Three Blocks, Soil 1: Soil Pressure Measurements (Test 2.1)

In Figure 6.121 - Figure 6.124 total saturated soil pressure measurements for each frequency are presented.

Figure 6.120 show the general view of the experiment set up of the three blocks tests for Soil 1.



Figure 6.120: Block, instruments, dummies and Soil 1

As it is seen from the Figure 6.121 - Figure 6.124, total saturated soil pressure measurements ranges under dynamic loading for 3 Hz-6 Hz are shown in Table 6.17 for Soil 1.

Table 6.17: Total saturated soil pressure measurements ranges for 3 Hz – 6 Hz for Soil 1

Frequency	Soil Pressure Cells	Ranges of Total Saturated Soil Pressure Measurements
3 Hz	SP1	5.87 kpa – 7.36 kpa
	SP2	3.82 kpa – 4.84 kpa
	SP3	2.61 kpa – 3.21 kpa
	SP4	0.60 kpa – 1.12 kpa
4 Hz	SP1	4.74 kpa – 9.21 kpa
	SP2	3.35 kpa – 12.78 kpa
	SP3	2.13 kpa – 6.06 kpa
	SP4	0.65 kpa – 4.95 kpa
5 Hz	SP1	5.30 kpa – 7.46 kpa
	SP2	3.79 kpa – 7.57 kpa
	SP3	2.61 kpa – 7.29 kpa
	SP4	0.73 kpa – 2.86 kpa
6 Hz	SP1	6.03 kpa – 8.80 kpa
	SP2	4.63 kpa – 5.47 kpa
	SP3	2.84 kpa – 3.19 kpa
	SP4	0.37 kpa – 0.28 kpa

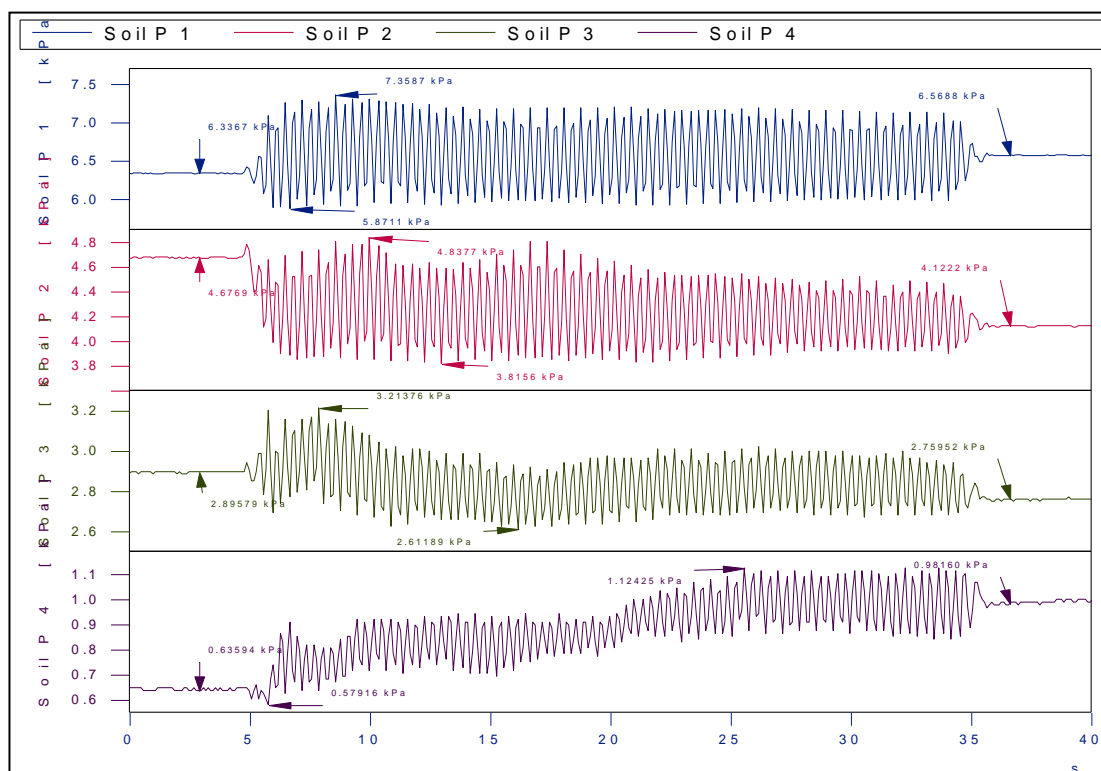


Figure 6.121: Soil pressure measurements for SP1, SP2, SP3 and SP4 for 3 Hz for Soil 1 (Test 3.1.1)

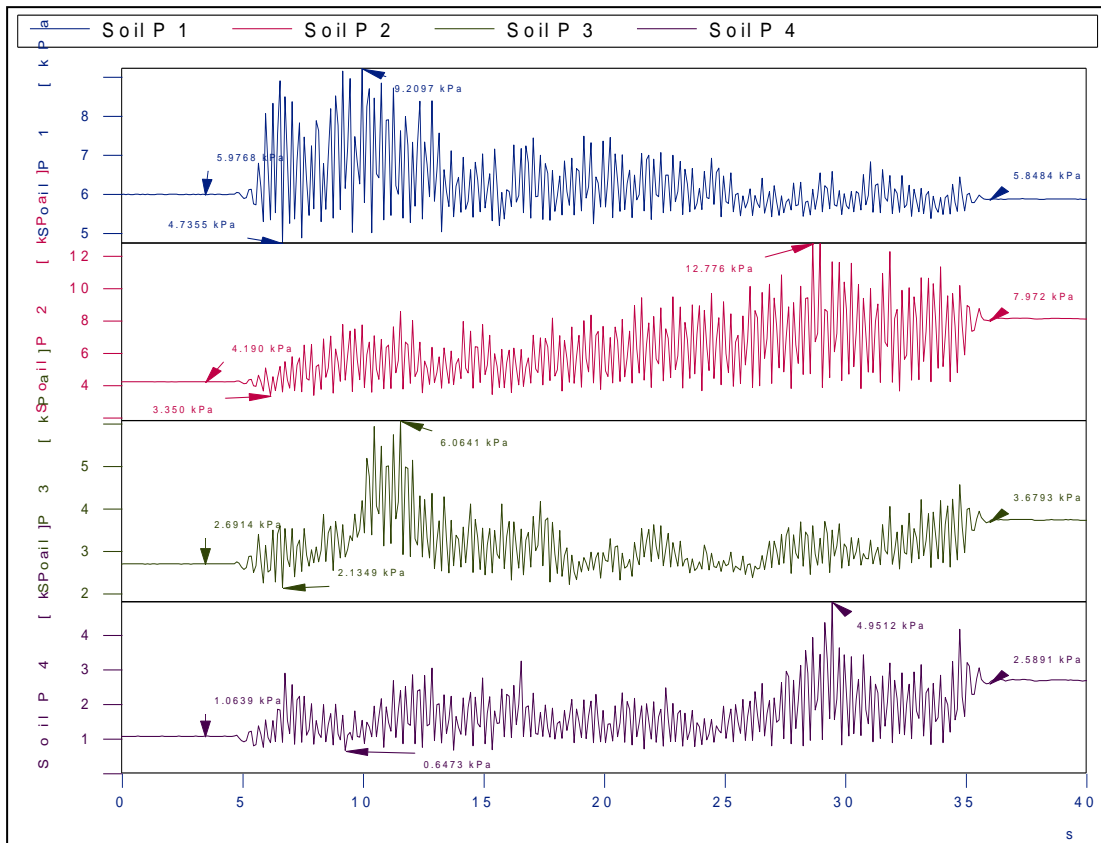


Figure 6.122: Soil pressure measurements for SP1, SP2, SP3 and SP4 for 4 Hz for Soil 1 (Test 3.1.2)

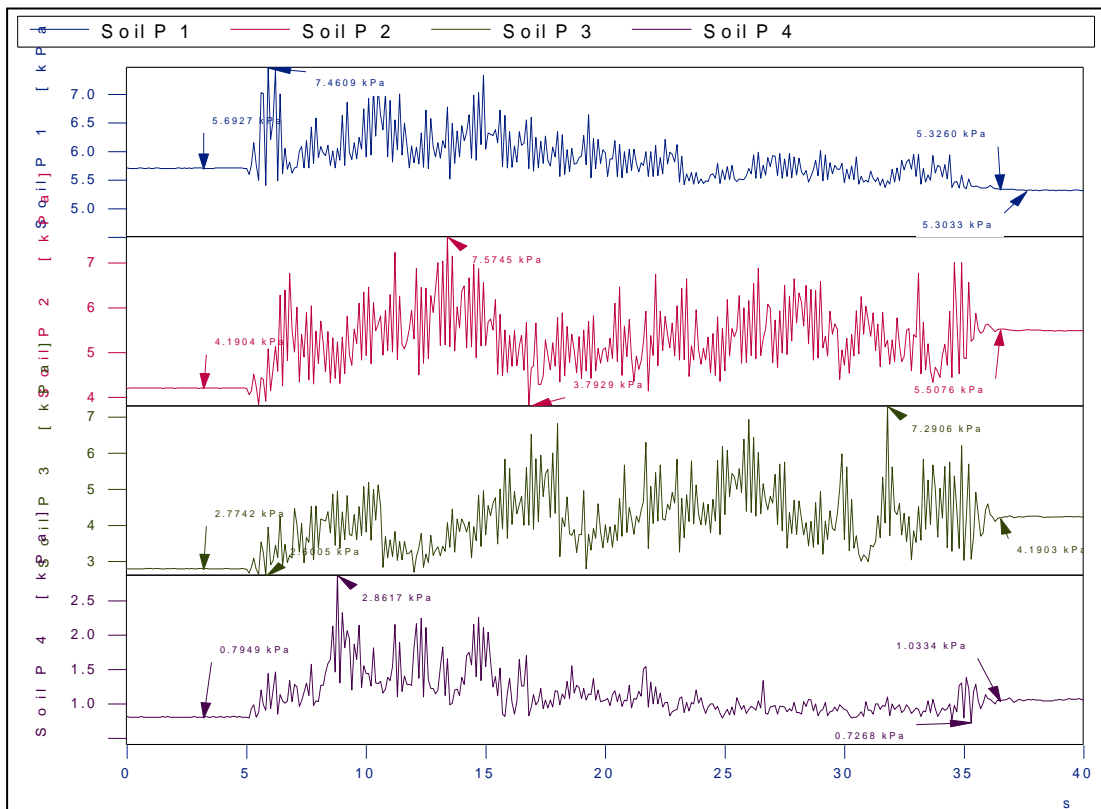


Figure 6.123: Soil pressure measurements for SP1, SP2, SP3 and SP4 for 5 Hz for Soil 1 (Test 3.1.3)

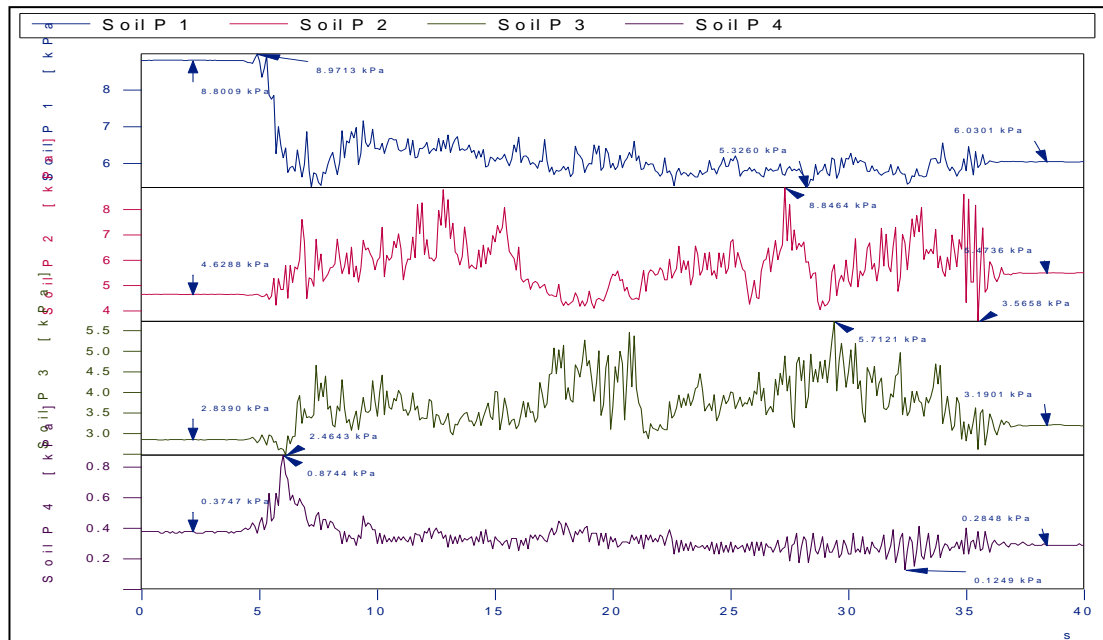


Figure 6.124: Soil pressure measurements for SP1, SP2, SP3 and SP4 for 6 Hz for Soil 1 (Test 3.1.4)

6.4.1.1 Results of Soil Pressure Measurements (Soil 1)

4 soil pressure cells namely SP1, located on the Block 1, and SP2 and SP3, located on the Block 2 and SP4, located on the Block 3, were used to define the total saturated soil pressure distribution acting on blocks for Soil 1 for each frequency (3 Hz - 6 Hz). In case of three blocks experiments, sudden changes were observed during the measurements as explained for one block case.

For the frequencies 3 Hz - 6 Hz, the saturated soil pressure measured for two different conditions - before dynamic loading and at the end of (after) dynamic loading - are given in Table 6.18 for Soil 1.

Table 6.18: Total saturated soil pressure measurements for different frequencies before and after dynamic loading for Soil 1

Frequency (Hz)	Soil Pressure Numbers	Total Saturated Soil Pressures (kpa)	
		Before Dynamic Loading (kpa)	After Dynamic Loading (kpa)
3	SP1	6.34	6.57
	SP2	4.67*	4.12
	SP3	2.90	2.76
	SP4	0.64	0.98
4	SP1	5.98	5.85
	SP2	4.19	7.97
	SP3	2.69	3.68
	SP4	1.06	2.59
5	SP1	5.69	5.30
	SP2	4.19	5.51
	SP3	2.77	4.19
	SP4	0.79	1.03
6	SP1	8.81*	6.03
	SP2	4.63	5.47
	SP3	2.84	3.19
	SP4	0.37	0.28

*sudden changes in pressure measurements

Total saturated soil pressure measurements for before dynamic loading and after dynamic loading acting on blocks for each frequency (3 Hz, 4 Hz, 5 Hz, 6 Hz) for Soil 1 versus depth relations are given in Figure 6.125 for Soil 1.

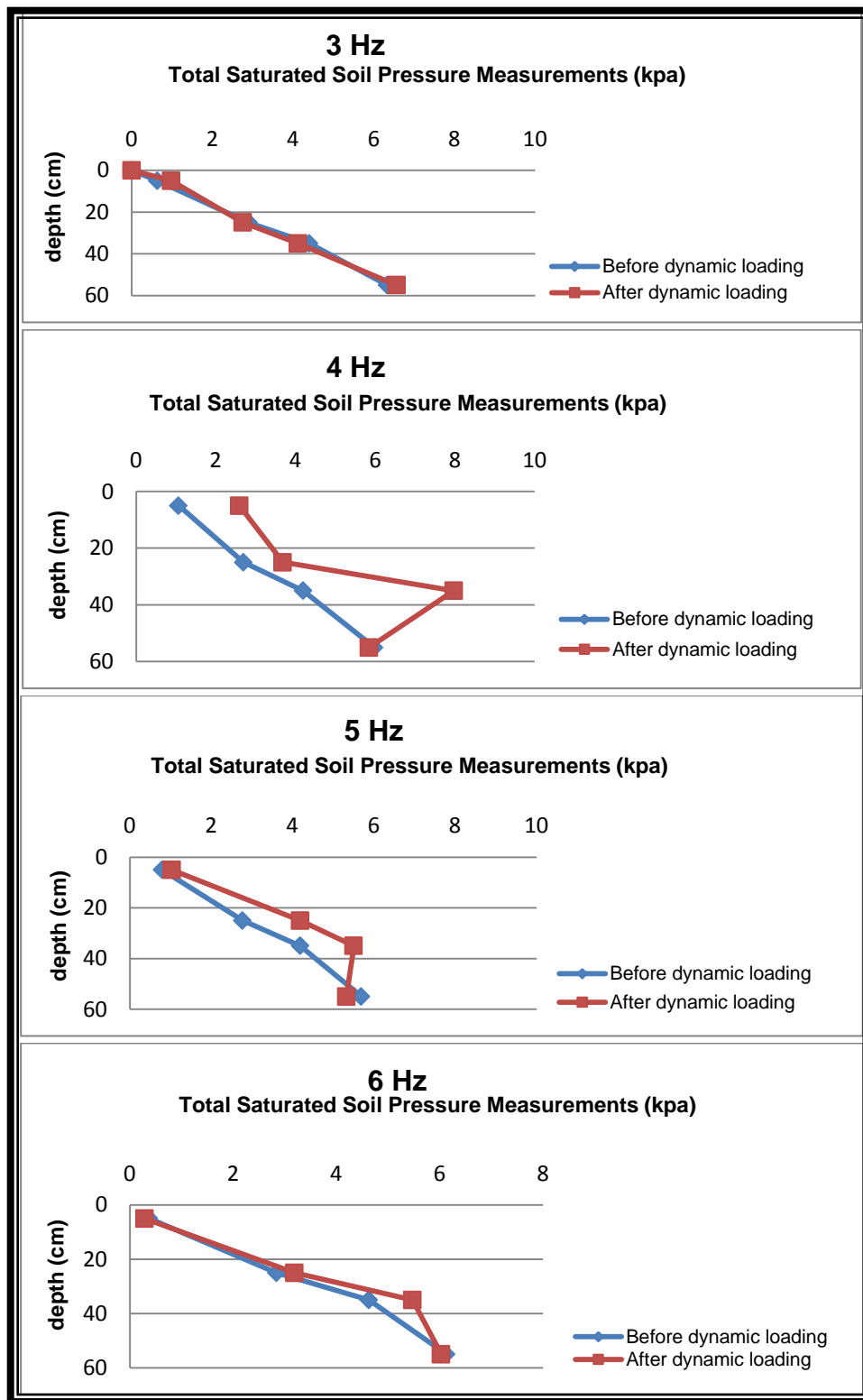


Figure 6.125: Saturated soil pressure measurements acting on block 1, block 2 and block 3 for 3, 4, 5, 6 Hz for Soil 1

As it is seen from the Figure 6.125 and Table 6.18 for Soil 1;

In general:

- *The total saturated soil pressure measurements increase while depth and frequency are increasing for both before and after dynamic loading.*
- *Total saturated soil pressure measurements for both before and after dynamic loading are almost same and these values increase while depth is increasing for 3 Hz.*
- *The pressure values of after dynamic loading is greater than the pressure values for before dynamic loading.*
- *If the final pressures are compared, the pressure values of before and after dynamic loading is close to each other.*

6.4.1.2 Three Blocks- Fluctuating and Non-fluctuating Components of Total Saturated Soil Pressure for Soil 1

Total saturated soil pressures, fluctuating and non-fluctuating components of total saturated soil pressures are given in APPENDIX H for Soil 1.

6.4.1.2.1 Maximum Fluctuating Components of Total Saturated Soil Pressures for Soil 1

Figures given in APPENDIX H show the total saturated soil pressures, non-fluctuating and fluctuating components of total saturated soil pressures versus depth for each frequency are shown in Table 6.19 and Figure 6.126 for Soil 1.

Table 6.19: Maximum fluctuating components of total saturated soil pressures and before dynamic loading pressure measurements for SP1, SP2, SP3 and SP4 for Soil 1

Frequency (Hz)	Soil Pressure Numbers	Before Dynamic Loading (kpa)	Maximum Fluctuating Comp. of Total Saturated Soil Pressure (kpa)
3	SP1	6.34	0.77
	SP2	4.40	0.55
	SP3	2.90	0.29
	SP4	0.64	0.19
4	SP1	5.98	2.47
	SP2	4.19	5.72
	SP3	2.69	2.47
	SP4	1.06	2.93
5	SP1	5.69	1.48
	SP2	4.19	1.85
	SP3	2.77	2.98
	SP4	0.79	1.40
6	SP1	6.13	0.78
	SP2	4.63	2.92
	SP3	2.84	1.48
	SP4	0.37	0.37

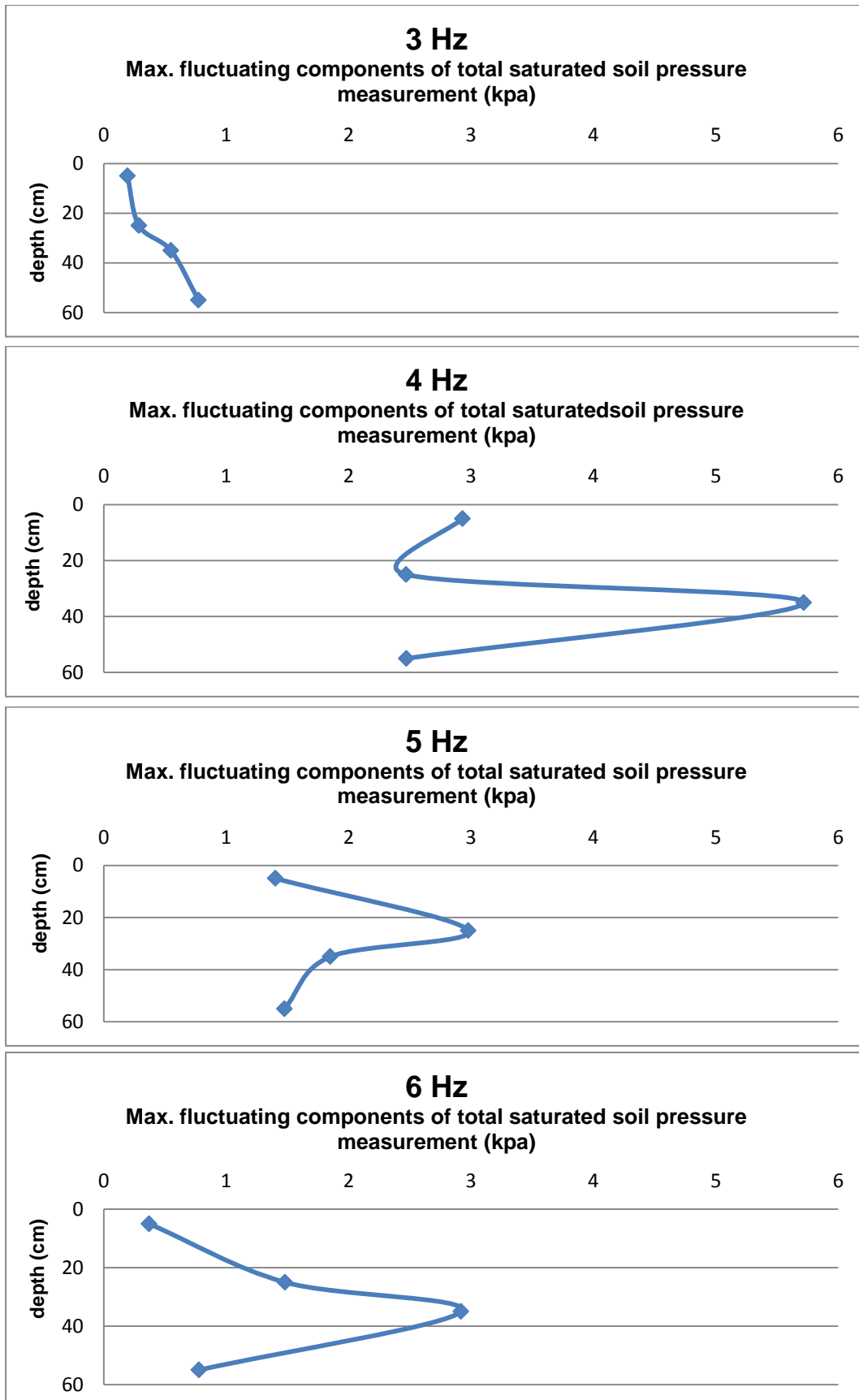


Figure 6.126: Relation between maximum fluctuating component of total lateral earth pressure and depth for Soil 1

As it is seen from Table 6.19 – Figure 6.126 for Soil 1;

- Only for 3 Hz, there is no significant motion on block during dynamic loading, maximum fluctuating component of total saturated soil pressure increases and then while depth is increasing.
- For 4 Hz, 5 Hz and 6 Hz, maximum fluctuating component of total saturated soil pressure increases until a “certain depth”. After a certain depth, fluctuating component of total saturated soil pressures decrease and in general the pressure values at the bottom of the blocks are greater than the pressure values at the top of the blocks. This certain depth is;

Frequency (Hz)	Depth (cm)
4 Hz	35 cm
5 Hz	25 cm
6 Hz	35 cm

Depth ranges are defined as 25 cm – 35 cm. The total height of the blocks is 60 cm, thus the application point of the fluctuating components of total saturated soil pressure (a) is;

$$60 \text{ cm} \times a = 25 \text{ cm} \quad a = 0.42$$

$$60 \text{ cm} \times a = 35 \text{ cm} \quad a = 0.58$$

“Application point of the fluctuating components of total saturated soil pressure is almost between 0.40 H – 0.60 H”.

6.4.1.2.2 Maximum Non-Fluctuating Components of Total Saturated Soil Pressures for Soil 1

The relation between maximum non-fluctuating components of total saturated soil pressures versus depth for each frequency are shown in Table 6.20 and Figure 6.127 for Soil 1.

Table 6.20: Maximum non-fluctuating components of total saturated soil pressures and before dynamic loading pressure measurements for SP1, SP2, SP3 and SP4 for Soil 1

Frequency (Hz)	Soil Pressure Numbers	Before Dynamic Loading (kpa)	Maximum Non-Fluctuating Comp. of Total Saturated Soil Pressure (kpa)
3	SP1	6.34	6.61
	SP2	4.40	4.67
	SP3	2.90	2.93
	SP4	0.64	0.99
4	SP1	5.98	6.74
	SP2	4.19	7.78
	SP3	2.69	3.60
	SP4	1.06	2.33
5	SP1	5.69	6.20
	SP2	4.19	5.79
	SP3	2.77	4.81
	SP4	0.79	1.50
6	SP1	6.13	7.01
	SP2	4.63	6.66
	SP3	2.84	4.39
	SP4	0.37	0.50

As it is seen from Table 6.20 and Figure 6.127 for Soil 1;

- Maximum non-fluctuating components of total saturated soil pressures and the total saturated soil pressures before dynamic loading increase while depth and frequency are increasing.
- Maximum non-fluctuating components of total saturated soil pressures and total saturated soil pressure before dynamic loading are so close to each other for 3 Hz. That is simply because no motion is occurred on block(s) for 3 Hz.
- Maximum non-fluctuating components of total saturated soil pressures are greater than the saturated soil pressure before dynamic loading for 3 Hz, 4 Hz, 5 Hz and 6 Hz.

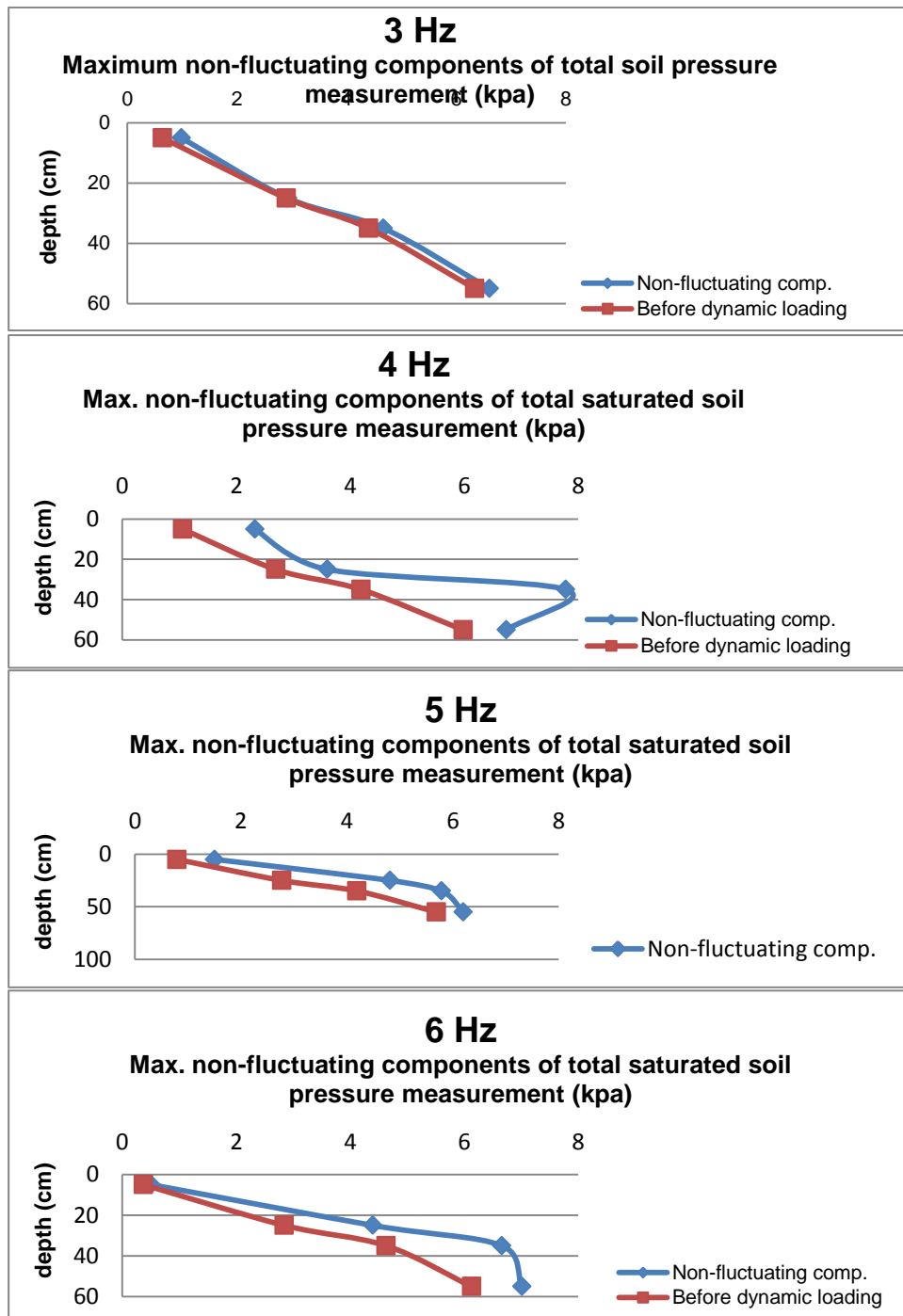


Figure 6.127: Maximum non-fluctuating components of total saturated soil pressure and total saturated soil pressure before dynamic loading for Soil 1

6.4.2 Three Blocks, Soil 2: Soil Pressure Measurements (Test 3.2)

Soil pressure measurements and results are presented for each series for Soil 2 with 3 tests (4 Hz, 5 Hz, and 6 Hz) for three blocks. In Figure 6.129 - Figure 6.131, total saturated soil pressure measurements for each frequency are presented for SP1, SP2, SP3 and SP4 (Figure 6.119).

Figure 6.128 show the general view of the experiment set up of the three blocks tests for Soil 2.



Figure 6.128: Block, instruments, dummies and Soil 2

As it is seen from the Figure 6.129 - Figure 6.131, soil pressure measurements ranges for 4 Hz – 6 Hz are shown in Table 6.21 for Soil 2.

Table 6.21: Soil pressure measurements ranges for 4 Hz – 6 Hz for Soil 2

Frequency	Soil Pressure Cells	Ranges of Total Saturated Soil Pressure Measurements
4 Hz	SP1	5.41 kpa – 9.74 kpa
	SP2	3.12 kpa – 8.79 kpa
	SP3	2.03 kpa – 6.08 kpa
	SP4	0.32 kpa – 1.11 kpa
5 Hz	SP1	4.66 kpa – 8.52 kpa
	SP2	3.69 kpa – 7.78 kpa
	SP3	2.51 kpa – 8.15 kpa
	SP4	0.16 kpa – 1.51 kpa
6 Hz	SP1	5.31 kpa – 7.92 kpa
	SP2	3.56 kpa – 9.91 kpa
	SP3	2.51 kpa – 7.14 kpa
	SP4	1.42 kpa – 0.20 kpa

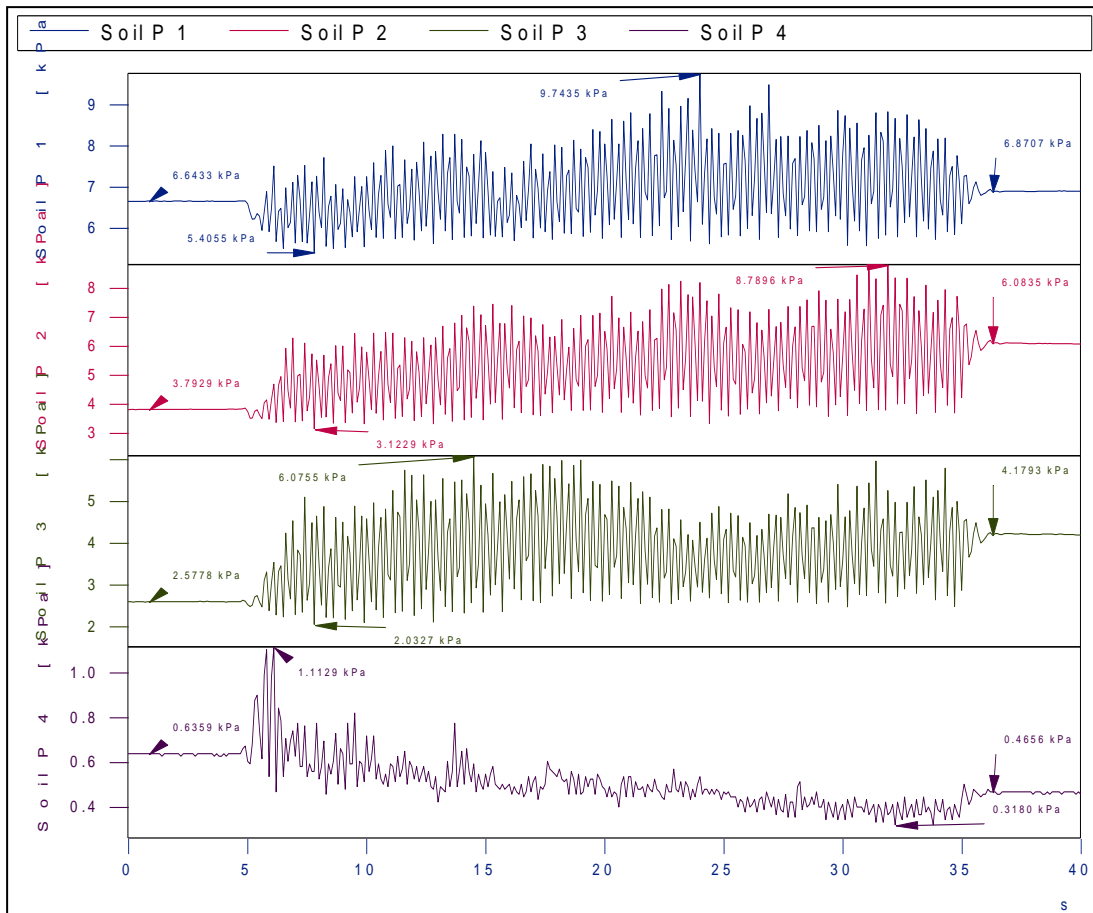


Figure 6.129: Soil pressure measurements for SP1, SP2, SP3 and SP4 for 4 Hz for Soil 2 (Test 3.2.1)

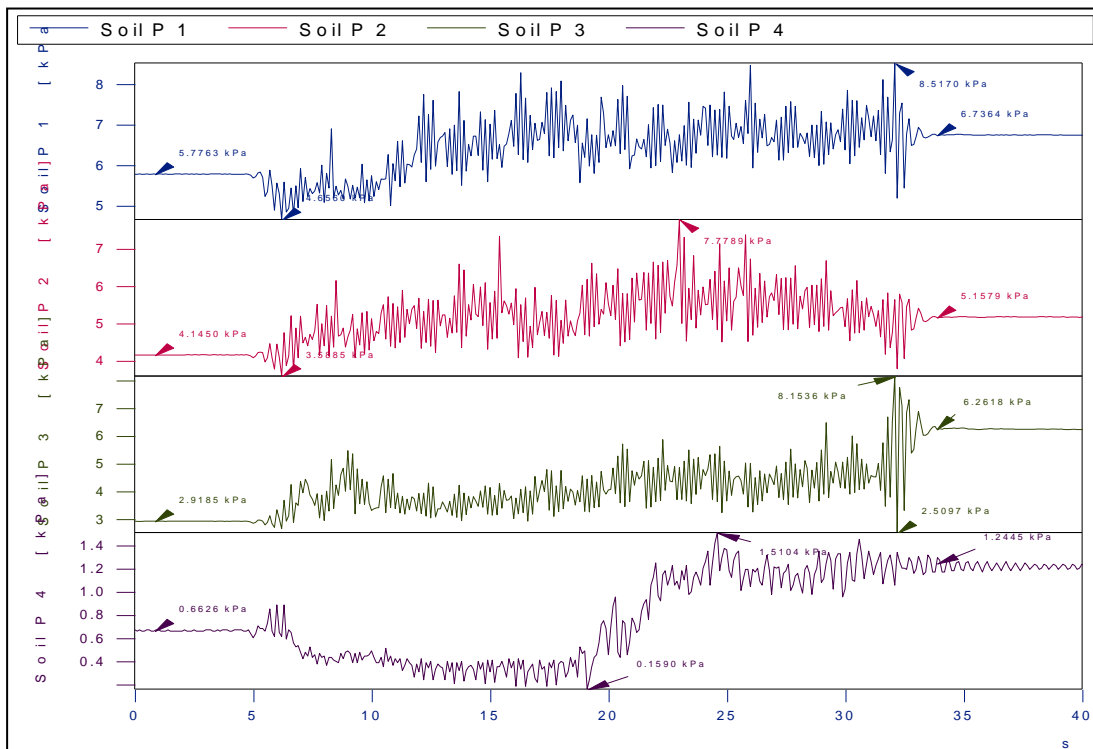


Figure 6.130: Soil pressure measurements for SP1, SP2, SP3 and SP4 for 5 Hz for Soil 2 (Test 3.2.2)

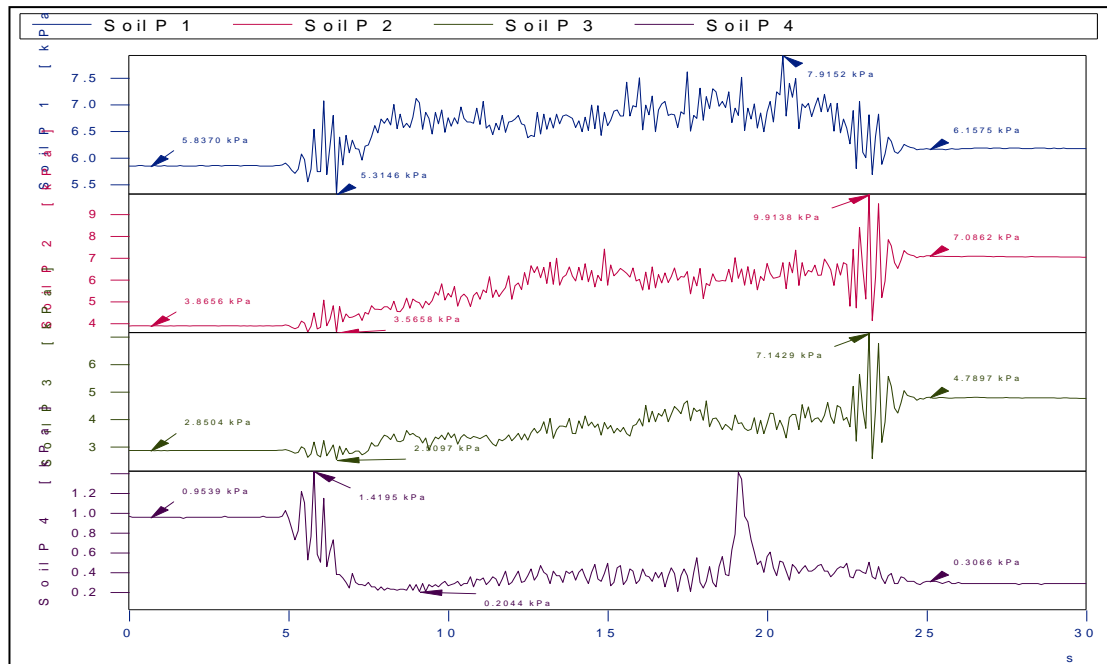


Figure 6.131: Soil pressure measurements for SP1, SP2, SP3 and SP4 for 6 Hz for Soil 2 (Test 3.2.3)

6.4.2.1 Results of Soil Pressure Measurements (Soil 2)

4 soil pressure cells namely SP1, located on the Block 1, and SP2 and SP3, located on the Block 2 and SP4, located on the Block 3, were used to define the total saturated soil pressure distribution acting on blocks for Soil 2 for each frequency (4 Hz - 6 Hz).

In contrary to Soil 1, for Soil 2, there is no significant sudden decrease are observed within a few seconds on total saturated soil pressure measurements obtained before dynamic loading. Because of this, finer material was used as backfill material.

For the frequencies 4 Hz - 6 Hz, the total saturated soil pressure measured for two different conditions -before dynamic loading and at the end of (after) dynamic loading - are given in Table 6.22.

Table 6.22: Total saturated soil pressure measurements for different frequencies before and after dynamic loading for Soil 2

Frequency (Hz)	Soil Pressure Numbers	Total Saturated Soil Pressures (kpa)	
		Before Dynamic Loading (kpa)	After Dynamic Loading (kpa)
4	SP1	6.64	6.87
	SP2	3.79	6.08
	SP3	2.58	4.18
	SP4	0.64	0.47
5	SP1	5.78	6.74
	SP2	4.15	5.16
	SP3	2.92	6.26
	SP4	0.66	1.25
6	SP1	5.83	6.16
	SP2	3.87	7.09
	SP3	2.85	4.79
	SP4	0.95	0.31

Total saturated soil pressure measurements for before dynamic loading and after dynamic loading acting on blocks for each frequency (4 Hz, 5 Hz, 6 Hz) for Soil 2 versus depth relations are given in Figure 6.132.

As it is seen from the Figure 6.132 and Table 6.22 for Soil, in general:

- Total saturated soil pressure values for both before and after dynamic loading are increase while depth and frequency are increasing.
- The pressure values of after dynamic loading is greater than the pressure values of before dynamic loading.
- if the final pressures are compared, it is realized that the pressure values for before dynamic loading is close to after dynamic loading.
- if the final pressures are compared, it is realized that the pressure values for before dynamic loading is nearly same or smaller than the pressure values for after dynamic loading. This results show that different from the Soil 1, Soil 2 (finer backfill material) exhibits irregular profile due to scattering of backfill material instead of showing regular profile due to compaction of backfill material for frequency increment. Compaction does not occur efficiently and relative density (D_r) decreases for Soil 2 due to dynamic loading.

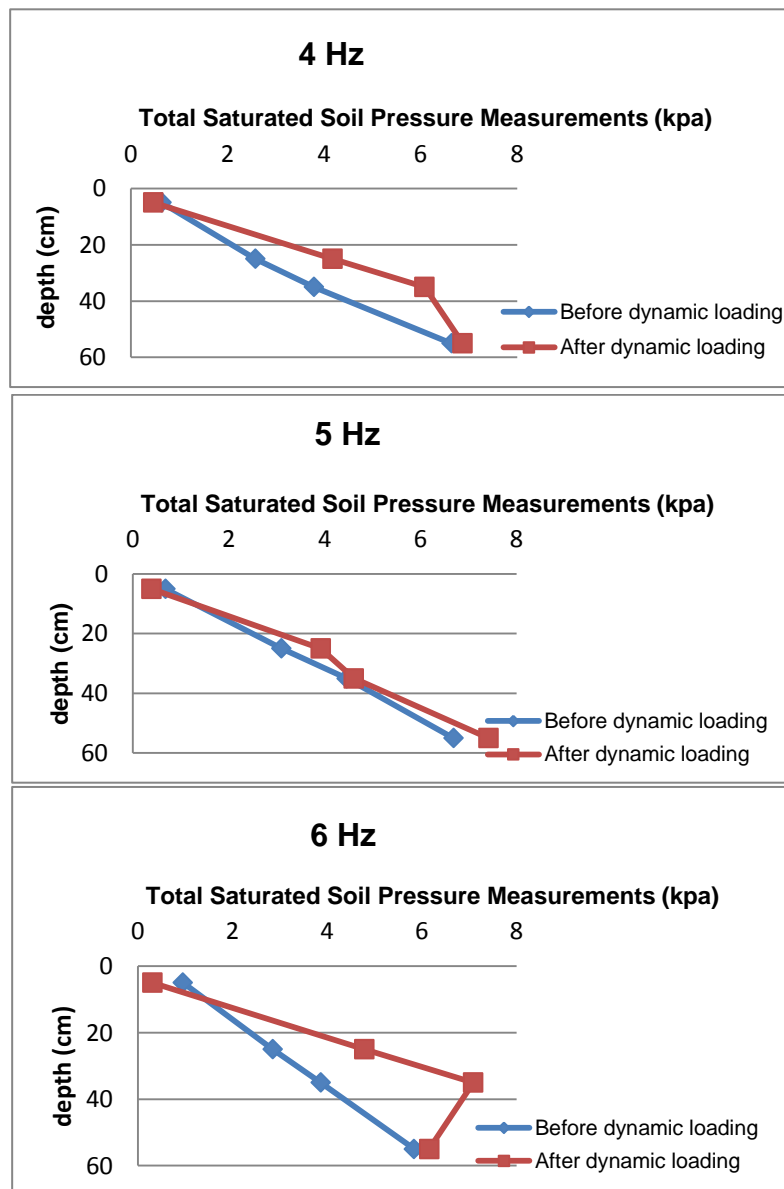


Figure 6.132: Total saturated soil pressure measurements acting on block 1, block 2 and block 3 for 4, 5, 6 Hz for Soil 2

6.4.2.2 Three Blocks- Fluctuating and Non-fluctuating Components of Total Saturated Soil Pressure for Soil 2

Total saturated soil pressures, fluctuating and non-fluctuating components of total saturated soil pressures are shown in APPENDIX H for different frequencies for Soil 2.

6.4.2.2.1 Maximum Fluctuating Components of Saturated Total Soil Pressures for Soil 2

The relation between maximum fluctuating components of total saturated soil pressures and depth for each frequency are shown in Table 6.23 and Figure 6.133 for Soil 2.

Table 6.23: Maximum fluctuating components of total saturated soil pressures and before dynamic loading pressure measurements for SP1, SP2, SP3 and SP4 for Soil 2

Frequency (Hz)	Soil Pressure Numbers	Before Dynamic Loading (kpa)	Maximum Fluctuating Comp. of Total Saturated Soil Pressure (kpa)
4	SP1	6.64	2.75
	SP2	3.79	2.99
	SP3	2.58	2.09
	SP4	0.64	0.46
5	SP1	5.78	1.75
	SP2	4.15	2.13
	SP3	2.92	2.71
	SP4	0.66	0.37
6	SP1	5.83	1.00
	SP2	3.87	3.28
	SP3	2.85	2.67
	SP4	0.95	0.89

As it is seen from Table 6.23 and Figure 6.133 for Soil 2;

- *Maximum fluctuating component of saturated soil pressure increases until a “certain depth” for 4 Hz, 5 Hz and 6 Hz. After a certain depth, dynamic effect of the saturated soil pressures decreases and in general the pressure values at the bottom of the blocks are greater than the pressure values at the top of the blocks.*

This certain depth is;

Frequency (Hz)	Depth (cm)
4 Hz	35 cm
5 Hz	27 cm
6 Hz	32 cm

Depth ranges are defined as 25 cm – 35 cm. The total height of the blocks is 60 cm, thus the application point of the fluctuating components of total saturated soil pressure (a) is;

$$\begin{aligned}
 60 \text{ cm} \times a &= 35 \text{ cm} & a &= 0.58 \\
 60 \text{ cm} \times a &= 27 \text{ cm} & a &= 0.45 \\
 60 \text{ cm} \times a &= 32 \text{ cm} & a &= 0.53
 \end{aligned}$$

“Application point of the fluctuating components of total saturated soil pressure is almost between 0.45 H – 0.60 H”.

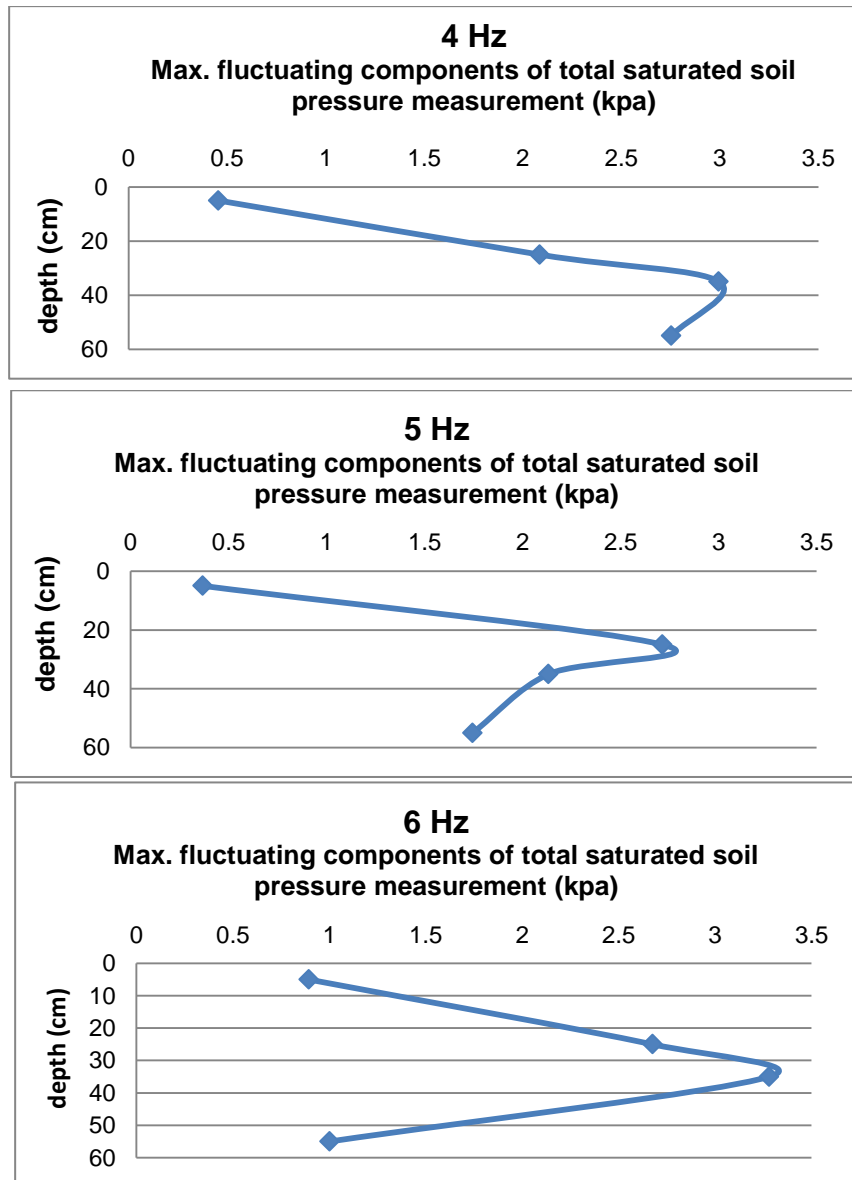


Figure 6.133: Relation between maximum fluctuating component of total saturated soil pressure and depth for Soil 2

6.4.2.2.2 Maximum Non-Fluctuating Components of Total Saturated Soil Pressures for Soil 2

The relation between maximum fluctuating components of total saturated soil pressures versus depth for each frequency are shown in Table 6.24 and Figure 6.134 for Soil 2.

As it is seen from Table 6.24 and Figure 6.134 for Soil 2;

- Maximum non-fluctuating components of total saturated soil pressures and the total saturated soil pressures before dynamic loading increase while depth is increasing for each frequency.
- Maximum non-fluctuating components of total saturated soil pressures are greater than the saturated soil pressure before dynamic loading for 4 Hz, 5 Hz and 6 Hz.

Table 6.24: Maximum non-fluctuating components of total saturated soil pressures and before dynamic loading pressure measurements for SP1, SP2, SP3 and SP4 for Soil 2

Frequency (Hz)	Soil Pressure Numbers	Before Dynamic Loading (kpa)	Maximum Non-fluctuating Comp. of Total Saturated Soil Pressure (kpa)
4	SP1	6.64	6.99
	SP2	3.79	5.96
	SP3	2.58	4.08
	SP4	0.64	0.66
5	SP1	5.78	6.78
	SP2	4.15	5.73
	SP3	2.92	6.00
	SP4	0.66	1.23
6	SP1	5.83	6.94
	SP2	3.87	6.95
	SP3	2.85	4.73
	SP4	0.95	0.88

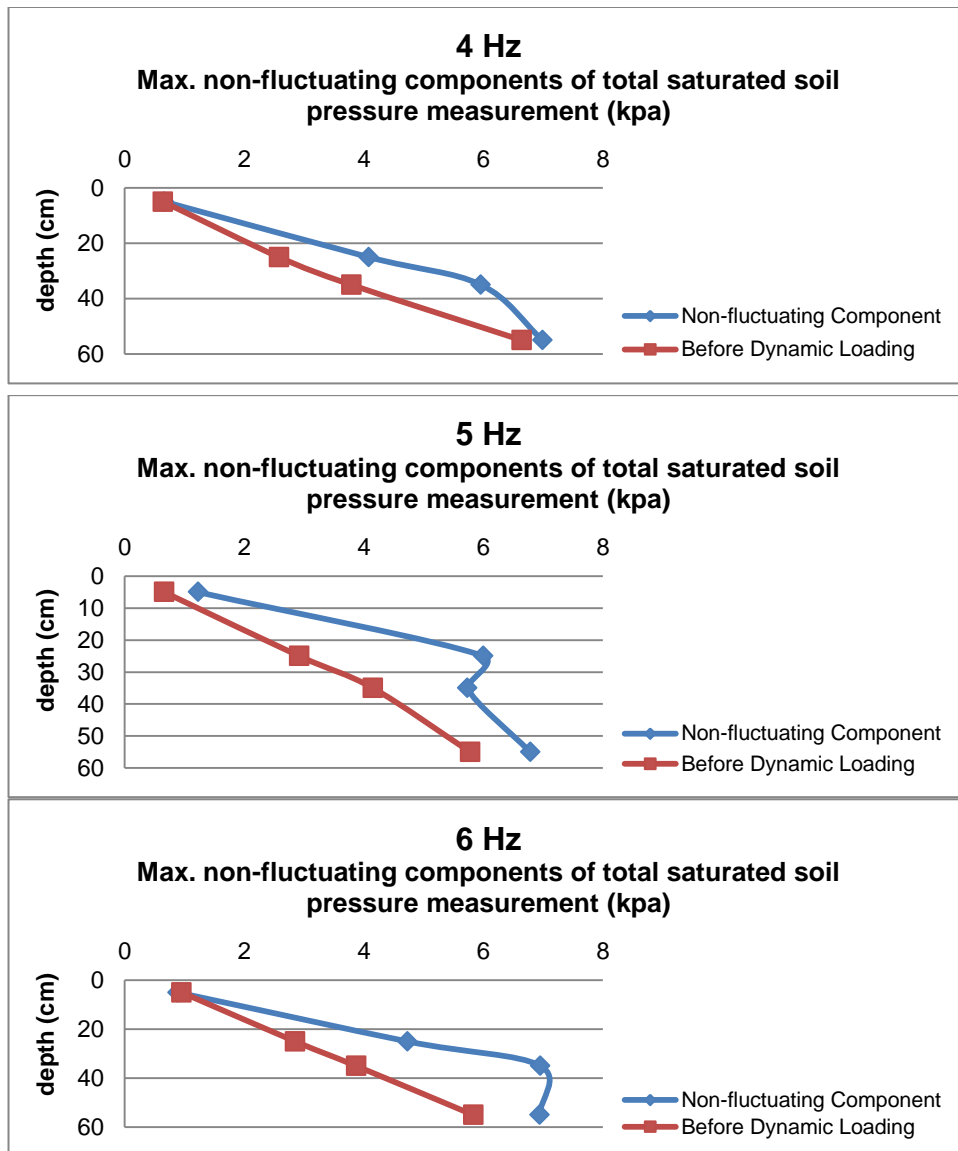


Figure 6.134: Maximum non-fluctuating components of total saturated soil pressure and total saturated soil pressure before dynamic loading for Soil 2

6.4.2.2.3 Presentation and Discussion of the Soil Pressure Measurement Results

In the design of block type quay walls under dynamic loading are found to be not fully understood. Therefore experimental studies (Table 4.9) were carried out for one block, two blocks and three blocks for Soil 1 and Soil 2 used as backfill material for different frequencies to shed a light to ambiguity of the pressure distribution for block type quay walls under dynamic loading.

Relative density (D_r) and internal friction angle (ϕ) of the backfill material placed an important role on saturated soil pressure as observed from the experiments.

Total saturated soil pressure for Soil 1 (coarser) was higher than Soil 2 (finer) for 2 Hz – 4 Hz. The higher pressure measurements during the experiments indicated the lower relative density and related internal friction angle during dynamic loading for Soil 1, even though, these properties ($D_r=0.60 - 0.70$ and $\phi=40^\circ - 42^\circ$) were almost the same in the preparation of the experiments..

Total saturated soil pressures for Soil 1 was almost same as Soil 2 for higher frequencies (5 Hz – 6 Hz). This can be explained by having almost the same relative density and related internal friction angle during dynamic loading for higher frequencies (5 Hz – 6 Hz).

Increase in frequency means that number of cycles of dynamic loading increases which causes an increase in acceleration measurements.

Test results were presented by considering the non-fluctuating and fluctuating components of total saturated soil pressure under dynamic loading for each frequency for one, two and three block(s). The most important outcome of these measurements were the distribution of the fluctuating component of the total saturated soil pressure together with the point of application resulting from dynamic loading for seismic design of block type quay walls which were left to be understood clearly.

Currently, there is only some suggested assumptions for practical applications for the seismic design of block type quay walls (Technical Seismic Specifications on Construction of Coastal and Harbor Structures, Railways And Airports, 2008) based on conventional seismic design method that has to be reviewed.

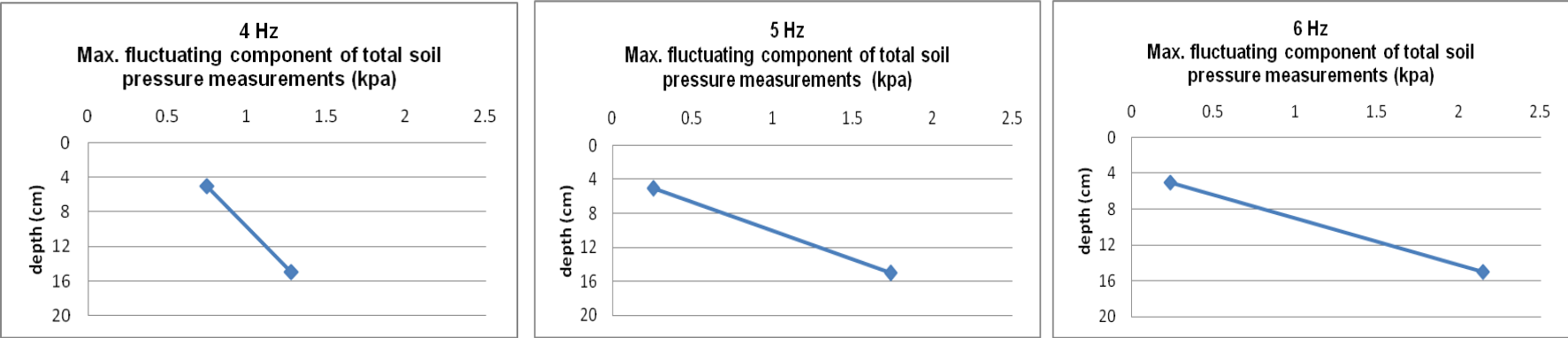
At present seismic design of block type quay wall as given in Technical Seismic Specifications on Construction of Coastal and Harbor Structures, Railways And Airports (2008) has no suggestion of the distribution of the saturated soil pressure under dynamic loading. It uses saturated soil pressure distribution under dynamic loading based on Mononobe – Okabe Method which linearly increases towards the foundation. The moment obtained from the saturated soil pressure under dynamic loading is then increased by multiplying by a coefficient equal to 1.5. This approach however results in larger dimension for the blocks to satisfy the factor of safety for sliding and overturning larger than at least 1 and 1.1, respectively.

The distribution of the fluctuating component of total saturated soil pressure under dynamic loading however will be the fundamental input to pass on to the performance based design. These findings on distribution of the fluctuating component of the total saturated soil pressure together with the point of application will be input to performance based methodology which is the ultimate aim of this study.

Results of maximum fluctuating components of the total saturated soil pressure for these tests are presented in summary in Figure 6.135 - Figure 6.137.

In view of the experimental results of the present study, maximum fluctuating component of the total saturated soil pressure for multi blocks type quay walls, up to a certain depth increases and then decreases for each frequency for Soil 1 and Soil 2. The application point of the fluctuating components of total saturated soil pressure is obtained almost between $0.40 H - 0.63 H$ (above the foundation) for Soil 1 (coarser) and $0.375 H$ and $0.65 H$ (above the foundation) for Soil 2 (finer), where H is the height of the structure.

SOIL 1



SOIL 2

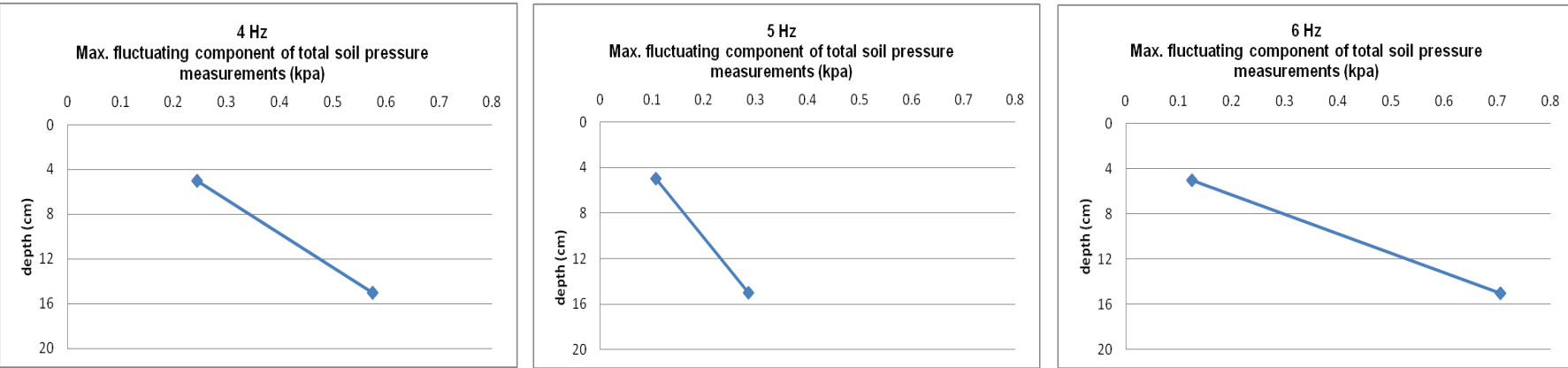
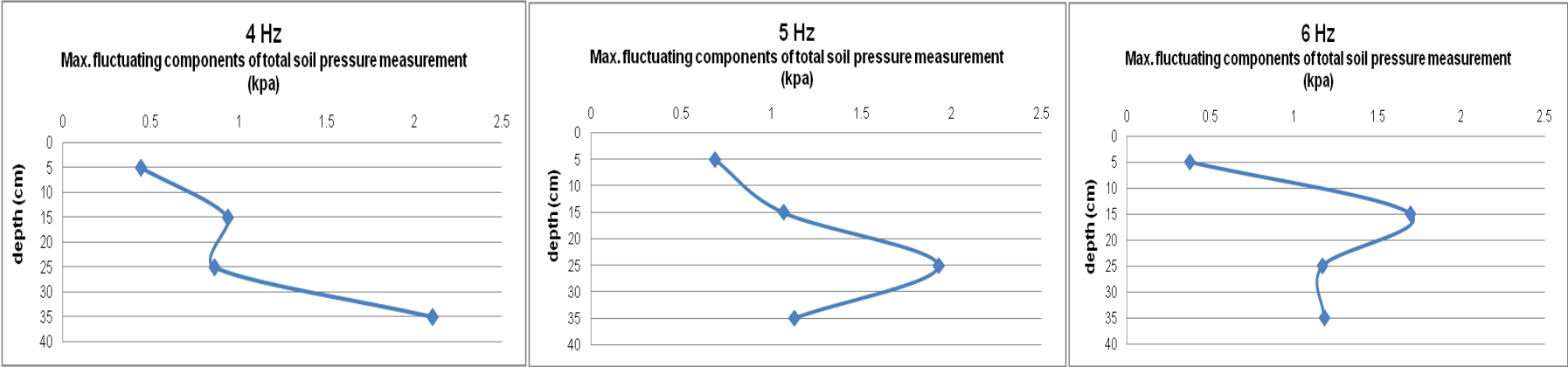


Figure 6.135: Maximum fluctuating component of total saturated soil pressure for Soil 1 and Soil 2 for one block

SOIL 1



SOIL 2

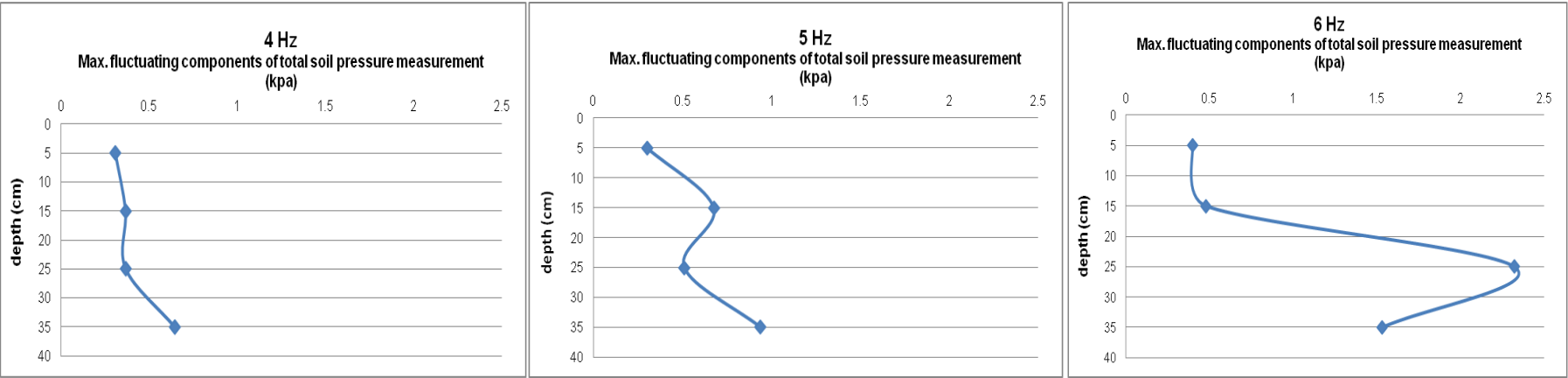


Figure 6.136: Maximum fluctuating component of total saturated soil pressure distribution acting on two blocks

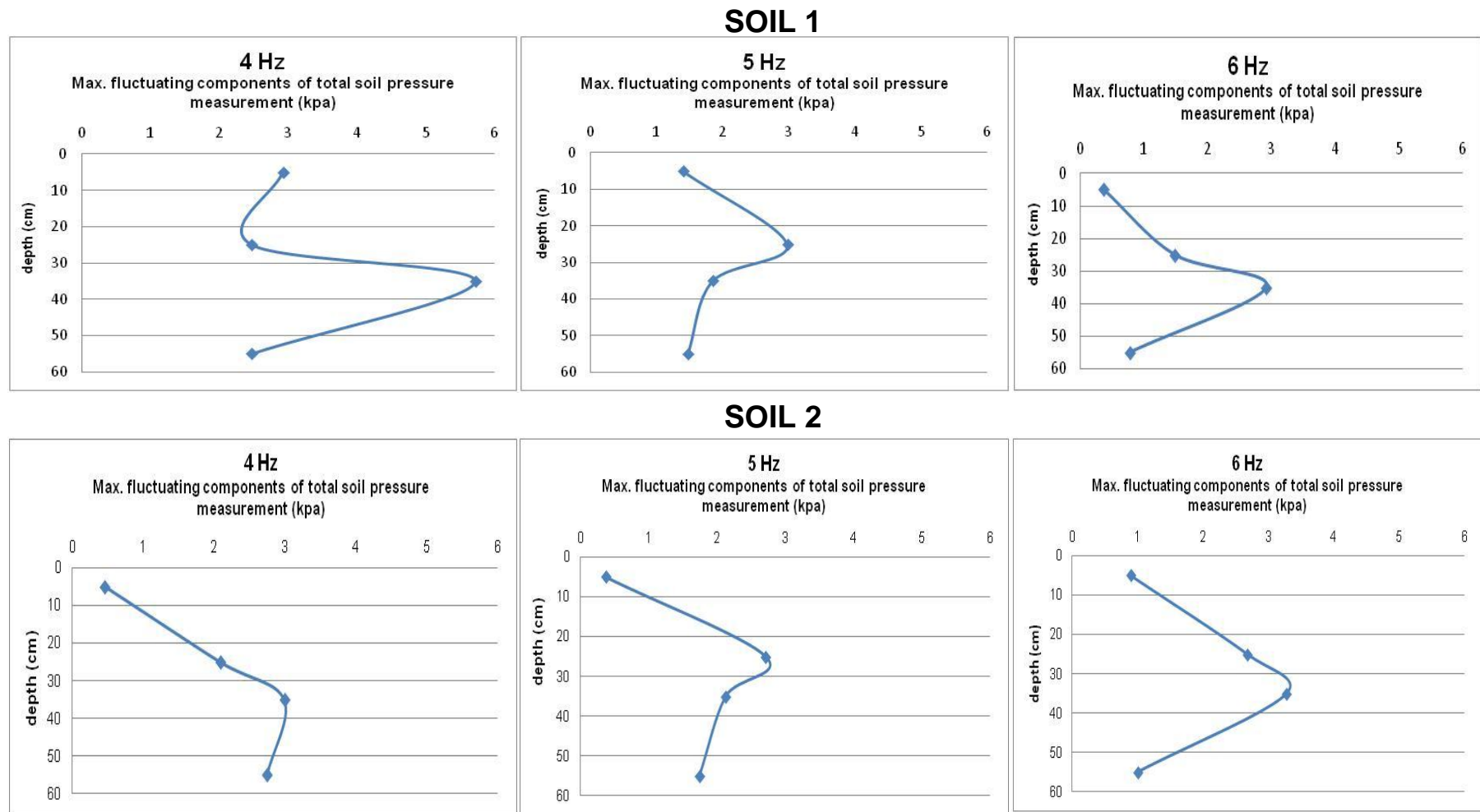


Figure 6.137: Maximum fluctuating component of total saturated soil pressure distribution acting on three blocks

CHAPTER 7

PRESENTATION AND DISCUSSION OF THE RESULTS OF POSITION TRANSDUCERS MEASUREMENTS

In this chapter, position transducers measurements and results are presented for each series for Soil 1 with 5 tests (2 Hz, 3 Hz, 4 Hz, 5 Hz, 6 Hz) for one block and two blocks, 4 tests (3 Hz, 4 Hz, 5 Hz, 6 Hz) for three blocks. Position transducers measurements and results are presented for each series for Soil 2 with 3 tests (4 Hz, 5 Hz, 6 Hz) for one block and two blocks, 3 tests (3 Hz, 4 Hz, 5 Hz) for three blocks.

7.1 One Block: Position Transducers Measurements (Test 1.1 and Test 1.2)

1g shaking table tests were performed with two position transducers – one of them was used for measuring the horizontal displacement, the other one was used for measuring the vertical displacement and tilting – for each frequency for one block tests for Soil 1. Due to the modification of the experimental set-up, it could not be performed the vertical displacement measurements for Soil 2.

7.1.1 One Blok, Soil 1: Position Transducers Measurements (Test 1.1)

General view of position transducers namely P1 (for vertical displacement measurements) located edge point of the block 1 and P2 (for horizontal displacement measurements) located near block for one block tests for Soil 1- Tests 1 are shown in Figure 7.1. The tests results are shown in Figure 7.3 – Figure 7.7 for Soil 1.

Figure 7.2 shows the placements of the position transducers for one block tests for Soil 1.

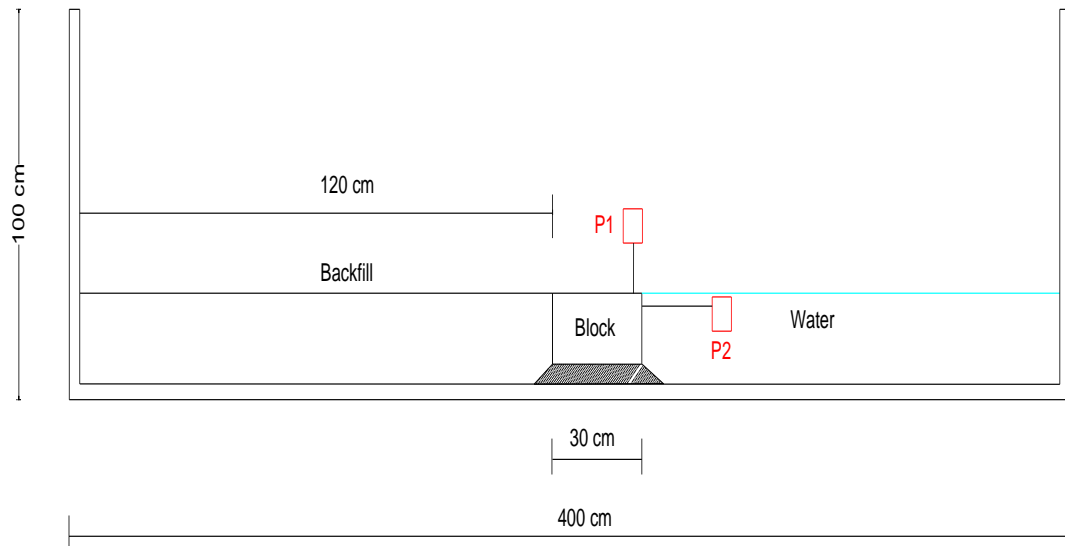


Figure 7.1: General view of position transducers (P1 and P2) for one block tests for Soil 1



Figure 7.2: Position transducers for one block tests for Soil 1

Position transducers measurements results for each frequency are presented by using two position transducers, P1 and P2, are shown in Figure 7.3 – Figure 7.7 for Soil 1 (Figure 7.1).

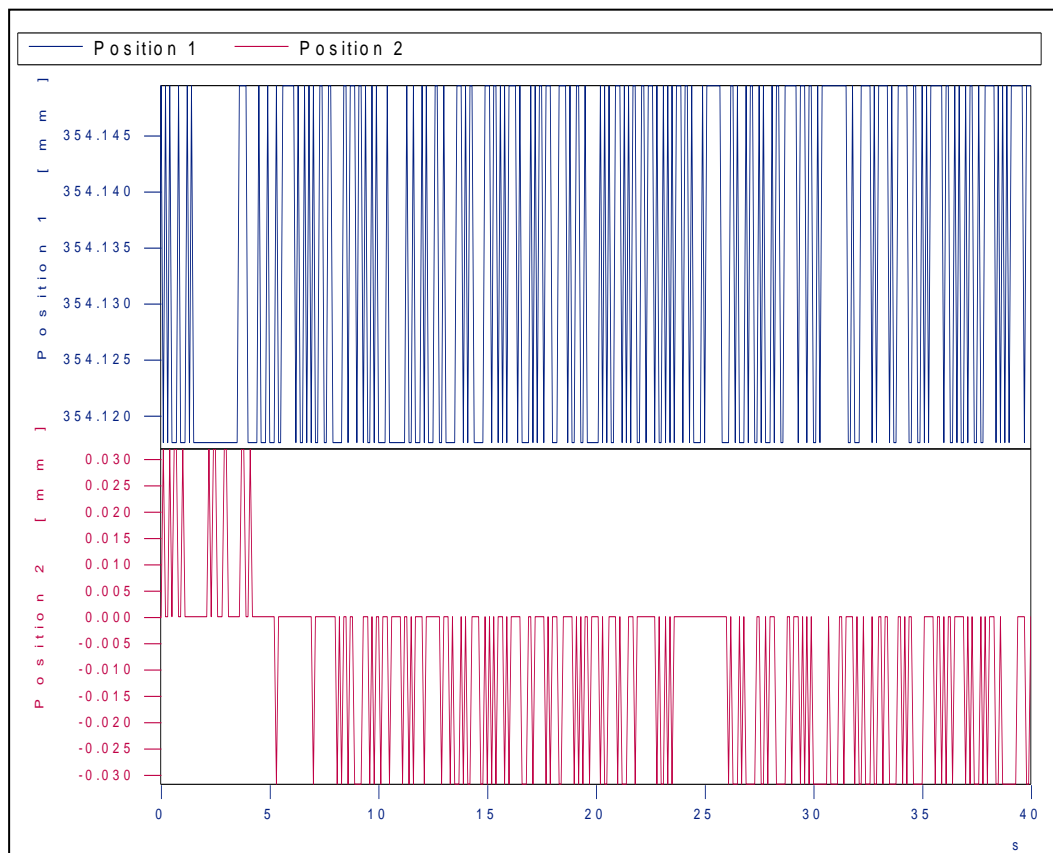


Figure 7.3: Horizontal and vertical displacement measurements for one block for 2 Hz

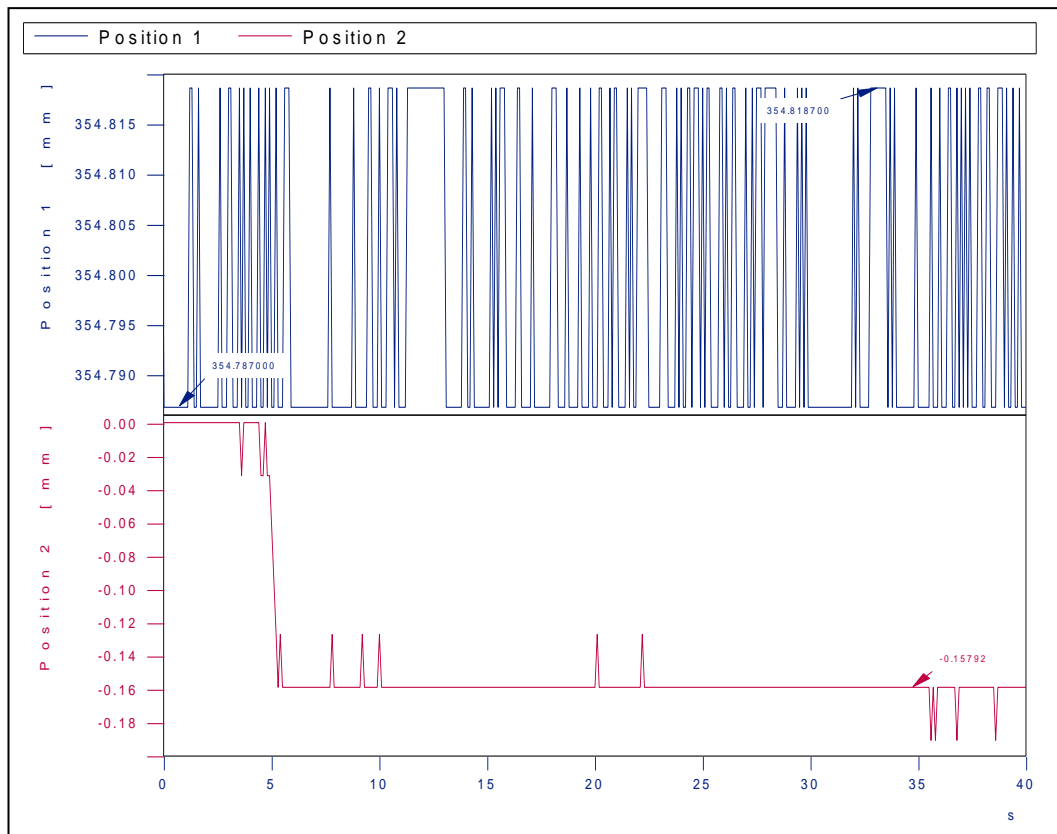


Figure 7.4: Horizontal and vertical displacement measurements for one block for 3 Hz

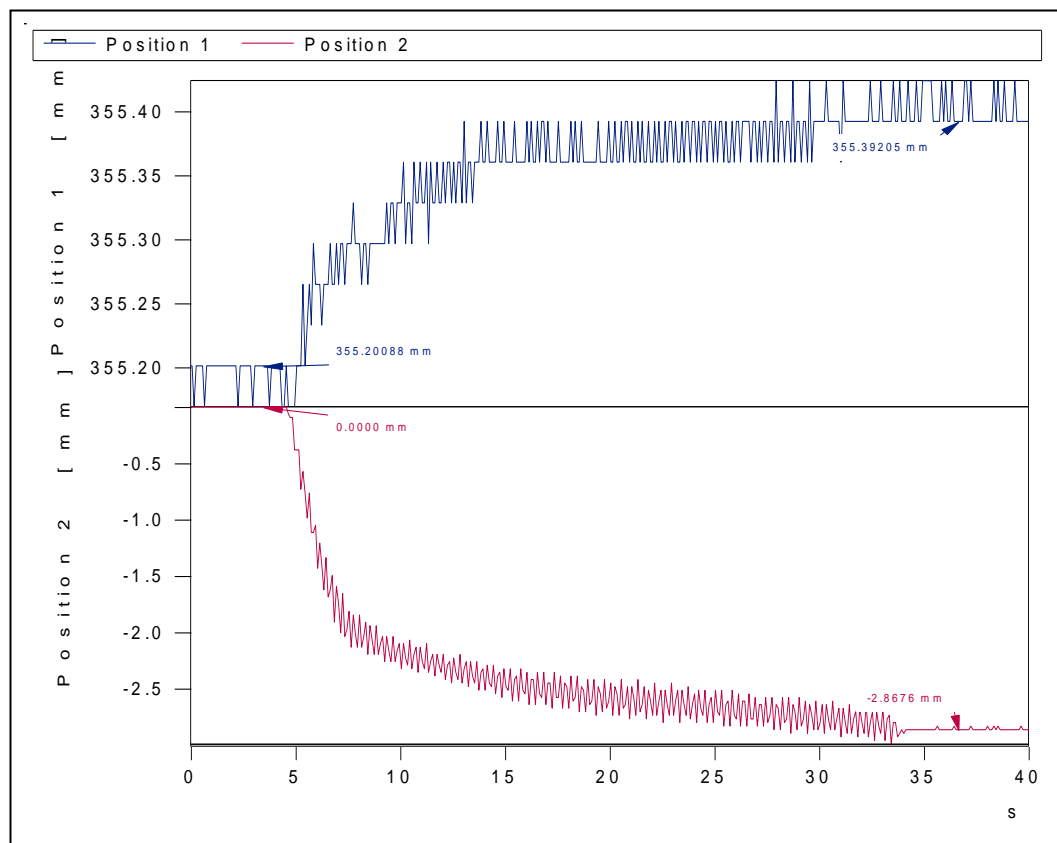


Figure 7.5: Horizontal and vertical displacement measurements for one block for 4 Hz

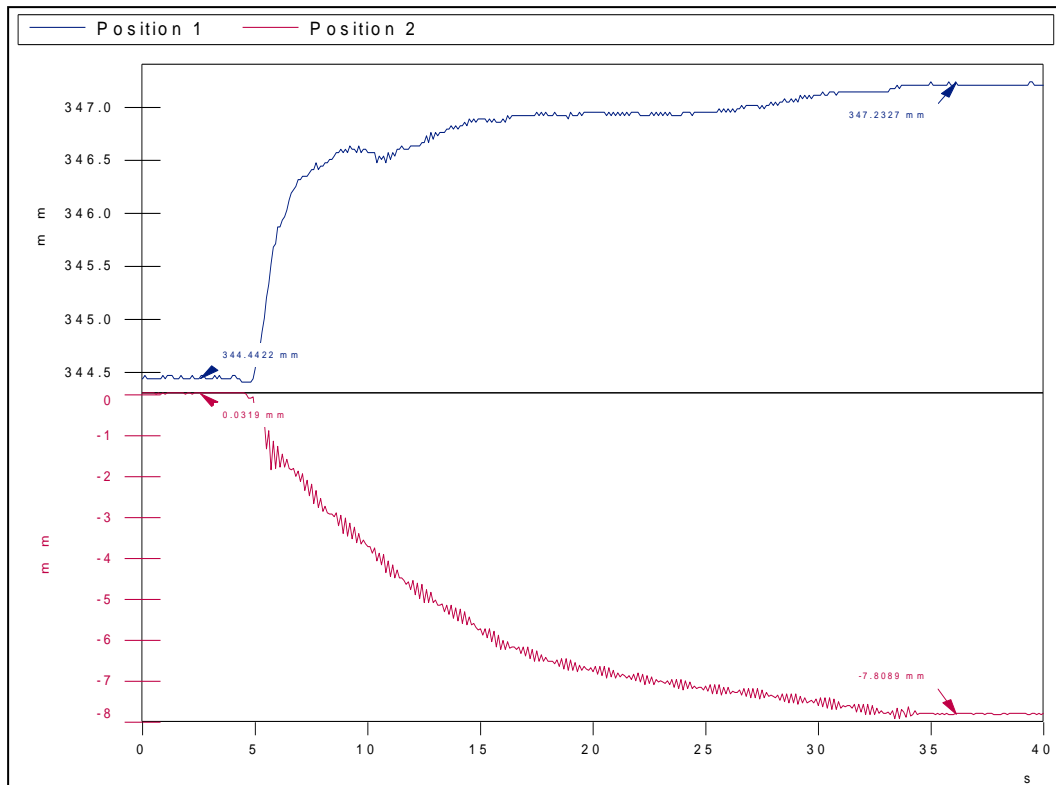


Figure 7.6: Horizontal and vertical displacement measurements for one block for 5 Hz

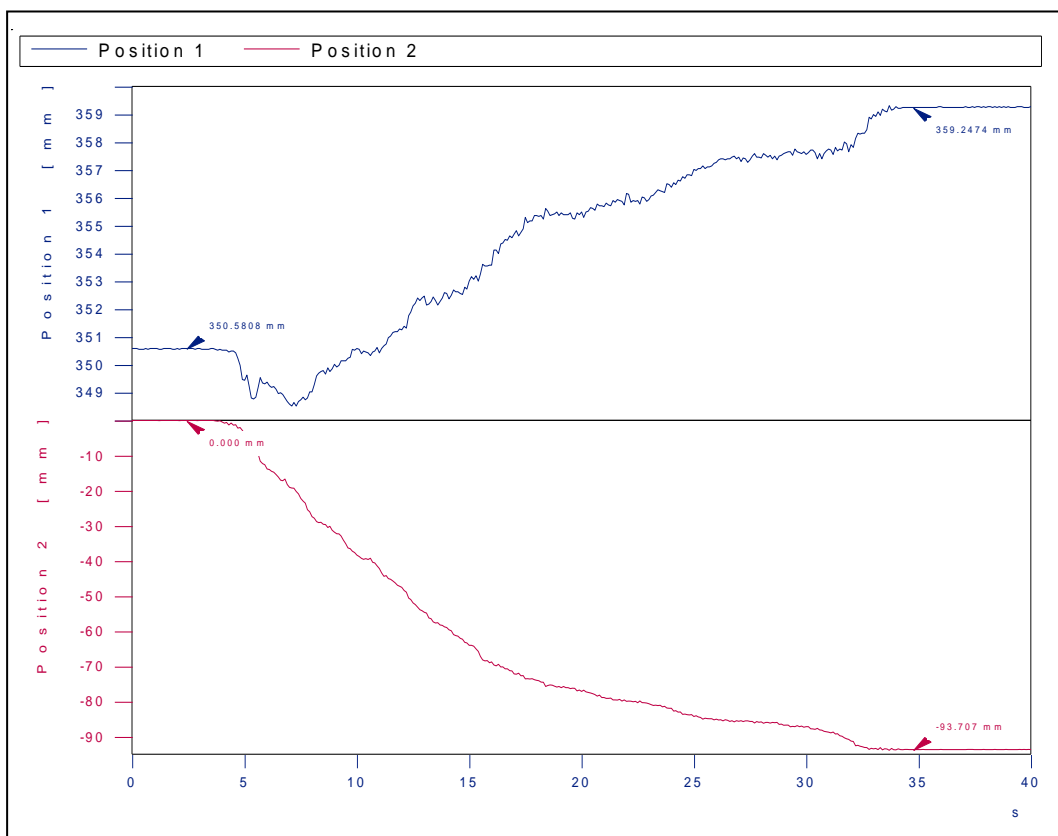


Figure 7.7: Horizontal and vertical displacement measurements for one block for 6 Hz

7.1.1.1 Horizontal, Vertical Displacements Measurements and Tilting Degree

Table 7.1 shows the horizontal, vertical displacement measurements results and calculated tilting values for each frequency for one block for Soil 1. Figure 7.9, Figure 7.10, Figure 7.11 show the horizontal, vertical displacement measurements results and calculated tilting values respectively. Figure 7.8 shows how to horizontal displacement measurements were observed for one block tests for Soil 1.



Figure 7.8: Position transducers for one block tests for Soil 1

Table 7.1: Horizontal, vertical displacement measurements results and calculated tilting values for each frequency for one block for Soil 1

Frequency (Hz)	Horizontal Disp. (mm)	Vertical Disp. (mm)	Tilting (degree)
2	0	0	0
3	0.16	0	0
4	2.87	0.18	0.07
5	7.78	2.7	1.03
6	93.71	-	-

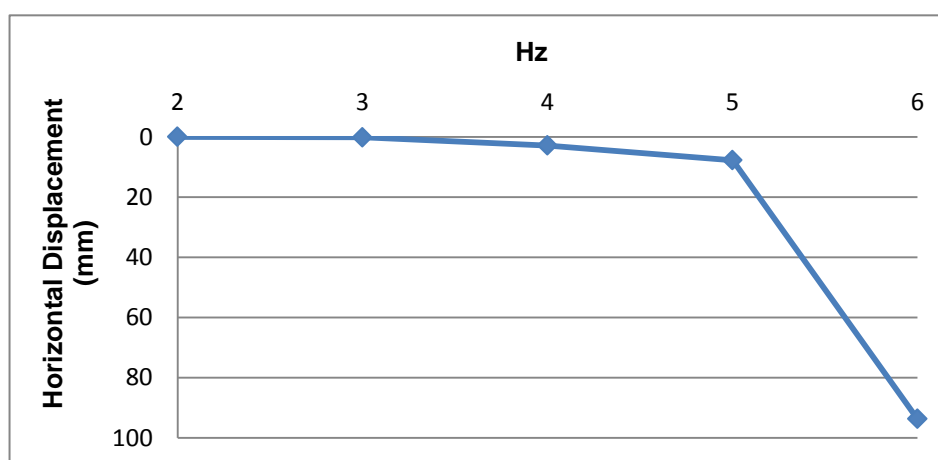


Figure 7.9: Horizontal displacement measurements for one block for Soil 1

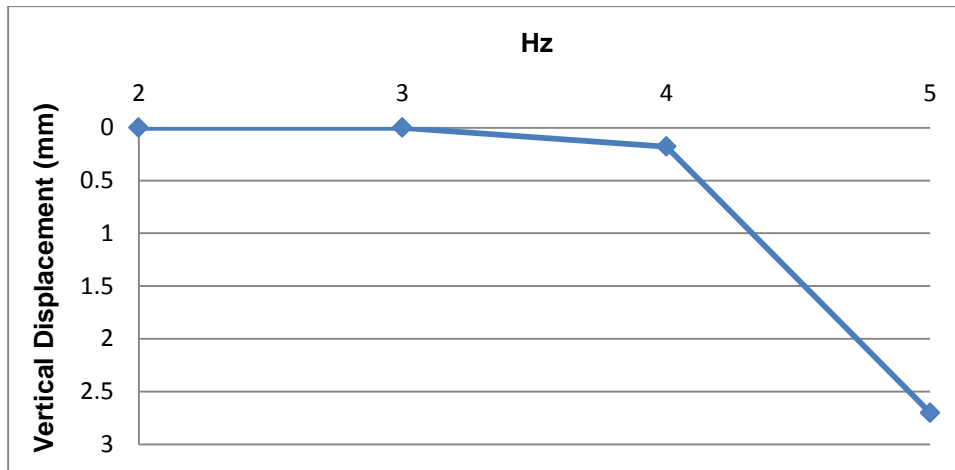


Figure 7.10: Vertical displacement measurements for one block for Soil 1

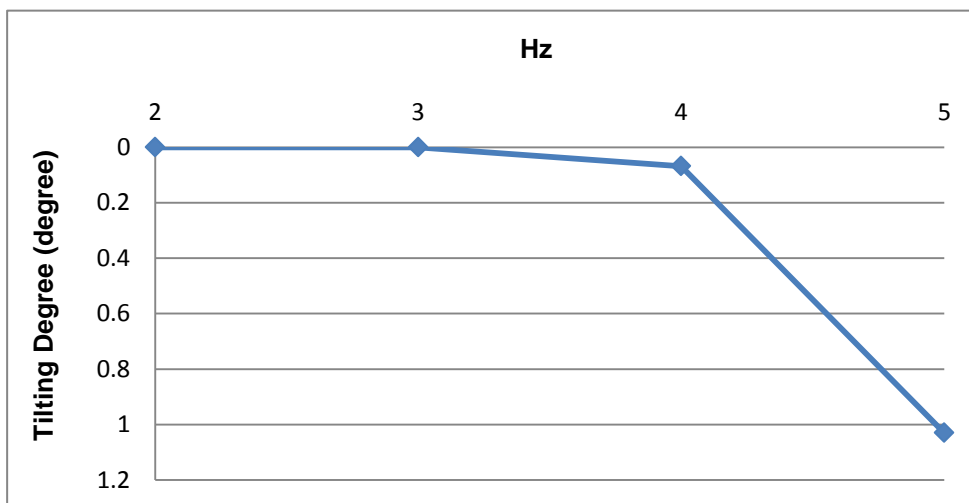


Figure 7.11: Tilting degree for one block for Soil 1

7.1.2 One Block, Soil 2: Position Transducers Measurements (Test 1.2)

General views of position transducers (P2) for one block tests for Soil 2- Tests 1.2 are shown in Figure 7.12 . The tests results are shown in APPENDIX I for Soil 2.

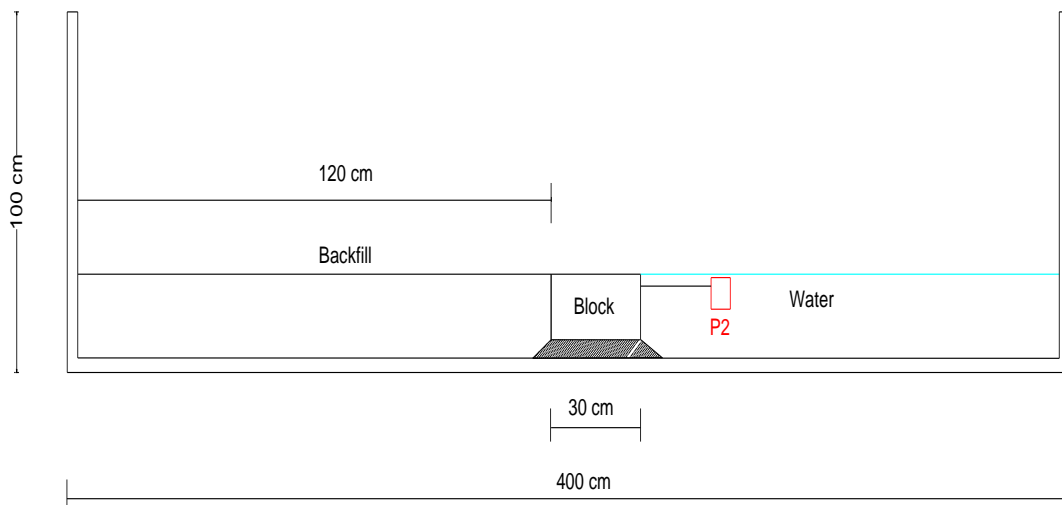


Figure 7.12: General view of position transducers (P2) for one block tests for Soil 2

Figure 7.13 shows the placements of the position transducer for one block tests for Soil 2.



Figure 7.13: Position transducer for one block test for Soil 2

7.1.2.1 Horizontal, Vertical Displacements and Tilting Degree

Table 7.2 shows the horizontal, vertical displacement measurements and tilting values for each frequency for one block for Soil 2. Figure 7.14 show the horizontal, vertical displacement measurements and tilting values respectively.

Table 7.2: Horizontal displacement measurements for each frequency for one block tests for Soil 2

Frequency (Hz)	Horizontal Disp. (mm)	Vertical Disp. (mm)	Tilting (degree)
4	2.12	-	-
5	17.07	-	-
6	114.14	-	-

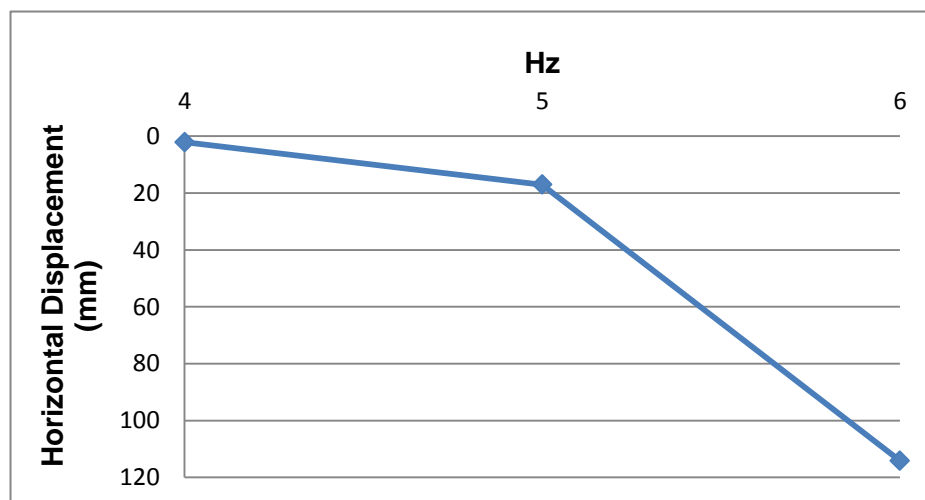


Figure 7.14: Horizontal displacement measurements for one block tests for Soil 2

7.1.3 Comparisons of Results for Position Transducers for One Block for Soil 1 and Soil 2

Table 7.3 shows the horizontal and vertical displacement measurements and calculated tilting values for one block for Soil 1 and Soil 2.

Table 7.3: Comparisons of tests results of one block for Soil 1 and Soil 2

FREQUENCY	DISPLACEMENTS	SOIL 1	SOIL 2
4 Hz	Horizontal Displacement (mm)	2.87	2.12
	Vertical Displacement (mm)	0.18	-
	Tilting (degree)	0.07	-
5 Hz	Horizontal Displacement (mm)	7.78	17.07
	Vertical Displacement (mm)	2.7	-
	Tilting (degree)	1.03	-
6 Hz	Horizontal Displacement (mm)	93.71	114.141
	Vertical Displacement (mm)	-	-
	Tilting (degree)	-	-

- the horizontal displacement measurements increase, while frequency is increasing for Soil 1 and Soil 2,
- the vertical displacement measurements and tilting degree also increase while frequency is increasing for Soil 1 and Soil 2,
- for 2 Hz, there is no motion for Block 1 for Soil 1,
- for 3 Hz, Block 2, starts to slide for Soil 1,
- for 4 Hz, the horizontal displacement measurements are same for Soil 1 and Soil 2,
- for 5 Hz, sudden increment occurs for horizontal and vertical displacement measurements and tilting degree for Soil 1 and Soil 2,
- It is not possible to evaluate the vertical displacement and tilting degree for 6 Hz due to the big horizontal displacement measurements. Thus, the vertical displacement measurements and tilting degree are given for 2 Hz to 5 Hz for Soil 1 and Soil 2,
- for 5 Hz and 6 Hz, the horizontal and vertical displacement measurements are greater for Soil 2 than Soil 1. However, both backfill material (Soil 1 and Soil 2) are selected as gravel, Soil 2 is selected as finer than Soil 1. Soil 2 can more easily fulfill the space occurring due to the sliding of the block during dynamic loading and Soil 2 can push the block more strongly.

7.2 Two Blocks: Position Transducers Measurements (Test 2.1 and Test 2.2)

1g shaking table tests were performed with three position transducers – two of them were used for measuring the horizontal displacements, the other one was used for measuring the vertical displacement and tilting – for each frequency for two blocks tests for Soil 1 and Soil 2.

General view of position transducers namely P1 (for vertical displacement measurements) located edge point of the block 2, P2 and P3 (for horizontal displacement measurements) located near blocks for two blocks tests for Soil 1- Tests 2.1 and for Soil 2 - Test 2.2 are shown in Figure 7.15.

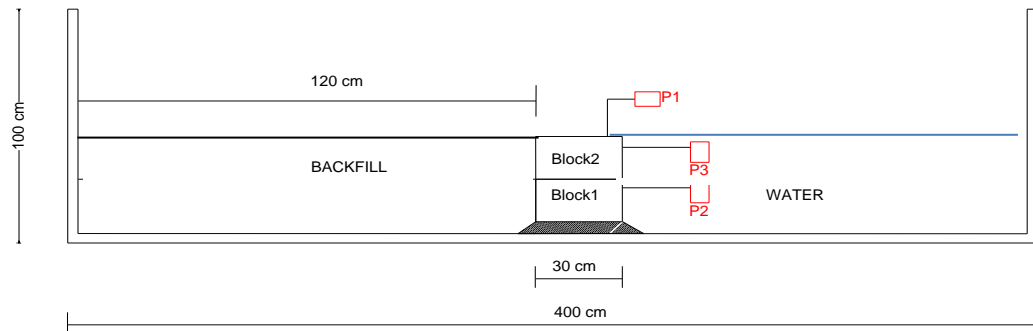


Figure 7.15: General view of position transducers (P1, P2, P3) for two blocks tests for Soil 1 and Soil 2

Figure 7.16 shows the the placements of the position transducers for two blocks tests for Soil 1 and Soil 2.

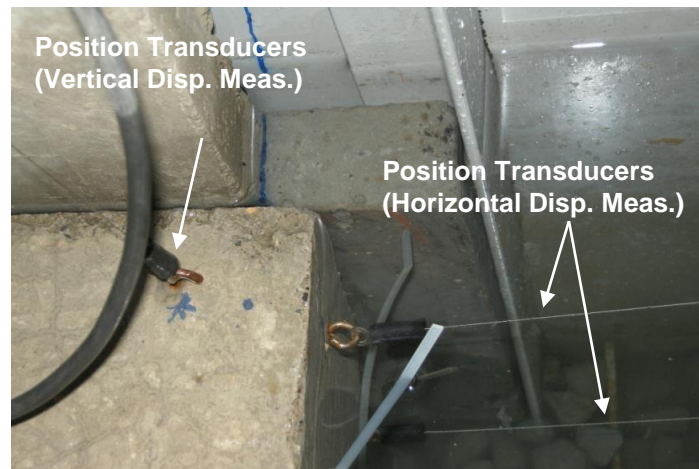


Figure 7.16: Position transducers for two blocks for Soil 1 and Soil 2

7.2.1 Two Blocks, Soil 1: Position Transducers Measurements (Test 2.1)

Position transducers measurements results for each frequency are presented by using three position transducers P1, P2 and P3 are shown in Figure 7.17– Figure 7.21 for Soil 1 (Figure 7.15).

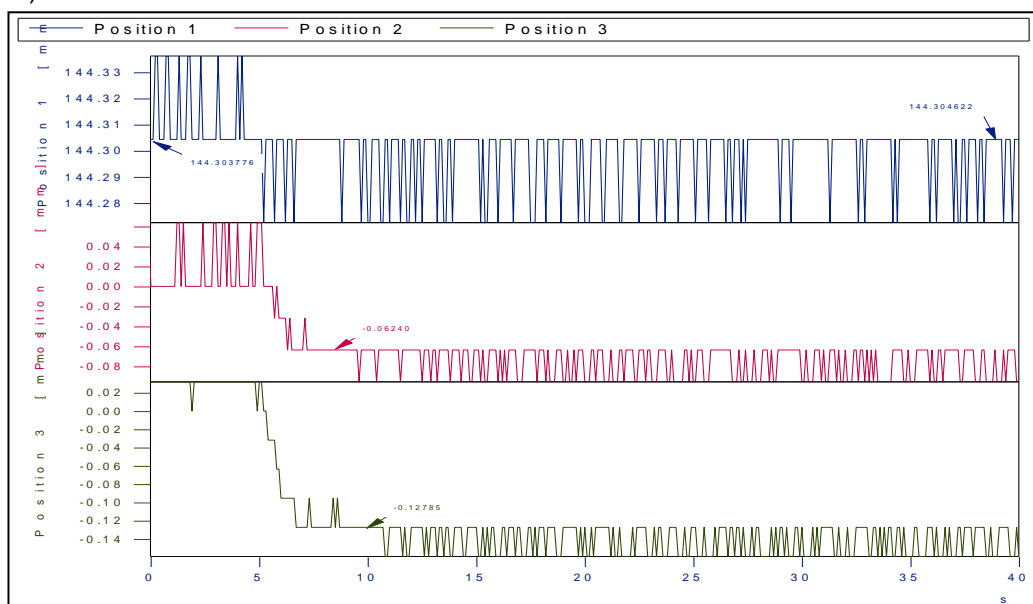


Figure 7.17: Horizontal and vertical displacement measurements for two blocks for 2 Hz

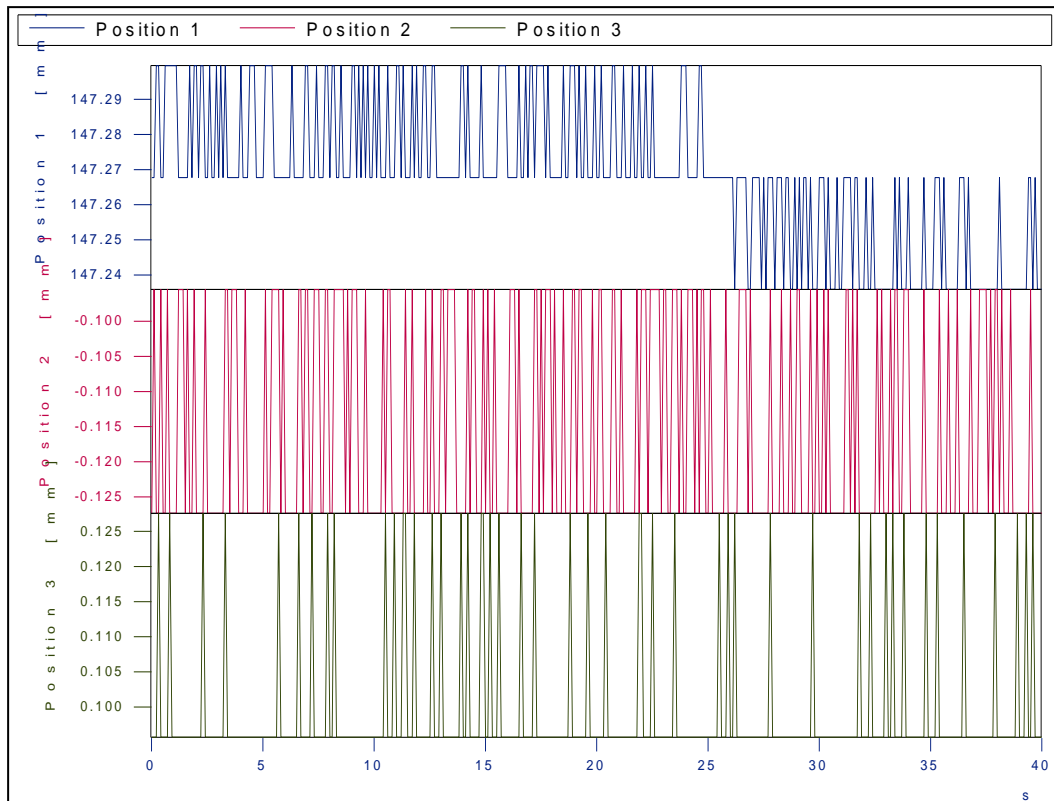


Figure 7.18: Horizontal and vertical displacement measurements for two blocks for 3 Hz

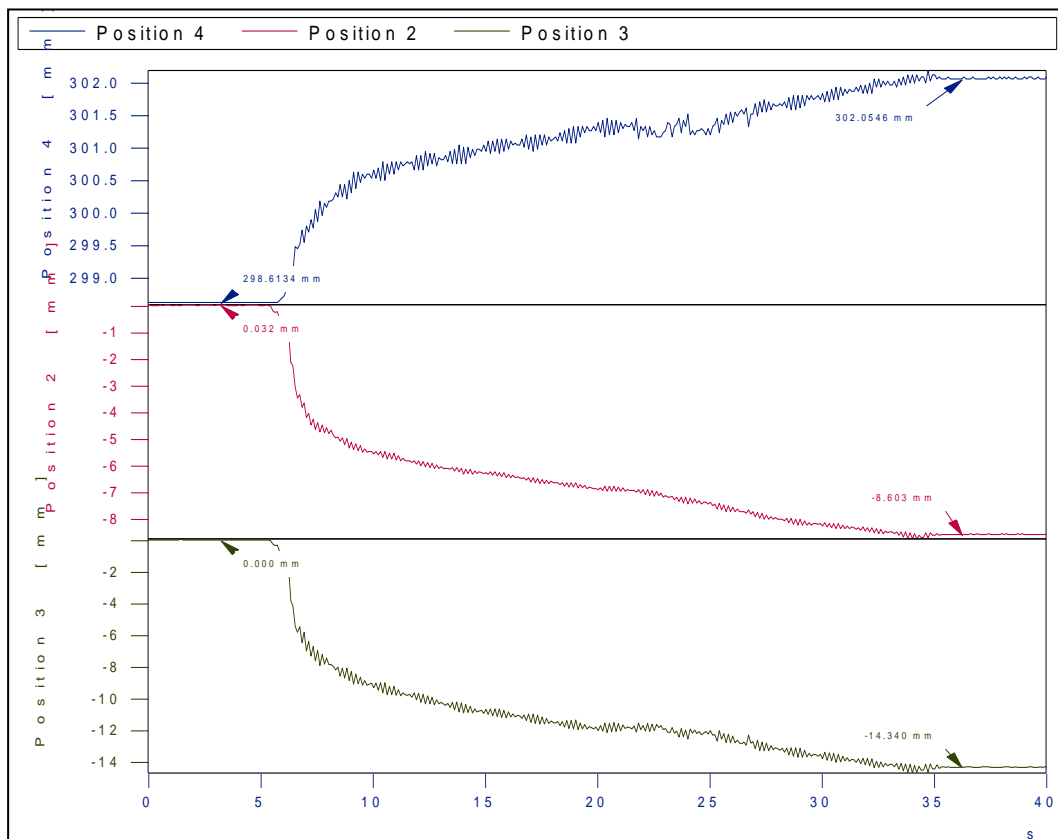


Figure 7.19: Horizontal and vertical displacement measurements for two blocks for 4 Hz

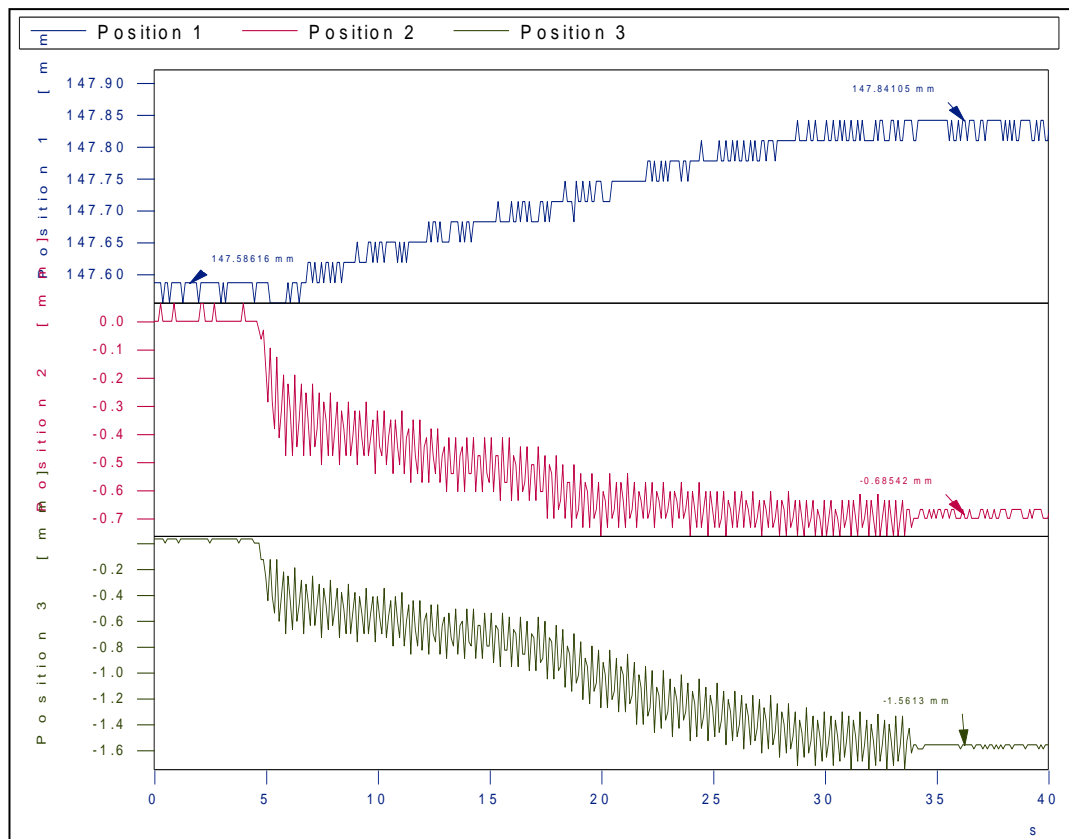


Figure 7.20: Horizontal and vertical displacement measurements for two blocks for 5 Hz

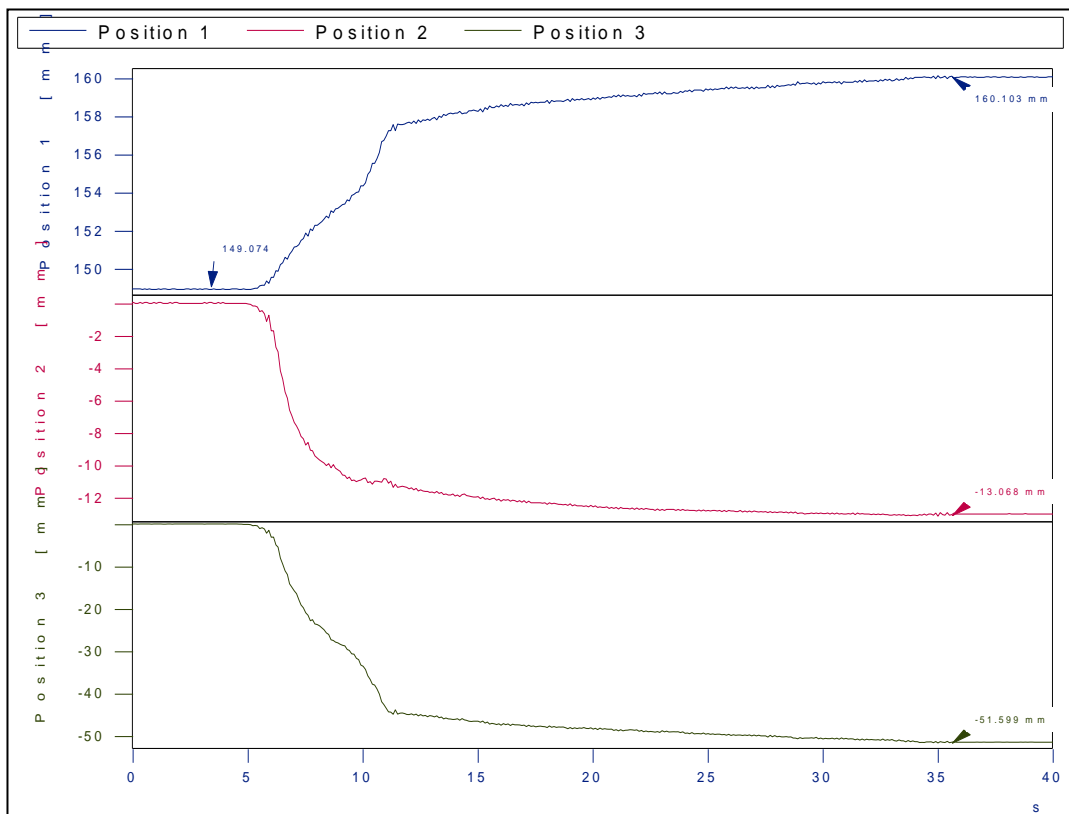


Figure 7.21: Horizontal and vertical displacement measurements for two blocks for 6 Hz

7.2.1.1 Horizontal, Vertical Displacements and Tilting Degree

Table 7.4 shows the horizontal, vertical displacement measurements and tilting values for each frequency for two blocks for Soil 1. Figure 7.25, Figure 7.26, Figure 7.27 show the horizontal, vertical displacement measurements and tilting values respectively. Figure 7.22, Figure 7.23 and Figure 7.24 show the horizontal displacement measurement for two blocks (Block 2) for Soil 1.



Figure 7.22: Horizontal displacement measurement for two blocks (Block 2) for Soil 1

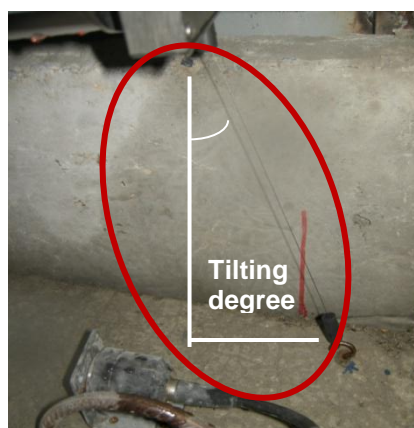
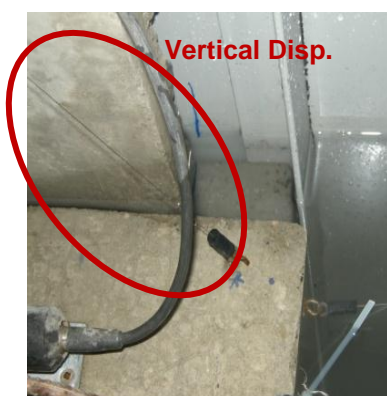


Figure 7.23: Horizontal displacement measurement for two blocks (Block 2) for Soil 1



Figure 7.24: Position of the Block 2 after dynamic loading (after 5 Hz)

Table 7.4: Horizontal, vertical displacement measurements and tilting values for each frequency for one block for Soil 1

Frequency (Hz)	Horizontal Disp. Block 1 (mm)	Horizontal Disp. Block 2 (mm)	Vertical Disp. (mm)	Tilting (degree)
2	0	0	0	0
3	0	0.13	0	0
4	0.68	1.56	0.25	0.2
5	8.6	14.34	3.1	1.32
6	13.07	51.56	-	-

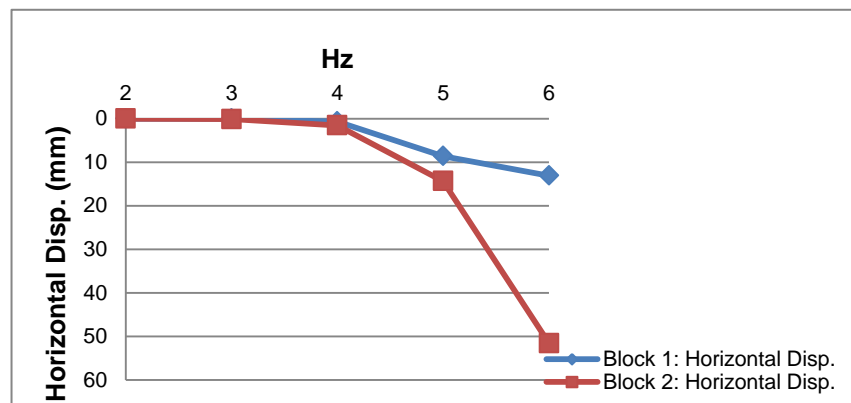


Figure 7.25: Horizontal displacement measurements for two blocks for Soil 1

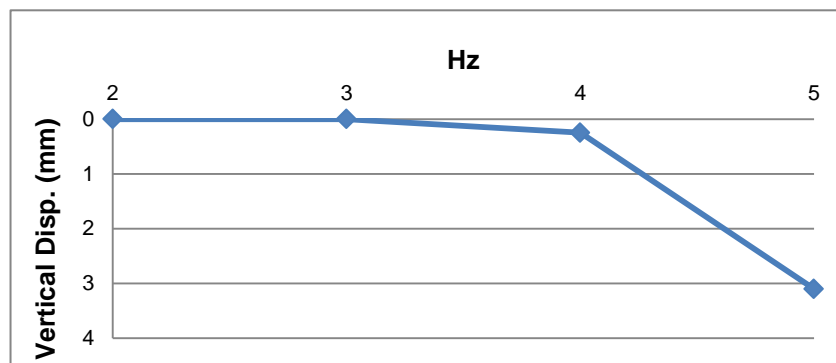


Figure 7.26: Vertical displacement measurements for two blocks for Soil 1

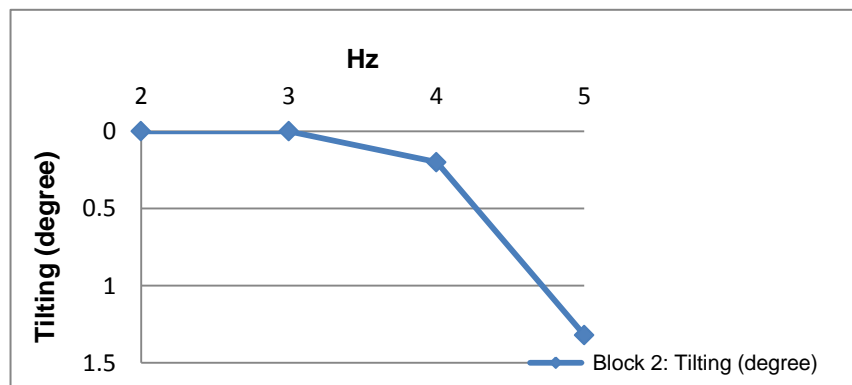


Figure 7.27: Tilting degree for two blocks for Soil 1

7.2.2 Two Blocks, Soil 2: Position Transducers Measurements (Test 2.2)

Position transducers measurements for each frequency are presented by using three position transducers located on block vertically (P1) and horizontally (P2 and P3) (Figure 7.15) are shown in APPENDIX J for Soil 2.

7.2.2.1 Horizontal, Vertical Displacements and Tilting Degree

Table 7.5 shows the horizontal, vertical displacement measurements and tilting values for each frequency for two blocks for Soil 2. Figure 7.28, Figure 7.29 and Figure 7.30 and Table 7.5 show the horizontal, vertical displacement measurements and tilting values respectively.

Table 7.5: Horizontal, vertical displacement measurements and tilting values for each frequency for one block for Soil 2

Frequency (Hz)	Horizontal Disp. Block 1 (mm)	Horizontal Disp. Block 2 (mm)	Vertical Disp. (mm)	Tilting (degree)
4	1.64	3.36	0.25	0.39
5	13.32	27.94	3.1	3.35
6	23.32	141.21	-	-

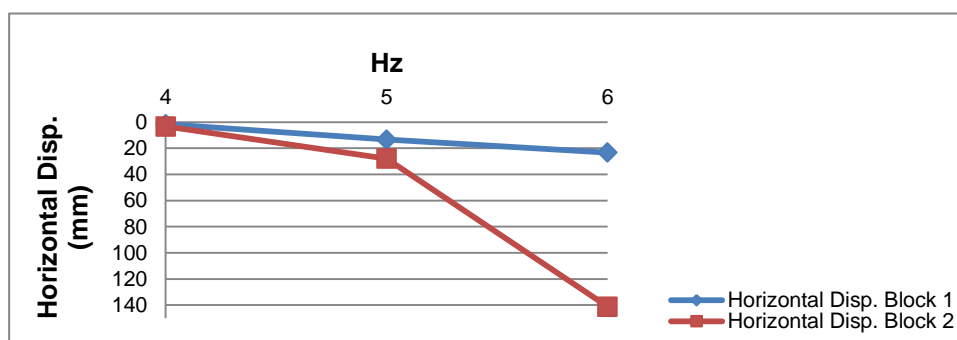


Figure 7.28: Horizontal displacement measurements for two blocks for Soil 2

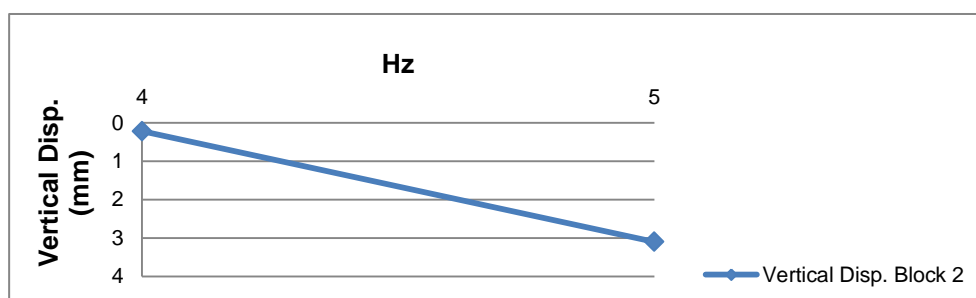


Figure 7.29: Vertical displacement measurements for two blocks for Soil 2

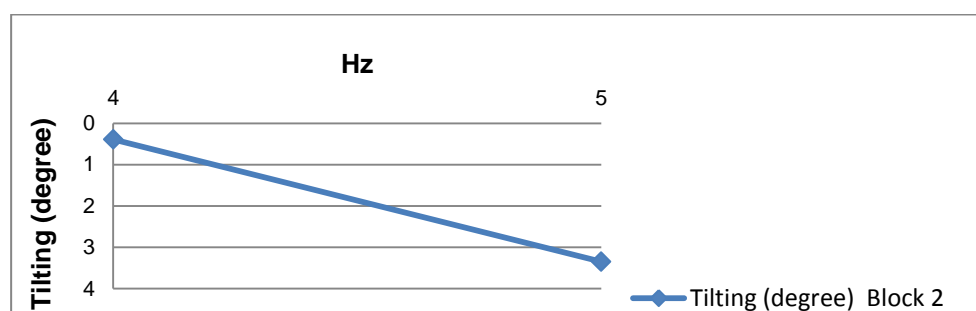


Figure 7.30: Tilting degree for two blocks for Soil 2



Figure 7.31: Two blocks experimental results for Soil 2

7.2.3 Comparisons of Results for Position Transducers for Two Blocks for Soil 1 and Soil 2

Table 7.4 and Table 7.5 shows the horizontal and vertical displacement measurements and tilting values for two blocks for Soil 1 and Soil 2.

- the horizontal displacement measurements increase for Block 1 and Block 2, while frequency is increasing for Soil 1 and Soil 2,
- the vertical displacement measurements and tilting degree also increase while frequency is increasing for Soil 1 and Soil 2,
- for 2 Hz, there is no motion for Block 1 and Block 2 for Soil 1,
- for 3 Hz, there is no motion for Block 1. Block 2, starts to slide for Soil 1,
- for 5 Hz, sudden increment occurs for horizontal and vertical displacement measurements and tilting degree,
- it is not possible to evaluate the vertical displacement and tilting degree for 6 Hz due to the big horizontal displacement measurements. Thus, the vertical displacement measurements and tilting degree are given for 4 Hz and 5 Hz,
- the horizontal displacement for Block 2, which is located on Block 1, is greater than the horizontal displacement for Block 1 for Soil 1 and Soil 2,
- the horizontal and vertical displacement measurements for Soil 2 are greater than the horizontal and vertical displacement measurements for Soil 1. However, both backfill material are selected as gravel, Soil 2 is finer than Soil 1. And, Soil 2 slumped down towards the structure more easily and the space between the blocks and backfill occurring due to the sliding of the blocks during dynamic loading can be filled by Soil 2. Thus, Soil 2 can push the blocks more strongly. Moreover, two blocks are placed without any shear key between blocks and Soil 2 can replace the space between the blocks and can increase the slipping condition between the blocks.

7.3 Three Block: Position Transducers Measurements (Test 3.1 and Test 3.2)

1g shaking table tests were performed with four position transducers – three of them were used for measuring the horizontal displacements, the other one was used for measuring the vertical displacement and tilting – for each frequency for three blocks tests for Soil 2. Due to the limitation of the experimental set-up, vertical displacement measurement could not be performed for Soil 1, however tilting degree are calculated by using the horizontal displacement measurements (Chapter 4).

7.3.1 Three Blocks, Soil 1: Position Transducers Measurements (Test 3.1)

General view of position transducers P1, P2 and P3 (for horizontal displacement measurements) located near blocks for three blocks tests for Soil 1- Tests 3.1 are shown in Figure 7.32.

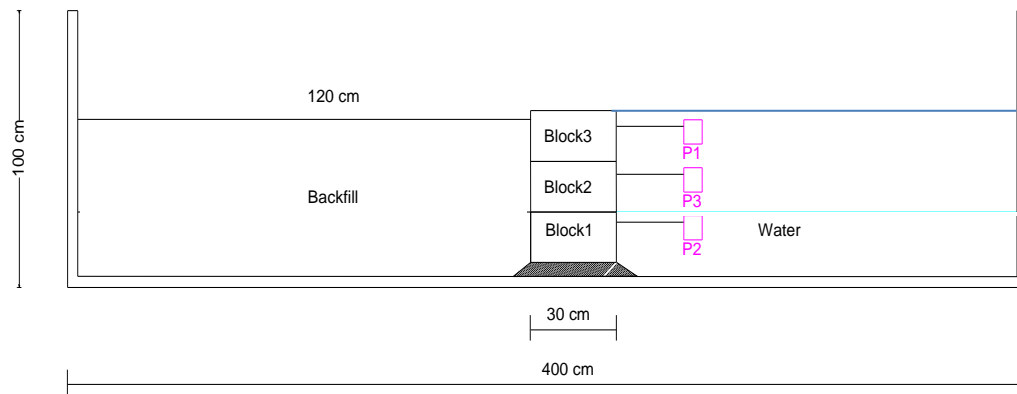


Figure 7.32: General view of position transducers (P1, P2 and P3) for three blocks tests for Soil 1

Figure 7.33 shows the placements of the position transducers (P1, P2, P3) for three block tests for Soil 1.



Figure 7.33: Placements of the position transducers (P1, P2, P3) for three block tests for Soil 1

Position transducers measurements results for each frequency are presented by using three position transducers; P1, P2 and P3 are shown in Figure 7.34 – Figure 7.37 for Soil 1 (Figure 7.32).

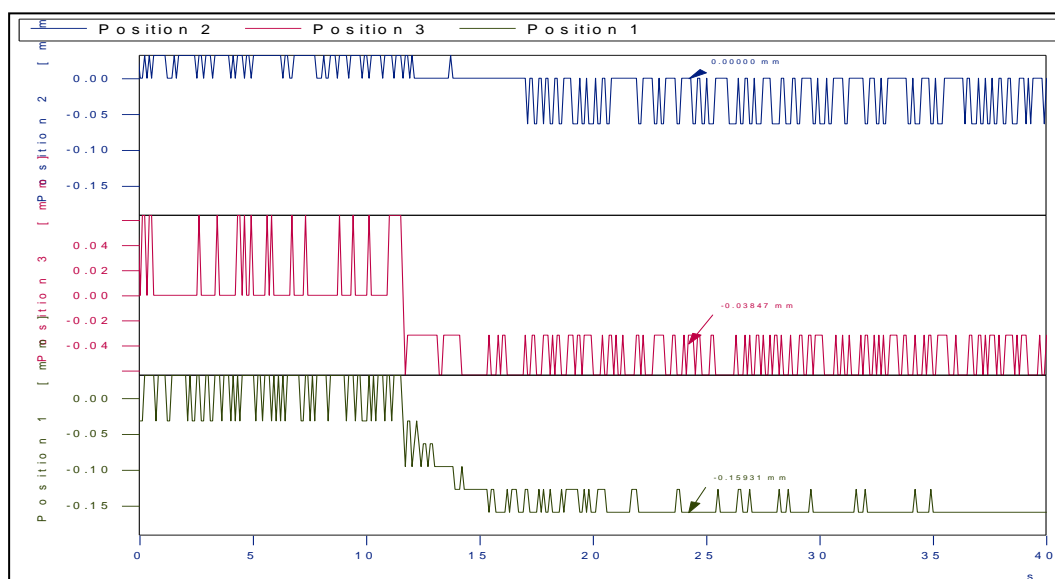


Figure 7.34: Horizontal and vertical displacement measurements for three blocks for 3 Hz

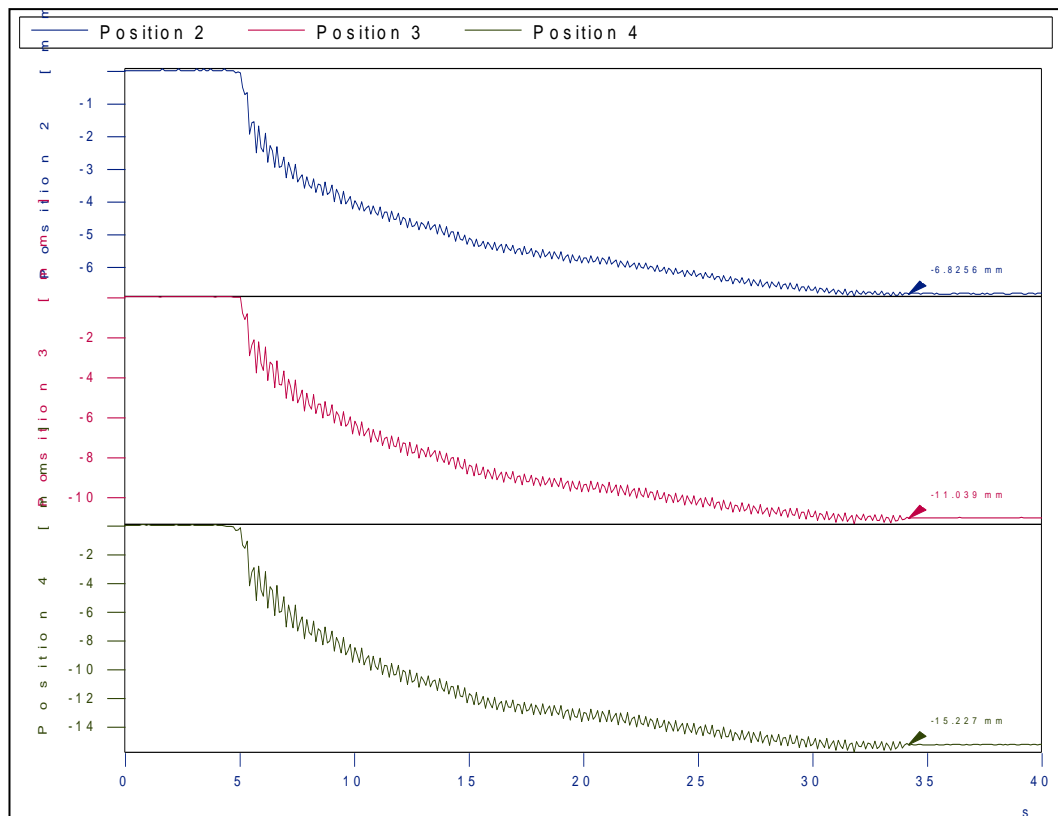


Figure 7.35: Horizontal and vertical displacement measurements for three blocks for 4 Hz

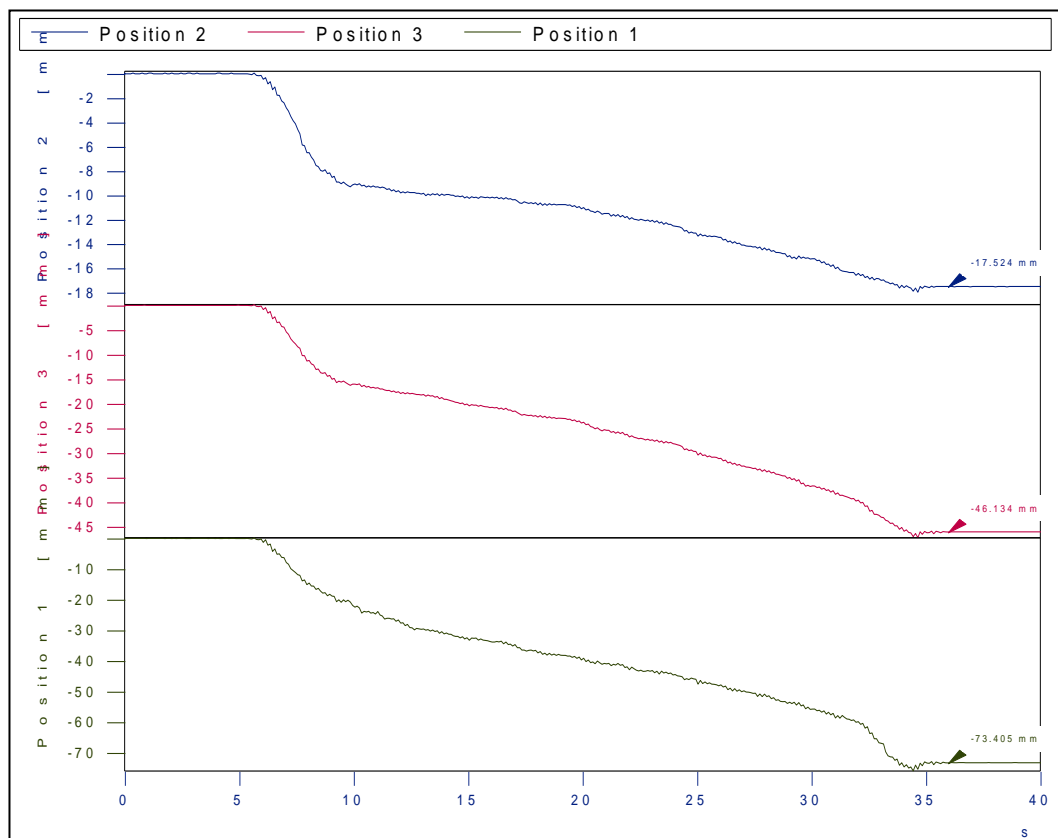


Figure 7.36: Horizontal and vertical displacement measurements for three blocks for 5 Hz

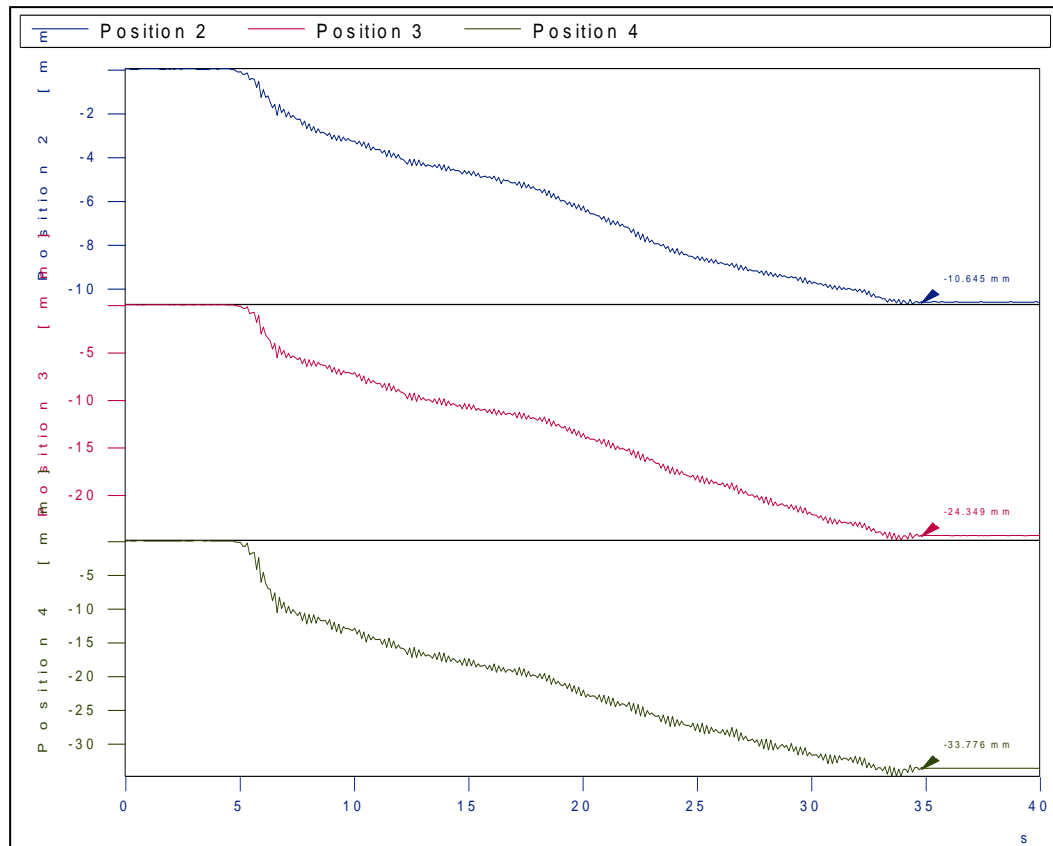


Figure 7.37: Horizontal and vertical displacement measurements for three blocks for 6 Hz

7.3.1.1 Horizontal, Vertical Displacements and Tilting Degree

Table 7.6 shows the horizontal displacement measurements and calculated tilting values for each frequency for three blocks for Soil 1.

Table 7.6: Horizontal displacement measurements and tilting values for each frequency for three blocks for Soil 1

Frequency (Hz)	Hor. Disp. Block 1 (mm)	Hor. Disp. Block 2 (mm)	Hor. Disp. Block 3 (mm)	Tilting Block 2 (degree)	Tilting Block 3 (degree)
3	0	0.039	0.16	0.009	0.028
4	6.83	11.04	15.23	0.96	0.96
5	10.65	24.35	33.78	3.13	2.06
6	17.52	46.13	73.4	-	-

Figure 7.38 and Figure 7.39 show the horizontal displacement measurements and calculated tilting values respectively.

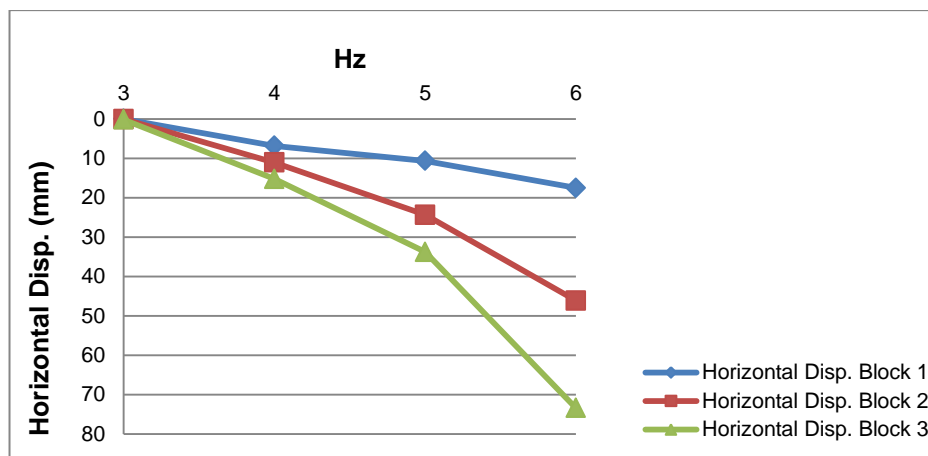


Figure 7.38: Horizontal displacement measurements for three blocks for Soil 1

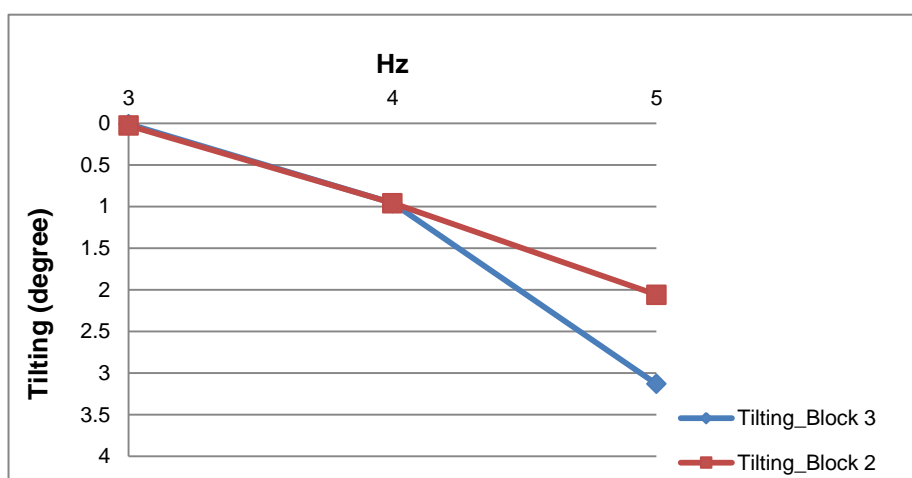


Figure 7.39: Tilting degree for three blocks for Soil

Figure 7.40 shows the horizontal displacement measurement for three blocks for Soil 1.

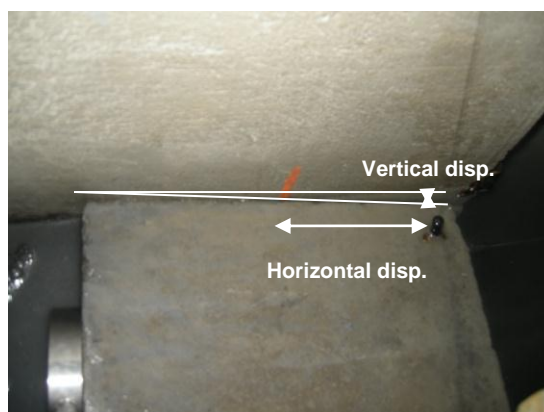


Figure 7.40: Horizontal displacement measurement for two blocks (Block 2) for Soil 1

7.3.2 Three Blocks, Soil 2: Position Transducers Measurements (Test 3.2)

General view of position transducers P1, P2, P3 (for horizontal displacement measurements) located near blocks and P4 (for vertical displacement measurements) located on edge point of block 3 for three blocks tests for Soil 2- Tests 3.1 are shown in Figure 7.41. The tests results are shown in APPENDIX K for Soil 2.

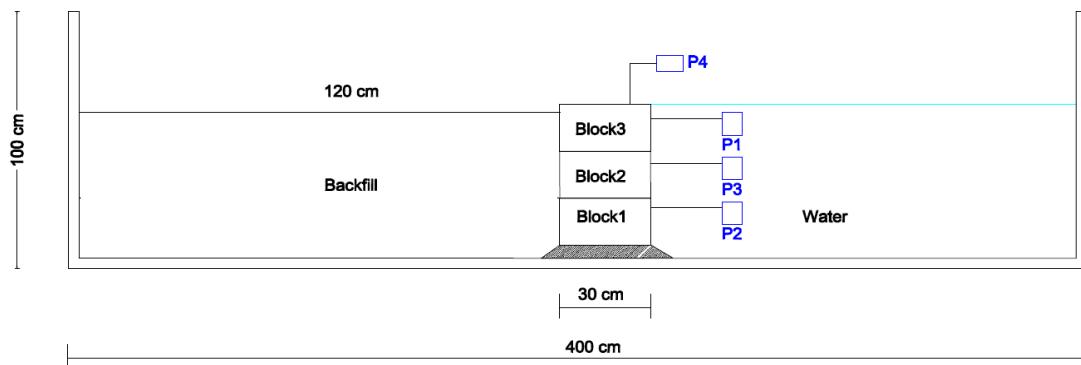


Figure 7.41: General view of position transducers (P1, P2, P3, P4) for three blocks tests for Soil 2

7.3.2.1 Horizontal, Vertical Displacements and Tilting Degree

Table 7.7 shows the horizontal displacement measurements and calculated tilting values for each frequency for three blocks for Soil 2.

Table 7.7: Horizontal displacement measurements and tilting values for each frequency for three blocks for Soil 2

Frequency (Hz)	Hor. Disp. Block 1 (mm)	Hor. Disp. Block 2 (mm)	Hor. Disp. Block 3 (mm)	Tilting Block 2 (degree)	Tilting Block 3 (degree)
3	1.27	1.46	2.07	0.04	0.14
4	4.43	8.35	13.43	0.9	1.16
5	32.8	41.28	78.96	1.94	8.57

Figure 7.42 and Figure 7.43 show the horizontal displacement measurements and tilting values respectively.

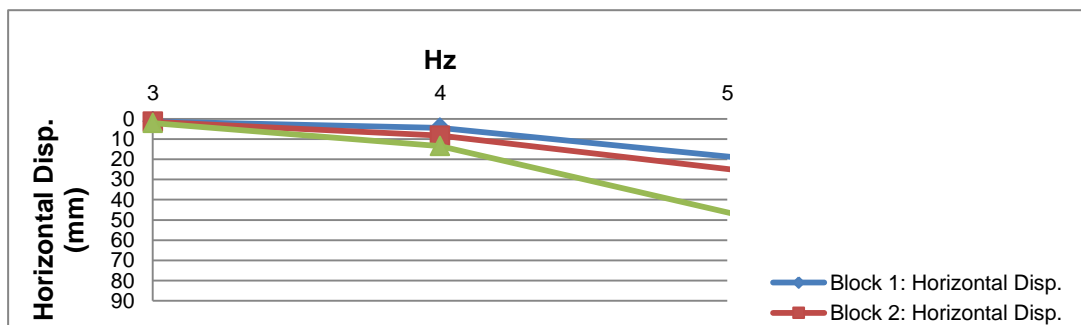


Figure 7.42: Horizontal displacement measurements for three blocks for Soil 2

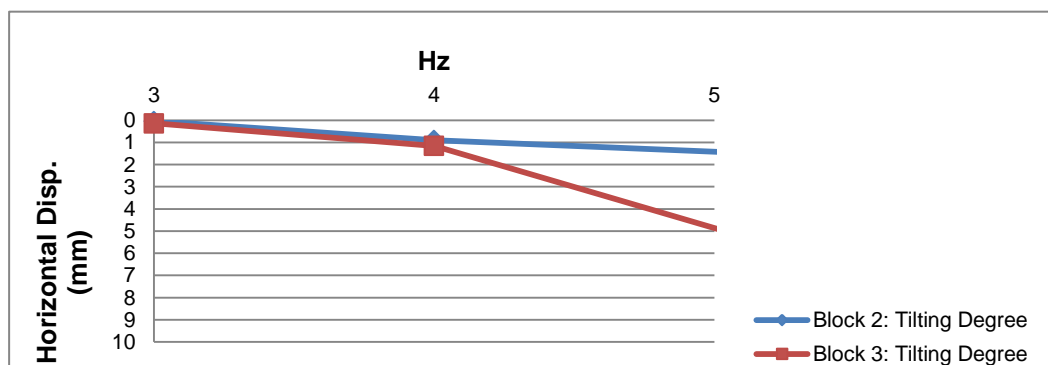


Figure 7.43: Tilting degree for three blocks for Soil 2

7.3.3 Comparisons of Results for Position Transducers for Three Blocks for Soil 1 and Soil 2

Table 7.6 and Table 7.7 show the horizontal and vertical displacement measurements and calculated tilting values for three blocks for Soil 1 and Soil 2.

- the horizontal displacement measurements increase for Block 1, Block 2, Block 3 while frequency is increasing for Soil 1 and Soil 2,
- the vertical displacement measurements and tilting degree also increase while frequency is increasing for Soil 1 and Soil 2,
- for 3 Hz, there is no motion for Block 1. Block 2, Block 3 start to slide for Soil 1,
- for 3 Hz, Block 1 starts to slide for Soil 2,
- for 5 Hz, sudden increment occurs for horizontal and vertical displacement measurements and tilting degree,
- the horizontal displacement for Block 3, which is located on Block 2, is greater than the horizontal displacement for Block 1 for Soil 1 and Soil 2,
- the horizontal displacement for Block 2, which is located on Block 1, is greater than the horizontal displacement for Block 1 for Soil 1 and Soil 2,
- the horizontal and vertical displacement measurements for Soil 2 are greater than the horizontal and vertical displacement measurements for Soil 1 (except 4 Hz for Soil 2). However, both backfill material are selected as gravel, Soil 2 is finer than Soil 1. And, Soil 2 slumped down towards the structure more easily and the gaps between the block(s) and backfill occurring due to the sliding of the block(s) during dynamic loading can be filled by Soil 2. Thus, Soil 2 can push the block(s) more strongly. Moreover, two blocks are placed without any shear key between block(s) and Soil 2 can replace the gaps between the blocks and can increase the slipping condition between the blocks.

7.4 Summary and Discussion of the Position Measurements

Table 7.8 and Table 7.9 show the summary of the horizontal displacement measurements and calculated tilting values with different frequencies for Soil 1 and Soil 2 for one block, two blocks and three blocks. During the evaluation of the results, the observations given below should be taken into consideration.

- For comparison of the results, a time based was selected as 30 sec. All the discussions based on 30 sec which is taken as a representative duration for a devastating earthquake which might be taken as representative of the most critical condition. For shorter durations the available measurements presented in APPENDIX I could be used for the any required duration.
- Horizontal displacement measurements increase while frequency is increasing for Soil 1 and Soil 2. Increase in frequency means that number of cycles of dynamic loading increases which causes an increase in acceleration measurements.
- In general, calculated tilting degree and vertical displacement measurements increase while frequency is increasing for Soil 1 and Soil 2.
- The horizontal displacement measurements of the block(s), located at the top, are always greater for the horizontal displacement measurements of the block(s) located at the bottom.

In conclusion, after 20 sec. which corresponds to approximately 60 sec in prototype, Soil 2 slumped down towards the structure causing higher horizontal displacement measurements on the block(s) compared to Soil 1 behavior. Thus, the horizontal, vertical displacement measurements and calculated tilting degree for Soil 2 is almost twice as much larger than the horizontal, vertical displacement measurements and calculated tilting degree for Soil 1.

Table 7.8: Horizontal displacement measurements for one block, two blocks and three blocks for Soil 1 and Soil 2

SOIL 1							SOIL 2			
BLOCK (S)	FREQ.	2 Hz	3 Hz	4 Hz	5 Hz	6 Hz	3 Hz	4 Hz	5 Hz	6 Hz
One Block	Block 1	0	0.16	2.87	7.78	93.71	-	2.12	17.07	114.14
Two Blocks	Block 1	0	0	0.68	8.60	13.07	-	1.64	13.32	23.32
	Block 2	0	0.13	1.56	14.34	51.56	-	3.36	27.94	141.21
Three Blocks	Block 1	-	0	6.83	10.65	17.53	1.27	4.43	32.80	-
	Block 2	-	0.039	11.04	24.35	46.13	1.46	8.35	41.28	-
	Block 3	-	0.16	15.23	33.78	73.40	2.07	13.43	78.96	-

Table 7.9: Calculated tilting degree for one block, two blocks and three blocks for Soil 1 and Soil 2

SOIL 1							SOIL 2			
BLOCK (S)	FREQ.	2 Hz	3 Hz	4 Hz	5 Hz	6 Hz	3 Hz	4 Hz	5 Hz	6 Hz
One Block	Block 1	0	0	0.07	1.03	-	-	-	-	-
Two Blocks	Block 2	0	0	0.2	1.32	-	-	0.39	3.35	-
Three Blocks	Block 2	-	0.009	0.96	3.13	-	0.04	0.9	1.94	-
	Block 3	-	0.028	0.96	2.06	-	0.14	1.16	8.57	-

7.4.1 Evaluation of the Position Transducers Results

Results of measurements for displacement and tilting were evaluated and discussed in view of “acceptable level of damage in performance-based design” (PIANC, 2001). In the design of quay walls, the normalized residual horizontal displacement defined as $(d/H)^*$ and tilting degree values are controlled by using the “acceptable level of damage in performance based design” and “proposed damage criteria” in (Table 4.6 and Table 4.7) given in PIANC (2001).

Similar to PIANC, (2001) the level of damage for gravity wall is also given in “Technical Seismic Specifications on Construction of Coastal and Harbor Structures, Railways And Airports (2008)”. The ‘sliding block analysis’ method or empirical approaches based on this method can be used to calculate the approximate rigid horizontal displacements of the gravity wall under the dynamic loading. Permitted levels of the performance for the displacement / strain limits for minimum and controlled damage level is given in Table 4.8.

Acceleration versus horizontal displacement figures are used for Soil 1 and Soil 2, to evaluate the minimum damage and controlled damage limits by considering the horizontal displacement measurements and tilting degrees for one block, two blocks and three blocks.

According to Table 7.8 and Table 4.8 horizontal displacement measurements are more critical than the tilting degree. Thus, only horizontal displacement measurements are evaluated.

7.4.1.1 For One Block

Acceleration versus horizontal displacement figure (Figure 7.44) are used for Soil 1 and Soil 2, to evaluate the minimum damage and controlled damage limits by considering the horizontal displacement measurements and tilting degrees for one block (Table 7.10). The scale is selected as 1/10 and the height of the block is $h = 20$ cm in model.

- Horizontal Displacement Measurements for Soil 1 and Soil 2:

For Minimum Damage (MD); $d / h < 0.015 \Rightarrow d = 3$ mm

For Controlled Damage (CD); $d / h < 0.05 \Rightarrow d = 10$ mm

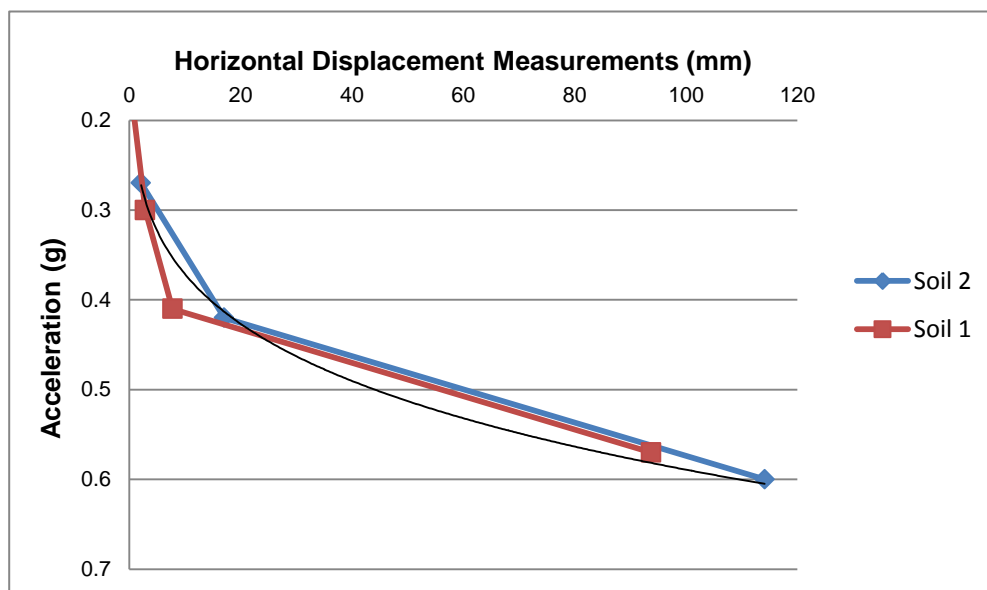


Figure 7.44: Horizontal displacement measurement vs. acceleration for Soil 1 and Soil 2 for one block (one block tests)

- **Tilting Degree for Soil 1 and Soil 2:**

According to Table 7.9 and Table 4.8 calculated tilting degree is smaller than given limit value.

7.4.1.2 For Two Blocks

Acceleration versus horizontal displacement figures (Figure 7.45 and Figure 7.46) are used for Soil 1 and Soil 2, to evaluate the minimum damage and controlled damage limits by considering the horizontal displacement measurements and tilting degrees for two blocks (Table 7.10)

The scale is selected as 1/10 and the height of the block 1 is $h_1 = 20$ cm and height of the block 2 is $h_2 = 40$ cm in model.

- **Horizontal Displacement Measurements for Soil 1 and Soil 2:**

For Block 1:

$h = 20$ cm;

For Minimum Damage (MD); $d / h < 0.015 \implies d = 3$ mm

For Controlled Damage (CD); $d / h < 0.05 \implies d = 10$ mm

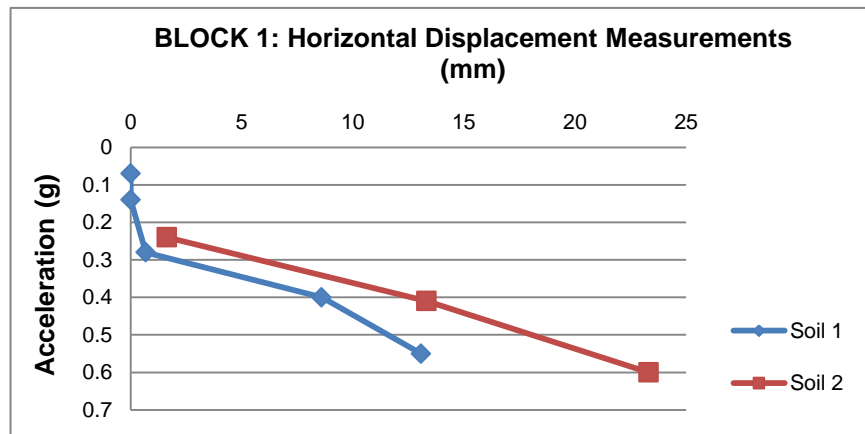


Figure 7.45: Horizontal displacement measurement vs. acceleration for Soil 1 and Soil 2 for Block 1 (two blocks tests)

For Block 2:

$h = 40$ cm;

For Minimum Damage (MD); $d / h < 0.015 \implies d = 6$ mm

For Controlled Damage (CD); $d / h < 0.05 \implies d = 20$ mm

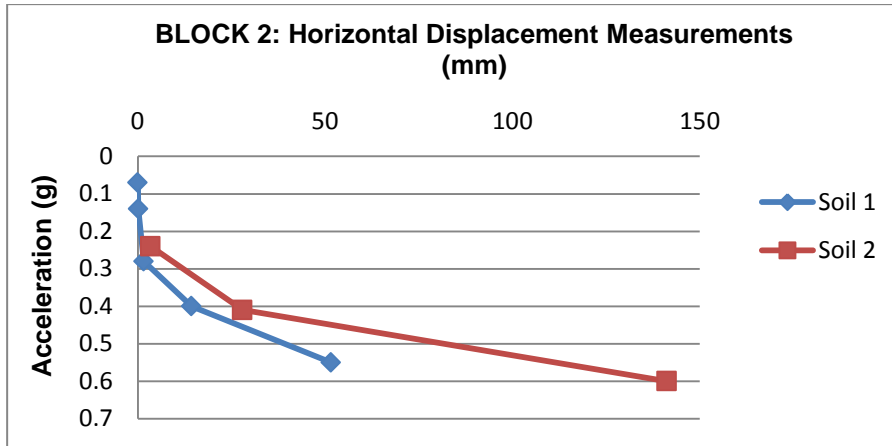


Figure 7.46: Horizontal displacement measurement vs. acceleration for Soil 1 and Soil 2 for Block 2 (two blocks tests)

After 5 Hz and 6 Hz, extensive damage in near collapse or complete loss of structure type damage level are observed.

7.4.1.3 For Three Blocks

Acceleration versus horizontal displacement figures (Figure 7.47, Figure 7.48, Figure 7.49) are used for Soil 1 and Soil 2, to evaluate the minimum damage and controlled damage limits by considering the horizontal displacement measurements and tilting degrees for two blocks (Table 7.10)

The scale is selected as 1/10 and the height of the block 1 is $h_1 = 20$ cm, the height of the block 2 is $h_2 = 40$ cm and the height of the block 3 is $h_3 = 60$ cm in model.

- Horizontal Displacement Measurements for Soil 1 and Soil 2:

For Block 1:

$h_1 = 20$ cm;

For Minimum Damage (MD); $d / h < 0.015 \implies d = 3$ mm

For Controlled Damage (CD); $d / h < 0.05 \implies d = 10$ mm

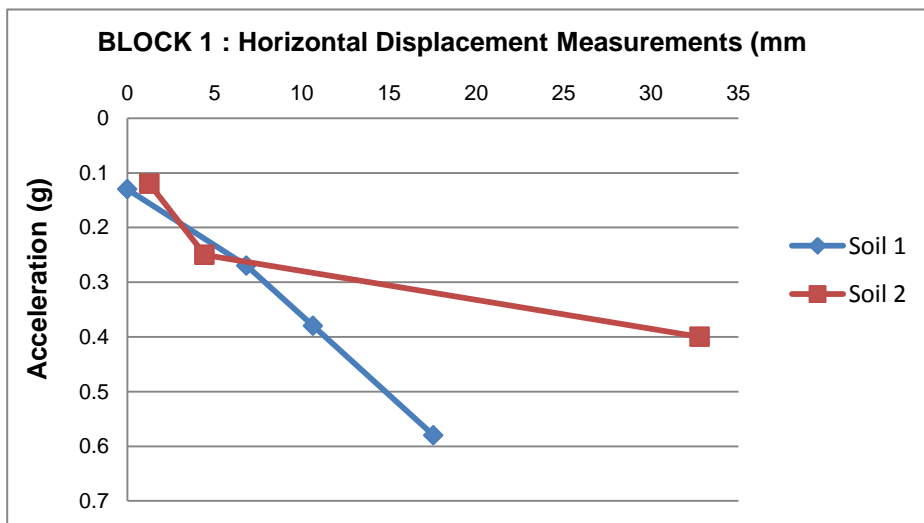


Figure 7.47: Horizontal displacement measurement vs. acceleration for Soil 1 and Soil 2 for Block 1 (three blocks tests)

For Block 2:

$h_2 = 40$ cm;

For Minimum Damage (MD); $d / h < 0.015 \implies d = 6$ mm

For Controlled Damage (CD); $d / h < 0.05 \implies d = 20$ mm

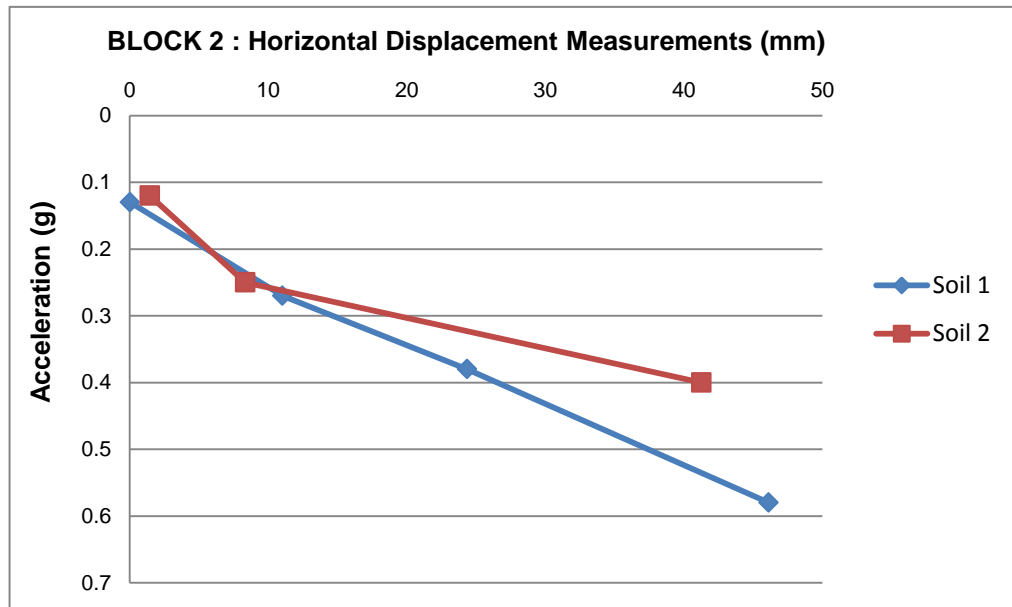


Figure 7.48: Horizontal displacement measurement vs. acceleration for Soil 1 and Soil 2 for Block 2 (three blocks tests)

For Block 3:

$h_3 = 60$ cm;

For Minimum Damage (MD); $d / h < 0.015 \implies d = 9$ mm

For Controlled Damage (CD); $d / h < 0.05 \implies d = 30$ mm

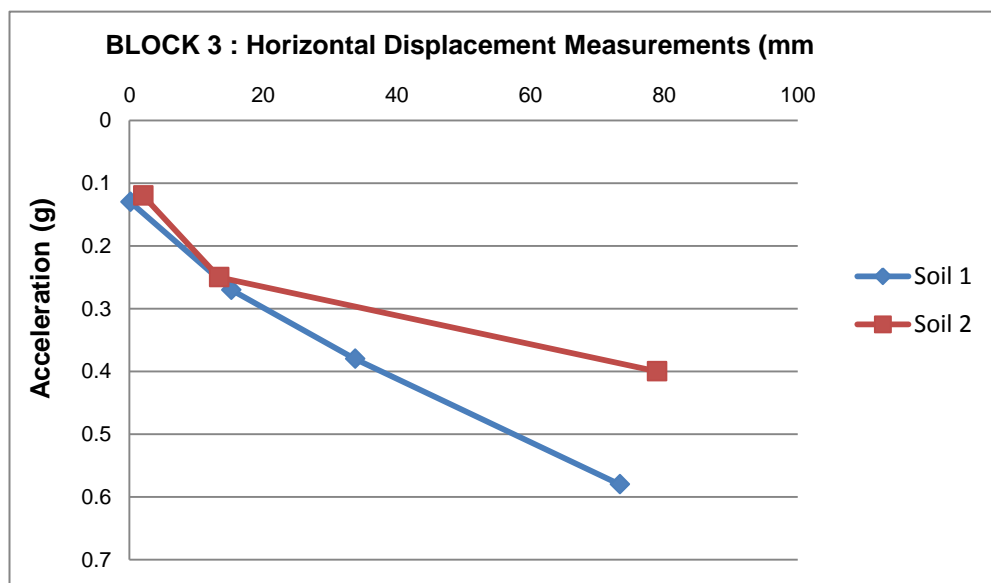


Figure 7.49: Horizontal displacement measurement vs. acceleration for Soil 1 and Soil 2 for Block 3 (three blocks tests)

Table 7.10: Damage level of block(s) for Soil 1 and Soil 2

SOIL TYPE		SOIL 1	SOIL 2	SOIL 1	SOIL 2
BLOCK (S)		MD	MD	CD	CD
One Block	Block 1	0.30g	0.29g	0.41g	0.37g
Two Blocks	Block 1	0.33g	0.28g	0.44g	0.37g
	Block 2	0.32g	0.26g	0.43g	0.36g
Three Blocks	Block 1	0.20g	0.20g	0.37g	0.30g
	Block 2	0.20g	0.20g	0.35g	0.30g
	Block 3	0.22g	0.20g	0.35g	0.28g

When experimental results of level damage of this study is compared with the level damage table given PIANC (2001), it is seen that minimum and controlled level damage of Soil 2 is critical than Soil 1 in terms of given damage criteria.

CHAPTER 8

FRICTION COEFFICIENTS

The friction coefficient is one of the key parameter for analyzing of the seismic design of block type quay walls. The stabilities of the block type quay walls are provided by the friction between blocks and friction at the bottom of the structure.

Recent studies about friction coefficients point out that static condition defines a system which does not change with time however dynamic condition defines a system in motion. Thus, using only static friction coefficients can cause misleading outputs for seismic design of block type quay walls.

In this chapter, the static friction coefficients were calculated with Coulomb Law and the dynamic friction coefficients were calculated with Proposed Friction Law (Hsieh et al., 2011) by using 1 g shaking table tests results and these obtained friction coefficients by using both methods were compared and discussed.

8.1 Static Friction Coefficient

Static friction coefficients were calculated by evaluating the 1 g shaking table tests results. The accelerations, displacements and soil pressure measurements for one block, two blocks and three blocks for Soil 1 were used to compute the static friction coefficients by using Coulomb Law.

Coulomb Law governed by the Eq. 8.1:

$$F_f \leq \mu F_n \quad (8.1)$$

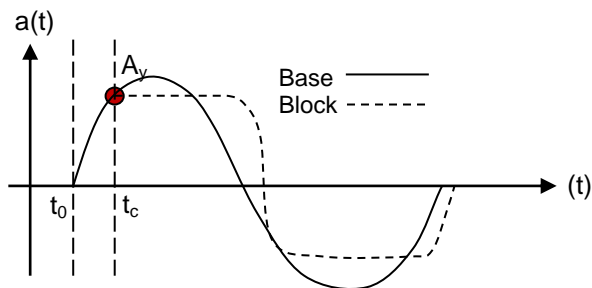
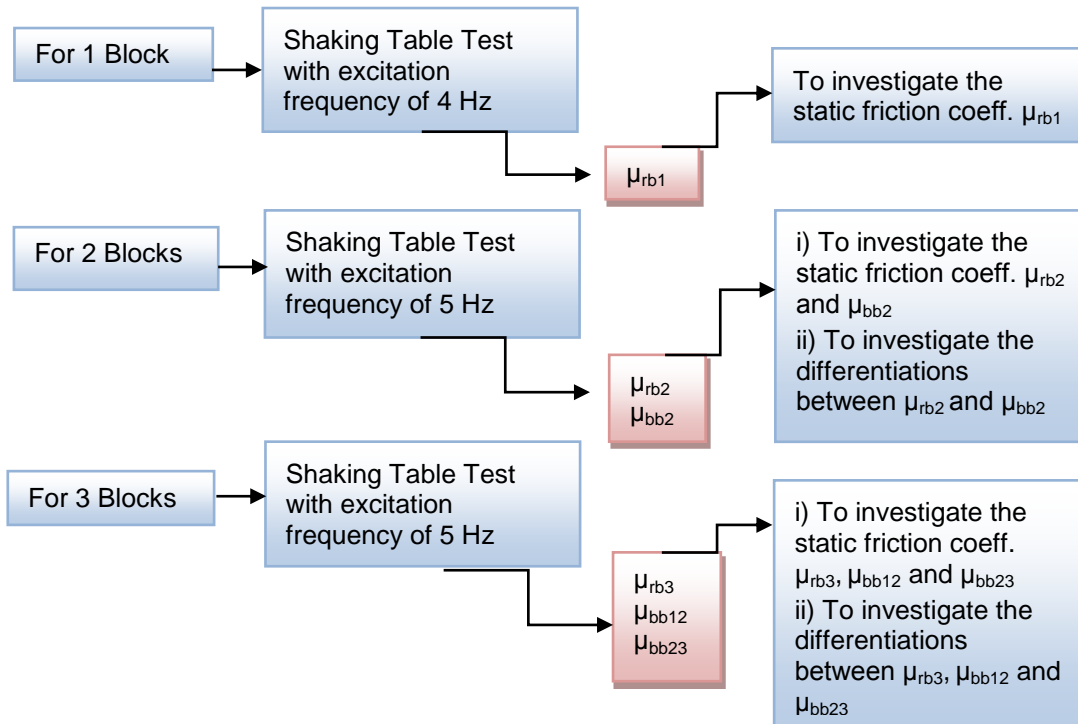
where;

F_f is the force exerted by friction, μ is the friction coefficient, F_n is the normal force.

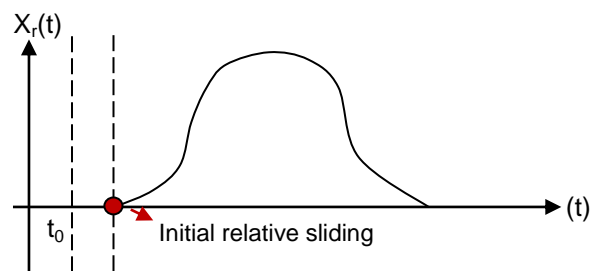
For one block, the static friction coefficient between rubble-block (μ_{rb1}); for two blocks, the static friction coefficient between rubble-block (μ_{rb2}) and the static friction coefficient between block-block (μ_{bb2}); for three blocks, the static friction coefficient between rubble-block (μ_{rb3}), the static friction coefficient between block 1 – block 2 (μ_{bb12}), the static friction coefficient between block 2 – block 3 (μ_{bb23}) were calculated with Coulomb Law. (Table 8.1).

The most important point is to determine the moment of the block begins to slide. For this purpose, the value of yield acceleration is to be specified. When the factor of safety against sliding is 1.0, the block acceleration at this time is defined as yield acceleration (A_y). Kim et al., (2005) says that “when the yield acceleration is greater than the input acceleration, the wall acceleration is the same as the input acceleration. But when the yield acceleration becomes less than the input acceleration, the wall acceleration fluctuates due to the dynamic interaction between the backfill soil with pore water and the wall”. And, it is assumed that block displacement occurs if the base of the acceleration exceeds the yield acceleration and the instantaneous critical friction coefficient (μ_c) is computed for the initiation time of sliding (t_c) (Figure 8.1).

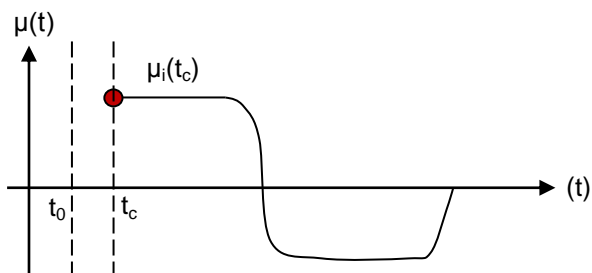
Table 8.1: The computation steps of the static friction coefficients for one block, two blocks and three blocks



A_y is the yield acceleration and can be defined by using Newmark (1965), $a(t)$ is the temporal acceleration



t_c is the initiation time of sliding, X_r is the temporal relative displacement of block to base.



μ_c is the instantaneous critical friction coefficient and $\mu_c = \mu_i(t_c)$ is the instantaneous friction coefficient at the initiation of sliding $t = t_c$

Figure 8.1: Schematic form of yield acceleration, initiation time of sliding, temporal relative displacement of block to the base (Hsieh et al., (2011))

However, it is too difficult to distinguish a clear moment as a starting point of sliding; therefore it is also too difficult to distinguish of yield acceleration. "Comparison of the horizontal displacement and acceleration time histories showed that the first major sliding took place at the time that the larger acceleration records have already been experienced without any major sliding at Peak 1 and Peak 2 in Figure 8.2 and major sliding started only when the rocking action of the block started" (Mohajeri et al., 2004).

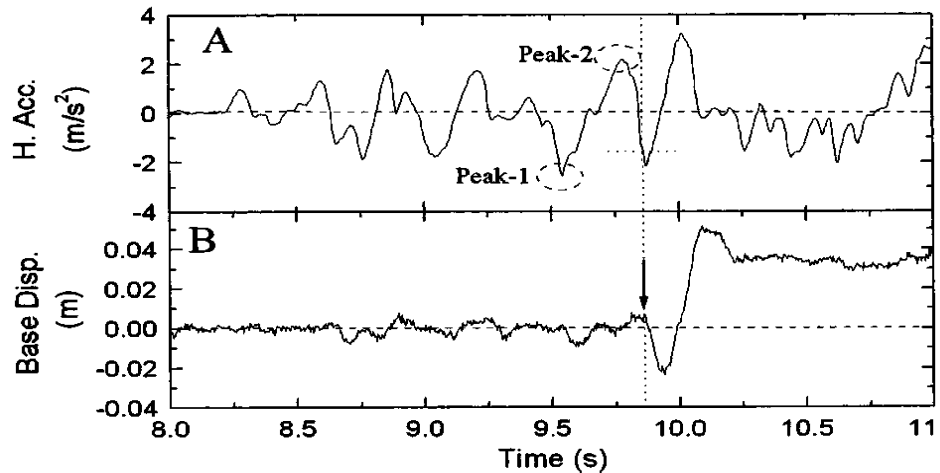


Figure 8.2: "Base displacement and horizontal acceleration time history for typical results of second series of shake table tests" (Mohajeri et al., 2004)

In this study, yield acceleration and starting point of sliding were recognized by using the same approach suggested by Mohajeri et al., (2004).

The static friction coefficients for one block, two blocks and three blocks were computed with Coulomb Theorem by following the steps given below.

Calculation Steps of Static Friction Coefficient

1. Determination of the time when the block starts sliding
2. Determination of the base and block(s) accelerations for this time
3. Determination of the soil pressures for this time
4. Determination of the hydrodynamic forces
5. Determination of the inertia forces
6. Determination of the horizontal forces
7. Determination of the block(s) weight
8. Determination of the vertical forces
9. Determination of the static friction coefficient

8.1.1 One Block

The static friction coefficients between rubble-block was computed by using the results of 1 g shaking table tests results for one block for 4 Hz.

8.1.1.1 Rubble – Block

Concrete rigid block slides down on rubble inclined plane to determine the static friction coefficient between rubble - block. According to tests results, the static friction angle (μ_s) was about 29° and static friction coefficient $\mu_s = 0.55$ for rubble-block.

1. Determination of the time when the block starts sliding

According to 1 g shaking table tests results for one block tests, the sliding time of block for 4 Hz (0.30 g for base) was determined as 11.426 sec. for Soil 1 (Table 8.2 and Figure 8.3).

Table 8.2: Sliding time of block for 4 Hz for Soil 1

Time (sec)	Horizontal Disp. (mm)
11.026	0
11.126	0
11.226	0
11.326	0
11.426	-6.37E-02
11.526	-9.56E-02
11.626	-9.56E-02
11.726	-0.382348
11.826	-0.382348
11.926	-0.382348
12.026	-0.732833

2. Determination of the base and block(s) accelerations

The base and block accelerations were also determined for 11.426 sec. when the block starts to slide for Soil 1 (Table 8.3 and Figure 8.3).

Table 8.3: Base and block accelerations for specified sliding time for Soil 1

Time (sec)	Base Acc. (g)	Block Acc. (g)	Time (sec)	Base Acc. (g)	Block Acc. (g)	Time (sec)	Base Acc. (g)	Block Acc. (g)
11.334	-0.009	-0.008	11.366	-0.006	0.019	11.398	-0.086	-0.110
11.336	-0.004	0.015	11.368	-0.005	-0.002	11.4	-0.088	-0.108
11.338	0.005	0.034	11.37	-0.016	-0.007	11.402	-0.088	-0.110
11.34	0.005	0.051	11.372	-0.010	-0.006	11.404	-0.089	-0.111
11.342	0.014	0.055	11.374	-0.024	-0.012	11.406	-0.074	-0.096
11.344	0.015	0.044	11.376	-0.035	-0.024	11.408	-0.060	-0.077
11.346	0.015	0.046	11.378	-0.040	-0.030	11.41	-0.077	-0.072
11.348	0.021	0.028	11.38	-0.055	-0.032	11.412	-0.055	-0.063
11.35	0.014	0.013	11.382	-0.058	-0.047	11.414	-0.043	-0.045
11.352	0.017	0.004	11.384	-0.063	-0.057	11.416	-0.057	-0.037
11.354	0.017	-0.007	11.386	-0.071	-0.066	11.418	-0.034	-0.039
11.356	0.018	-0.010	11.388	-0.076	-0.074	11.42	-0.035	-0.035
11.358	0.018	-0.016	11.39	-0.080	-0.080	11.422	-0.032	-0.030
11.36	0.007	0.004	11.392	-0.085	-0.094	11.424	-0.009	-0.025
11.362	0.009	0.029	11.394	-0.088	-0.100	11.426	-0.009	-0.016
11.364	-0.005	0.031	11.396	-0.087	-0.105	11.428	-0.005	-0.009

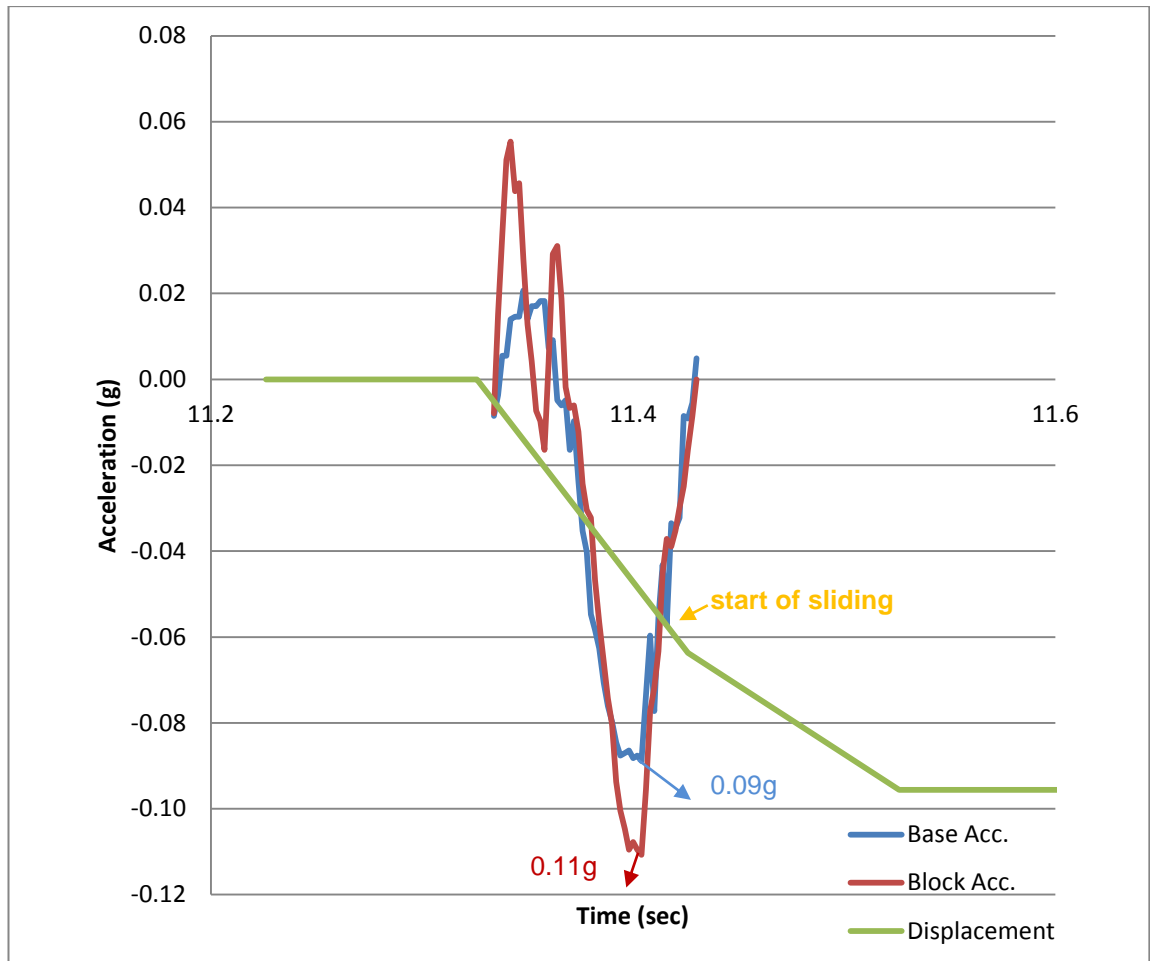


Figure 8.3: Base and block acceleration and start of sliding point

As it seen from the Figure 8.3, the base and block acceleration were assumed as 0.09g and 0.11g respectively.

3. Determination of the soil pressures and soil forces

The soil pressure measurements were also determined for 11.426 sec. when the block starts to slide for Soil 1 (Table 8.4).

The total soil pressure measurements with respect to elevation of soil pressure cells (SP1: located at 5 cm below the top of the block and SP2 located at 15 cm below the top of the block) for 11.42 sec are given in Table 8.5. The last point where depth is 20 cm is also computed (Figure 8.4).

Table 8.4: The soil pressure measurements for 11.426 sec for SP1 and SP2 for Soil 1

Time (sec)	SP1 (kpa)	SP2 (kpa)
11.226	2.77	1.16
11.326	2.57	0.99
11.426	2.13	0.91

Table 8.5: Total soil pressure measurements versus elevation for 4 Hz for Soil 1

Elevation (m)	Total Pressure (kN/m ²)
0	0
-0.05	0.9
-0.15	2.13
-0.2	2.86

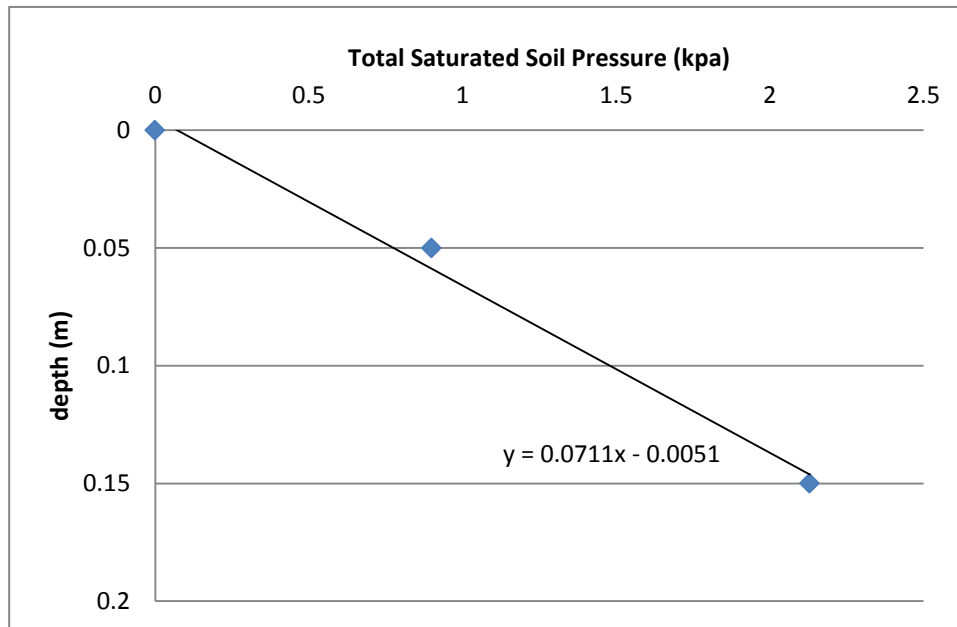


Figure 8.4: Total soil pressure versus depth

Soil Force:

$$F = 0.5 \times 2.86 \times 0.2 \times 0.25 = 0.071 \text{ kN}$$

Horizontal Component of Soil Force: $0.071 \times \cos 13.67 = 0.069 \text{ kN}$

Vertical Component of Soil Force: $0.071 \times \sin 13.67 = 0.017 \text{ kN}$

(block dimension is 20, 25, 30 cm)

4. Determination of the hydrodynamic forces

$$\begin{aligned}
 F_{\text{water}} &= \frac{7}{12} \times \gamma_w \times kh \times H^2 \\
 &= \frac{7}{12} \times 10 \times 0.09 \times 0.2^2 = 0.052 \text{ kN/m}
 \end{aligned}$$

$$F_{\text{water}} = 0.052 \times 0.25 = 0.013 \text{ kN}$$

5. Determination of the inertia forces

$$F_{\text{inertia}} = ma$$

$$F_{\text{inertia}} = 0.035 \times 0.11 \times 9.81 = 0.038 \text{ kN}$$

6. Determination of the total horizontal forces

$$F_{total-horizontal} = 0.069 + 0.038 + 0.013 = 0.120 \text{ kN}$$

7. Determination of the block(s) weight

$$W = (23 - 10) \times 0.2 \times 0.3 \times 0.25 = 0.195 \text{ kN}$$

8. Determination of the total vertical forces

$$F_{total-vertical} = 0.195 + 0.017 = 0.212 \text{ kN}$$

9. Determination of the static friction angles

$$\mu_s = \frac{0.120}{0.212} = 0.57$$

8.1.2 Two Blocks

8.1.2.1 Static Friction Coefficient: Rubble - Block 1

The static friction coefficient between rubble - block 1 was computed by using the results of 1 g shaking table tests results for two blocks for 5 Hz for Soil 1. Results of the static friction coefficients calculations are summarized in Table 8.6.

Table 8.6: Results of the static friction coefficients calculations for rubble-block 1 for 5 Hz

STATIC FRICTION COEFFICIENTS, RUBBLE-BLOCK 1, TWO BLOCKS, 5 HZ	
Sliding Time	30.6820 sec
Accelerations	Base Acceleration: - 0.1186 g
	Block Acceleration: - 0.098 g
Soil Forces	Horizontal Comp. : 0.16 kN
	Vertical Comp. : 0.038 kN
Hydrodynamic Forces	0.02 kN
Inertia Forces	0.067 kN
Block(s) Weight	0.39 kN
Total Horizontal Forces	0.25 kN
Total Vertical Forces	0.43 kN
Static Friction Coefficient	0.58

8.1.2.2 Static Friction Coefficient: Block 1 - Block 2

Concrete rigid block slides down on rubble inclined plane to determine the static friction coefficient between rubble-block. According to tests results, the static friction angle (μ_s) was about 25° and static friction coefficient $\mu_s = 0.47$ for block-block.

The static friction coefficient between block 1 - block 2 was computed by using the results of 1 g shaking table tests results for two blocks for 5 Hz for Soil 1. Results of the static friction coefficient calculations are summarized in Table 8.7.

Table 8.7: Results of the static friction coefficients calculations
for block 1-block 2 for 5Hz

STATIC FRICTION COEFFICIENTS, BLOCK 1-BLOCK 2, TWO BLOCKS, 5 HZ	
Sliding Time	30. 842 sec
Accelerations	(bottom)Block 1 Acceleration: - 0.1041 g
	(top) Block 2 Acceleration: - 0.085 g
Soil Forces	Horizontal Comp. : 0.062 kN
	Vertical Comp. : 0.0145 kN
Hydrodynamic Forces	0.013 kN
Inertia Forces	0.029 kN
Block(s) Weight	0.195 kN
Total Horizontal Forces	0.104 kN
Total Vertical Forces	0.21 kN
Static Friction Coefficient	0.50

8.1.3 Three Blocks

8.1.3.1 Static Friction Coefficient: Rubble - Block 1

The static friction coefficient between rubble - block 1 was computed by using the results of 1 g shaking table tests results for three blocks for 5 Hz for Soil 1. Results of the static friction coefficient calculations are summarized in Table 8.8.

Table 8.8: Results of the static friction coefficients calculations
for rubble-block 1 for 5Hz

STATIC FRICTION COEFFICIENTS, RUBBLE - BLOCK 1, THREE BLOCKS, 5 HZ	
Sliding Time	21. 854 sec
Accelerations	Base Acceleration: - 0.1126 g
	Block Acceleration: - 0.1095 g
Soil Forces	Horizontal Comp. : 0.17 kN
	Vertical Comp. : 0.038 kN
Hydrodynamic Forces	0.059 kN
Inertia Forces	0.11 kN
Block(s) Weight	0.585 kN
Total Horizontal Forces	0.34 kN
Total Vertical Forces	0.623 kN
Static Friction Coefficient	0.55

8.1.3.2 Static Friction Coefficient: Block 1 - Block 2

The static friction coefficient between block 1 – block 2 was computed by using the results of 1 g shaking table tests results for three blocks for 5 Hz for Soil 1. Results of the static friction coefficient calculations are summarized in Table 8.9.

Table 8.9: Results of the static friction coefficients calculations
for block 1-block 2 for 5Hz

STATIC FRICTION COEFFICIENTS, BLOCK 1 - BLOCK 2, TWO BLOCKS, 5 HZ	
Sliding Time	21. 858 sec
Accelerations	Block 1 Acceleration: - 0.1131 g
	Block 2 Acceleration: - 0.0955 g
Soil Forces	Horizontal Comp. : 0.12 kN
	Vertical Comp. : 0.028 kN
Hydrodynamic Forces	0.012 kN
Inertia Forces	0.066 kN
Block(s) Weight	0.39 kN
Total Horizontal Forces	0.198 kN
Total Vertical Forces	0.418 kN
Static Friction Coefficient	0.47

8.1.3.3 Static Friction Coefficient: Block 2 - Block 3

The static friction coefficient between block 2 - block 3 was computed by using the results of 1 g shaking table tests results for three blocks for 5 Hz for Soil 1. Results of the static friction coefficient calculations are summarized in Table 8.10.

Table 8.10: Results of the static friction coefficients calculations
for block 2 - block 3 for 5 Hz

STATIC FRICTION COEFFICIENTS, BLOCK 2 - BLOCK 3, TWO BLOCKS, 5 HZ	
Sliding Time	21. 858 sec
Accelerations	Base Acceleration: - 0.0955 g
	Block Acceleration: - 0.0785 g
Soil Forces	Horizontal Comp. : 0.057 kN
	Vertical Comp. : 0.013 kN
Hydrodynamic Forces	0.0072 kN
Inertia Forces	0.027 kN
Block(s) Weight	0.195 kN
Total Horizontal Forces	0.0912 kN
Total Vertical Forces	0.208 kN
Static Friction Coefficient	0.44

8.2 Dynamic Friction Coefficient

Dynamic friction coefficients were calculated by evaluating the 1 g shaking table tests results for one block, two blocks, and three blocks for Soil 1. The accelerations, displacements and soil pressure measurements results were used to compute the dynamic friction coefficients by using Proposed Friction Law (Hsieh et al., 2011)

- Proposed Friction Law (Hsieh et al., 2011)

“Forces acting on rigid block sliding on an inclined plane are shown in Figure 8.5.”

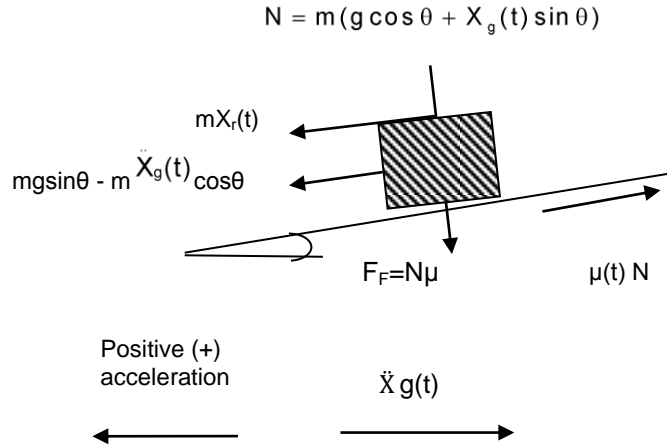


Figure 8.5: Forces acting on rigid block sliding on an inclined plane (Hsieh et al., 2011)

N is the normal force, m is the mass of the sliding block, g is the gravitational acceleration, θ is the slope angle, $\ddot{X}_g(t)$ is the absolute temporal acceleration at base and $\ddot{X}_b(t)$ is the absolute temporal acceleration of the sliding block.

Normal force is;

$$N = m(g \cos \theta + \ddot{X}_g(t) \sin \theta) \quad (8.2)$$

and instantaneous friction coefficient is;

$$m g \sin \theta - m \ddot{X}_g(t) \cos \theta - \mu_i(t) N \text{sign}(\dot{x}(t)) = m \ddot{X}_r(t) \quad (8.3)$$

$$\ddot{X}_b(t) = \ddot{X}_g(t) + \ddot{X}_r(t) \quad (8.4)$$

In these equations N is 343.35 N, m is 35 kg, g is 9.81 m/s², θ is 0°, the absolute temporal acceleration at base $\ddot{X}_g(t)$ and the absolute temporal acceleration of the sliding block $\ddot{X}_b(t)$ are determined according to 1 g shaking table tests results for one block, two blocks and three blocks.

Figure 8.6 shows the static and dynamic friction coefficients between rubble –block 1 and for one block for 4 Hz.

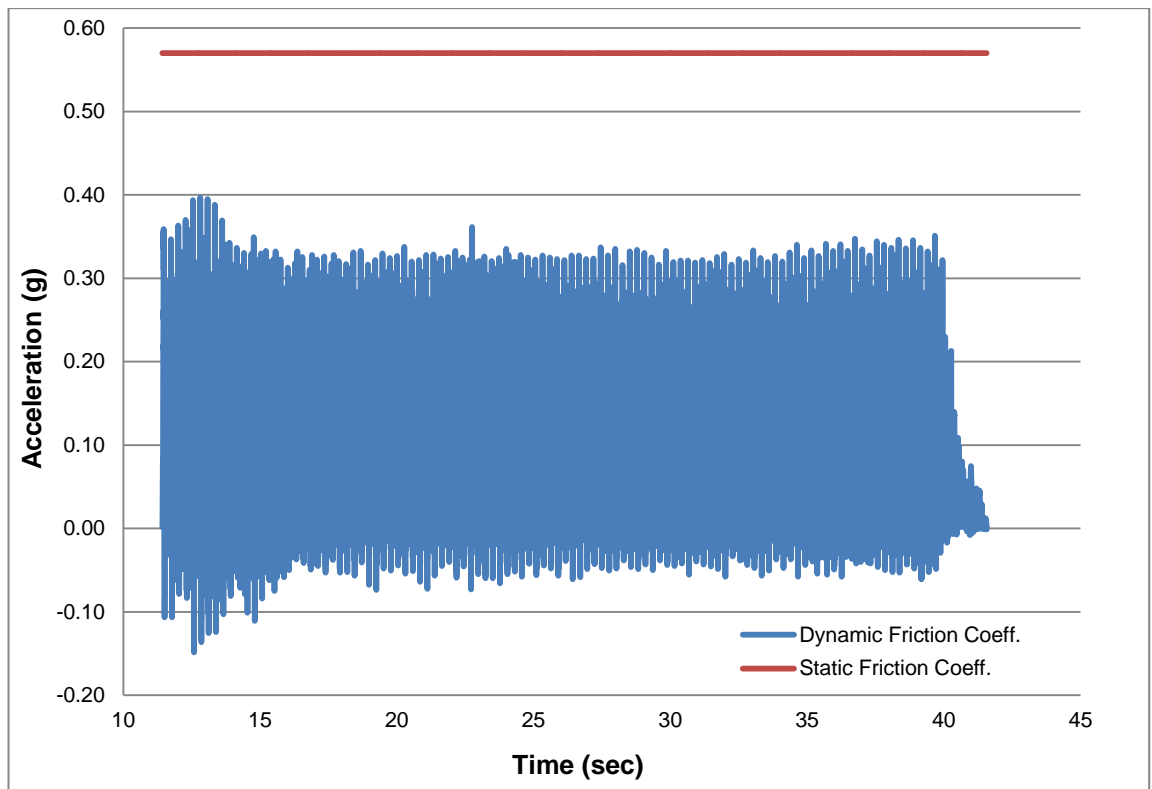


Figure 8.6: Dynamic and static friction coefficients between rubble-block 1 for one block for 4 Hz.

Figure 8.7 and Figure 8.8 show the static and dynamic friction coefficients between rubble – block 1 and block 1 – block 2 for two blocks for 5 Hz.

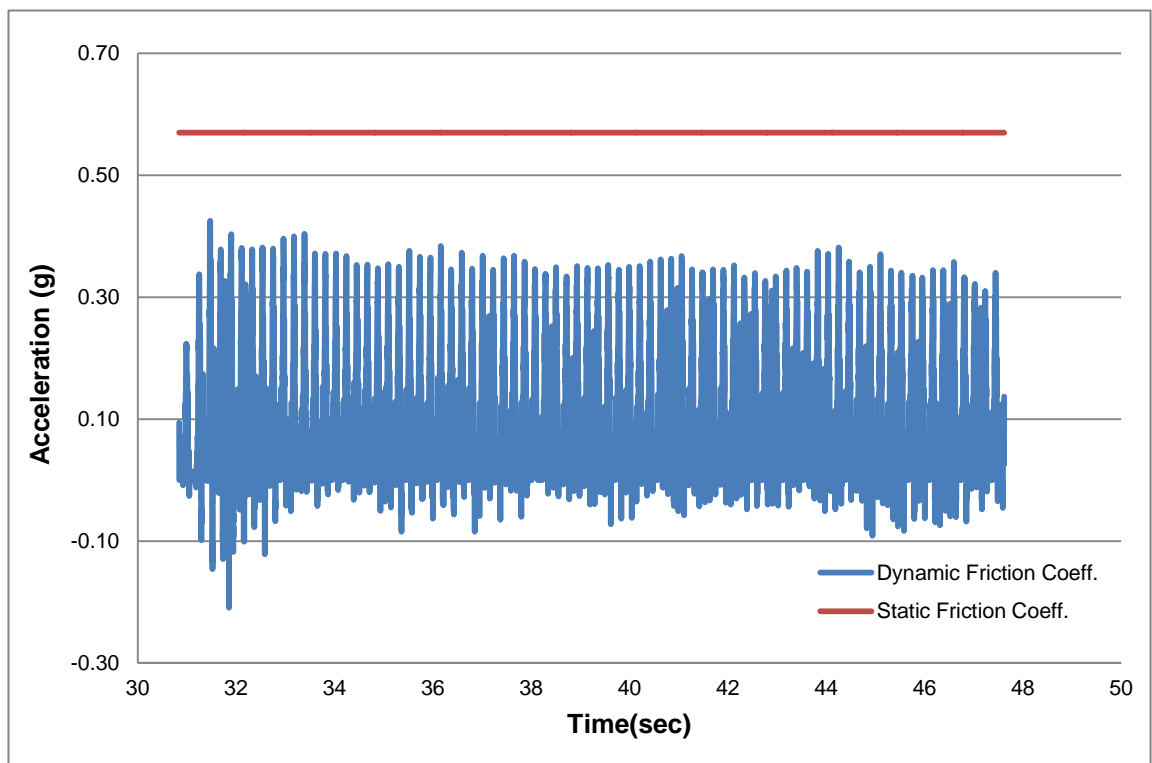


Figure 8.7: Dynamic and static friction coefficients between rubble-block 1 for two blocks for 5 Hz

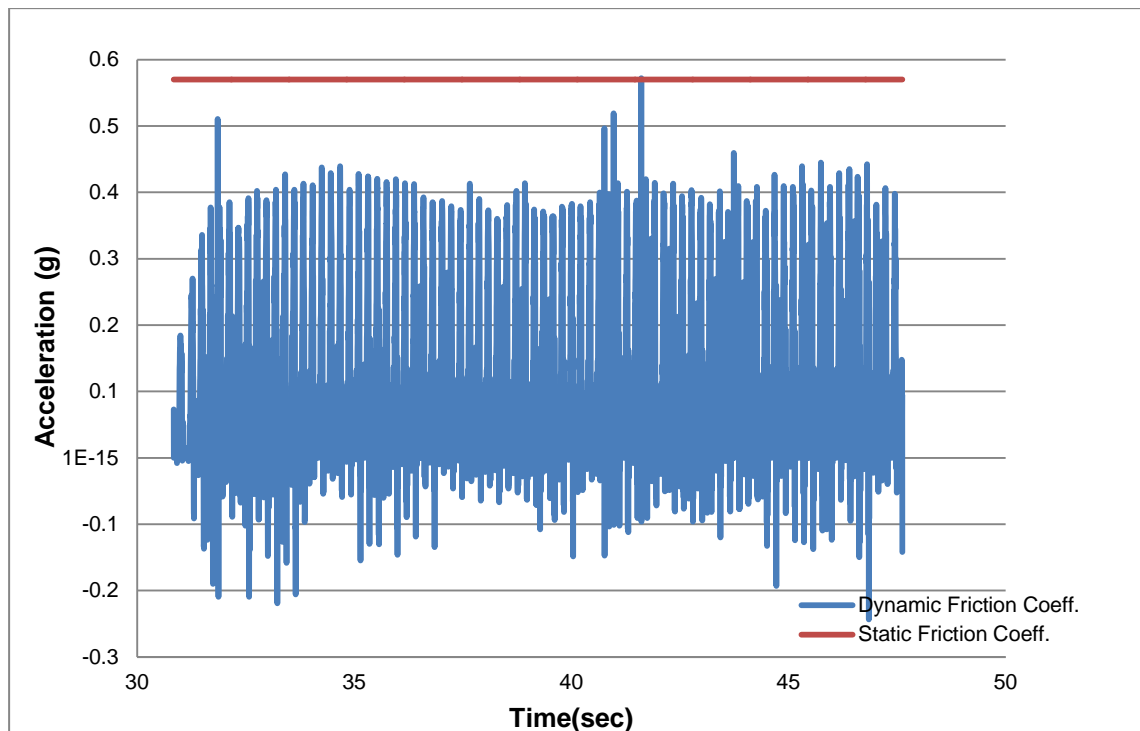


Figure 8.8: Dynamic and static friction coefficients between block 1- block 2 for two blocks for 5 Hz.

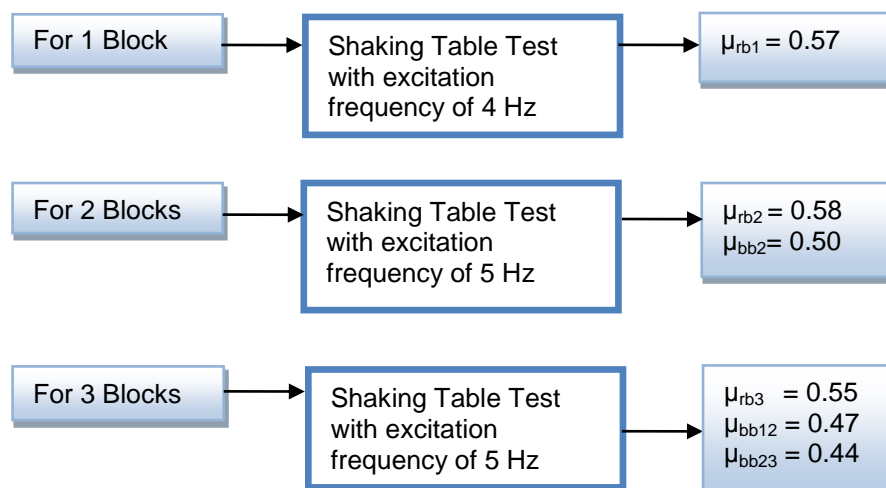
Figure 8.6 - Figure 8.8 show that in general calculated dynamic friction coefficients are smaller than calculated static friction coefficients. “The negative values of friction coefficients arise when input acceleration is much larger than block’s response acceleration, which indicate the vanishing of the interface friction. At this point the friction coefficient starts oscillating around a value near zero” (Mendez et al., 2009).

8.3 Comparisons Of Static And Dynamic Friction Coefficients

The static friction coefficients were calculated with Coulomb Law and the dynamic friction coefficients were calculated with Proposed Friction Law (Hsieh et al., 2011) by using 1 g shaking table tests results for Soil 1. These computed static and dynamic friction coefficients between rubble-block and block-block were compared and discussed below.

The calculated static friction coefficients are given in Table 8.11.

Table 8.11: Static friction coefficients for rubble-block and block-block for one block, two blocks and three blocks



- As it is seen from Table 8.11, the static friction coefficients for rubble-block and block-block were calculated between 0.55-0.58 and 0.44-0.50, respectively. The static friction coefficient for rubble-block and block-block can be proposed as 0.57 and 0.47.
- The static friction coefficient between block-block is smaller than the static friction coefficient between block-foundation.
- These static friction coefficients results are also compared with the static friction coefficients recommended in Technical Seismic Specifications on Construction of Coastal and Harbor Structures, Railways And Airports (2008) and OCDI (2009) (Table 8.12).

Table 8.12: Comparisons of static friction coefficients with the standards

Surface	Tilting Tests	1 g Shaking Table Tests	Turkish Regulations, (2008)	OCDI, (2009)
Block - Rubble	0.55	0.57	0.60	0.60
Block - Block	0.47	0.47	0.50	0.50

As it is seen from Table 8.12 the calculated static friction coefficients are close to recommended values given in Technical Seismic Specifications on Construction of Coastal and Harbor Structures, Railways And Airports (2008) and OCDI (2009).

- Static friction coefficients were computed with inclined surface as 0.55 for rubble-block and 0.47 for block-block.
- In general constant force should be applied to move the block in static condition then block moves when the force exerted on block exceeds this constant force value. It is certain that smaller forces should be applied to ensure the continuity of the movement of the block in dynamic condition. Thus, the static friction coefficient is generally higher than the dynamic friction coefficient.
- Calculated dynamic friction coefficients are smaller than calculated static friction coefficients
- Increment in the block number (bottom to the upper side) causes the decrement in the friction coefficient. Due to the decrement of the friction coefficient cause increment of the net force acting of the block placed upper side and this simply because the horizontal displacement measurements of the block(s), located at the top, are always greater for the horizontal displacement measurements of the block(s) located at the bottom.
- A steady decrease from the static condition to dynamic condition in friction angle cause block acceleration increment

CHAPTER 9

NUMERICAL MODELING

In this study, a two-dimensional (2D) reference model has been developed to simulate seismic performance of block type quay walls.

Over the last decade, important developments have been achieved in several commercial computer programs which are used seismic analysis of the structures and some of these programs can also be used for the seismic analysis of gravity type quay walls. These commercial computer programs are based on numerical modeling techniques namely finite element analysis and finite difference analysis. By using these commercial computer programs, it is possible to analyze the very complex problems, such as modeling of the behavior of gravity type quay walls, understanding of the soil-structure-fluid interaction mechanism, computing the displacement on the gravity type quay walls and obtaining the design parameters for dynamic loading. "The finite element method is certainly the most comprehensive approach to analyze the performance of soil structures subjected to seismic loading and has some advantages in considering the natural failure mechanisms and the interaction of structure-soil system" (Li et al., 2010).

Although, several commercial computer programs can be used for seismic design of gravity type quay walls, these programs still have some disadvantages in defining the basic design parameters. "Programs like PLAXIS, FLAC, SHAKE , SASSI, etc... are simpler than the general purpose finite element software, but each has its own limitations (Maleki and Mahjoubi, 2010).

In this study, nonlinear time history analysis has been conducted with this 2D plain strain analysis model using the computer program PLAXIS V8.2. The displacements and soil pressure measurements obtained from PLAXIS V8.2 software program were also compared with the displacements and soil pressure measurements obtained from 1 g shaking table tests. In addition, a case study were carried out using PLAXIS V8.2 and site measurements were compared with the numerical results.

9.1 Modeling of the System

PLAXIS V8.2 is a program based on the finite element method. This program is divided into four subprograms; *Input, Calculations, Output and Curves*.

9.1.1 Subprogram 1 : Input

PLAXIS V8.2 computer program that uses the finite-element method (FEM), was utilized for horizontal dynamic loading of only one input, which had displacement amplitude of 3 mm and a frequency of 5 Hz for models for one block, two blocks and three blocks for Soil 1.

Fifteen noded, triangular, 2D plane-strain elements were used in the PLAXIS V8.2 computer program. Backfill width of models are selected 10 times of structures height. In this way, test results such as displacements and soil pressures were simulated approximately. At the end of the backfill, triangular load distribution is placed instead of standard boundary conditions. Thus, swelling on backfill during dynamic loading was prevented. In Figure 9.1, Figure 9.2 and Figure 9.3 numerical models are shown for model with one block, two blocks, three blocks.

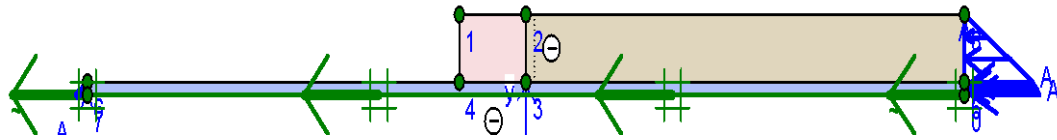


Figure 9.1: Numerical model for one block

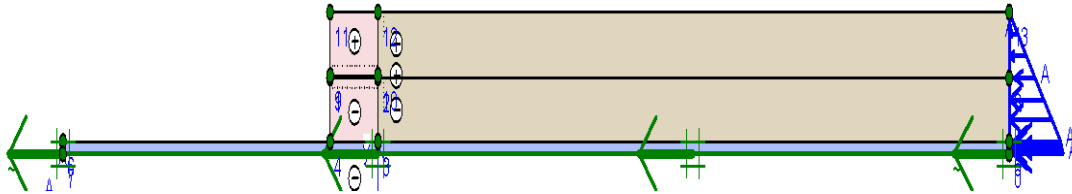


Figure 9.2: Numerical model for two blocks

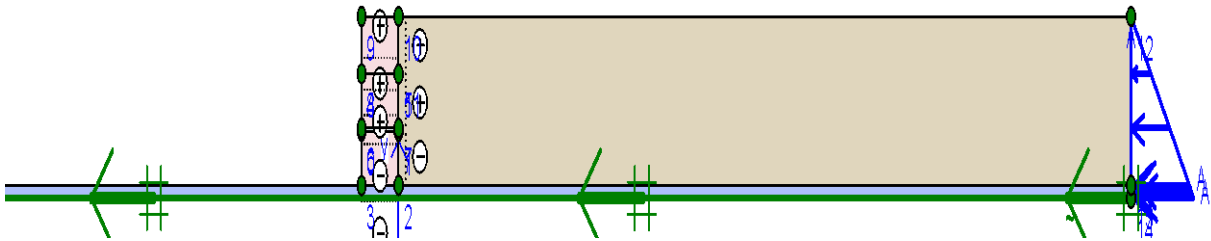


Figure 9.3: Numerical model for three blocks

In numerical model runs were carried out for 10 sec. duration in accordance with the model characteristics and limitations. Thus, comparisons of the displacements and soil pressure results between numerical and experimental studies were made for test duration 10 sec which corresponding to almost 30 sec. duration in prototype. When the experimental results are examined, it is seen that within 10 sec. the representative horizontal displacement values are reached close to total horizontal displacement values occurred in 30 sec. Therefore for horizontal displacement results duration of numerical model as 10 sec is found to be accurate enough.

Typical input acceleration data obtained from 1 g shaking table tests are shown for one block, two blocks and three blocks for 5 Hz as an example for Soil 1 in Figure 9.4 - Figure 9.6).

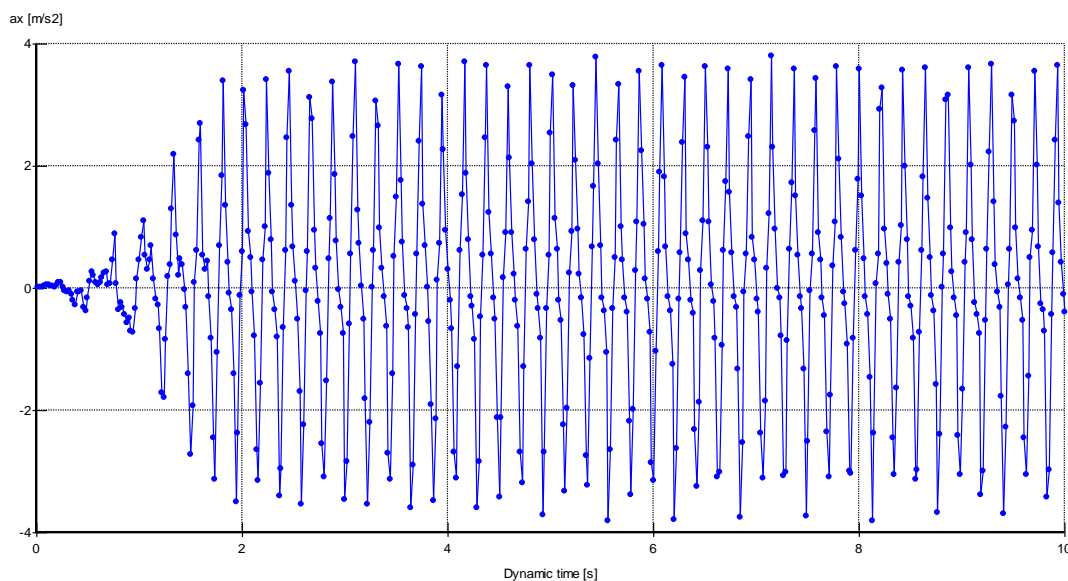


Figure 9.4: Input motion for one block

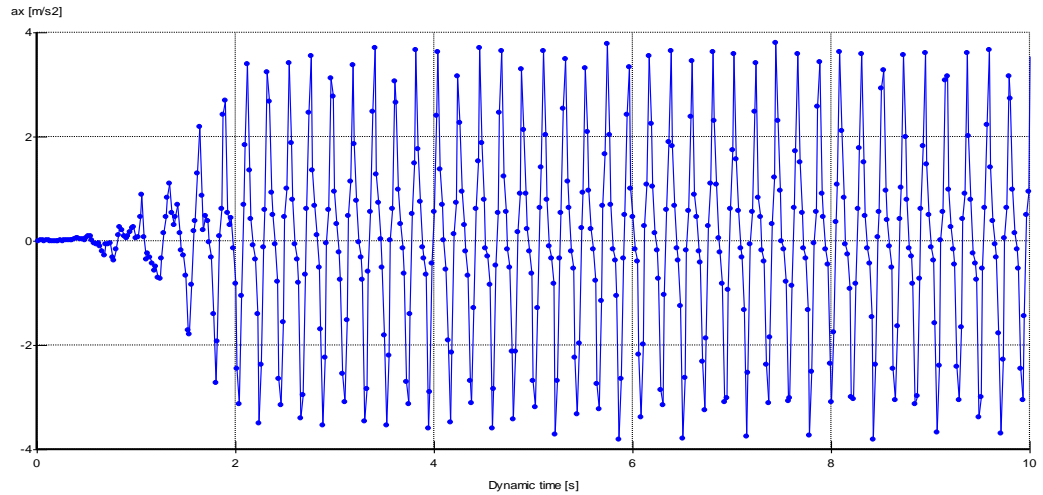


Figure 9.5: Input motion for two blocks

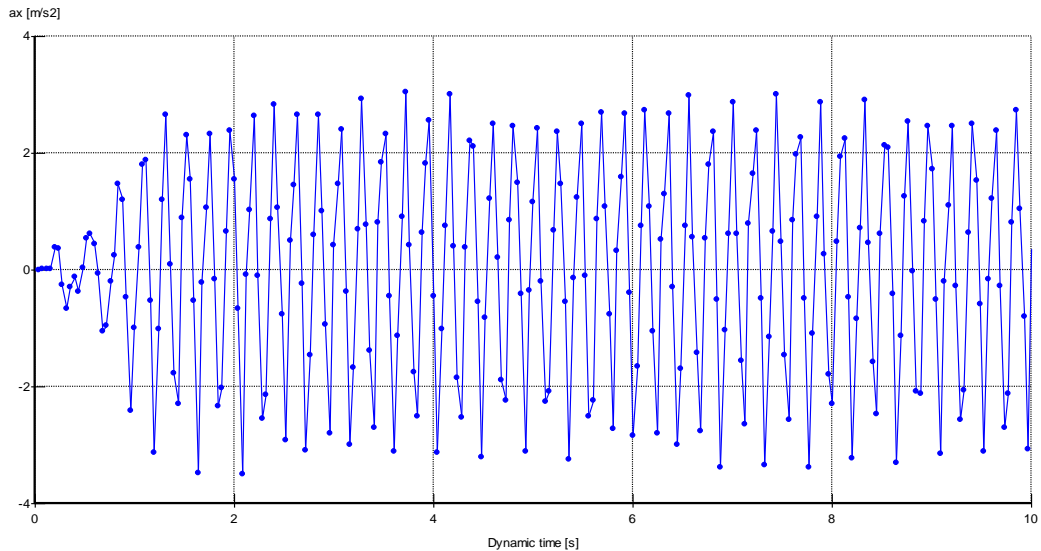


Figure 9.6: Input motion for three blocks

In order to simulate the behavior of the soil, a suitable soil model and appropriate design material (soil and concrete) parameters should be assigned as input parameters in the model. Soil is the most complicated material and during the analytical and numerical analysis, there are different types of material models, which can be applied to the solution of geotechnical problems. The available soil models in PLAXIS V8.2 computer program are linear elastic model, Mohr-Coulomb model, Hardening Soil model, soft soil model, soft soil creep model, and jointed rock model (Table 9.1).

Based on the properties of the material model presented in Table 9.1, hardening soil model was chosen as recommended in PLAXIS V8.2 Manual under dynamic loading and a linear-elastic stress-strain behavior was assumed for the retaining walls using a high enough Young's modulus to simulate a rigid block.

Interface finite elements were used to model soil-block interaction. These are defined with a strength reduction factor R_{inter} that models the roughness of the interaction. In this study, $R_{inter} \times \tan \phi$ was defined as 0.5-0.6 as described in Chapter 8.

Additionally, simulating friction between block-block, a very thin soil layer is defined as interface. The properties of interface and all other material properties are summarized in Table 9.2. All the material properties were determined given in APPENDIX L.

Table 9.1: Material models given in PLAXIS V8.2
(PLAXIS GID, Material Models Manual)

MODEL	PROPERTIES
“Linear Elastic Model	Soil behaviour is non-linear and irreversible. The linear elastic model is insufficient to capture the essential features of soil.
Mohr-Coulomb Model	This is a first order model and only a limited number of features that soil behaviour shows reality. For each layer one estimates a constant average stiffness. But this assumption is not exactly true for the material behaviour of soils.
Hardening Soil Model	“Hardening-soil model is an advanced model for simulating the behaviour of different types of soil, both soft soil and stiff soil” (Schanz, 1998). Soil stiffness is described much more accurately. In contrast to Mohr-Coulomb model, all stiffness increase with pressure. Although this is an advanced soil model, there are a number of features of real soil behaviour the model does not include.
Soft Soil Model	Soft soil model is superseded by Hardening Soil model.
Soft Soil Creep Model	This is especially the case for excavation problems, including tunneling.
Jointed Rock Model	Especially meant to simulate the behaviour of rock layers”

When the input parameters (geometry, material properties) of the model is complete, the finite element model or *mesh* can be generated. There are several options depending on how coarse or fine mesh the user wishes to adapt. The use of a finer mesh however requires a longer calculation time. In this study, 15 noded, triangular elements were used to optimise the run time of the numerical model.

The last step before calculation is defining the initial condition. The initial conditions cover the initial values for *effective stress*, *tension* and *pore pressure*. The initial pore pressure can in the simplest case be determined by drawing the ground water level and assuming hydrostatic pore pressure increase.

Table 9.2: The properties of interface and all other material properties

Symbol	Parameters	Units	Hardening-Soil			Linear Elastic
			backfill	foundation	interface	concrete block
γ_{unsat}	Unsaturated unit weight	kN/m ³	16	20	16	24
γ_{sat}	Saturated unit weight	kN/m ³	19	22	19	24
$E_{50\text{ref}}$	Reference secant Young's modulus	kN/m ²	100000	150000	200000	40000
E_{oedref}	Reference constraint modulus	kN/m ²	66627.93	148244.41	200000	-
E_{urref}	Reference unloading-reloading modulus	kN/m ²	300000	450000	600000	-
φ	Shear strength angle	°	40	45	40	-
ψ	Dilatancy angle	°	10	15	10	0.2
ν_{ur}	Poisson rate	-	0.2	0.2	0.2	
p_{ref}	Reference stress	kN/m ²	100	100	100	-
Power	Power for stress level dependency	-	0.5	0.5	0.5	
$K_{0\text{nc}}$	Earth pressure coefficient at rest	-	0.29	0.31	0.36	
R_f	Failure ratio	-	0.9	0.9	0.9	

9.1.2 Subprogram 2 : Calculation

The calculation subprogram can be used to define calculation steps. There are three different calculation types that can be chosen : *plastic*, *consolidation* and ϕ/c -*reduction* where the last one is helpful for computing *safety factors*. In this study, “plastic calculation” were used as calculation type.

9.1.3 Subprogram 3 : Outputs

Response of block(s) during dynamic loading due to block(s)-soil-water interaction were studied by using finite element program (PLAXIS V8.2) to investigate the effects of soil-block-water interaction on soil pressures and block(s) displacements.

Figure 9.7, Figure 9.8 and Figure 9.9 show the outputs of PLAXIS V8.2 computer program for one block, two blocks and three blocks for 5 Hz for Soil 1, respectively.

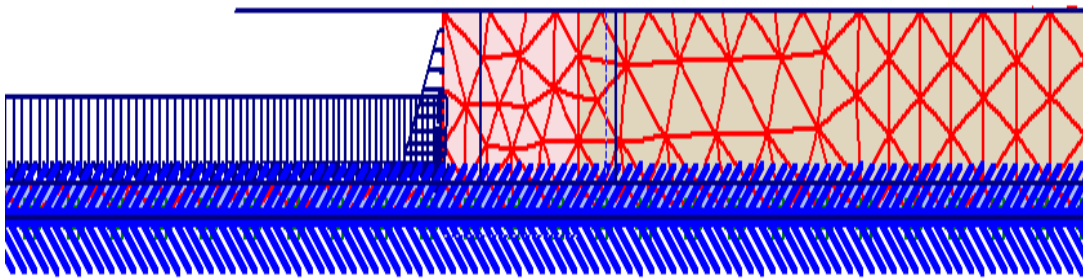


Figure 9.7: Outputs of PLAXIS V8.2 computer program for one block for Soil 1

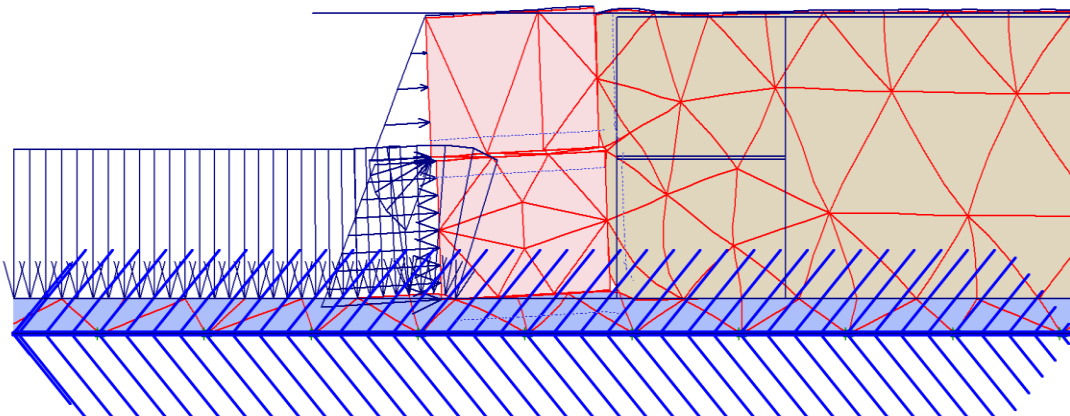


Figure 9.8: Outputs of PLAXIS V8.2 computer program for two blocks for Soil 1

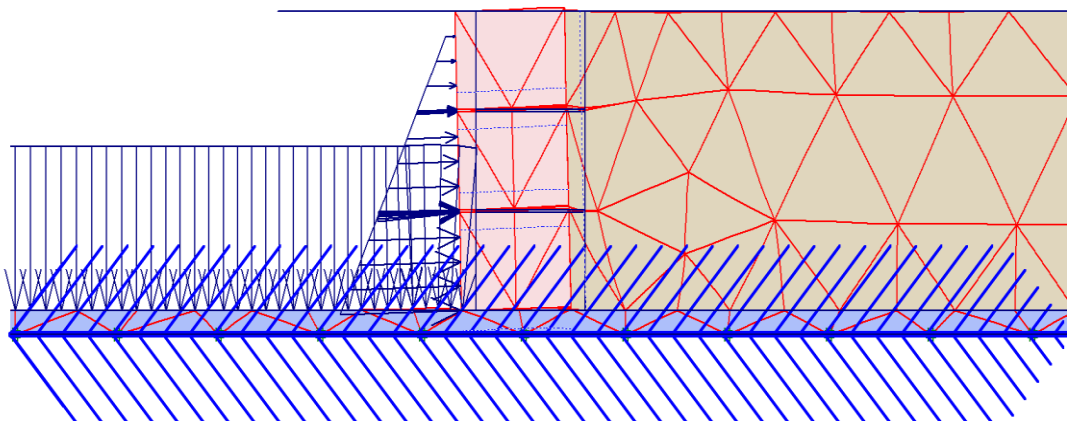


Figure 9.9: Outputs of PLAXIS V8.2 computer program for three blocks for Soil 1

Contours of total displacements for one block, two blocks and three blocks are also shown in Figure 9.10, Figure 9.11 and Figure 9.12. It is seen that largest displacements on backfill occurs just behind the structures (red color).

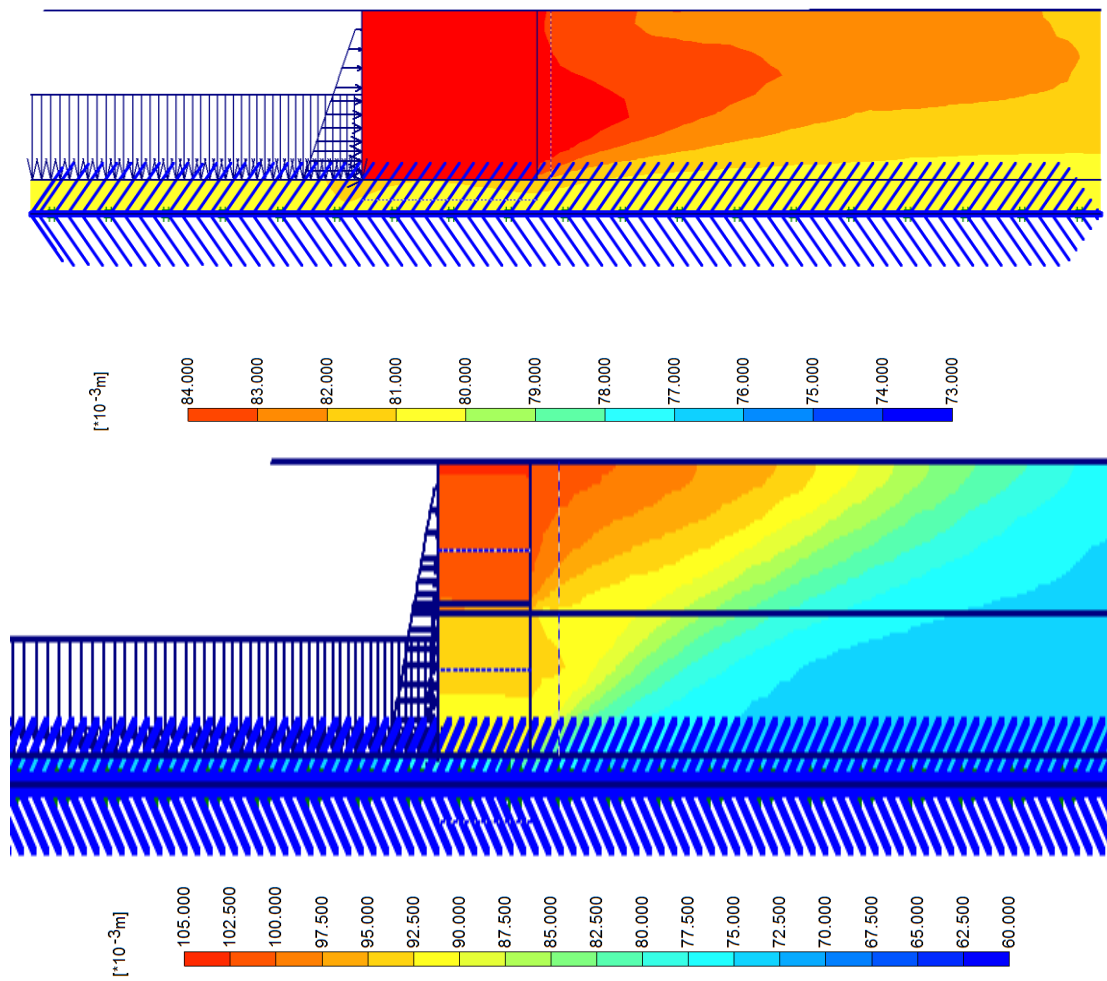


Figure 9.11: Contours of total displacement for two blocks for Soil 1

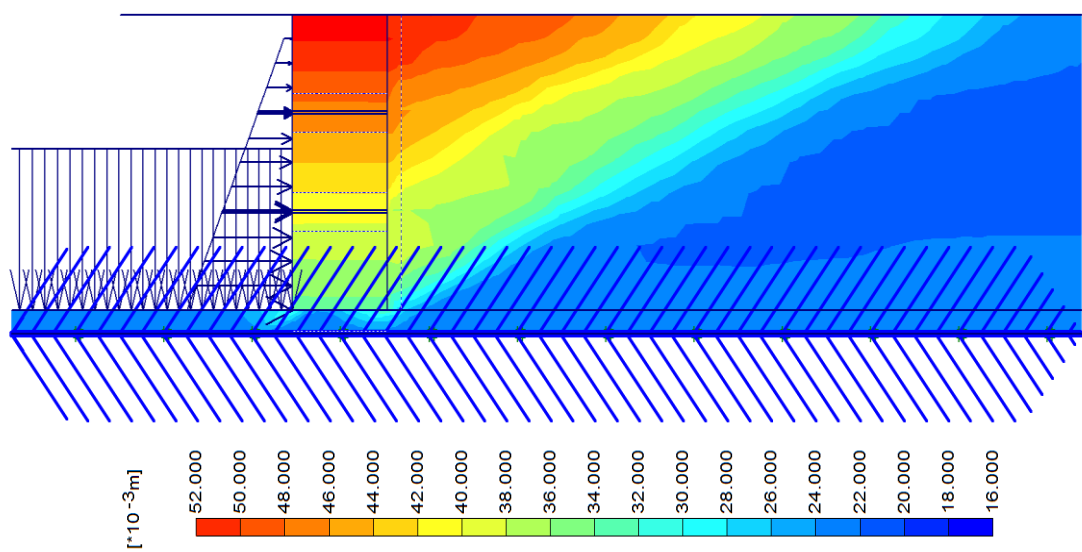


Figure 9.12: Contours of total displacement for three blocks for Soil 1

Soil profile measurements which show the initial position of the soil and after dynamic loading position of the soil (for 5 Hz for three blocks) are shown in Figure 9.13.

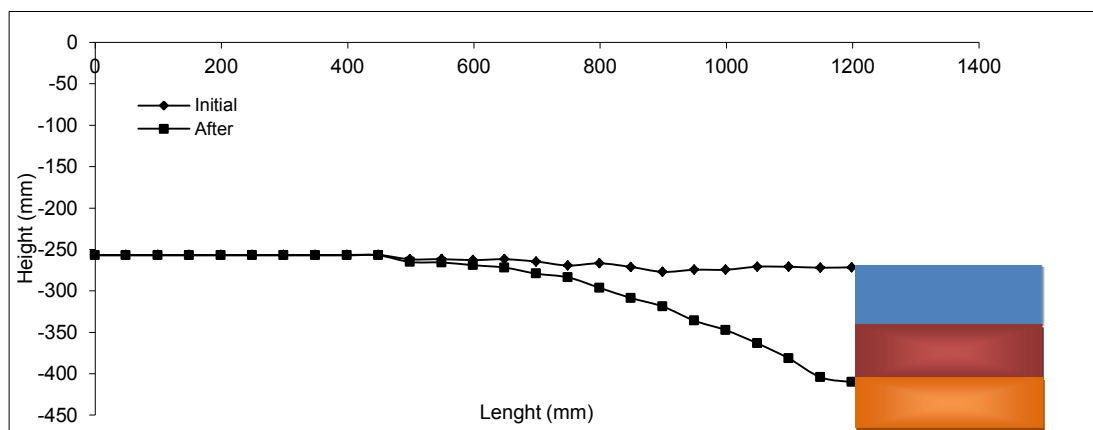


Figure 9.13: Soil profile measurements for three blocks for 5 Hz for Soil 1

If maximum total displacement area of backfill from PLAXIS V8.2 and backfill settlement behind the structures from experiment are compared, it is seen that active thrust zones on backfill are almost same for numerical and physical model. However, calculated vertical displacements are not equal to measured vertical displacement because backfill profile is measured at the end of 30 second. Nevertheless, results are found to be compatible finding to have an idea about damage area on backfill.

Discussions of the outputs of the numerical modeling for one block, two blocks and three blocks in 10 sec. for 5 Hz performed by PLAXIS V8.2 were carried out in two groups, i) soil pressure outputs and ii) displacements outputs.

9.1.3.1 Soil Pressure Outputs

The soil pressure outputs obtained from PLAXIS V8.2 for one block, two blocks and three blocks for 5 Hz for Soil 1 showed in Figure 9.14, Figure 9.15, and Figure 9.16.

ONE BLOCK

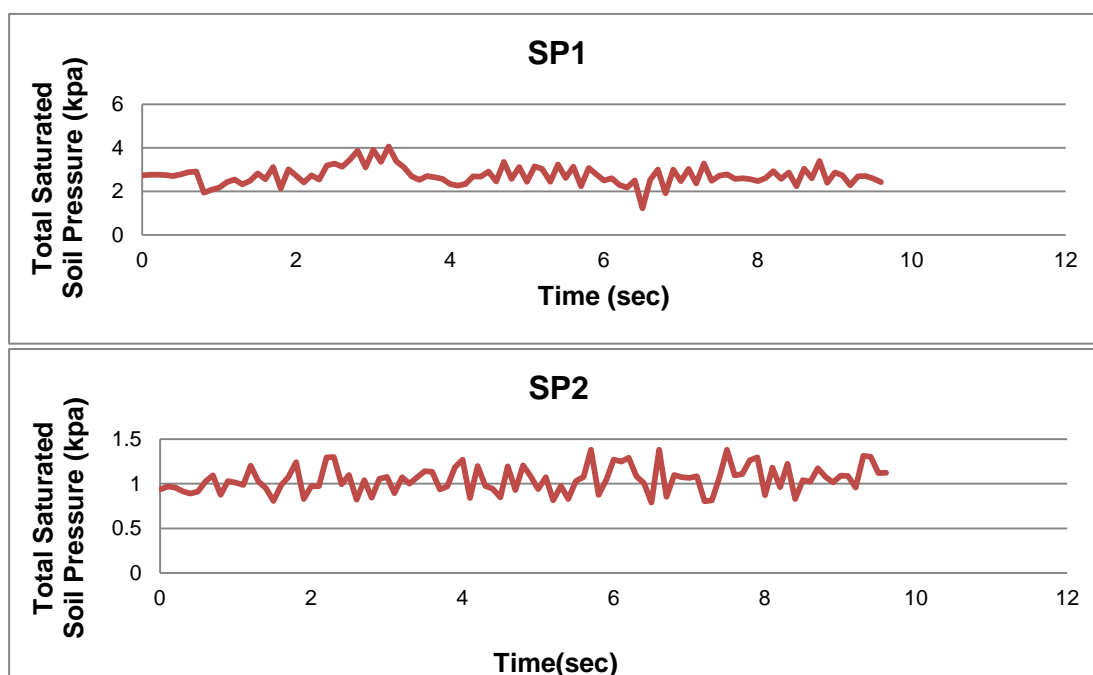


Figure 9.14: Total saturated soil pressure results (SP1 and SP2) for one block for 5 Hz for Soil 1

TWO BLOCKS

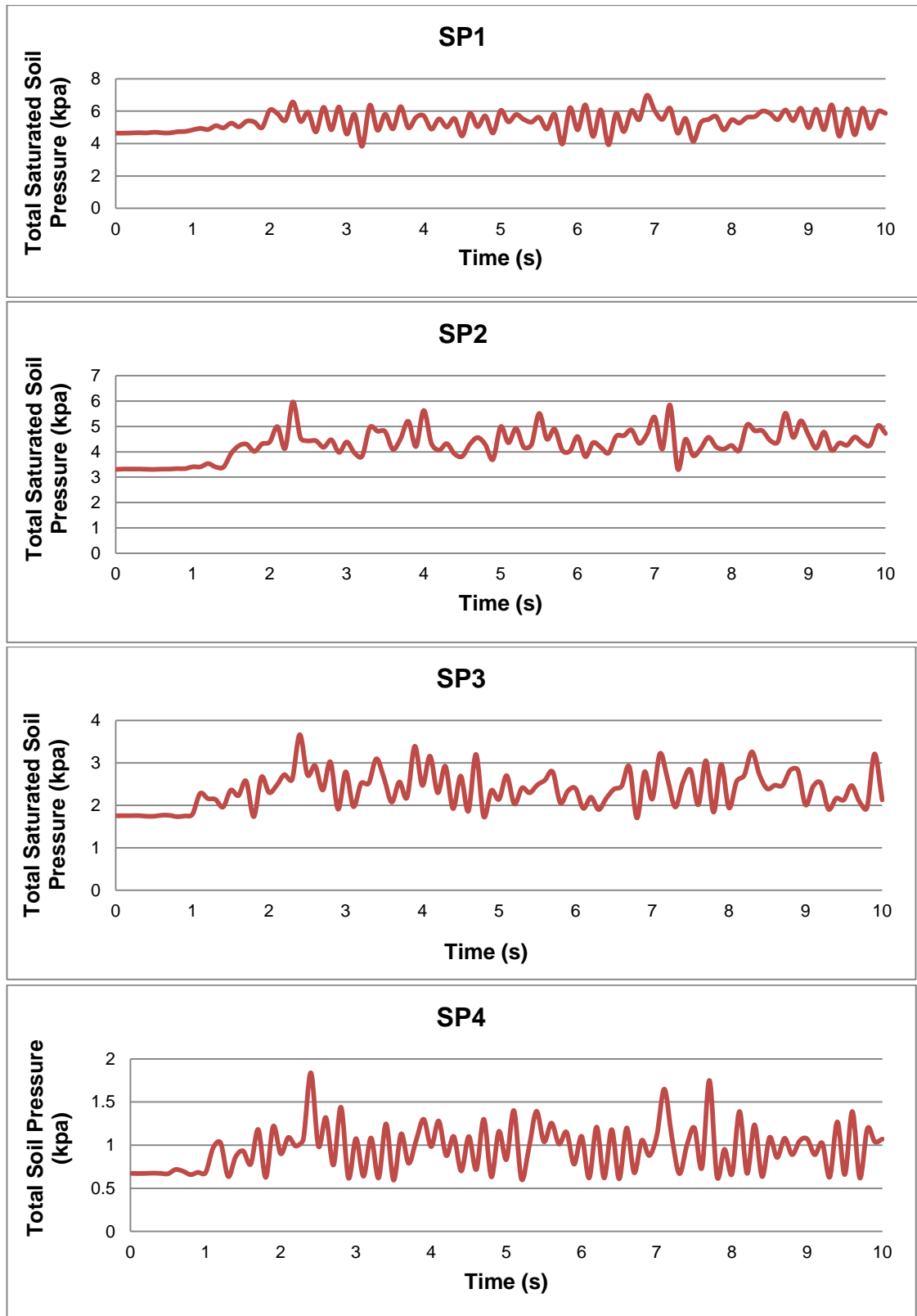


Figure 9.15: Total saturated soil pressure results (SP1, SP2, SP3 and SP4) for two blocks for 5 Hz for Soil 1

THREE BLOCKS

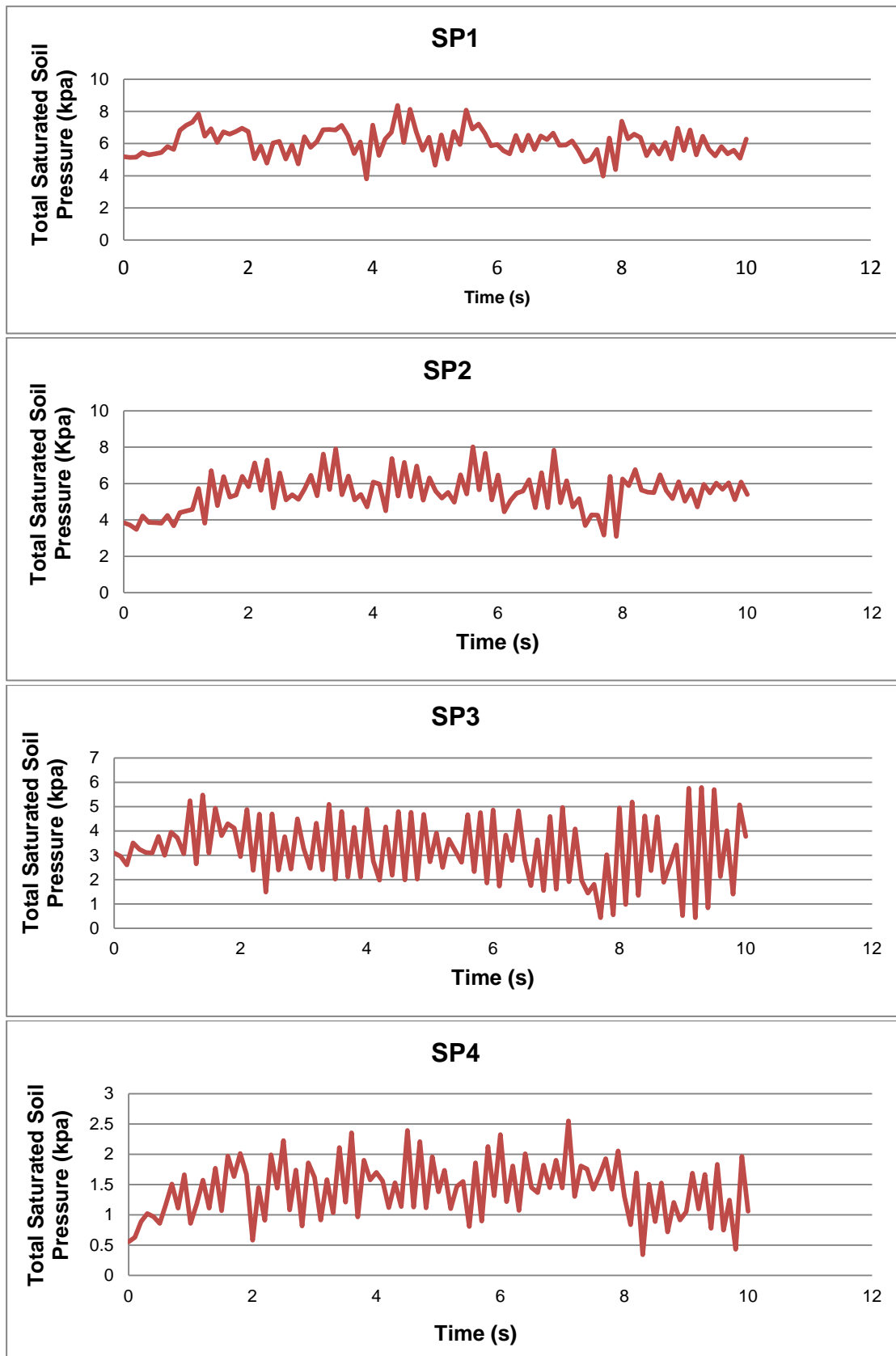


Figure 9.16: Total saturated soil pressure results (SP1, SP2, SP3 and SP4) for three blocks for 5 Hz for Soil 1

9.1.3.2 Displacement Outputs

The displacement outputs of each block obtained from PLAXIS V8.2 computer program for one block, two blocks and three blocks for 5 Hz for Soil 1 showed in Figure 9.17, Figure 9.18, Figure 9.19 and Table 9.3.

One Block

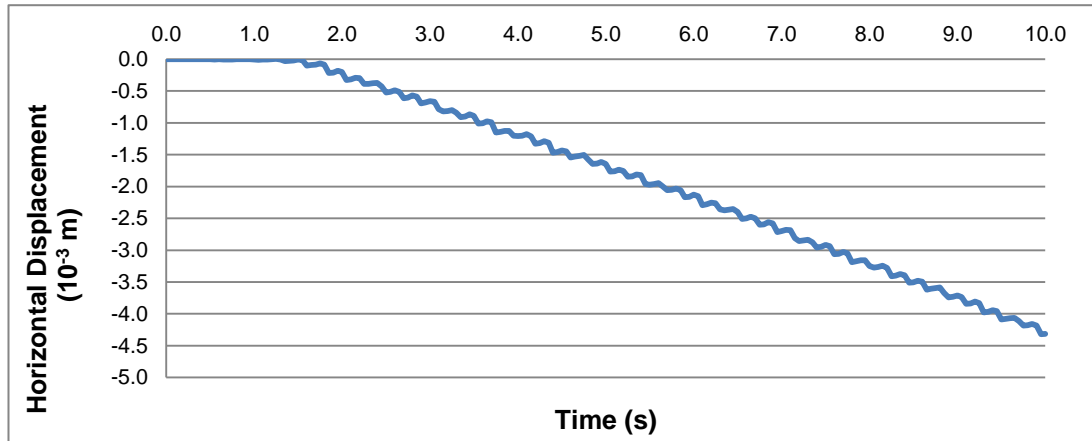


Figure 9.17: Displacement results for one block for 5 Hz for Soil 1

Two Blocks

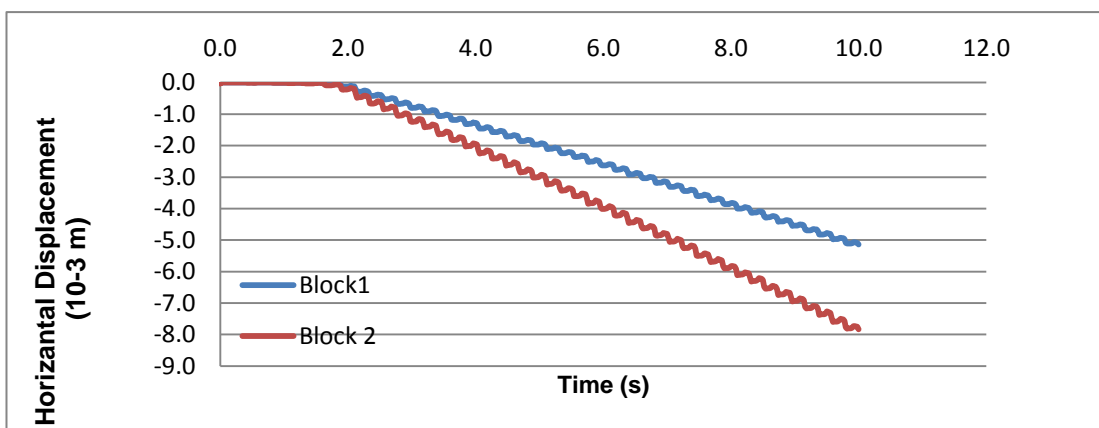


Figure 9.18: Displacement results for two blocks for 5 Hz for Soil 1

Three Blocks

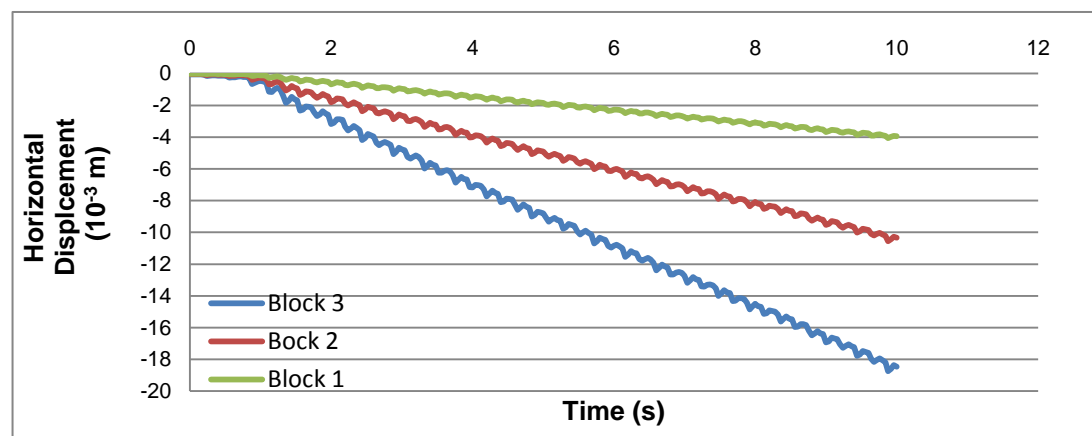


Figure 9.19: Displacement results for three blocks for 5 Hz for Soil 1

Table 9.3: The displacement results obtained from PLAXIS V8.2 for one block, two blocks and three blocks for 5 Hz for Soil 1

STRUCTURE	BLOCK NUMBER	HORIZONTAL DISPLACEMENT (mm)
One Block	Block 1	4.3
Two Blocks	Block 1	5.0
	Block 2	7.8
Three Blocks	Block 1	4.0
	Block 2	11
	Block 3	19 .0

Using the numerical results given in Table 9.3 are compared with the experimental results (Table 7.8) are compared.

9.2 Comparisons of the Experimental and Numerical Results

Soil pressure and displacements results obtained by using the 1 g shaking table tests results (experimental study) are given in Chapter 7 and displacements and soil pressure results obtained by using the PLAXIS V8.2 (numerical study) computer program are given between Figure 9.20 - Figure 9.22. The 1 g shaking table tests results were used as the verification tools.

9.2.1 Comparisons of Soil Pressure Results

In Figure 9.20, Figure 9.21 and Figure 9.22, soil pressure results obtained from 1 g shaking table tests and PLAXIS V8.2 computer program are shown together for one block, two blocks, three blocks for 5 Hz for Soil 1.

ONE BLOCK

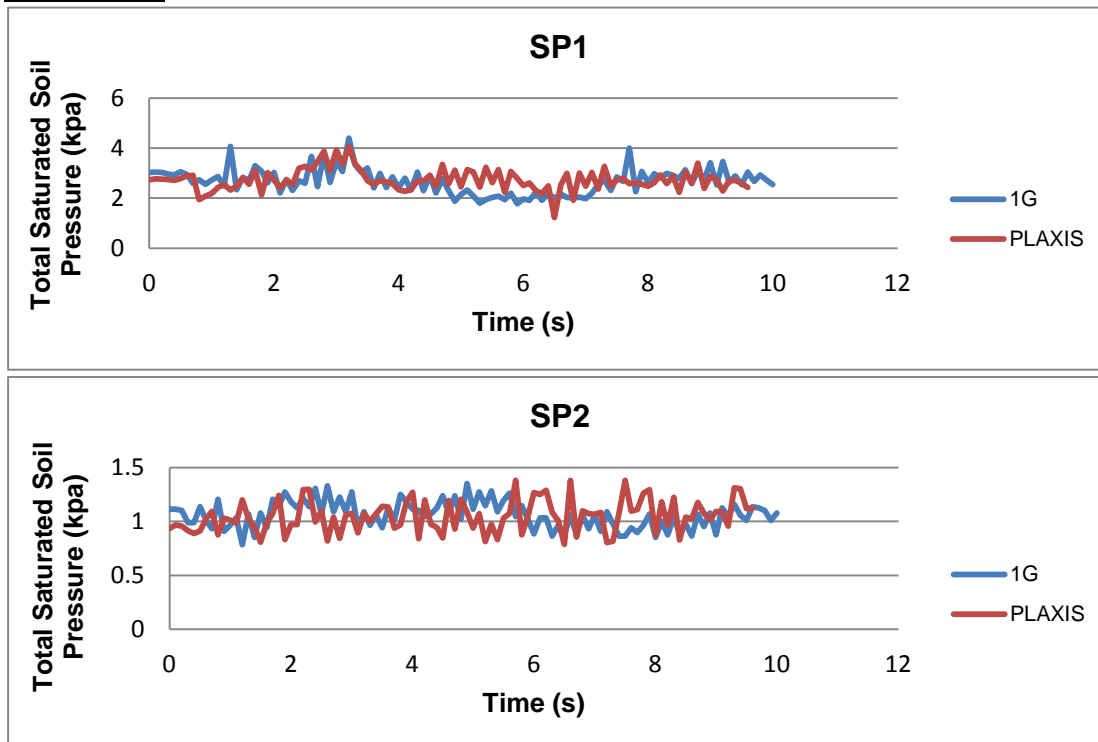


Figure 9.20: Comparisons of soil pressure cells (SP1 and SP2) measurements for one block

TWO BLOCKS

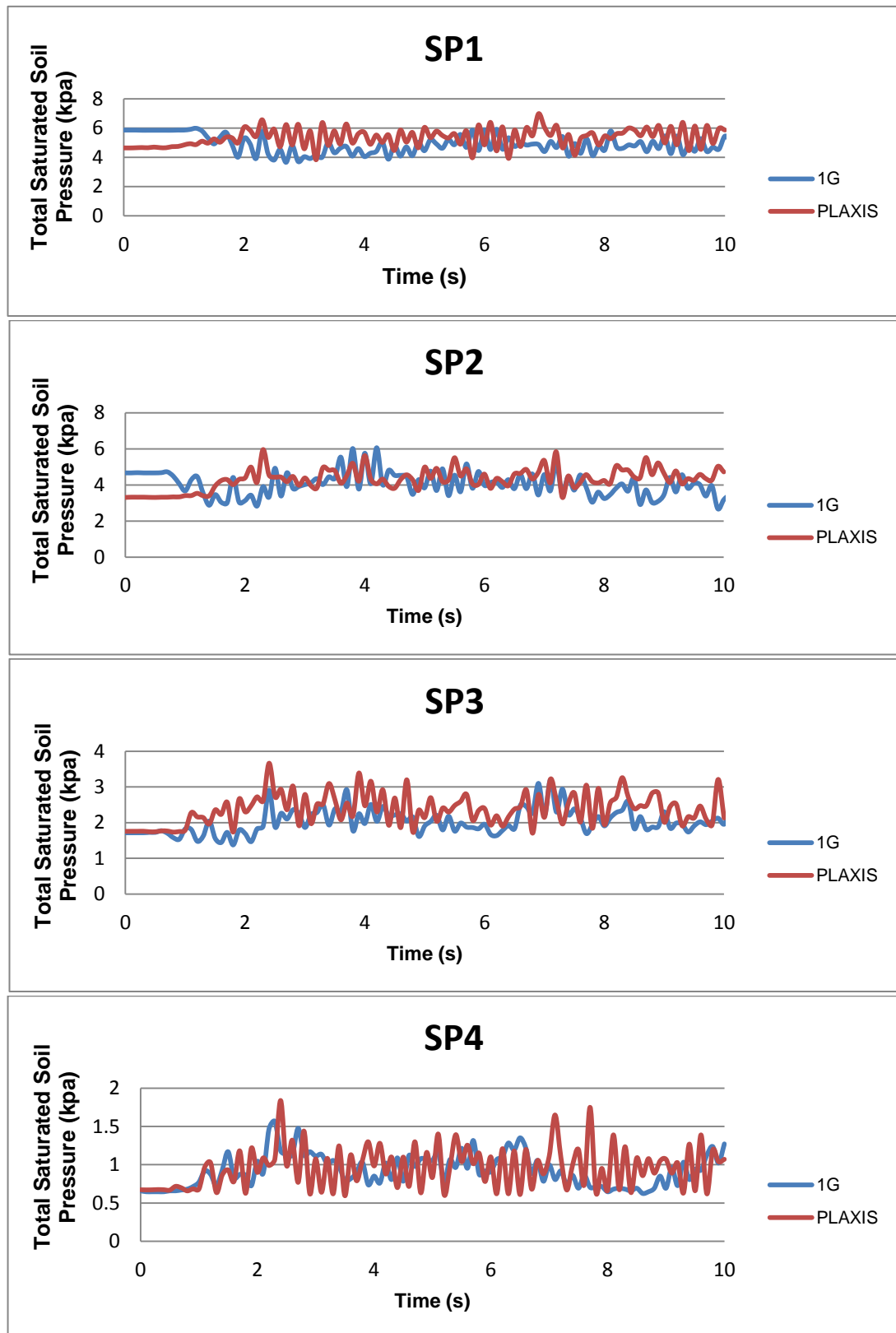


Figure 9.21: Comparisons of soil pressure cells (SP1, SP2, SP3, SP4) measurements for two blocks

THREE BLOCKS

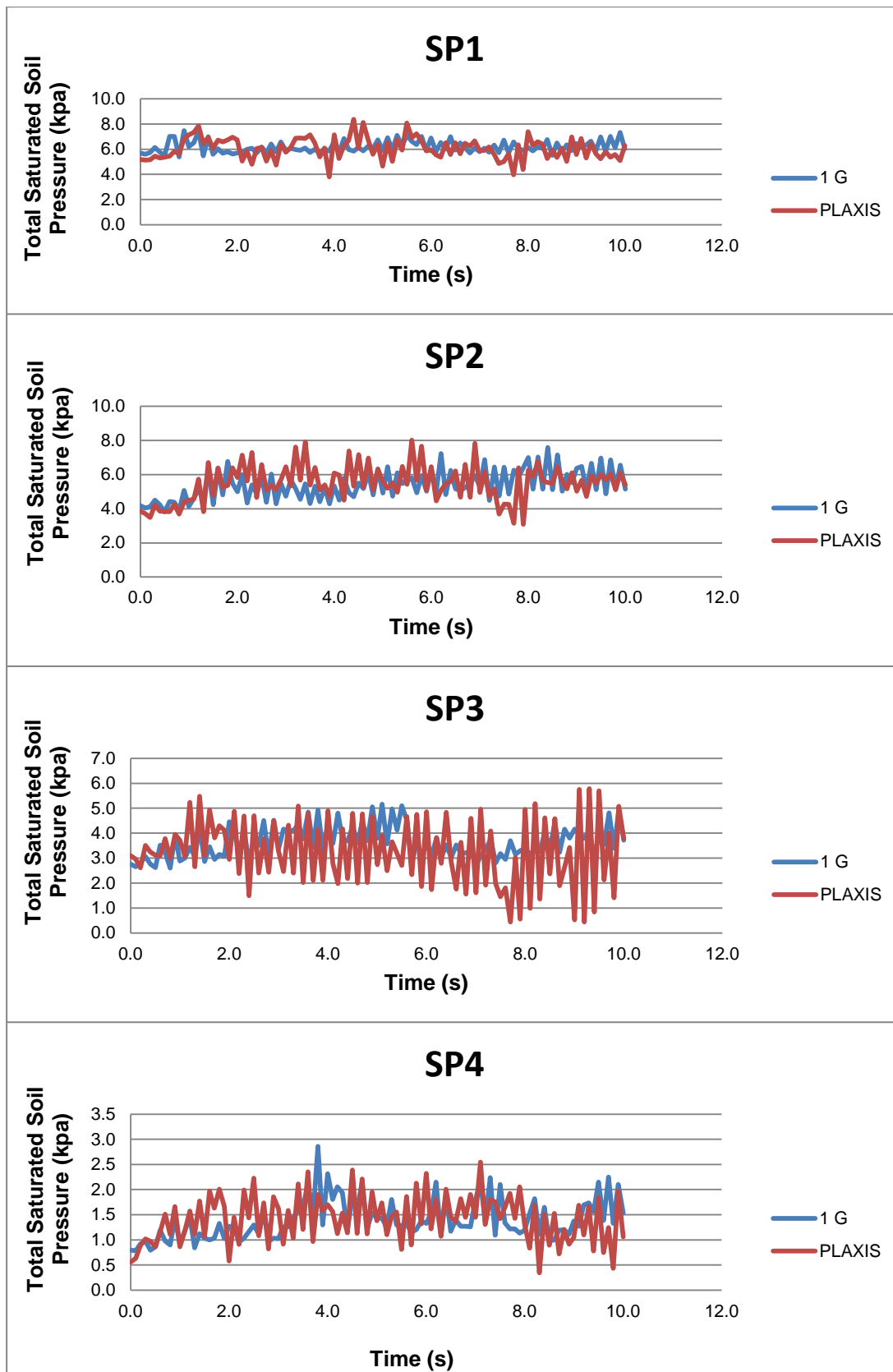


Figure 9.22: Comparisons of soil pressure cells (SP1, SP2, SP3, SP4) measurements for three blocks

Although, there is no perfect similarity between obtained instantaneous saturated soil pressures presented in Figure 9.20 - Figure 9.22 for one, two, three block(s) respectively, it can be assumed that average total saturated soil pressures obtained from experimental and numerical studies are compatible. Even in the case of maximum deviation between experimental and numerical results are between (%2 and %9) for SP1, (%1 and %4.8) for SP2, (%12 and %17) for SP3 and (%2 and %4.3) for SP4 in case of one block (Table 9.4), two blocks (Table 9.5), three blocks (Table 9.6) respectively which can be considered to be very small.

Table 9.4: Maximum deviation between experimental and numerical studies for one block

Soil Pressure Name	SP1	SP2
Max. Total Soil Pressure Results		
PLAXIS 8.2	2.72	1.05
1 G SHAKING TABLE TESTS	2.66	1.06
Max. Deviation (%)	2	1

Table 9.5: Maximum deviation between experimental and numerical studies for two blocks

Soil Pressure Name	SP1	SP2	SP3	SP4
Max. Total Soil Pressure Results				
PLAXIS 8.2	5.35	4.30	2.37	0.96
1 G SHAKING TABLE TESTS	4.89	4.10	2.02	0.92
Max. Deviation (%)	9	4.8	17	4.3

Table 9.6: Maximum deviation between experimental and numerical studies for three blocks

Soil Pressure Name	SP1	SP2	SP3	SP4
Max. Total Soil Pressure Results				
PLAXIS 8.2	6.05	5.48	3.25	1.42
1 G SHAKING TABLE TESTS	6.18	5.39	3.64	1.39
Max. Deviation (%)	2	1	12	2

9.2.2 Comparisons of Displacements Results

Table 9.7, Figure 9.23, Figure 9.24 and Figure 9.25 show the displacements results comparisons between 1 g shaking table tests and PLAXIS V8.2 computer program for one block, two blocks and three blocks for 5 Hz for Soil 1, respectively.

Table 9.7: Comparisons of displacements results

Structure	Block Number	Horizontal Displacement (mm)	
		PLAXIS V8.2 Results	1 g Shaking Table Tests Results
One Block	Block 1	4.3	5.8
Two Blocks	Block 1	5.0	6.3
	Block 2	8.0	11
Three Blocks	Block 1	4.0	5.0
	Block 2	10.0	11.0
	Block 3	18.0	18.0

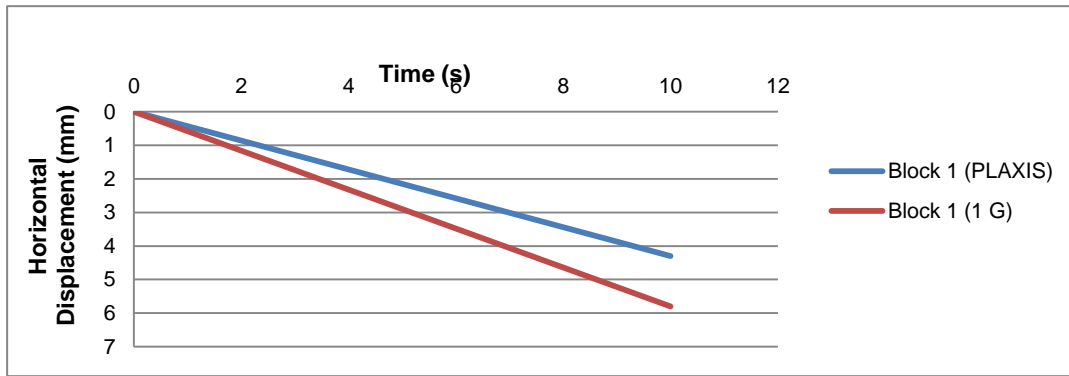


Figure 9.23: Displacements results comparisons between 1 g shaking table tests and PLAXIS V8.2 computer program for one block for 5 Hz for Soil 1.

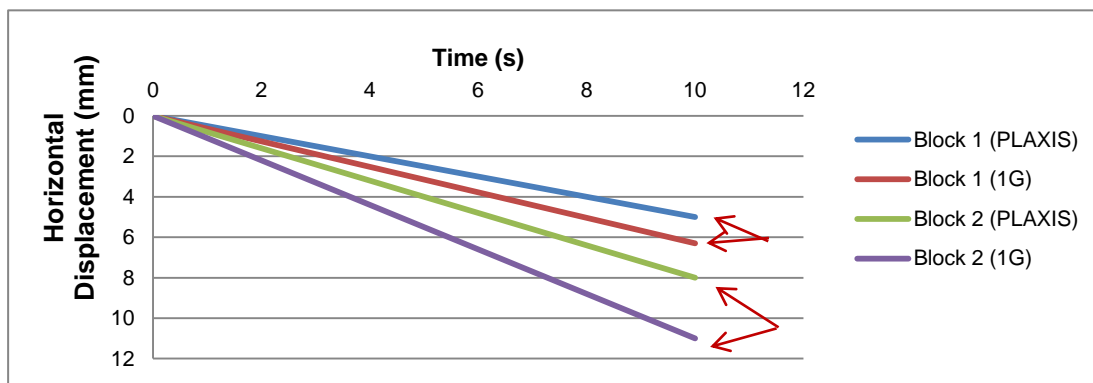


Figure 9.24: Displacements results comparisons between 1 g shaking table tests and PLAXIS V8.2 computer program for two blocks for 5 Hz for Soil 1.

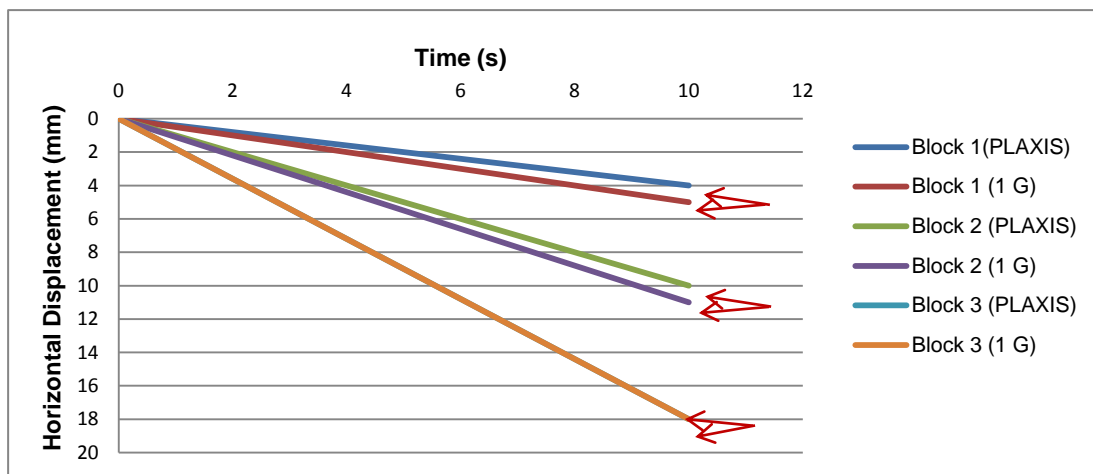


Figure 9.25: Displacements results comparisons between 1 g shaking table tests and PLAXIS V8.2 computer program for three blocks for 5 Hz for Soil 1.

Comparison of the experimental and numerical results for displacements show that, although several assumptions and approaches were defined to model soil-water-structure interaction in PLAXIS V8.2 computer program, it is certain that displacement results are compatible to each other. Especially in case of three blocks results are found to be almost perfectly matching.

Comparisons of all soil pressure and horizontal displacement results show that experimental conditions are simulated successfully with numerical study. Unknown material properties were

determined by using 1 g shaking table tests results and 1 g shaking table tests results were verified by using PLAXIS V8.2.

9.3 A Case Study on Derince Port Block Type Quay Wall

The recorded bedrock motions of the August 17, 1999 the Eastern Marmara Earthquake, which caused serious damaged on Derince Port block type quay wall, were used as an input for the PLAXIS V8.2 software program to compare the horizontal displacement results of numerical model and real site measurements. Further, these results are discussed in view of the definitions of the damage levels as given in PIANC (2001).

9.3.1 Derince Port

“The Eastern Marmara Earthquake occurred on with an $M_w=7.4$ and struck the İzmit Bay and eastern Marmara Sea region, north-west Turkey. The main fault is a single strike-slip fault approximately 140 km long, starting from Sapanca Lake in the east and ending in İzmit Bay in the west” (Yüksel et al., 2002). “During Kocaeli Earthquake 1999, over 15.000 fatalities and 20 billion US dollars in losses were observed. “The earthquake occurred in İzmit, 1999 caused serious damage mostly on block type quay wall in Derince Port”.
http://www.jsceint.org/Report/report/kocaeli/kocaeli_chap6.pdf).

“Derince Port is located near İzmit and the largest port in the area with about 1.5 km of waterfront structures and with eight wharves (Figure 9.26). The peak ground accelerations were obtained approximately 0.25g to 0.3g” (Yüksel et al., 2002).

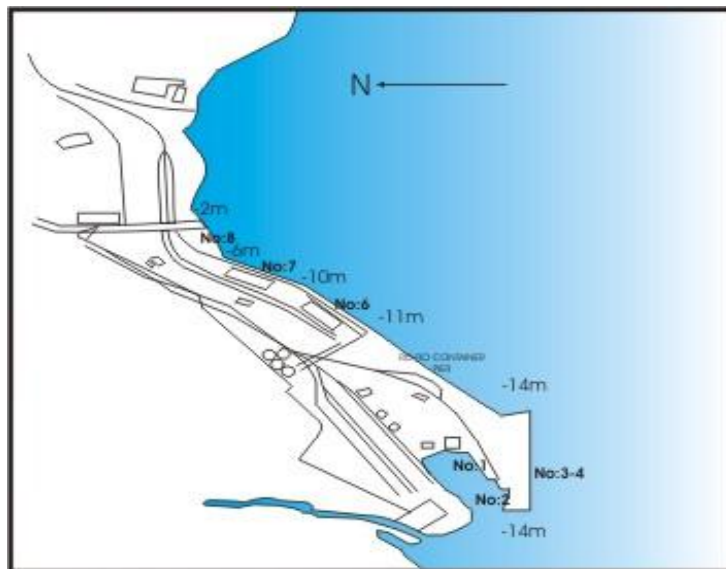


Figure 9.26: Derince Port

The soil profiles beneath the 12 m deep and crosssection of the block type quay wall are given in Figure 9.27 and Figure 9.28.

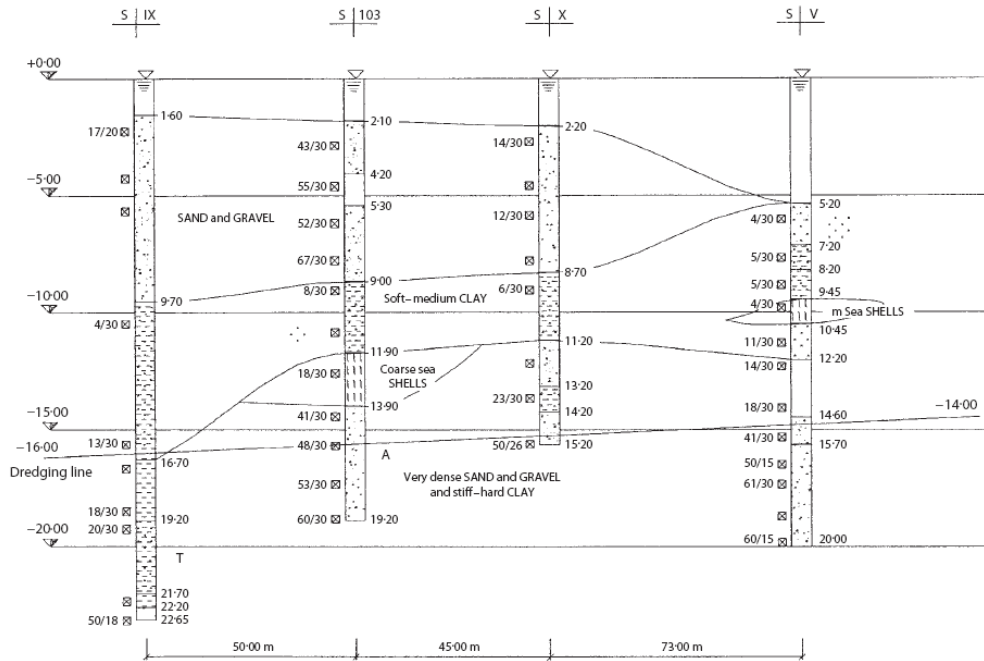


Figure 9.27: Cross section of block type quay walls (Yüksel et al., 2002)

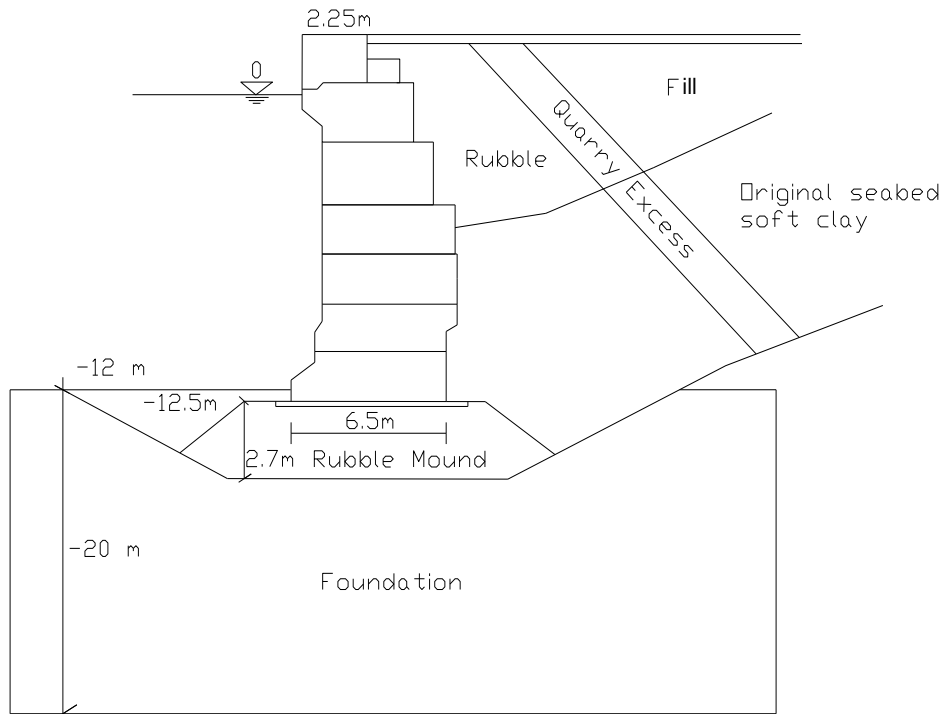


Figure 9.28: Cross section of block type quay walls (Yüksel et al., 2002)

Site measurements show that the block type quay wall moved seaward without any vertical displacement. However, 0.5 m lateral displacement towards the sea and 0.5-0.8 m settlement on the backfill behind the quay wall were observed (Yüksel et al., 2002). PIANC (2001), states that 0.7 m lateral displacement was occurred at Derince Port. At some quays

mid-span deflections and relative corner movements were observed. The settlement of backfill caused the tilting of a crane on rails. One of the cranes was overturned while others were derailed due to the rocking response to the earthquake shaking. Damages of these cranes caused important loss of serviceability. There was one crane that was fixed to the foundation that did not suffer apparent damage. Also liquefaction was serious problem for the backfill behind the quay wall. The most liquefaction occurs at a location where near a river basin mainly caused by the complexity of sedimentation of the soil. However, the major problem is sandy backfill material behind the quay walls dredged from a river mount by the sea probably a kind of delta sediment”
(http://www.jsceint.org/Report/report/kocaeli/kocaeli_chap6.pdf).

9.3.2 Numerical Modeling of Derince Port, Block Type Quay Wall

First step of the numerical modeling is defining the input parameters, in this part geometry was defined and acceleration data was ensured. To define the geometry by using PLAXIS V8.2 software program, the thickness of the firm foundation and sea bed rock foundation were taken as 2.7 m and 20 m for the numerical modeling of block type quay walls (Figure 9.26). The input acceleration data obtained from <http://peer.berkeley.edu/svbin/Detail?id=P1103> web site was used to define unknown earthquake parameter for the Plaxis V8.2, (Figure 9.29, APPENDIX M).

P1103 : Earthquake and Station Details

Kocaeli, Turkey 1999/08/17 Magnitude: M (7.4) Ml () Ms (7.8)	Station: Izmit Data Source: ERD
Distance (km): Closest to fault rupture (4.8) Hypocentral () Closest to surface projection of rupture (4.8)	Site conditions: Geomatrix or CWB (A) USGS (A)

A newer version of this record is available in the PEER NGA database: [NGA1165](#)

Download Files

Record/Component	HP (Hz)	LP (Hz)	PGA (g)	PGV (cm/s)	PGD (cm)	Acceleration	Velocity	Displacement	Spectra
KOCAELI/IZT-UP	0.1	30.0	0.146	13.1	6.66	ATH	VTH	DTH	0.5% 1% 2% 3% 5% 7% 10% 15% 20%
KOCAELI/IZT180	0.1	30.0	0.152	22.6	9.81	ATH	VTH	DTH	0.5% 1% 2% 3% 5% 7% 10% 15% 20%
KOCAELI/IZT090	0.1	30.0	0.22	29.8	17.12	ATH	VTH	DTH	0.5% 1% 2% 3% 5% 7% 10% 15% 20%

HP = High Pass and LP = Low Pass Filters
Spectra are available for 0.5 - 20% damping.
Source record processed by Pacific Engineering.

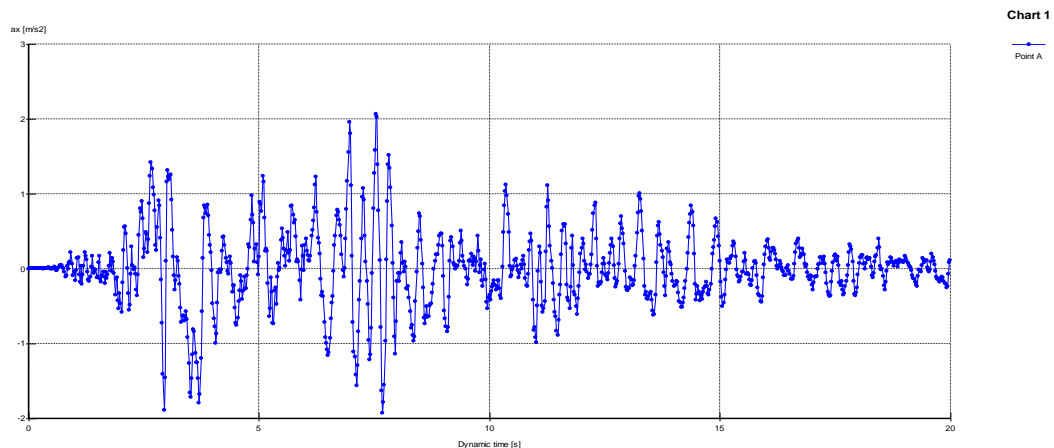


Figure 9.29: Acceleration data for Kocaeli Earthquake, 1999
(<http://peer.berkeley.edu/svbin/Detail?id=P1103>)

Fifteen noded, triangular, 2D plane-strain elements were used in the PLAXIS V8.2 computer program. Backfill width of models were selected 3 times of total height of the structures, bed rock and sea bed (20+12= 32).

The geometric model of Derince Port block type quay wall for PLAXIS V8.2 software program is prepared as shown in Figure 9.30. The surcharge load was defined as 3 t/m².

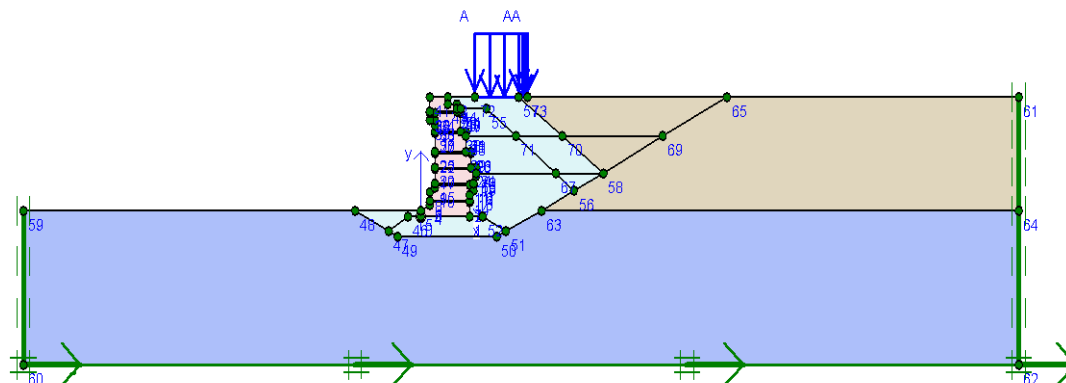


Figure 9.30: The geometric model of Derince Port block type quay wall

The properties and placements of the materials used in PLAXIS V8.2 are shown in Table 9.8 and Figure 9.31.

Table 9.8: Properties of the materials used in PLAXIS V8.2

Parameter	Layer 1 (backfill)	Layer 2 (Rock Fill)	Layer 3 (Dense Sand)
	Drained	Drained	Drained
γ_{unsat} (kN/m ³)	16	16	20
γ_{sat} (kN/m ³)	19	19	22
ϕ (internal friction angle, degree)	40	40	45
ν (poisson ratio, degree)	0.2	0.2	0.2
ψ (dilatancy angle, degree)	10	10	15
$E_{50\text{ref}}$ (kN/m ²)	100000	500000	1000000
E_{oedref} (kN/m ²)	45244.01	494148	957210.6
E_{urref} (kN/m ²)	300000	1500000	3000000

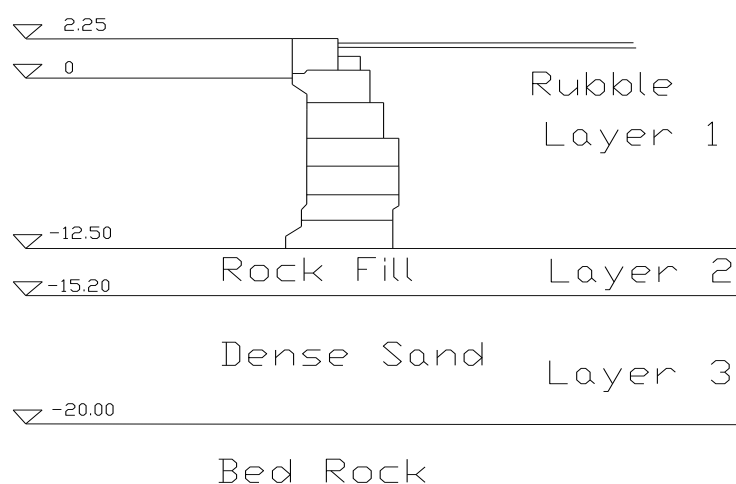


Figure 9.31: Crossection of the Derince Port, block type quay wall

Hardening soil model was chosen for under dynamic loading and a linear-elastic stress–strain behavior was assumed for the retaining walls using a high enough Young’s modulus to simulate a rigid block.

Interface finite elements were used to model soil–block interaction. R_{inter} was defined as 0.5–0.6 as obtained from the present experimental study.

Additionally, simulating friction between block–block, a very thin soil layer is defined as interface. The properties of interface and all other material properties are summarized in Table 9.2.

The initial conditions cover the initial values for *effective stress*, *tension* and *pore pressure*.

In calculation step, “plastic calculation” were used. In numerical model runs were carried out for 10 sec. Figure 9.32 shows the outputs of PLAXIS V8.2 computer program for Derince Port, block type quay wall.

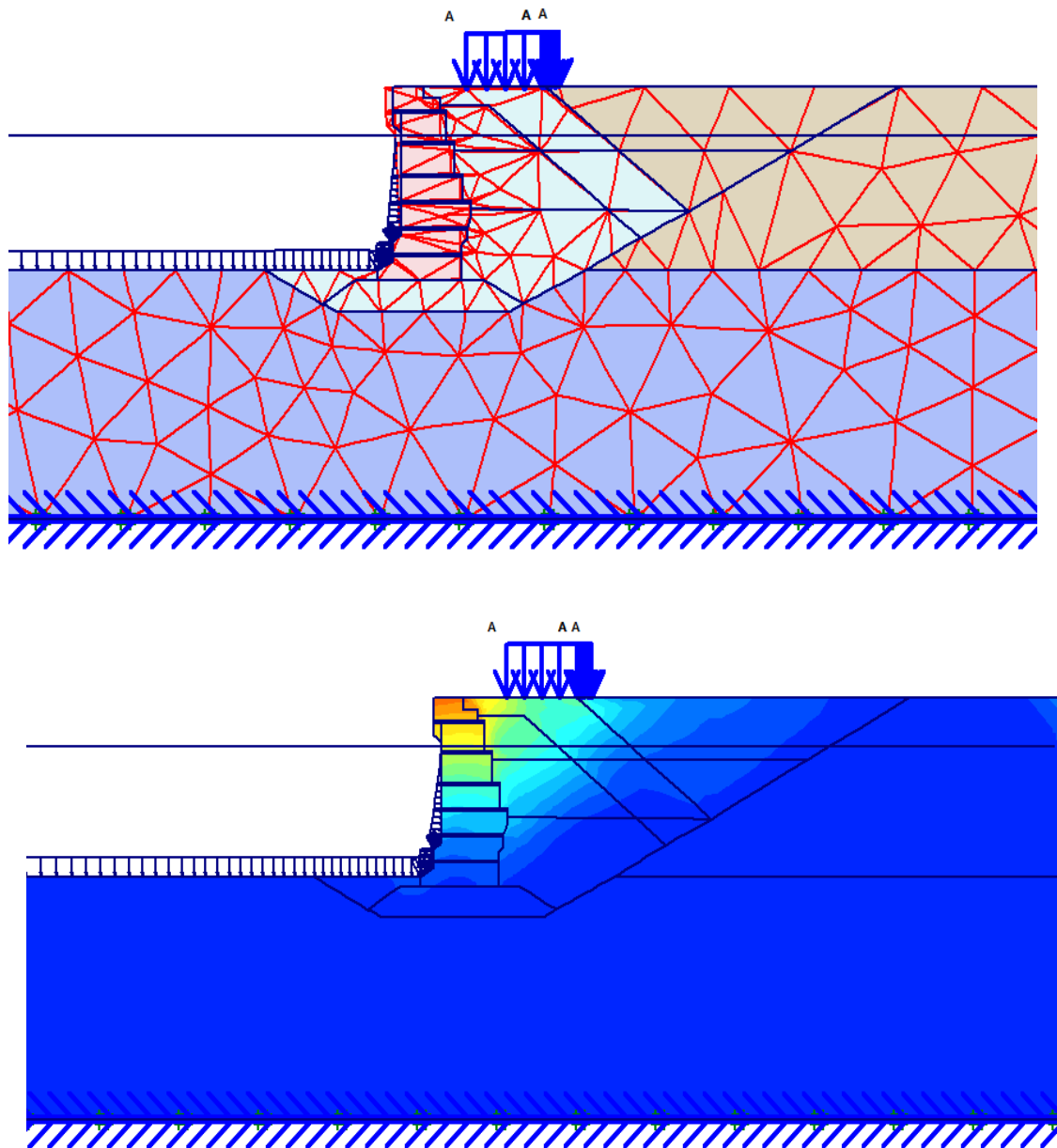


Figure 9.32: Outputs of PLAXIS V8.2 computer program for Derince Port, block type quay wall

9.3.2.1 Result of Derince Port, Block Type Quay Wall

The horizontal relative displacement results obtained by using PLAXIS V8.2 are shown in Figure 9.33.

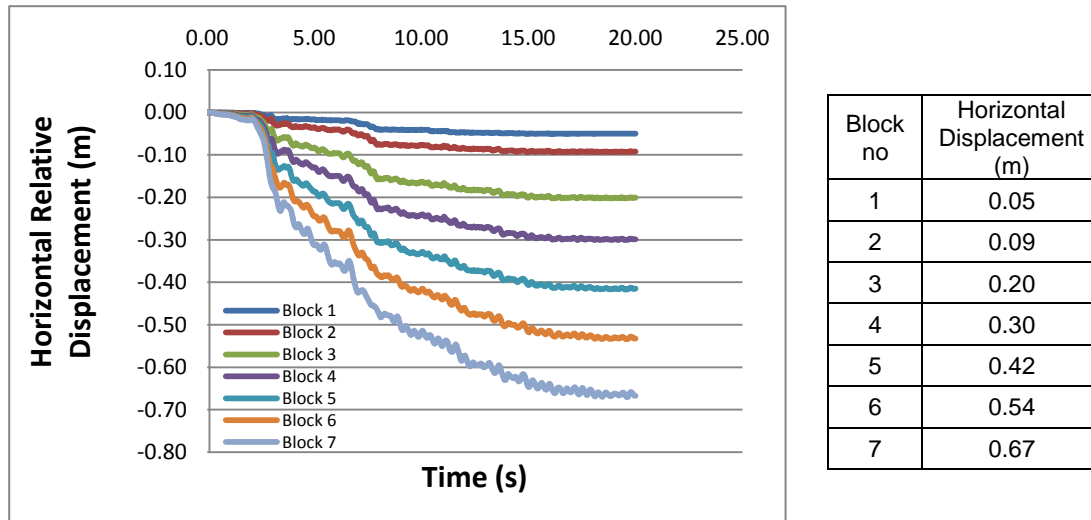


Figure 9.33: The horizontal displacement results

PIANC (2001), states that 0.7 m lateral displacement was occurred at Derince Port, block type quay wall. As it is seen from the Figure 9.33, the max. horizontal relative displacement occurred on block 7 (placed on top of the structure) is 0.67 m.

Compatibility of the results obtained from experimental and numerical model proves that the numerical model with the design parameters obtained from 1g shaking table tests could be successfully used for the multiple block type quay wall.

9.3.2.2 Discussions on Acceptable Level of Damage Derince Port, Block Type Quay Wall

In the design of quay walls, the normalized residual horizontal displacement defined as $(d/H)^*$ (where d is residual horizontal displacement at the top of the wall; h is height of gravity wall) and tilting degree values are controlled by using the “acceptable level of damage in performance-based design” and “proposed damage criteria” in given in PIANC (2001). The acceptable level of damage in performance based design was determined for Derince Port, block type quay walls by considering the horizontal displacement and tilting measurements (Table 4.8, PIANC, 2001).

- Horizontal Displacement

PIANC (2001), Yüksel et al., (2002), states that 0.7 m lateral displacement measured at Derince Port, block type quay wall as occurred after the earthquake. As it is seen from the Figure 9.33, the maximum horizontal relative displacement of block 7 (placed on top of the structure) was $d = 0.67$ m from the numerical computations.

The total height of the block type quay wall was $h = 14.75$ m (Figure 9.27) and the minimum and controlled damage levels were calculated as (PIANC, 2001):

$$d / h < 0.047 \quad (h = 14.75 \text{ m and } d = 0.70 \text{ m})$$

d : residual horizontal displacement (m), h : structure height (m)

As defined in PIANC (2001);

For Minimum Damage (MD); $d / h < 0.015$

For Controlled Damage (CD); $d / h < 0.05$

Acceptable level of damage on block type quay wall ($0.047 < 0.05$) was obtained as “controlled damaged”.

- Tilting

Tilting degree occurred on Derince Port, block type quay wall was calculated as $\alpha = 2.7^\circ$ ($\arctan(0.7/14.5)$).

As defined in PIANC (2001);

For Minimum Damage (MD); tilting degree $< 3^\circ$

For Controlled Damage (CD); tilting degree $< 3^\circ - 5^\circ$

According to calculated tilting result on Derince Port, block type quay wall, acceptable level of damage was obtained as “minimum damaged” yet can be considered very close to controlled damage.

Acceptable level damage of the structure is determined by considering the most critical condition. In Derince Port, block type quay wall, horizontal displacement is more critical than tilting, thus acceptable level of damage on block type quay wall was obtained as “controlled damaged”.

PIANC (2001) gives the damaged levels in terms of structural and operational level. According to these definition, Derince Port, block type quay wall damaged falls into “controlled damaged” as for structural level. In view of “operational damaged” the block type quay wall damage was short-term loss of serviceability. This result is also compatible with the site measurements. Because even if the Derince Port block type quay wall had been damaged due to earthquake, it was still in use for berthing and mooring purposes after the earthquake which is inconformity with the above given definitions.

This result is a good evidence of the reliability of the definitions of damaged levels given in PIANC (2001) to be used in performance based of approaches for seismic design of block type quay walls.

- Conventional Seismic Design of Derince Port, Block Type Quay Wall

“Conventional seismic design” based on providing a capacity of the structure to resist a design seismic force, but it does not provide any information on the performance of a structure when the limit of the force-balance is exceeded. Not to exceed the limit equilibrium (factors of sliding and overturning) in conventional seismic design for the relatively high intensity ground motions associated with a very rare seismic event, the construction cost will most likely be too high as discussed in the case study of Derince Port.

The factor of safety against sliding and overturning values for Derince Port, block type quay wall were calculated by using the conventional seismic design method given in “Technical Seismic Specifications on Construction of Coastal and Harbor Structures, Railways And Airports (2008)” (Karakuş, 2007).

Factor of safety against sliding and overturning values for the blocks were calculated equal to 1 or less than 1 (Karakuş, 2007) indicating in conventional terminology as failure of the structure. From these results do not reveal the damage of level of the structure. Horizontal displacement and uniform vertical settlement of block type quay wall may not significantly reduce the stability, and may be generally acceptable from a structural point of view. Site measurements of Derince Port, block type quay wall show that damage occurred on blocks, but, damage level did not cause critical results since Derince Port, block type quay wall is still serviceable.

In “conventional seismic design method”, factor of safety against sliding and overturning values for the blocks are recommended greater than 1 normally. In view of this practice, larger block sizes should have been used for Derince Port. However, in view of performance base design method the block sizes are satisfactory the fulfill the requirements for operational and structural damage definitions.

CHAPTER 10

RESULTS AND CONCLUSIONS

Block type quay walls are the simplest and the mostly used type of gravity quay walls resulting in economic solutions in most of the coastal engineering applications considering their practical construction possibilities. Parallel to trend in the world, in Turkey as well, block type quay walls are designed under dynamic loading by using conventional seismic design method in engineering applications.

In this study, the dynamic response of block type quay wall was investigated considering basically accelerations, pore pressures, soil pressures and displacements for one block, two blocks, three blocks for different frequencies for Soil 1 and Soil 2 experimentally to form the base for the “performance based design for block type quay walls under dynamic loads”. The experimental studies completed with numerical studies and case study were carried out for block type quay wall under dynamic loading. Site data of Derince Port, block type quay wall damaged during Eastern Marmara Earthquake, 1999 were used as input carried for case study.

Stages of the study are summarized below.

1st stage: Experimental Studies

At this stage, a series of 1g shaking table tests were carried out to investigate the acceleration, pore pressure, soil pressure and displacement measurements on a block type quay wall model constructed with 1/10 scale. In these tests one, two, three blocks were tested for Soil 1 and Soil 2 under dynamic loading for selected frequencies between 2 Hz to 6 Hz (Table 4.9) for 30 seconds.

In seismic design of block type quay wall, since the soil properties are very important, in practice, granular backfill material was used as recommended to avoid liquefaction effect. In this study, two type of soils were used as backfill, Soil 1 and Soil 2 with two different nominal diameter (D_{n50}) of Soil 1 ($D_{n50}=2.2$ cm) and Soil 2 ($D_{n50}=1.0$ cm) corresponding ($D_{n50} = 22$ cm and $D_{n50} = 10$ cm) in prototype, respectively as recommended in practical engineering applications.

2nd stage: Numerical Studies

At this stage, result of the total saturated soil pressures and displacements of 1 g shaking table tests were verified with the numerical studies. The acceleration and friction results of 1 g shaking table tests were used as input parameters for the numerical modelling (PLAXIS V8.2). Result of these studies are presented in Table 9.3 and Table 9.7.

3th stage: Case Study on Derince Port, Block Type Quay Wall

At this stage, a case study was carried out with the site data of the Eastern Marmara Earthquake, 1999 for Derince Port, block type quay wall by using the PLAXIS V8.2 software program. Result of the studies are presented Figure 9.33.

4th stage: Acceptable Level of Damage

At this stage, results of measurements for displacement were calculated and discussed in view of “acceptable level of damage in performance-based design” (PIANC, 2001). Result of this studies are presented in Table 7.10.

PIANC (2001) gives the damaged levels in terms of structural and operational level. According to these definition, Derince Port, block type quay wall damaged falls into "controlled damaged" as for structural level. In view of "operational damaged" the block type quay wall damage was "short-term loss of serviceability".

Conclusions obtained from 4 stages are summarized as given below.

10.1 Experimental Studies

Conclusions based on the experimental results of accelerations, pore pressures, soil pressures, displacements and friction coefficients are given below. In all the experiments increase in frequency means that number of cycles of dynamic loading increases which causes an increase in acceleration measurements.

10.1.1 Acceleration

Acceleration and frequency relations for Soil 1 (coarser material) and Soil 2 (finer backfill) for one block, two blocks and three blocks: The acceleration measurements of the block(s) were defined with the maximum absolute acceleration, $|a_{max}|$, measured during the experiment.

- As the frequency increases, $|a_{max}|$ increases for both Soil 1 and Soil 2 for all blocks.
- For frequencies less than 2, 3 Hz, the maximum $|a_{max}|$ remains almost constant for all block(s) and base.
- For frequencies between 4 Hz – 6 Hz, the maximum $|a_{max}|$ is recorded on the top blocks having minimum values at the base.
- After 20 sec. test duration corresponds to approximately 60 sec in prototype, as the frequency increases behavior of the Soil 2 changed totally compared to Soil 1. Soil 2 slumped down towards the structure causing higher and irregular acceleration measurement on the block(s) compared to Soil 1.
- For frequencies (2 Hz, 3 Hz, 4 Hz, 5 Hz), $|a_{max}|$ of block(s)' for Soil 1 are in general slightly greater than $|a_{max}|$ of block(s)' accelerations for Soil 2.
- For 6 Hz, $|a_{max}|$ of block(s)' for Soil 2 are almost twice as much than for Soil 1 except for base where $|a_{max}|$ is almost the same.

In conclusion;

- Accelerations of the block(s) depend on the placement of the blocks ordered from the top to the base (foundation) where the acceleration of the blocks above is larger than the acceleration of the block(s) below. Hence, minimum acceleration is recorded at the base.
- Using Soil 1 (coarser) or Soil 2 (finer) backfill material does not cause significant different in the behavior of the material during seismic loading between 2 Hz - 5 Hz. However, for larger frequency (6 Hz) this difference becomes significant resulting higher accelerations for Soil 2.

10.1.2 Pore Pressure

According to experimental and numerical results show no significant effect of excess pore pressure on block(s) for Soil 1 and Soil 2. Thus, in this study the effect of excess pore pressure is neglected.

10.1.3 Saturated Soil Pressures

- Total saturated soil pressure increases towards the base both for Soil 1 and Soil 2.
- Application point of the fluctuating components of total saturated soil pressure is obtained between 0.40 H – 0.63 H for Soil 1 (coarser) and 0.375H and 0.65 H (H is the structure height) for Soil 2 (finer). This result has a practical importance in the seismic design of block type quay walls.

The choice of the backfill material in case of smaller peak ground acceleration ($< 0.4 \text{ g Hz}$) depends of the cost optimization of the material however in case of regions where the seismic loading is critical then the choice of the coarser backfill material (Soil 1) is recommended.

These findings on distribution of the fluctuating component of the total saturated soil pressure together with the point of application will be the input to performance based methodology which is the ultimate aim of this study.

10.1.4 Displacements

- Horizontal displacement measurements increase while frequency is increasing for Soil 1 and Soil 2.
- The horizontal displacement measurements of the block(s), located at the top, are always greater for the horizontal displacement measurements of the block(s) located at the bottom.

In general, calculated tilting degree and vertical displacement measurements increase while frequency is increasing both for Soil 1 and Soil 2.

In conclusion, after 20 sec. which corresponds to approximately 60 sec in prototype, Soil 2 slumped down towards the structure causing higher horizontal displacement measurements on the block(s) contrary to Soil 1 behavior. Thus, the horizontal, vertical displacement measurements and calculated tilting degree for Soil 2 is greater than the horizontal, vertical displacement measurements and calculated tilting degree for Soil 1 for especially for 5 Hz and 6 Hz.

10.1.5 Friction Coefficient Results

- The static friction coefficient between block-block is smaller than the static friction coefficient between block-foundation.
- Static friction coefficients were computed with inclined surface as 0.55 for rubble-block and 0.47 for block-block close to recommended values given in Technical Seismic Specifications on Construction of Coastal and Harbor Structures, Railways And Airports (2008) and OCDI (2009) (Table 8.11 and Table 8.12).
- Increase in the block number (bottom to the top) causes the decrease in the friction coefficient.
- Increment in the block number (bottom to the upper side) causes the decrement in the friction coefficient. Due to the decrement of the friction coefficient cause increment of the net force acting of the block placed upper side and this simply because the horizontal displacement measurements of the block(s), located at the top, are always greater for the horizontal displacement measurements of the block(s) located at the bottom (Table 8.11).
- A steady decrease from the static condition to dynamic condition in friction angle cause block acceleration increment.

10.2 Numerical Analysis

PLAXIS V8.2 computer program that uses the finite-element method (FEM) was used for horizontal dynamic loading of only one input for frequency of 5 Hz for Soil 1 for one, two, three block(s) cases and 4 Hz for three block(s).

Comparisons of model results obtained for total saturated soil pressure and displacements the of the block(s) show that experimental conditions are simulated succesfully with the numerical study (Table 9.7).

10.3 Case Study

PLAXIS V8.2 software program was used with site data of the block type quay wall of Derince Port, Eastern Marmara Earthquake, 1999, as inputs (Yüksel et al., 2002 and PIANC, 2001). Horizontal displacement result was obtained as 0.67 m for the top of the block which is in very close agreement with the site measurements given in references (0.70 m).

10.4 Acceptable Level of Damage

The experimental results of level damage of this study is compared with the level damage table given PIANC (2001), it is seen that minimum and controlled level damage of Soil 2 is critical than Soil 1 in terms of given damage criteria.

The acceptable level of damage in performance based design (Table 4.6) (PIANC, 2001) is also determined for Derince Port, block type quay walls. According to calculated result, if the horizontal displacement of the block (placed at top of the structure) is $d=70$ cm classified as controlled damage (CD) for the block type quay wall.

This result is compatible with site measurements. Although, Derince Port, block type quay wall had been damaged during the earthquake it was still serviceable after the earthquake which fulfills the definition of "acceptable level of damage" given in PIANC (2001) (Table 4.6). Conformity of the limit of performance (level of damage) (PIANC, 2001) by the above given results is the indication of the reliability of the limit of damage level definitions for the coastal engineers to be used with confidence.

This result is a good evidence of the reliability of the definitions of damaged levels given in PIANC (2001) to be used in performance based of approaches for seismic design of block type quay walls.

Design parameters obtained in this study by experimentally and numerically will be useful tools for the coastal engineers in the performance based design of block type quay wall under dynamic loads.

10.5 Future Studies

The complex nature of the problem studied was rather challenging at the intersection of coastal engineering, geotechnical engineering left the below given recommendations as future studies.

It is certain that, the most significant parameter is backfill properties. In this study, two different backfill materials (Soil 1, $D_{n50} = 2.2$ cm and Soil 2 $D_{n50} = 1.0$ cm) were used to define the saturated soil pressure distribution parallel to practical applications. However, to define the effect of the backfill properties on design parameters, diameter of the backfill can be selected finer than Soil 2 and coarser than Soil 1. In general, the nominal diameter of the backfill can be selected as $7\text{cm} < D_{n50} < 34$ cm in future studies.

In this study only rectangular block(s) are used by placing them on top of each other with with aligned centroids. Since the placement pattern and shape which might be effective in the stability of the structure. Thus, more comprehensive studies should include tests with different block(s) dimensions, shapes and different placement patterns of blocks.

The quay wall must be able to bear safely the loads of cranes, vehicles and stored goods. Thus, for further studies the effect of the these loads can be investigated under dynamic loading.

The quay walls exposed to waves and tsunami can be another study area where by including the wave forces most critical design conditions can be investigated.

Another study can be to focus on the use of 1 g shaking table tests based on irregular (unsteady random time history) acceleration data to study the dynamic response of block type quay wall.

The analytical solutions based on performance based design for seismic design of block type quay walls can be developed by using the both experimental and numerical results presented in this study.

Finally, studies with successive dynamic loading on the block type quay wall have to be carried out to have the time history of the damage of the structure.

REFERENCES

- Alyami, M., Rouainia, M., Wilkinson, S.M., (2009). "Numerical Analysis of Deformation Behavior of Quay walls under Earthquake Loading." *Soil Dynamics and Earthquake Engineering* 29 (2009) 525–536.
- Anastasopoulos, I., Georgarakos, T., Georgiannou, V., Drosos, V., Kourkoulis, R., (2010). "Seismic Performance of Bar-Mat Reinforced-Soil Retaining wall: Shaking Table Testing Versus Numerical Analysis With Modified Kinematic Hardening Constitutive Model." *Soil Dynamics and Earthquake Engineering*, 30 (2010) 1089–1105.
- Arablouei, A., Gharabaghi, A.R.M., Abedi, K., Ghalandarzeh, A., (2006). "The Dynamic Response of Gravity Type Quay Wall during Earthquake Including Soil-Sea-Structure Interaction." *7th International Congress on Civil Engineering*.
- Arablouei, A., Ghalandarzadeh, A., and Gharabaghi, A.R.M., (2008). "A Numerical Study of Liquefaction Induced Deformation on Caisson-Type Quay Wall Using a Partially Coupled Solution." *ASME 2008, 27th International Conference on Offshore Mechanics and Arctic Engineering Ocean, Offshore and Arctic Engineering Division Volume 4: Ocean Engineering; Offshore Renewable Energy* ISBN: 978-0-7918-4821-0 pp. 589-597.
- Ashford, S.A., Sitar, N., (2002). "Simplified Method for Evaluating Seismic Stability of Steep Slopes." *Journal of Geotechnical and Geoenvironmental Engineering*, 119–128.
- Ausilio, E., Conte, E., Dente, G., (2000). "Seismic Stability Analysis of Reinforced Slopes." *Soil Dynamics and Earthquake Engineering*, 2000, 19:159–72.
- Bhasin, R., Kaynia, A.M., (2004). "Static and Dynamic Simulation of a 700-m High Rock Slope in Western Norway." *Engineering Geology*, 71, 213–226.
- Center for Civil Engineering Research and Codes (CUR), (2005). "Quay Wall Hand Book." 717 Pages, published by CUR, PO Box 420, 2800 AK, Gouda, The Netherland, ISBN 0 415 364396.
- Chen. B.F., (1995). "The Significance of Earthquake-Induced Dynamic Forces in Coastal Structures Design." *Department of Marine Environment*, National Sun Yat-Sen University, *Ocean Engng*, Vol. 22, No. 4, pp. 301-315, 1995.
- Choudhury, D., Ahmad S.M., (2007). "Design of Waterfront Retaining Wall for the Passive Case under Earthquake and Tsunami." *Applied Ocean Research*, 29 (2007) 37–44.
- Choudhury, D., Nimbalkar, S., (2007). "Seismic Rotational Displacement of Gravity Walls by Pseudo-Dynamic Method: Passive Case." *Soil Dynamics and Earthquake Engineering*, 27 (2007) 242–249.
- Corigliano, M., (2007). "Seismic Response of Deep Tunnels in Near-fault Conditions" (Research Doctorate in Geotechnical Engineering)
- Dewoolkar, M.M., Ko H.Y., Pak R.Y.S., (2000), "Experimental Developments for Studying Static and Seismic Behavior of Retaining Walls With Liquefiable Backfills", *Soil Dynamics and Earthquake Engineering*, 19 (2000) 583-593.
- Engineering and Design - Geotechnical Investigations, EM 1110-1-1804, (2001).

- Ertugrul, O., (2006). "A Finite Element Modeling Study on the Seismic Response of Cantilever Retaining Walls." (The Degree of Master of Science).
- Gazetas, G., Psarropoulos, P.N., Anastasopoulos, I., Gerolymos, N., (2004). "Seismic Behavior of Flexible Retaining Systems Subjected to Short-Duration Moderately Strong Excitation." *Soil Dynamics and Earthquake Engineering*, 24 (2004) 537–550.
- Ghosh, S., (2010). "Pseudo-Dynamic Active Force and Pressure behind Battered Retaining Wall Supporting Inclined Backfill Soil." *Dynamics and Earthquake Engineering* 30(2010)1226–1232.
- Girsang, C.H., (2001). "A Numerical Investigation of the Seismic Response of the Aggregate Pier Foundation System." *Master of Science Thesis in Civil Engineering*, December 20, 2001.
- Green R.A., Olgun C.G., Ebeling R.M., Cameron W. I., (2003). "Seismically Induced Lateral Earth Pressures on a Cantilever Retaining Wall", *Proceedings of the Sixth US Conference and Workshop on Lifeline Earthquake Engineering* (TCLEE 2003), ASCE.
- Hazarika, H., Kohama, E., and Sugano, T. (2008). "Underwater Shake Table Tests on Waterfront Structures Protected with Tire Chips Cushion." *J. Geotech. Geoenviron. Eng.*, 134(12), 1706–1719.
- Hsieh, Y.M., Lee, K.C., Jeng, F.S., Huang, T.H., (2010). "Can Tilt Tests Provide Correct Insight Regarding Frictional Behavior of Sliding Rock Block Under Seismic Excitation?." *Engineering Geology*.
- Iai, S., Ichii K., (1998). "Performance Based Design for Port Structures." *U.S. Department of Commerce*, Editors: Raufaste N.J.
- Ichii, K., (2004). "Application of Risk Density Analysis for Seismic Design: A Gravity-Type Quay Wall Case." *Proceedings of the 4th International Conference on Computer Simulation in Risk Analysis and Hazard Mitigation*, Rhodes, Greece; 2004. p. 41–50.
- International Navigation Association (PIANC) (2001). "Seismic Design Guidelines for Port Structures." *Technical Commentary 7, Analysis Methods*, Balkema, Tokyo.
- Itasca Consulting Group, Inc. (2000). "FLAC (Fast Lagrangian Analysis of Continua)." *User's Manuals*, Minneapolis, MN, USA (2000).
- Kagawa, T., (1978). "On the Similitude in Model Vibration Tests of Earth-Structures." *Proceeding of Japan Society of Civil Engineering*, No.275, pp.69-77, 1978 (in Japanese).
- Karakuş, H., (2007). "New Seismic Design Approaches for Block Type Quay Walls." *M.S., Department of Civil Engineering*, p:173.
- Kastranta, G., (2000). "Seismic Effective-Stress Deformation Analysis of Waterfront Retaining Structures." *Master of Science*, Rice University, Texas.
- Kim S.R., Kwon O.S., Kim M.M., (2004). "Evaluation of Force Components Acting on Gravity Type Quay Walls During Earthquakes." *Soil Dynamics and Earthquake Engineering* 24 (2004) 853–866.
- Kim S.R., Jang I.S., Chung C.K., Kim M.M., (2005). "Evaluation of Seismic Displacements of Quay Walls." *Soil Dynamics and Earthquake Engineering* 25 (2005) 451–459.

- Kim, S.R., Kwon, O.S., Kim, M.M., (2004). "Evaluation of Force Components Acting on Gravity Type Quay Walls During Earthquakes." *Soil Dynamics and Earthquake Engineering* 24 (2004) 853–866
- Kokusho, T., and Iwatate, T., (1979). "Scaled Model Tests and Numerical Analysis on Nonlinear Dynamic Response of Soft Grounds.", *Proceeding of Japan Society of Civil Engineers*, No.285, pp.57-67, 1979 (in Japanese).
- Kramer, S.L., (1996). "Geotechnical Earthquake Engineering." Upper Saddle River, NJ: Prentice-Hall Inc.; 1996. pp. 653.
- Leung, C.F., Shen, R.F., (2008). "Performance of Gravity Caisson on Sand Compaction Piles." *Canadian Geotechnical Journal*, 45, no.3 (2008): 393 – 407.
- Leynoud, D., Mienert, J., Nadim, F., (2004). "Slope Stability Assessment of the Hellandd Hansen Area Offshore the Mid-Norwegian Margin." *International Journal of Marine Geology, Geochemistry and Geophysics*, September, 2004.
- Li, X., Wu, Y., He, S., (2010). "Seismic Stability Analysis of Gravity Retaining Walls." *Soil Dynamics and Earthquake Engineering*, 30(2010) 875–878.
- Lysmer, J., Ostadan, F. and Chen, C.C. (1999). "SASSI2000- A system for Analysis of Soil-Structure Interaction." *University of California, Department of Civil Engineering*, Berkeley, California, USA (1999).
- Ma, G.W., An, X.M., Wang, M.Y., (2009). "Analytical Study of Dynamic Friction Mechanism in Blocky Rock Systems." *International Journal of Rock Mechanics & Mining Sciences* 46 (2009) 946–951.
- Maleki, S., and Mahjoubi, S., (2010). "A New Approach for Estimating the Seismic Soil Pressure on Retaining Walls." *Transaction A: Civil Engineering* Vol. 17, No. 4, pp. 273, 284, Sharif University of Technology, August 2010.
- Matsuo, M., Kenmochi, S., Yagi, H., (1978). "Experimental Study on Earth Pressure of Retaining Wall by Field Tests." *Soils Found*, 18(3): 27–41.
- Me´ndez, B.C., Romo, M.P., (2005). "Transition from the Static to the Kinetic Coefficient of Friction". *Proceedings of the 11th International Conference of the International Association of Computer Methods and Advances in Geomechanics*, Turin, Italy, 2005, paper 234.
- Me´ndez, B.C., Romo, M.P., (2006). "Experiments on Frictional Behavior of a Sliding Block". *Serie Investigacio´n y Desarrollo del Instituto de Ingenierı´a, UNAM, Me´xico*, DF 2006; p. 39, ISBN 970-32-3251-5, ISSN 970-32-0196-2 (SID/647).
- Me´ndez, B.C., Botero, E., Romo, M.P., (2009). "A New Friction Law for Sliding Rigid Blocks Under Cyclic Loading." *Soil Dynamics and Earthquake Engineering*, 29 (2009) 874–882.
- Mohajeri, M., Ichii, K., and Tamura, T., (2004). "Experimental Study on Sliding Block Concept for Caisson Walls." *Journal of Waterway, Port, Coastal and Ocean Engineering*, ASCE / MAY/JUNE 2004.
- Moghadam, A.M., Ghalandarzadeh, A., Towhata, I., Moradi, M., Ebrahimian, B., Hajjalikhani, P., (2009). "Studying the Effects of Deformable Panels on Seismic Displacement of Gravity Quay walls." *Ocean Engineering*, 36 (2009) 1129–1148

- Moss, R. E. S., Kayen, R. E., Tong, L.Y., Liu, S.Y., Cai, G.J., and Wu, J.,(2011). "Retesting of Liquefaction and Nonliquefaction Case." *Journal of Geotechnical and Geoenvironmental Engineering*, ASCE, April 2011
- Motta E., (1993), "Generalized Coulomb Active Earth Pressure for Distanced Surcharge." *Journal of Geotechnical Engineering*, Vol.120, No.6, June, 1994, ISSN 0733-9410/94/0006-1072, technical note No. 5597.
- Mylonakis, G., Kloukinas P., Papantonopoulos C., (2007). "An alternative to the Mononobe Okabe Equations for Seismic Earth Pressures." *Soil Dynamics and Earthquake Engineering*, 27 (2007) 957–969.
- Na, U.J., Chaudhuri, S.R., Shinozuka, M.,(2008). "Probabilistic Assessment for Seismic Performance of Port Structures." *Soil Dynamics and Earthquake Engineering*, 28 (2008) 147–158.
- Naboulsi, S., Nicholas, T., (2003). "Limitations of the Coulomb Friction Assumption in Fretting Fatigue Analysis." *Int. J. Solids Struct.* 2003,40 (23):6497–512.
- National Research Council (U.S.), (1968). "The Great Alaska Earthquake of 1964." *Committee on the Alaska Earthquake*, Volume 1, Part 1, National Academies, 1968 p. 285.
- Nazarian, H.N. and A.H. Hadjian, (1979). "Earthquake-Induced Lateral Soil Pressures on Structures." *ASCE Journal of Geotechnical Engineering*, Vol. 105, No. GT9, pp. 1049-1066, September, 1979.
- Nergiz, C., (2009). "Development of a Stability Analysis Program for Block Type Quay Walls and Comparison of Block Placing Methods." Msc Thesis, Middle East Technical University.
- Newmark, N.M., (1965). "Effects of Earthquake on Dams and Embankments." *Geotechnique*, 1965; 15:139–60.
- Okabe, S., (1926). "General Theory of Earth Pressure." *J. Jpn. Soc. Civ. Eng.*, 12(1) (in Japanese)
- Psarropoulosa, P.N., Klonarisb, G., Gazetasa, G., (2005). "Seismic Earth Pressures on Rigid and Flexible Retaining Walls." *Soil Dynamics and Earthquake Engineering*, 25 (2005) 795–809.
- Rabinowicz, E., (1951). "The Nature of Static and Kinetic Coefficients of Friction". *J.Appl.Phys*, 1951, 22(11):1373–9.
- Richards, R., Elms, D.G., (1979). "Seismic Behavior of Gravity Retaining Walls." *Journal of the Geotechnical Engineering Division*, 1979, 105(GT4):449–64
- Sadrekarami, A., Ghalandarzadeh, A., Sadrekarami, J., (2008). "Static and Dynamic Behavior of Hunchbacked Gravity Quay Walls." *Soil Dynamics and Earthquake Engineering*, 28 (2008) 99–117.
- Sawicki, A., Chybicki, W., Kulczykowski, M., (2007). "Influence of Vertical Ground Motion on Seismic-Induced Displacements of Gravity Structures." *Computers and Geotechnics*, 34 (2007) 485–497.
- Schnabel, P.B., Lysmer, J. and Seed, H.B., (1972). "SHAKEA, Computer Program for Earthquake Response Analysis of Horizontally Layered Sites." *Earthquake Engineering Research Center*, University of California, Berkeley, California, USA.

- Sherif, M.A., Fang, Y.S., (1984). "Dynamic Earth Pressures on Rigid Walls Rotating about the Base." *Proceedings of the 8th World Conference on Earthquake Engineering*, Vol. 6. San Francisco, 993–1000.
- Sumer, B.M., Kaya, Ai, Hansen, N.E.O., (2002). "Impact of Liquefaction on Coastal Structures in the 1999 Kocaeli, Turkey Earthquake." *Proceedings of The Twelfth (2002) International Offshore and Polar Engineering Conference*, ISBN 1-880653-58-3 (Set); ISSN 1098-6189 (Set)
- The Overseas Coastal Area Development Institute of Japan (OCDI), (2002). "Technical Standards and Commentaries for Port and Harbor Facilities in Japan." Editors for Translation Version: Goda, Y., Tabata, T., Yamamoto, S., printed by Daikousha Printing Co., Ltd.
- Tiznado, F., Roa R., (2011). "Seismic Lateral Movement Prediction for Gravity Retaining Walls on Granular Soils." *Soil Dynamics and Earthquake Engineering*, 31(2011)391–400.
- Torisu, S.S., Sato, J., Towhata, I., Honda, T., (2010). "1-G Model Tests and Hollow Cylindrical Torsional Shear Experiments on Seismic Residual Displacements of Fill Dams From the View Point of Seismic Performance-Based Design" *Soil Dynamics and Earthquake Engineering*, 30 (2010) 423–437.
- Towhata, I., Ghalandarzadeh, A., Sundarraj, K.P., Vargas-Monge, W, (1996). "Dynamic Failures of Subsoils Observed in Waterfront Areas". *Soils Found* , 1: 149–60.
- Trandafir, A.C., Kamai, T., Sidle R.C., (2009). "Earthquake-induced Displacements of Gravity Retaining Walls and Anchor-Reinforced Slopes." *Soil Dynamics and Earthquake Engineering* 29 (2009) 428–437.
- Villalobosi, F., (2011). "Crustal Deformation Associated With The 1960 Earthquake Events in the South of Chile." *5th International Conference on Earthquake Geotechnical Engineering*, January 2011, 10-13, Santiago, Chile.
- Whitman, R. V., and Liao, S. (1985). (Jan). "Seismic Design of Gravity Retaining Walls." *Miscellaneous Paper GL-85-1, U.S. Army Engineer Waterways Experiment Station*, Vicksburg, MS.
- Wood, D.M., (2004). "Geotechnical Modelling".
- Zeng, X., (1998). "Seismic Response of Gravity Quay Walls, I: Centrifuge Modeling", *Journal of Geotechnical and Geoenvironmental Engineering*.
- Yang, Z., Elgamal, A., Abdoun, T., Lee, C.J., (2001). "A Numerical Study of Lateral Spreading Behind a Caisson Type Quay Wall." *Proceedings: 4th International Conference on Recent Advances in Geotechnical Earthquake Engineering and Soil Dynamics and Symposium in Honor of Prof. W.D. Liam Finn*, San Diego, California, March 26-31, 2001.
- Yüksel, Y., Alpar B., Yalçiner A.C., Çevik E., Özgüven O., Çelikoğlu Y., (2002), "Effects of the Eastern Marmara Earthquake on Marine Structures and Coastal Areas." *Proceedings of The Institution of Civil Engineers, Water & Maritime Engineers* 156, June 2002, Issue WM2, pages 147-1
- http://www.jsceint.org/Report/report/kocaeli/kocaeli_chap6.pdf (last visited on January, 2003)
- <http://www.stanford.edu/~tyzhu/Documents/Some%20Useful%20Numbers.pdf> (last visited on January, 2003)

APPENDIX A

ADVANTAGES AND DISADVANTAGES

Advantages and disadvantages of 1 g shaking table tests and some possible solutions preventing the negative effects are summarized in Table A1 and Table A2.

Table A1 : Advantages of shaking table tests

Advantage of Shaking Table Tests

well controlled large amplitude motions,

their use is justified if the purpose of the test is to validate the numerical model or to understand the basic failure mechanisms,

easier experimental measurements,

soil can be placed, compacted and instrumented relatively easily,

valuable insight into liquefaction, post-earthquake settlement, foundation response and lateral earth pressure problems.

Table A2 : Disadvantages of shaking table tests and possible solutions

Disadvantage of Shaking Table Tests and Possible Solutions

Problem : “reduced effective stress results in reduced shear strength

Solution: This is not a major problem because the load is reduced as well and the impact on overall slope stability is insignificant,

Problem : dilatancy of sand and development of excess pore water pressure

Solution: Under reduced stress level, dilatancy changes from negative (contractive) to positive (expansion) and, in water- saturated sand, the excess pore water pressure is reduced, making sand unrealistically resistant against seismic loading. This problem is solved by compacting sand in the model looser than in the corresponding real-life structure” (Torisu et al., 2010).

Problem : “It is difficult to simulate the stress–strain behavior of granular soil over a wide range of strain and different confining stress levels. The behavior of soil is highly nonlinear and confining stress dependent, and the soil volume may probably change due to the pure shearing, known as dilatancy” (Verdugo,1992). “Dilatancy is important when the soil is saturated and it is subjected to the rapid and repeating shear deformations” (Moghadam et al., 2009).

Solution: According to Towhatam (1995), “the density of sand should be reduced in the model scale in order to create a similar type of stress–strain behavior in the lower confining stress level”. “The value of reduced density is calculated by the formula proposed by Ghalandarzadeh (1997)” (Moghadam et al., 2009).

Problem: The boundary effects formed by the physical modeling might affect the responses of the whole model” (Moghadam et al., 2009).

Solution : According to Dewoolkar et al.,(2000), “If the ratio of backfill length to the wall height is high enough (over 2), then the boundary has no significant effect on the wall structure response”.

Problem: “Dissipation of excess pore pressure is faster in the model comparing with that of prototype when the pore fluid and soil particles in model and prototype are the same” (Yoshimi and Tokimatsu (1977)).

Solution : According to Ghalandarzadeh (1997), “Regarding the fast dissipation problem, occurring in excess pore pressure, the input shaking is recommended to be applied in a longer duration time”.

higher gravitational stresses cannot be produced

“With scaling down the size of prototype, the dynamic loading frequency increases” (Moghadam et al., 2009).

APPENDIX B

SCALING

“A similitude is derived for the shaking table tests on saturated soil structure fluid model in 1 g gravitational field. The main tool used for deriving the similitude is the basic equations which govern the equilibrium and the mass balance of soil skeleton, pore water, pile and sheet pile and sheet pile structures, and external waters such as sea. In addition to the basic equations, an assumption is made upon the constitutive law of soil; i.e. the stress strain relation is determined irrespective of the confining pressures if appropriate scaling factors are introduced for the stress and the strain for taking the effect of the confining pressures into account” (Iai, 1989).

Table B.1: Scale factors (Wood, 2004)

quantity	general	1g (laboratory)
length	n_ℓ	$1/n$
mass density	n_ρ	1
acceleration	n_g	1
stiffness	n_G	$1/n^\alpha$
stress	$n_\rho n_g n_\ell$	$1/n$
force	$n_\rho n_g n_\ell^3$	$1/n^3$
force/unit length	$n_\rho n_g n_\ell^2$	$1/n^2$
strain	$n_\rho n_g n_\ell / n_G$	$1/n^{1-\alpha}$
displacement	$n_\rho n_g n_\ell^2 / n_G$	$1/n^{2-\alpha}$
pore fluid viscosity	n_μ	1 or* $n^{1-\alpha/2}$
pore fluid density	$n_{\rho f}$	1
permeability (Darcy's Law)	$n_{\rho f} n_g / n_\mu$	1 or* $1/n^{1-\alpha/2}$
hydraulic gradient	$n_\rho / n_{\rho f}$	1
time (diffusion)	$n_\mu n_\ell^2 / n_G$	$1/n^{2-\alpha}$ or* $1/n^{1-\alpha/2}$
time (creep)	1	1
time (dynamic)	$n_\ell (n_\rho / n_G)^{1/2}$	$1/n^{1-\alpha/2}$
velocity	$n_g n_\ell (n_\rho / n_G)^{1/2}$	$1/n^{1-\alpha/2}$
frequency	$(n_G / n_\rho)^{1/2} / n_\ell$	$n^{1-\alpha/2}$
shear wave velocity	$(n_G / n_\rho)^{1/2}$	$1/n^{\alpha/2}$

*scaling of pore fluid viscosity introduced in order force identity of scale factors for diffusion time and dynamic time

“If strains are identical in model and prototype then the displacements will scale with the linear scale of the model n_ℓ ”

If we are concerned about concepts such as stresses and strains then we are assuming that the soil is behaving as a continuous material so that such concepts have some clear meaning and relevance. If the geotechnical system under study leads to relative movement on interfaces either between separate blocks of soil forming part of a failure mechanism, or between the soil and a structural element such as a pile or section of reinforcement then the

interface behavior will be controlled by relative displacement across the interface and a small model may have difficulty in correctly reproducing the system response” (Wood, 2004). Thus, in this study similitude for model tests in 1g gravitational field in the special case in which $\lambda_p = 1$ if ($\alpha = 0.5$), $\lambda_e = \lambda^{0.5}$. Since the scale is 1/10, λ is taken as 10.

“Experimental experience suggests that the exponent α might be of the order of 0.5 for sands but of the order of 1 for clays. Evidently a value $\alpha = 0$ implies that the stiffness is independent of stress level” (Wood, 2004).

The corresponding scaling of parameters between the prototype and model used in this experiment are derived as follows for length, time, displacement, force:

1. Length

$$\frac{L_p}{L_m} = \lambda$$

where; L: length, λ : the linear scale ratio between the prototype and model

2. Time

$$\frac{T_p}{T_m} = \frac{L_p / V_{sp}}{L_m / V_{sm}} = \frac{L_p}{L_m} \frac{V_{sm}}{V_{sp}} = \lambda \lambda^{-1/2} = \lambda^{1/2}$$

where; T: time, L: length

3. Displacement

$$\frac{\varepsilon_p}{\varepsilon_m} = \frac{\Delta u_p / u_p}{\Delta u_m / u_m} = \lambda^{0.5}$$

$$\frac{\varepsilon_p}{\varepsilon_m} = \frac{\Delta u_p}{\Delta u_m} \frac{u_m}{u_p} \Rightarrow \lambda^{0.5} = \frac{\Delta u_p}{\Delta u_m} \frac{1}{\lambda} \Rightarrow \frac{\Delta u_p}{\Delta u_m} = \lambda^{1.5}$$

4. Force

$$\frac{F_p}{F_m} = \frac{m_p a_p}{m_m a_m} = \frac{\rho_p V_p^3}{\rho_m V_m^3} = \frac{\lambda^3}{1} = \lambda^3$$

where;

F: force

m: mass

a: acceleration

ρ : density

V: volume

λ : the linear scale ratio between the prototype and model

APPENDIX C

RELATIVE DENSITY

Relative density and percent compaction are commonly used for evaluating the state of compactness of a given soil mass and relative density is calculated as:

- ρ_{dmin}

$$W_{cap} = 4235 \text{ g}, W_{total} = 13830 \text{ g}$$

$$W_{soil} = 13830 - 2 * 4235 = 5360 \text{ g} = 5.36 \text{ kg}$$

$$V = \frac{\pi \times 0.16}{4} \times 0.19 = 0.0038 \text{ m}^3$$

$$\rho_{dmin} = \frac{5.36}{0.0038} = 1410 \text{ kg/m}^3 = 1.41 \text{ t/m}^3$$

- ρ_{dmax}

$$W_{cap} = 4235 \text{ g}, W_{total} = 14950 \text{ g}$$

$$W_{soil} = 14950 - 2 * 4235 = 6480 \text{ g} = 6.48 \text{ kg}$$

$$V = \frac{\pi \times 0.16}{4} \times 0.19 = 0.0038 \text{ m}^3$$

$$\rho = \frac{6.48}{0.0038} = 1705 \text{ kg/m}^3 = 1.7 \text{ t/m}^3$$

- ρ

$$W_{cap} = 4235 \text{ g}, W_{total} = 14550 \text{ g}$$

$$W_{soil} = 14550 - 2 * 4235 = 6080 \text{ g} = 6.08 \text{ kg}$$

$$V = \frac{\pi \times 0.16}{4} \times 0.19 = 0.0038 \text{ m}^3$$


$$\rho = \frac{6.08}{0.0038} = 1600 \text{ kg/m}^3$$

Relative Density:

$$D_r = \frac{1/\rho_{min} - 1/\rho}{1/\rho_{min} - 1/\rho_{max}} = \frac{1/1.41 - 1/1.60}{1/1.41 - 1/1.71} = 0.68$$

Table D.2 : The technical specifications of position transducers


All external anodized aluminum parts of transducer were replaced with stainless steel and corrosion resistant plastic (Table D.3).

MEASUREMENT RANGE DESIGNATOR	STANDARD MEASUREMENT RANGES (in) (mm)	APPLICABLE SERIES			WIRE ROPE TENSION (NOMINAL) (oz) (N)	WIRE ROPE DIAMETER (in) (mm)		WEIGHT (lb) (Kg)		Product Photo
		HX-PA HX-PB HX-P420 HX-P510 HX-P1010	HX-EP	HX-V HX-VP						
2	2 50	✓	-	✓	34 9.4	.016	0.4	2 0.9		
3	3 75	✓	-	✓	24 6.7	.016	0.4	2 0.9		
4	4 100	✓	-	✓	24 6.7	.016	0.4	2 0.9		
5	5 125	✓	-	✓	19 5.3	.016	0.4	2 0.9		
6	6 150	✓	-	✓	24 6.7	.016	0.4	2 0.9		
10	10 250	✓	✓	✓	34 9.4	.016	0.4	2 0.9		
15	15 390	✓	✓	✓	24 6.7	.016	0.4	2 0.9		
20	20 500	✓	-	✓	24 6.7	.016	0.4	2 0.9		
25	25 640	✓	✓	✓	19 5.3	.016	0.4	2 0.9		
30	30 750	✓	-	✓	24 6.7	.016	0.4	2 0.9		
40	40 1000	✓	-	✓	24 6.7	.016	0.4	2 0.9		
50	50 1250	✓	✓	✓	19 5.3	.016	0.4	2 0.9		
60	60 1500	✓	✓	✓	24 6.7	.016	0.4	2 0.9		
80	80 2.0m	✓	✓	✓	21 5.8	.016	0.4	2 0.9		

Model Number 626B13	INDUSTRIAL ICP® ACCELEROMETER		Revision A ECN #: 27012
Performance Sensitivity (±5%) 1000 mV/g 102 mV/(m/s²) [2] Measurement Range ±5 g ±49.1 m/s² Frequency Range (±5%) 30 to 120000 cpm 0.5 to 2000 Hz [3] Frequency Range (±10%) 22 to 240000 cpm 0.37 to 4000 Hz Frequency Range (±3 dB) 12 to 380000 cpm 0.2 to 8000 Hz Resonant Frequency 720 kcpm 12 kHz Broadband Resolution (1 to 10000 Hz) 11 µg 107.9 µm/s² [1] Non-Linearity ±1% ±1% [4] Transverse Sensitivity ≤7% ≤7%		Optional Versions (Optional versions have identical specifications and accessories as listed for standard model except where noted below. More than one option may be used.) LB - Low Bias Voltage M - Metric Mount TO - Temperature Output Notes [1] Typical. [2] Conversion Factor 1g = 9.81 m/s². [3] The high frequency tolerance is accurate within ±10% of the specified frequency. [4] Zero-based, least-squares, straight line method. [5] 1/4-28 has no equivalent in S.I. units. [6] Twisted shielded pair. [7] See PCB Declaration of Conformance PS023 for details.	
Environmental Overload Limit (Shock) 2500 g pk 24525 m/s² pk Temperature Range -86 to +250 °F -54 to +121 °C Temperature Response See Graph See Graph [1] Enclosure Rating IP68 IP68			

DRUCK-PDCR81 type pore pressure cells were used to obtain pore pressure distributions. The technical specifications of selected accelerometer is given in Table D.5 (DRUCK- PDCR 81).

Table D.5 : Technical Specifications of pore pressures

Technical Specifications		
Dynamic Range	0-100 kPa	 PDCR 81
Sensitivity	0.020 mV/V/mba	
Accuracy	%0.2	
Temperature	-20 °C - +120 °C	

5. Software and Hardware System

In this study a software and hardware system were also used. The technical specification is given in Table D.6.

Table D.6: Technical specification of Spartan software and hardware program

Technical Specification of Spartan Software and Hardware Program TESTBOX 2010
2 all the instruments were connected to each other by SPARTAN software and hardware system Gb memory card
16 digital entrance channels
TESTLAB – DYNAMIC
200 Hz Sampling

APPENDIX E

MATHCAD SOFTWARE PROGRAM

MathCAD software program was used to obtain fluctuating and non fluctuating component of total soil pressure. Program details are given below.

data :=

	0	1
0	51.04	1.04
1	51.14	1.07
2	51.24	1.11
3	51.34	1.06
4	51.44	0.92
5	51.54	1.01
6	51.64	1.23
7	51.74	1.12
8	51.84	0.92
9	51.94	1.14

DATA := csort(data,0)

X := DATA $\langle 0 \rangle$

Y := DATA $\langle 1 \rangle$

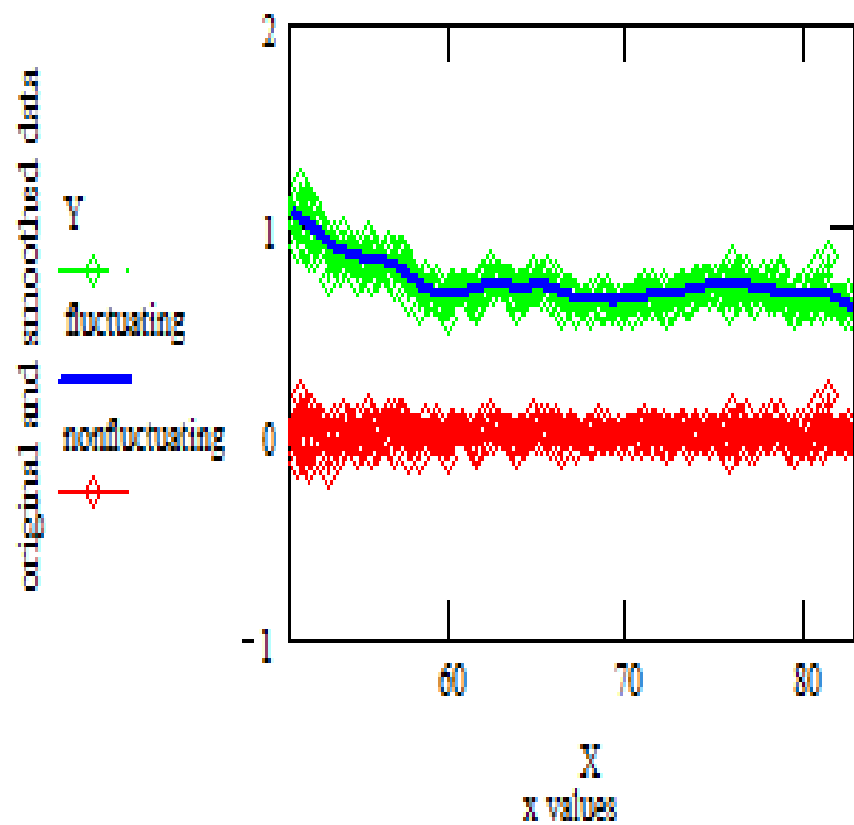
fluctuating := supsmooth(X,Y)

nonfluctuating := Y – fluctuating

		0			0
	0	1.084		0	-0.039
	1	1.077		1	-9.951·10 ⁻³
	2	1.071		2	0.042
	3	1.064		3	-7.919·10 ⁻³
	4	1.057		4	-0.137
	5	1.051		5	-0.04
	6	1.044		6	0.183
fluctuating =	7	1.037	nonfluctuating =	7	0.087
	8	1.031		8	-0.111
	9	1.024		9	0.112
	10	1.016		10	0.085
	11	1.008		11	-0.157
	12	1		12	0.112
	13	0.993		13	-0.118
	14	0.985		14	-0.042
	15	0.978		15	0.044

sonuc ⁽⁰⁾ := X sonuc ⁽¹⁾ := Y
 sonuc ⁽²⁾ := fluctuating sonuc ⁽³⁾ := nonfluctuating

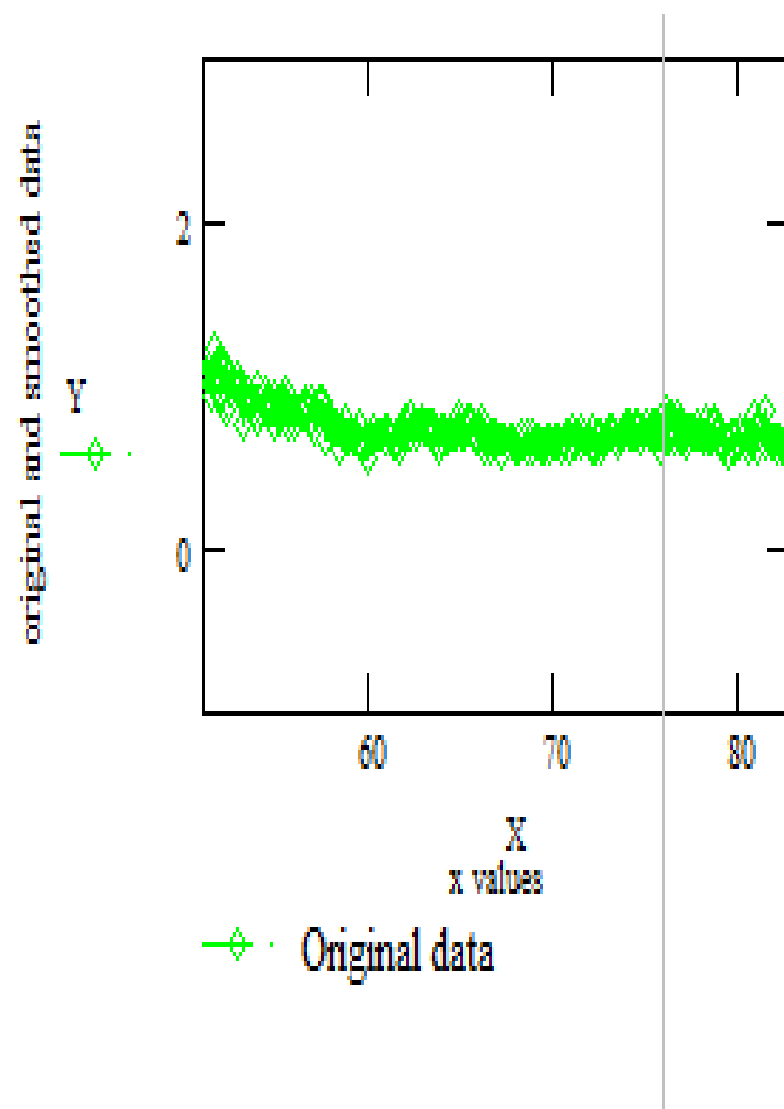
		0	1	2	3
	0	51.042	1.045	1.084	-0.039
	1	51.142	1.067	1.077	-9.951·10 ⁻³
	2	51.242	1.113	1.071	0.042
	3	51.342	1.056	1.064	-7.919·10 ⁻³
	4	51.442	0.92	1.057	-0.137
	5	51.542	1.011	1.051	-0.04
	6	51.642	1.226	1.044	0.183
sonuc =	7	51.742	1.124	1.037	0.087
	8	51.842	0.92	1.031	-0.111
	9	51.942	1.136	1.024	0.112
	10	52.042	1.102	1.016	0.085
	11	52.142	0.852	1.008	-0.157
	12	52.242	1.113	1	0.112
	13	52.342	0.874	0.993	-0.118
	14	52.442	0.943	0.985	-0.042
	15	52.542	1.022	0.978	0.044

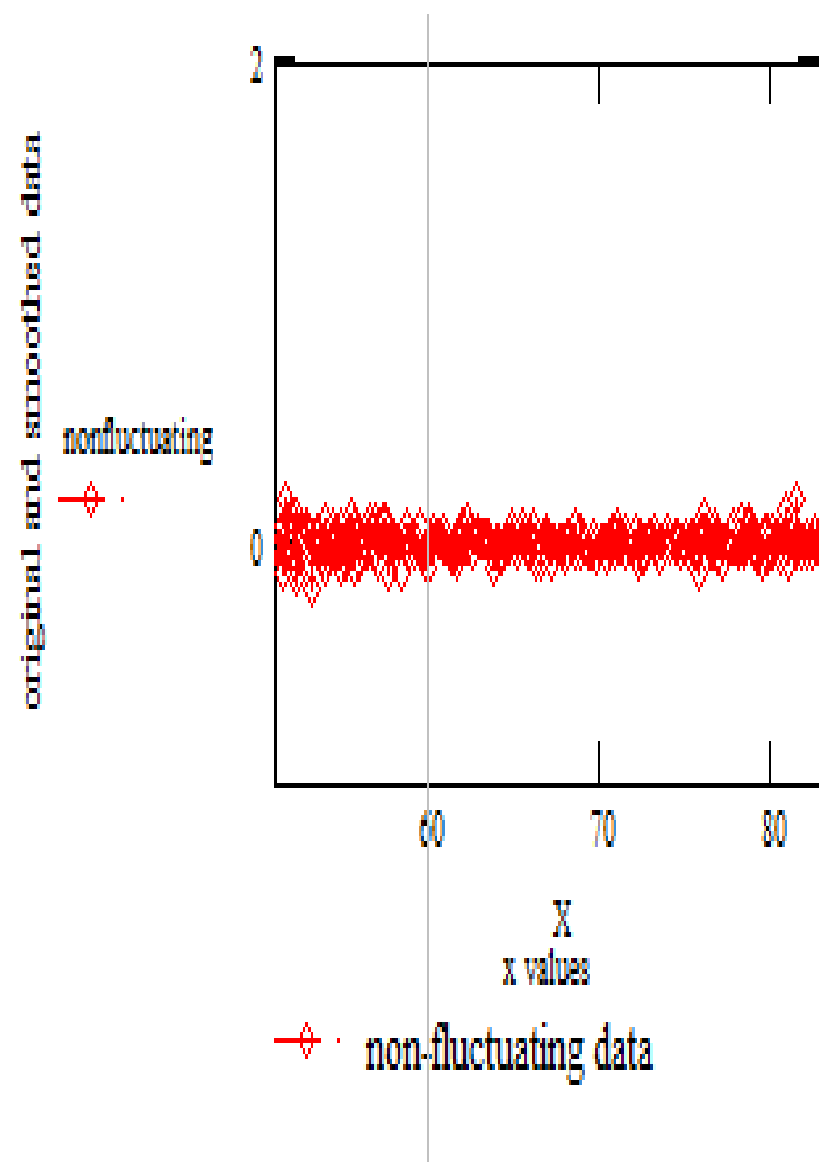
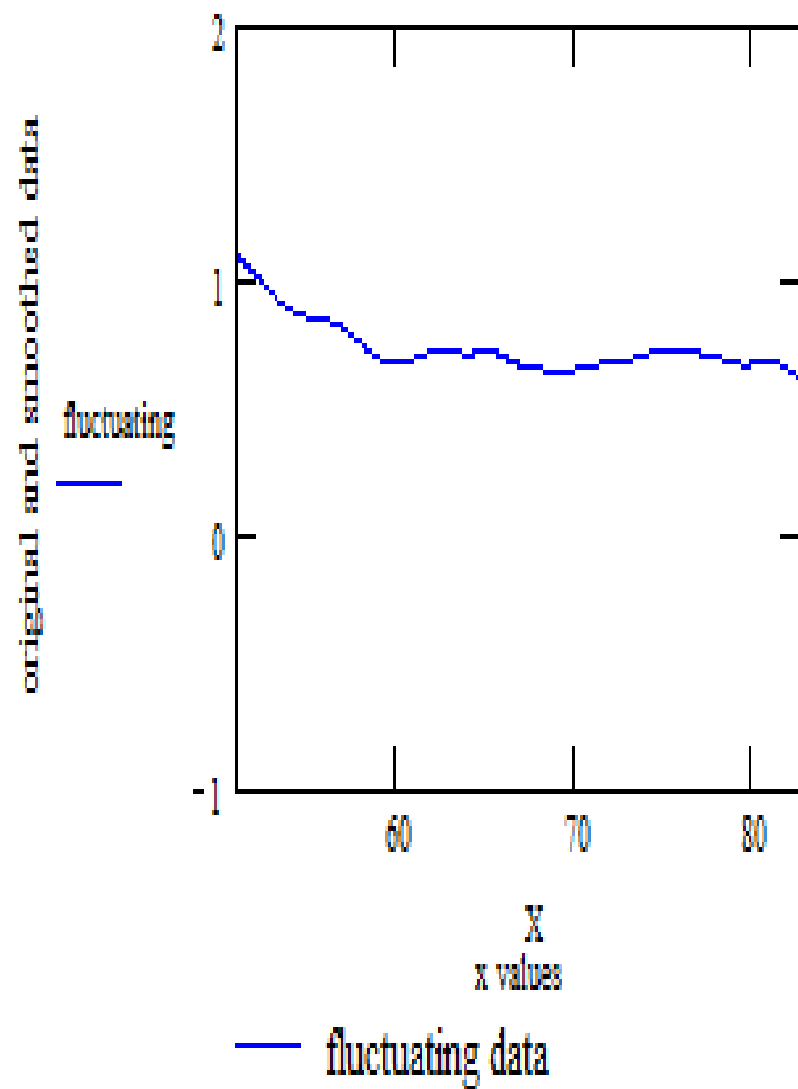


Original data

fluctuating data

non-fluctuating data





APPENDIX F

ACCELERATION RESULTS

Acceleration measurements for two blocks and three blocks for Soil 1 and Soil 2 are presented in this chapter.

1. TWO BLOCKS

Test 2.1 was carried out with 2 Hz, 3 Hz, 4 Hz, 5 Hz, 6 Hz for Soil 1 and Test 2.2 was carried out and 4 Hz, 5 Hz, 6 Hz for Soil 2.

SOIL 1

Results of acceleration measurements for two blocks for Soil 1 (Test 2.1) under dynamic loading are presented in Figure F1 – Figure F5.

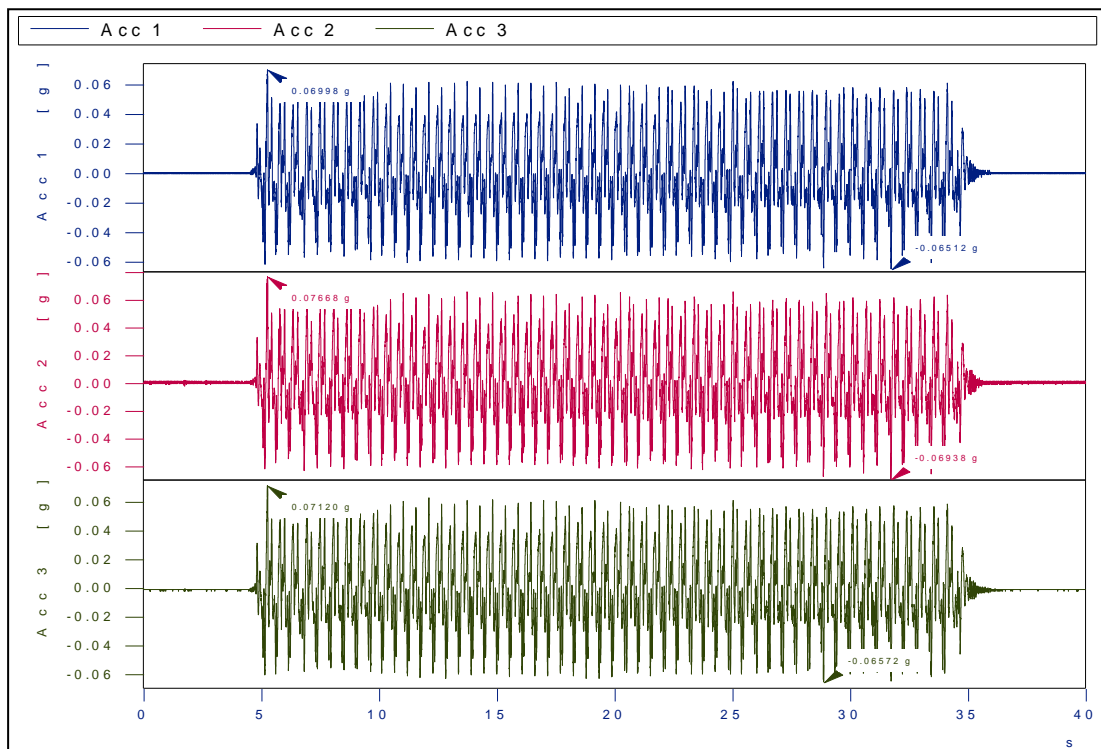


Figure F1 : Acceleration values of Base (Acc 1), Block 1 (Acc 3) and Block 2 (Acc 2) for 2 Hz (Test 2.1.1)

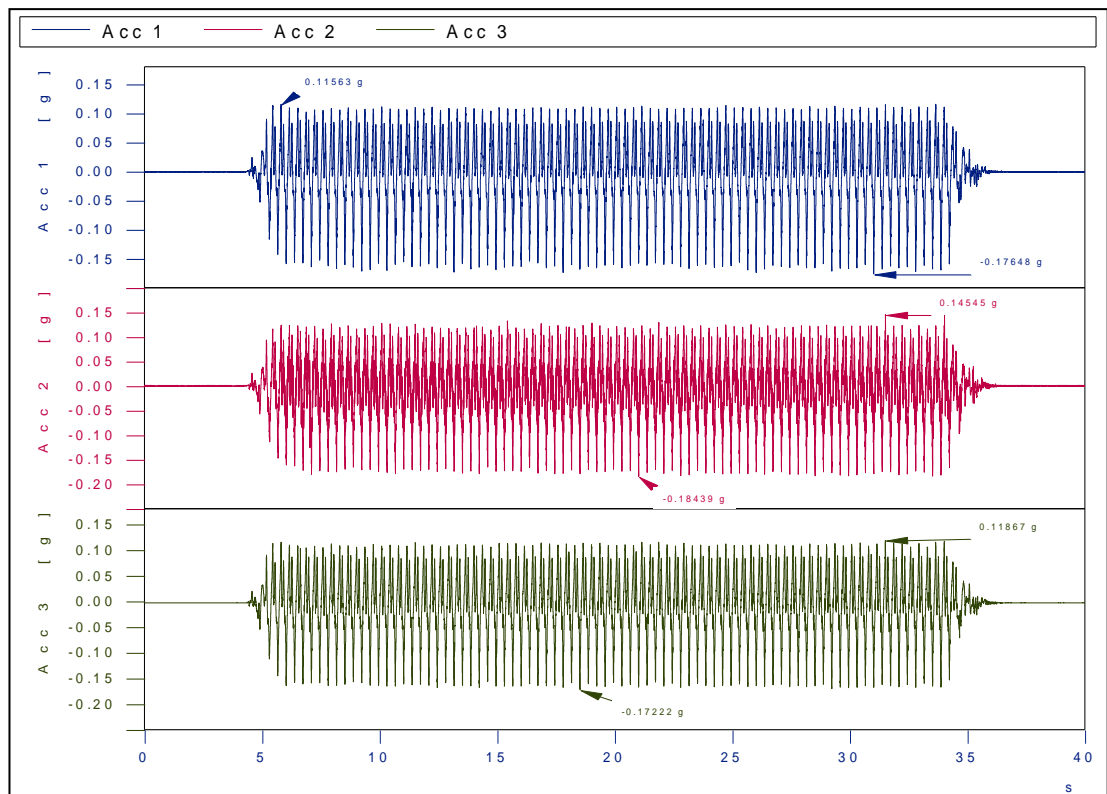


Figure F2 : Acceleration values of Base (Acc 1), Block 1 (Acc 3) and Block 2 (Acc 2) for 3 Hz (Test 2.1.2)

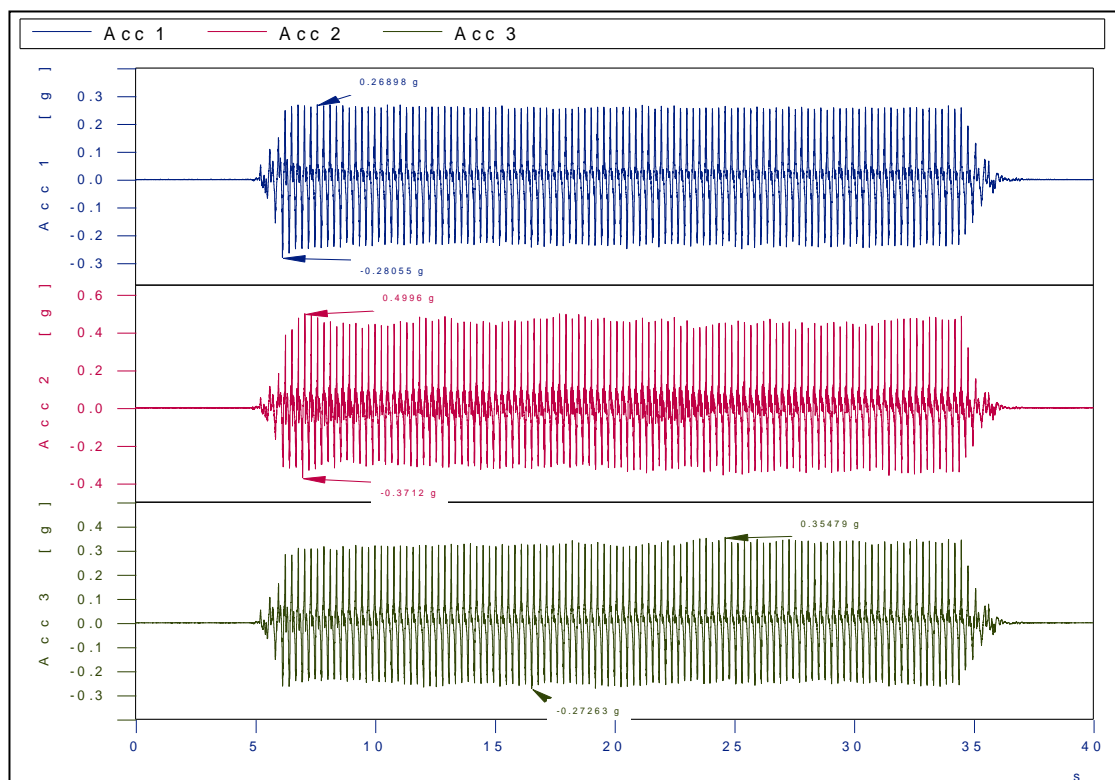


Figure F3 : Acceleration values of Base (Acc 1), Block 1 (Acc 3) and Block 2 (Acc 2) for 4 Hz (Test 2.1.3)

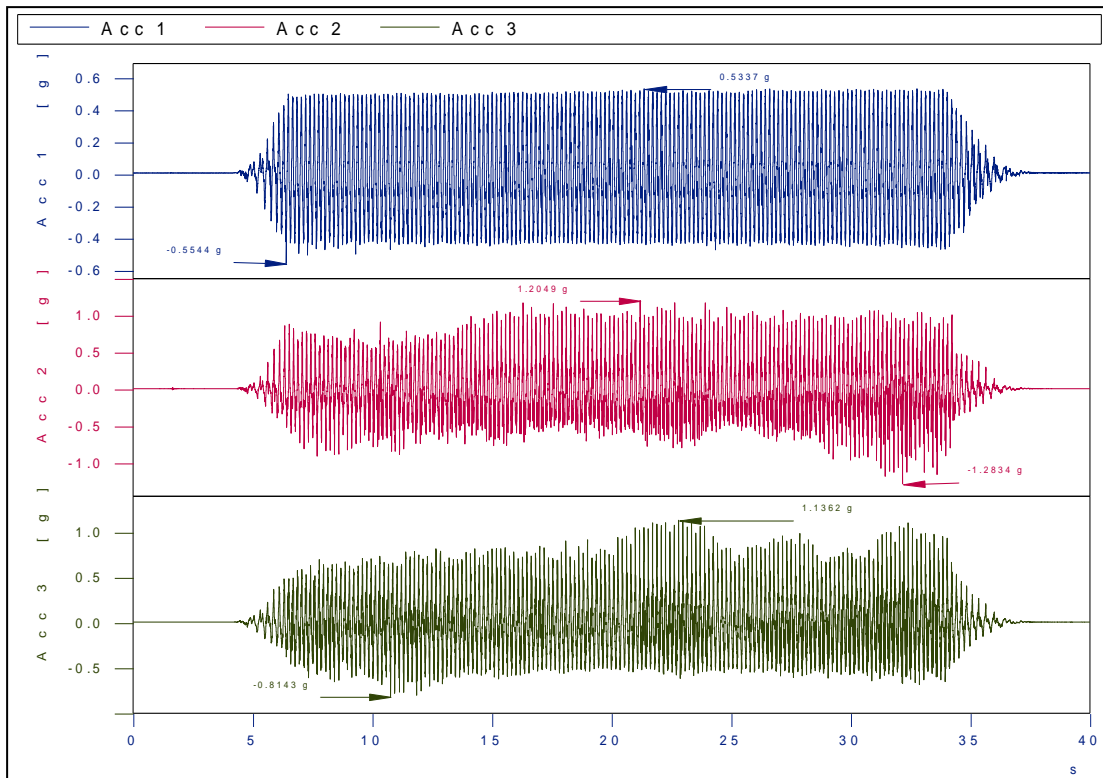


Figure F4 : Acceleration values of Base (Acc 1), Block 1 (Acc 3) and Block 2 (Acc 2) for 5 Hz (Test 2.1.4)

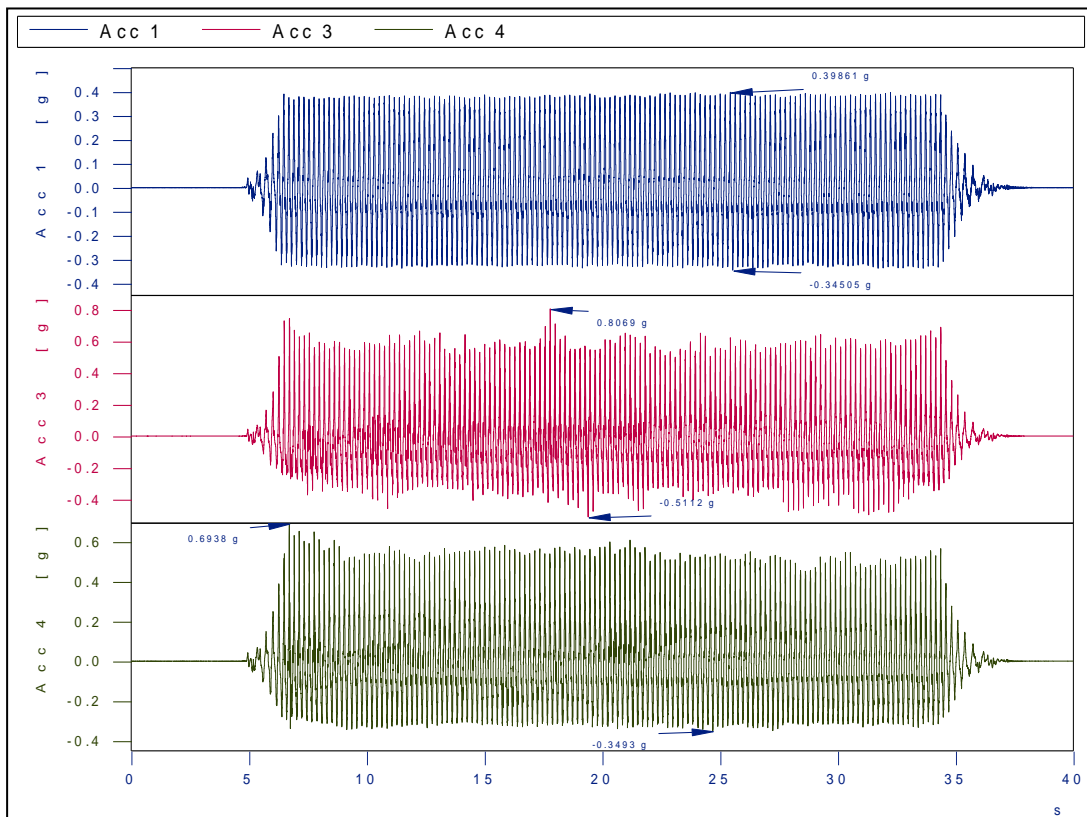


Figure F5 : Acceleration values of Base (Acc 1), Block 1 (Acc 3) and Block 2 (Acc 2) for 6 Hz (Test 2.1.5)

SOIL 2

Results of acceleration measurements for two blocks for Soil 2 (Test 2.2) under dynamic loading are presented in Figure F6 – Figure F8.

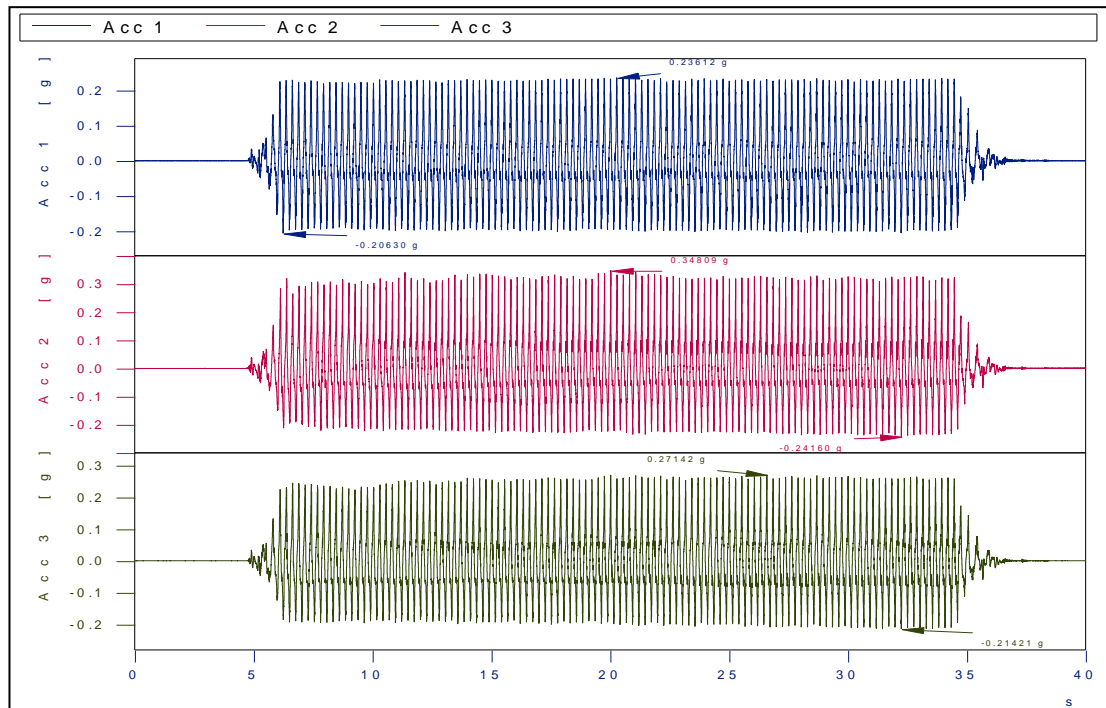


Figure F6 : Acceleration values of Base (Acc 1), Block 1 (Acc 3) and Block 2 (Acc 2) for 4 Hz (Test 2.2.1)

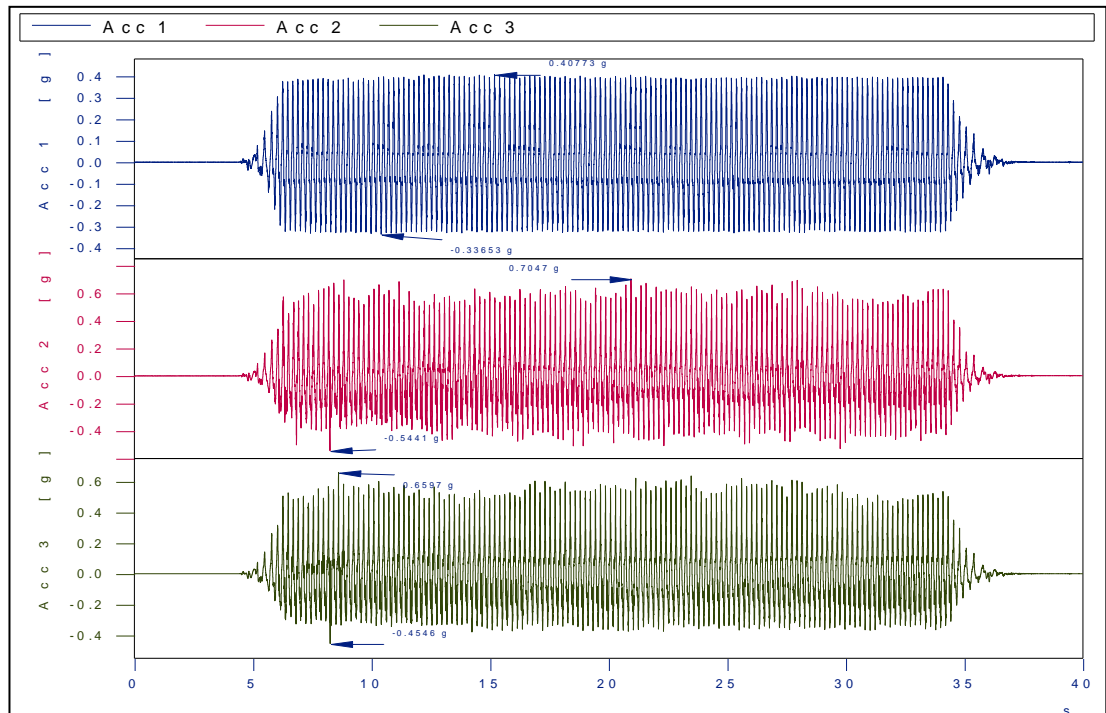


Figure F7 : Acceleration values of Base (Acc 1), Block 1 (Acc 3) and Block 2 (Acc 2) for 5 Hz (Test 2.2.2)

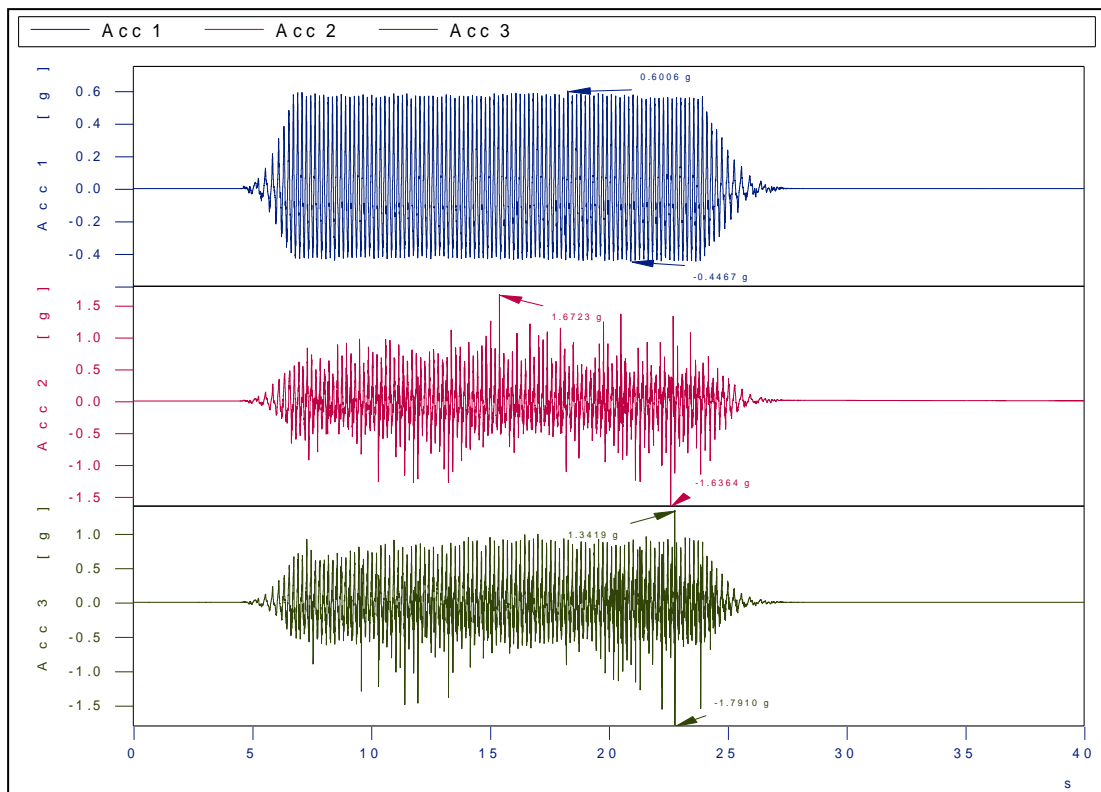


Figure F8 : Acceleration values of Base (Acc 1), Block 1 (Acc 3) and Block 2 (Acc 2) for 6 Hz (Test 2.2.3)

2. THREE BLOCKS

Test 3.1 was carried out with 3 Hz, 4 Hz, 5 Hz, 6 Hz for Soil 1 and Test 3.2 was carried out and 3 Hz, 4 Hz, 5 Hz for Soil 2.

SOIL 1

Results of acceleration measurements for three blocks for Soil 1 (Test 3.1) under dynamic loading are presented in Figure F9 – Figure F12.

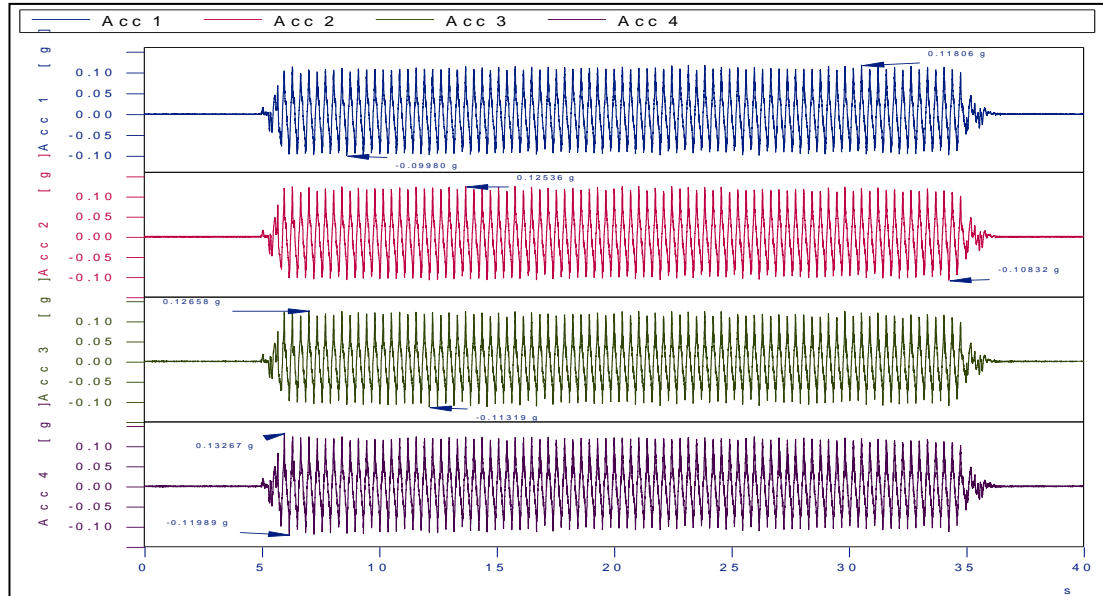


Figure F9: Acceleration values of base (Acc 1), block 1 (Acc 2) and block 2 (Acc 3) and block 3 (Acc 4) for 3 Hz (Test 3.1.1)

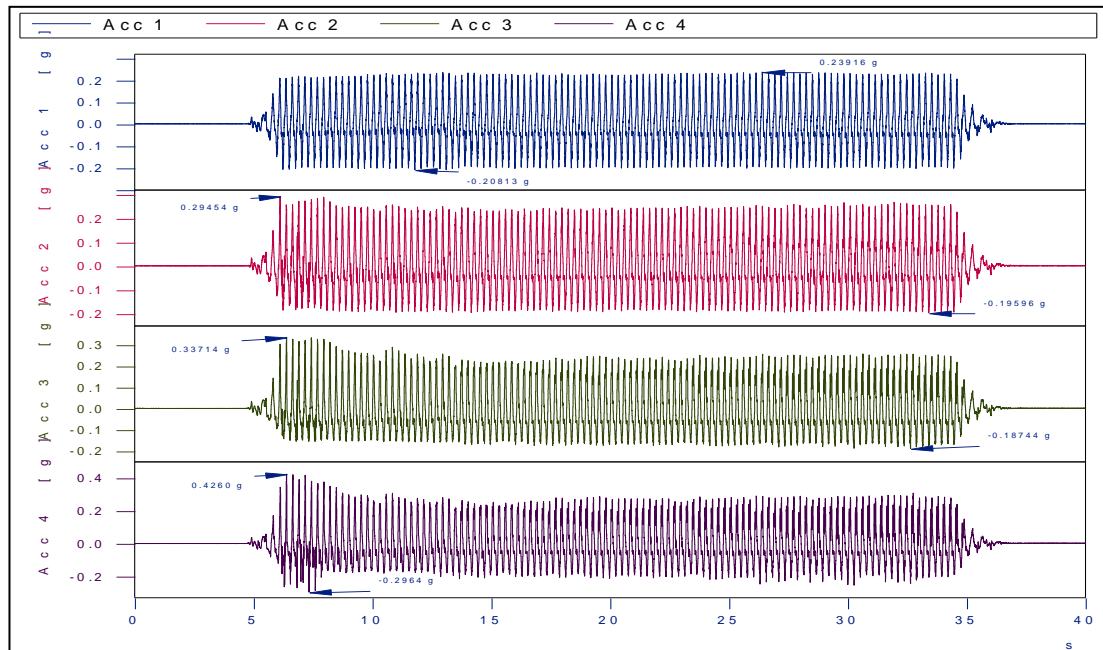


Figure F10: Acceleration values of base (Acc 1), block 1 (Acc 2) and block 2 (Acc 3) and block 3 (Acc 4) for 4 Hz (Test 3.1.2)

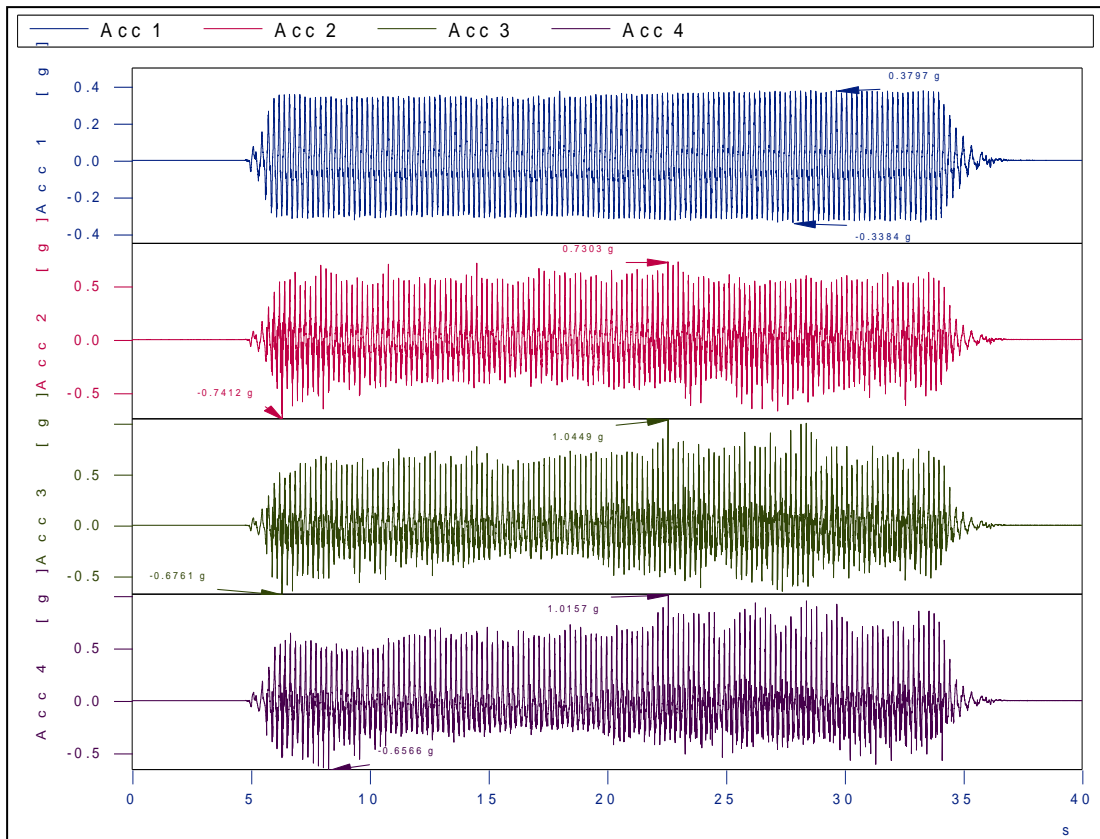


Figure F11: Acceleration values of base (Acc 1), block 1 (Acc 2) and block 2 (Acc 3) and block 3 (Acc 4) for 5 Hz (Test 3.1.3)

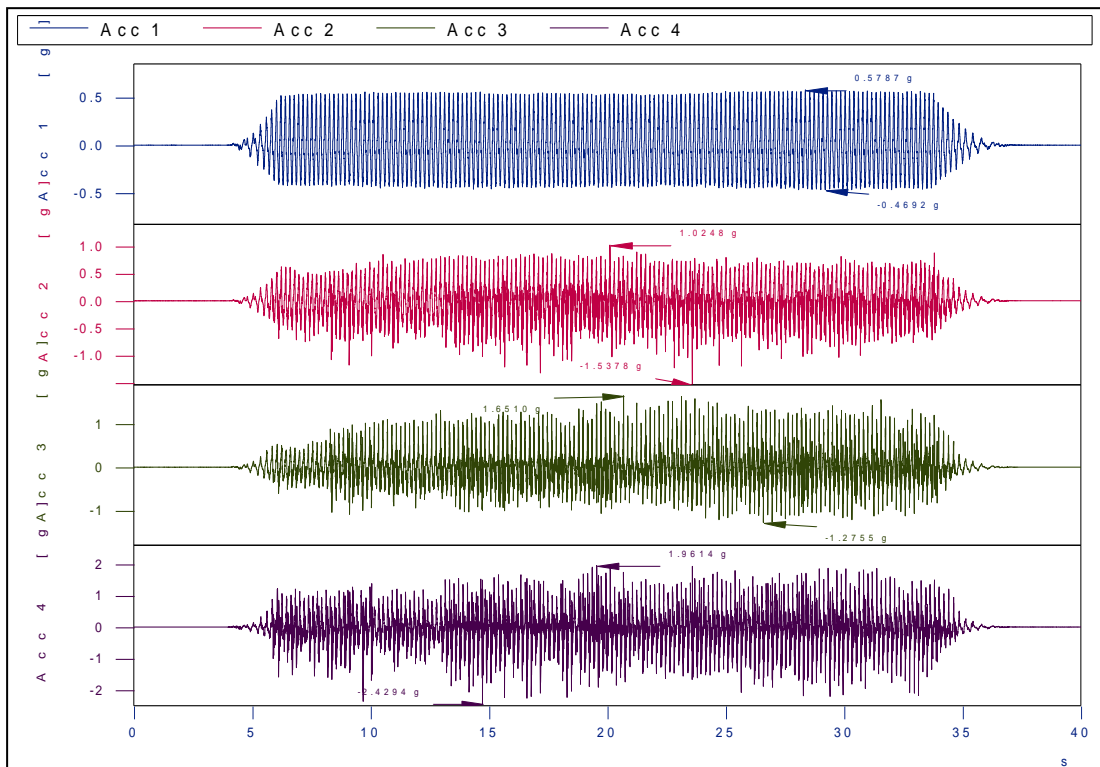


Figure F12: Acceleration values of base (Acc 1), block 1 (Acc 2) and block 2 (Acc 3) and block 3 (Acc 4) for 6 Hz (Test 3.1.4)

SOIL 2

Results of acceleration measurements for three blocks for Soil 2 (Test 3.2) under dynamic loading are presented in Figure F13 – Figure F15.

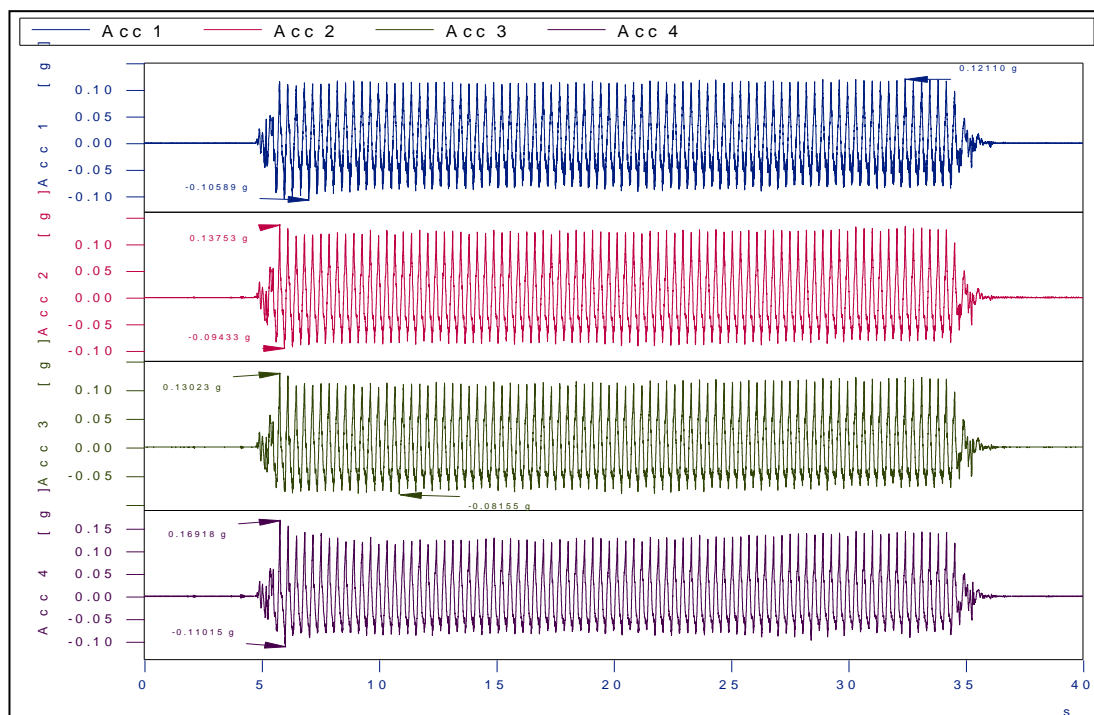


Figure F13: Acceleration values of base (Acc 1), block 1 (Acc 2) and block 2 (Acc 3) and block 3 (Acc 4) for 3 Hz (Test 3.2.1)

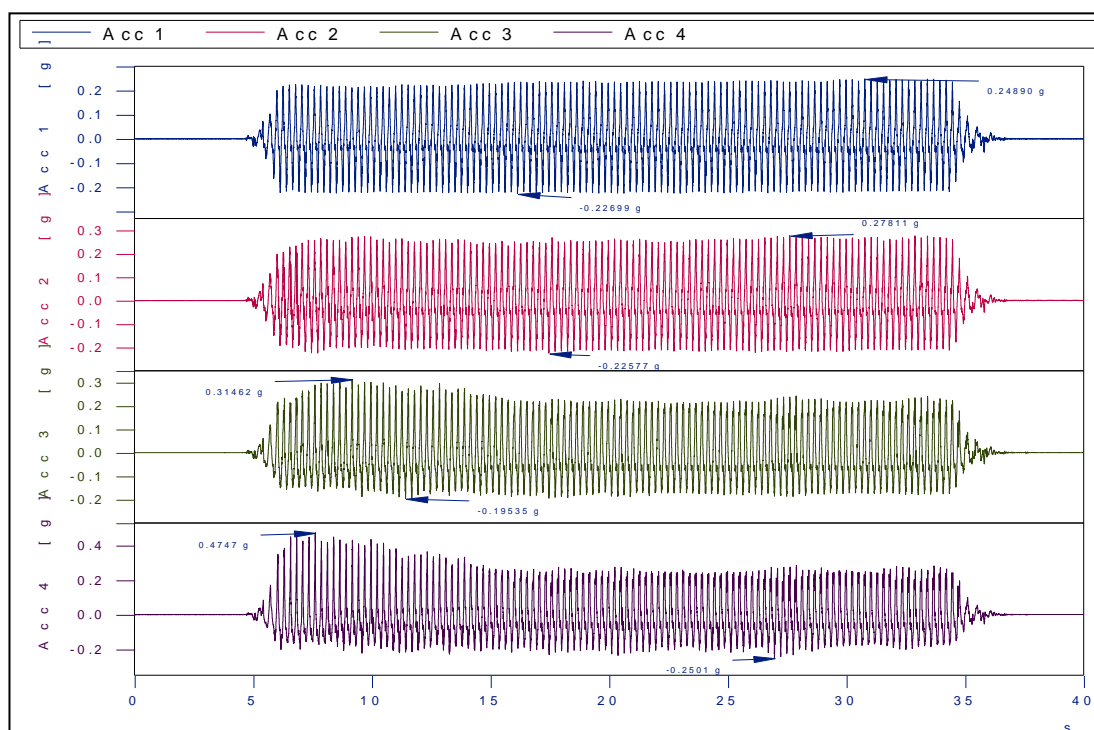


Figure F14: Acceleration values of base (Acc 1), block 1 (Acc 2) and block 2 (Acc 3) and block 3 (Acc 4) for 4 Hz (Test 3.2.2)

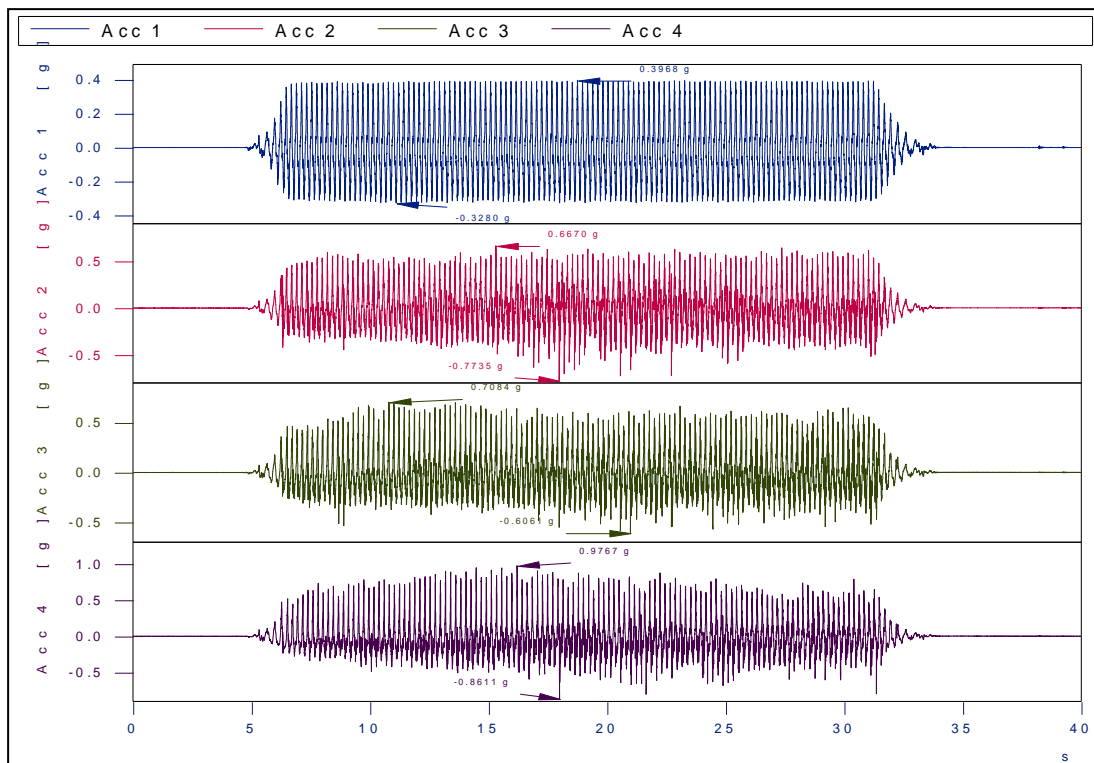


Figure F15: Acceleration values of base (Acc 1), block 1 (Acc 2) and block 2 (Acc 3) and block 3 (Acc 4) for 5 Hz (Test 3.2.3)

APPENDIX G

TWO BLOCKS: FLUCTUATING AND NON-FLUCTUATING COMPONENTS

By using MathCAD software program, these components were computed and total saturated soil pressures, fluctuating and non-fluctuating components of total saturated soil pressures are shown between Figure G1- Figure G112 for 2, 3, 4 and 6 Hz for Soil 1 and 4, 5, 6 Hz for Soil 2.

1. SOIL 1

1.1. Two Blocks- Fluctuating and Non-fluctuating Components of Total Saturated Soil Pressure for 2 Hz for Soil 1

Fig. G1 - G4 show the total saturated soil pressure, non-fluctuating and fluctuating components of total saturated soil pressure for SP1 for 2 Hz.

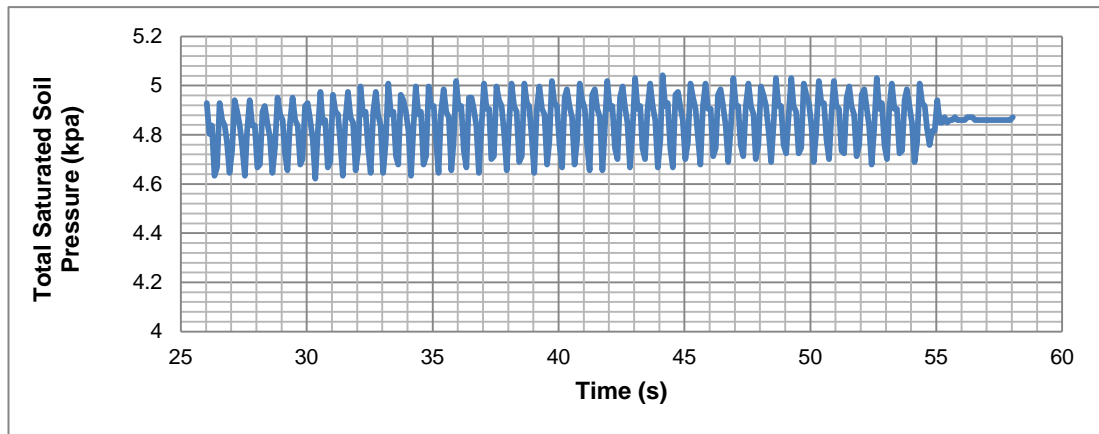


Figure G1: Total saturated soil pressure for SP1 for 2 Hz

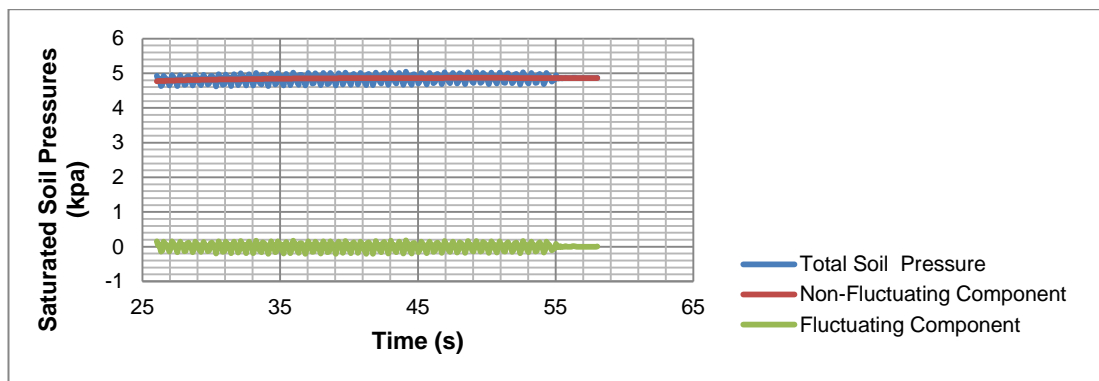


Figure G.2: Total saturated soil pressure, non fluctuating and fluctuating components of total saturated soil pressure for SP1 for 2 Hz

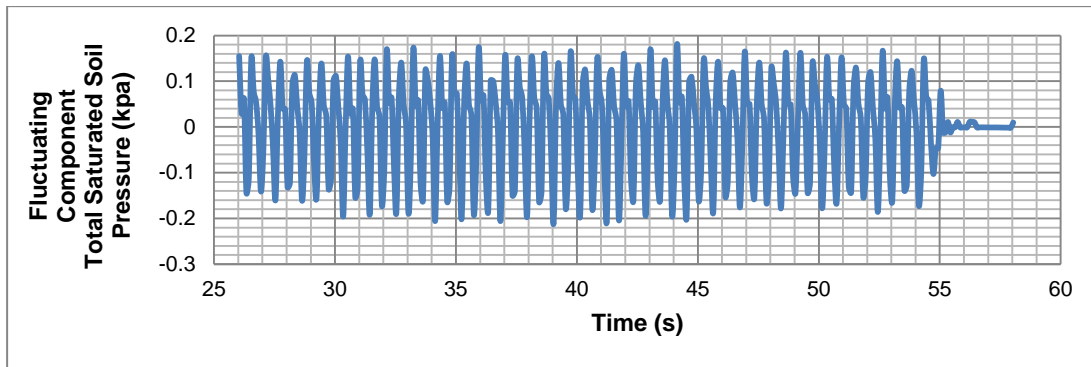


Figure G3: Fluctuating components of total saturated soil pressures for SP1 for 2 Hz

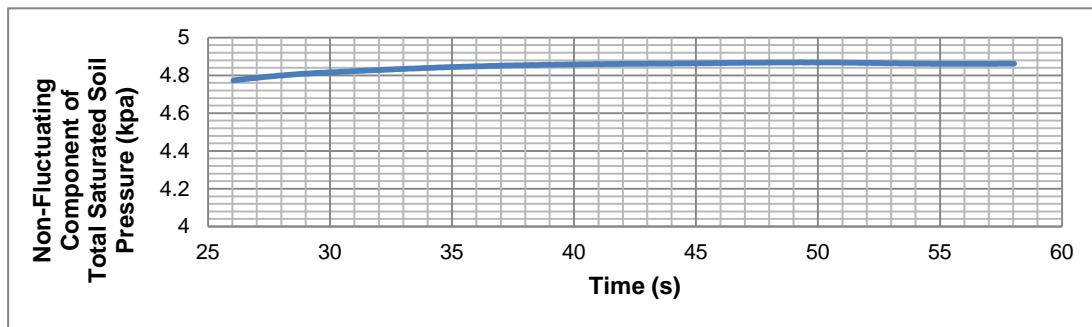


Figure G4: Non fluctuating components of total saturated soil pressures for SP1 for 2 Hz

Fig. G5 – G8 show the total saturated soil pressure, non fluctuating and fluctuating components of total saturated soil pressure for SP2 for 2 Hz.

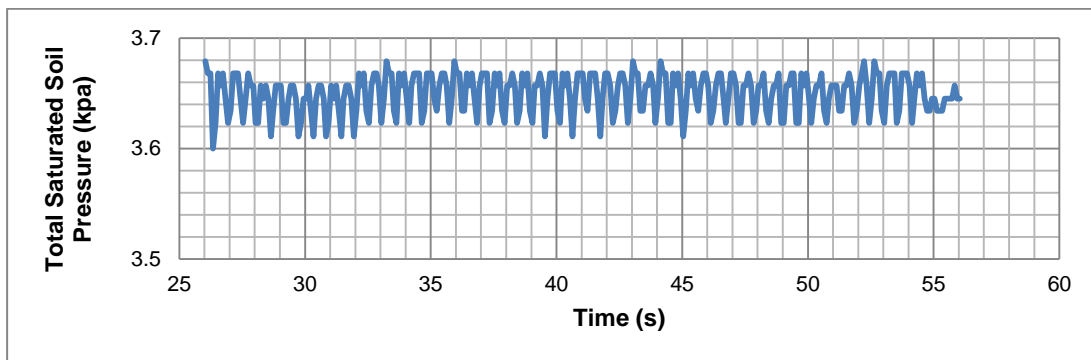


Figure G5: Total saturated soil pressure for SP2 for 2 Hz

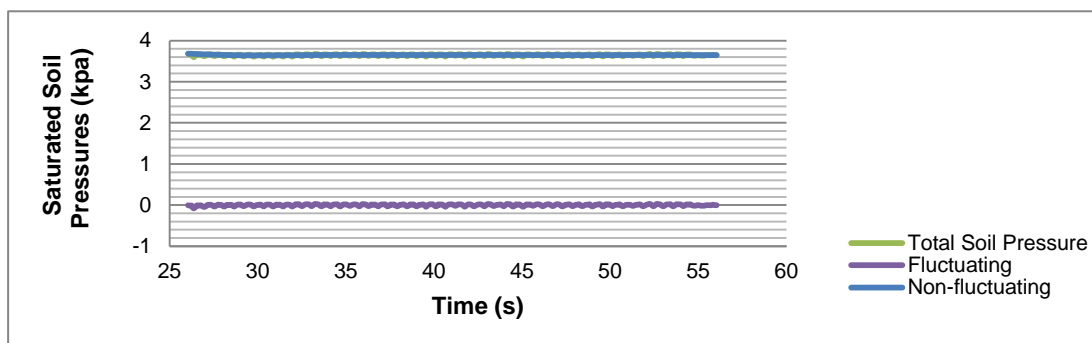


Figure G6: Total saturated soil pressure, non fluctuating and fluctuating components of total saturated soil pressure for SP2 for 2 Hz

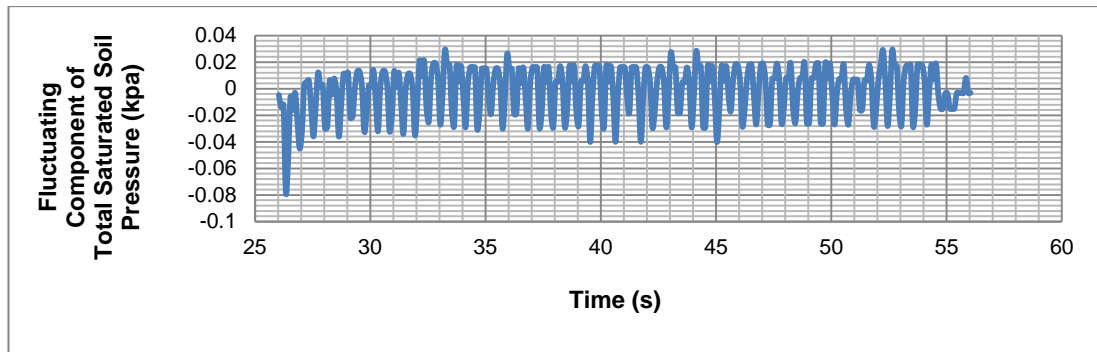


Figure G7: Fluctuating components of total saturated soil pressures for SP2 for 2 Hz

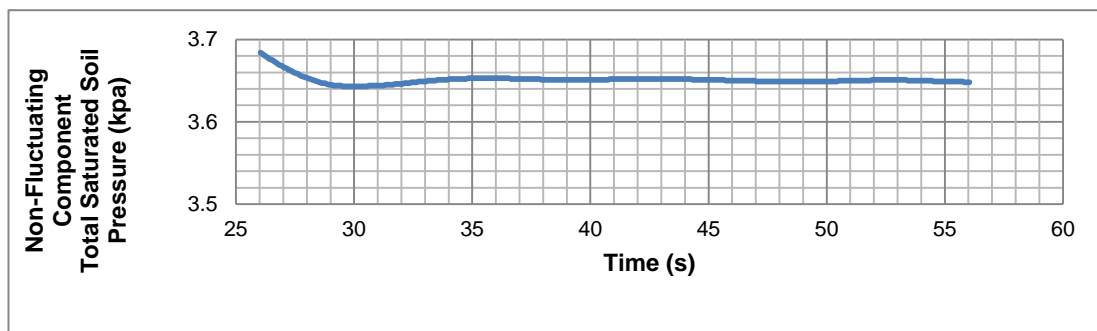


Figure G8: Non fluctuating components of total saturated soil pressures for SP2 for 2 Hz

Fig. G9 – G12 show the total saturated soil pressures, non fluctuating and fluctuating components of total saturated soil pressures for SP3 for 2 Hz.

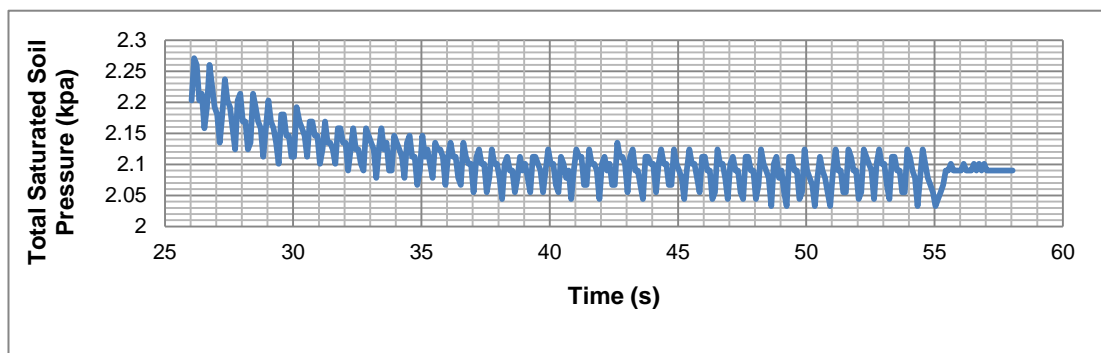


Figure G9: Total saturated soil pressure for SP3 for 2 Hz

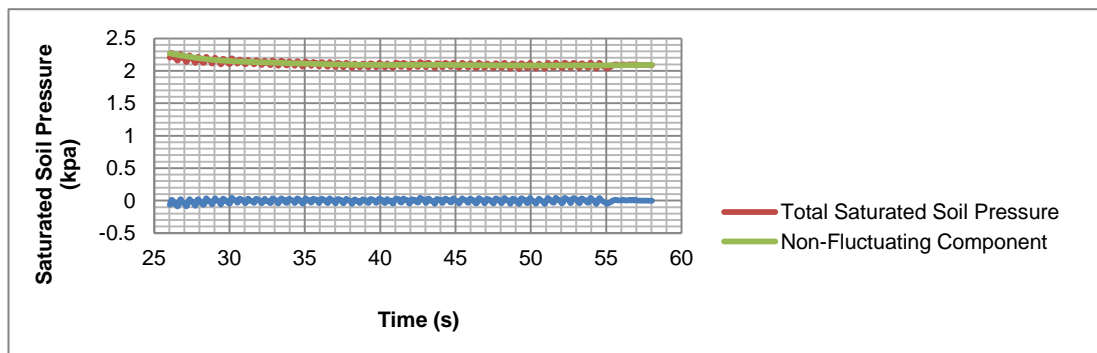


Figure G10: Total saturated soil pressure, non fluctuating and fluctuating components of total saturated soil pressure for SP3 for 2 Hz

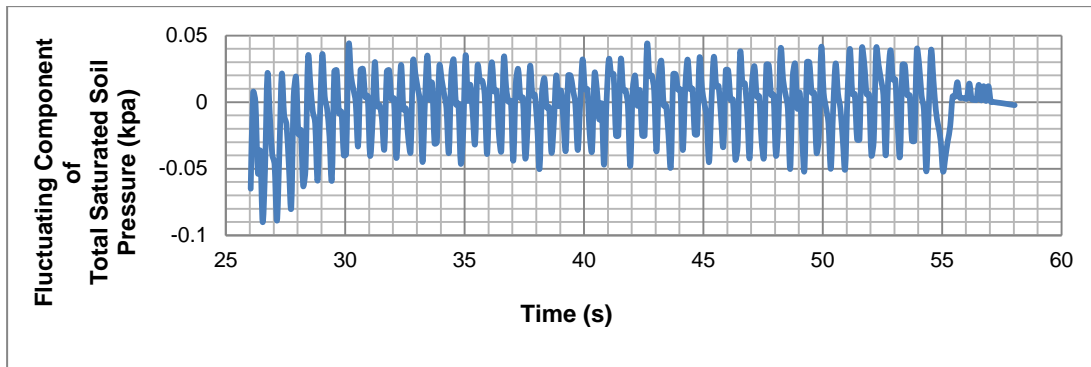


Figure G11: Fluctuating components of total saturated soil pressures for SP3 for 2 Hz

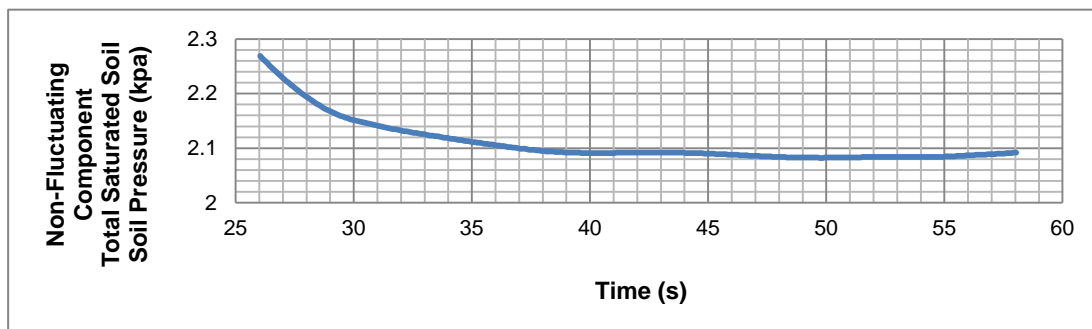


Figure G12: Non fluctuating components of total saturated soil pressures for SP3 for 2 Hz

Fig. G13 - G16 show the total saturated soil pressures, non fluctuating and fluctuating components of total saturated soil pressures for SP4 for 2 Hz.

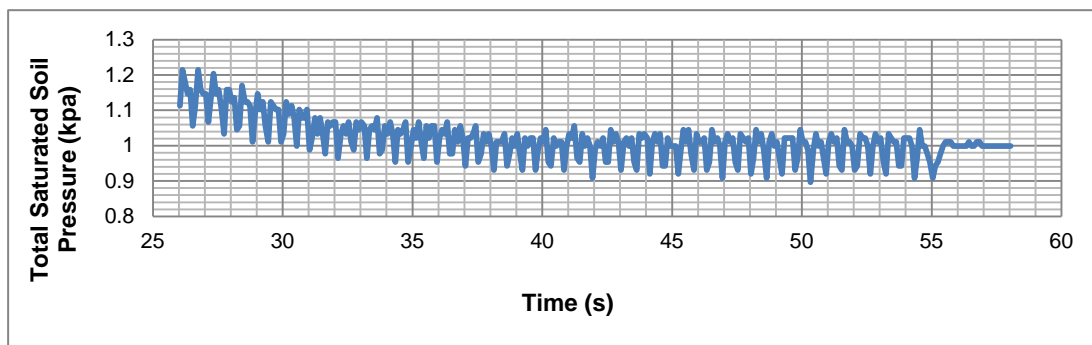


Figure G13: Total saturated soil pressure for SP4 for 2 Hz

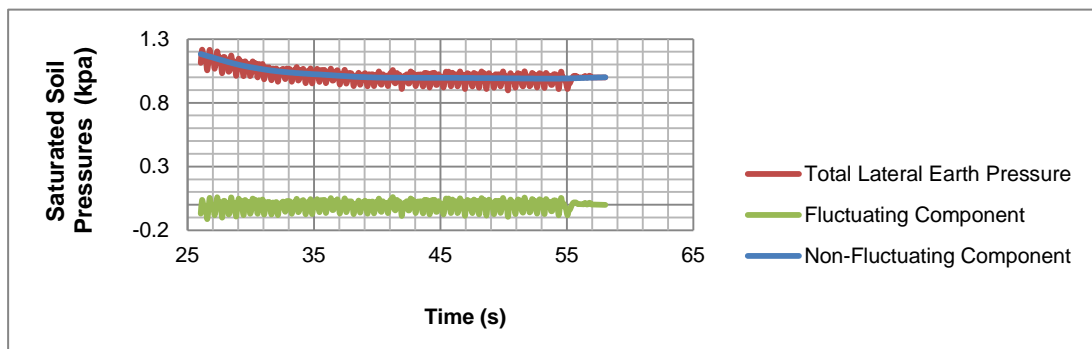


Figure G14: Total saturated soil pressure, non fluctuating and fluctuating components of total saturated soil pressure for SP4 for 2 Hz

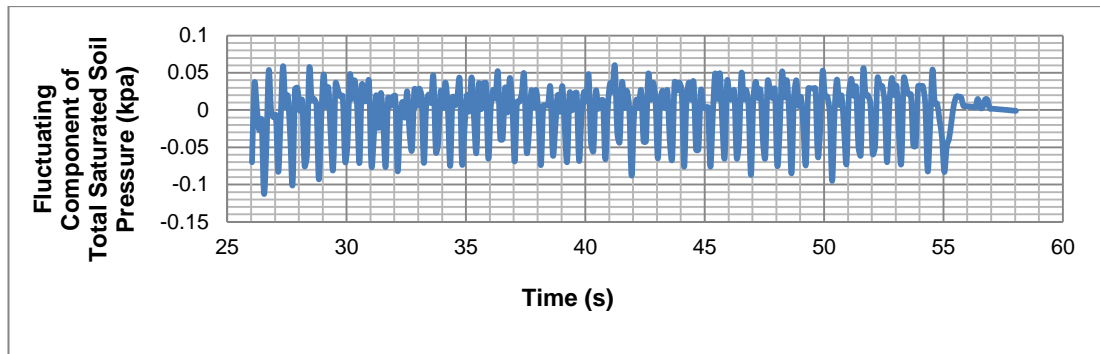


Figure G15: Fluctuating components of total saturated soil pressures for SP4 for 2 Hz

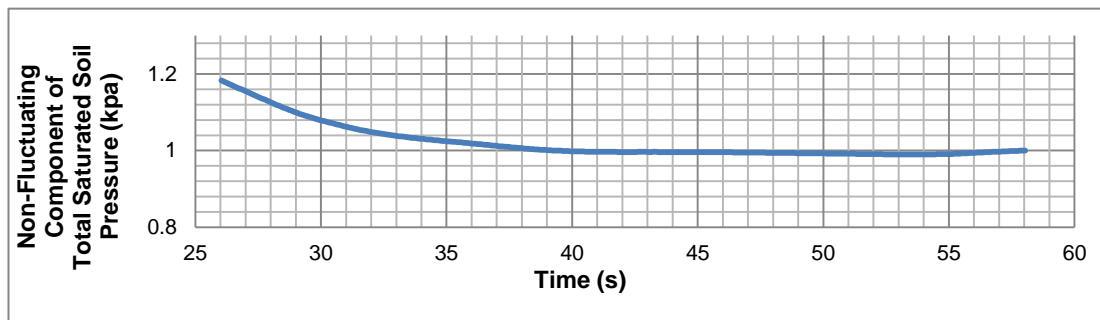


Figure G16: Non fluctuating components of total saturated soil pressures for SP4 for 2 Hz

1.2. Two Blocks- Fluctuating and Non-Fluctuating Components of Total Soil Pressure for 3 Hz for Soil 1

Fig. G17 – G20 show the total saturated soil pressures, non fluctuating and fluctuating components of total saturated soil pressures for **SP1 for 3Hz**.

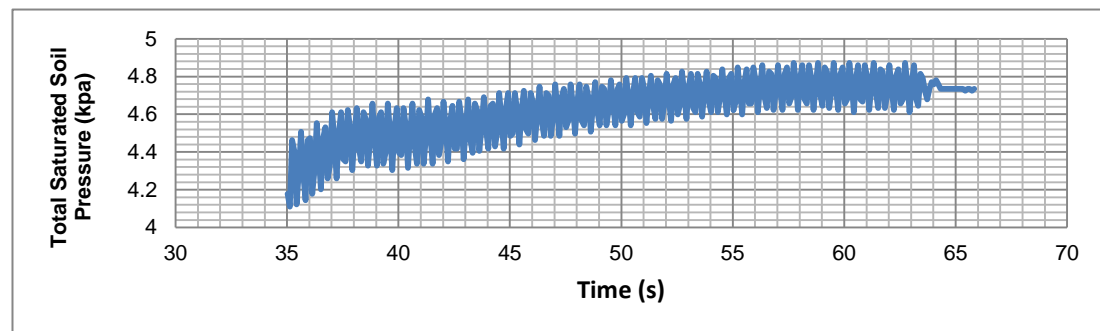


Figure G17: Total saturated soil pressure for SP1 for 3 Hz

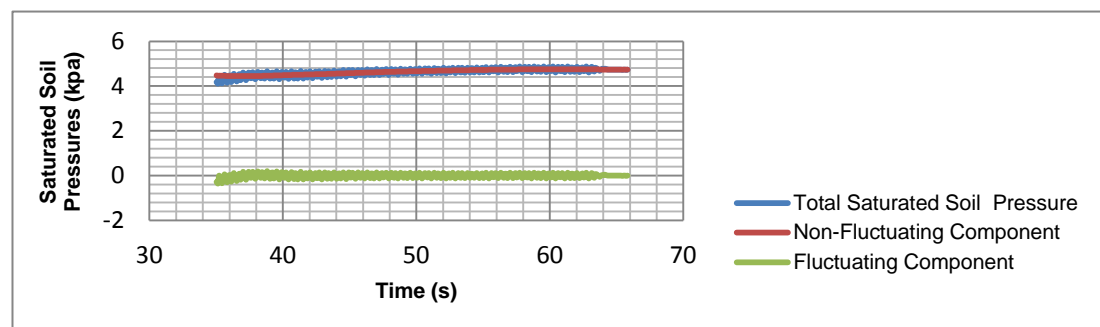


Figure G18: Total saturated soil pressure, non fluctuating and fluctuating components of total saturated soil pressure for SP1 for 3 Hz

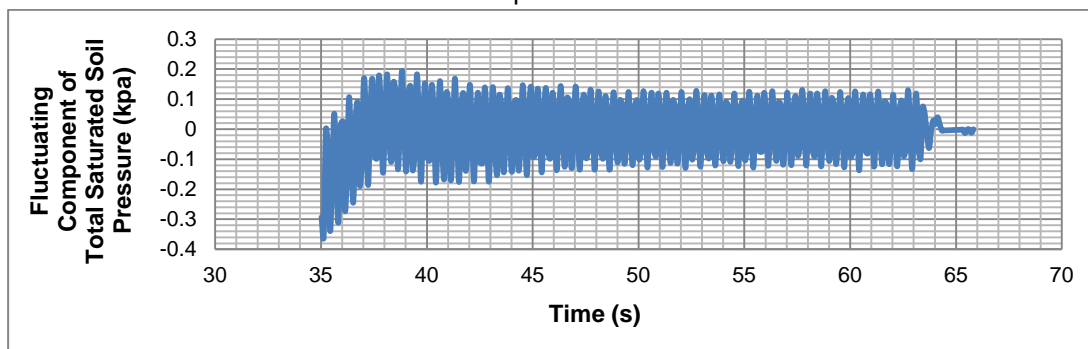


Figure G19: Fluctuating components of total saturated soil pressures for SP1 for 3 Hz

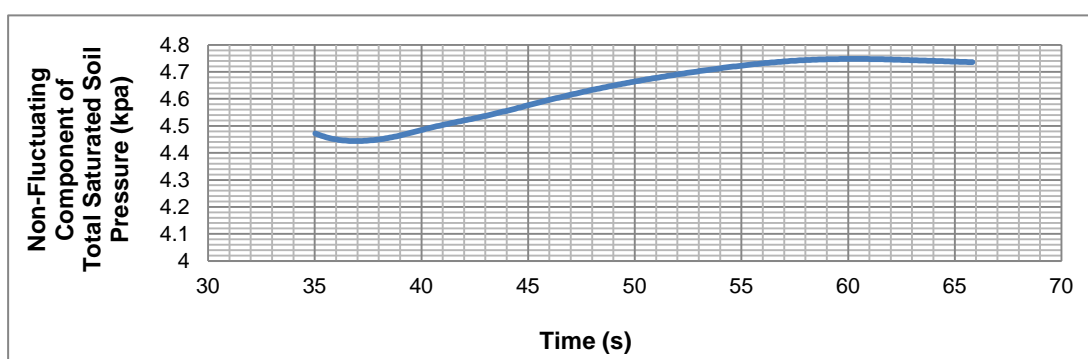


Figure G20: Non fluctuating components of total saturated soil pressures for SP1 for 3 Hz

Fig. G21 – G24 show the total saturated soil pressures, non fluctuating and fluctuating components of total saturated soil pressures for SP2 for 3 Hz.

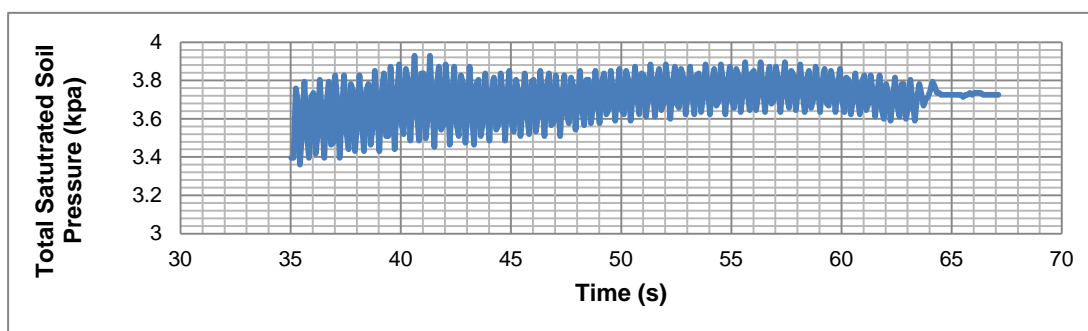


Figure G21: Total saturated soil pressure for SP2 for 3 Hz

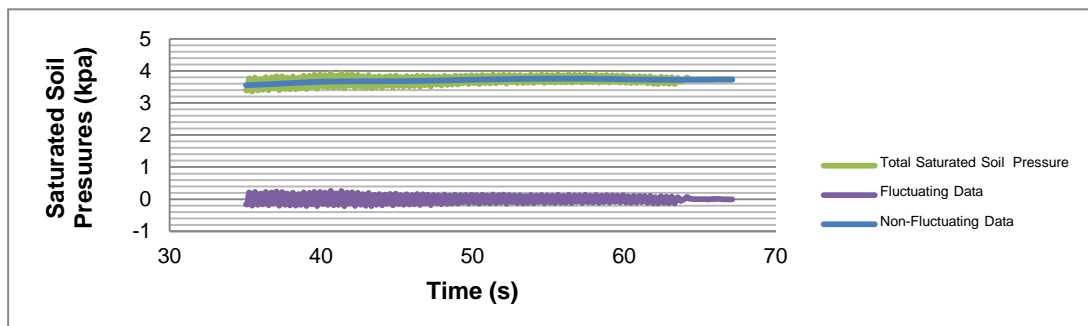


Figure G.22: Total saturated soil pressure, non fluctuating and fluctuating components of total saturated soil pressure for SP2 for 3 Hz

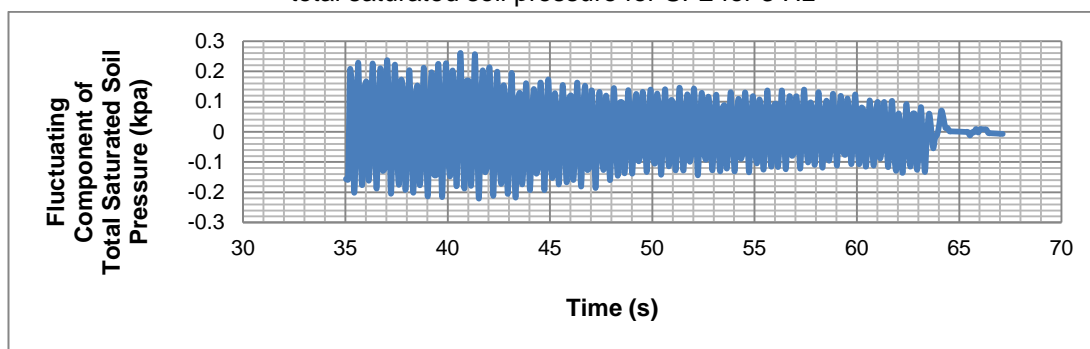


Figure G23: Fluctuating components of total saturated soil pressures for SP2 for 3 Hz

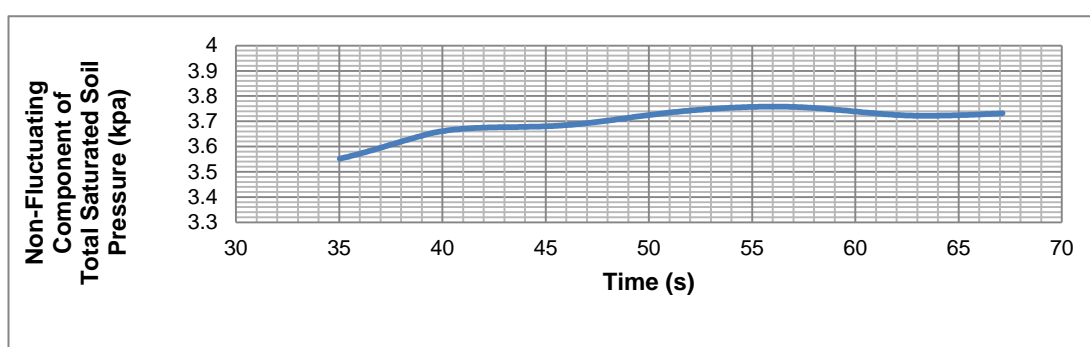


Figure G.24: Non fluctuating components of total saturated soil pressures for SP2 for 3 Hz

Fig. G.25 – G.28 show the total saturated soil pressures, non fluctuating and fluctuating components of total saturated soil pressures for **SP3 for 3 Hz**.

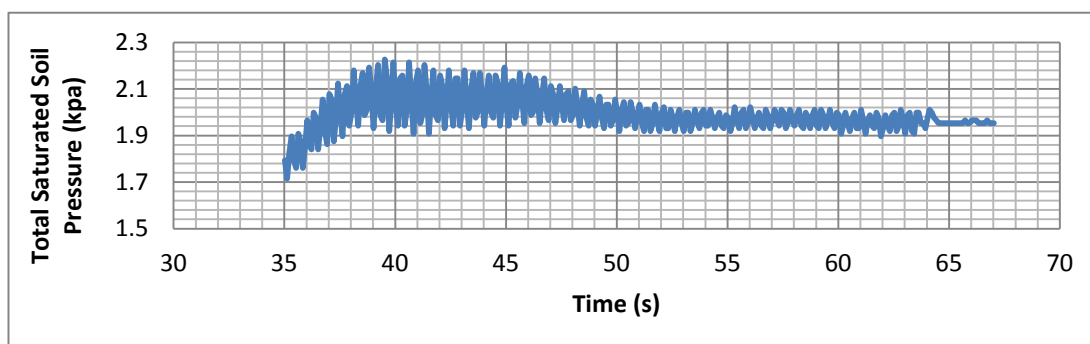


Figure G25: Total saturated soil pressure for SP3 for 3 Hz

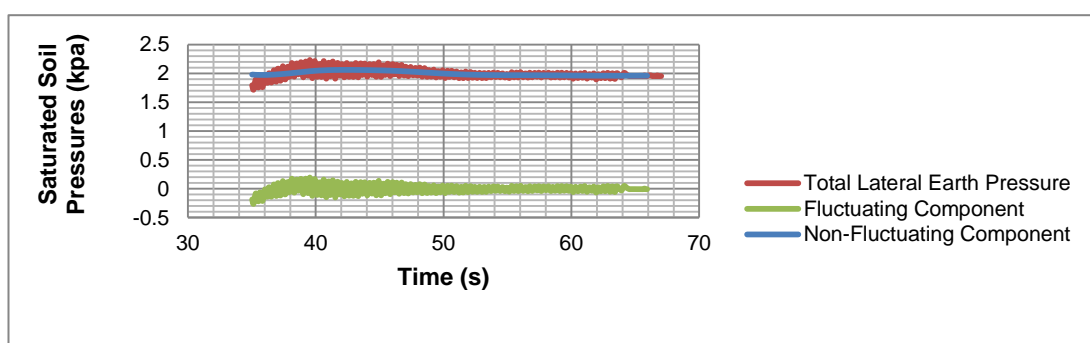


Figure G.26: Total saturated soil pressure, non fluctuating and fluctuating components of total saturated soil pressure for SP3 for 3 Hz

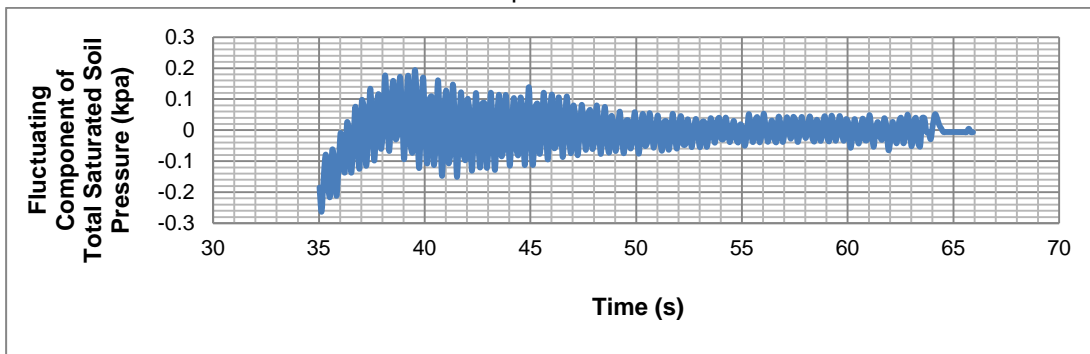


Figure G.27: Fluctuating components of total saturated soil pressures for SP3 for 3 Hz

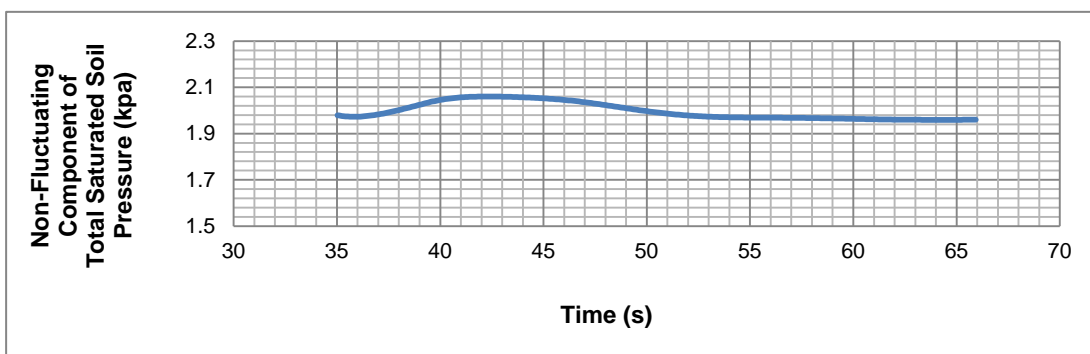


Figure G.28: Non-fluctuating components of total saturated soil pressures for SP3 for 3 Hz

Fig. G.29 – G.32 show the total saturated soil pressures, non fluctuating and fluctuating components of total saturated soil pressures for **SP4 for 3 Hz**.

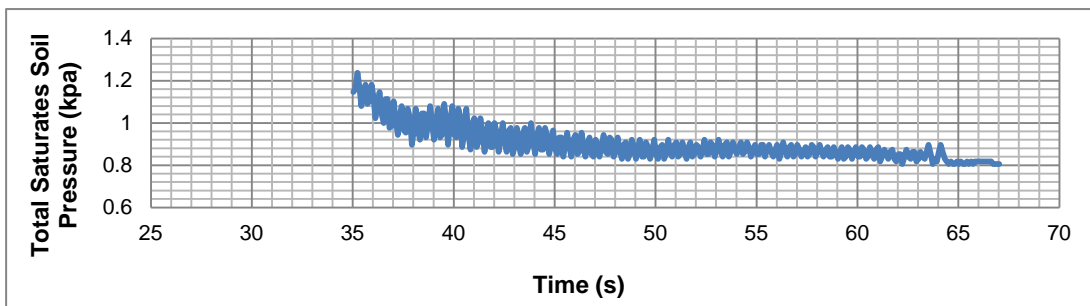


Figure G.29: Total saturated soil pressure for SP4 for 3 Hz

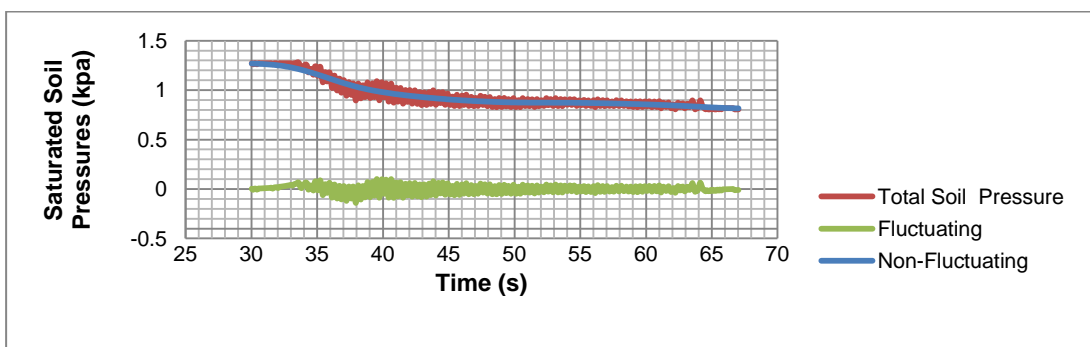


Figure G30: Total saturated soil pressure, non fluctuating and fluctuating components of total saturated soil pressure for SP4 for 3 Hz

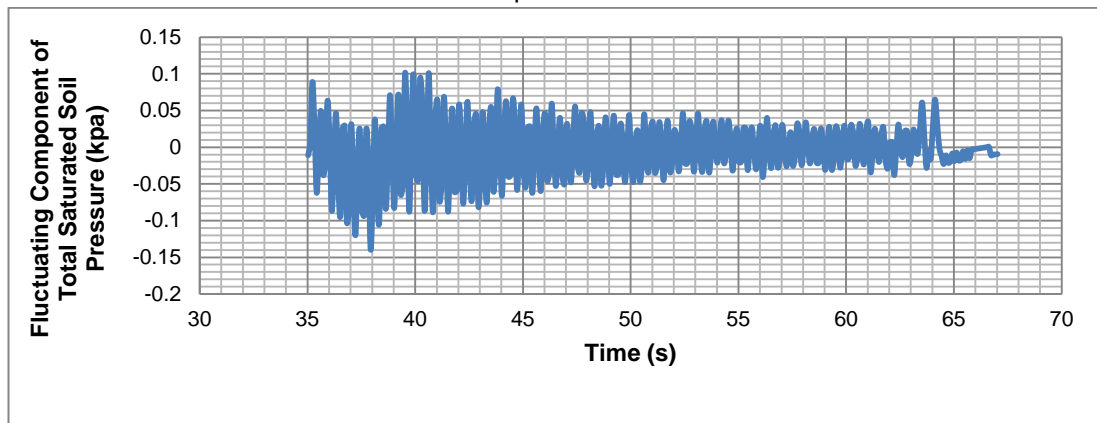


Figure G31: Fluctuating components of total saturated soil pressures for SP4 for 3 Hz

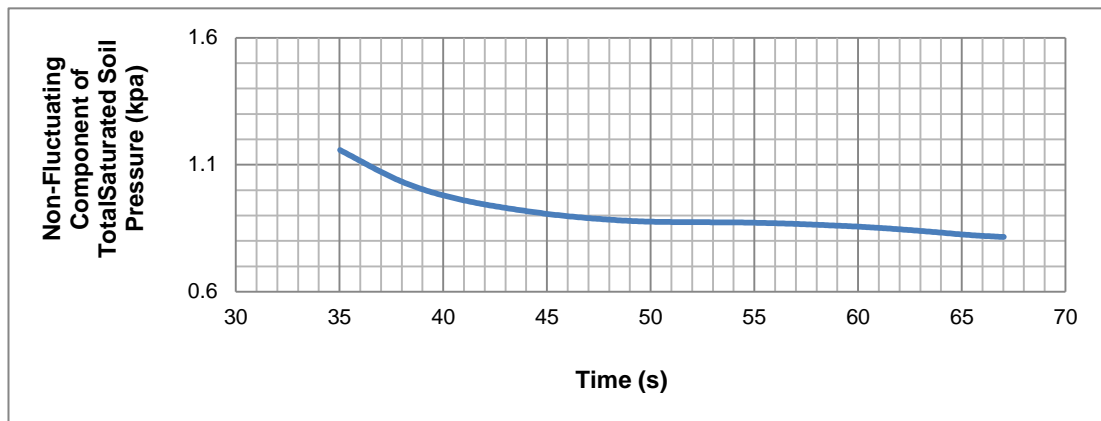


Figure G32: Non fluctuating components of total saturated soil pressures for SP4 for 3 Hz

1.3. Two Blocks- Fluctuating and Non-Fluctuating Components of Total Soil Pressure for 4 Hz for Soil 1

Fig. G33 – G36 show the total saturated soil pressures, non fluctuating and fluctuating components of total saturated soil pressures for **SP1 for 4 Hz.**

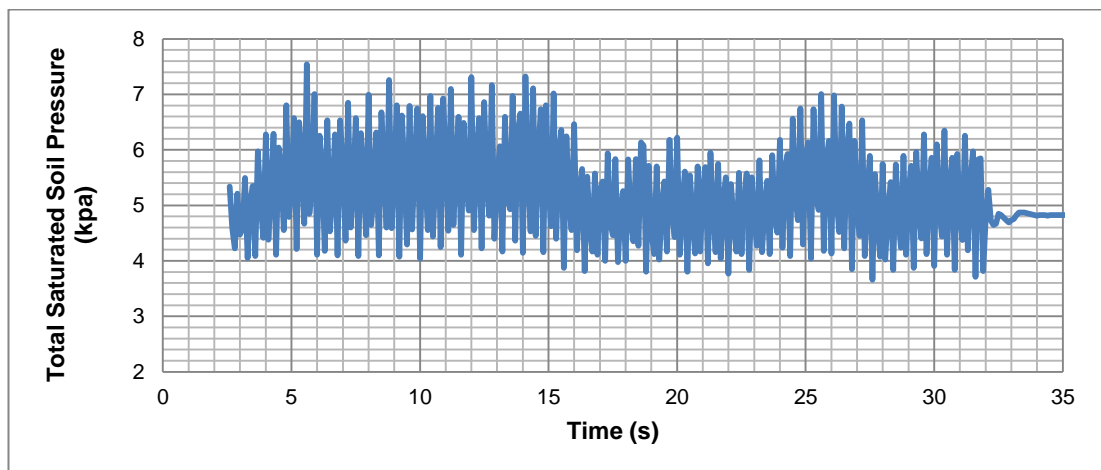


Figure G33: Total saturated soil pressure for SP1 for 4 Hz

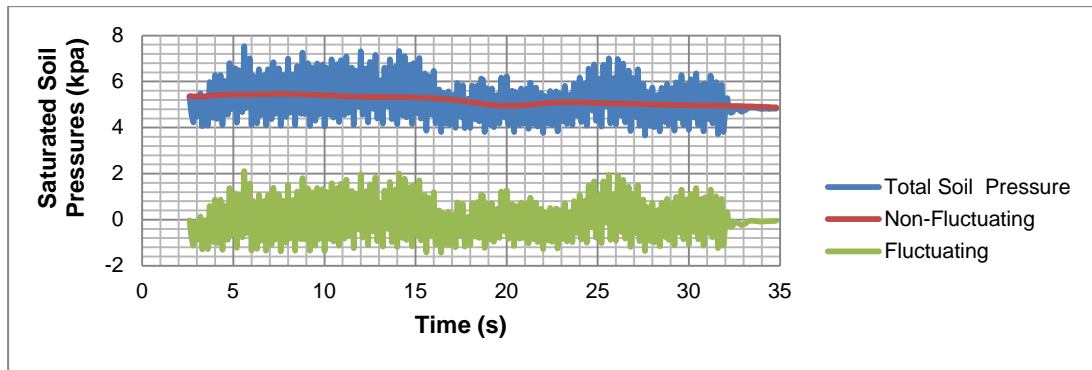


Figure G.34: Total saturated soil pressure, non fluctuating and fluctuating components of total saturated soil pressure for SP1 for 4 Hz

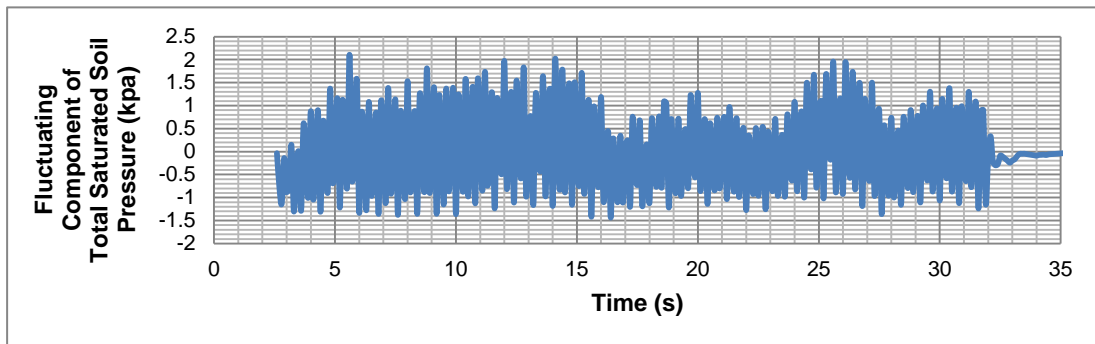


Figure G35: Fluctuating components of total saturated soil pressures for SP1 for 4 Hz

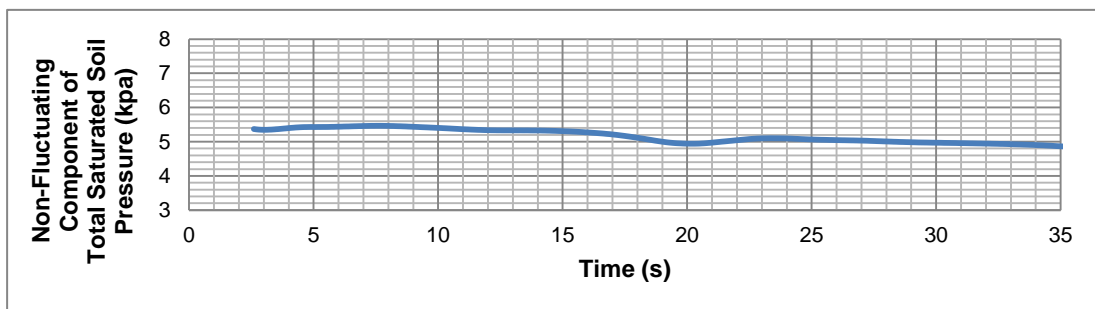


Figure G36: Non fluctuating components of total saturated soil pressures for SP4 for 4 Hz

Fig. G37 – G40 show the total saturated soil pressures, non fluctuating and fluctuating components of total saturated soil pressures for SP2 for 4 Hz.

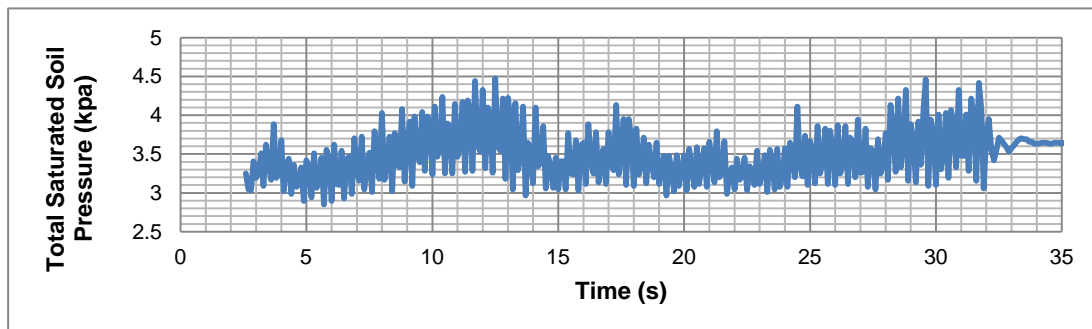


Figure G37: Total saturated soil pressure for SP2 for 4 Hz

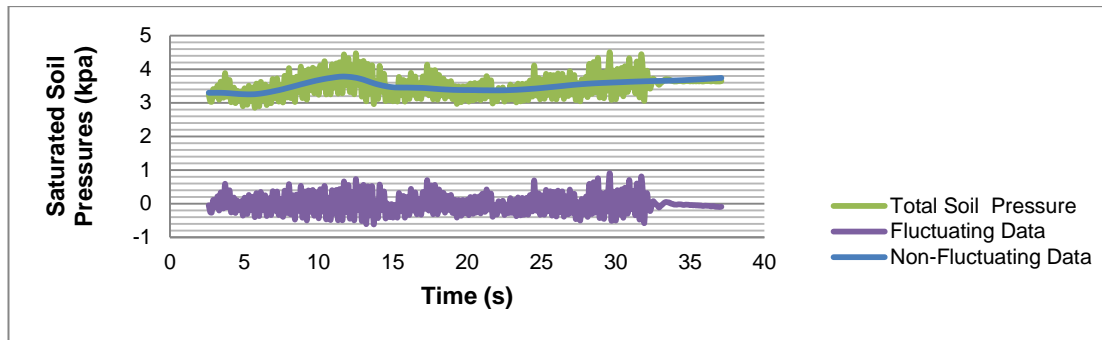


Figure G38: Total saturated soil pressure, non fluctuating and fluctuating components of total saturated soil pressure for SP2 for 4 Hz

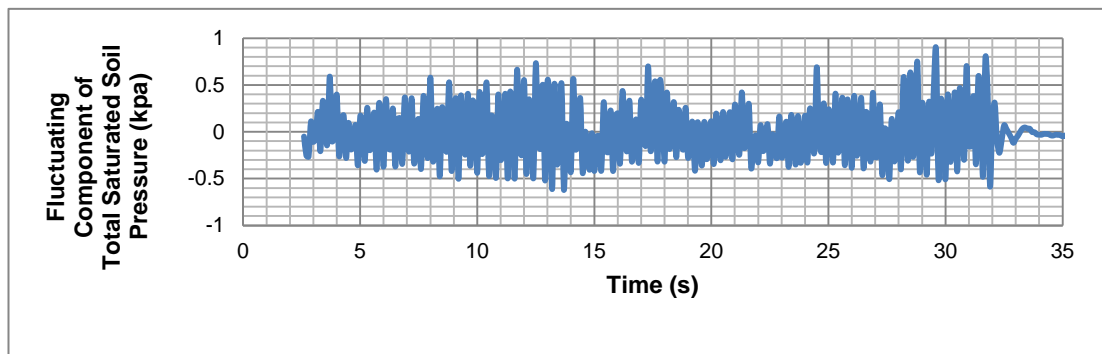


Figure G39: Fluctuating components of total saturated soil pressures for SP2 for 4 Hz

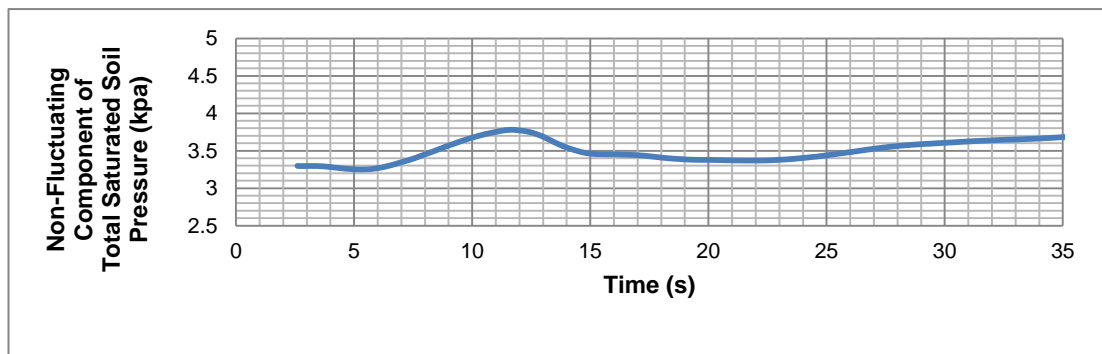


Figure G40: Non fluctuating components of total saturated soil pressures for SP2 for 4 Hz

Fig. G41 – G44 show the total saturated soil pressures, non fluctuating and fluctuating components of total saturated soil pressures for **SP3 for 4 Hz**.

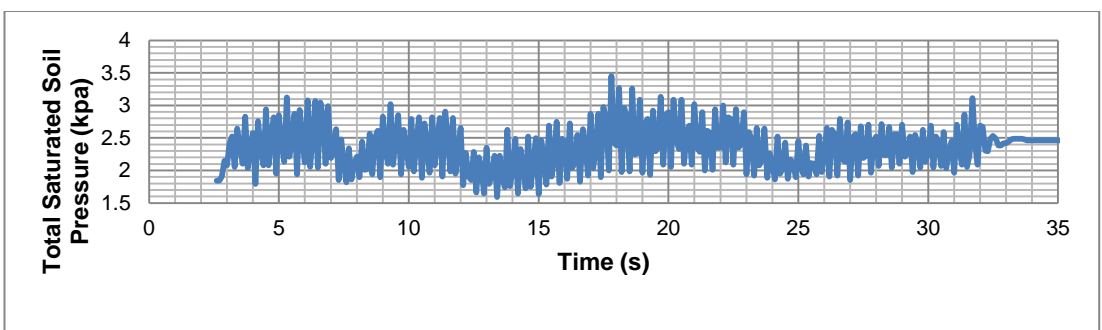


Figure G41: Total saturated soil pressure for SP3 for 4 Hz

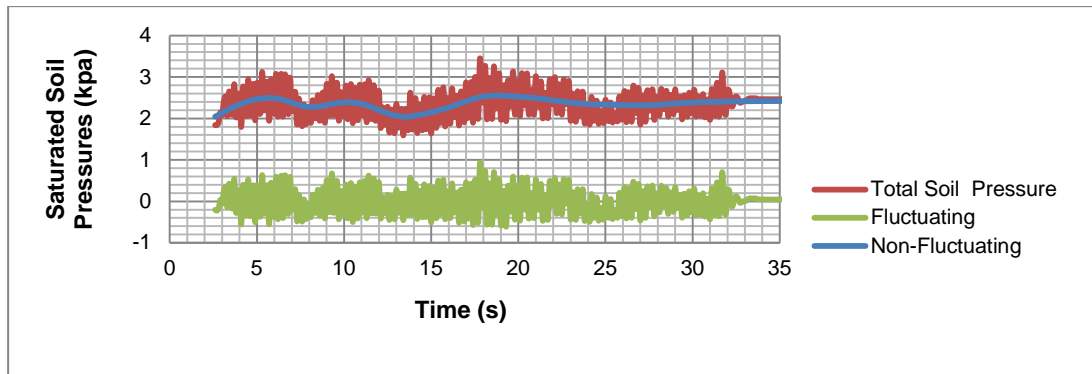


Figure G42: Total saturated soil pressure, non fluctuating and fluctuating components of total saturated soil pressure for SP3 for 4 Hz

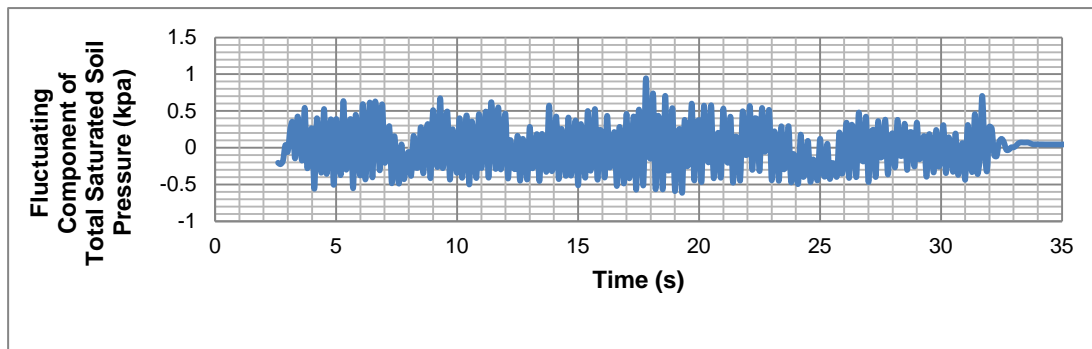


Figure G43: Fluctuating components of total saturated soil pressures for SP3 for 4 Hz

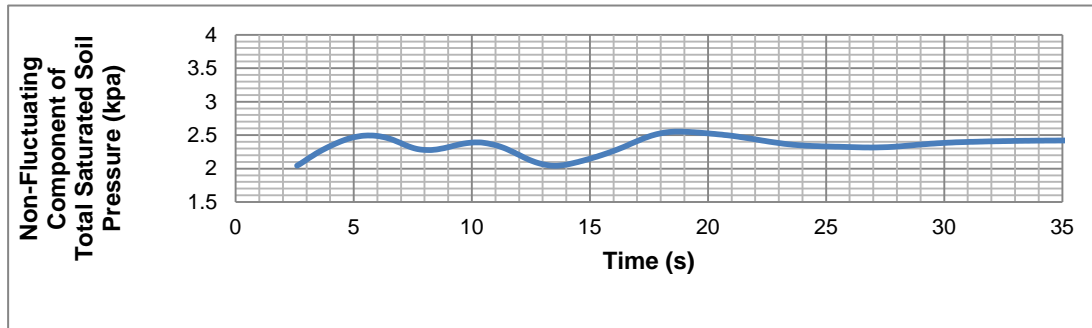


Figure G44: Non fluctuating components of total saturated soil pressures for SP3 for 4 Hz

Fig. G45 – G48 show the total saturated soil pressures, non fluctuating and fluctuating components of total saturated soil pressures for SP4 for 4 Hz.

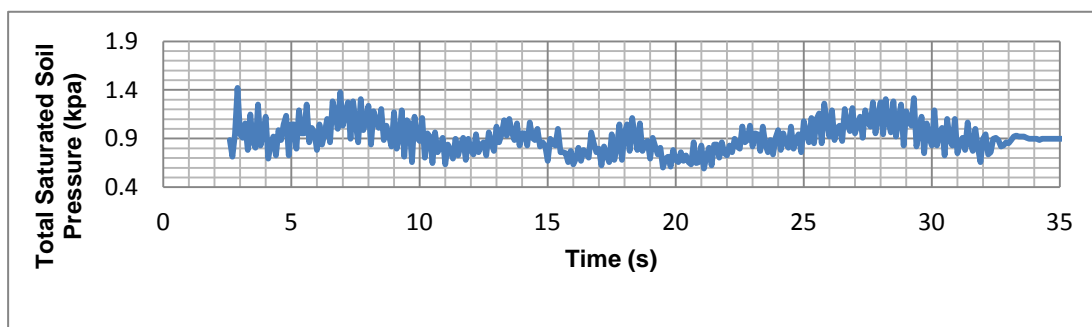


Figure G45: Total saturated soil pressure for SP4 for 4 Hz

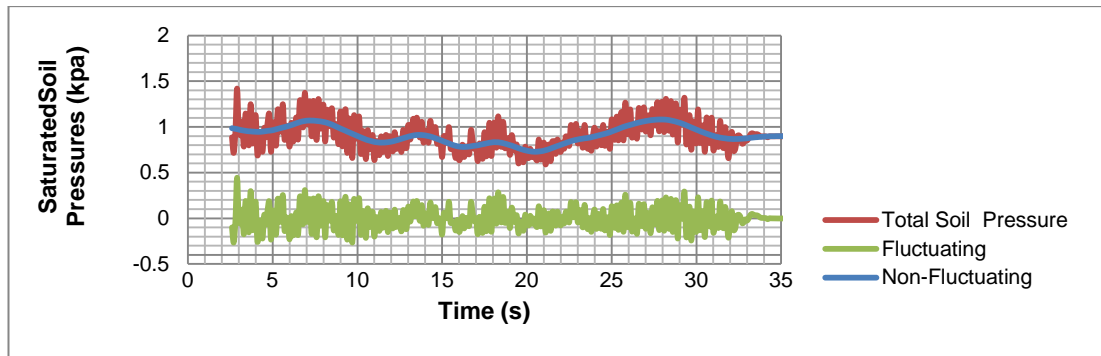


Figure G46: Total saturated soil pressure, non fluctuating and fluctuating components of total saturated soil pressure for SP4 for 4 Hz

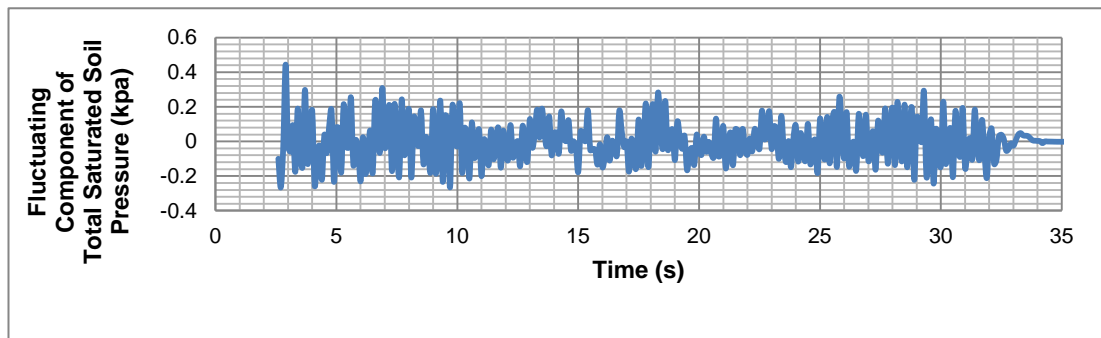


Figure G47: Fluctuating components of total saturated soil pressures for SP4 for 4 Hz

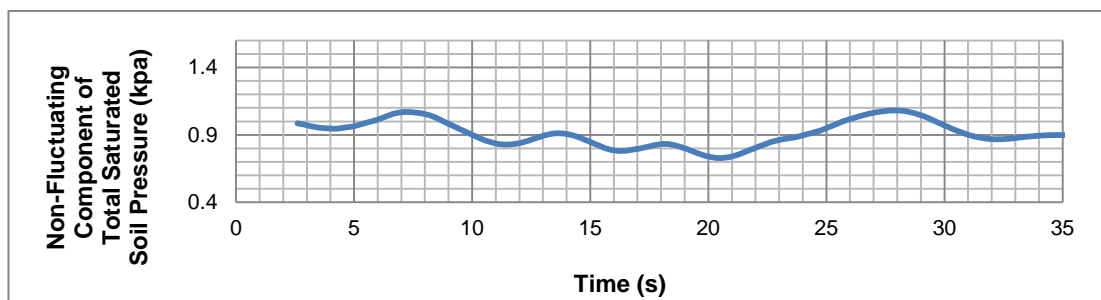


Figure G48: Non fluctuating components of total saturated soil pressures for SP4 for 4 Hz

1.4. Two Blocks- Fluctuating and Non-Fluctuating Components of Total Soil Pressure for 6 Hz for Soil 1

Fig. G49 – G52 show the total saturated soil pressures, non fluctuating and fluctuating components of total saturated soil pressures for **SP1 for 6 Hz**.

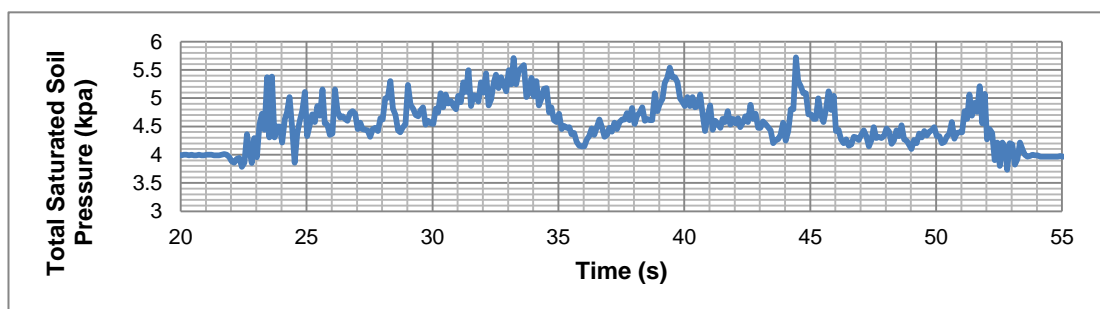


Figure G49: Total saturated soil pressure for SP1 for 6 Hz

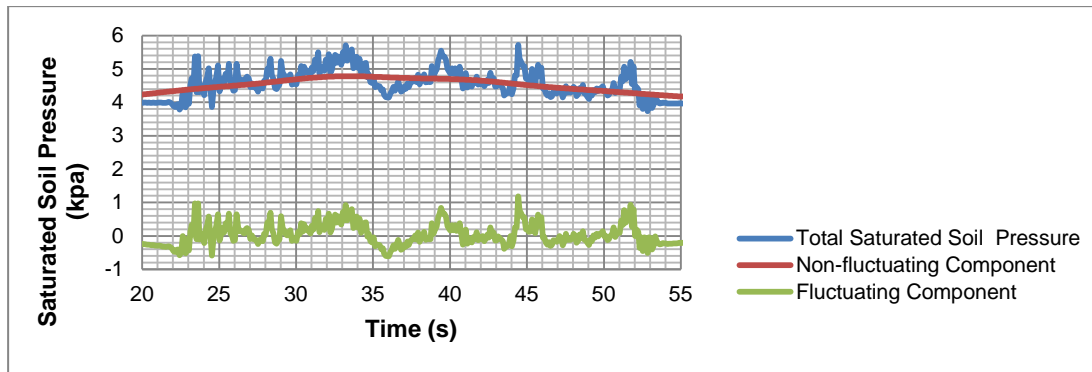


Figure G50: Total saturated soil pressure, non fluctuating and fluctuating components of total saturated soil pressure for SP1 for 6 Hz

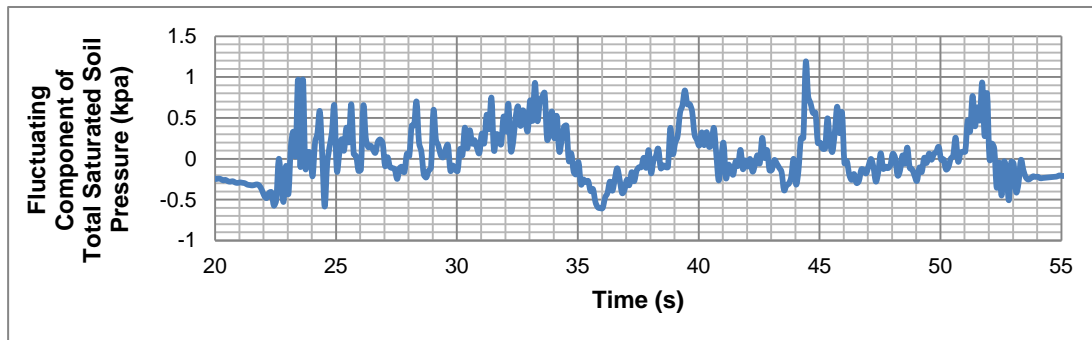


Figure G51: Fluctuating components of total saturated soil pressures for SP1 for 6 Hz

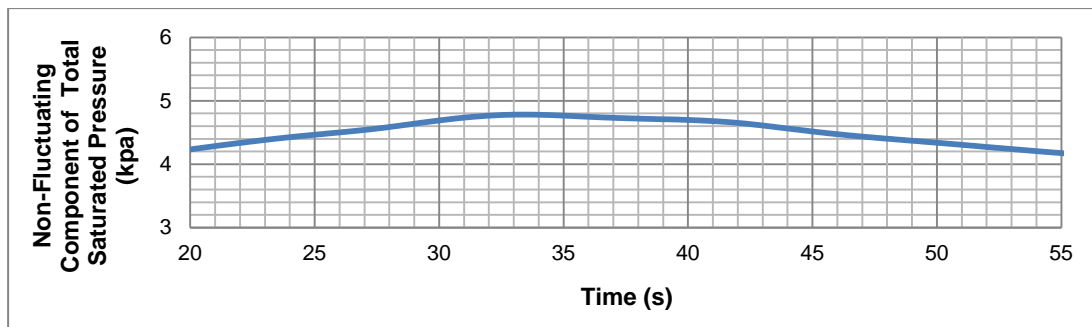


Figure G52: Non-fluctuating components of total saturated soil pressures for SP1 for 6 Hz

Fig. G53 – G56 show the total saturated soil pressures, non fluctuating and fluctuating components of total saturated soil pressures for **SP2 for 6 Hz.**

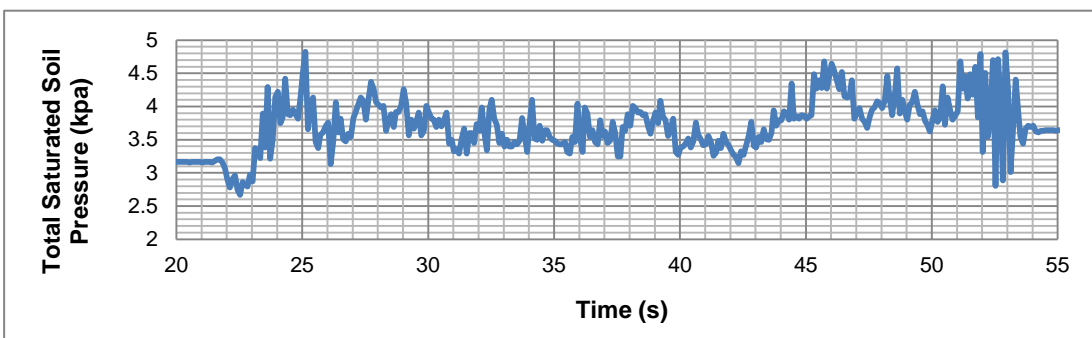


Figure G53: Total saturated soil pressure for SP2 for 6 Hz

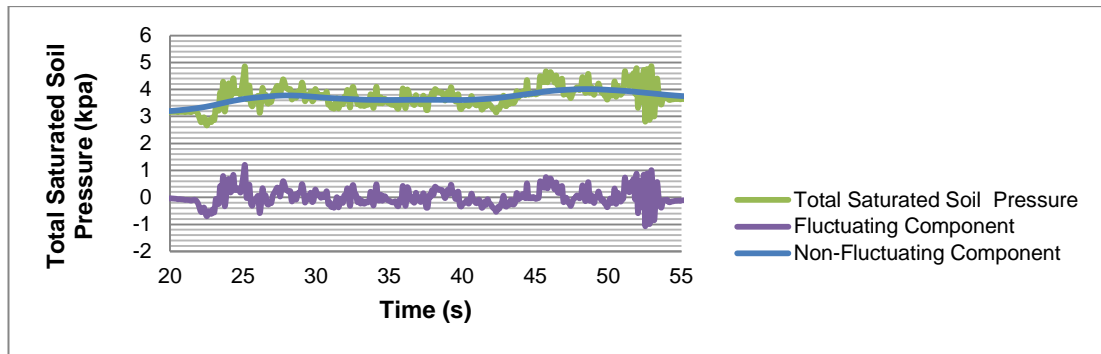


Figure G54: Total saturated soil pressure, non fluctuating and fluctuating components of total saturated soil pressure for SP2 for 6 Hz

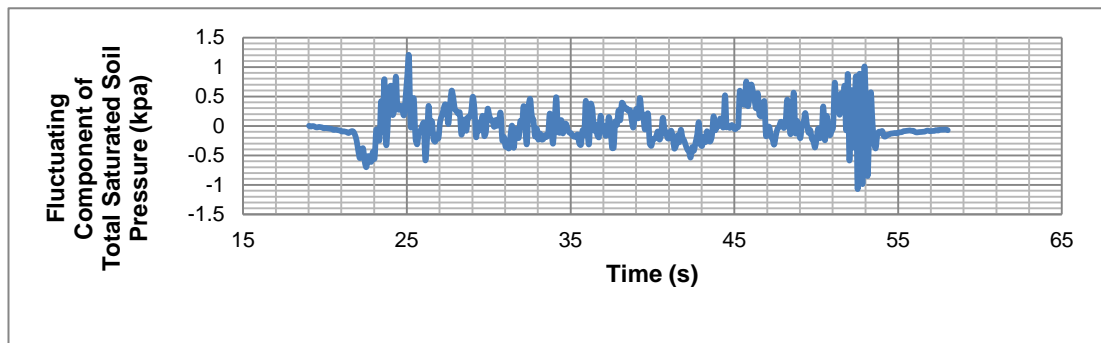


Figure G55: Fluctuating components of total saturated soil pressures for SP2 for 6 Hz

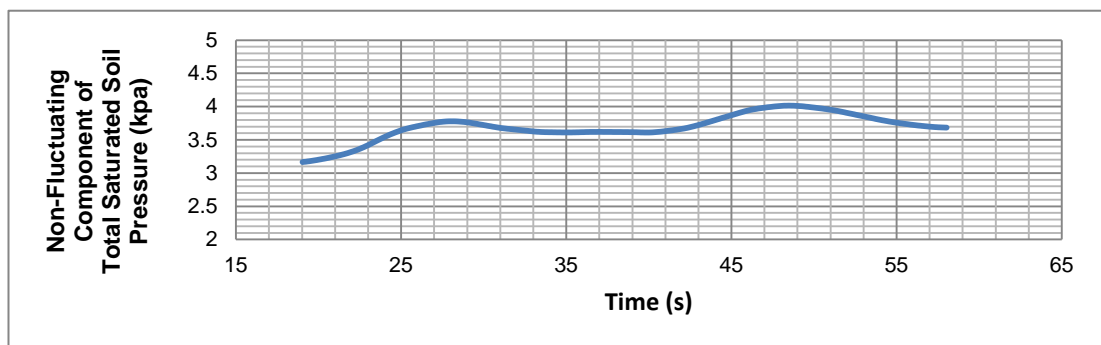


Figure G56: Non-fluctuating components of total saturated soil pressures for SP1 for 6 Hz

Fig. G57- G60 show the total saturated soil pressures, non fluctuating and fluctuating components of total saturated soil pressures for **SP3 for 6 Hz**.

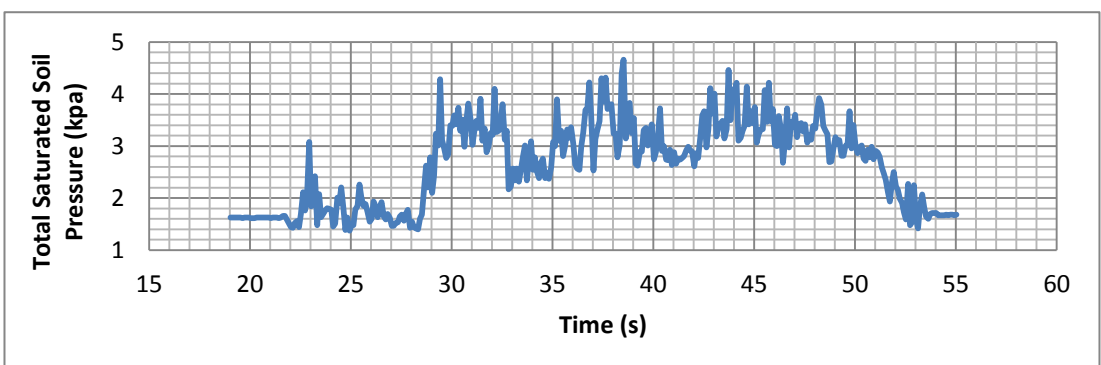


Figure G57: Total saturated soil pressure for SP3 for 6 Hz

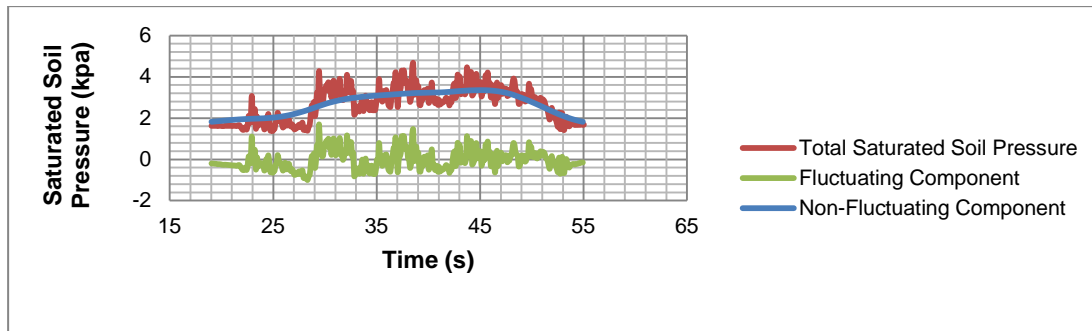


Figure G58: Total saturated soil pressure, non fluctuating and fluctuating components of total saturated soil pressure for SP3 for 6 Hz

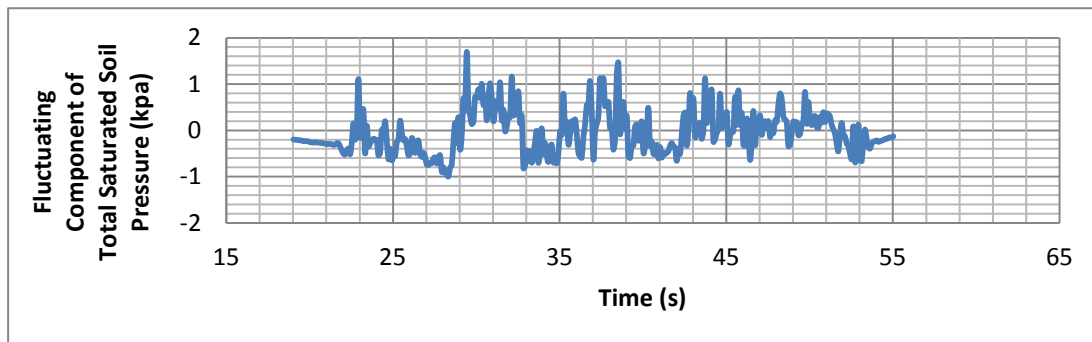


Figure G59: Fluctuating components of total saturated soil pressures for SP3 for 6 Hz

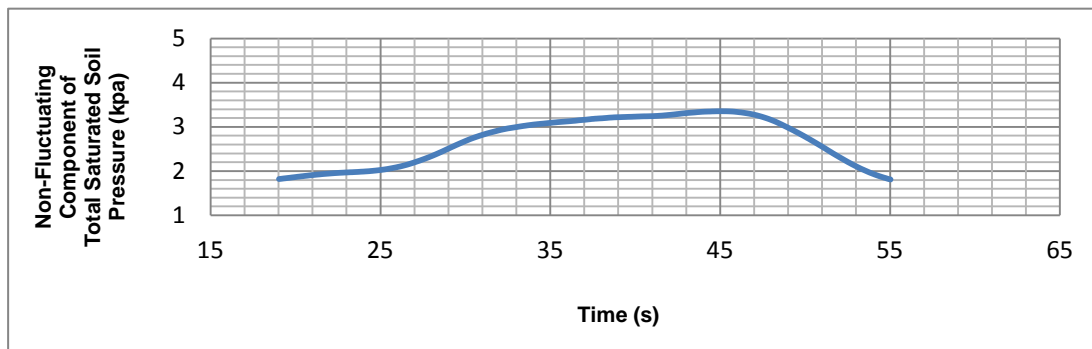


Figure G60: Non-fluctuating components of total saturated soil pressures for SP1 for 6 Hz

Fig. G61 – G64 show the total saturated soil pressures, non fluctuating and fluctuating components of total saturated soil pressures for SP4 for 6 Hz.

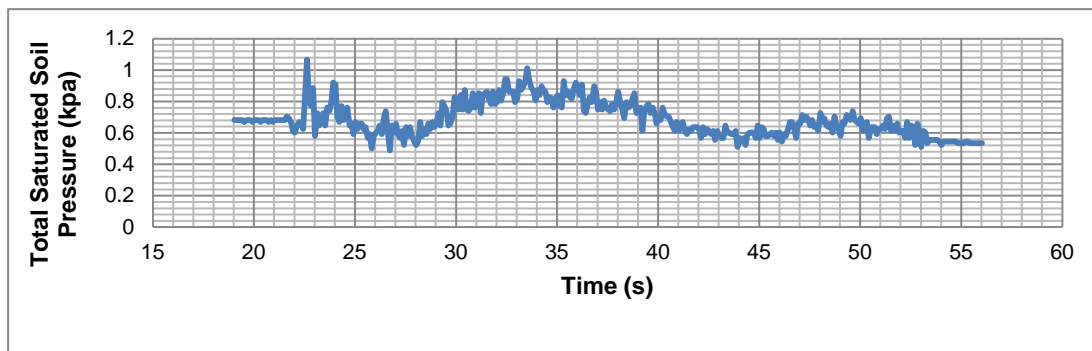


Figure G61: Total saturated soil pressure for SP4 for 6 Hz

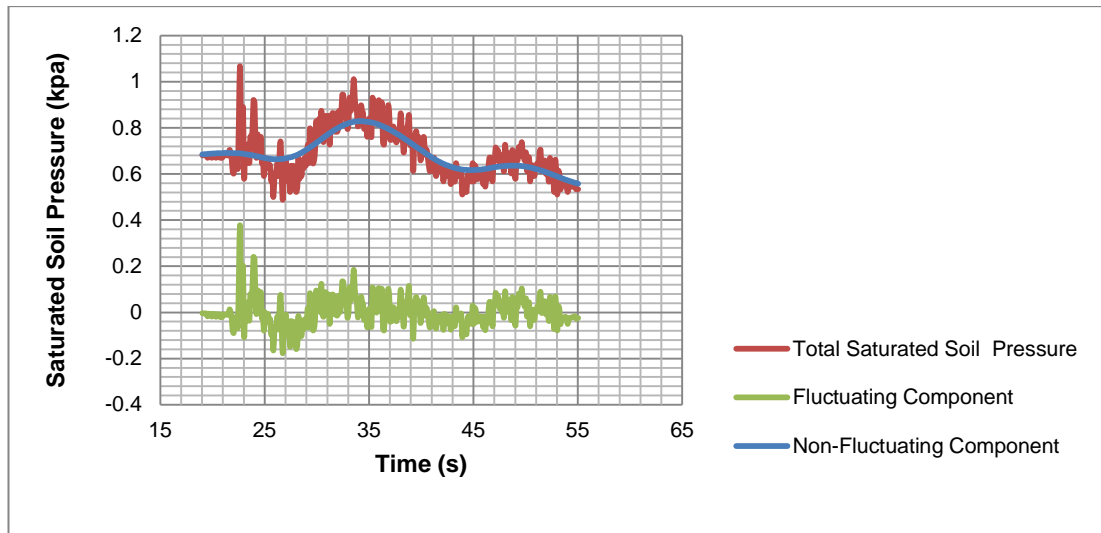


Figure G62: Total saturated soil pressure, non fluctuating and fluctuating components of total saturated soil pressure for SP3 for 6 Hz

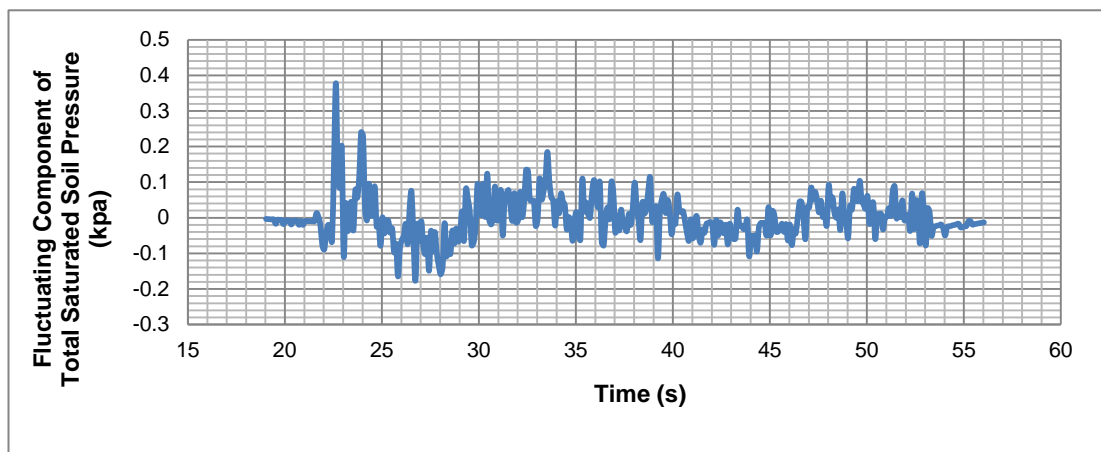


Figure G63: Fluctuating components of total saturated soil pressures for SP4 for 6 Hz

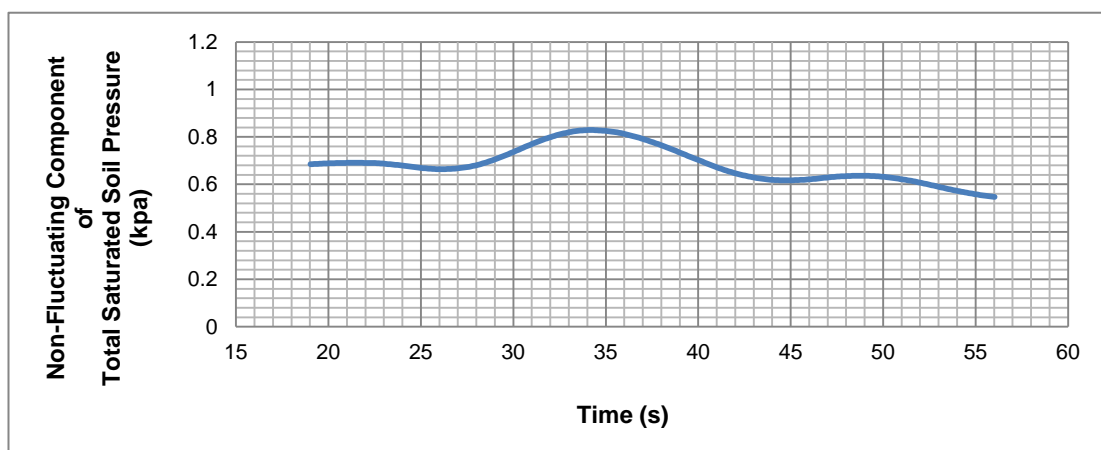


Figure G64: Non-fluctuating components of total saturated soil pressures for SP4 for 6 Hz

2. SOIL 2

2.1. Two Blocks- Fluctuating and Non-fluctuating Components of Total Saturated Soil Pressure for 4 Hz for Soil 2

Fig. G65 – G112 show the total saturated soil pressure, non fluctuating and fluctuating components of total saturated soil pressure for SP1 for 4 Hz.

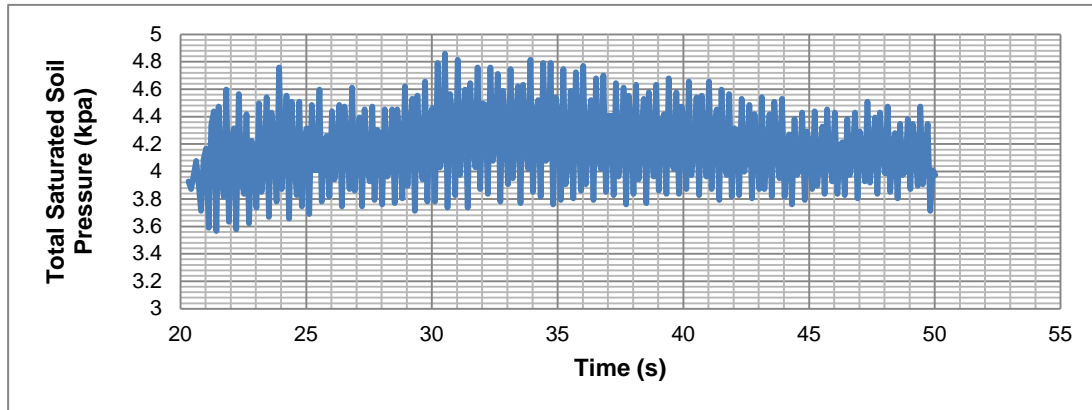


Figure G65: Total saturated soil pressure for SP1 for 4 Hz

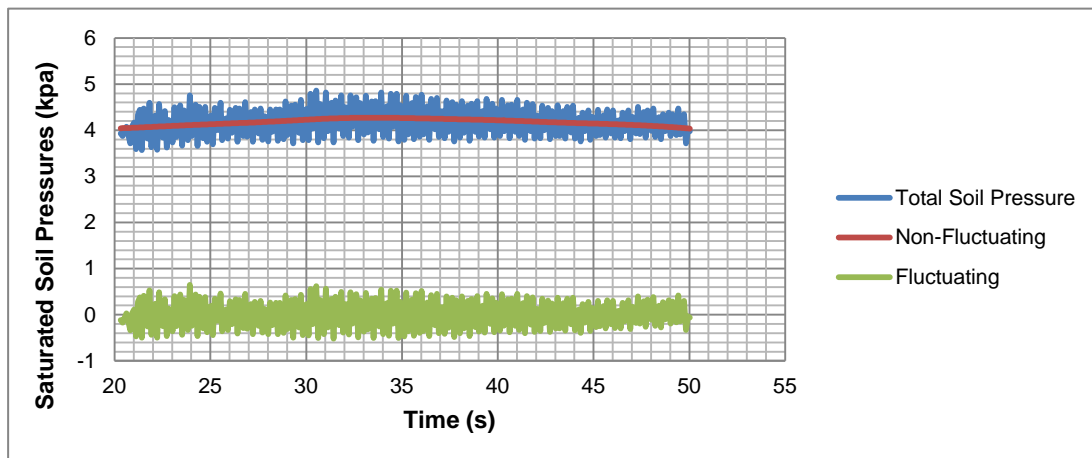


Figure G66: Total saturated soil pressure, non fluctuating and fluctuating components of total saturated soil pressure for SP1 for 4 Hz

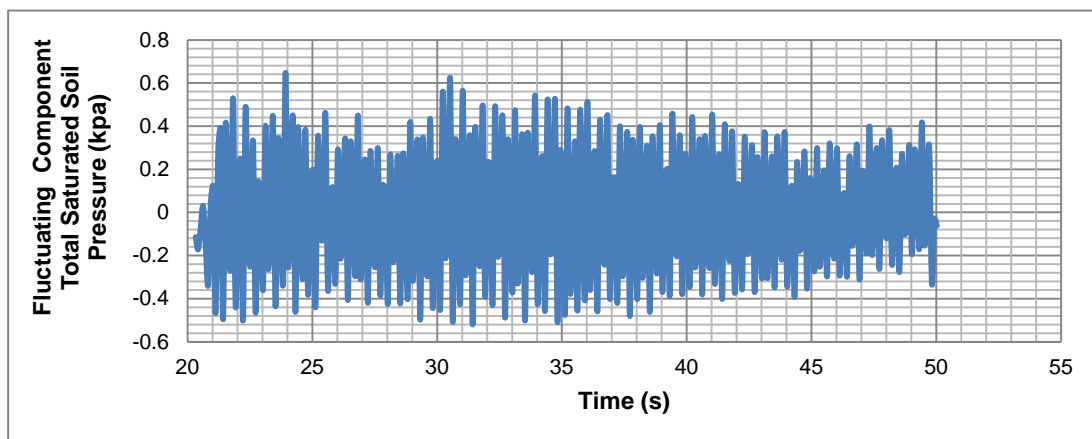


Figure G67: Fluctuating components of total saturated soil pressures for SP1 for 4 Hz

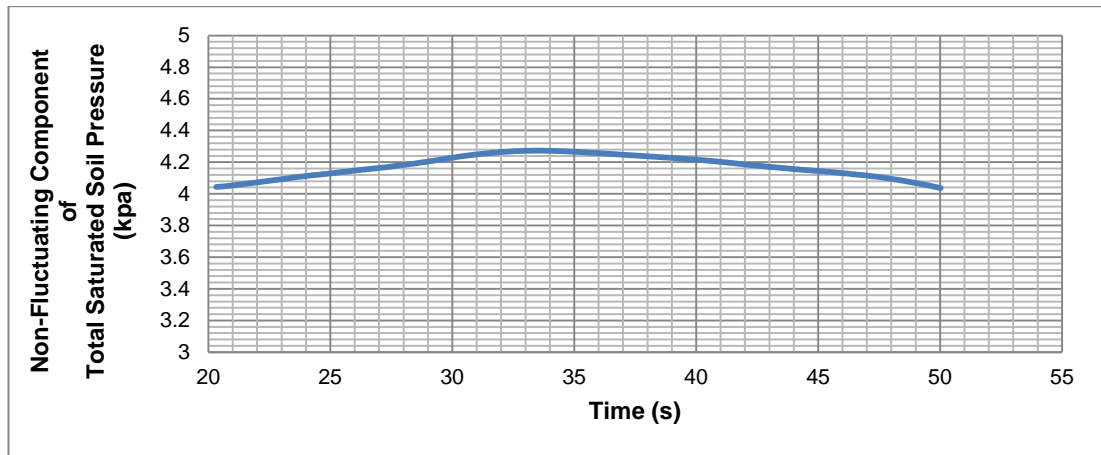


Figure G68: Non fluctuating components of total saturated soil pressures for SP1 for 4 Hz

Fig. G69 – G72 show the total saturated soil pressure, non fluctuating and fluctuating components of total saturated soil pressure for **SP2 for 4 Hz**.

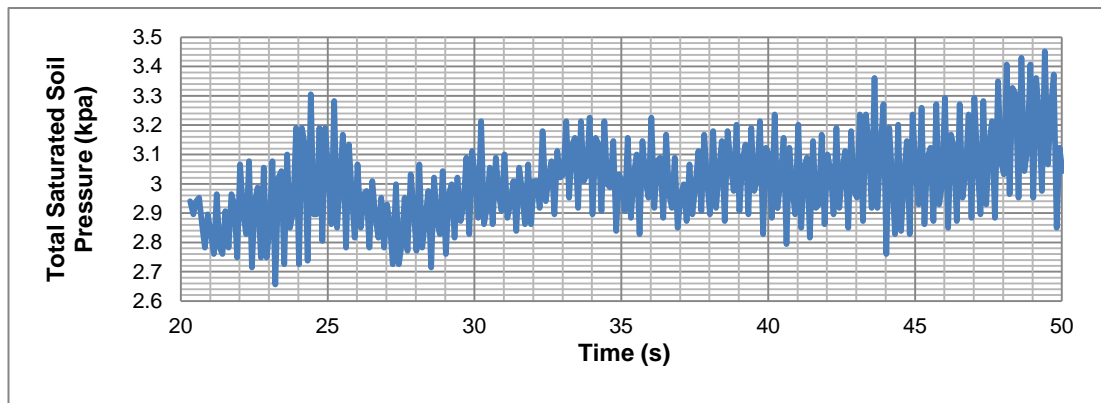


Figure G69: Total saturated soil pressure for SP2 for 2 Hz

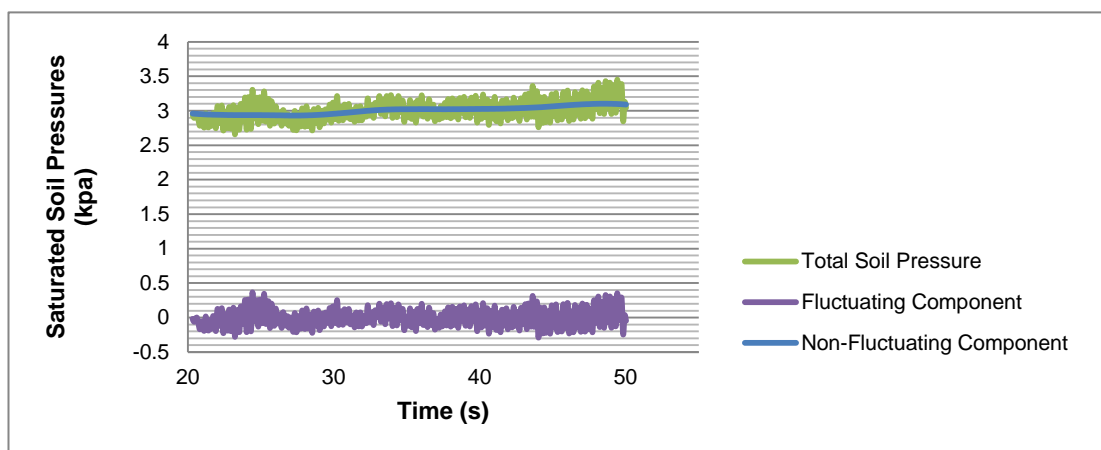


Figure G70: Total saturated soil pressure, non fluctuating and fluctuating components of total saturated soil pressure for SP2 for 4 Hz

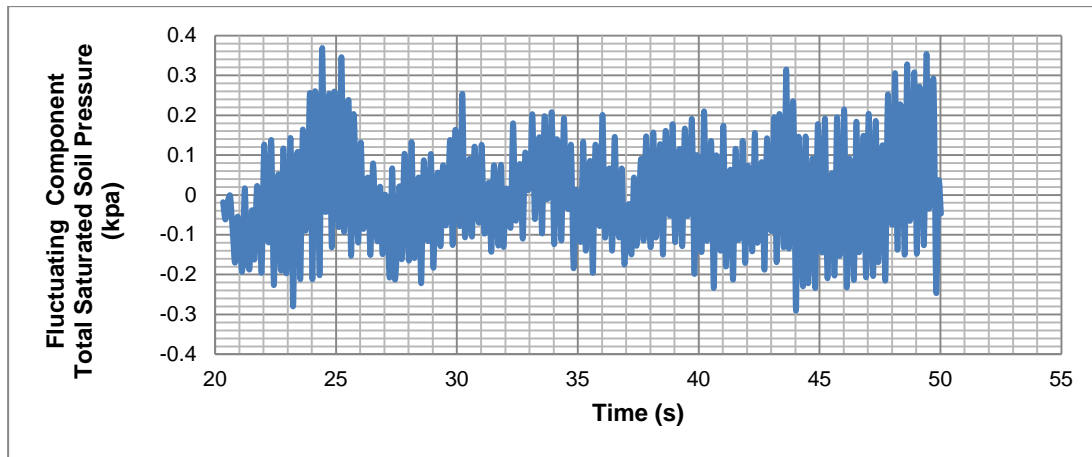


Figure G71: Fluctuating components of total saturated soil pressures for SP2 for 4 Hz

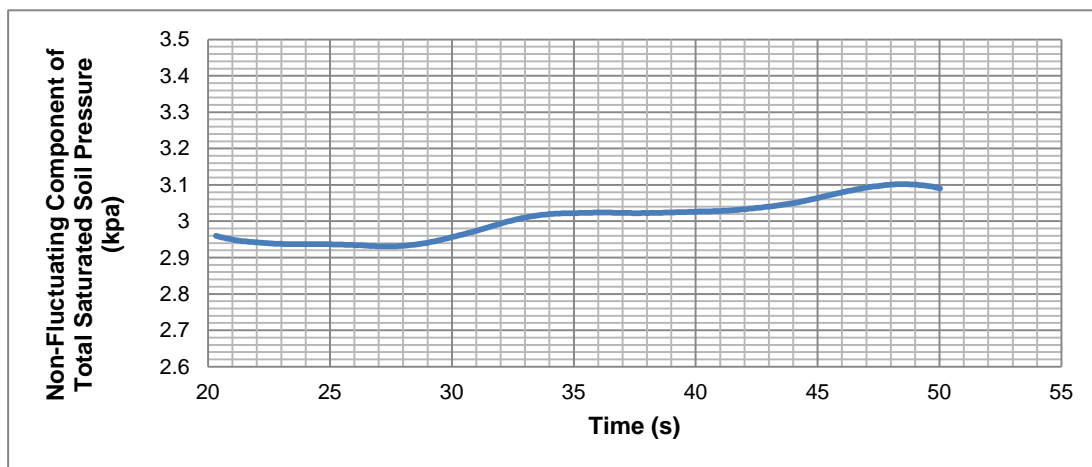


Figure G72: Non fluctuating components of total saturated soil pressures for SP2 for 4 Hz

Fig. G73 – G76 show the total saturated soil pressures, non fluctuating and fluctuating components of total saturated soil pressures for SP3 for 4 Hz.

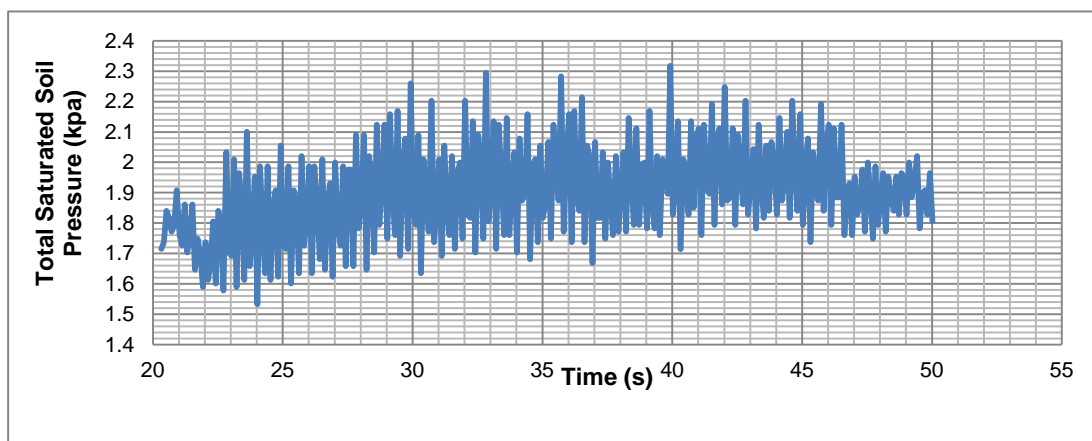


Figure G73: Total saturated soil pressure for SP3 for 4 Hz

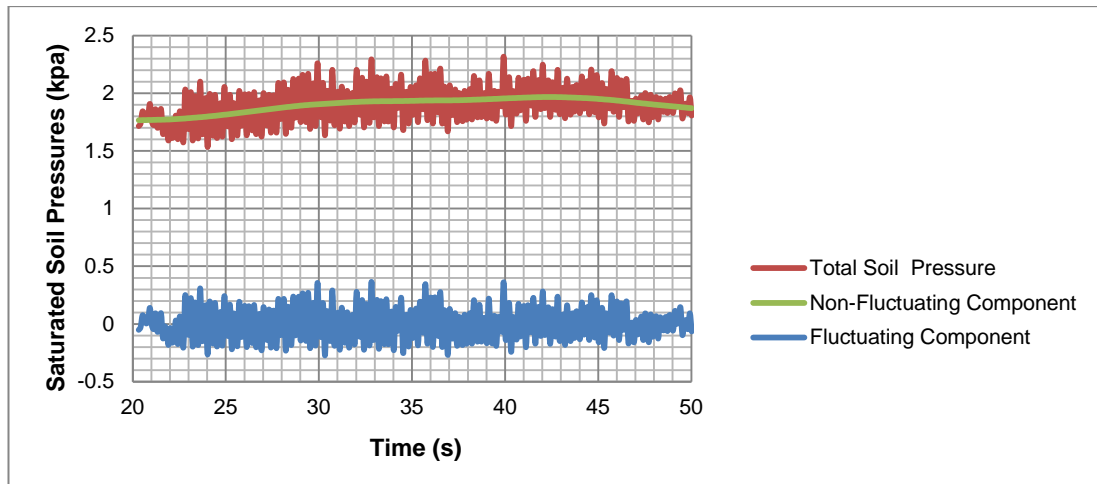


Figure G74: Total saturated soil pressure, non fluctuating and fluctuating components of total saturated soil pressure for SP3 for 4 Hz

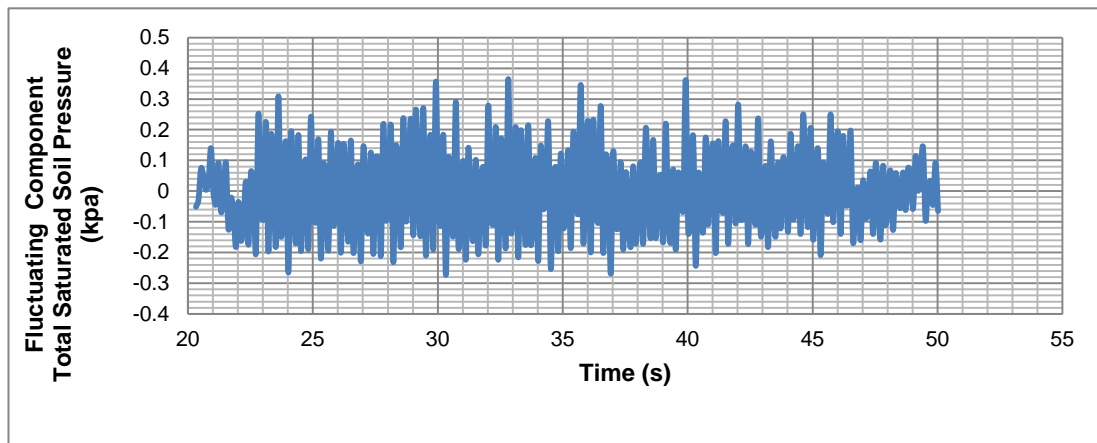


Figure G75: Fluctuating components of total saturated soil pressures for SP3 for 4 Hz

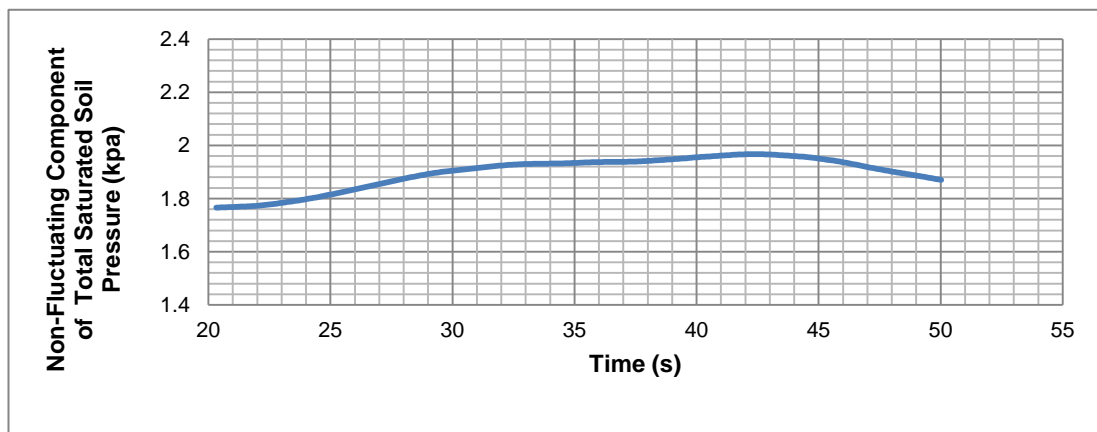


Figure G76: Non fluctuating components of total saturated soil pressures for SP3 for 4 Hz

Fig. G77 – G80 show the total saturated soil pressures, non fluctuating and fluctuating components of total saturated soil pressures for **SP4 for 4Hz.**

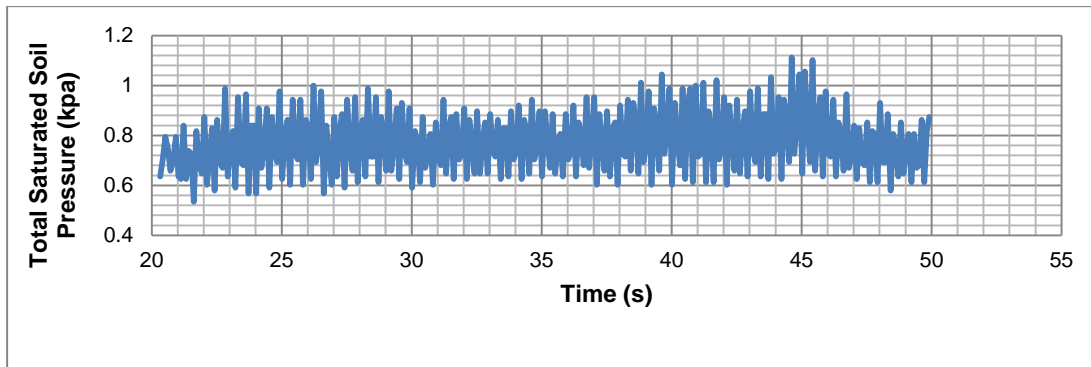


Figure G77: Total saturated soil pressure for SP4 for 4 Hz

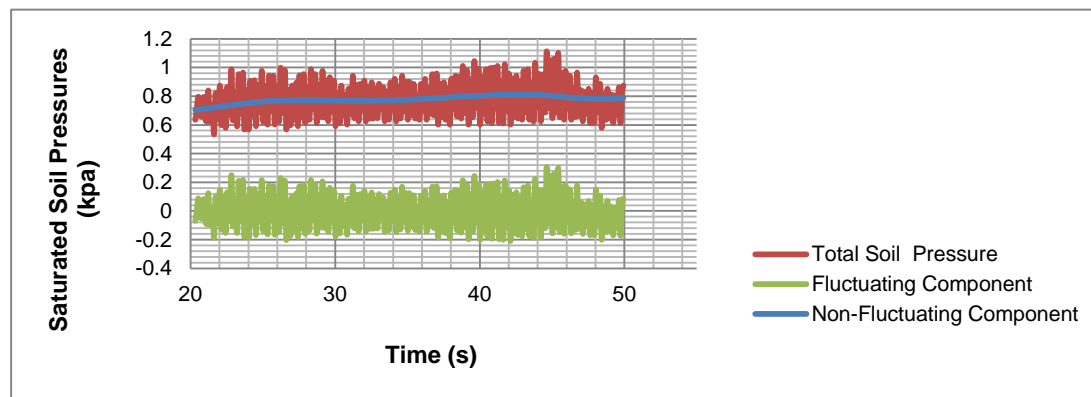


Figure G78: Total saturated soil pressure, non fluctuating and fluctuating components of total saturated soil pressure for SP4 for 4 Hz

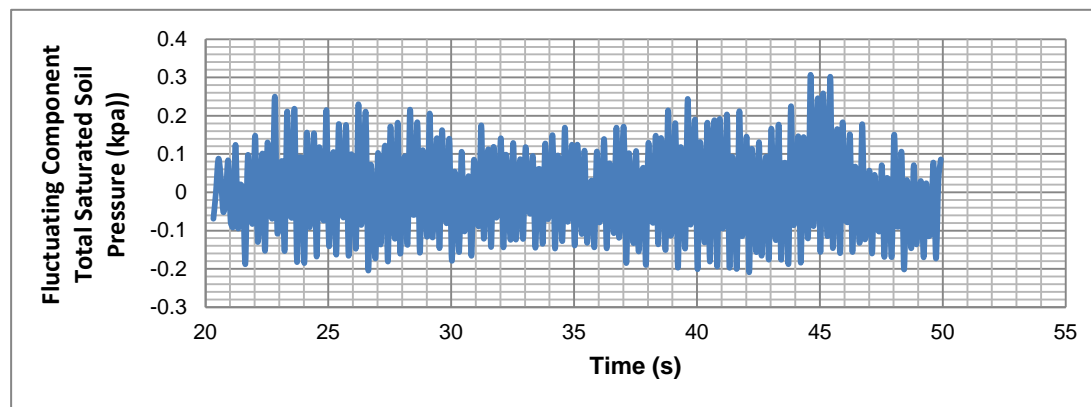


Figure G79: Fluctuating components of total saturated soil pressures for SP4 for 4 Hz

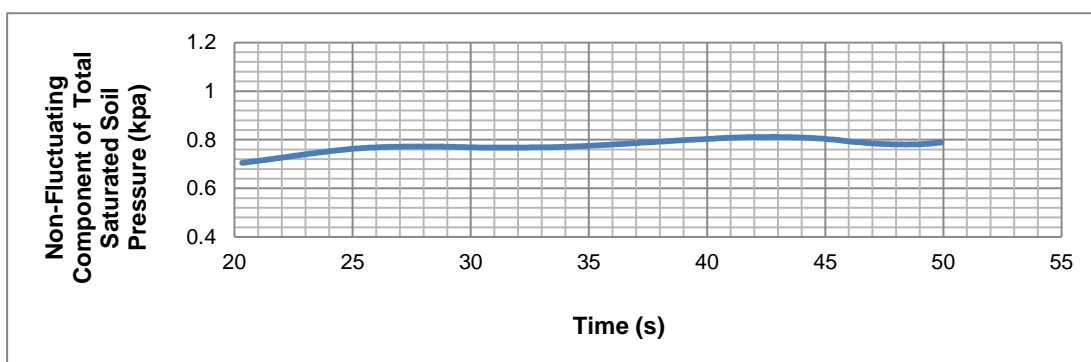


Figure G80: Non fluctuating components of total saturated soil pressures for SP4 for 4 Hz

2.2. Two Blocks- Fluctuating and Non-Fluctuating Components of Total Soil Pressure for 5 Hz for Soil 2

Fig. G81 – G84 show the total saturated soil pressures, non fluctuating and fluctuating components of total saturated soil pressures for **SP1 for 5 Hz**.

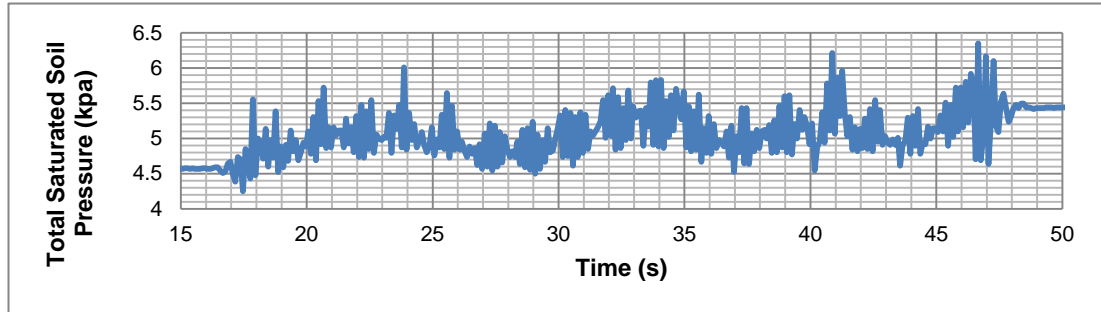


Figure G81: Total saturated soil pressure for SP1 for 5 Hz

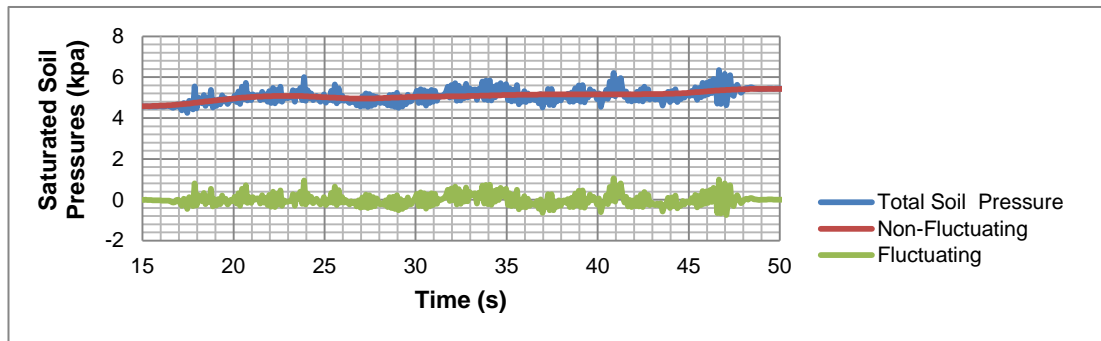


Figure G82: Total saturated soil pressure, non fluctuating and fluctuating components of total saturated soil pressure for SP1 for 5 Hz

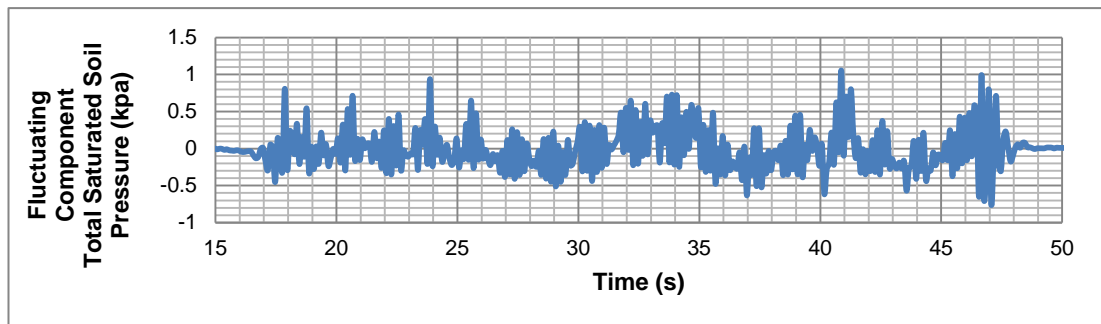


Figure G83: Fluctuating components of total saturated soil pressures for SP1 for 5 Hz

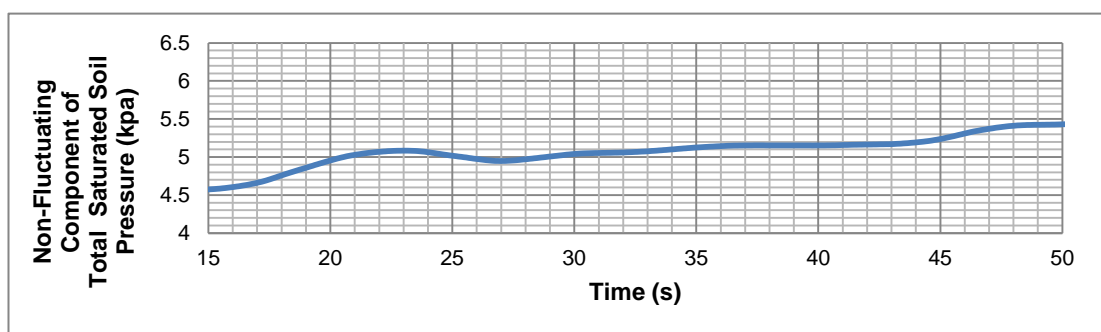


Figure G84: Non fluctuating components of total saturated soil pressures for SP1 for 5 Hz

Fig. G85 – G.88 show the total saturated soil pressures, non fluctuating and fluctuating components of total saturated soil pressures for SP2 for 5 Hz.

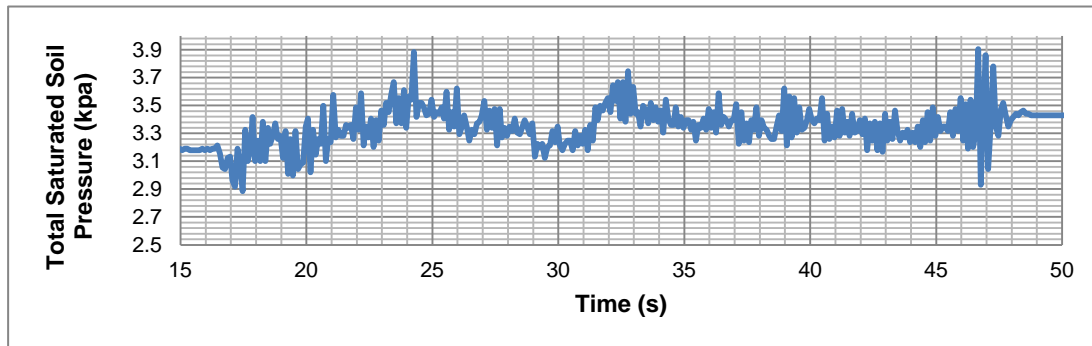


Figure G85: Total saturated soil pressure for SP2 for 5 Hz

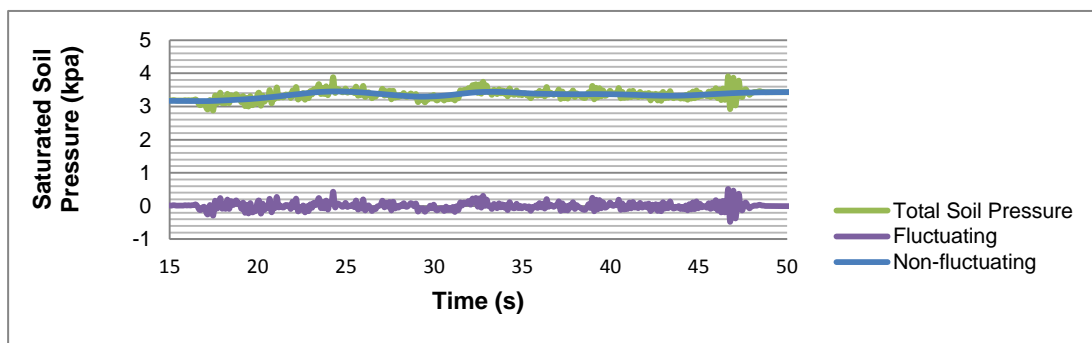


Figure G86: Total saturated soil pressure, non fluctuating and fluctuating components of total saturated soil pressure for SP2 for 5 Hz

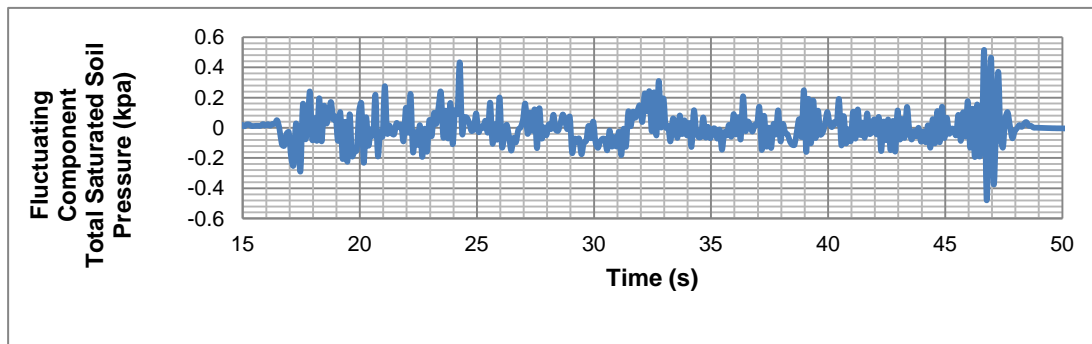


Figure G87: Fluctuating components of total saturated soil pressures for SP2 for 5 Hz

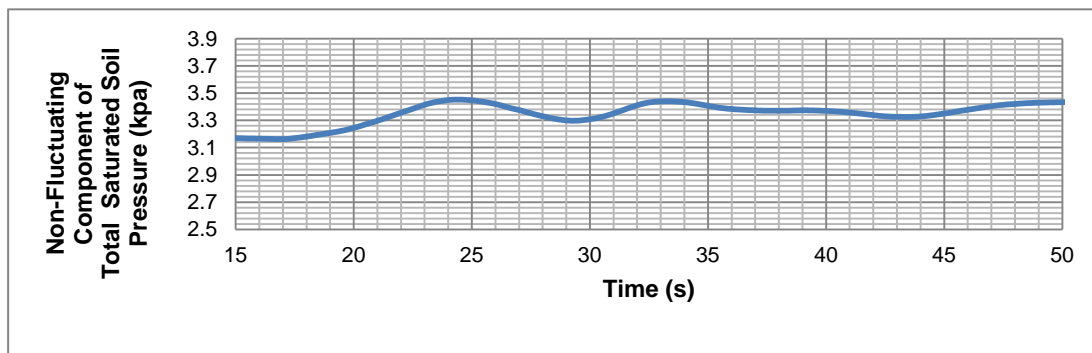


Figure G88: Non fluctuating components of total saturated soil pressures for SP2 for 5 Hz

Fig. G89 – G92 show the total saturated soil pressures, non fluctuating and fluctuating components of total saturated soil pressures for SP3 for 5 Hz.

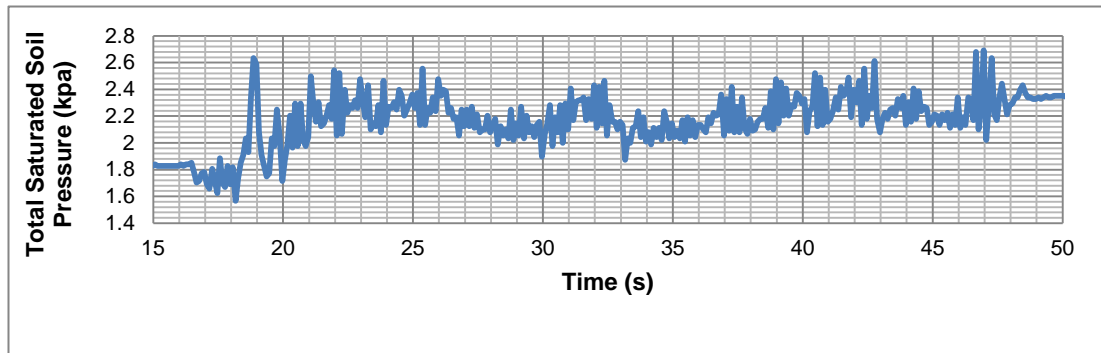


Figure G89: Total saturated soil pressure for SP3 for 5 Hz

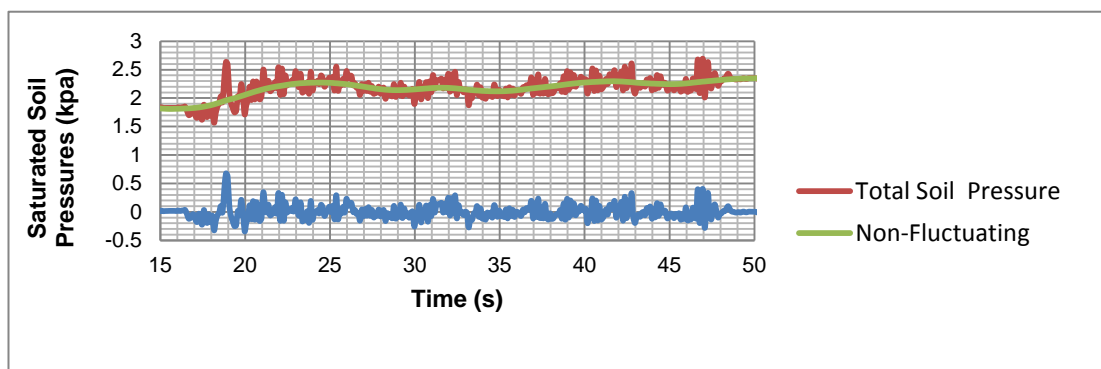


Figure G90: Total saturated soil pressure, non fluctuating and fluctuating components of total saturated soil pressure for SP3 for 5 Hz

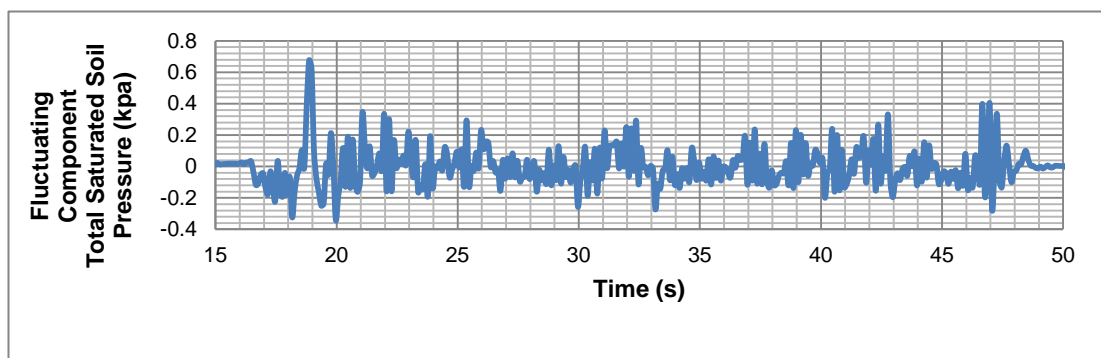


Figure G91: Fluctuating components of total saturated soil pressures for SP3 for 5 Hz

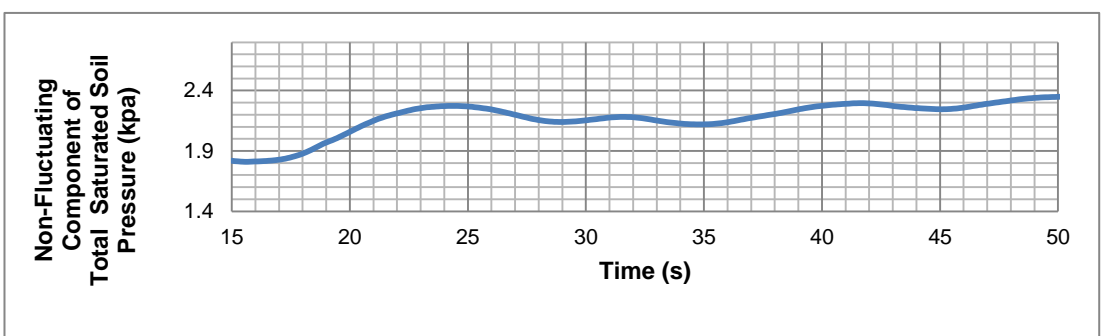


Figure G92: Non fluctuating components of total saturated soil pressures for SP3 for 5 Hz

Fig. G.93 - G96 show the total saturated soil pressures, non fluctuating and fluctuating components of total saturated soil pressures for SP4 for 5 Hz.

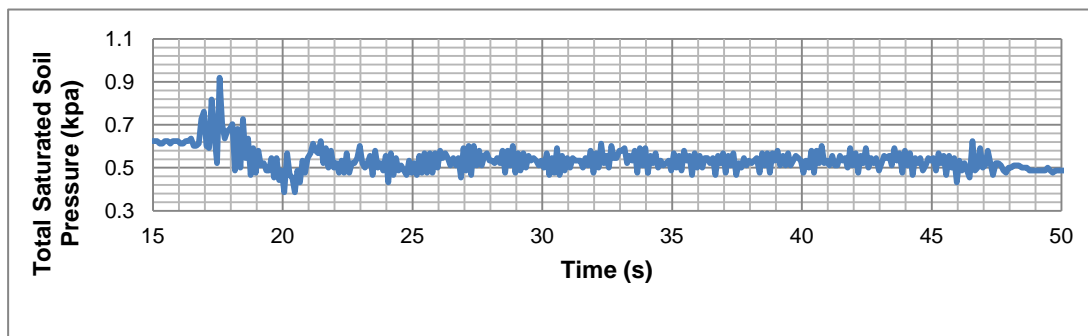


Figure G.93: Total saturated soil pressure for SP4 for 5 Hz

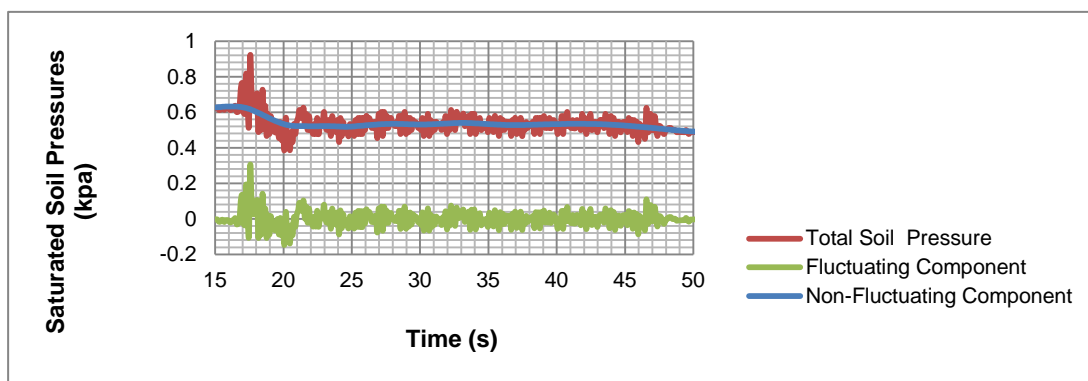


Figure G.94: Total saturated soil pressure, non fluctuating and fluctuating components of total saturated soil pressure for SP4 for 5 Hz

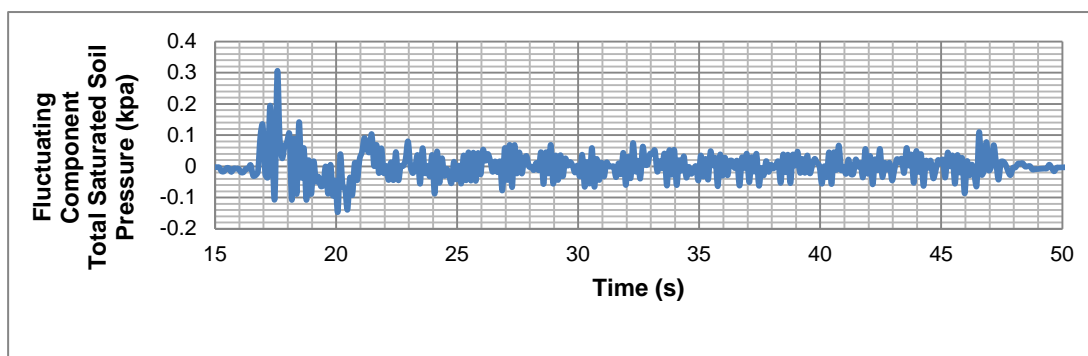


Figure G.95: Fluctuating components of total saturated soil pressures for SP4 for 4 Hz

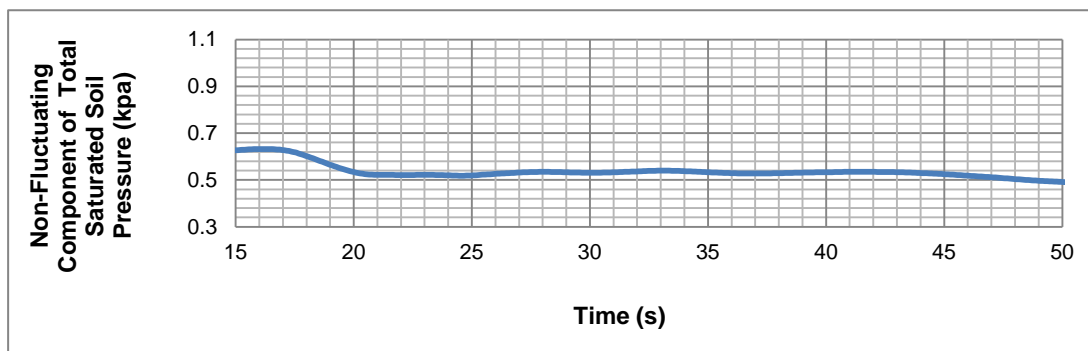


Figure G.96: Non fluctuating components of total saturated soil pressures for SP4 for 5 Hz

2.3. Two Blocks- Fluctuating and Non-fluctuating Components of Total Saturated Soil Pressure for 6 Hz for Soil 2

Fig. G.97 – G.100 show the total saturated soil pressures, non fluctuating and fluctuating components of total saturated soil pressures for **SP1 for 6 Hz**.

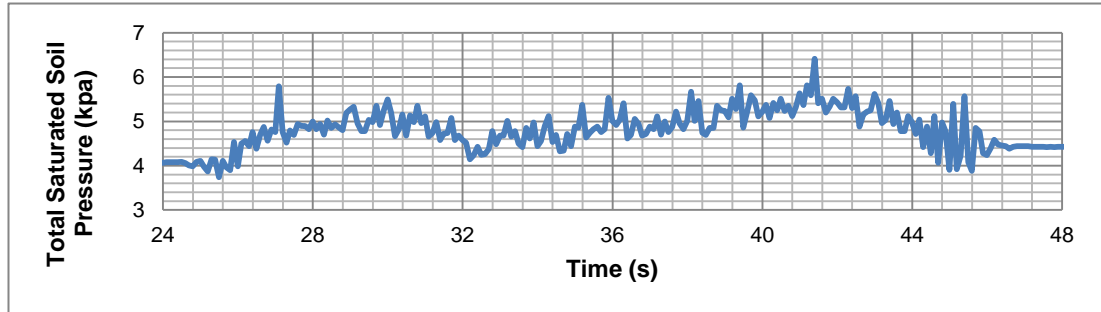


Figure G.97: Total saturated soil pressure for SP4 for 5 Hz

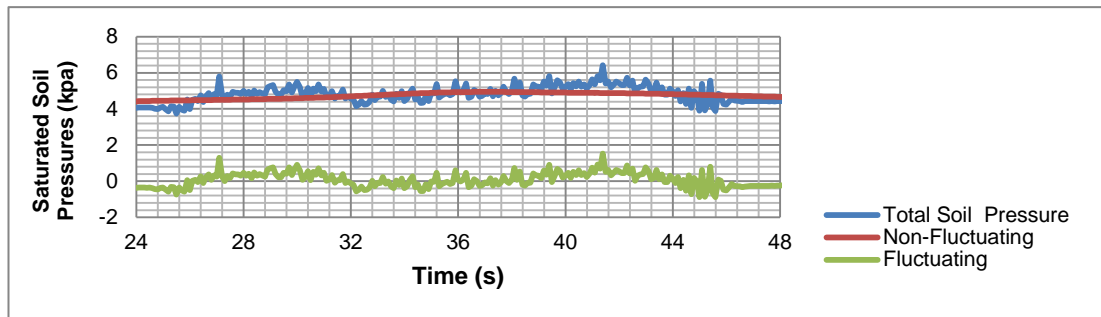


Figure G.98: Total saturated soil pressure, non fluctuating and fluctuating components of total saturated soil pressure for SP1 for 6 Hz

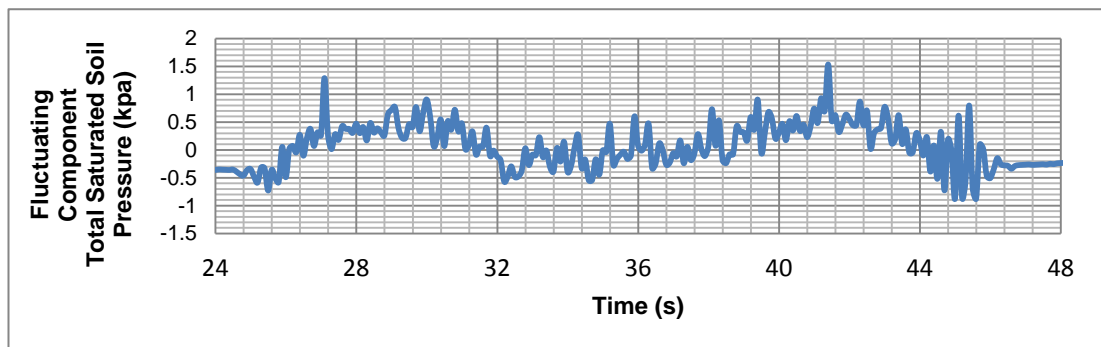


Figure G.99: Fluctuating components of total saturated soil pressures for SP1 for 6 Hz

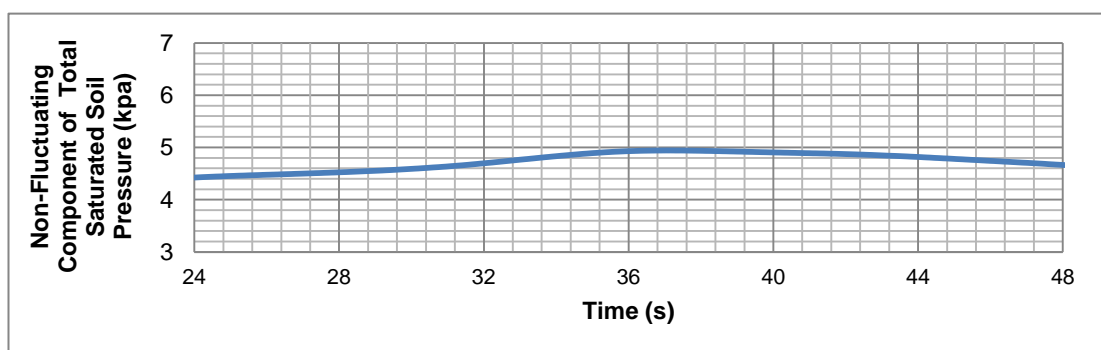


Figure G.100: Non fluctuating components of total saturated soil pressures for SP1 for 6 Hz

Fig. G.101 - 104 show the total saturated soil pressures, non fluctuating and fluctuating components of total saturated soil pressures for SP2 for 6 Hz.

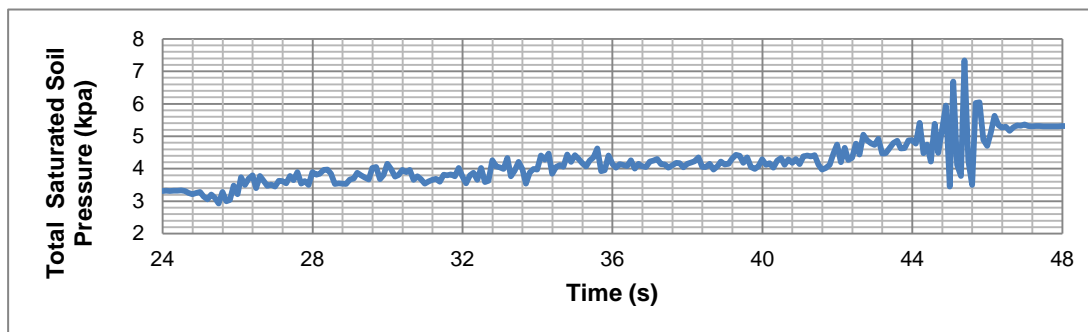


Figure G.101: Total saturated soil pressure for SP1 for 6 Hz

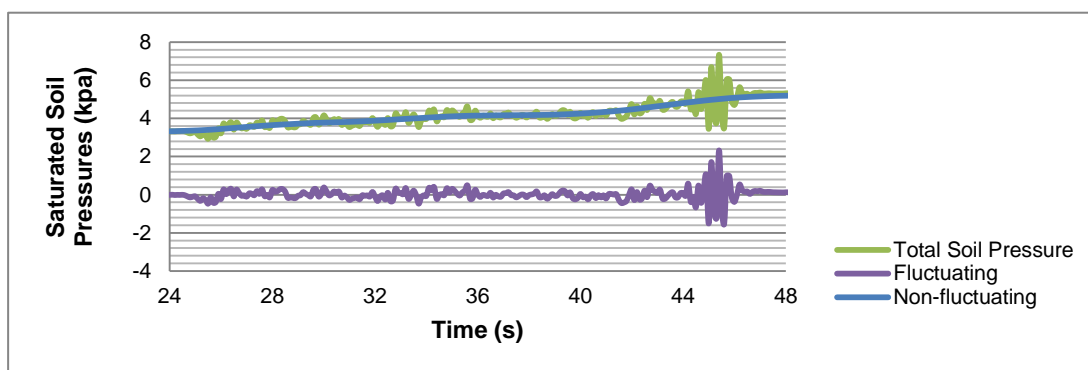


Figure G.102: Total saturated soil pressure, non fluctuating and fluctuating components of total saturated soil pressure for SP2 for 6 Hz

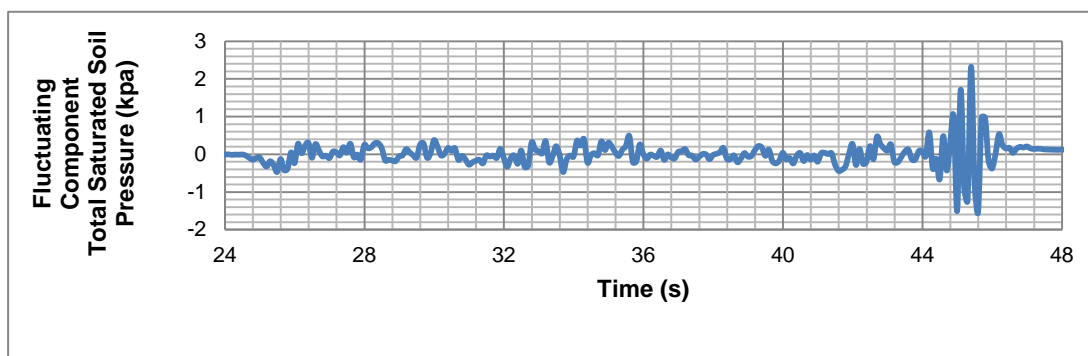


Figure G.103: Fluctuating components of total saturated soil pressures for SP2 for 6 Hz

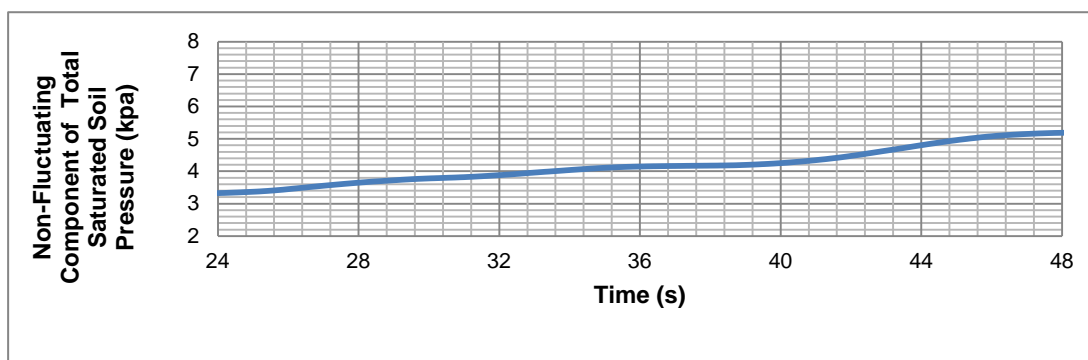


Figure G.104: Non fluctuating components of total saturated soil pressures for SP2 for 6 Hz

Fig. G105 – G108 show the total saturated soil pressures, non fluctuating and fluctuating components of total saturated soil pressures for SP3 for 6 Hz.

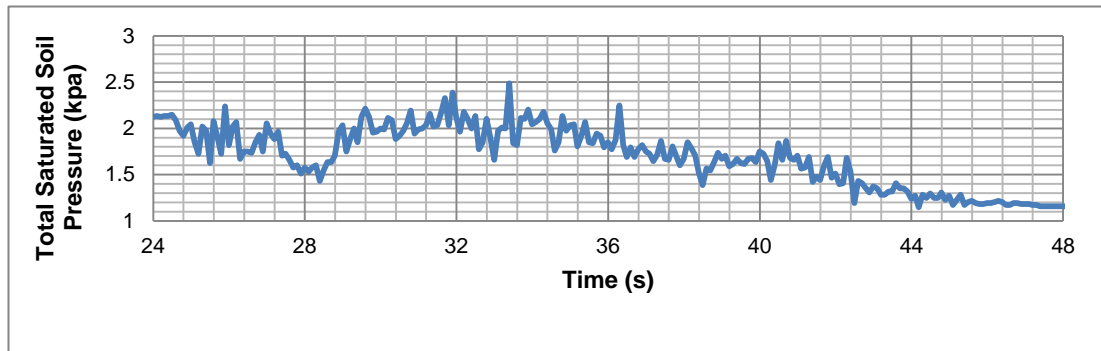


Figure G105: Total saturated soil pressure for SP3 for 6 Hz

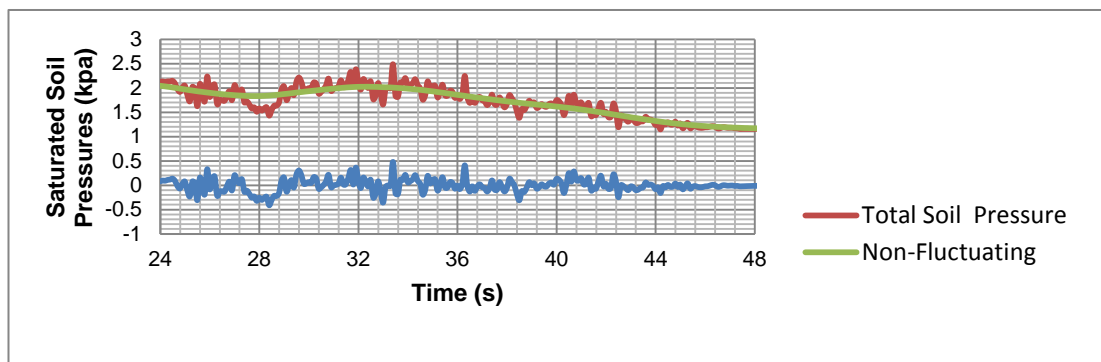


Figure G106: Total saturated soil pressure, non fluctuating and fluctuating components of total saturated soil pressure for SP3 for 6 Hz

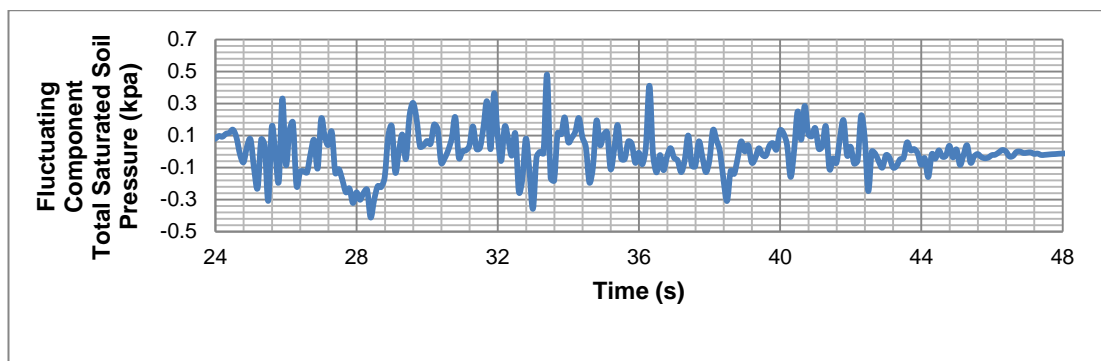


Figure G107: Fluctuating components of total saturated soil pressures for SP3 for 6 Hz

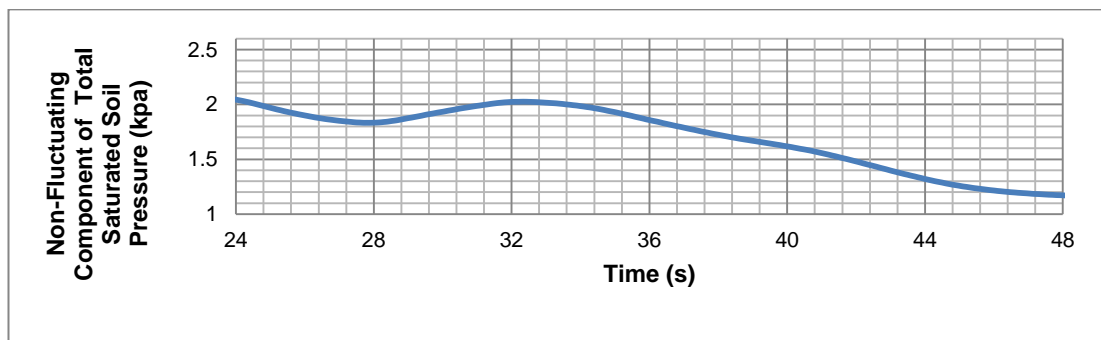


Figure G108: Non-fluctuating components of total saturated soil pressures for SP3 for 6 Hz

Fig. G109 – G112 show the total saturated soil pressures, non fluctuating and fluctuating components of total saturated soil pressures for SP4 for 6 Hz.

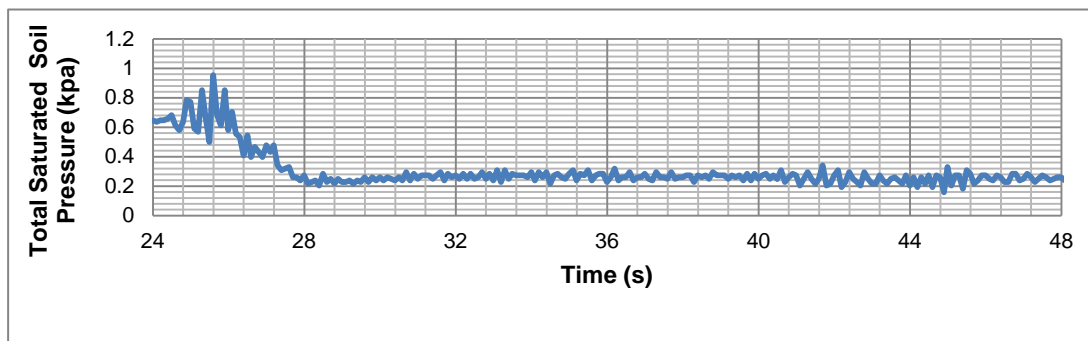


Figure G109: Total saturated soil pressure for SP4 for 6 Hz

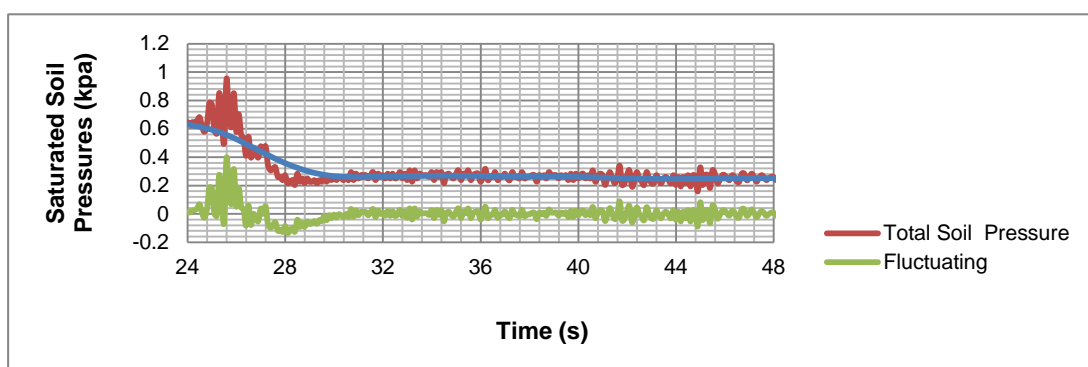


Figure G110: Total saturated soil pressure, non fluctuating and fluctuating components of total saturated soil pressure for SP4 for 6 Hz

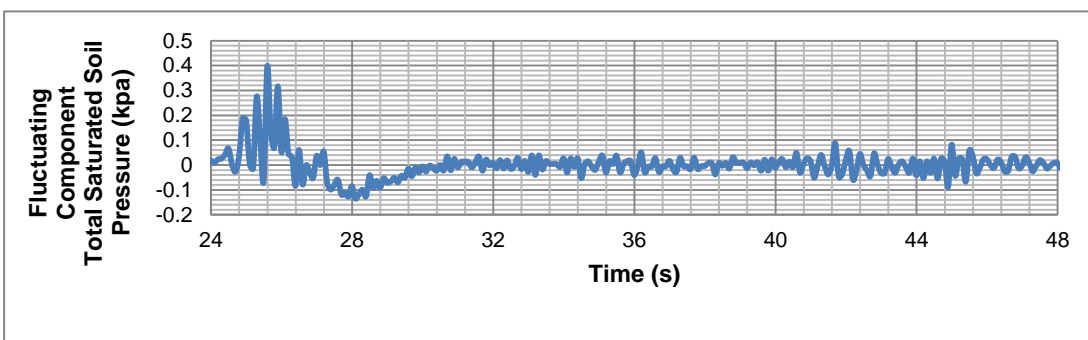


Figure G111: Fluctuating components of total saturated soil pressures for SP4 for 6 Hz

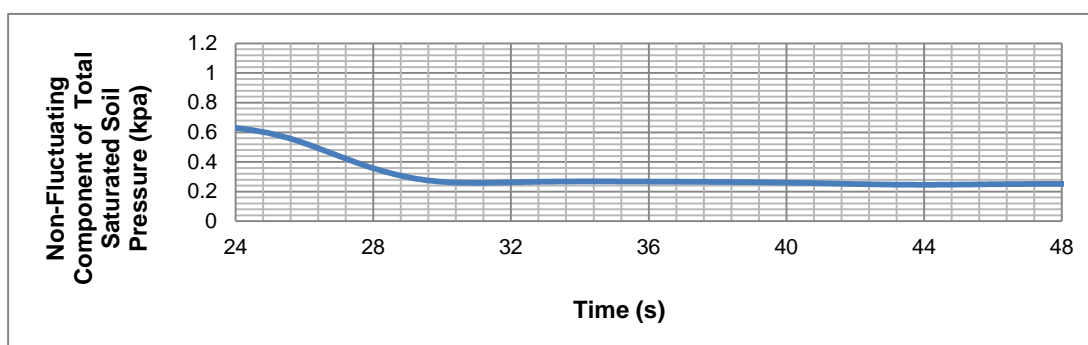


Figure G112: Non-fluctuating components of total saturated soil pressures for SP4 for 6 Hz

APPENDIX H

THREE BLOCKS: FLUCTUATING AND NON-FLUCTUATING COMPONENTS

By using MathCAD software program, these components were computed and total saturated soil pressures, fluctuating and non-fluctuating components of total saturated soil pressures are shown between Figure H1- Figure G112 for 3, 4, 5 and 6 Hz for Soil 1 and 3, 4, 5 Hz for Soil 2.

2. SOIL 1

1.1. Three Blocks- Fluctuating and Non-fluctuating Components of Total Saturated Soil Pressure for 3 Hz for Soil 1

Figure H1 – Figure H4 show the total saturated soil pressure, non fluctuating and fluctuating components of total saturated soil pressure for SP1 for 3 Hz.

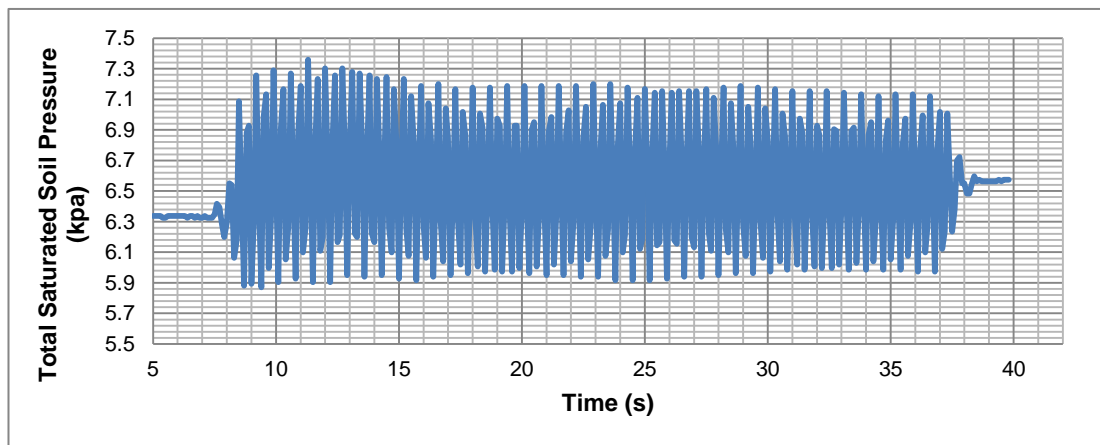


Figure H1: Total saturated soil pressure for SP1 for 3 Hz

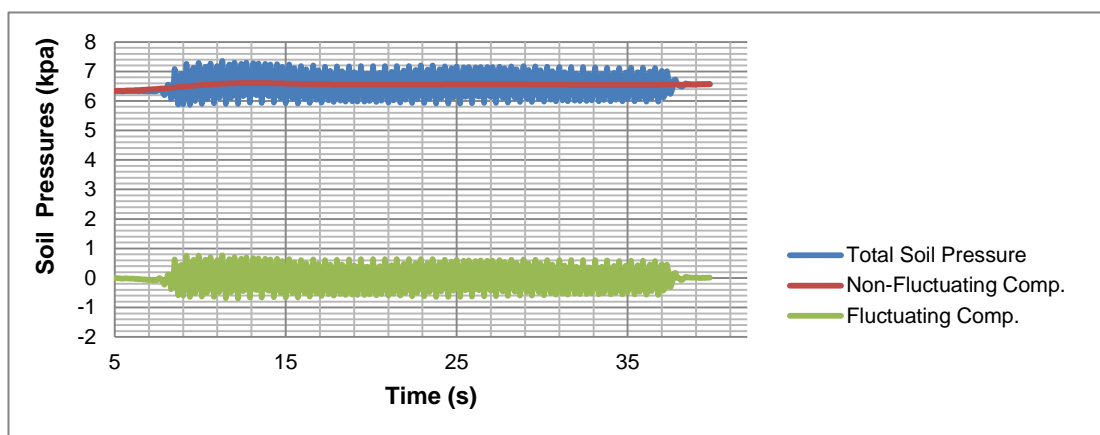


Figure H2: Total saturated soil pressure, non fluctuating and fluctuating components of total saturated soil pressure for SP1 for 3 Hz

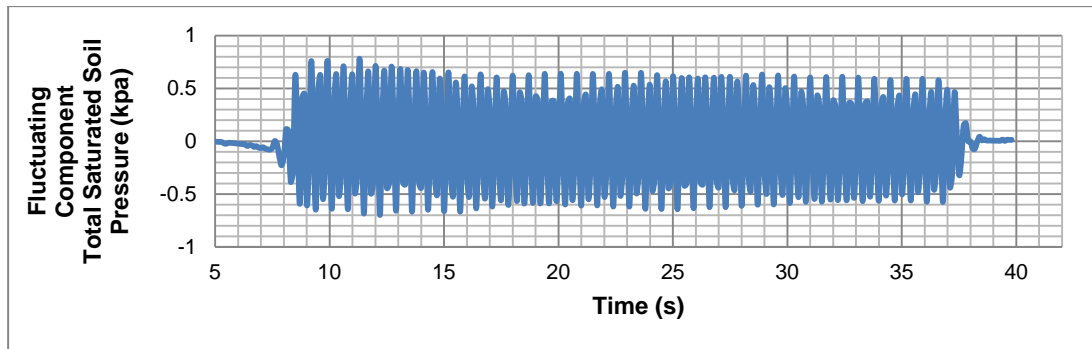


Figure H3: Fluctuating components of total saturated soil pressures for SP1 for 3 Hz

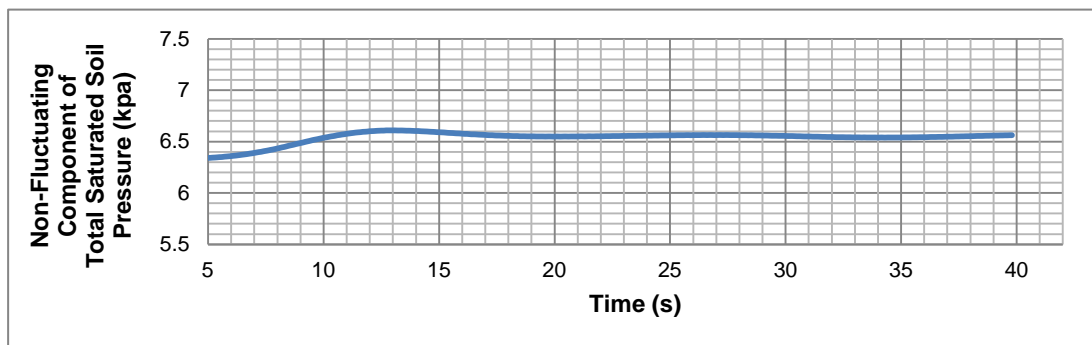


Figure H.4: Non fluctuating components of total saturated soil pressures for SP1 for 3 Hz

Fig. H.5 – H.8 show the total saturated soil pressure, non fluctuating and fluctuating components of total saturated soil pressure for SP2 for 3 Hz.

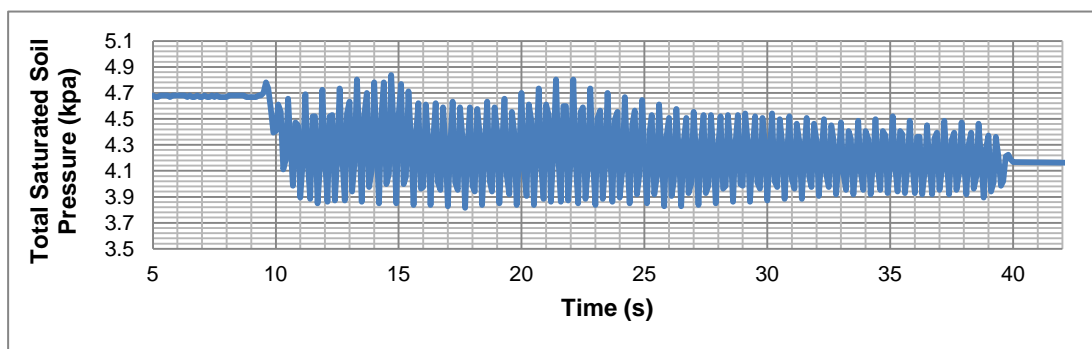


Figure H5: Total saturated soil pressure for SP2 for 3 Hz

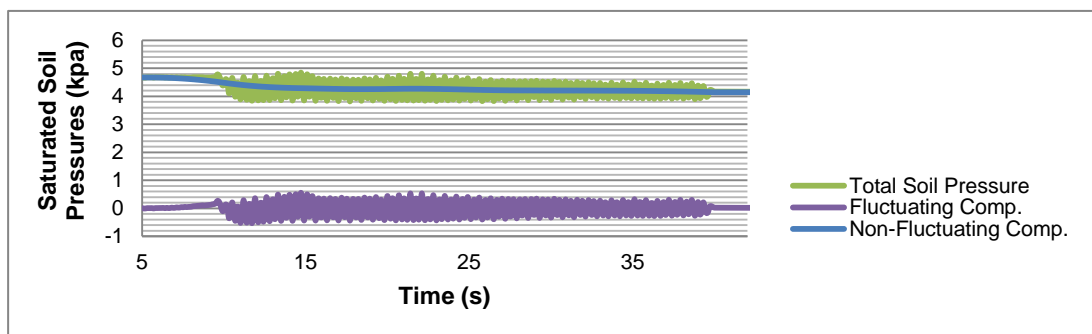


Figure H6: Total saturated soil pressure, non fluctuating and fluctuating components of total saturated soil pressure for SP2 for 3 Hz

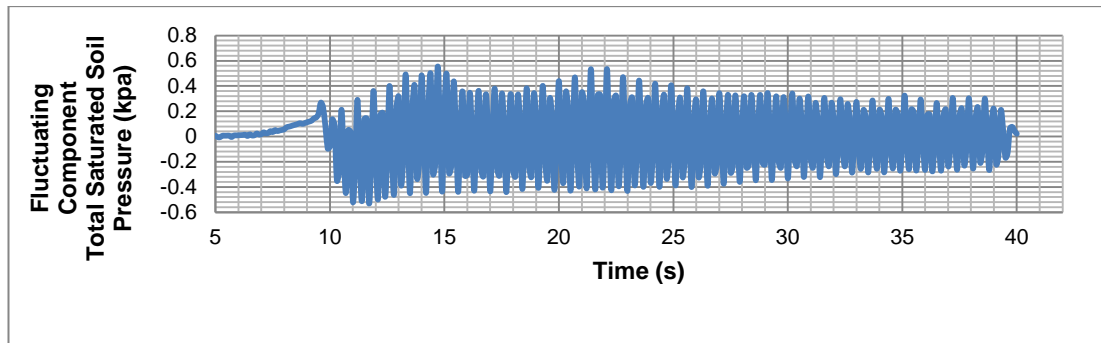


Figure H7: Fluctuating components of total saturated soil pressures for SP2 for 3 Hz

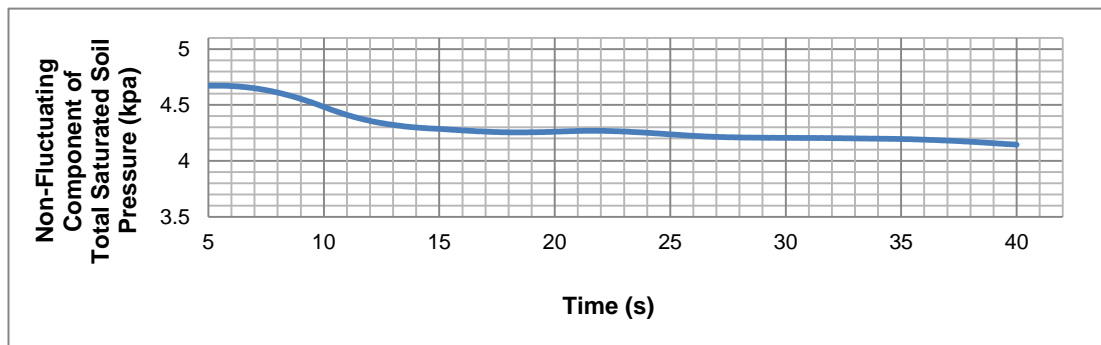


Figure H8: Fluctuating components of total saturated soil pressures for SP2 for 3 Hz

Fig. H9 – 7H12 show the total saturated soil pressure, non fluctuating and fluctuating components of total saturated soil pressure for SP3 for 3 Hz.

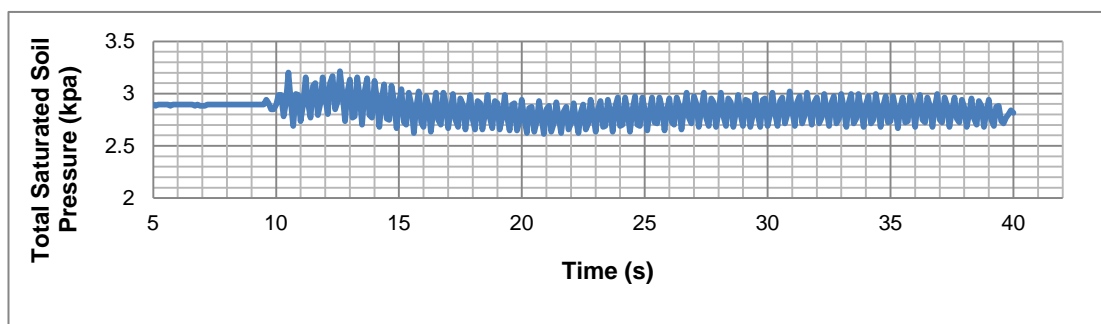


Figure H9: Total saturated soil pressure for SP3 for 3 Hz

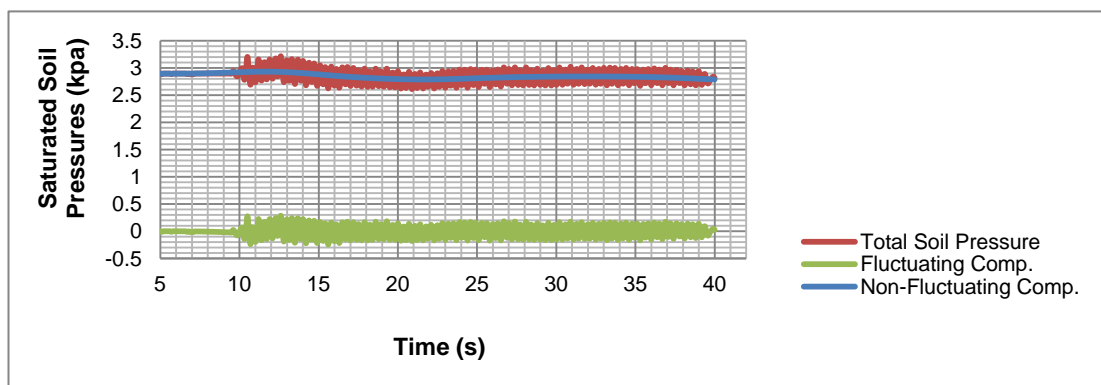


Figure H10: Total saturated soil pressure, non fluctuating and fluctuating components of total saturated soil pressure for SP3 for 3 Hz

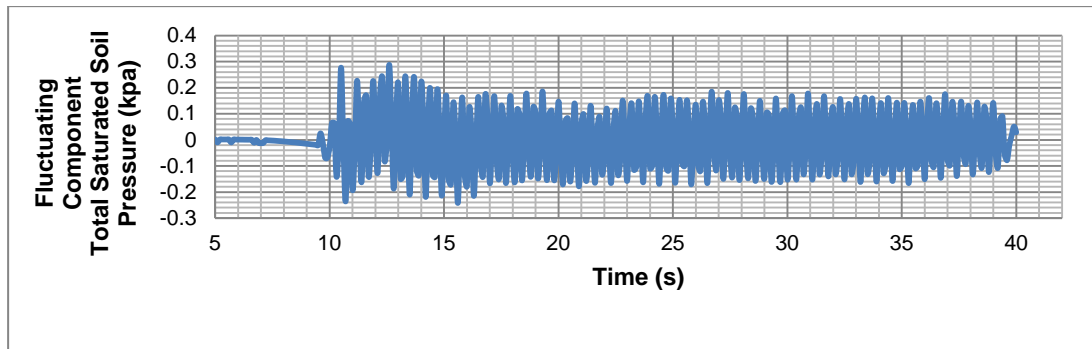


Figure H11: Fluctuating components of total saturated soil pressures for SP3 for 3 Hz

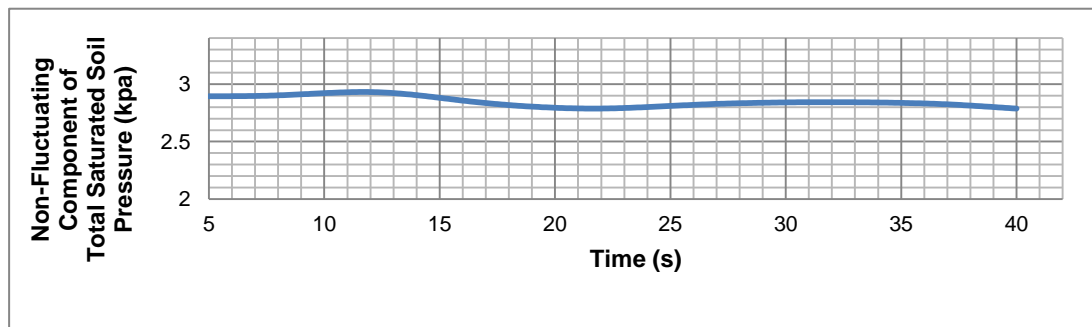


Figure H12: Non- fluctuating components of total saturated soil pressures for SP3 for 3 Hz

Fig. H13 – H16 show the total saturated soil pressure, non fluctuating and fluctuating components of total saturated soil pressure for SP4 for 3 Hz.

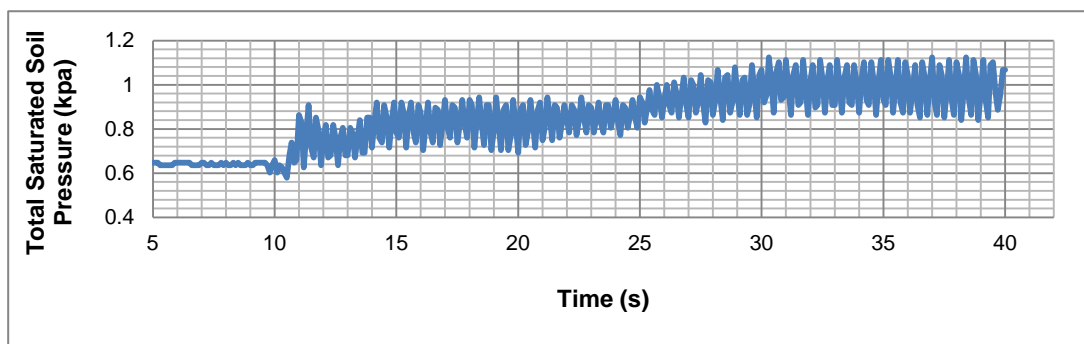


Figure H13: Total saturated soil pressure for SP4 for 3 Hz

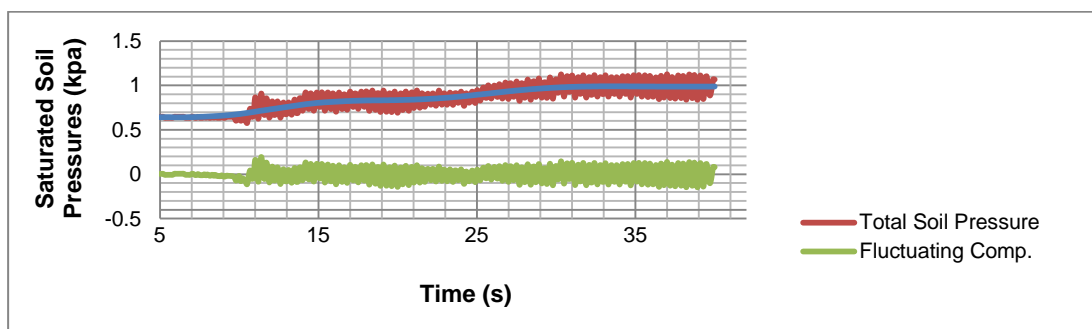


Figure H14: Total saturated soil pressure, non fluctuating and fluctuating components of total saturated soil pressure for SP1 for 3 Hz

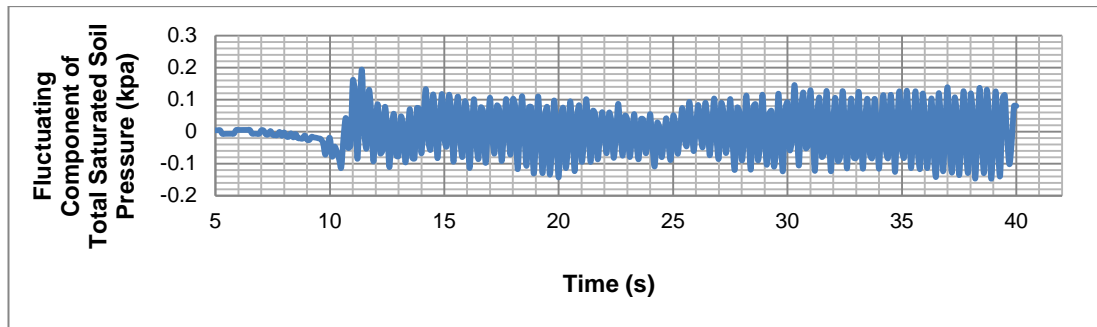


Figure H15: Fluctuating components of total saturated soil pressures for SP1 for 3 Hz

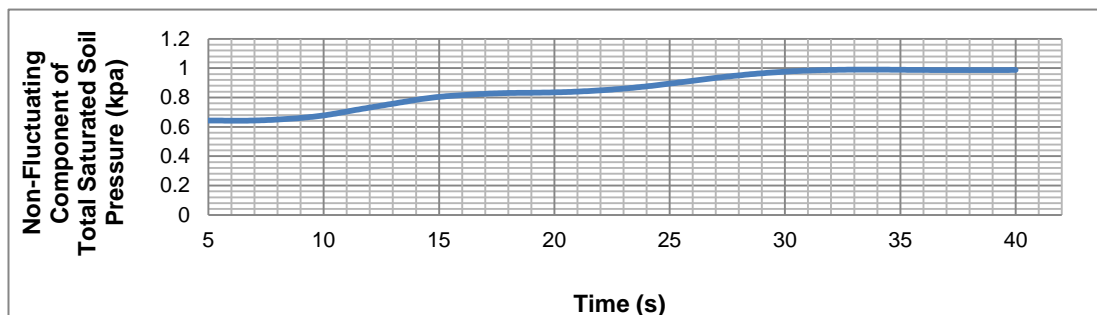


Figure H16: Non fluctuating components of total saturated soil pressures for SP1 for 3 Hz

1.2. Three Blocks- Fluctuating and Non-fluctuating Components of Total Saturated Soil Pressure for 4 Hz for Soil 1

Fig. H.17 – H.20 show the total saturated soil pressure, non fluctuating and fluctuating components of total saturated soil pressure for SP1 for 4 Hz.

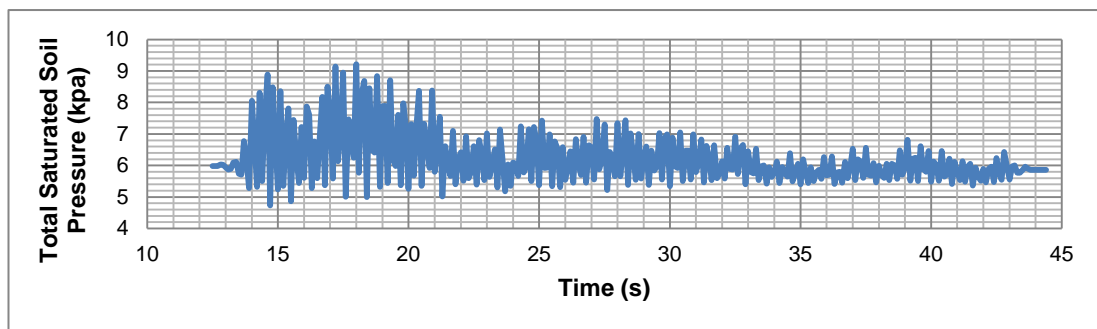


Figure H17: Total saturated soil pressure for SP1 for 4 Hz

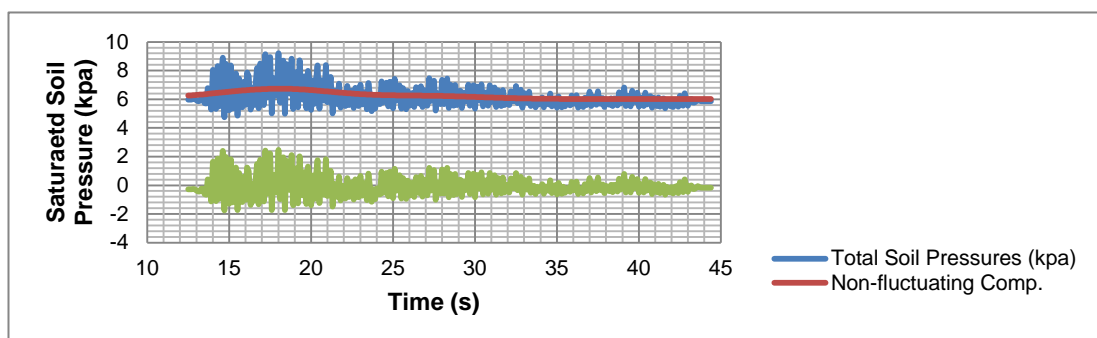


Figure H18: Total saturated soil pressure, non fluctuating and fluctuating components of total saturated soil pressure for SP1 for 4 Hz

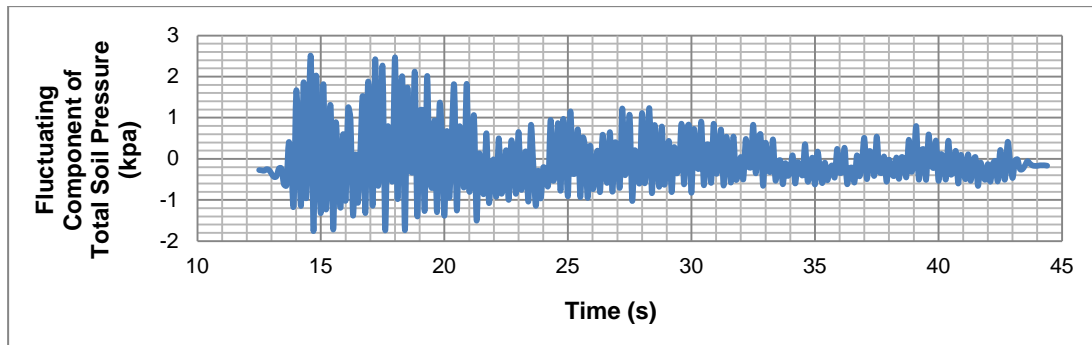


Figure H19: Fluctuating components of total saturated soil pressures for SP1 for 4 Hz

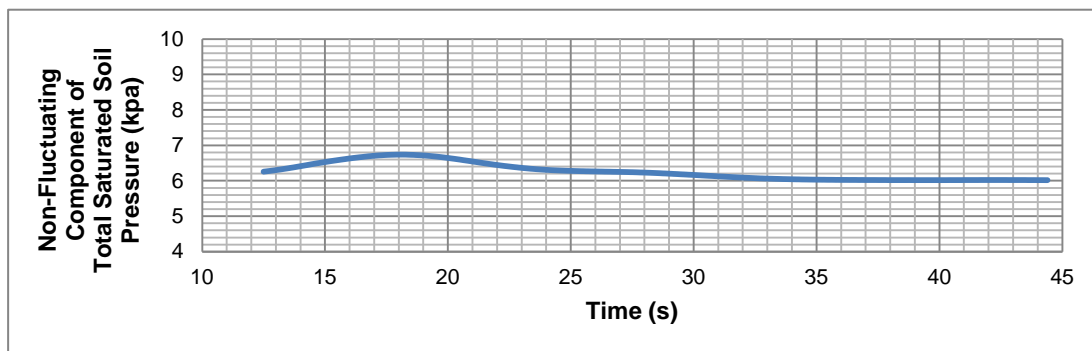


Figure H20: Non fluctuating components of total saturated soil pressures for SP1 for 4 Hz

Fig. H21 – H24 show the total saturated soil pressure, non fluctuating and fluctuating components of total saturated soil pressure for SP2 for 4 Hz.

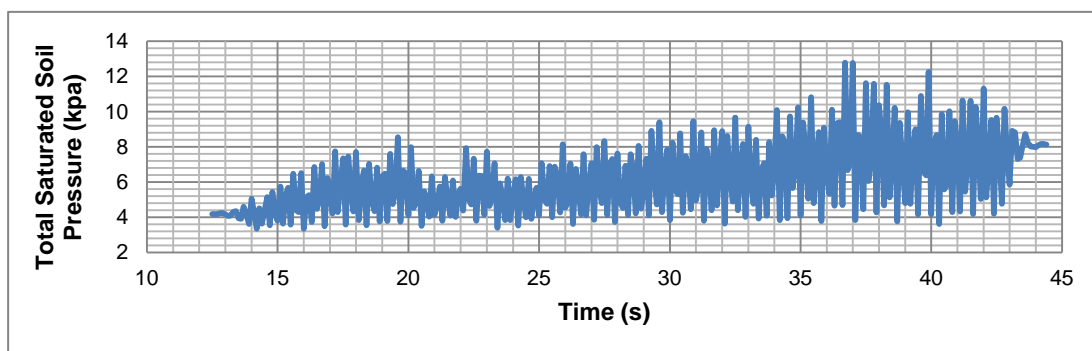


Figure H21: Total saturated soil pressure for SP2 for 4 Hz

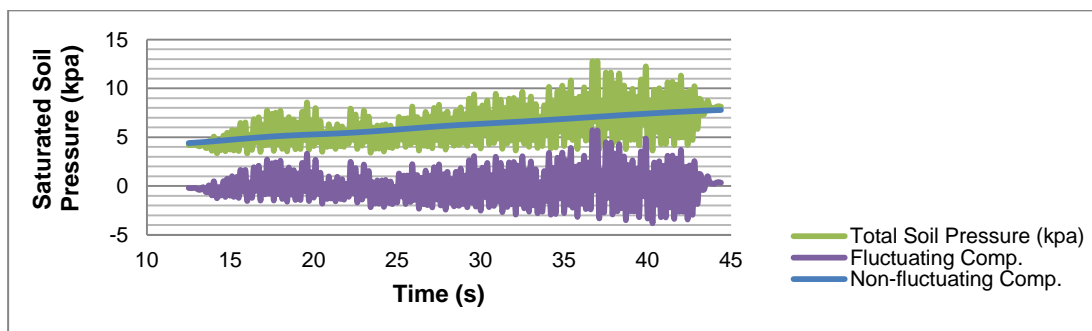


Figure H22: Total saturated soil pressure, non fluctuating and fluctuating components of total saturated soil pressure for SP2 for 4 Hz

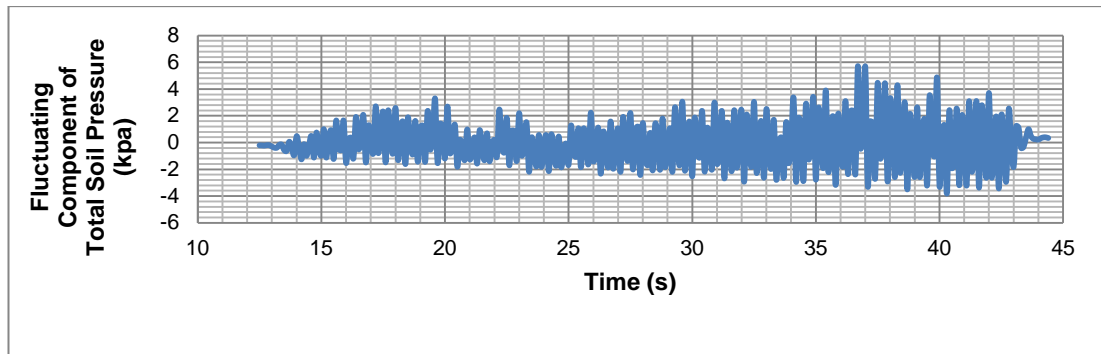


Figure H23: Fluctuating components of total saturated soil pressures for SP2 for 4 Hz

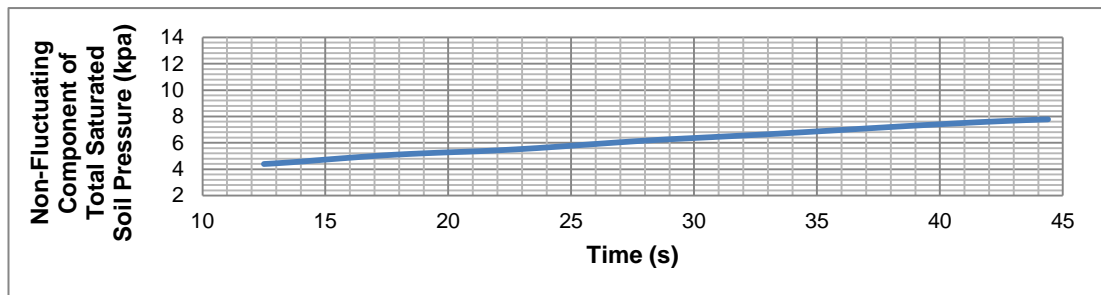


Figure H24: Non- fluctuating components of total saturated soil pressures for SP2 for 4 Hz

Fig. H25 – H28 show the total saturated soil pressure, non fluctuating and fluctuating components of total saturated soil pressure for SP3 for 4 Hz.

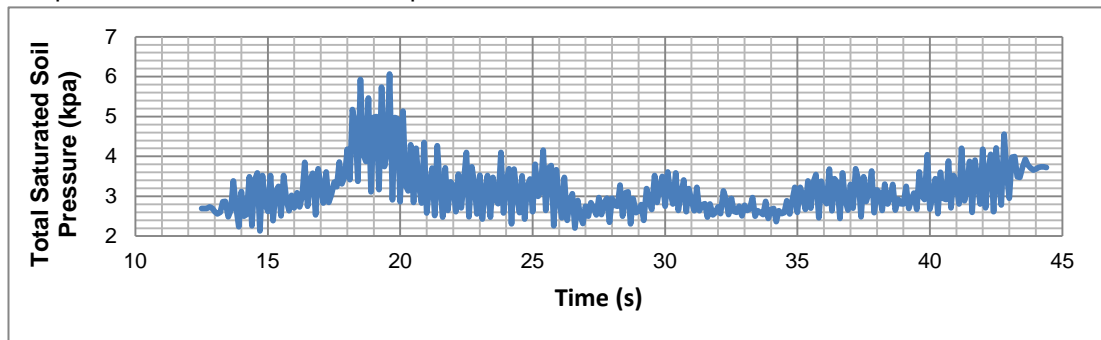


Figure H25: Total saturated soil pressure for SP2 for 4 Hz

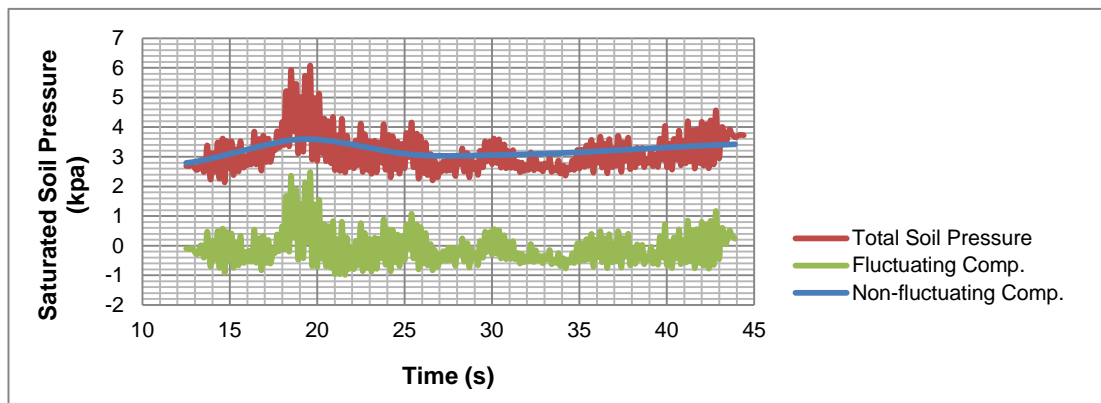


Figure H26: Total saturated soil pressure, non fluctuating and fluctuating components of total saturated soil pressure for SP3 for 4 Hz

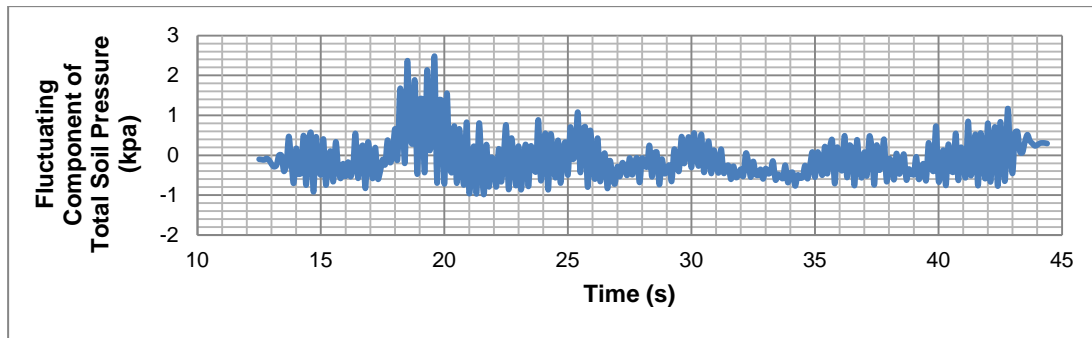


Figure H27: Fluctuating components of total saturated soil pressures for SP2 for 4 Hz

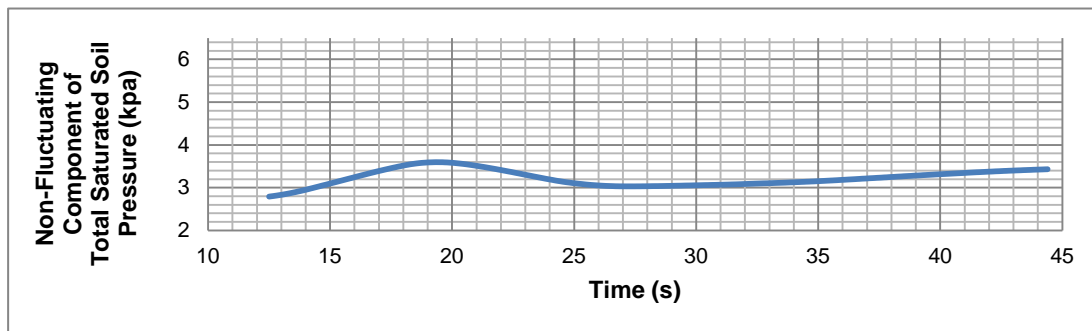


Figure H28: Non- fluctuating components of total saturated soil pressures for SP3 for 4 Hz

Fig. H29 – H32 show the total saturated soil pressure, non fluctuating and fluctuating components of total saturated soil pressure for SP4 for 4 Hz.

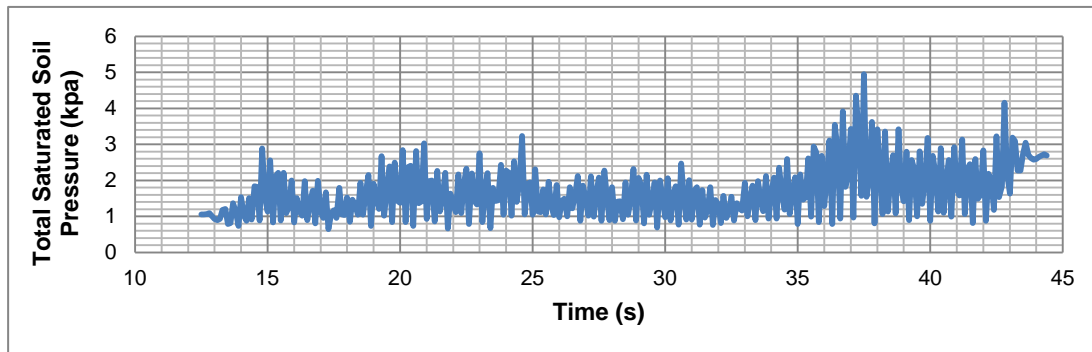


Figure H29: Total saturated soil pressure for SP4 for 4 Hz

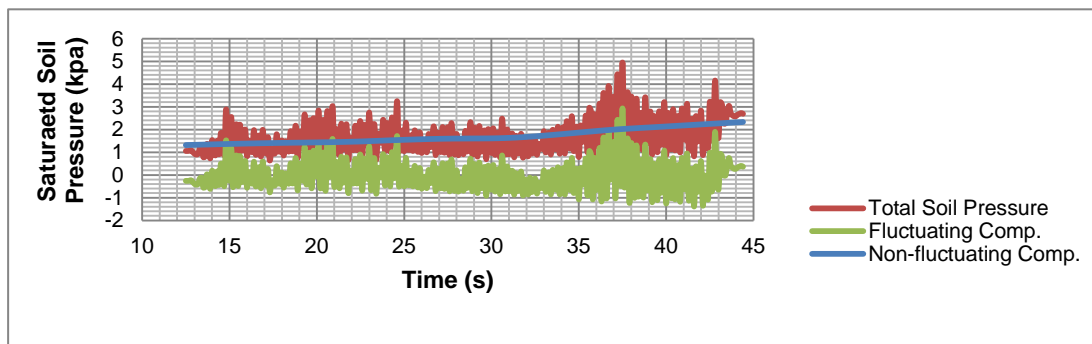


Figure H30: Total saturated soil pressure, non fluctuating and fluctuating components of total saturated soil pressure for SP4 for 4 Hz

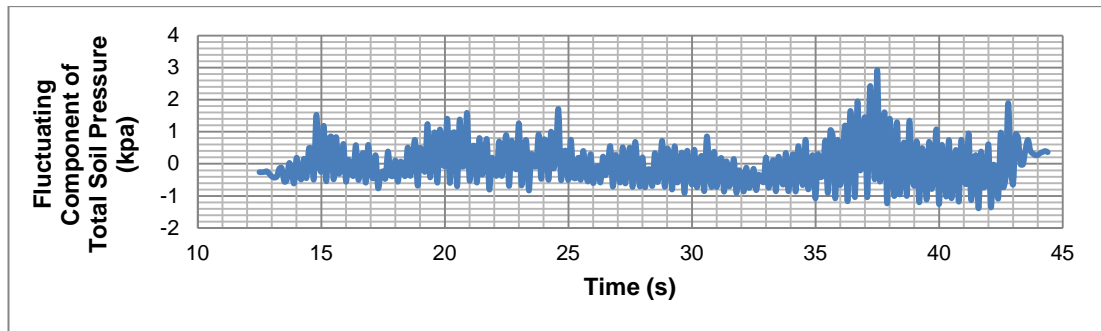


Figure H31: Fluctuating components of total saturated soil pressures for SP4 for 4 Hz

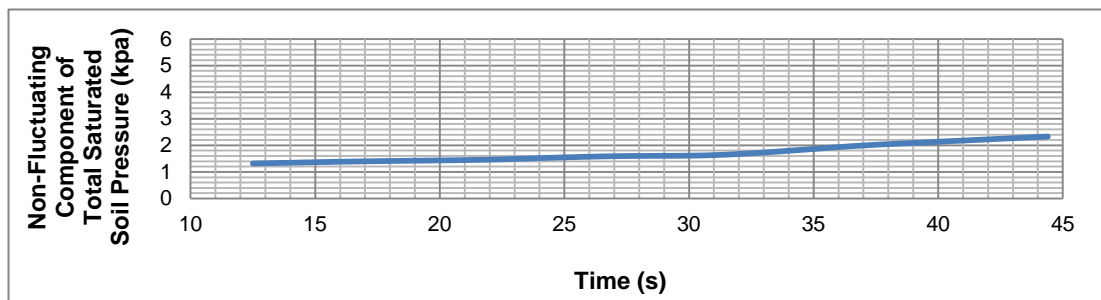


Figure H32: Non-fluctuating components of total saturated soil pressures for SP4 for 4 Hz

1.3. Three Blocks- Fluctuating and Non-fluctuating Components of Total Saturated Soil Pressure for 5 Hz for Soil 1

Fig. H33 – H36 show the total saturated soil pressure, non fluctuating and fluctuating components of total saturated soil pressure for SP1 for 5 Hz.

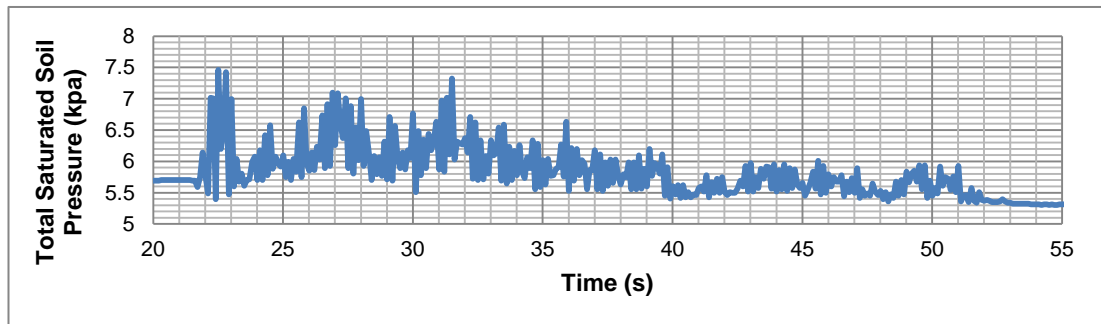


Figure H33: Total saturated soil pressure for SP1 for 5 Hz

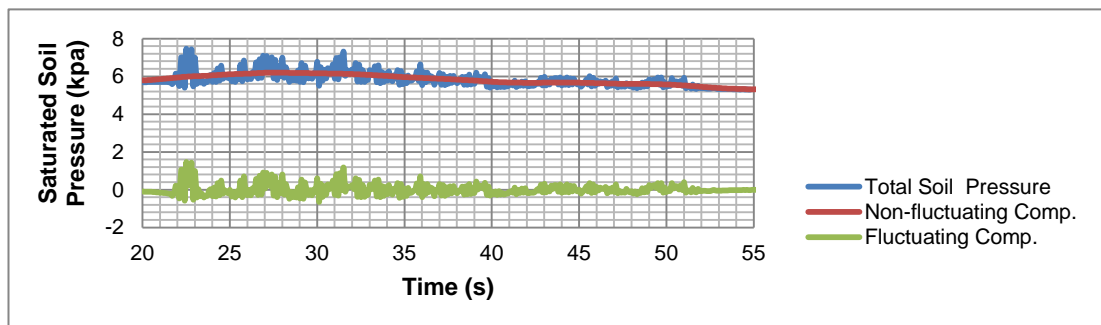


Figure H34: Total saturated soil pressure, non fluctuating and fluctuating components of total saturated soil pressure for SP1 for 5 Hz

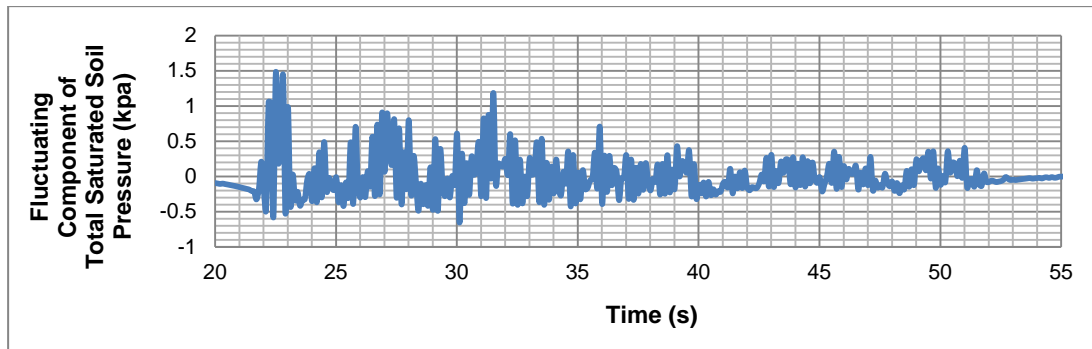


Figure H35: Fluctuating components of total saturated soil pressures for SP1 for 5 Hz

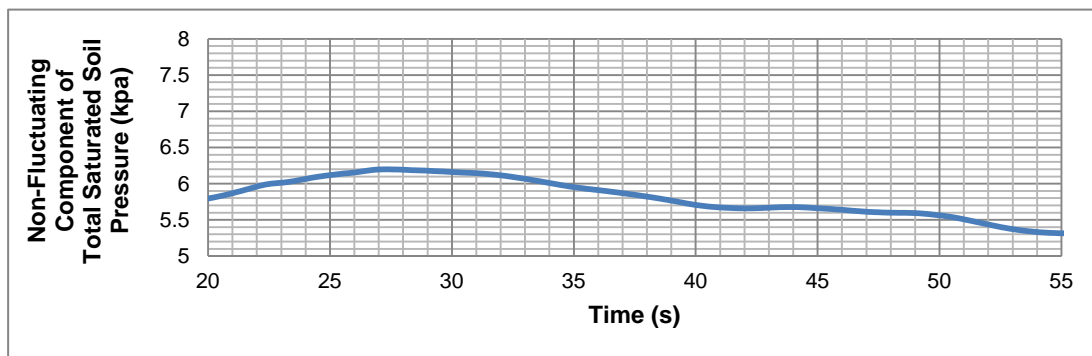


Figure H36: Non-fluctuating components of total saturated soil pressures for SP1 for 5 Hz

Fig. H37 – H40 show the total saturated soil pressure, non fluctuating and fluctuating components of total saturated soil pressure for SP2 for 5 Hz.

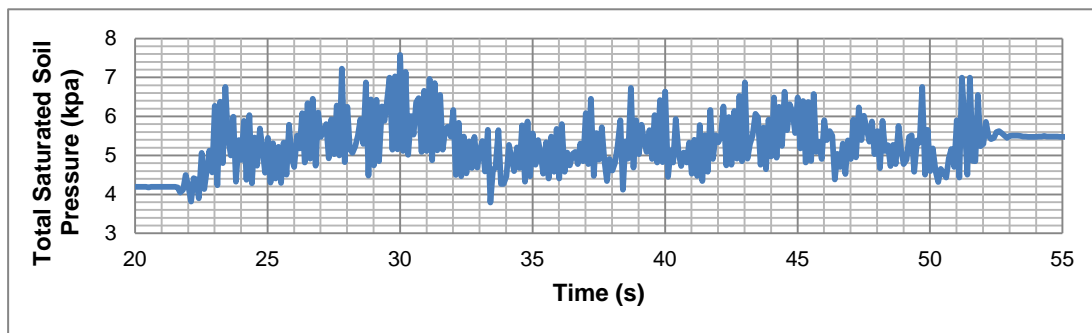


Figure H37: Total saturated soil pressure for SP2 for 5 Hz

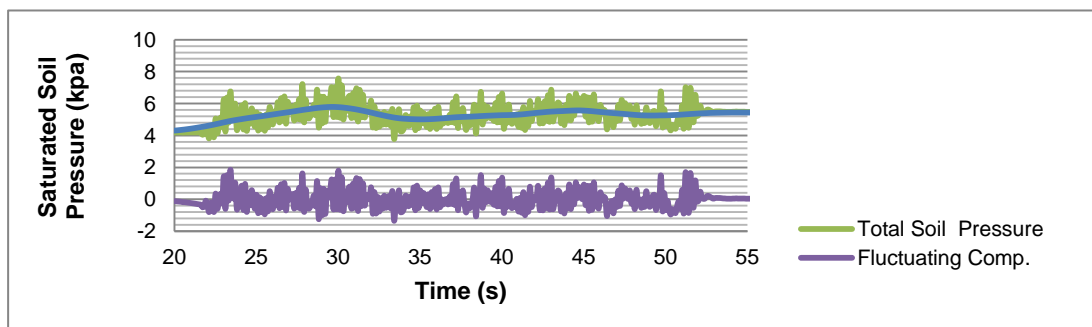


Figure H38: Total saturated soil pressure, non fluctuating and fluctuating components of total saturated soil pressure for SP2 for 5 Hz

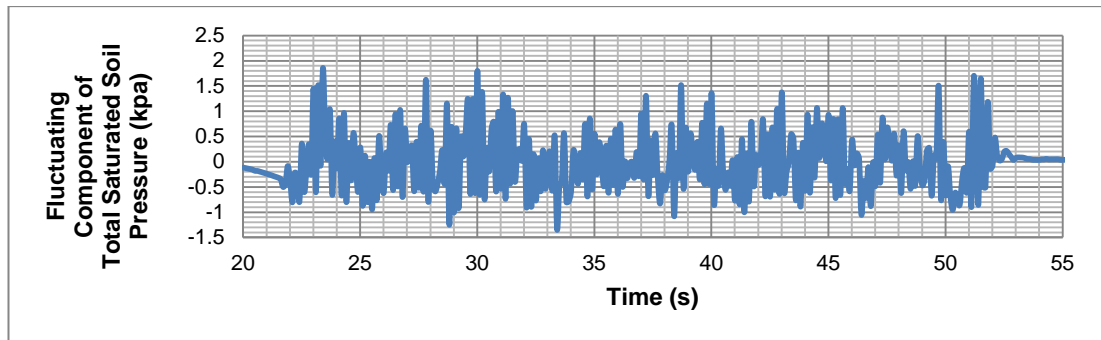


Figure H39: Fluctuating components of total saturated soil pressures for SP2 for 5 Hz

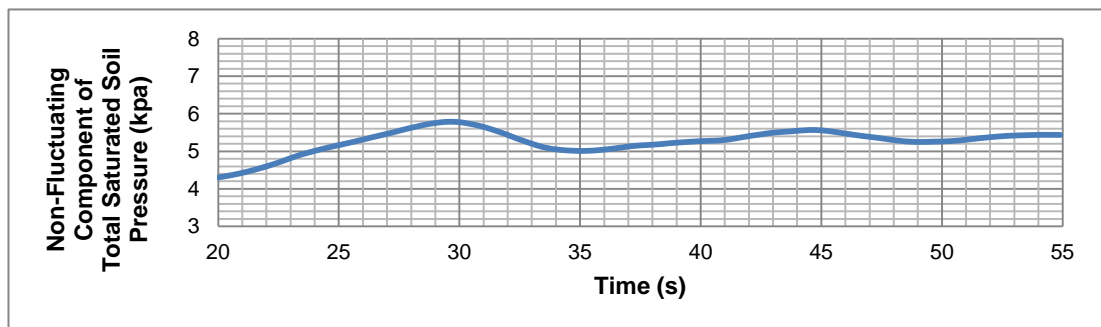


Figure H40: Non-fluctuating components of total saturated soil pressures for SP2 for 5 Hz

Fig. H41 – H44 show the total saturated soil pressure, non fluctuating and fluctuating components of total saturated soil pressure for SP3 for 5 Hz.

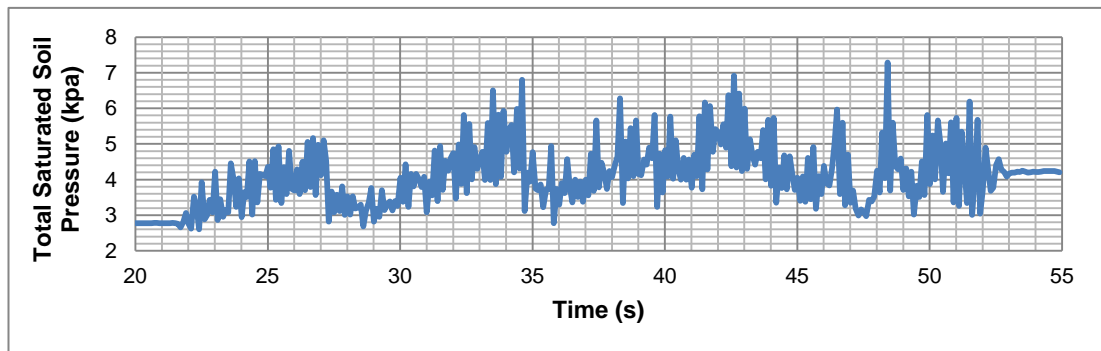


Figure H41: Total saturated soil pressure for SP3 for 5 Hz

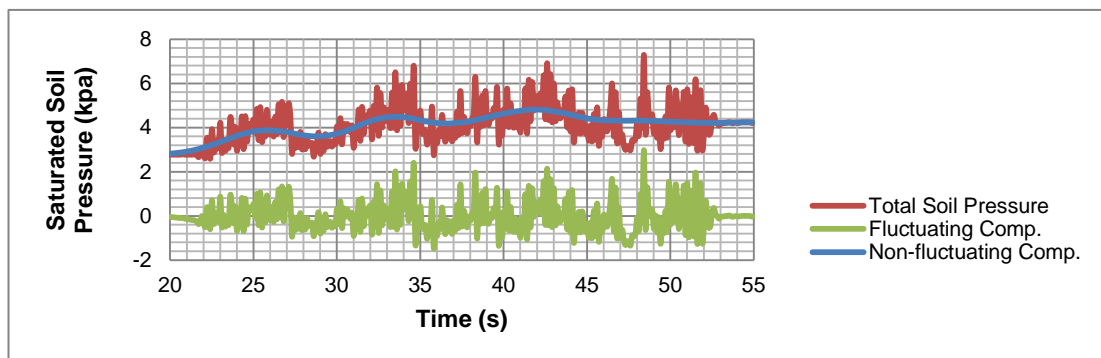


Figure H42: Total saturated soil pressure, non fluctuating and fluctuating components of total saturated soil pressure for SP3 for 5 Hz

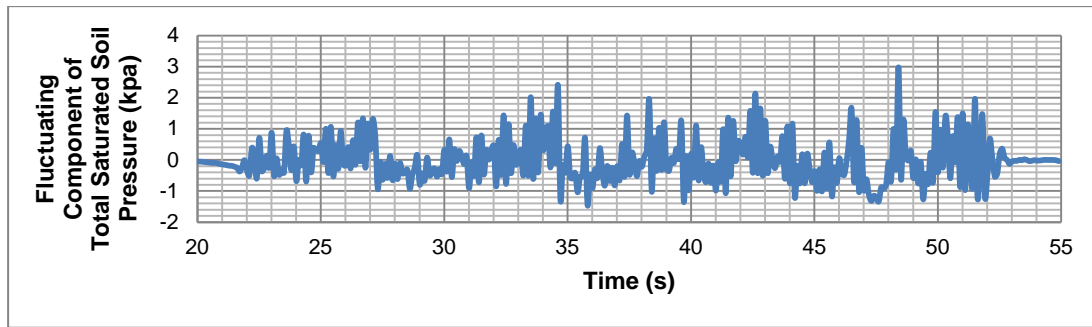


Figure H43: Fluctuating components of total saturated soil pressures for SP3 for 5 Hz

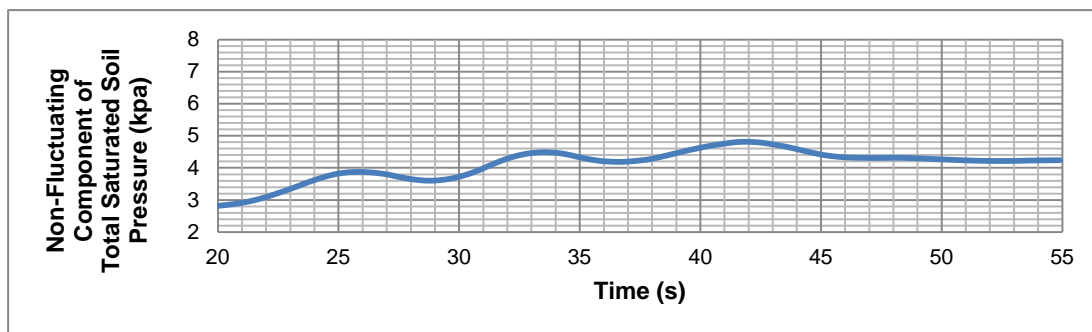


Figure H44: Non-fluctuating components of total saturated soil pressures for SP3 for 5 Hz

Fig. H45 – H48 show the total saturated soil pressure, non fluctuating and fluctuating components of total saturated soil pressure for SP4 for 5 Hz.

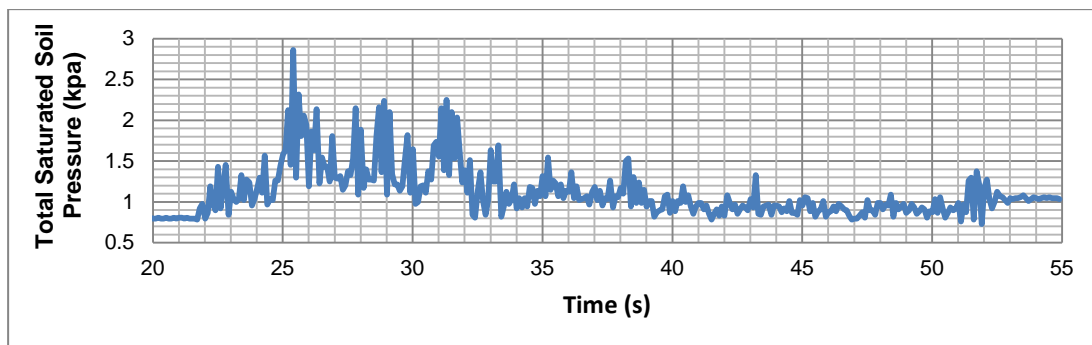


Figure H45: Total saturated soil pressure for SP4 for 5 Hz

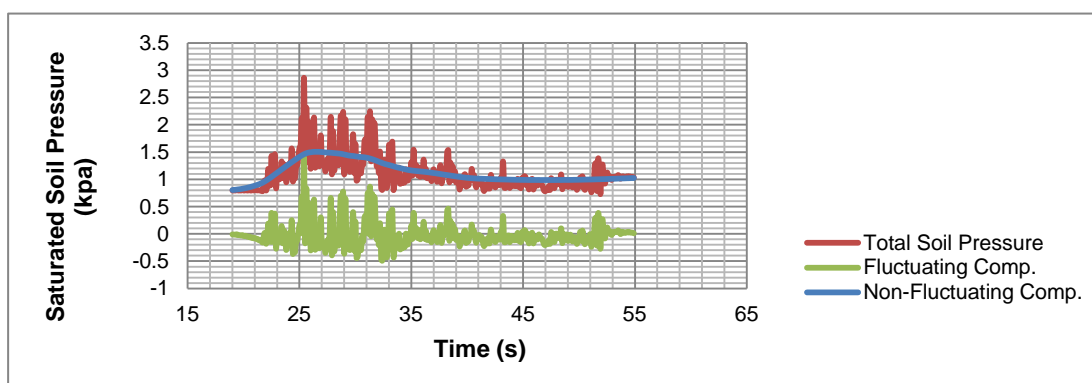


Figure H46: Total saturated soil pressure, non fluctuating and fluctuating components of total saturated soil pressure for SP4 for 5 Hz

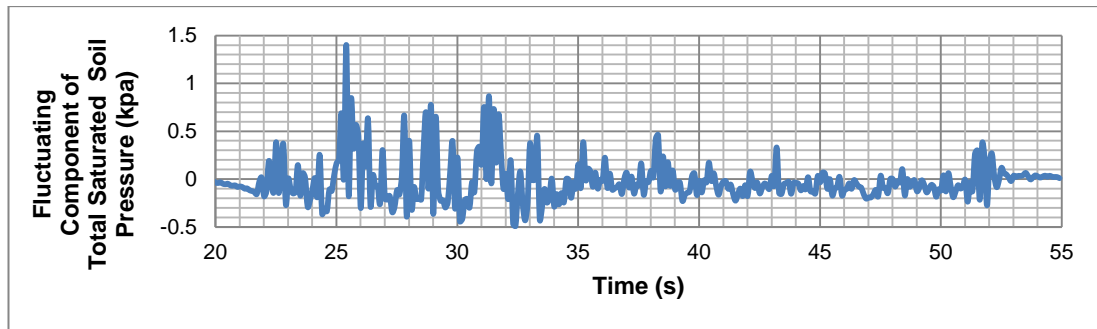


Figure H47: Fluctuating components of total saturated soil pressures for SP4 for 5 Hz

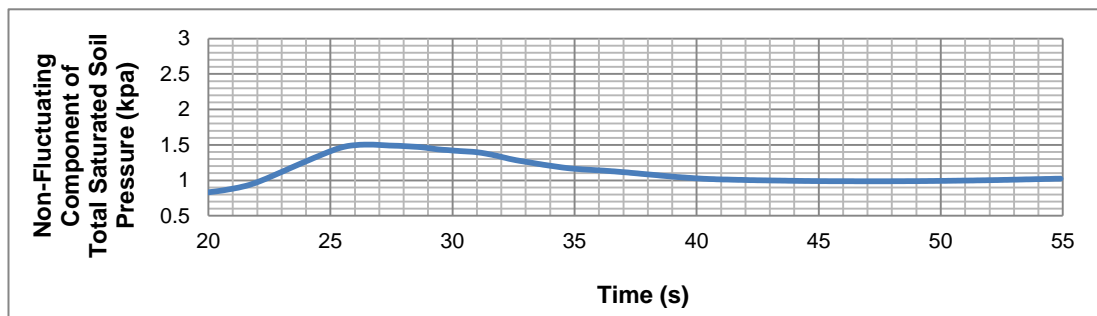


Figure H48: Non-fluctuating components of total saturated soil pressures for SP4 for 5 Hz

1.4. Three Blocks- Fluctuating and Non-fluctuating Components of Total Saturated Soil Pressure for 6 Hz for Soil 1

Fig. H49 – H52 show the total saturated soil pressure, non fluctuating and fluctuating components of total saturated soil pressure for SP1 for 6 Hz.

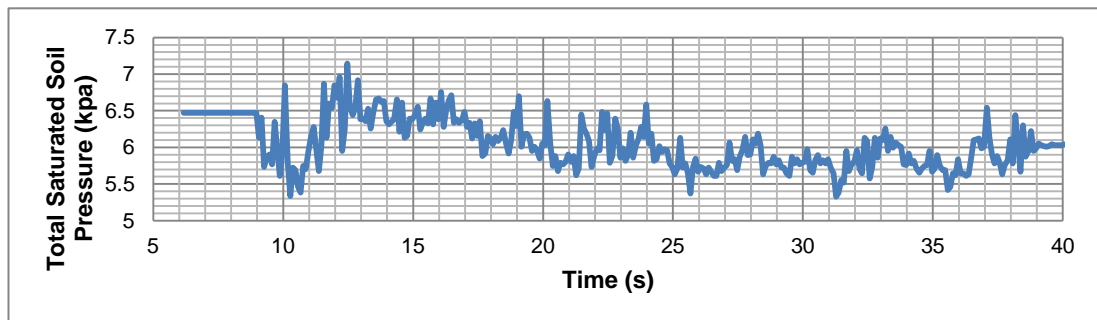


Figure H49: Total saturated soil pressure for SP1 for 6 Hz

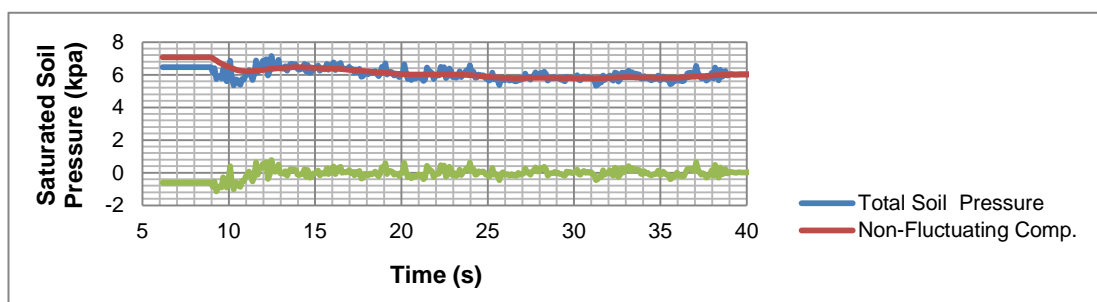


Figure H50: Total saturated soil pressure, non fluctuating and fluctuating components of total saturated soil pressure for SP1 for 6 Hz

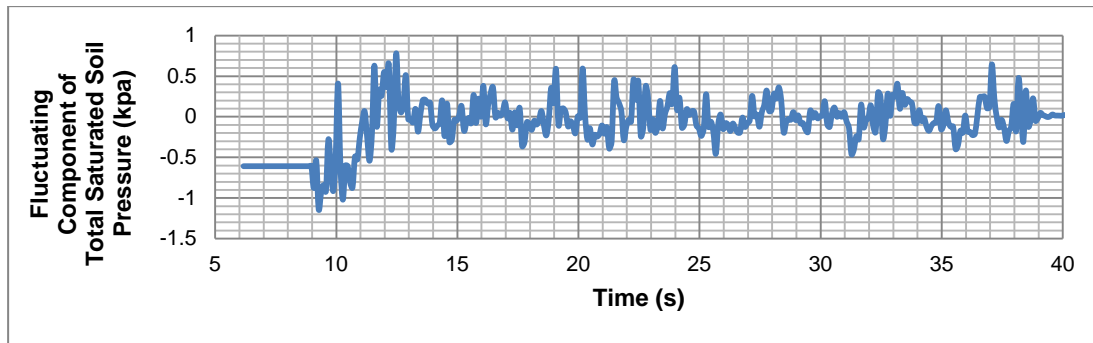


Figure H51: Fluctuating components of total saturated soil pressures for SP1 for 6 Hz

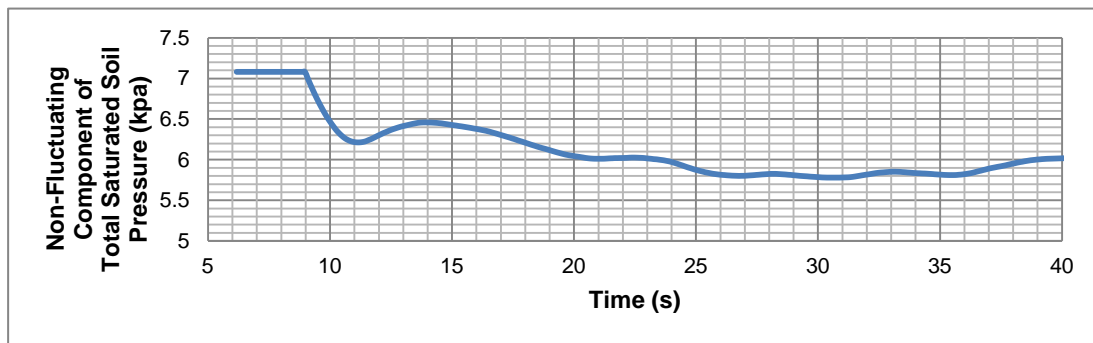


Figure H52: Non-fluctuating components of total saturated soil pressures for SP1 for 6 Hz

Fig. H53 – H56 show the total saturated soil pressure, non fluctuating and fluctuating components of total saturated soil pressure for SP2 for 6 Hz.

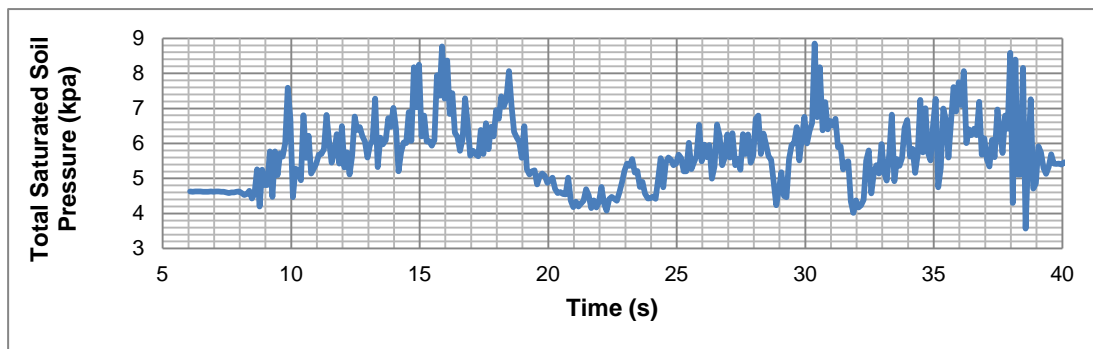


Figure H53: Total saturated soil pressure for SP2 for 6 Hz

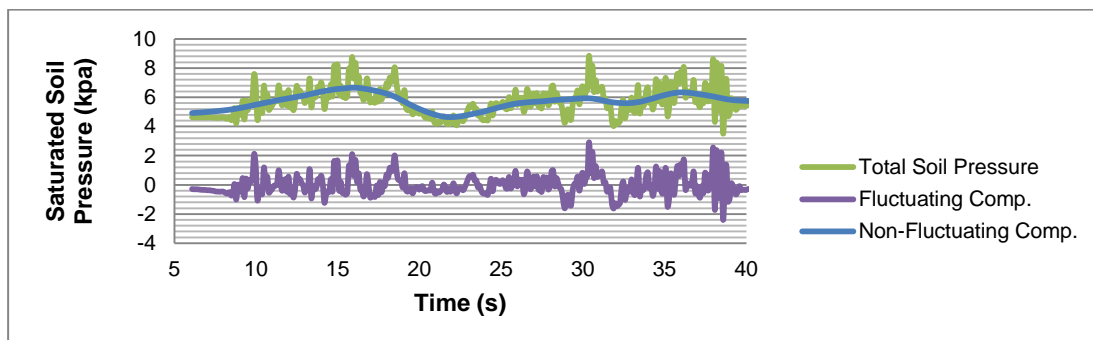


Figure H54: Total saturated soil pressure, non fluctuating and fluctuating components of total saturated soil pressure for SP2 for 6 Hz

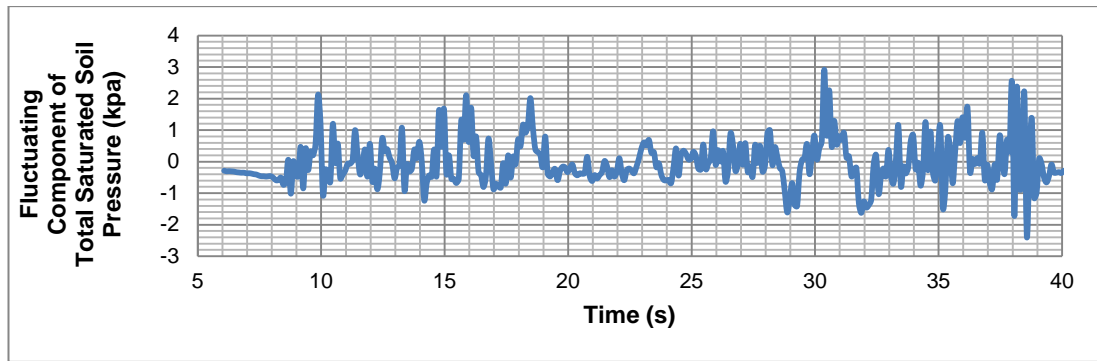


Figure H55: Fluctuating components of total saturated soil pressures for SP2 for 6 Hz

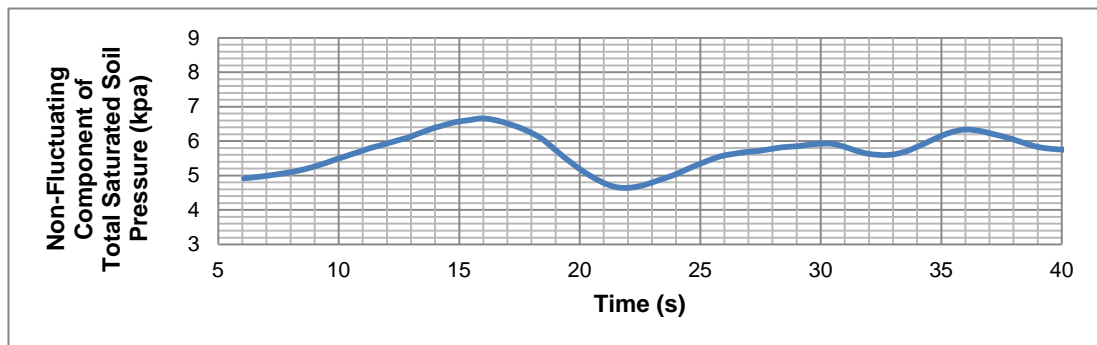


Figure H56: Non-fluctuating components of total saturated soil pressures for SP2 for 6 Hz

Fig. H57 – H60 show the total saturated soil pressure, non fluctuating and fluctuating components of total saturated soil pressure for SP3 for 6 Hz.

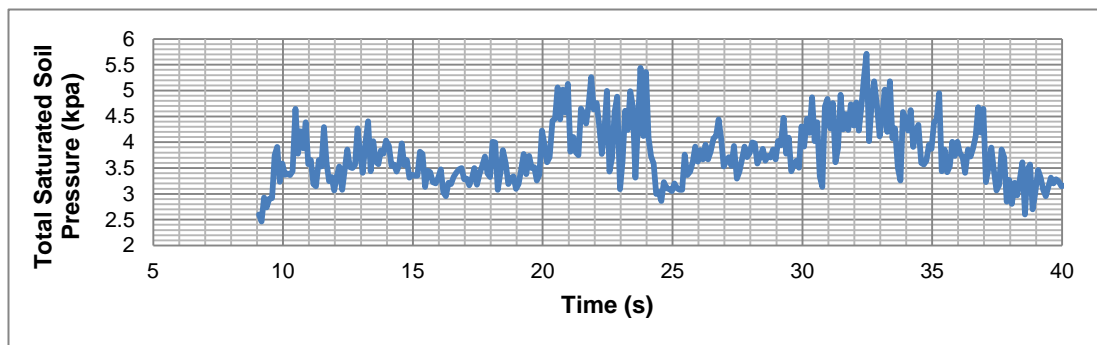


Figure H57: Total saturated soil pressure for SP3 for 6 Hz

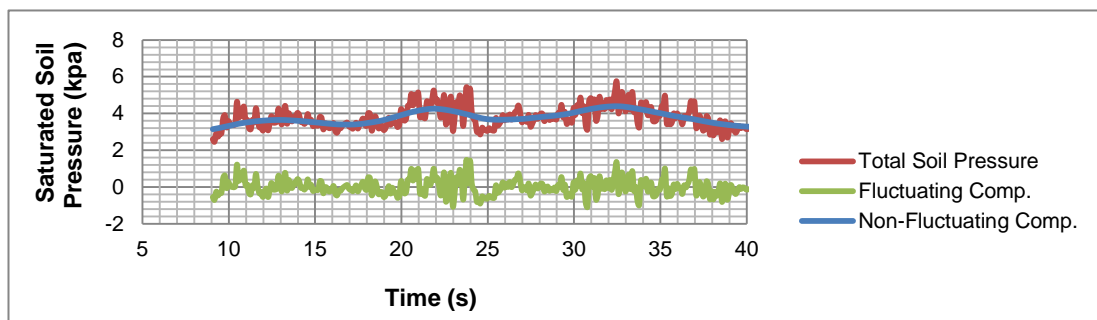


Figure H58: Total saturated soil pressure, non fluctuating and fluctuating components of total saturated soil pressure for SP3 for 6 Hz

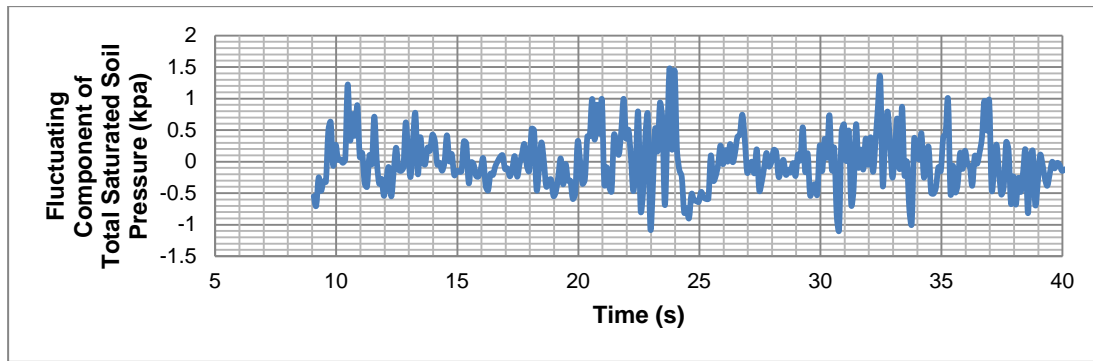


Figure H59: Fluctuating components of total saturated soil pressures for SP3 for 6 Hz

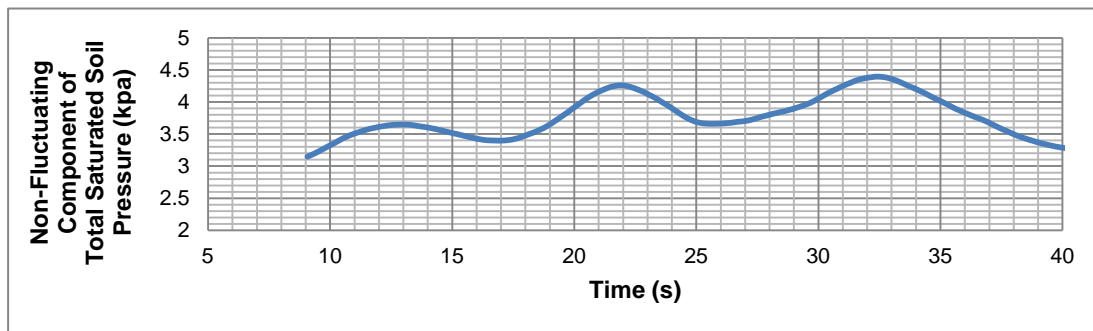


Figure H60: Non-fluctuating components of total saturated soil pressures for SP3 for 6 Hz

Fig. H61 – H64 show the total saturated soil pressure, non fluctuating and fluctuating components of total saturated soil pressure for SP4 for 6 Hz.

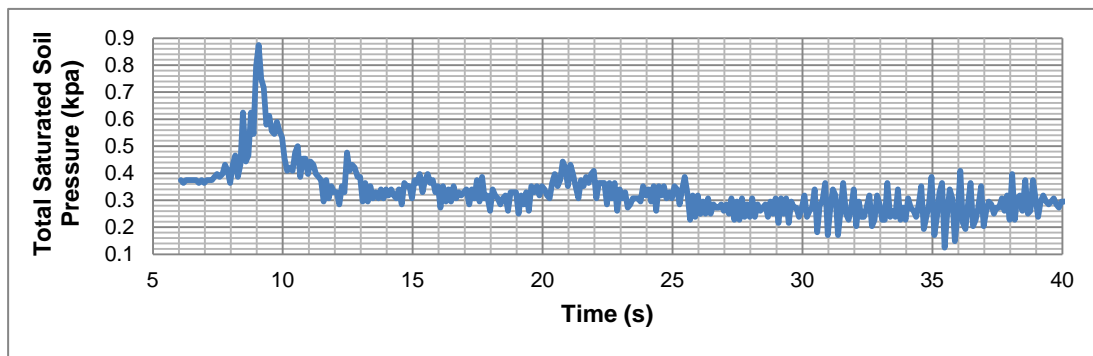


Figure H61: Total saturated soil pressure for SP4 for 6 Hz

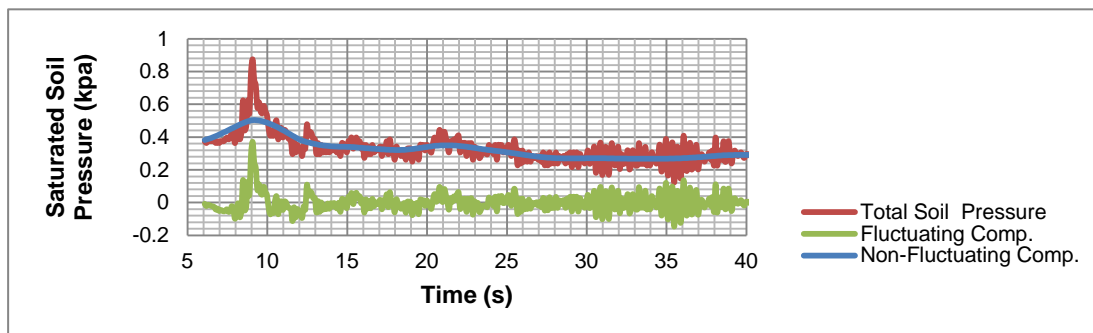


Figure H62: Total saturated soil pressure, non fluctuating and fluctuating components of total saturated soil pressure for SP4 for 6 Hz

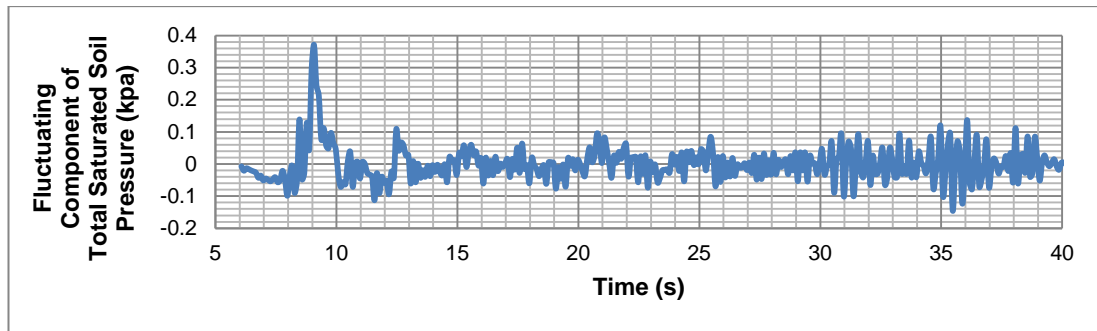


Figure H63: Fluctuating components of total saturated soil pressures for SP4 for 6 Hz

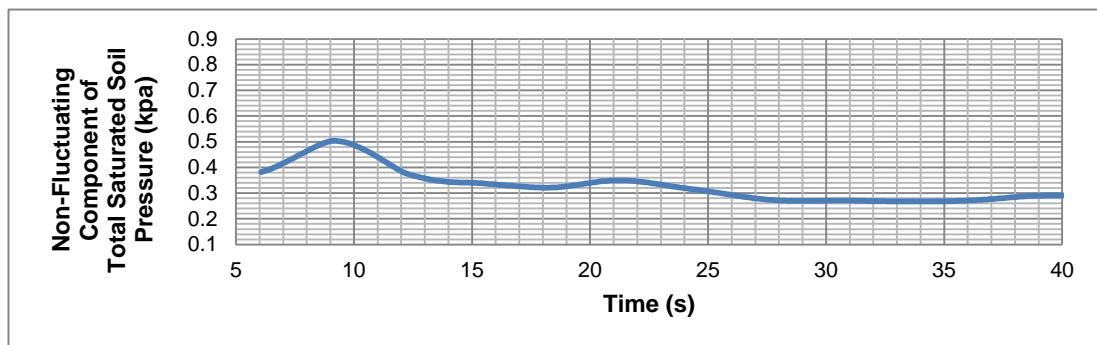


Figure H64: Non-fluctuating components of total saturated soil pressures for SP3 for 6 Hz

3. SOIL 1

2.1. Three Blocks- Fluctuating and Non-fluctuating Components of Total Saturated Soil Pressure for 4 Hz for Soil 2

Fig. H65 – H68 show the total saturated soil pressure, non fluctuating and fluctuating components of total saturated soil pressure for SP1 for 4 Hz.

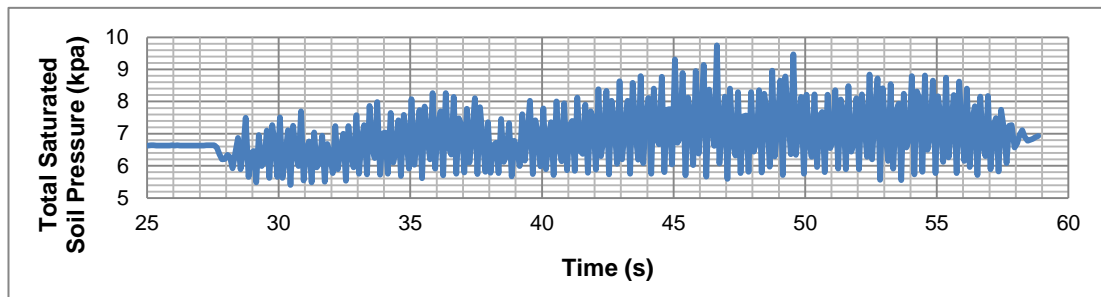


Figure H65: Total saturated soil pressure for SP1 for 4 Hz

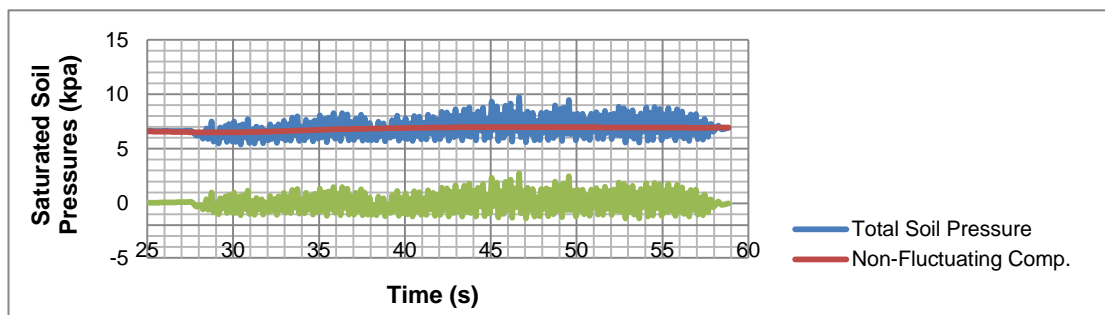


Figure H66: Total saturated soil pressure, non fluctuating and fluctuating components of total saturated soil pressure for SP1 for 4 Hz

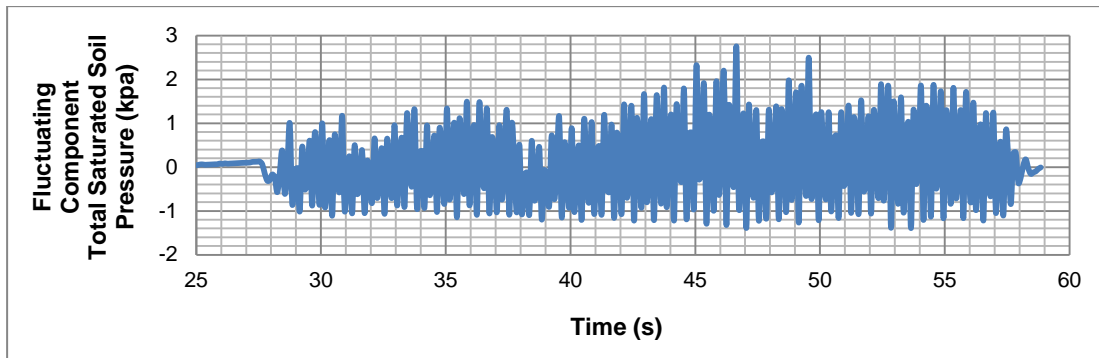


Figure H67: Fluctuating components of total saturated soil pressures for SP1 for 4 Hz

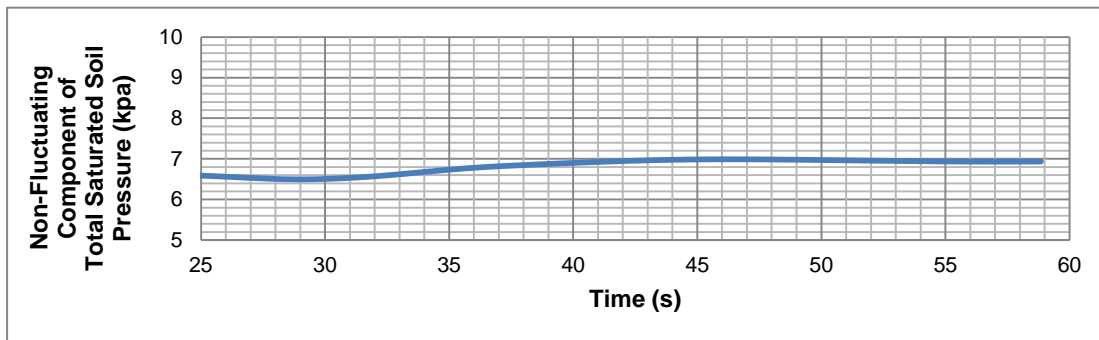


Figure H68: Non fluctuating components of total saturated soil pressures for SP1 for 4 Hz

Fig. H69 – H72 show the total saturated soil pressure, non fluctuating and fluctuating components of total saturated soil pressure for SP2 for 4 Hz.

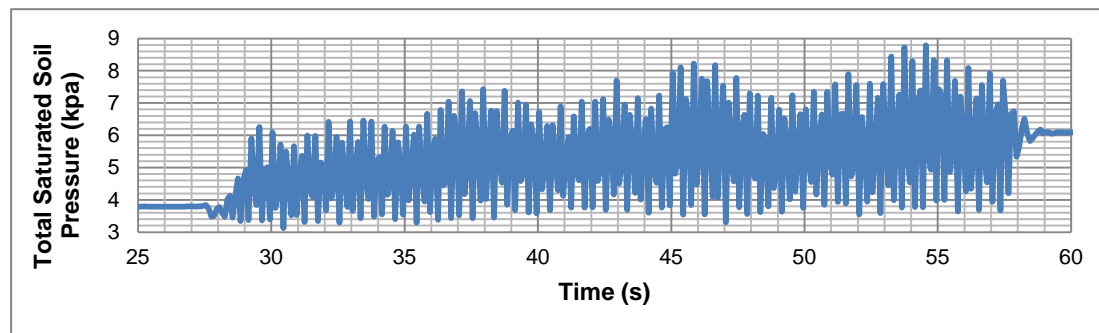


Figure H69: Total saturated soil pressure for SP2 for 4 Hz

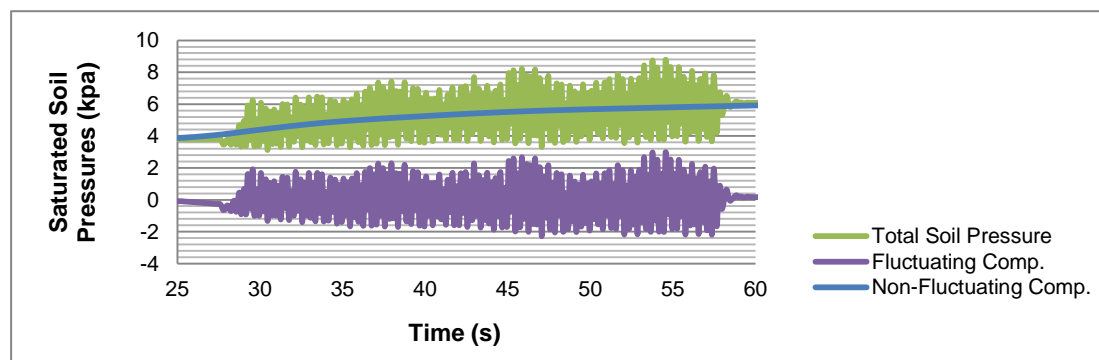


Figure H70: Total saturated soil pressure, non fluctuating and fluctuating components of total saturated soil pressure for SP2 for 4 Hz

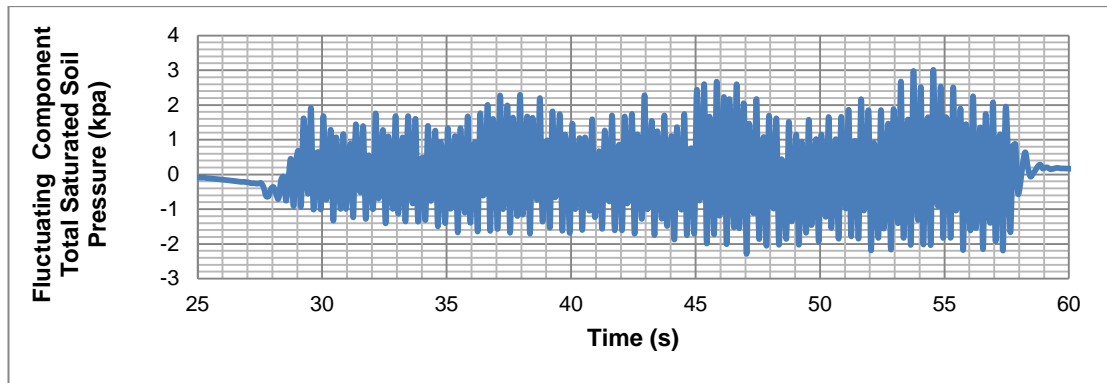


Figure H71: Fluctuating components of total saturated soil pressures for SP2 for 4 Hz

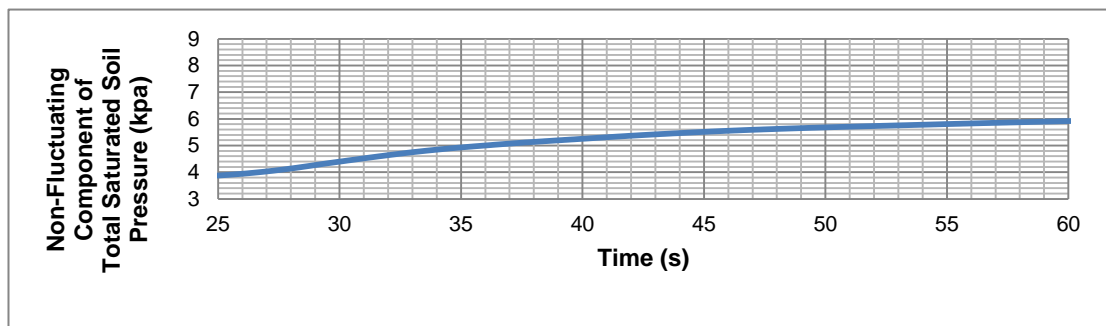


Figure H72: Non fluctuating components of total saturated soil pressures for SP2 for 4 Hz

Fig. H73 – H76 show the total saturated soil pressure, non fluctuating and fluctuating components of total saturated soil pressure for SP3 for 4 Hz.

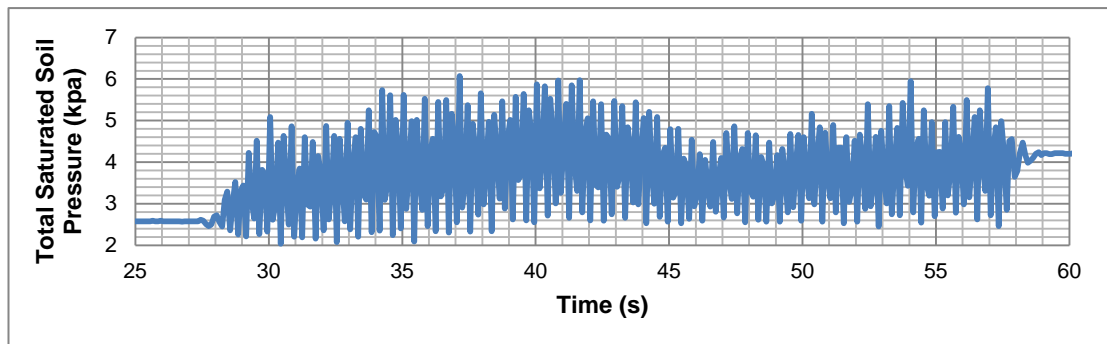


Figure H73: Total saturated soil pressure for SP3 for 4 Hz

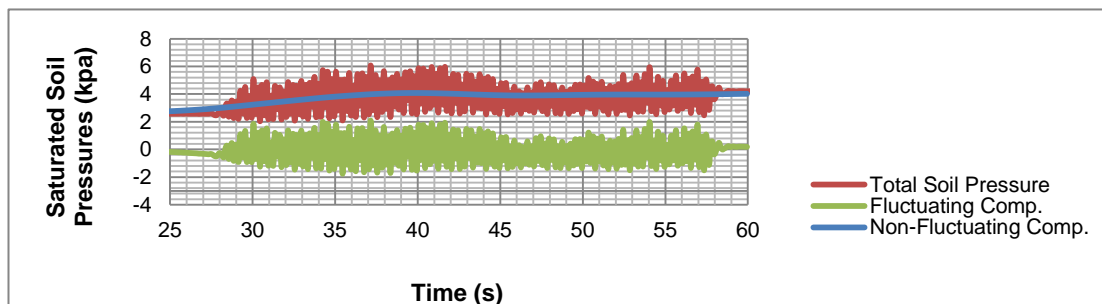


Figure H74: Total saturated soil pressure, non fluctuating and fluctuating components of total saturated soil pressure for SP3 for 4 Hz

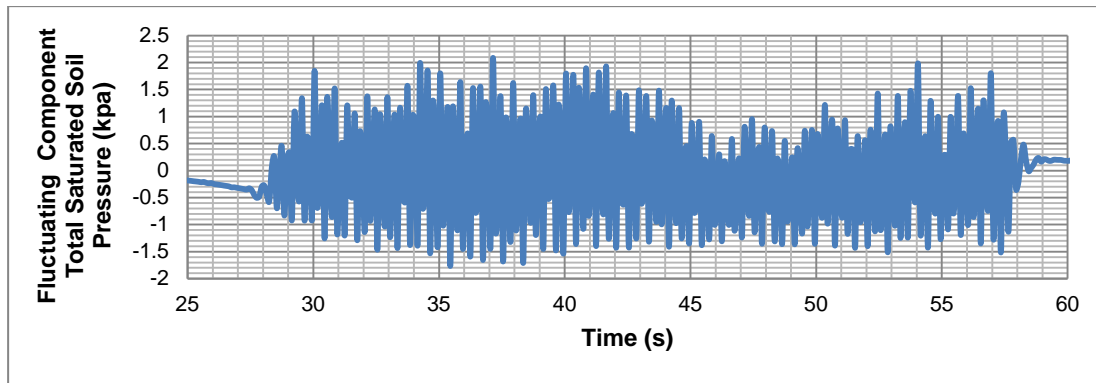


Figure H75: Fluctuating components of total saturated soil pressures for SP3 for 4 Hz

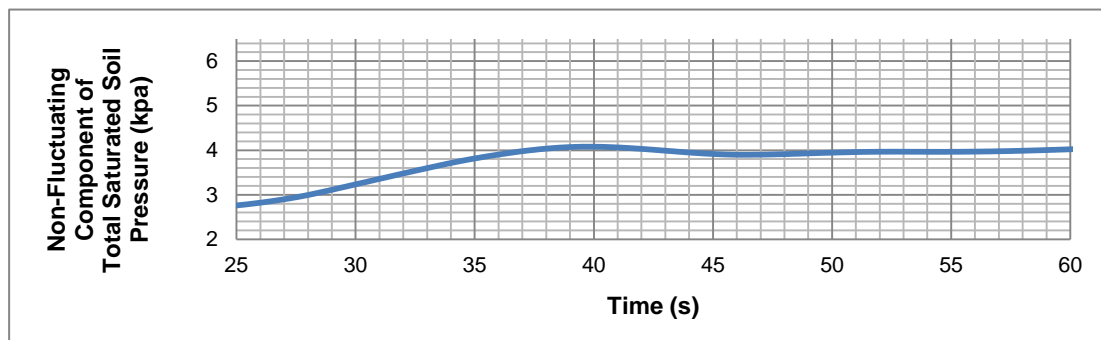


Figure H76: Non fluctuating components of total saturated soil pressures for SP3 for 4 Hz

Fig. H77 – H80 show the total saturated soil pressure, non fluctuating and fluctuating components of total saturated soil pressure for SP4 for 4 Hz.

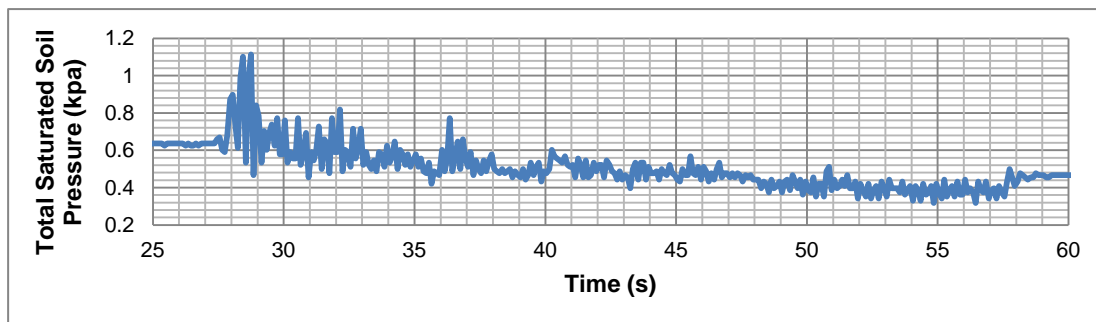


Figure H77: Total saturated soil pressure for SP4 for 4 Hz

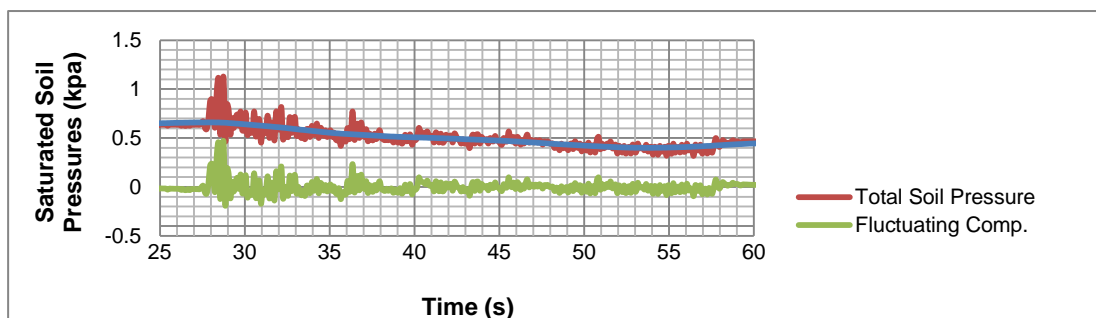


Figure H78: Total saturated soil pressure, non fluctuating and fluctuating components of total saturated soil pressure for SP4 for 4 Hz

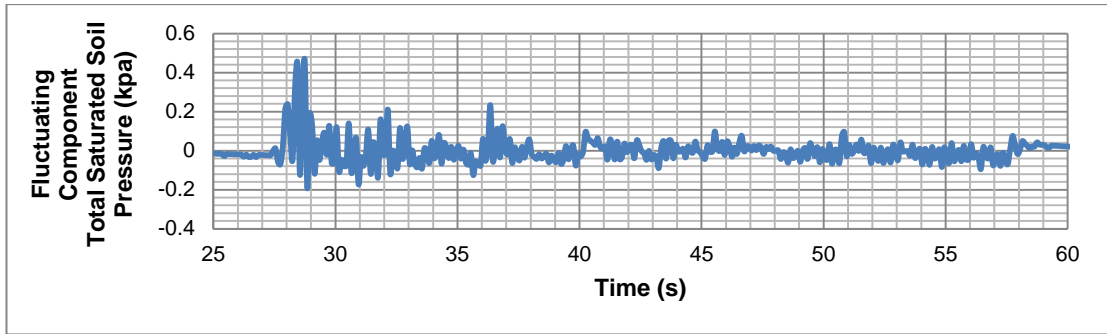


Figure H79: Fluctuating components of total saturated soil pressures for SP4 for 4 Hz

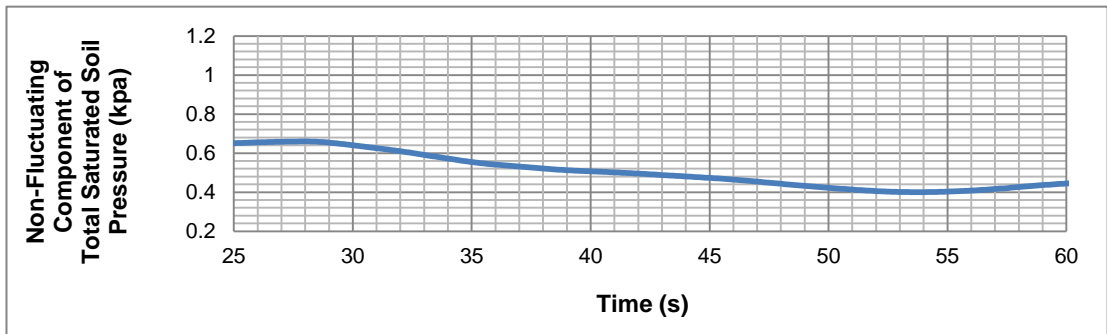


Figure H80: Non fluctuating components of total saturated soil pressures for SP4 for 4 Hz

2.2. Three Blocks- Fluctuating and Non-fluctuating Components of Total Saturated Soil Pressure for 5 Hz for Soil 2

Fig. H81 – H84 show the total saturated soil pressure, non fluctuating and fluctuating components of total saturated soil pressure for SP1 for 5 Hz.

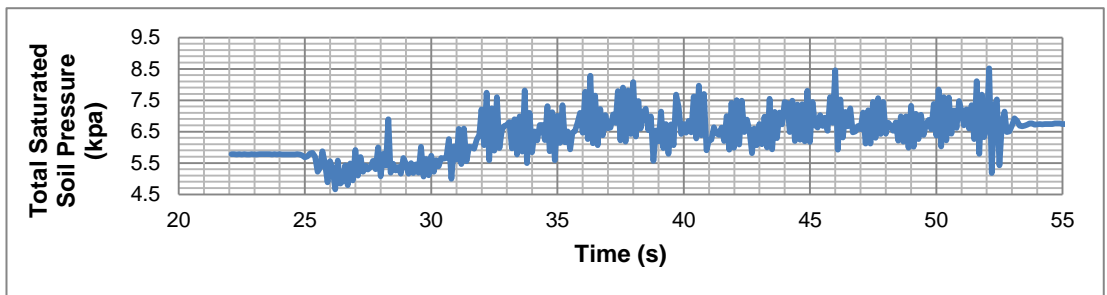


Figure H81: Total saturated soil pressure for SP1 for 5 Hz

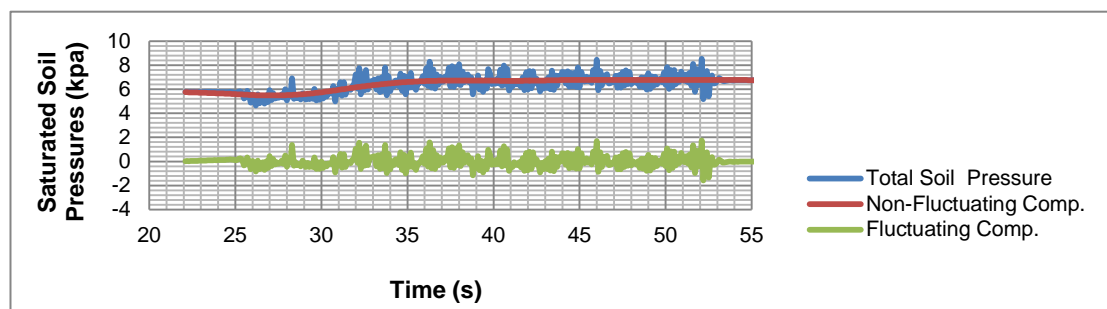


Figure H82: Total saturated soil pressure, non fluctuating and fluctuating components of total saturated soil pressure for SP1 for 5 Hz

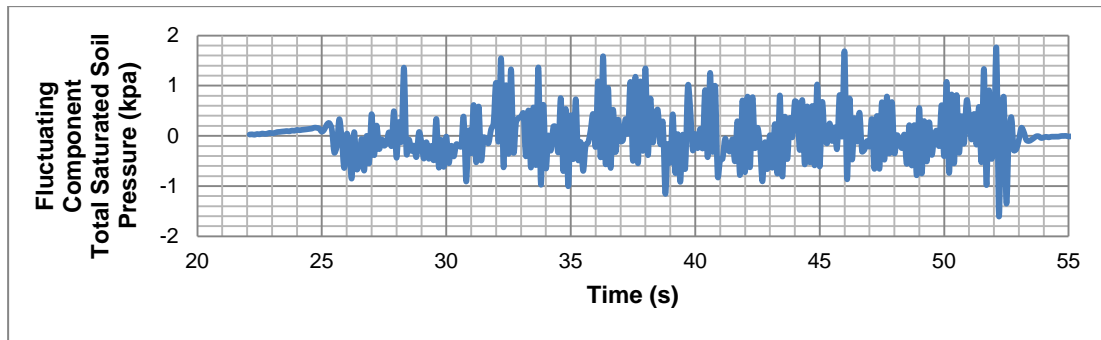


Figure H83: Fluctuating components of total saturated soil pressures for SP1 for 5 Hz

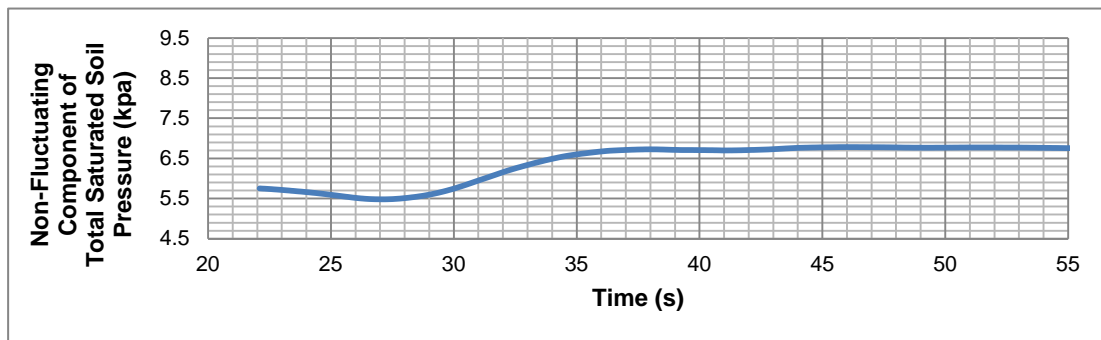


Figure H84: Non fluctuating components of total saturated soil pressures for SP1 for 5 Hz

Fig. H85 - H88 show the total saturated soil pressure, non fluctuating and fluctuating components of total saturated soil pressure for SP2 for 5 Hz.

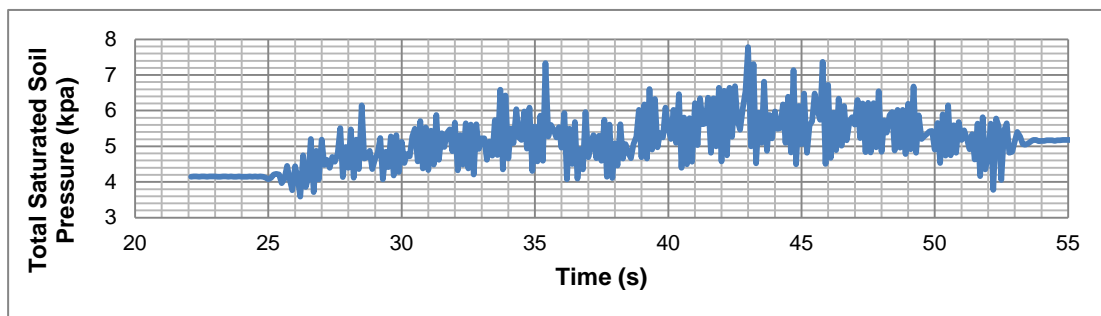


Figure H.85: Total saturated soil pressure for SP2 for 5 Hz

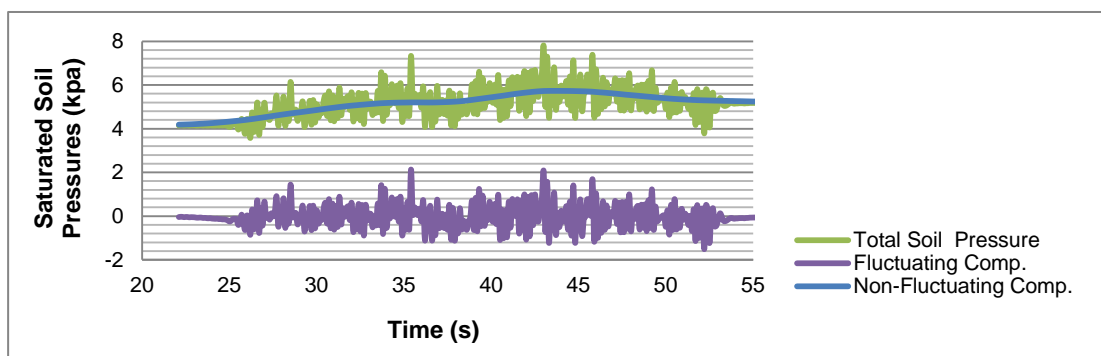


Figure H86: Total saturated soil pressure, non fluctuating and fluctuating components of total saturated soil pressure for SP2 for 5 Hz

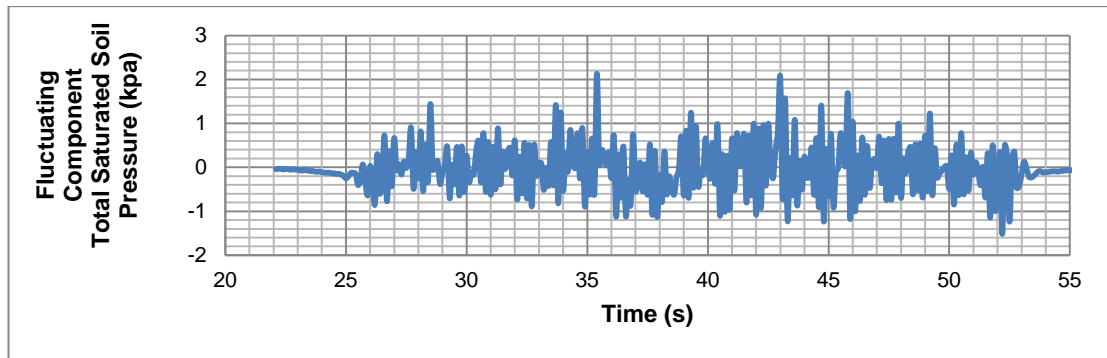


Figure H87: Fluctuating components of total saturated soil pressures for SP2 for 5 Hz

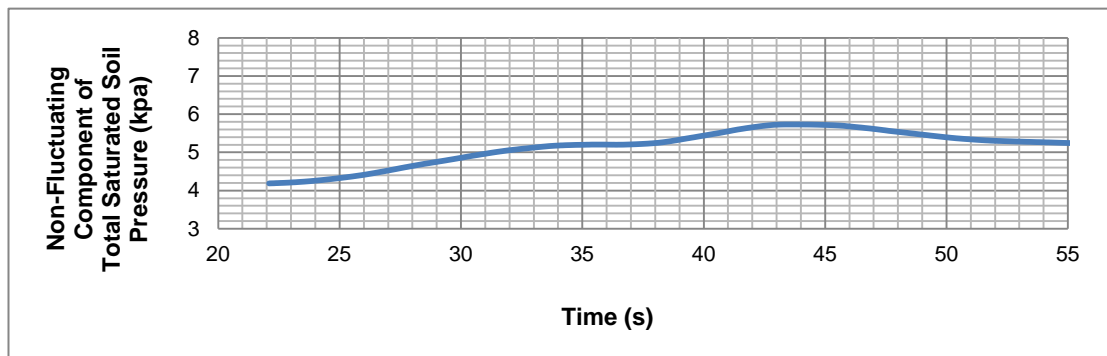


Figure H88: Non fluctuating components of total saturated soil pressures for SP2 for 5 Hz

Fig. H89 – H92 show the total saturated soil pressure, non fluctuating and fluctuating components of total saturated soil pressure for SP3 for 5 Hz.

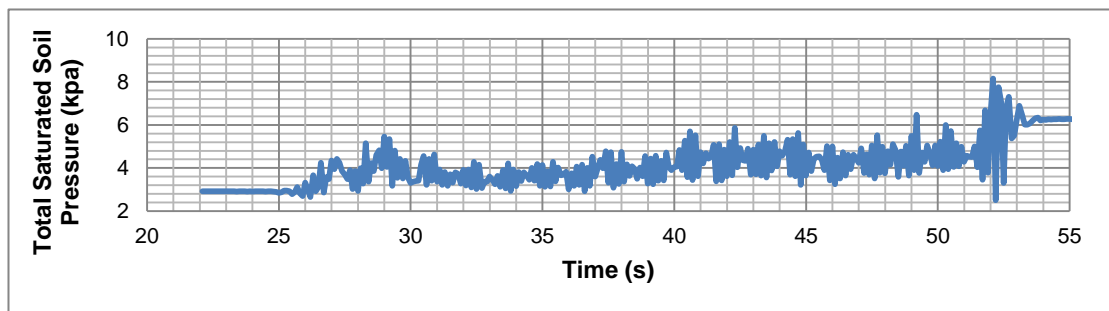


Figure H89: Total saturated soil pressure for SP3 for 5 Hz

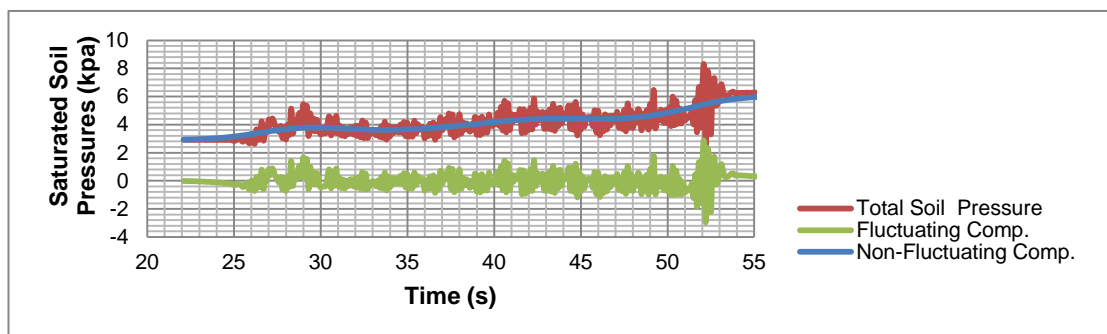


Figure H90: Total saturated soil pressure, non fluctuating and fluctuating components of total saturated soil pressure for SP3 for 5 Hz

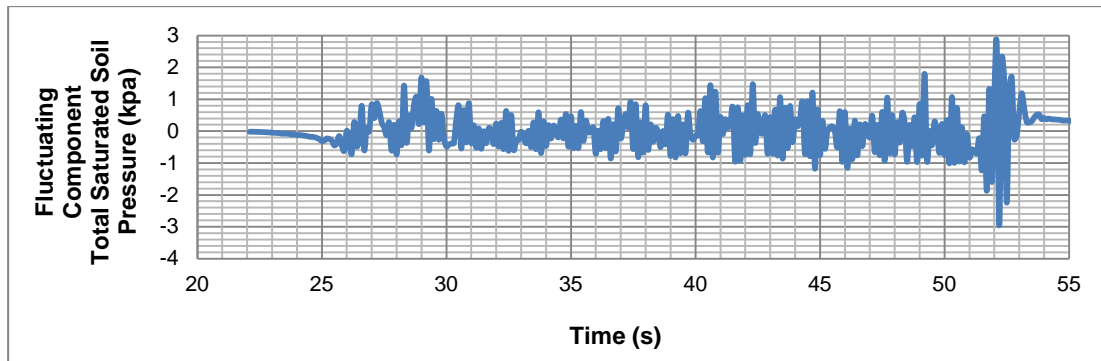


Figure H91: Fluctuating components of total saturated soil pressures for SP3 for 5 Hz

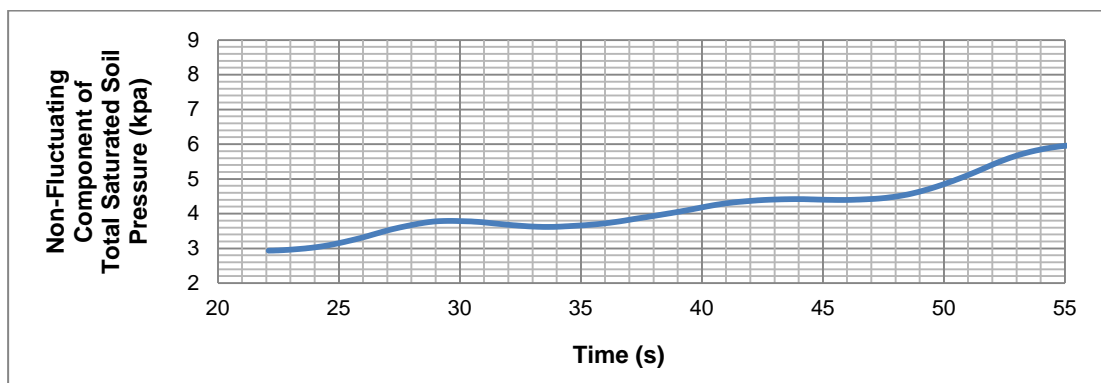


Figure H92: Non fluctuating components of total saturated soil pressures for SP3 for 5 Hz

Fig. H93 – H96 show the total saturated soil pressure, non fluctuating and fluctuating components of total saturated soil pressure for SP4 for 5 Hz.

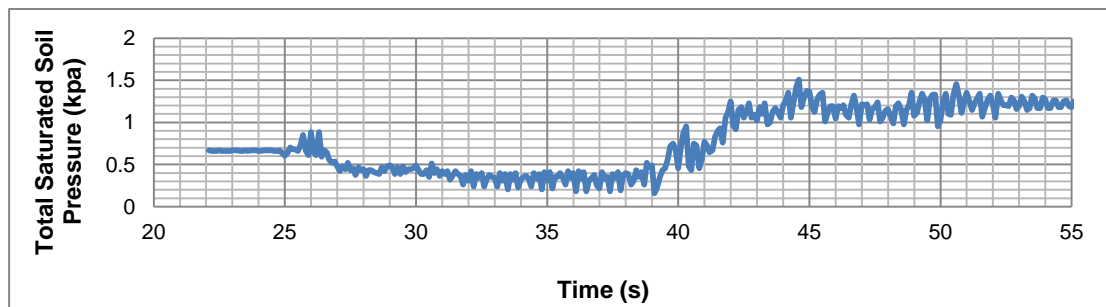


Figure H93: Total saturated soil pressure for SP4 for 5 Hz

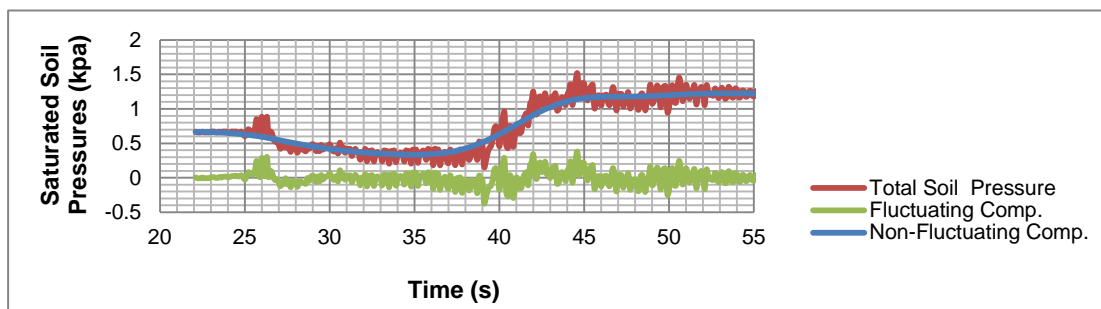


Figure H94: Total saturated soil pressure, non fluctuating and fluctuating components of total saturated soil pressure for SP4 for 5 Hz

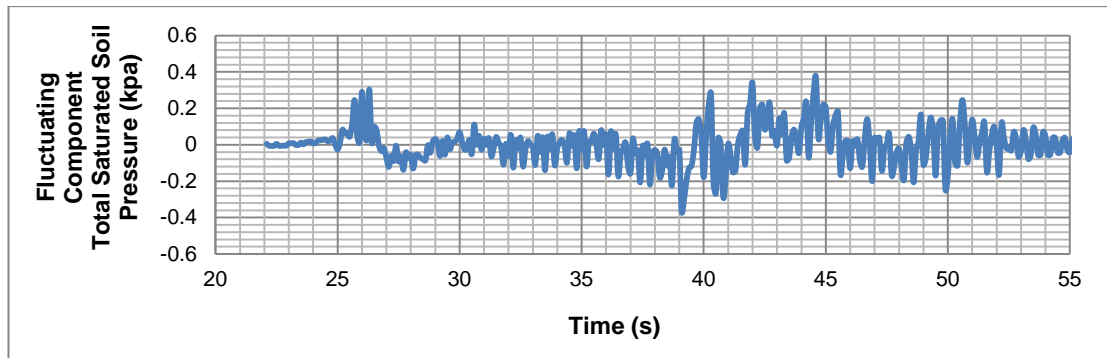


Figure H95: Fluctuating components of total saturated soil pressures for SP4 for 5 Hz

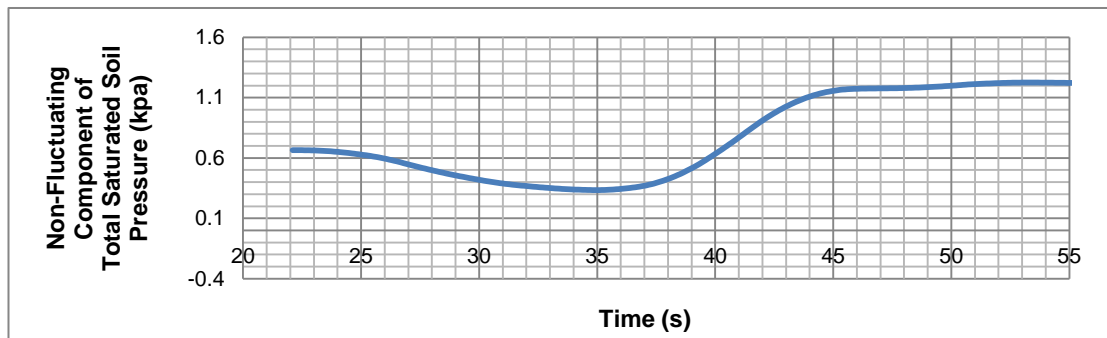


Figure H96: Non fluctuating components of total saturated soil pressures for SP4 for 5 Hz

2.3. Three Blocks- Fluctuating and Non-fluctuating Components of Total Saturated Soil Pressure for 6 Hz for Soil 2

Fig. H97 – H100 show the total saturated soil pressure, non fluctuating and fluctuating components of total saturated soil pressure for SP1 for 6 Hz.

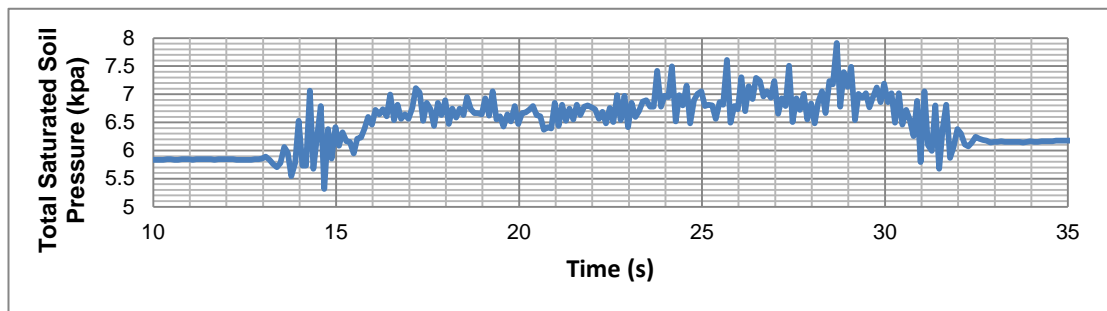


Figure H97: Total saturated soil pressure for SP1 for 6 Hz

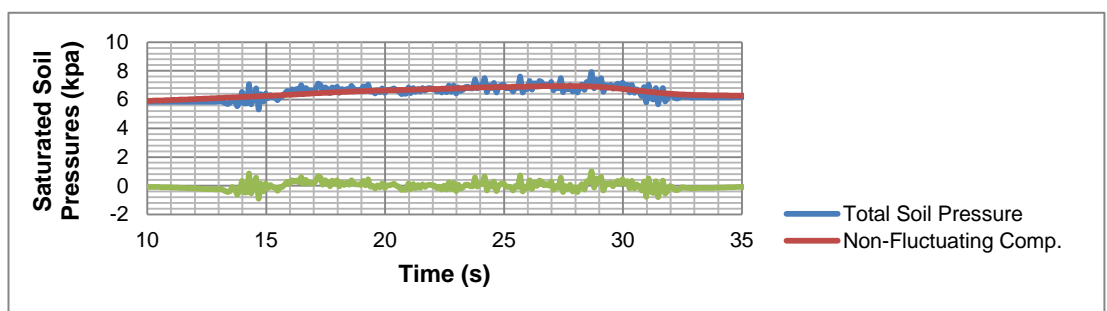


Figure H98: Total saturated soil pressure, non fluctuating and fluctuating components of total saturated soil pressure for SP1 for 6 Hz

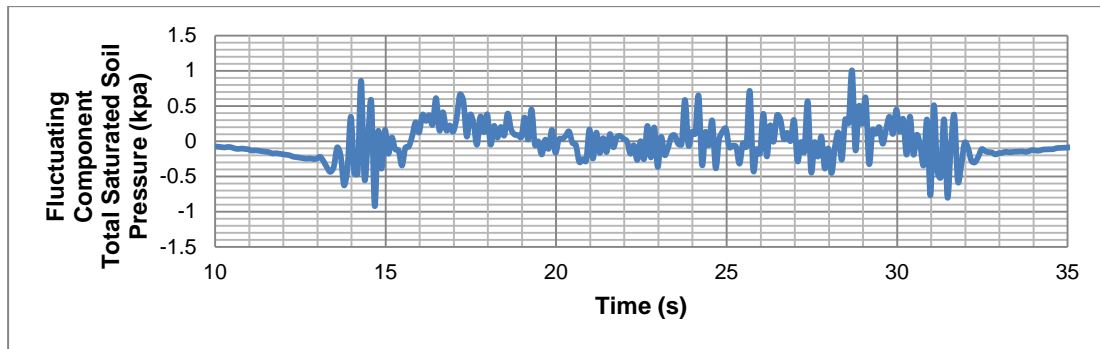


Figure H99: Fluctuating components of total saturated soil pressures for SP1 for 6 Hz

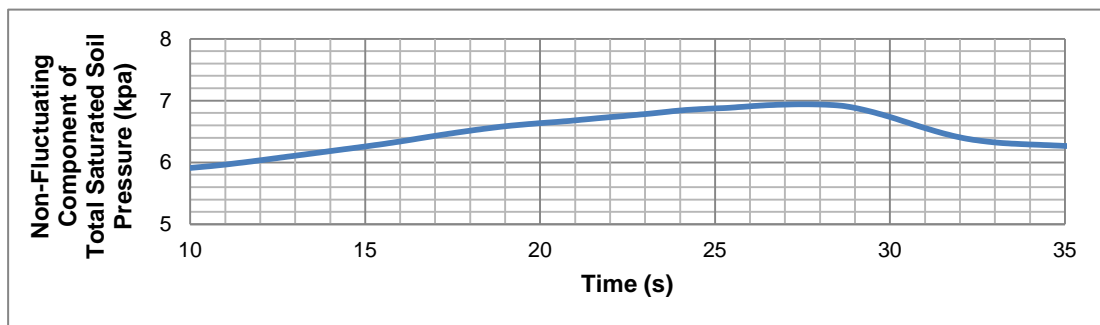


Figure H100: Non fluctuating components of total saturated soil pressures for SP1 for 6 Hz

Fig. H101 – H104 show the total saturated soil pressure, non fluctuating and fluctuating components of total saturated soil pressure for SP2 for 6 Hz.

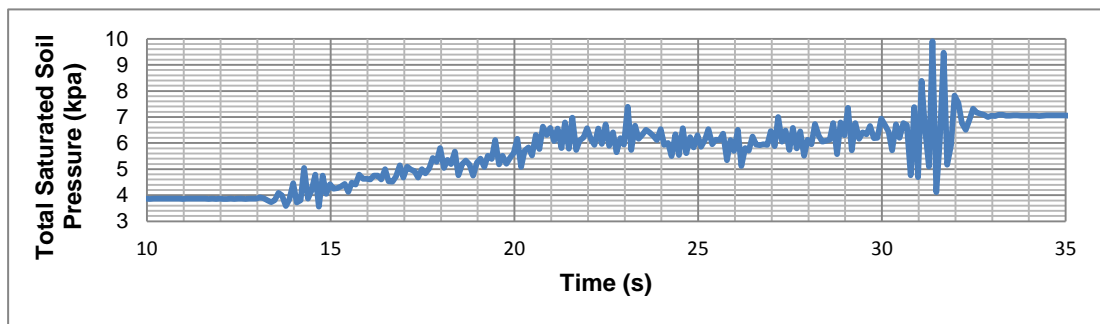


Figure H101: Total saturated soil pressure for SP2 for 6 Hz

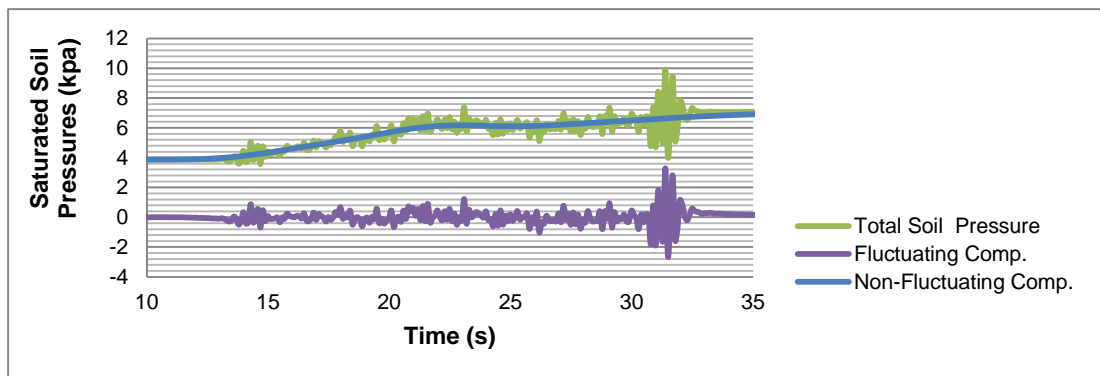


Figure H102: Total saturated soil pressure, non fluctuating and fluctuating components of total saturated soil pressure for SP2 for 6 Hz

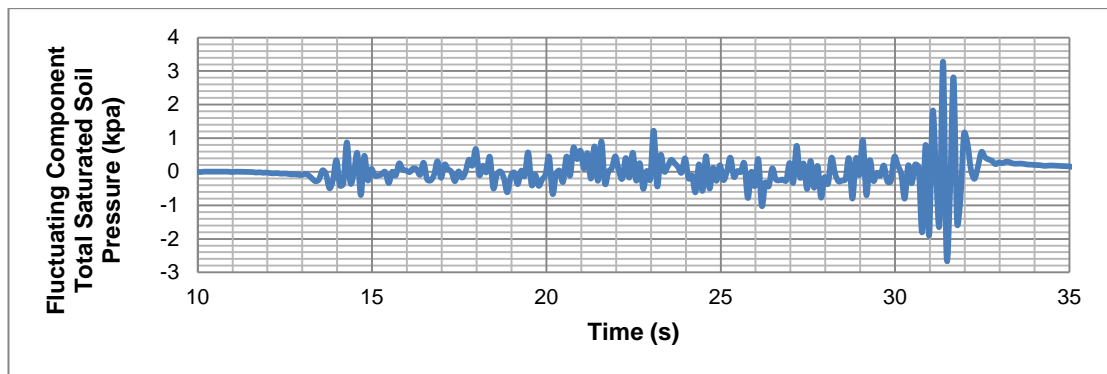


Figure H103: Fluctuating components of total saturated soil pressures for SP2 for 6 Hz

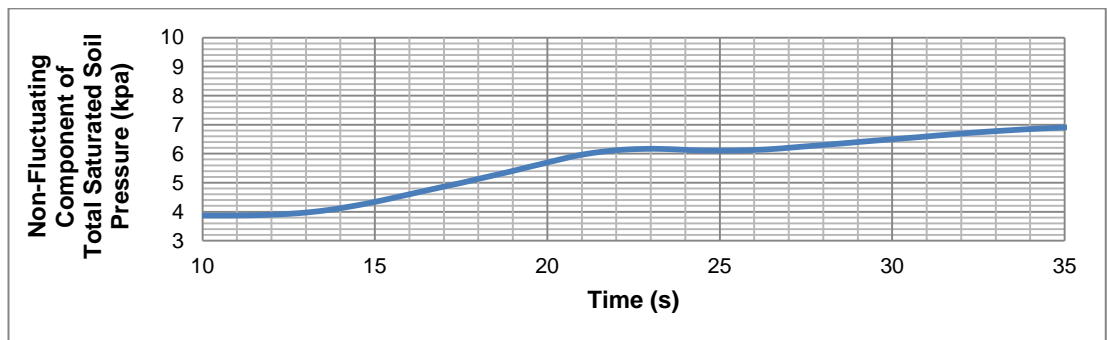


Figure H104: Non fluctuating components of total saturated soil pressures for SP2 for 6 Hz

Fig. H105 – H108 show the total saturated soil pressure, non fluctuating and fluctuating components of total saturated soil pressure for SP3 for 6 Hz.

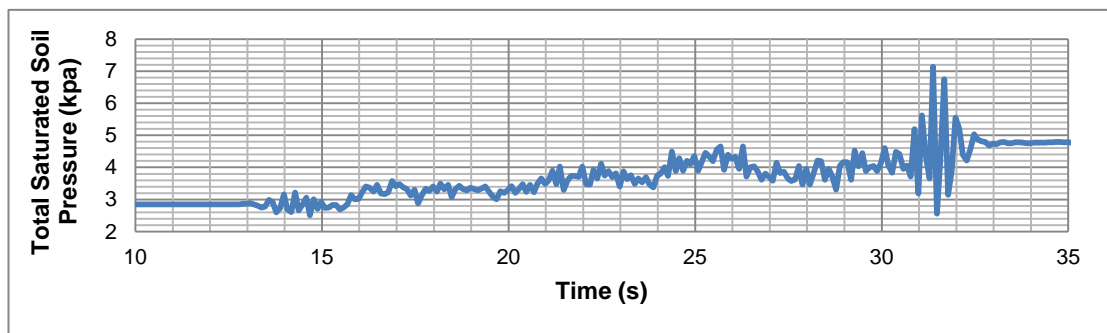


Figure H105: Total saturated soil pressure for SP3 for 6 Hz

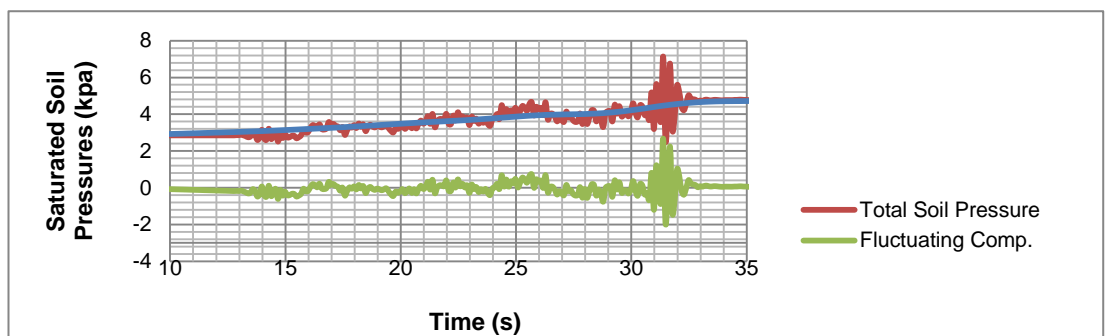


Figure H106: Total saturated soil pressure, non fluctuating and fluctuating components of total saturated soil pressure for SP3 for 6 Hz

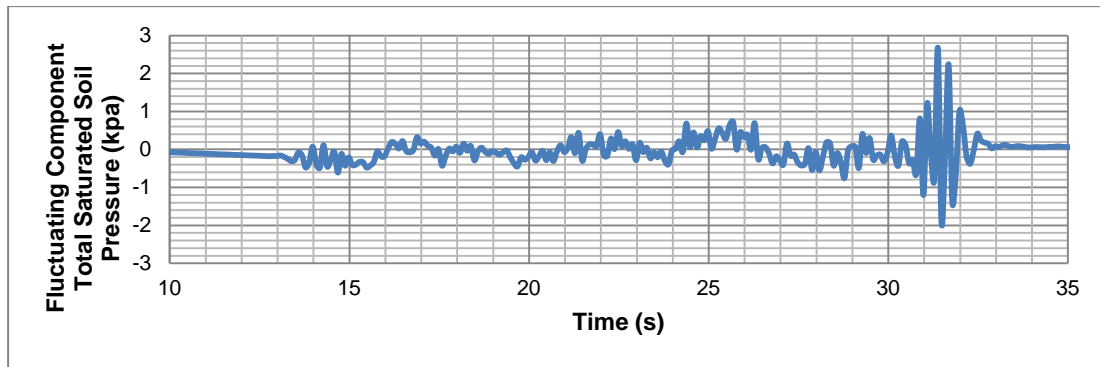


Figure H107: Fluctuating components of total saturated soil pressures for SP3 for 6 Hz

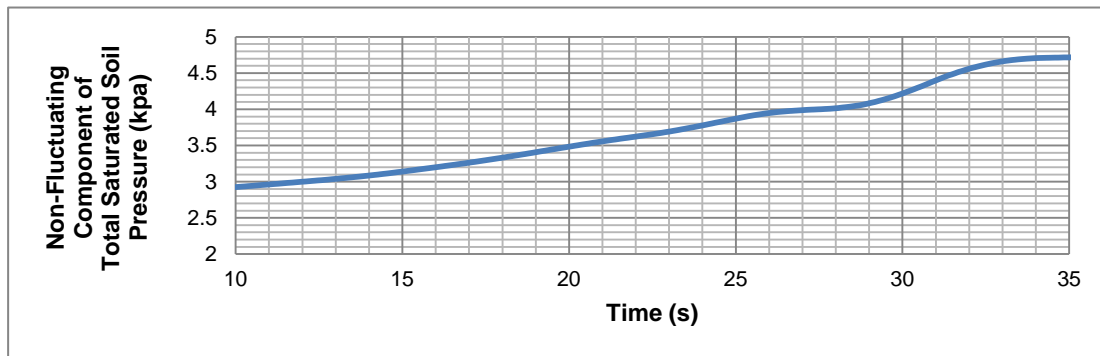


Figure H108: Non fluctuating components of total saturated soil pressures for SP3 for 6 Hz

Fig. H109 – 112 show the total saturated soil pressure, non fluctuating and fluctuating components of total saturated soil pressure for SP4 for 6 Hz.

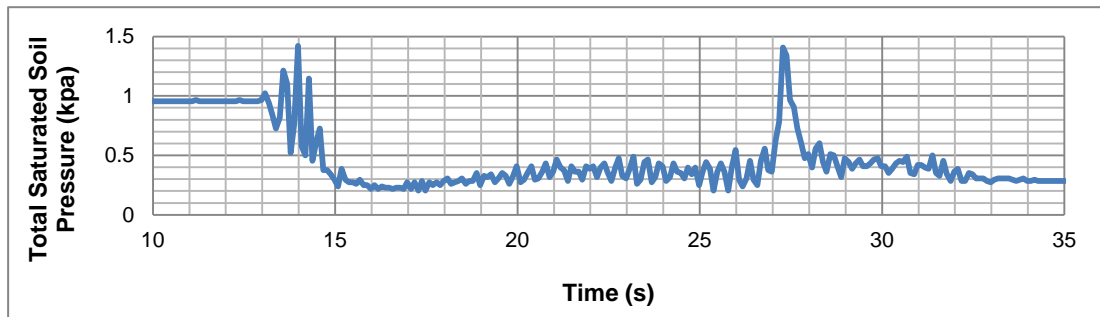


Figure H109: Total saturated soil pressure for SP4 for 6 Hz

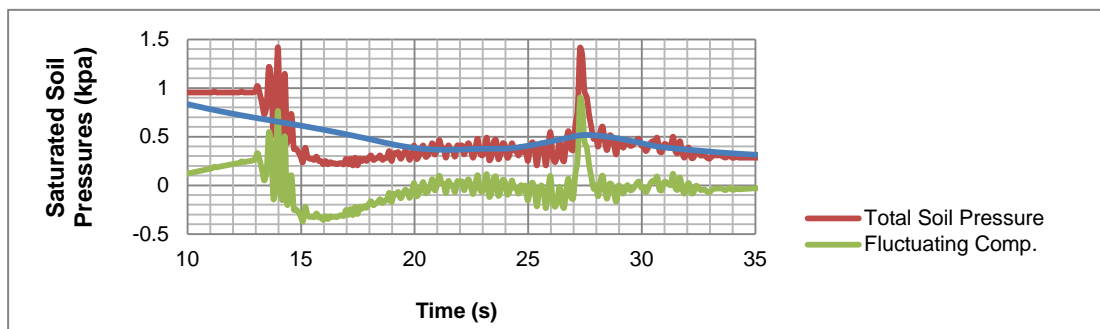


Figure H110: Total saturated soil pressure, non fluctuating and fluctuating components of total saturated soil pressure for SP4 for 6 Hz

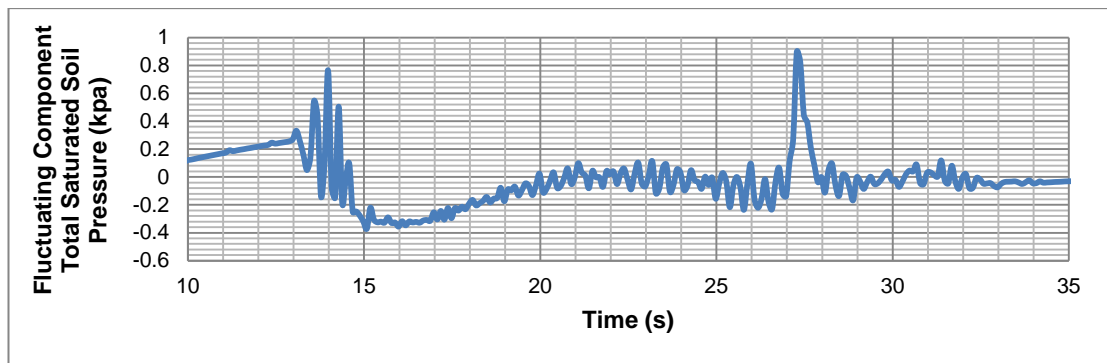


Figure H111: Fluctuating components of total saturated soil pressures for SP4 for 6 Hz

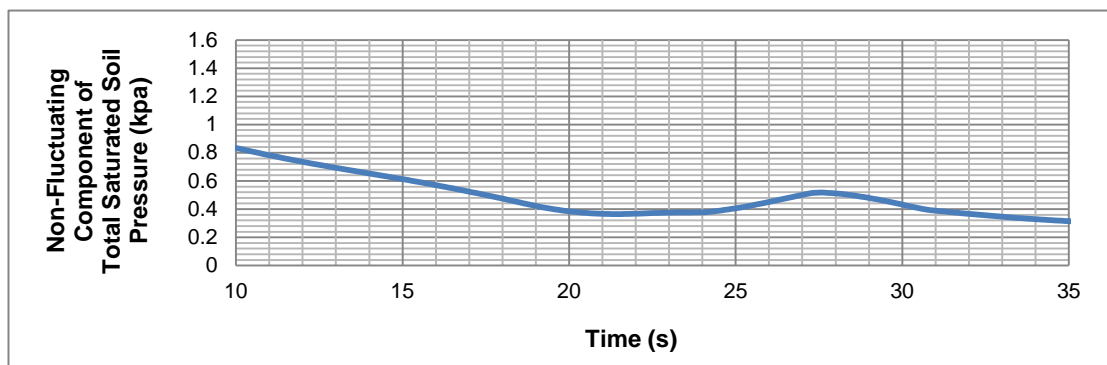


Figure H112: Non fluctuating components of total saturated soil pressures for SP4 for 6 Hz

APPENDIX I

POSITION MEASUREMENTS

Position transducers measurements for one block tests for Soil 2- Tests 2.1 are shown in Figure I1 – I3.

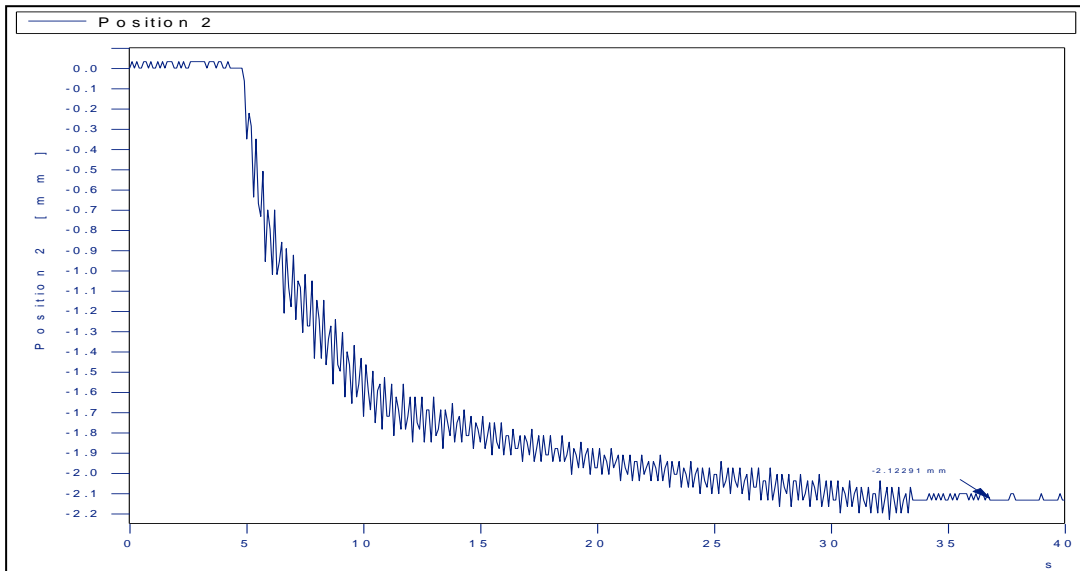


Figure I1: Horizontal displacement measurements for one block for 4 Hz

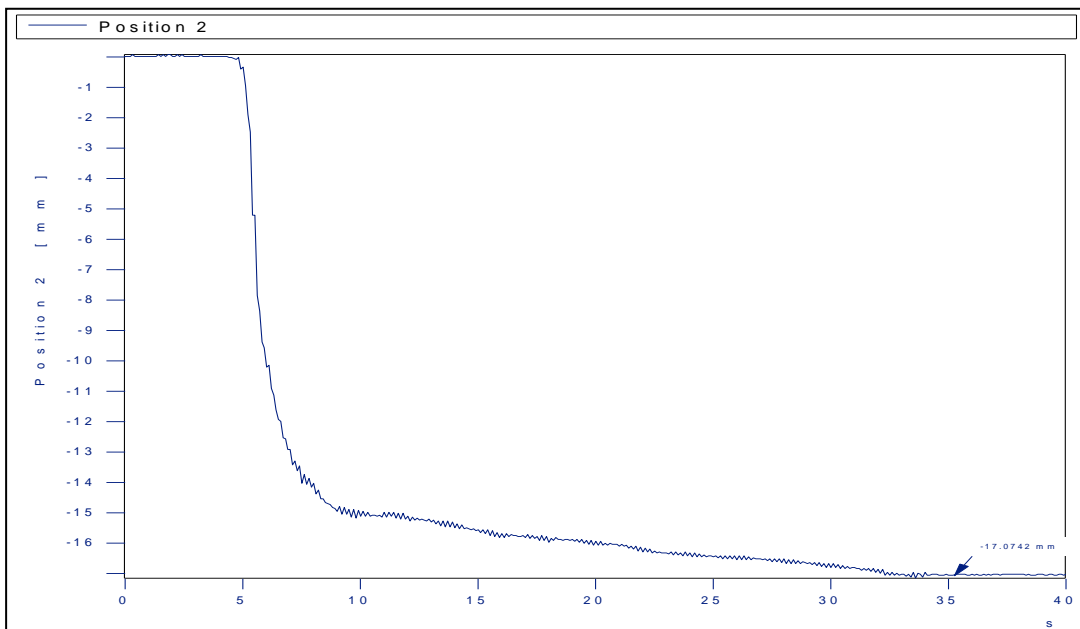


Figure I2: Horizontal displacement measurements for one block for 5 Hz

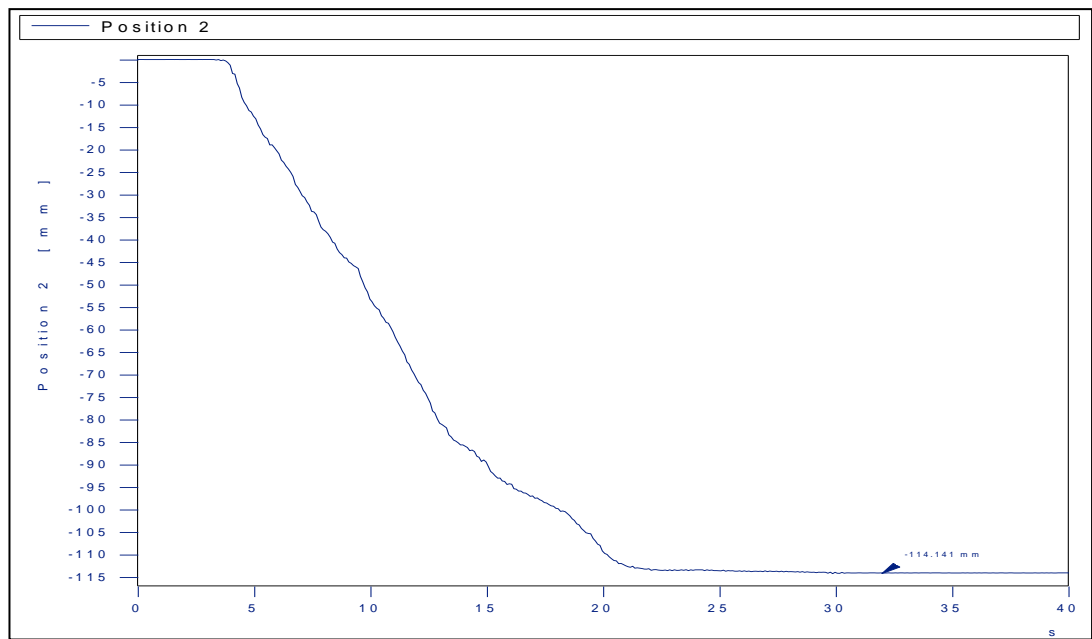


Figure I3: Horizontal displacement measurements for one block for 6 Hz

APPENDIX J

POSITION MEASUREMENTS

Position transducers measurements for two blocks tests for Soil 2- Tests 2.2 are shown in Figure J1 – I3.

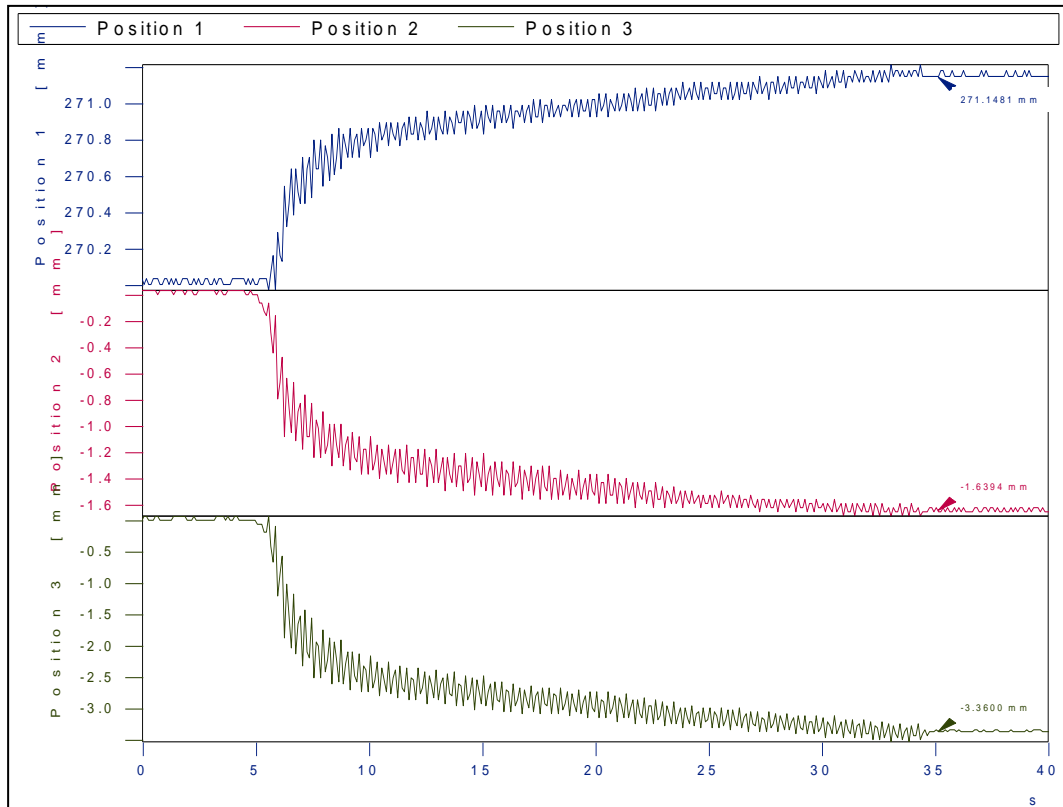


Figure J1: Horizontal and vertical displacement measurements for two blocks for 4 Hz

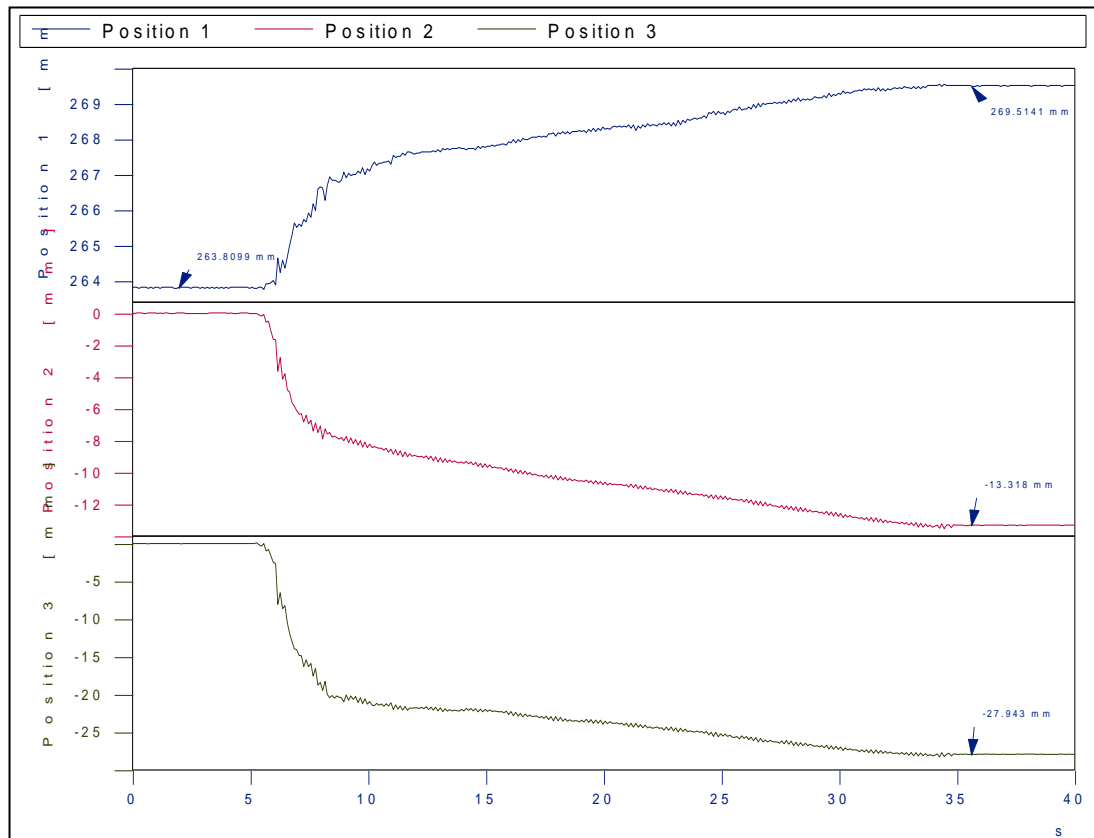


Figure J2: Horizontal and vertical displacement measurements for two blocks for 5 Hz

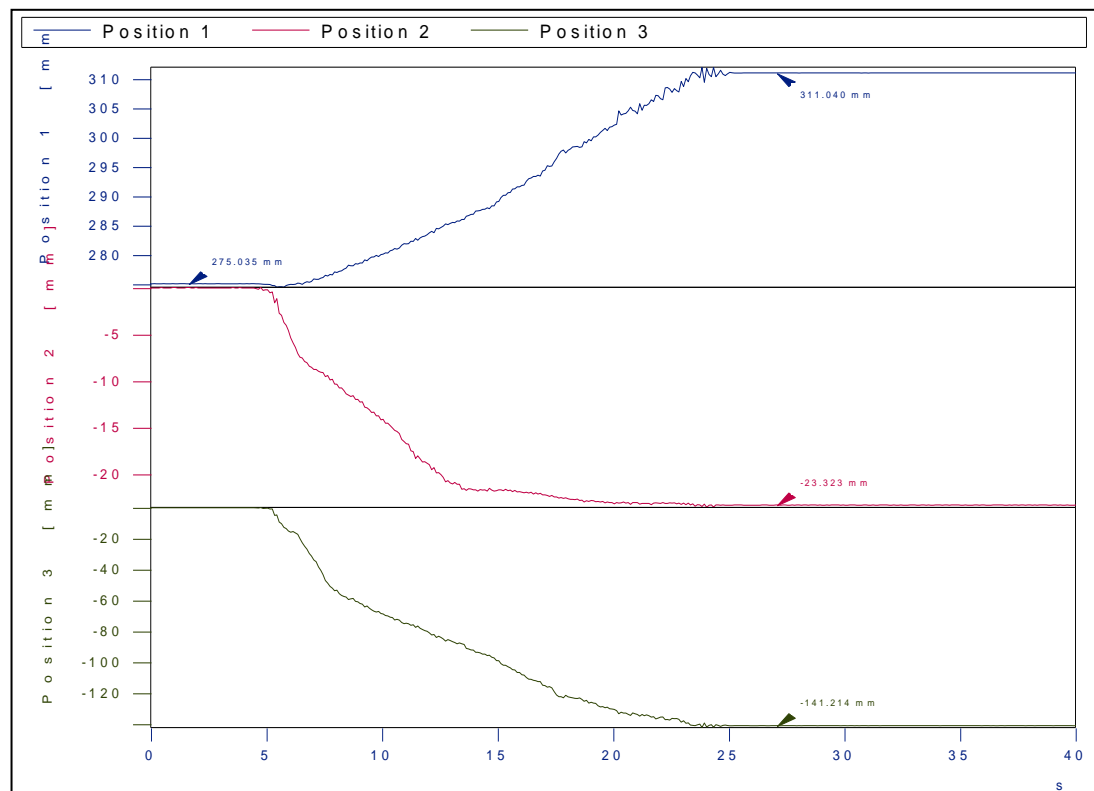


Figure J3: Horizontal and vertical displacement measurements for two blocks for 5 Hz

APPENDIX K

POSITION MEASUREMENTS

Position transducers measurements for two blocks tests for Soil 2- Tests 3.2 are shown in Figure K1 – K3.

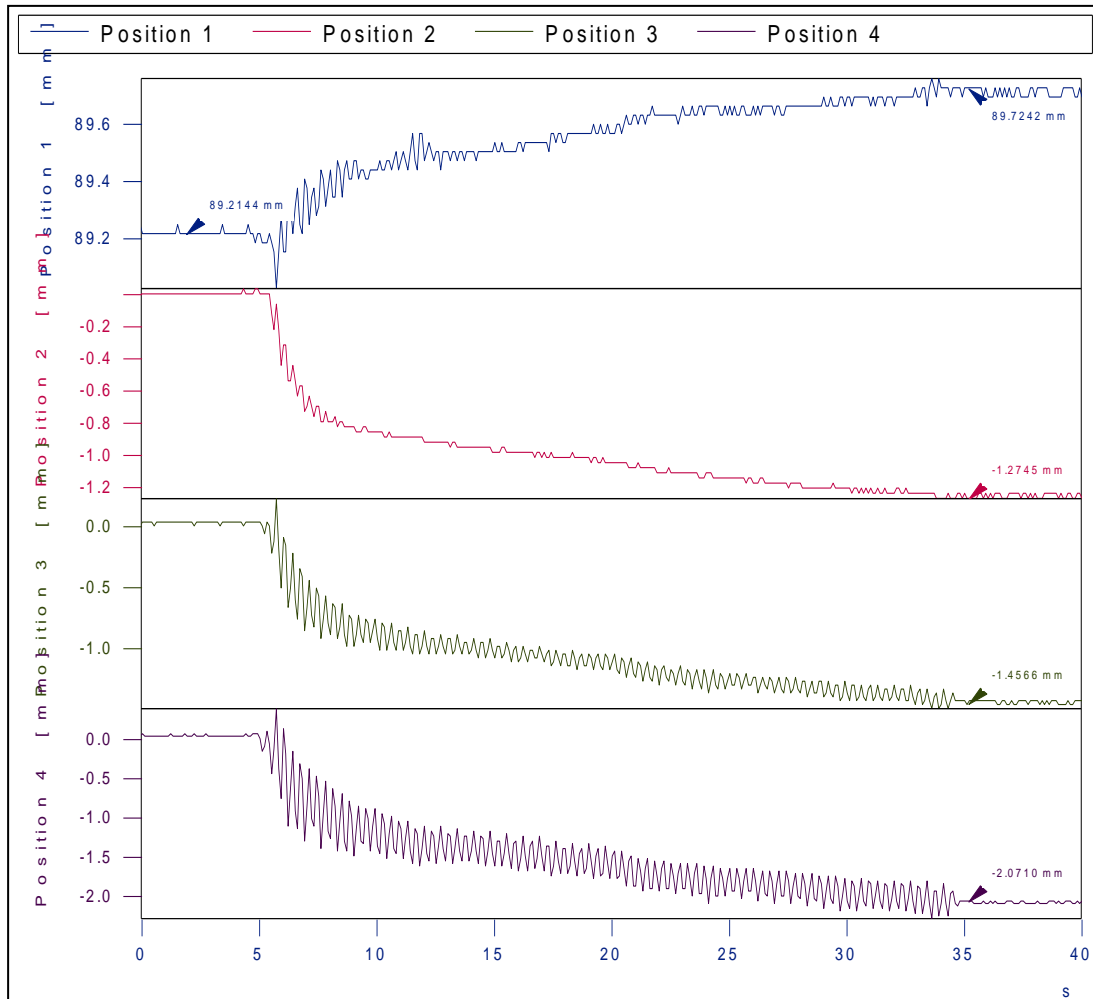


Figure K1: Horizontal and vertical displacement measurements for three blocks for 3 Hz

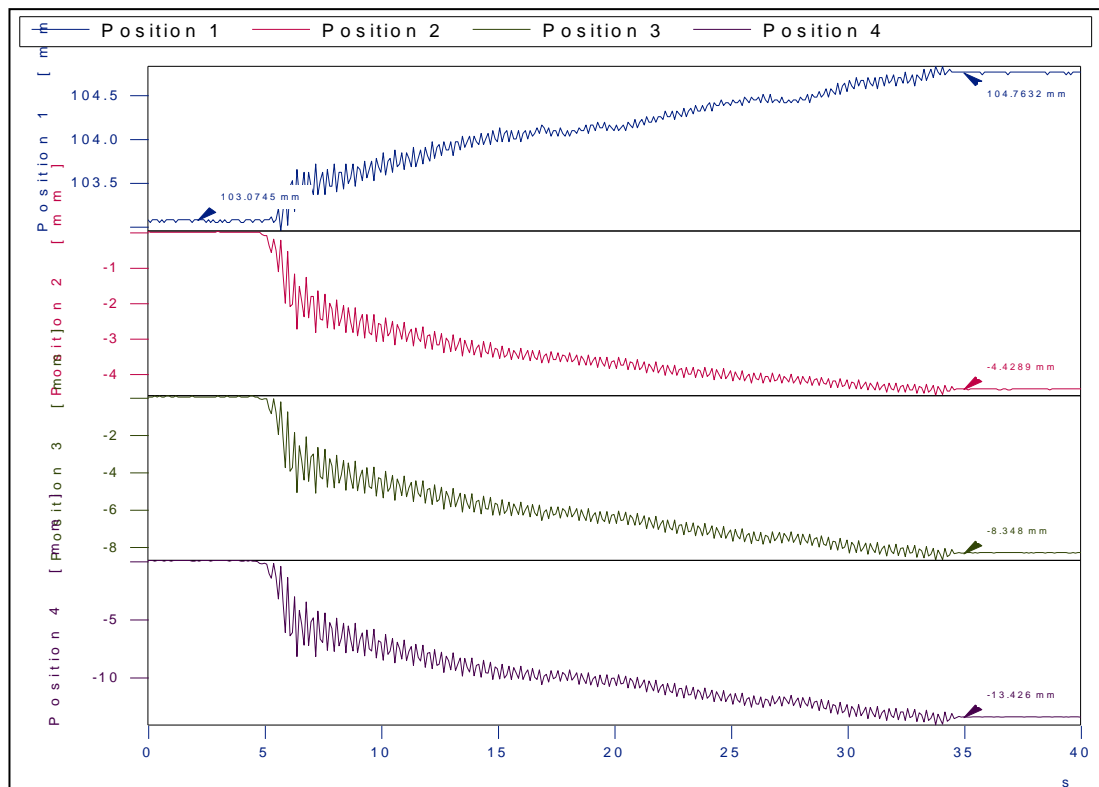


Figure K2: Horizontal and vertical displacement measurements for three blocks for 4 Hz

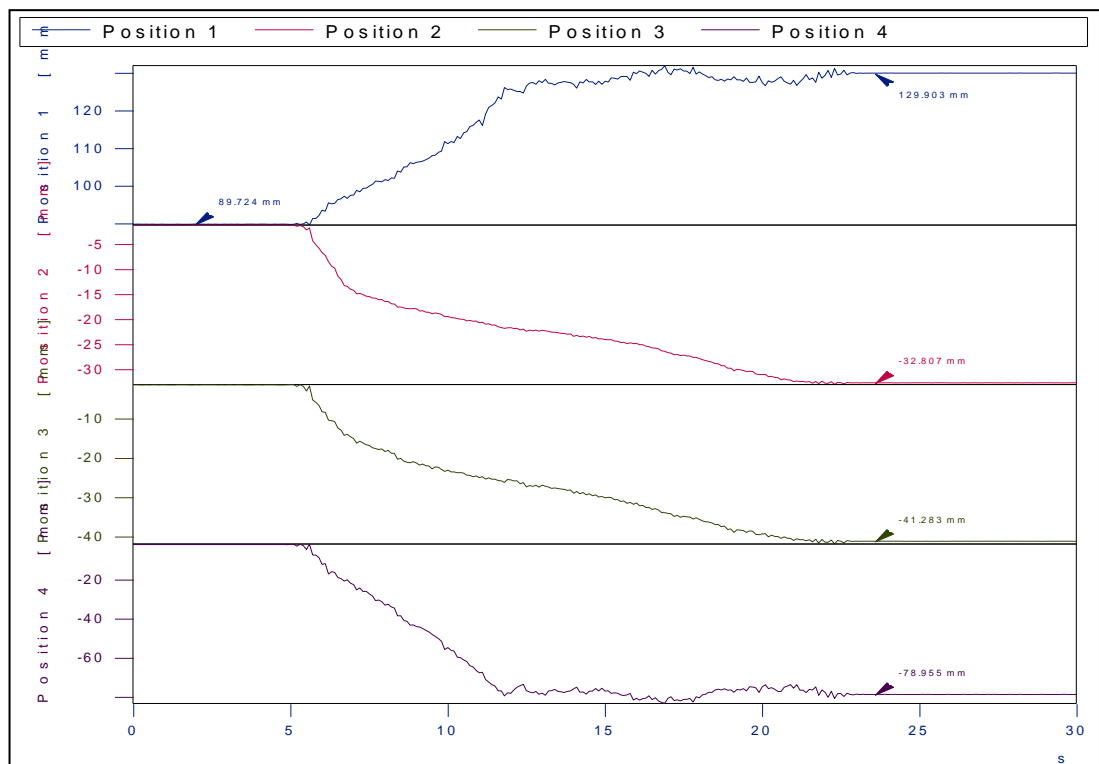


Figure K3: Horizontal and vertical displacement measurements for three blocks for 5 Hz

APPENDIX L

MATERIAL PROPERTIES

<http://www.stanford.edu/~tyzhu/Documents/Some%20Useful%20Numbers.pdf>

Some Useful Numbers on the Engineering Properties of Materials (Geologic and Otherwise)
GEOL 615

Coefficient of sliding friction (μ)

For most rocks, μ varies between 0.8 and 0.5. A value of 0.60 would be a good number for general use.

Glass on glass	0.4
Rubber on concrete	0.75
Steel on steel	0.55

Angle of internal friction (ϕ)

Rock	30°
Sand	30-40°
Gravel	35°
Silt	34°
Clay	20°
Loose sand	30-35°
Medium sand	40°
Dense sand	35-45°
Gravel with some sand	34-48°
Silt	26-35°

Because the angle of internal friction, ϕ , is typically around 25-35°, the coefficient of internal friction ($\tan\phi$) is 0.5 to 0.7

Cohesive strength (τ_0)

Rock	10,000 kPa
Silt	75 kPa
Clay	10-20 kPa
Very soft clay	0-48 kPa
Soft clay	48-96 kPa
Medium clay	96-192 kPa
Stiff clay	192-384 kPa
Very stiff clay	384-766 kPa
Hard clay	>766 kPa

Density (ρ)

Sandy soil	1800 kg/m ³
Gravel soil	2000 kg/m ³
Silty soil	2100 kg/m ³
Clay soil	1900 kg/m ³
Mafic igneous rocks	3000 kg/m ³
Felsic igneous rocks	2700 kg/m ³
Metamorphic rocks	2700 kg/m ³
Sedimentary rocks	2600 kg/m ³
Granite	2700 kg/m ³
Shale	2500 kg/m ³

Limestone	2700 kg/m ³
Chalk	2100 kg/m ³
Sandstone	2000 kg/m ³
Steel	8000 kg/m ³
Concrete	1680-3000 kg/m ³
Water	1000 kg/m ³

Unit weight (γ) (recall that $\gamma = \rho g$)

"Rock"	26.5 kN/m ³
Gravel soil	19 kN/m ³
Sandy soil	16 kN/m ³
Silty soil	20 kN/m ³
Clay soil	18 kN/m ³
Water	9.8 kN/m ³
Concrete	23 kN/m ³
Steel	78 kN/m ³

Porosity

Gravel	30-40%
Sand	20-35 %
Silt	35-50 %
Clay	33-60 %
Sand and gravel, mixed	20-35 %
Glacial till	10-20 %
Sandstone	5-30%
Limestone	5-30%
Shale	10-30 %
Fractured igneous rock	10-40%
Granite	0.5-1.5 %
Diabase	0.1-0.5 %
Gabbro	0.1-0.2 %
Basalt	0.1-1.0 %
Gneiss	0.5-1.5 %
Marble	0.5-2 %
Slate	0.1-0.5 %
Quartzite	0.1-0.5 %

----- (Unfractured) -----

Permeability

Well-sorted gravel	10 ⁻² to 1 cm/sec
Well-sorted sands, glacial outwash	10 ⁻³ to 10 ⁻¹ cm/sec
Silty sands, fine sands	10 ⁻⁵ to 10 ⁻³ cm/sec
Silt, sandy silts, clayey sands, till	10 ⁻⁶ to 10 ⁻⁴ cm/sec
Clay	10 ⁻⁹ to 10 ⁻⁶ cm/sec

Soil Sensitivity

Insensitive clays	<1
Low sensitive clays	1-2
Medium sensitive clays	2-4
Sensitive clays	4-8
Extra sensitive clays	8-16
Quick clay	>16

Compressibility (C_c)

Soft clay	>0.3
Clay	0.3-0.15
Silty clay	0.15-0.075
Sandy clay	<0.075

Poisson's ratio (ν)

Sandy Soil	0.25-0.4
Gravel soil	0.15-0.35
Granite	0.1-0.3
Sandstone	0.21-0.38
Shale	0.2-0.4
Limestone	0.18-0.33
Chalk	0.35
Marble	0.06-0.22
Steel	0.3

Young's Modulus (E)

Clay soil	10-200 MPa (soft to stiff)
Sandy soil	10-50 MPa (loose to compact)
Gravel soil	70-170 MPa (loose to compact)
Soft clay	1-3 MPa
Hard clay	6-14 MPa
Loose sand	10-28 MPa
Dense sand	35-69 MPa
Granite	10-70 GPa
Sandstone	1-20 GPa
Shale	1-70 GPa
Limestone	15-55 GPa
Marble	50-70 GPa
Steel	200 GPa
Glass	45 GPa
Wood	6,000-15,000 MPa

Bulk modulus (K)

Granite	50 GPa
Shale	10 GPa
Limestone	65 GPa
Chalk	9 GPa
Sandstone	0.7 GPa

Modulus of rigidity (μ)

Granite	24 GPa
Shale	1.6 GPa
Limestone	24 GPa
Chalk	3.2 GPa
Sandstone	0.4 GPa
Steel	80 GPa
Wood	4 GPa
Glass	19 GPa

Lithostatic pressure gradient

26.46 MPa/km (for $\rho = 2.70$)

Hydrostatic pressure gradient

9.8 MPa/km

Unconfined compressive strength

Granite	100-250 MPa
Basalt	100-300 MPa
Quartzite	150-300 MPa
Sandstone	20-170 MPa
Shale	5-100 MPa
Limestone	30-250 MPa
Marble	35-60 MPa
Slate	100-200 MPa
Quartzite	150-300 MPa
Concrete	14-42 MPa
High strength concrete	70 MPa
Steel	250 MPa
Wood	5 MPa

Field test for compressive strength of soils and rocks

Term	Diagnostic features	Undrained compressive strength
Very soft soil	Exudes between fingers when squeezed	<25 kPa
Soft soil	Easily indented by fingers	25-50 kPa
Firm soil	Indented only by strong finger pressure	50-100 kPa
Stiff soil	Indented by thumb pressure	100-200 kPa
Very stiff soil	Indented by thumb nail	200-400 kPa
<u>Hard soil</u>	<u>Difficult to indent by thumbnail</u>	<u>400-1000 kPa</u>
Very strong rock	Very hard rock, requires repeated hammer blows	>100 MPa
Strong rock	Hand specimen can be broken with single blow	50-100 MPa
Mod. strong rock	5 mm indentations with hammer pick end	12.5-50 MPa
Mod. weak rock	Too hard to cut by hand	5-12.5 MPa
Weak rock	Crumbles with blows of pick end of hammer	1.25-5 MPa

Shear strength

Granite	14-50 MPa
Diabase	25-60 MPa
Basalt	20-60 MPa
Slate	15-30 MPa
Quartzite	20-60 MPa
Sandstone	8-40 MPa
Shale	3-30 MPa
Limestone	10-50 MPa
Gravel	200-600 kPa
Sand	100-300 kPa
Very soft clay	0-25 kPa
Soft clay	25-50 kPa
Medium clay	50-100 kPa
Stiff clay	100-200 kPa
Very Stiff clay	200-400 kPa
Hard clay	>400 kPa
Wood	10 MPa
Concrete	2 MPa
Steel	230 MPa

Tensile strength

Granite	7-25 MPa
Basalt	10-30 MPa
Gneiss	5-20 MPa
Quartzite	10-30 MPa
Sandstone	4-25 MPa
Shale	2-10 MPa
Limestone	5-25 MPa
Marble	15 MPa
Steel	400 MPa
High strength steel	750 MPa
Cast iron	170 MPa
Aluminum	450 MPa
Concrete	5 MPa
Rubber	15 MPa

P-wave velocity

Soil	100-500 m/sec
Glacier ice	3000-4000 m/sec
Clay (dry)	200-1400 m/sec
Clay (wet)	1200-2200 m/sec
Alluvium	3000-5000 m/sec
Water	1450-1500 m/sec
Sand	400-2300 m/sec
Oil	1300 m/sec
Air	320-340 m/sec
Granite	3000-5900 m/sec
Basalt	4500-6500 m/sec

Quartzite	5000-6500 m/sec
Sandstone	1400-4000 m/sec
Shale	1400-3000 m/sec
Limestone	2500-6000 m/sec
Marble	3500-6000 m/sec
Salt	4500 m/sec

S-wave velocity

Clay (dry)	410 m/sec
Clay (saturated)	390 m/sec
Alluvium	1900 m/sec
Water	0 m/sec (because no shear strength)
Oil	0 m/sec (because no shear strength)
Air	0 m/sec (because no shear strength)
Limestone	3100 m/sec
Sandstone	2400 m/sec
Dolomite	3000 m/sec
Shale	2600 m/sec
Granite	3400-3600 m/sec
Dolerite	3500-3600 m/sec
Salt	2700 m/sec

Resistivity

Marble	5×10^7 - 10^9 Ohm-m
Mica	10^{11} - 10^{14} Ohm-m
Quartz	10^{12} - 10^{14} Ohm-m
Slate	1 - 2×10^6 Ohm-m
Petroleum	2×10^{14} Ohm-m
Distilled water	5000 Ohm-m
Saltwater 2 ppm	3.4 Ohm-m
Saltwater 10 ppm	0.72 Ohm-m
Saltwater 20 ppm	0.38 Ohm-m
Saltwater 100 ppm	0.09 Ohm-m

APPENDIX M

AUGUST 17, 1999 EARTHQUAKE DATA

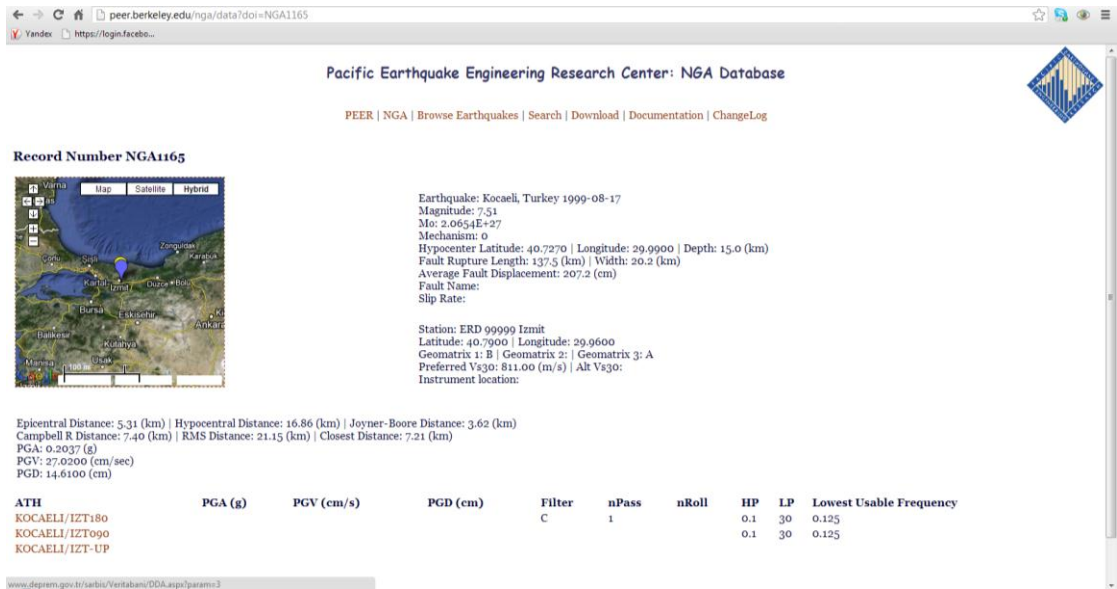


Figure M1: August 17, 1999 Earthquake Data

CURRICULUM VITAE

PERSONAL INFORMATION

Surname, Name: Karakuş, Hülya

Nationality: Turkish (TC)

Date and Place of Birth: August 08, 1980, Eskişehir

Marital Status: Engaged

Phone: +90 312 441 45 96

email: hulya_karakus@hotmail.com

EDUCATION

Degree	Institution	Year of Graduation
MS	METU Civil Engineering	2007
BS	University of Osmangazi Civil Engineering	2003
High School	Muhittin Güzelkılınç High School, Konya	1998

WORK EXPERIENCE

Year	Place	Enrollment
2011- Present	YÜKSEL PROJE ULUSLARARASI A.Ş.	Project Engineer
2004-2011	METU Department of Civil Engineering	Research Assistant
200 July	DSİ / Eskişehir	Intern Engineering Student
200 August	Kışınbay İnş.Lim.Ltd.Şti./Eskişehir	Intern Engineering Student

FOREIGN LANGUAGES

Advanced English

PUBLICATIONS

Karakuş, H., Ergin, A., Guler, I., Cihan, K., Yüksel, Y., (2012). "Dynamic Response of Block Type Quay Wall." *PIANC-COPEDEC VIII*, Chennai, Hindistan, pp: 1561-157220-24, February 2012.

Yüksel, Y., Cihan, K., Uluşan, A., Bulgurlar, B. ve Karakuş, H., (2011). "Keson ve L Tipi Rıhtım Yapılarının Sismik Yükler Altında Davranışı." *7th National Coastal Engineering Symposium*, Trabzon, pp: 247-256, 21-23, 2011.

Karakuş, H., Ergin, A., Güler, I., Cihan, K., Yüksel, Y., (2011). "Blok Tipi Kıyı Yapılarının Dinamik Davranışında 1G Sarsma Deneyleri." *7th National Coastal Engineering Symposium*, Trabzon, pp: 209-219, 21-23, Kasım 2011.

Karakuş, H., Ergin, A., Guler, I., Cetin, K.O., Yalçiner, A.C.,(2010). "New Seismic Design Approaches for Block Type Quay Walls and Performance Based Design Methodology." *5th Sakhalin Youth Scientific School*, Yuzno Sakhalin- Rusya, 2010

Yalçiner, A. C., Özer, C., Karakuş, H., Zaytsev, A., Guler, I., (2010). "Evaluation Of Coastal Risk At Selected Sites Against Eastern Mediterranean Tsunamis." *Proceedings of 32nd International Conference on Coastal Engineering (ICCE 2010)*, Shanghai, China, <http://journals.tdl.org/ICCE/issue/current/showToc>.

Dilmen, D. I., Yalçiner, A. C., Zaytsev, A., Chernov, A., Özer, C., Insel, I.,Pelinovsky, E., Kurkin, A., Karakuş, H., Kanoğlu, U., Imamura, F., (2009). "CBS Tabanlı Tsunami Baskın Haritalarının Geliştirilmesi; Fethiye Örneği." *Proceedings of 62th Turkey Geology Congress*.

Dilmen, D. I., Yalçiner, A. C., Zaytsev, A., Chernov, A., Özer, C., Insel, I.,Pelinovsky, E., Kurkin, A., Karakuş, H., (2009). "Tsunami Modeling and Inundation Mapping for Fethiye Town, SW Turkey." *Proceedings of International Symposium on Historical Earthquakes and Conservation of Monuments and Sites in the Eastern Mediterranean Region, 500th Anniversary Year of the 1509 September 10, Marmara Earthquake*, Istanbul, Turkey, September 10-12, 2009, pp. 242-245

Karakuş, H., Ergin, A., Guler, I., Cetin, K.O., (2008). „New Seismic Design Approaches for Block Type Quay Walls." *Conference on Marine Problems and Specific Solutions, COMPASS*, Maldives, 2008.

Zaytsev, A., Karakuş, H., Yalçiner, A. C., Chernov, A., Pelinovsky, E., Kurkin, A., Özer, C., Insel, I., Özyurt, G., and Dilmen, D.I., (2008). "Tsunamis in Eastern Mediterranean, Histories, Possibilities And Realities." *COPEDEC VII, 2008*, Dubai, UAE. paper number: Z-01.

Özer, C., Karakuş, H., Yalçiner A. C., (2008). "Investigation of Hydrodynamic Demands of Tsunamis in Inundation Zone." *Proceedings of 7th International Conference on Coastal and Port Engineering in Developing Countries*, Dubai, UAE, February 24-28, 2008.

Karakuş, H., Ergin, A., Guler, I., Cetin, K.O., (2007). " New Seismic Design Approaches for Block Type Quay Walls." *MS Thesis* in Middle East Technical University, Ankara, Turkey.

Yalçiner, A.C., Pelinovsky, E., Zaytsev, A., Kurkin, A., Özer, C., Karakuş, H., Özyurt, G., (2007). "Modelling and Visualization of Tsunamis: Mediterranean Examples." *Tsunami and Nonlinear Waves*, Anjan Kundu (Ed.), Springer, 2007, pp.273-283

A. Zaytsev, H. Karakuş, A.C. Yalçiner, A.Chernov, E. Pelinovsky, A. Kurkin, Yalçiner, A.Chernov, E. Pelinovsky, A. Kurkin, C. Özer, I. Insel, G. Özyurt and D.I. Dilmen (2008). "Tsunamis In Eastern Mediterranean, Histories, Possibilities And Realities." *Proceedings of COPEDEC VII, 2008*, Dubai, UAE.

Karakuş, H., Ergin, A., Guler I., Cetin, K.O., (2007). "New Seismic Design Approaches for Block Type Quay Walls." *Proceedings of 6th National Coastal Engineering Symposium*, İzmir, Turkey.

Karakuş, H., Yalçiner, A.C., Pelinovsky, E., Zaytsev, A., Kurkin, A., Kuran, U., Özer, C., Özyurt, G., (2006). "Understanding And Mitigation of Tsunamis in the Eastern Mediterranean." *Proceedings of Hazards, 2006 Symposium*, Patras, Greece.

Yalçiner, A. C., Karakuş, H., Özer, C., Özyurt, G., (2005). "Understanding The Generation, Propagation, Near and Far Field Impacts of Tsunamis, Planning Strategies and Preparedness for Future Events." *The Course Notes of the Short Course* on July, 11-12, 2005, for University Teknologi Malaysia, Kuala Lumpur.

Tuncay, T., Tan, O., Yolsal, S., Yalçiner, A.C., Özer, C., Karakuş, H., Kuran, U., (2005). "Bizde de Olur mu?" TUBITAK Bilim- Teknik Dergisi, 2005.

Yalçiner, A. C., Kuran, U., and Karakuş, H., (2005). "Tsunamis in the Mediterranean and Comparison with Caribbean." *Proceedings of the NSF Caribbean Tsunami Workshop*, 2004.

ACADEMIC PRESENTATION:

"Dynamic Response of Block Type Quay Wall" presentation in India for 8th International Conference on Coastal and Port Engineering in Developing Countries COPEDEC, India, 2012.

1g Shaking Table Tests for Block Type Quay Walls" 7th National Coastal Engineering Symposium, Trabzon, Turkey, 2011.

"Seismic Analysis of Block Type Quay Walls" 5th Sakhalin Youth Scientific School, Russian Academy of Sciences, Far East Branch Institute of Marine Geology and Geophysics, Yuzhno Sakhalinsk, Russia, June 8-11, 2010.

"Tsunamis In Eastern Mediteranean, Histories, Possibilities And Realities" 7th International Conference on Coastal and Port Engineering in Developing Countries, Dubai, UAE, (2008).

"New Seismic Design Approaches for Block Type Quay Walls" presentation in Maldives for COMPASS 2008 (Conference on Marine Problems and Specific Solutions) , June 2008.

"Understanding and Mitigation of Tsunamis in the Eastern Mediterranean" presentation in Greece for Hazards, 2006.

"Coastal Defense Structure" course notes and presentation for "Coastal and Harbor Structures Design" lecture. 2004-2005 spring term.

"Beach Erosion near Tidal Inlets Selected Case Studies along Southwest Florida Coastline" presentation for "Coastal Sediment Transport" lecture 2004-2005 spring terms.

COURSES, CONFERENCES and SYMPOSIUM

7th International Workshop on Coastal Disaster Prevention organized by Port and Airport Research Insititute (PARI), Asia Pacific Center for Coastal Disaster Research, Tokyo, Japan, January 26-28, 2011.

European Geosciences Union General Assembly 2010, Vienna, Austria, May 03–07, 2010.

UNESCO-IOC Sixth Session of the Intergovernmental Coordination Group for the Tsunami Early Warning and Mitigation System in the North Eastern Atlantic, the Mediterranean and Connected Seas (ICG/NEAMTWS-VI), Istanbul, Turkey , November 11-13, 2009.

Closing Meeting of European Commission Project “TRANSFER” Tsunami Risk AND Strategies For the European Region, Istanbul, Turkey, September 14-16, 2009.

International Symposium on Historical Earthquakes and Conservation of Monuments and Sites in the Eastern Mediterranean Region, 500th Anniversary Year of the 1509 September 10, Marmara Earthquake, Istanbul, Turkey, September 10-12, 2009.

Short course at Yildiz Technical University, Istanbul by Dr. J. Van der MEER (2007).

6th National Coastal Engineering Symposium, Izmir, Turkey (2007).

5th National Coastal Engineering Symposium, Bodrum, Turkey (2005).